GUIDEBOOK

50th. Annual Field Conference Of Pennsylvania Geologists

CENTRAL PENNSYLVANIA GEOLOGY REVISITED

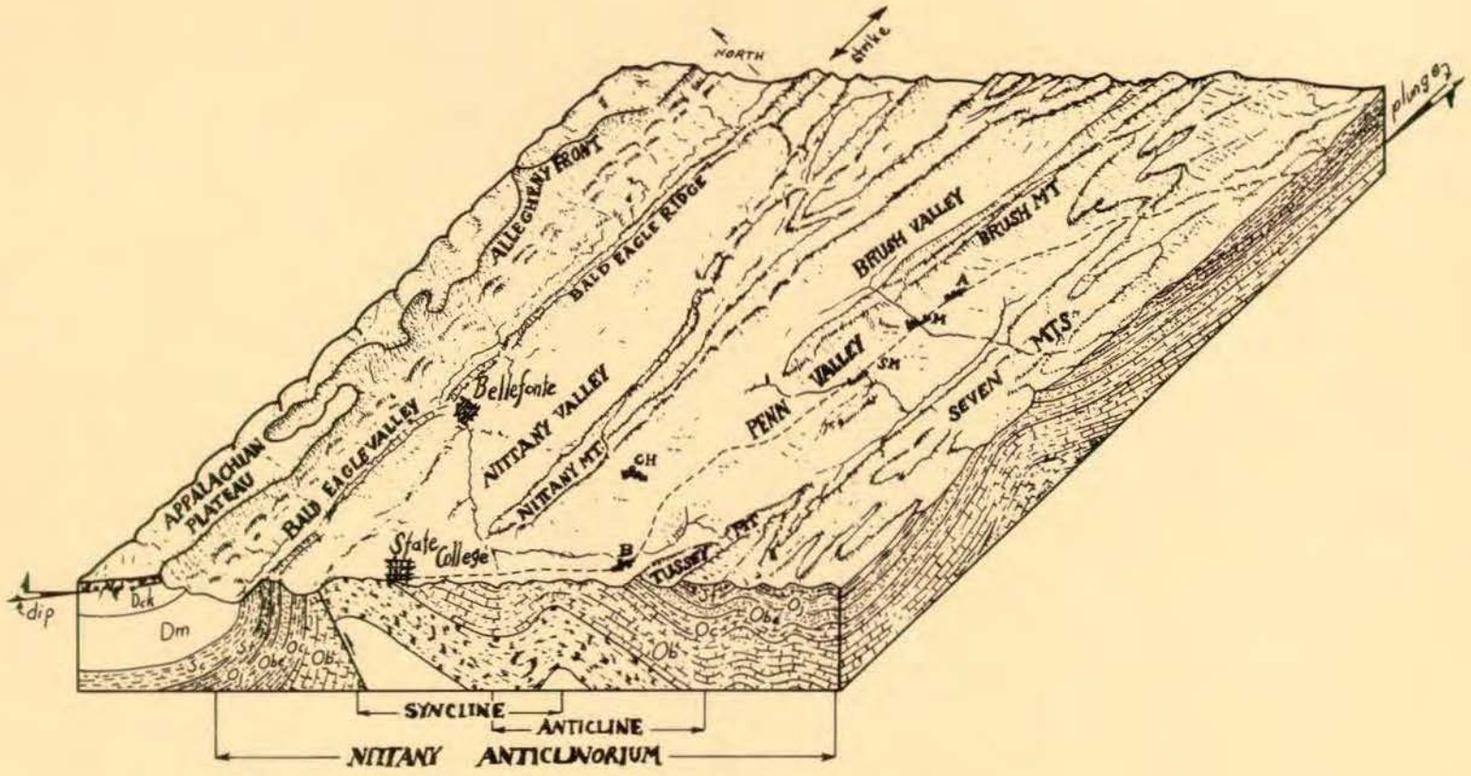

October 4, 5, and 6, 1985

State College, Pa.

Host: Department of Geosciences,
Pennsylvania State University

ACKNOWLEDGEMENTS

We would like to make a special acknowledgement to Victor Rahmanian, whose work constitutes the basis for the Catskill sedimentation discussion and field trip. Victor desired to attend the conference but foreign assignments prevent him from participating.

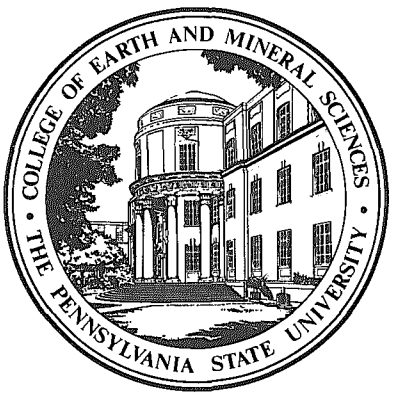

Printing of the

50th Field Conference of Pennsylvania Geologists

Guidebook

has been partially provided by a grant from the

College of Earth and Mineral Sciences,

Pennsylvania State University

Guidebook for the

50th ANNUAL FIELD CONFERENCE OF PENNSYLVANIA GEOLOGISTS

CENTRAL PENNSYLVANIA GEOLOGY REVISITED

Field Trip Leaders:

David P. Gold, Pennsylvania State University, Local Committee Chairman
Michael R. Canich,
Cabot Oil and Gas Company
Roger J. Cuffey, P.S.U.
Alan Davis, P.S.U.
Thomas W. Gardner, P.S.U.
Albert L. Guber, P.S.U.
Richard R. Parizek, P.S.U.
Howard A. Pohn, U.S.G.S.
Arthur W. Rose, P.S.U.
Rudy Slingerland, P.S.U.
Barry Voight, P.S.U.
Eugene G. Williams, P.S.U.
William B. White, P.S.U.

October 3-5, 1985

Host: Dept. of Geosciences, Pennsylvania State University

Headquarters: Holiday Inn, State College, Pennsylvania

Guidebook Distributed By:

Field Conference of Pennsylvania Geologists
c/o Department of Environmental Resources
Bureau of Topographic and Geologic Survey
P. O. Box 2357
Harrisburg, PA 17120

Reprinted February 1987

Contents

FIELD TRIP #1

A MID-SILURIAN CORAL-BRYOZOAN REEF IN CENTRAL PENNSYLVANIA

by
Roger J. Cuffey, Carolyn E. Davidheiser,
Shirley S. Fonda, Anne B. Lutz,
Laurie S. Zimmerman, and Barbara B. Skerky

Significance and Purpose

Central Pennsylvania lies just beyond the borders of the Great Lakes district, renowned for its development as one of the world's earliest major coral reef provinces. Nonetheless, Silurian rocks in our state also contain a few small bioherms, which apparently represent scattered outliers from those major Midwestern reef tracts (Cuffey and Davidheiser, 1979; Inners, 1984).

One in particular among our local bioherms is of wider interest scientifically, for two reasons. First, unlike the Great Lakes Silurian reefs, this Pennsylvania one--near Lock Haven (Clinton County; Fig. 1)--is undolomitized and hence provides a good view of the organisms and sediments involved in reefs at that time. Second, bryozoans participated significantly in the construction of the Lock Haven reef, a rather unusual and hence intriguing situation, because reef-building represents a paleoecologic extreme for that phylum, and because bryozoan-built structures are exotic variants among bioherms through geologic time (Cuffey, 1977, 1985).

Consequently, we wish to showcase the Lock Haven reef here, so that its unique features and potential contributions can be appreciated both by Pennsylvania geologists and also by reef- and bryozoan-oriented scientists in general. Our chapter will therefore serve for overall summary, this conference field trip, and future self-guided individual visits. After briefly outlining the overall setting, we will discuss implications of our studies of the Lock Haven reef (Cuffey and Davidheiser, 1979; Davidheiser, 1980; Davidheiser and Cuffey, 1981; Cuffey, 1985), and then present its observable characteristics in the format of several field-trip stops.

Initially cut into years ago by the road (then dirt or gravel) running eastward from Castanea, the Lock Haven reef remained rather poorly exposed until mid-1972. Then, the extremely heavy rains from Hurricane Agnes provoked much slumping along the road cuts at the foot of Bald Eagle Mountain. These slumps, combined with subsequent road repairs and reconstruction, improved the reef exposures significantly for a few years. Recently, however, weathering and continued slumping are again obscuring and covering parts of the outcrop.

In the years spent examining the Lock Haven reef, we have been assisted by many individuals; we wish to particularly thank L. Brant, W. Bruck, G. Burgess, T. Davies, R. Dunay, J. Head, J. Jobling, S. Krajewski, P. Kremer, R. Lanning, R. Lowright, J. Malkames, C. McKee, G. Mertz, J. Morrison, G. Moser, G. Newton, M. Podwysocki, J. Shultz, D. Siegel, J. Swinehart, A. Thorn, K. Wilson, and M. Zeigler.

Overall Setting

In current terminology (Cuffey, 1985), the Lock Haven reef consists of a favositid crust-mound center, surrounded by cladoporid and trepostome frame-

thickets. The exposed surface of the Lock Haven reef displays lateral variations in both rock and fossil characteristics, variations which can be expressed well by grouping those materials into several lithotypes, each interpretable as having formed within a different environmental zone. Commencing at the outer edge of the reef (i.e., at the eastern end of the currently available outcrops), and progressing inward (westward) toward the central or thickest part of the reef, the sequence of lithotypes--and inferred equivalent ecozones--is platy shale and limestone (off-reef mud bottom), massive calcarenite (surrounding sand apron), trepostome branch coquina (deeper reef flank), cladoporid branch coquina (shallower reef flank), favositid reef-rock (reef crest or core), and stromatolitic rubbly limestone (reef cap) Fig. 1; Table 1).

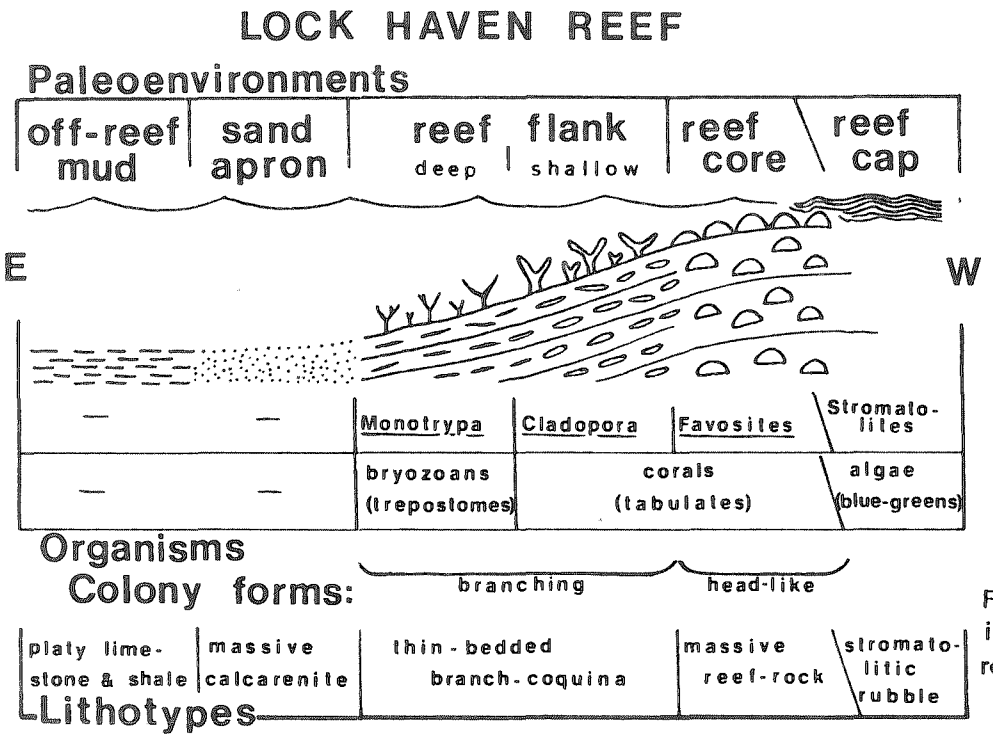

Figure 1. Ecozonation inferred for Lock Haven reef; also compare Table 1.

The Lock Haven reef is a thick carbonate, surrounded by thinly interbedded shales and limestones, which represent the Rochester Shale overlain by the lower limestone-and-shale member of the McKenzie Formation (or equivalent portions of the more broadly conceived Mifflintown Formation of recent usage). These strata are of Middle Silurian age (specifically middle Wenlockian). The reef mass can be correlated with particular biozones (as discussed later under Stop 6); it appears to be founded on approximately the Rochester-McKenzie boundary and projects upward (hence as a knob of "Rochester") into the basal McKenzie.

Regional stratigraphic correlations tie the Rochester-McKenzie contact into the New York standard section just above the Clinton-Lockport boundary (Berry and Boucot, 1970, at the level of the Gasport Dolomite, basal Lockport). The Gasport, in westernmost New York state and adjacent Ontario, contains well-developed small reefs (Crowley, 1973; Crowley and Poore, 1974), partly resembling the Lock Haven reef with which they are contemporaneous. (Lichenaliid-bryozoan reefs described from the basal Rochester or uppermost Irondequoit in that area by Sarle, 1901, are somewhat older; Hewitt and Cuffey, 1985; Brett, 1982, 1983a, 1983b).

Moreover, as a mid-Silurian reef, the Lock Haven deposit is at least roughly correlative with the vast Great Lakes Silurian reef complex. Several different times of reef initiation and growth (reef "generations") can be distinguished within that reef complex (Shaver, 1977; Shaver and others, 1978). One early, short-lived generation, early in middle Wenlockian time, consists of the Gasport reefs, and hence also the Lock Haven reef as a contemporaneous southeastern outlier.

During the Middle Silurian, North America was in an equatorial position, mostly shallowly submerged, and dominated by carbonate sedimentation, much like the modern Bahama Banks. Still isolated from most other land masses, the continent was being approached closely by one other, the Baltic-shield craton (Ziegler and others, 1977; Dott and Batten, 1976). A large region, centered on the Michigan Basin but extending outward far across the surrounding shallow shelves, developed a vast reef complex. The edge of this reefal sea graded eastward into a shallow muddy bottom perhaps slightly deeper or basinal, which in turn abutted against mountainous islands along the eastern margin of the continent. A few small patch reefs developed in that mud-bottomed Appalachian sea, and one of them is now preserved and exposed as the Lock Haven reef.

TABLE 1. Summary of observed and inferred features of the Lock Haven reef

PRESERVED FACIES SUMMARY NAME (stop numbers)	OFF-REEF SHALE (5)	CALCARENITE APRON (4)	TREPOSTOME FLANK (3)	CLADOPORID FLANK (2)	FAVOSITID CORE (1)	REEF CAP (7,8,9)
environment	open level bottom		reef mound or bioherm			
ecozone	off-reef mud bottom	circum-reef sand apron	reef flank or slope: deep flank	reef flank or slope: shallow flank	reef top: reef crest or core	reef top: reef flat
habitat	barren mud	barren sand	bryozoan thickets	coral thickets	coral heads	algal domes
depth	deep (but see text)		moderately deep	moderately shallow	very shallow	intertidal
dominant phylum or class	--	--	bryozoans	corals		algae
dominant order	--	--	trepostomes	tabulates		stromatolites
dominant genus and species	--	--	*Monotrypa benjamini*	*Cladopora seriata*	*Favosites niagarensis*	*Collenia* sp.
dominant growth form	--	--	branches		heads or domes	
general rock type	shale	limestone				
particular lithotype	platy shale	massive calcarenite	branch coquina		massive biolithite	stromatolitic cap
specific reef-rock or carbonate-rock types	mudstone marlstone, micstone	grainstone	baffestone, rudstone, floatstone	rudstone	globstone	crutstone, bindstone, rudstone
bedding characteristics	shaly	massive	thin-bedded		massive	massive laminated

Reef Recognition

Recognition of the Lock Haven deposit as a fossil reef results from several detailed observational comparisons, rather than its geometric form (because that is so poorly exposed).

First, the suite of organisms preserved there abundantly--the coral heads, and coral and bryozoan branches--are typical of reef deposits in general, rather than of level bottoms. Indeed, this particular fact was what triggered Hoskins' (1964) original recognition of the reefal nature of this deposit.

Second, this assemblage does not occur as a coherent or consistent combination elsewhere in the enclosing formations, which yield a quite different brachiopod-ostracod fauna instead. Such sharp faunal contrast is characteristic of reef versus off-reef habitats. Patches of favositid heads are found elsewhere, but not the entire assemblage of favositids, cladoporids, and trepostomes.

Third, spatial or distributional variations within the coral-bryozoan assemblage here are the same as observed in other fossil and modern reef complexes, where they are clearly an ecozonation.

Fourth, the sedimentary matrix associated with each of the major coral and bryozoan types is typical of the organism-sediment combinations seen in ancient and modern reefs.

Fifth, fossil fragments from the zones interpreted as topographically higher occur occasionally in the matrix of zones thought to be lower, but not vice versa. This suggests downward transport along the flanks of a higher-standing, hence typically reefal, carbonate mass.

Sixth, the Lock Haven materials match analogous portions of the well-exposed Silurian reefs in the Great Lakes district. Detailed examination of a number of those reefs in Ohio, Indiana, and Illinois provided much comparative data helpful in precisely interpreting the Lock Haven reef after its exposures improved in 1972. (Hurricane Agnes that year triggered extensive slumping which temporarily much better exposed the reef than before or since.)

Seventh, the Lock Haven materials correspond nicely to comparable sections of modern Caribbean reefs on which we have dived extensively. This experience with modern counterparts proved especially useful in illustrating this paper (Figs. 4-5 of field guide).

Finally, Swartz (1970, pers. commun.; 1946, 1939, 1935b) had briefly noted "coralline lenses," with abundant Cladopora multipora [or seriata] and Favosites niagarensis, in the lower McKenzie near Lock Haven. He interpreted them as Lockport coral-rich limestone tongues from the north interfingering with McKenzie ostracod-bearing shales to the south, but did not label them as reefs. Most probably, his not stating the reefal character of these deposits was a function of his times, when reef geology was in an embryonic state, prior to the extensive biogeologic studies resulting from naval actions in the Pacific years later.

Reef Growth History

Only the outermost edge of the foundation underlying the Lock Haven reef is currently exposed; it is the platy shale and limestone typical of the off-reef habitat. The stratigraphic position of the reef mass suggests that such rocks extend underneath the entire reef. The lowest ecozone within the mound is the surrounding calcarenite sand apron; it is conceivable--though not demonstrated yet--that this rock type also goes across under the whole reef, as its basal zone. Apparently, therefore, the Lock Haven bioherm was initiated upon either a mud or sand bottom, mixed terrigenous and calcareous in composition, and likely soft or shifting (unstable, in either case). Such a foundation is not typical for modern coral reefs (though may possibly be approached by the rare Bahamian bryozoan reefs; Cuffey and others, 1977), but is encountered in many Paleozoic reefs. Various Great Lakes Silurian reefs, for example, were initiated upon terrigenous mud, carbonate mud, or carbonate sand (but not hardgrounds, so far as reported).

Once the reef foundation was in place, whether mud or sand, organic growth activities by colonial invertebrates became the predominant processes. Low on the reef flank, clumps of branching trepostomes (Monotrypa benjamini) trapped or baffled carbonate sands. Several such colonies are now visible, standing in place, still largely embedded in the calcarenitic matrix (Fig. 4J of field guide). Such sediment-trapping clumps may well have been the first reef organisms to occupy the barren sand patch on the overall muddy bottom. Higher on the reef flank, branching cladoporids (Cladopora seriata) apparently continued with the sediment-baffling role. In addition, throughout the flank, broken trepostome and cladoporid branches accumulated voluminously as skeletal sediment. However, outside of the branching colonies themselves (Fig. 4P of field guide), none appear to have formed an actual interlocking open framework here. In contrast, the head-like favositids (Favosites niagarensis) built a massive, dense, largely solid, lump-upon-lump reef frame in the reef core or crest, and also contributed some large loose boulders as reef-top loose rubble. Shells of other groups--particularly gastropods, calcispheres, and ostracods--added more skeletal sediment, especially around the foot of the reef flank. No bryozoans appear in the cryptic hidden-encrusting role seen elsewhere in some Silurian (Scoffin, 1972; Spjeldnaes, 1975) and most modern (Cuffey, 1977) reefs.

Zones within certain fossil reefs elsewhere have been interpreted as successive seral stages, from pioneer to climax communities. In contrast, the various ecologic zones seen within the Lock Haven reef appear to have been synchronously coexisting, rather than chronologically successive. As a result, except for possibly distinguishing an earlier normal-marine reefal stage (with several simultaneous ecozones) and a possibly slightly later intertidal stromatolitic-cap stage (reminiscent of several Michigan Basin reefs; Mesolella and others, 1974; Huh and others, 1977), little can be inferred concerning growth stages within that bioherm. Moreover, even if the Lock Haven ecozones were successional, difficulties would still remain in applying published developmental patterns to this reef. Mid-Ordovician reefs exhibit pioneer colonization and stabilization stages, followed by biotic diversification, and eventually climaxed with domination by a particular reef-building group (Alberstadt and others, 1974); at Lock Haven, however, each zone is occupied by only one major species, with no visible diversity changes from one to another. Great Lakes mid-Silurian reefs are described as growing from deep quiet-water pioneer, upward through semi-rough, into shallow rough-water climax stages (Lowenstam, 1957; Nicol, 1962). The reefs exhibiting this seral succession are hundreds of feet thick; in contrast, the Lock Haven reef is so thin or low that each zone could have

been only barely different in turbulence conditions from those preceding and following it.

Although regional studies indicate "shallow" waters for the Lock Haven reef, the actual reef form and zonation may imply a more precise figure for water depth there. In particular, stratigraphic relief over the mound can be interpreted as also being the during-life depositional relief; thus, a minimum of about 30 feet (10 meters) water depth is implied. Moreover, the algal stromatolite cap was probably intertidal; if this cap grew at the same time as (or very shortly after) the reef core which it partly covers, then mean sea level would have been right at the top of the mound, and hence the actual water depth immediately surrounding the reef would have been on the order of 25 or 30 feet, at least at the very end of reef growth.

Another intriguing but more complex possibility is suggested by recent studies of temporary low sea-level stands during Silurian time (Dennison and Head, 1975). Most of this time, the Appalachian sea may have been at a relatively constant depth, shallow but not extremely so--perhaps on the order of as much as 200 feet (60 meters). At several points in time, sea level dropped throughout the region (possibly due to world-wide eustatic changes or plate-tectonic movements, or to regional tectonic warpings) for a geologically short moment and then rapidly recovered to its "normal" level; some of the drops were apparently slight, but others may have virtually emptied the basin. Perhaps, the initial Lock Haven trepostome thickets baffling calcarenite sand grew under those deeper waters, and by coincidence sea level began to drop rapidly just after their establishment. As the water column shallowed to intermediate depth, the trepostomes were replaced by cladoporids, in turn giving way to favositids as shallowing continued; finally, the reef top became intertidally exposed to develop the stromatolites capping the reef. If rates of reef growth and sea-level change were comparable to those seen in the post-glacial Pleistocene-Holocene transition, the two processes might well have nearly balanced, thereby producing only a relatively thin reefal deposit during each rapidly shallowing depth interval.

The principal problem with this possible interpretation of Lock Haven reef history is that the inferred sea-level lowerings do not coincide with the geologic time of reef growth; lowered sea level is indicated by the Keefer sandstones well below, and next by the Rabble Run red beds well above, the horizon of the Lock Haven reef (Dennison and Head, 1975). Moreover, although the outcrops do not permit full disclosure, the Lock Haven reef rocks do not appear to exhibit any features suggesting episodes of exposure and drying of the reef mass (there are, for instance, no Barbados-type caliche horizons cutting across coral heads within the reef core). Therefore, the reef probably remained permanently or continuously submerged during its growth and development (unlike some of the Great Lakes Silurian reefs).

After full reef development, however, the stromatolitic cap indicates intertidal conditions and hence intermittent exposure (probably briefly, until resumed mud accumulation off-reef buried the reef mass early in McKenzie time, at most only a few thousand years following Rochester time). No obvious erosional surface or truncation was seen in the available outcrops; hence, while exposure may have contributed to reef termination, scouring does not seem to have been involved much (although the breccia or rubble in part of the reef cap suggests some erosion).

Overall duration of Lock Haven reef growth was probably quite short geologically, as implied both by the thinness of the reef mound (only 30 feet thick)

and by its being embedded entirely within the Rochester-McKenzie shale sequence (a small fraction of the total Middle Silurian interval). Moreover, the reef generation to which the Lock Haven (and the Gasport) reefs belong flourished entirely within the early part of mid-Wenlockian time, again a relatively short interval within the Silurian period. Thus, the life span of the Lock Haven bioherm seems comparable to that of many Holocene patch reefs, whose individual durations have been determined as on the order of a few hundred or very few thousands of years.

Comparison with Great Lakes Silurian Reefs

As noted previously, the Lock Haven reef can be regarded as an eastern outlier of the vast Silurian reef complex of the Great Lakes district, and hence can be profitably compared with well-developed reefs in that region (Briggs and others, 1978; Crowley, 1973; Droste and Shaver, 1977, 1983; Lowenstam, 1957; Shaver, 1977; Shaver and others, 1978). Indeed, many aspects of the Lock Haven reef became fully understood only after careful field examination of several of the Great Lakes reefs.

An obvious difference is the geographically isolated position of the Lock Haven reef, far away from contemporaneous reef tracts. The Lock Haven reef sat out on a sea floor dominated by terrigenous muds, while the Great Lakes reefs were surrounded by carbonate-sediment bottoms.

Moreover, the Lock Haven reef is relatively thin or low-standing, and small and possibly equidimensional in plan view, as are many similar patch reefs in the Great Lakes area. Other Great Lakes reefs are much thicker, up to several hundred feet stratigraphically, and extended laterally as elongate barrier reefs.

Another conspicuous contrast is the predominantly limestone composition of the Lock Haven reef, versus the thoroughly dolomitized character of the Great Lakes reefs.

Both the Pennsylvania and Midwestern bioherms exhibit well-developed ecologic zonations. The Lock Haven reef, and many Great Lakes reefs, have a deeper zone characterized by branching trepostomes and/or cladoporids, functioning as sediment trappers and as sediment formers. Shallower zones in these are dominated by massive frame-building heads, although the Lock Haven head-like colonies are favositid corals, while the Great Lakes ones are predominantly stromatoporoids with only minor favositids. And, numerous Michigan Basin reefs--like the Lock Haven reef--are capped by stromatolitic deposits, probably representing at least brief intertidal exposure at the end of reef growth. Zonations in the Lock Haven and many smaller Great Lakes reefs appear to have been contemporaneously coexisting ecologic zones on the surfaces of relatively short-lived reef mounds; in addition, zonation in many larger Midwestern reefs reflects successional seral stages in comparatively long-duration reef growth.

The organic communities building and inhabiting the Lock Haven and Great Lakes reefs, although comparable, are somewhat different. The same major groups, for the most part, are found in each. However, stromatoporoids, pelmatozoans or crinoids, and fenestrate bryozoans are missing from the Lock Haven reef but are present (and often abundant) on Midwestern Silurian reefs. Additionally, the Lock Haven assemblage is less diversified at lower taxonomic levels; among the tabulate corals, for example, only favositids and cladoporids occupied the reef mound, while those two plus halysitids, alveolitids, and others flourished on the Great Lakes reefs.

Other Pennsylvania Silurian Bioherms

Another small bioherm occurs at roughly the same horizon as the Lock Haven reef, about 25 miles further east near Allenwood (Inners, 1984). It is composed of Favosites heads, so that it appears comparable to the reef core at Lock Haven; however, it lacks the surrounding broken-branch rubble and calcarenite apron of the latter. It thus resembles the small satellite reef (Stop 10) adjacent to the Lock Haven reef (Fig. 5T of field guide).

At Lakemont, on the south side of Altoona, is a limestone lens (Swartz, 1935a, 1939), also approximately at the Rochester-McKenzie boundary. However, field examination of the highway cut exposure there shows mostly stromatolitic masses interbedded with shales and limestones more reminiscent of tidal-flat than reefal deposits; a couple of rolled favositid cobbles recovered from the base of the lens suggest possible nearby coral patches. Indeed, current excavations several hundred feet to the northeast are encountering scattered favositid heads heavily encrusted with algal stromatolites, materials which may occur in this stratigraphic interval relatively widely across central Pennsylvania (A. L. Guber, 1984, pers. commun.). If confirmed by further investigation, such would indicate scattered coral patches, some of which grew into small reef mounds like that at Allenwood, and a few into larger patch reefs like that at Lock Haven.

According to Swartz (1970, pers. commun.), three or four miles west of the Lock Haven reef may be another bioherm, 30-40 feet thick, behind the funeral home and agricultural office in the village of Mill Hall, but possibly covered or removed by recent highway construction (according to local residents). Several field visits have so far failed to yield anything other than typical non-reefal Rochester-McKenzie limestone slabs. Additionally, Swartz (1935b) referred to "coralline deposits" near Williamsport as well as Lock Haven, but no exact locations were given.

At a higher horizon (the Keyser Limestone), a small bioherm exposed in Altoona (Brezinski and Kertis, 1982) consists of a lower foliaceous bryozoan lettucestone zone overlain by an upper stromatoporoid reef-rock cap, and so presents quite a different combination of taxa than does the Lock Haven reef.

Finally, a few patch reefs have been noted in the West Virginia Silurian, and some at least have cladoporid zones resembling that at Lock Haven (Patchen and Smosna, 1975; Smosna and Warshauer, 1978, 1979, 1983).

FIELD TRIP #1

GUIDE TO THE LOCK HAVEN REEF

by
Roger J. Cuffey, Carolyn E. Davidheiser, Shirley S. Fonda,
Anne B. Lutz, Laurie S. Zimmerman, and Barbara B. Skerky

DRIVE TO LOCK HAVEN ON DIVIDED HIGHWAY U.S. 220; TAKE EXIT MARKED "LOCK HAVEN, PENNA. HWY. 120 WEST; CASTANEA, LOCK HAVEN UNIVERSITY"; TURN SOUTH (TOWARD MOUNTAIN, AWAY FROM CITY); IN 0.1 MILE, TURN LEFT (EAST) AT T-JUNCTION; 0.2 MILE FURTHER, TURN RIGHT (SOUTH) AT T-JUNCTION BESIDE CASTANEA FIRE COMPANY #1 BUILDING.

DRIVE SOUTH (TOWARD MOUNTAIN) FOR 0.2 MILE, ACROSS BALD EAGLE CREEK, INTO THE VILLAGE OF CASTANEA (WHERE THE ROAD BECOMES LOGAN AVENUE); TURN LEFT (EAST) ON BROWN STREET; IN 0.1 MILE, TURN RIGHT (SOUTH) ON McELHATTAN AVENUE; 0.1 MILE FURTHER, TURN LEFT (EAST) ON EAST KELLER STREET; PROCEED EASTWARD FOR 0.9 MILE TO PARKING PULLOUT AREA ON RIGHT (SOUTH) SIDE OF ROAD. PARK AND WALK BACK TOWARD CASTANEA TO SEE THE REEF EXPOSURES IN THE LOW ROADCUTS ALONG THE SOUTH SIDE OF THE ROAD (FIGS. 1 AND 2).

FROM THE CENTER OF THE PARKING AREA, WALK WESTWARD (BACK TOWARD CASTANEA) 490 FEET (149 METERS) TO PROMINENT EXPOSURE OF RUBBLY-WEATHERING MASSIVE LIMESTONE (STOP 1) IMMEDIATELY EAST OF TELEPHONE POLE NUMBERED "09209 N34998."

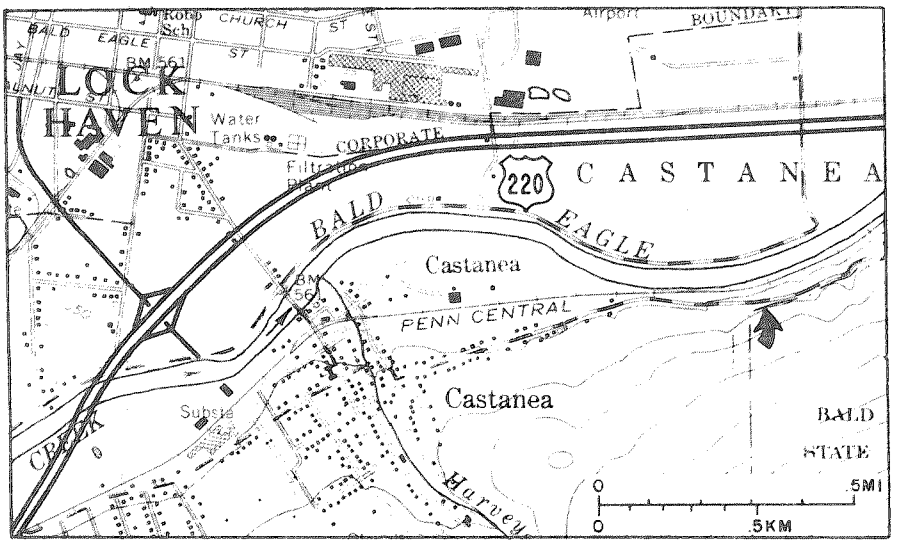

Figure 1. Location of Lock Haven reef (arrow); base modified from Lock Haven and Mill Hall (Pennsylvania) 7-1/2' topographic quadrangles, U.S. Geological Survey.

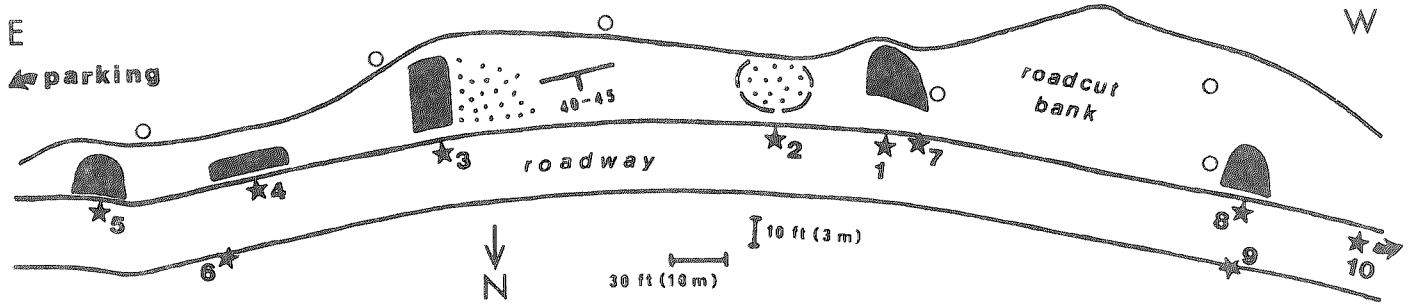

Figure 2. Detailed map of Lock Haven reef (rock exposures, black; float-strewn slopes, stippled); stops indicated by numbered stars; open circles are bases of telephone poles; strike-and-dip symbol indicates average for reef materials, mostly N75-80°E and 40-45°N; note exaggeration of cross-roadway versus along-roadway distances.

Stop 1: Favositid Reef-Core

This exposure shows the center of the Lock Haven reef deposit. That center is massive reef-rock or biolithite, made up of favositid coral heads, and represents the ancient reef crest (Fig. 5G-M).

The rock here is globstone, medium-gray, tough, hard, crystalline, and composed of in-place heads of tabulate corals (Favosites niagarensis, up to a foot in diameter). This lithotype weathers light brown, and bouldery, nodular, or rubbly appearing (due to weathering around the Favosites heads). The coral heads are separated by minor amounts of in-filling micrite mud and spar cement; occasional calcispheres and brachiopod fragments are embedded therein as well.

This massive favositid reef-rock, during life, was probably a rocky or rubbly surface almost completely covered with head-like coral colonies (Favosites niagarensis), and probably very shallow and wave-swept. The head-like brain corals (Diploria spp.) presently covering reef-knoll tops on the Bermuda outer reefs furnish a modern analogue to this ecozone (Fig. 5H).

WALK EASTWARD (BACK TOWARD PARK AREA) 55 FEET (17 METERS) TO FLOAT-STREWN SLOPE (STOP 2).

Stop 2: Cladoporid Reef-Flank

Although now largely covered, the bedrock here is indicated by the numerous float slabs of cladoporid branch coquina, which represent the original shallow reef flank (Fig. 5A-F).

Thin-bedded, dark-gray to medium-brown, tough to friable, densely fossiliferous limestones (mostly rudstones, a few floatstones; originally bafflestones, but not branchstones) comprise this lithotype, characterized by closely packed, broken, narrow branches lying parallel to bedding and making up the great bulk of the rock volume. The matrix in which the branch fragments are embedded appears aphanitic in hand specimen, but is varied in thin-section--partly clay-mineral mud, partly micrite, and partly finely crystalline spar cement. The branches are mud-filled, moderately finely tubular, moderately small apertured, cladoporid tabulate corals (Cladopora seriata). Local pockets or clusters of small brachiopods are scattered through the cladoporid coquinas. Near the top of this ecozone (adjacent to the reef core), a few overturned and fragmentary favositid heads intermingle with the cladoporid branches.

The cladoporid-branch coquina was the shallow, probably still turbulent portion of the old reef flank or side, gently sloping away from the crest into somewhat deeper water. Densely covered with the projecting tips of thinly branching colonies (Cladopora seriata), this ecozone must have closely resembled the dense branching Acropora thickets around the edge of the Heron Island (Australia) platform reef, or the tangled thickets of Acropora cervicornis on Caribbean reefs (Fig. 5B). Locally, clusters of small brachiopods nestled down among the cladoporid branches.

WALK EASTWARD AGAIN, 165 FEET (50 METERS) TO HIGH EXPOSURE OF SMOOTH-SURFACED MASSIVE LIMESTONE (STOP 3).

Stop 3: Trepostome Reef-Flank

The exposed limestone here is a trepostome bafflestone, with several large in-place bryozoan colonies embedded in the carbonate sands. To the right (west) of this exposure, the bedrock is mostly covered, but float blocks of trepostome floatstone and rudstone indicate that these branch coquinas extend over toward the cladoporid coquina seen at the previous stop. These bryozoan coquinas represent the ancient deep reef flank ecozone (Fig. 4I-R).

These rocks overall appear identical to the cladoporid coquina described at the preceding stop, except for the characteristics of the branches themselves. Here, they are spar-filled, very finely tubular, very small apertured branches identified as Monotrypa benjamini, a trepostome bryozoan. Near the base of this ecozone (adjacent to the massive calcarenite sand apron), the matrix is more calcarenitic, with many gastropod, ostracod, and calcisphere fragments, and a few branching-trepostome clumps or thickets (up to 3 feet or 1 meter across) still standing in place; these, again, are Monotrypa benjamini.

The trepostome-branch coquina also probably looked very much like the preceding ecozone when alive, but in somewhat deeper and probably a bit quieter waters. Finely branched thickets of Acropora prolifera in the reefs off St. Croix (Fig. 5K) furnish a modern analogue.

WALK EASTWARD AGAIN, 95 FEET (29 METERS) TO LOW EXPOSURE OF SMOOTH-SURFACED MASSIVE LIMESTONE (STOP 4).

Stop 4: Circum-Reef Calcarenite Apron

Superficially much like the limestone seen at the previous stop, the bedrock here, however, contains few or no bryozoan colonies and fragments. It is thus a massive calcarenite, a lithified carbonate sand originally deposited as a barren apron surrounding the reef mass (Fig. 4E-H).

This rock type is specifically a grainstone, dark-gray (weathering dark brown), massive, unfossiliferous, homogenous, hard, tough, and smooth-surfaced to vaguely ripple-marked. Freshly broken surfaces appear coarsely crystalline or obscurely clastic, with relatively uniform grain size; weathered surfaces become sandy textured. Nearer to the reef mass proper, occasional small trepostome-branch fragments may be found embedded in this calcarenite. A rather different appearance is presented by thin-sections of this lithotype, being composed of much fossil debris surrounded by subordinate matrix material. The fossils are small, broken, often recrystallized fragments of abundant gastropods, calcispheres (of uncertain affinities, but possibly algal or protozoan), and ostracods, accompanied by a few brachiopod or trilobite fragments. Most of the embedding matrix is clear crystalline spar, largely cement, but locally recrystallizing or even cross-cutting in origin.

The massive calcarenite represents the bottom flattening out at the foot of the reef flank. This area immediately surrounding the reef mass was level-bottom loose carbonate sand, open or barren (i.e., lacking any colonies growing in-place here), and locally ripple-marked. Many modern reefs--such as patch reefs within the Florida reef tract and on the shallow shelf east of Joulters Cays on the Great Bahama Bank--are surrounded by such barren sand aprons (Fig. 4F).

WALK EASTWARD AGAIN, 85 FEET (26 METERS) TO SIZEABLE EXPOSURE OF PLATY SHALE AND SHALY LIMESTONE (STOP 5).

Stop 5: Off-Reef Shale

The shaly bedrock here is not part of the Lock Haven reef itself, but rather represents the ancient deep off-reef muddy bottoms above which the reef grew (Fig. 4A-D).

The platy off-reef lithotype consists of calcareous shale, shaly limestone, and thin-bedded limestone (i.e., mudstones, marlstones, and micstones), all intergrading continuously with one another; they are medium brown to medium gray brown when fresh, but weather light gray brown. Evenly bedded, not rippled at all, the beds are hard, brittle, and platy. Their texture is aphanitic and argillaceous; they weather to a finely muddy surface. Largely unfossiliferous, these rocks exhibit only a few horizontal trails or burrows on some bedding planes. In thin-section, these platy strata consist partly of brownish, opaque, clay-mineral mud, and partly of grayish, homogeneous to clotted (pelleted) micrite, all thinly interbedded. No detrital quartz sand grains were seen. A few small fossil shell fragments appear in the sections, a few gastropods and occasional ostracods, but no bryozoans or corals.

These rocks represent off-reef mud bottoms. They were possibly barren but possibly vegetated (presumably with soft-bodied algae not now fossilized), certainly lacking colonies, but locally strewn with small shells, burrowed, level, and apparently at the same depth as the adjacent sand apron. Carbonate-mud bottoms under 12-15 feet (4-5 meters) of water on the Bahama Banks provide a suitable modern counterpart (Fig. 4B).

STEP BACK NORTHWARD, ACROSS THE ROAD (BEWARE OF ONCOMING TRAFFIC!); WALK WESTWARD AGAIN (BACK TOWARD STOP 1), BUT FOR ONLY 60 FEET (20 METERS); STOP AND FACE WESTWARD TO VIEW SPATIAL RELATIONSHIPS OF STRATA SO FAR EXAMINED (STOP 6).

Stop 6: Overview of Reef Form

The Lock Haven reef is poorly exposed, and therefore its overall mounded form is difficult to discern in the field. However, the best opportunity for doing so is from this spot, after the observer has examined each of the facies preserved at the previous stops.

Standing here, at the eastern end of the reef exposures and sighting back (westward, along strike) at the thickest portion of the reef, one recognizes about 30 feet (10 meters) distance stratigraphically between the base and top of the reefal limestone beds. Behind his back (further eastward), the winding road in places cuts through that same 30-foot interval, but there it consists entirely of shaly beds without evidence of reefal involvement. Moreover, some of the lower limestones--especially those at Stop 3 containing in-place branching trepostome clumps--exhibit a mounded upper surface (over a thickened portion of that bed, Fig. 4L, so that the mound is clearly not the upwarped surface of a small anticline). This mounding appears to slope gently upward toward the stratigraphically highest favositid reef bed; if the two are mentally connected, they form an upper surface (for the limestones) which is inclined slightly (perhaps only 5°) to the overall dip of the shaly sequence. It is, moreover, this limestone surface off of which the overlying shaly beds slumped after hurricane rainfall in 1972, thereby exposing the surface rather cleanly so that lateral variations within the limestones could be readily examined.

These observations suggest that the limestones exposed comprise one side or half of a lenticular or mound-like mass, still largely buried within the mountainside, but only thinly covered along the road by shales not significantly enough interfingered with the carbonates to prevent slumping off of that cover as a whole. By analogy with modern reefs similarly isolated from other contemporaneous reefs, a mound-like form of roughly circular plan view would be a reasonably likely shape for the Lock Haven reef; its dimensions would then be 30 feet (10 meters) high by approximately 1000 feet (300 meters) across. The lack of interfingered shale along the limestone surface implies lack of simultaneous reef and shale deposition. In other words, the reef mass probably stood up as a knob--perhaps nearly as high as its 30-foot (10 meter) thickness--above the surrounding mud-bottomed sea floor for a short time geologically. Later on, the reef became buried by further mud accumulation.

Another implication of these geometric relationships is that the exposed limestone surface approximates the ancient living surface of the reef mound, so that lateral variations exposed now within the limestone represent contemporaneous ecologic zones (ecozones) coexisting down the flank of the reef mass during its life. Again by analogy with living reefs of similar form, those ecozones probably had coexisted for some time prior to the instant represented by the exposed surface of growth and deposition; hence, each ecologic zone visible at the surface most likely extends below in lateral facies relationships like those typically seen in better exposed fossil reefs (Fig. 3). Future drilling or deeper cut exposures would, however, be necessary to fully test this interpretation. An alternative possibility would be to interpret the various limestone types as being flat layers resting one on top of the other; however, reefs seldom, if ever, grow in such fashion, so that this seems quite unlikely.

In addition to this paleoecologic zonation, the Lock Haven reef can be positioned within the biostratigraphic zonation (biozones) previously developed for these mid-Silurian units. F. M. Swartz (1970, pers. commun.) measured a section here many years ago when exposures were even less adequate than today. However, his section can be reinterpreted in terms of current understanding of this fossil reef (Fig. 3); in particular, he noted head-like colonies (reef core) at the level of the Velibeyrichia moodeyi biozone and branching colonies (deep reef flank) opposite the Whitfieldella marylandica biozone.

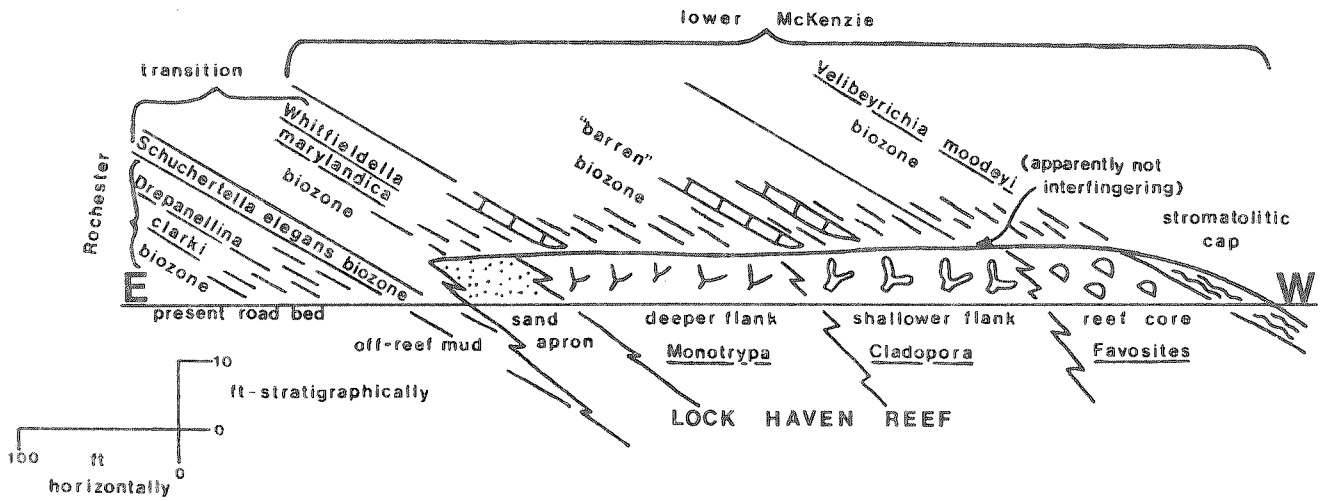

Figure 3. Coordination of ecozonation within, and biozonation adjacent to, the Lock Haven reef (adapted from Cuffey and Davidheiser, 1979, and F. M. Swartz, 1970, pers. commun.).

CONTINUE WALKING WESTWARD, FOR ANOTHER 350 FEET (106 METERS), BACK TO JUST BEYOND STOP 1, TO UPPER RIGHT (WESTERN) EDGE OF RUBBLY LIMESTONE EXPOSURE (STOP 7).

Stop 7: Stromatolitic Reef-Cap

Although now largely eroded away, a few blocks of massive, laminated, and stromatolitic limestone near the top of this exposure represent an algal reef cap developed after active reef growth had ceased, much as in certain Great Lakes Silurian reefs (Fig. 5J, N-P).

Light-gray to light-brown weathered, dark-gray fresh, and aphanitic, these limestones are homogeneous micrite (i.e., micstones) without shelly fossils. They are predominantly very low domed stromatolites (Collenia spp.), and form cruststones and bindstones. Such stromatolites suggest intertidal conditions, like the tidal flats covered by thin blue-green algal mats, in the Bahamas and Bonaire.

WALK WESTWARD AGAIN, 190 FEET (58 METERS) TO LIMESTONE EXPOSURE (STOP 8) AT ROAD LEVEL BELOW DOUBLE-BASED TELEPHONE POLE.

Stop 8: Rubble and "Oncolites" within Reef-Cap

Stratigraphically the topmost horizon of the Lock Haven reef, the bedrock here is a mixture of rubble breccia and bryozoan nodules or "oncolites" embedded in finer carbonate sediments. These materials seem most reasonably interpreted as reef-top or reef-flat rubble or cobble substrates (Fig. 5Q-S).

Varied in character, these are mostly dark gray fresh, weathering light gray to light brown, and aphanitic or finely crystalline; matrixes are diverse, including homogeneous micrite, pelleted micrite, and spar cement, while fossil contents range from negligible to abundant (shell fragments: brachiopods, gastropods, calcispheres, ostracods, and trilobites). Two variants, both rudstones, are especially notable among these reef-top limestones. One is composed of small round nodules, apparently algal oncolites, but actually rounded trepostome-bryozoan fragments (Monotrypa benjamini) (Fig. 5R-S), encrusted by vaguely cellular laminations (solenoporacean algae? chaetetid sponges? stromatoporoids?). Presumably, storm waters tossed broken bryozoan branches up from the deep flank, and those were further encrusted while being washed around upon the reef top. Another variant consists of subangular to rounded pebbles (up to 30 mm diameter) of favositid fragments, possibly a cemented reef-top rubble deposit (Fig. 5Q). The "oncolitic" and rubbly rock types suggest the cobble-strewn reef flats of Australian reefs like the Low Isles, intertidal and periodically quite turbulent.

STEP BACK NORTHWARD, ACROSS THE ROAD (BEWARE OF TRAFFIC!); FROM THE NORTH SIDE OF THE ROAD, LOOK OVER THE EDGE AND DOWN THE SLOPE (STOP 9).

Stop 9: Bryozoan "Oncolites" within Reef-Cap

Limestone float blocks composed of bryozoan "oncolites," again Monotrypa benjamini (Fig. 5R-S), weather out of the road fill below the pavement here. These apparently were originally part of the bedrock at the previous stop, but have since been displaced by road construction activities.

RETURN SOUTH ACROSS ROAD AGAIN (WATCH TRAFFIC!) TO ROADSIDE LIMESTONE EXPOSURE (STOP 8), AND CONTINUE ON WESTWARD FOR AN ADDITIONAL 215 FEET (66 METERS) ALONG THE SOUTHERN SIDE OF THE ROAD (STOP 10).

Stop 10: Favositid Satellite Bioherm

Approximately 110 feet (34 meters) horizontally south of, and 45 feet (14 meters) vertically above the roadside here is a small biohermal mound (Fig. 5T), interpreted as a satellite reef developed near the main Lock Haven reef mass. This mound consists of favositid coral heads embedded in a calcarenite matrix, but lacks any trepostome or cladoporid branch coquinas, and so resembles another small bioherm several miles farther east (Inners, 1984). Various other carbonate rock types, all non-reefal lithologies, can be seen in the bedrock exposures (apparently a small quarry) and float blocks in the mountainside woods surrounding the satellite reef.

WALK BACK EASTWARD, PAST ALL THE PREVIOUS STOPS, TO RETURN TO THE PARKING AREA: END OF FIELD TRIP NO. 1.

[see page 16]

Figure 4. Deeper-ecozone Lock Haven reef materials and modern analogues (scale of each photograph indicated as the actual width of the field of view shown). A-D, off-reef shale, Stop 5: A, platy shale and shaly limestone in vertical outcrop face (20 cm); B, modern analogue, shallow but far offshore carbonate mud resuspended in wake of shallow-draft research vessel out on interior of Great Bahama Bank (5-10 m); C, bedding surfaces of shale (7 cm); D, vertical peel-section of thin micstone bed (5 mm). E-H, calcarenite apron, Stop 4: E, massive grainstone weathering to sandy-textured surface (8 cm); F, modern analogue, barren sand ring around base of patch reef off St. Croix, grass-covered sand on left and base of reef on right (1.5 m); G, vaguely rippled bedding-plane surface (2 m); H, vertical peel-section (6 mm). I-R, trepostome flank, Stop 3: I, trepostome branch-coquina rudstone (9 cm); J, trepostome colony in growth position, embedded in calcarenitic matrix, thus forming bafflestone (11 cm); K, modern analogue, Acropora prolifera thickets off St. Croix (1 m); L, exposure of bedding plane containing in-place trepostome branching colonies, and C. Davidheiser on thickened mounded portion of bed (11 m); M, peel-section of trepostome branch-coquina rudstone, all Monotrypa benjamini fragments (11 mm); N-R, trepostome Monotrypa benjamini: N, half of large branching colony in upright growth position (48 cm); O, broken branch fragment showing characteristic finely tubular structure (13 mm); P, framework formed by colony branches in growth position (65 mm); Q, tangential peel-section (2.0 mm); R, longitudinal peel-section (2.0 mm).

[see page 17]

Figure 5. Shallow-ecozone Lock Haven reef materials and modern analogues (scale indicated as in Fig. 5). A-F, cladoporid flank, Stop 2: A, cladoporid branch-coquina rudstone (10 cm); B, modern analogue, Acropora cervicornis thicket off Grand Cayman (2 m); C, peel-section of cladoporid branch-coquina rudstone, all Cladopora seriata fragments (8 mm); D-F, tabulate Cladopora seriata: D, broken branch fragment showing typical coarsely tubular structure (14 mm); E, tangential peel-section (1.6 mm); F, longitudinal peel-section (2.3 mm). G-M, favositid core, Stop 1: G, favositid globstone (25 cm); H, modern analogue, Diploria heads on Bermuda (1 m); I, J, reef core as exposed in 1970 and 1983, respectively, with L. Zimmerman pointing to last remnant of stromatolitic reef cap (12 m, 3 m); K-M, tabulate Favosites niagarensis: K, head-like colony (50 cm); L, exterior surface approximating a tangential section (14 mm); M, longitudinal peel-section (7 mm). N-S, reef cap: N-P, stromatolite Collenia sp., Stop 7: N, very broad dome (40 cm); O, closely packed narrow columns (25 cm); P, vertical peel-section showing homogeneous micrite and subtle laminations (5 mm); Q, rubble-breccia rudstone, Stop 8 (25 cm); R-S, trepostome Monotrypa benjamini as rounded "oncolites" rather than branching colonies, Stop 9: R, "oncolite" rudstone (12 cm); S, tangential thin-section (3 mm). T, satellite bioherm west of main reef mass, Stop 10 (4 m).

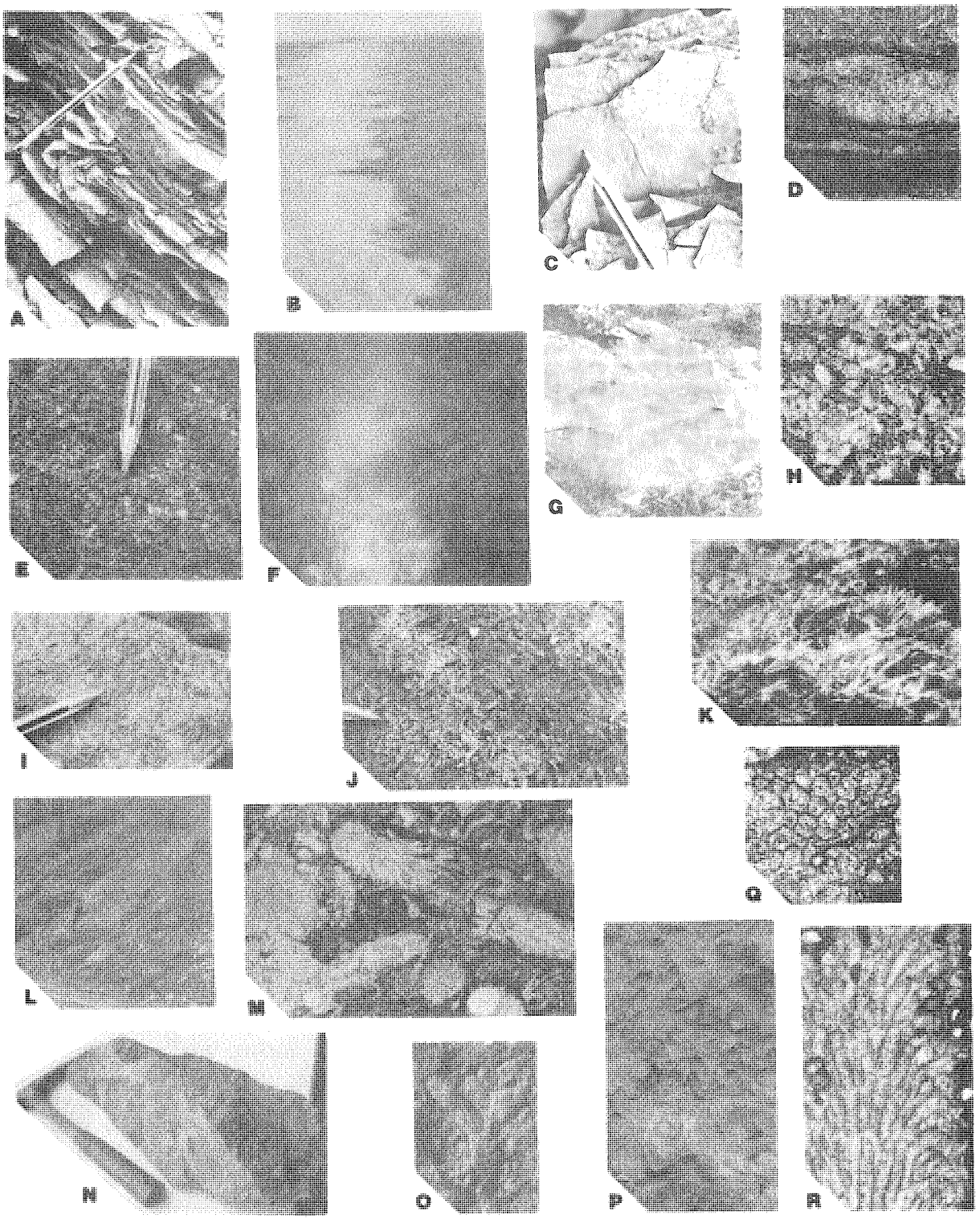

Figure 4.

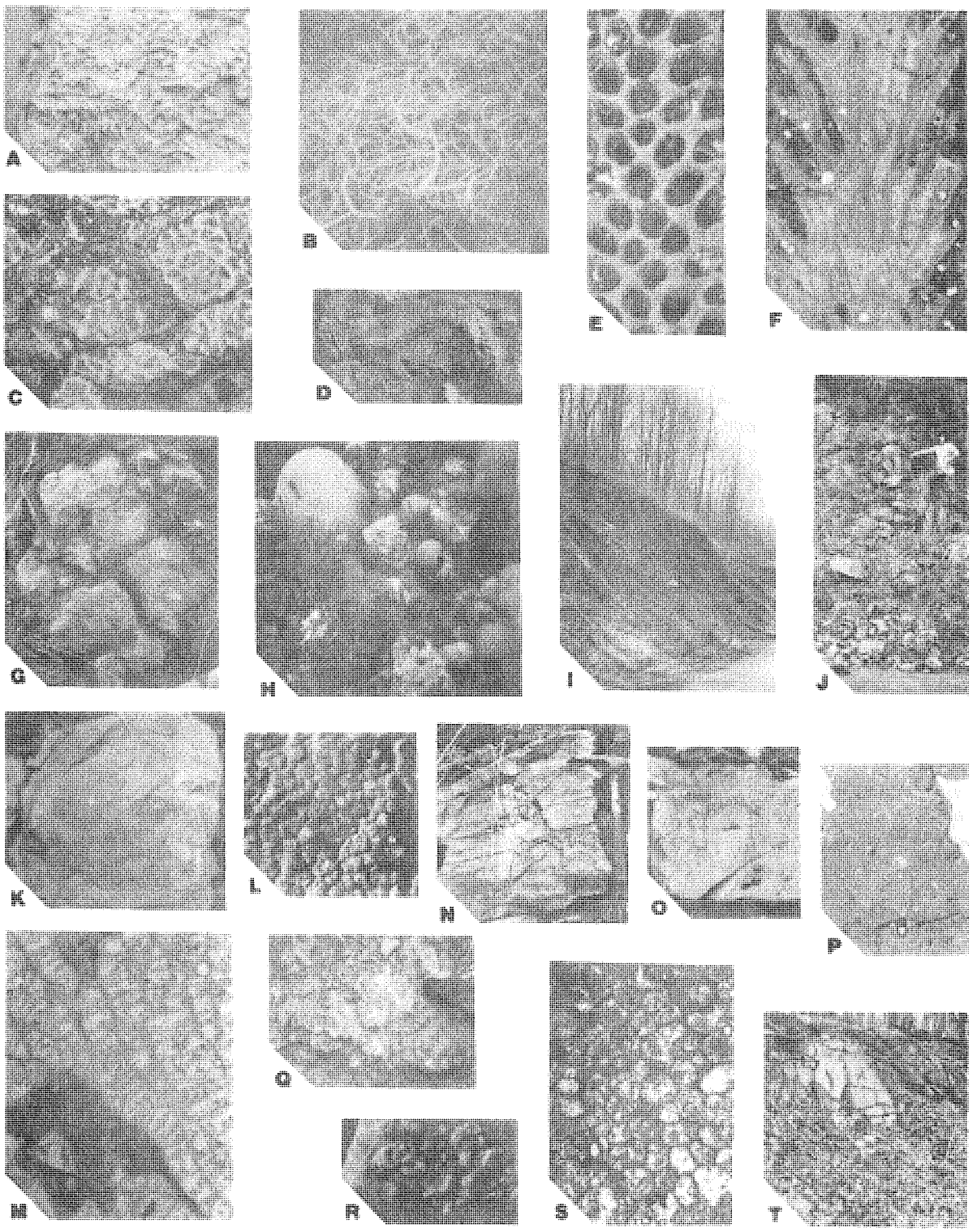

Figure 5.

REFERENCES

Alberstadt, L. P., Walker, K. R., and Zurawski, R. P., 1974, Patch reefs in the Carters Limestone (Middle Ordovician) in Tennessee, and vertical zonation in Ordovician reefs: Geological Society of America Bulletin, v. 85, p. 1171-1182.

Berry, W. B. N., and Boucot, A. J., eds., 1970, Correlation of the North American Silurian rocks: Geological Society of America Special Paper 102, p. 1-289.

Brett, C. E., 1982, Stratigraphy and facies variation of the Rochester Shale (Silurian: Clinton Group) along Niagara Gorge: New York State Geological Association, Annual Meeting, Guidebook, v. 54, p. 217-245.

_____, 1983a, Sedimentology, facies and depositional environments of the Rochester Shale (Silurian; Wenlockian) in western New York and Ontario: Journal of Sedimentary Petrology, v. 53, p. 947-971.

_____, 1983b, Stratigraphy and facies relationships of the Silurian Rochester Shale (Wenlockian; Clinton Group) in New York State and Ontario: Rochester Academy of Science Proceedings, v. 15, p. 118-141.

Brezinski, D. K., and Kertis, C. A., 1982, Environmental setting and succession in a Late Silurian patch reef from central Pennsylvania: Compass of Sigma Gamma Epsilon, v. 60, p. 13-24.

Briggs, L. I., Briggs, D. Z., Elmore, R. D., and Gill, D., 1978, Stratigraphic facies of carbonate platform and basinal deposits, late Middle Silurian, Michigan Basin: Geological Society of America, North-Central Section, Field Excursion Guidebook for 1978, p. 117-131.

Crowley, D. J., 1973, Middle Silurian patch reefs in Gasport Member (Lockport Formation), New York: American Association of Petroleum Geologists Bulletin, v. 57, p. 283-300.

Crowley, D. J., and Poore, R. Z., 1974, Lockport (Middle Silurian) and Onondaga (Middle Devonian) patch reefs in western New York: New York State Geological Association, 46th Annual Meeting, Guidebook, Geology of western New York State, p. A1-A41.

Cuffey, R. J., 1977, Bryozoan contributions to reefs and bioherms through geologic time: American Association of Petroleum Geologists Studies in Geology 4, p. 181-194.

_____, 1985, Expanded reef-rock textural classification and the geologic history of bryozoan reefs: Geology, v. 13, p. 307-310.

Cuffey, R. J., and Davidheiser, C. E., 1979, Paleoecologic zonation within a mid-Silurian (Rochester Shale) patch reef near Lock Haven, central Pennsylvania: Geological Society of America Abstracts with Programs, v. 11, p. 9.

Cuffey, R. J., Gebelein, C. D., Fonda, S. S., Bliefnick, D. M., Kosich, D. F., and Soroka, L. G., 1977, Modern tidal-channel bryozoan reefs at Joulters Cays (Bahamas): International Coral Reef Symposium, 3rd, Proceedings, v. 2, p. 339-345.

Davidheiser, C. E., 1980, Bryozoans and bryozoan-like corals--Affinities and variability of Diplotrypa, Monotrypa, Labyrinthites, and Cladopora (Trepostomata and Tabulata) from selected Ordovician-Silurian reefs in eastern North America (Newfoundland, Pennsylvania, Michigan): University Park, Pennsylvania State University, D.Ed. thesis, 673 p.

Davidheiser, C. E., and Cuffey, R. J., 1981, Coral versus bryozoan affinities of Coenites-like branches from northeastern North American Silurian reefs: Geological Society of America Abstracts with Programs, v. 13, p. 128.

Dennison, J. M., and Head, J. W., 1975, Sea-level variations interpreted from the Appalachian Basin Silurian and Devonian: American Journal of Science, v. 275, p. 1089-1120.

Dott, R. H., and Batten, R. L., 1976, Evolution of the earth: New York, McGraw-Hill, 2nd ed., 504 p.

Droste, J. B., and Shaver, R. H., 1977, Synchronization of deposition--Silurian reef-bearing rocks on Wabash Platform with cyclic evaporites of Michigan Basin: American Association of Petroleum Geologists Studies in Geology 5, p. 93-109.

_____, 1983, Atlas of early and middle Paleozoic paleo-geography of the southern Great Lakes area: Indiana Geological Survey Special Report 32, p. 1-32.

Hewitt, M. C., and Cuffey, R. J., 1985, Lichenalliid-fistuliporoid crust-mounds (Silurian, New York-Ontario), typical early Paleozoic bryozoan reefs: International Coral Reef Congress, 5th, Proceedings (in press).

Hoskins, D. M., 1964, Fossil collecting in Pennsylvania: Pennsylvania Geological Survey, 4th ser., General Geology Report 40, p. 1-126.

Huh, J. M., Briggs, L. I., and Gill, D., 1977, Depositional environments of pinnacle reefs, Niagara and Salina Groups, northern shelf, Michigan Basin: American Association of Petroleum Geologists Studies in Geology 5, p. 1-21.

Inners, J. D., 1984, A Niagaran (mid-Silurian) patch reef near Allenwood, Union County: Pennsylvania Geology, v. 15, no. 5, p. 12-16.

Lowenstam, H. A., 1957, Niagaran reefs in the Great Lakes area: Geological Society of America Memoir 67, v. 2 (Paleoecology), p. 215-248.

Mesolella, K. J., Robinson, J. D., McCormick, L. M., and Ormiston, A. R., 1974, Cyclic deposition of Silurian carbonates and evaporites in Michigan Basin: American Association of Petroleum Geologists Bulletin, v. 58, p. 34-62.

Nicol, D., 1962, The biotic development of some Niagaran reefs--an example of ecological succession or sere: Journal of Paleontology, v. 36, p. 172-176.

Patchen, D. G., and Smosna, R. A., 1975, Stratigraphy and petrology of Middle Silurian McKenzie Formation in West Virginia: American Association of Petroleum Geologists Bulletin, v. 59, p. 2266-2287.

Sarle, C. J., 1901, Reef structures in Clinton and Niagara strata of western New York: American Geologist, v. 28, p. 282-299.

Scoffin, T. P., 1972, Cavities in the reefs of the Wenlock Limestone (Mid-Silurian) of Shropshire, England: Geologische Rundschau, v. 61, p. 565-578.

Shaver, R. H., 1977, Silurian reef geometry--new dimensions to explore: Journal of Sedimentary Petrology, v. 47, p. 1409-1424.

Shaver, R. H., Ault, C. H., Ausich, W. I., Droste, J. B., Horowitz, A. S., James, W. D., Okla, S. M., Rexroad, C. B., Suchomel, D. M., and Welch, J. R., 1978, The search for a Silurian reef model, Great Lakes area: Indiana Geological Survey Special Report 15, p. 1-36.

Smosna, R., and Warshauer, S. M., 1978, The evolution of a carbonate shelf, Silurian McKenzie Formation, West Virginia: A cluster analytic approach: Journal of Sedimentary Petrology, v. 48, p. 127-142.

_____, 1979, A very Early Devonian patch reef and its ecological setting: Journal of Paleontology, v. 53, p. 142-152.

_____, 1983, Environment analysis of a Silurian patch reef, Lockport Dolomite of West Virginia: Society of Economic Paleontologists and Mineralogists Core Workshop 4, p. 26-52.

Spjeldnaes, N., 1975, Silurian bryozoans which grew in the shade: Docum. Lab. Geol. Fac. Sci. Lyon, h.s. 3, fasc. 2, p. 415-424.

Swartz, F. M., 1935a, Relations of the Silurian Rochester and McKenzie Formations near Cumberland, Maryland, and Lakemont, Pennsylvania: Geological Society of America Bulletin, v. 46, p. 1165-1194.

_____, 1935b, Silurian sections in north central Pennsylvania: Geological Society of America Proceedings 1934, p. 114.

_____, 1939, Silurian System (Tyrone quadrangle): Pennsylvania Geological Survey, 4th ser., Atlas 96, p. 29-56.

_____, 1946, Faunal development, conditions of deposition, and paleogeography of some Appalachian mid-Paleozoic sediments: Cong. Panamericano Engenharia de Minas e Geologia, 2nd, An., v. 3, com. 2, out. 1946, p. 9-33.

Ziegler, A. M., Scotese, C. R., McKerrow, W. S., Johnson, M. E., and Bambach, R. K., 1977, Paleozoic biogeography of continents bordering the Iapetus (pre-Caledonian) and Rheic (pre-Hercynian) Oceans, In West, R. M., ed., Paleontology and plate tectonics with special reference to the history of the Atlantic Ocean: Milwaukee Public Museum Special Publications in Biology and Geology 2, p. 1-22.

FIELD TRIP #2

CATSKILL SEDIMENTATION IN CENTRAL PENNSYLVANIA

Eugene G. Williams

(This report is a summary of the Ph.D. thesis by Victor Rahmanian, 1979).

The Upper Devonian deposits of north-central and central Pennsylvania have been the subject of several geological studies in the past 20 years. Most of these studies contributed significantly to an improved understanding of the sedimentologic and stratigraphic aspects. However, the models of the depositional environment of these deposits have become quite controversial. The main point of disagreement arises from studies of Allen and Friend (1968) and Walker and Harms (1971), in the Susquehanna Valley area of south-central Pennsylvania (Fig. 1).

Allen and Friend (1968) concluded that the Catskill facies is not deltaic but instead was deposited in a vast coastal plain of alluviation located between the Acadian Mountains in the east and the Devonian seas in the west. This coastal plain stretched for at least 500 miles between New York and Virginia. It was characterized at its western margin by a network of barrier islands, tidal flats, and lagoonal environments, and at its eastern parts by an alluvial environment consisting of a network of meandering and braided streams (Fig. 1).

Walker and Harms (1971), in their study of the Upper Devonian of the same area, not only rejected Allen and Friend's interpretation but also questioned the deltaic nature of Catskill deposits in south-central Pennsylvania. They suggested that the Upper Devonian depositional system in this area was a quiet, prograding muddy shoreline, similar to muddy coastlines of southwestern Louisiana. They proposed that progradation of the shoreline was made possible by a supply of mud from a distant (unrecognized) delta by means of longshore currents. The sea supposedly had a low wave and low tidal range (Fig. 1). The principal criterion for this interpretation was the presence of several cycles, called "motifs" in the lowermost members of the Catskill Formation. These cycles were reported to consist of an alternation of marine-nonmarine sediments and to be devoid of prominent sand bodies. Winnowed sand bodies thicker than 50 cm were reported to be especially rare or absent in nearshore or shoreline positions of each cycle, suggesting a rather muddy shoreline which shifted back and forth through the course of sedimentation.

Glaeser (1974) studied the Upper Devonian sedimentary environments in northeasten Pennsylvania. He suggested a fluvially dominated deltaic model as the environment of deposition of Trimmers Rock and Catskill deposits (Fig. 1). In the proposed model by Glaeser (1974), prodelta, coastal-margin (delta-front and delta-plain) and alluvial-plain environments comprise the three major depositional environments of the indicated deltaic system. Using mostly subsurface information, he also constructed a three-dimensional time-stratigraphic correlation diagram and isopach maps which showed the regional relationship of the proposed deltaic components in northeastern Pennsylvania.

Humphreys and Friedman (1975) studied Catskill deposits in north-central Pennsylvania. They classified the Upper Devonian Catskill into three lithofacies: 1) gray marine sandstone and siltstones and shale, interpreted as of tidal origin; 2) coarse-grained gray-green, nonmarine sandstones, red siltstones and shale, inferred to have accumulated in and adjacent to meandering streams; and 3) coarse-grained, gray-green nonmarine sandstones of braided-stream origin.

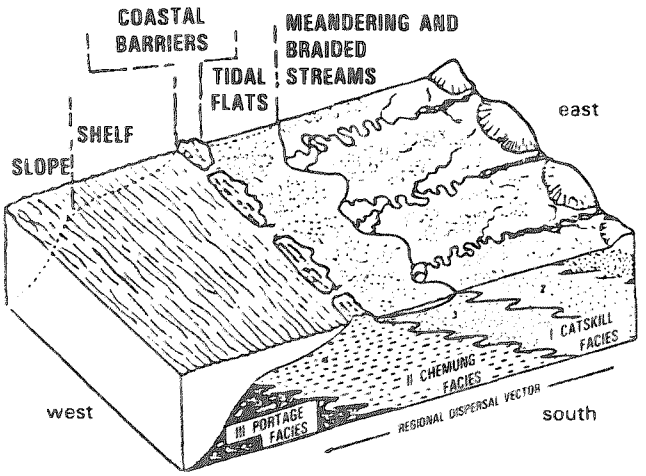

(a) (After Allen and Friend, 1968).

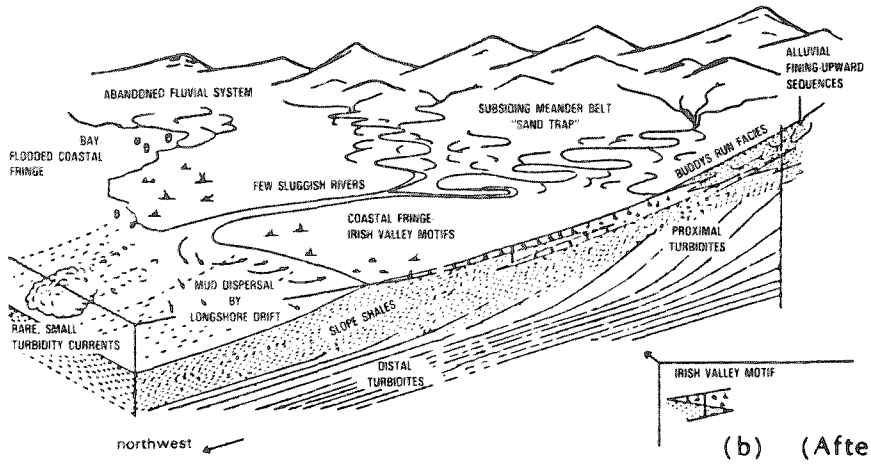

(b) (After Walker and Harms, 1971).

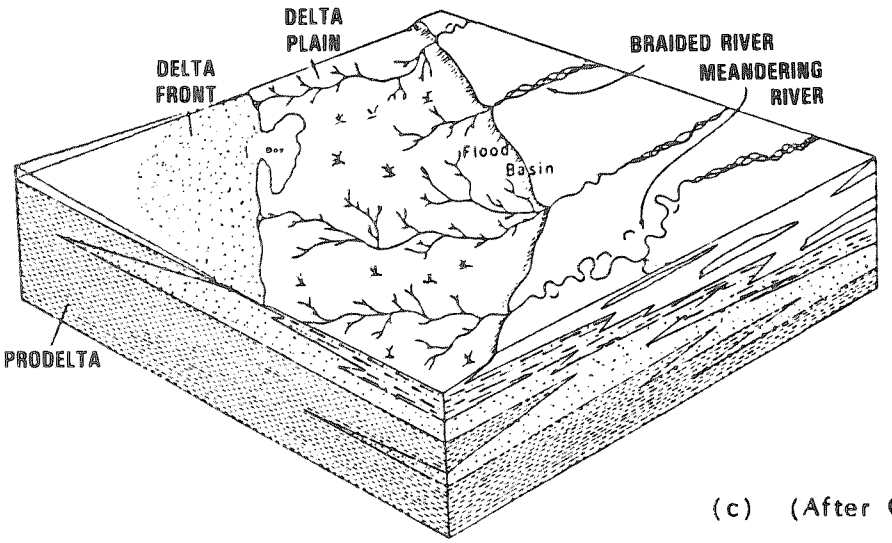

(c) (After Glaeser, 1974).

Figure 1. Depositional models proposed for the Upper Devonian sediments of Pennsylvania.

In the study area, strata of the Catskill Formation are exposed along two almost parallel, northeast-trending outcrop belts, one along the northwest limb of the Broadtop syncline, and the other along the Allegheny Front in Centre, Blair, and Bedford Counties (Fig. 2). A northwestward paleoslope for the

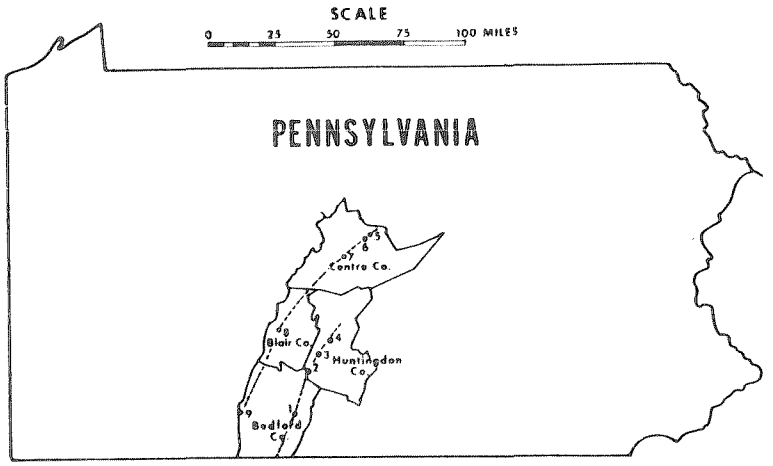

Figure 2. Index map of the study area. Numbers refer to the measured section (1-Everett, 2-Saxton, 3-Entriken, 4-Raystown Dam, 5-Milesburg, 6-Runville, 7-Port Matilda, 8-Horseshoe Curve, 9-New Baltimore). Dashed lines show the position of the Upper Devonian Catskill-Trimmers Rock formational boundary along the west flank of the Broadtop synclinorium (sections 1-4) and the Allegheny Front (sections 5-9) (from Rahmanian, 1979).

Upper Devonian depositional system has been documented by most of the studies on the Upper Devonian deposits in Pennsylvania and New York, and is confirmed by the paleocurrent measurements in the present study. Considering the northwestward paleoslope for these sediments, the northeast-trending outcrop belts of the study area provide a series of strike sections which give the opportunity to study the interrelationship of different depositional environments of the Upper Devonian rock in time and space. The average overall thickness of the Catskill Formation in this area is about 2000 feet, and the exposed thickness of this formation varies from 1200 to 1600 feet.

The Catskill Formation is divisible into three members in central Pennsylvania (Fig. 3). The basal Irish Valley Member consists of gray sandstone, siltstone, and shale, chocolate-brown siltstone and silty claystones, and red silty sandstone, siltstone, and claystone, all of which are arranged in several marine-nonmarine transitional cycles. The middle member (Sherman Creek Member) of this formation, where developed in the area, consists of a sequence of interbedded red siltstone and very fine grained sandstone, arranged in thin fining-upward cycles. The Duncannon Member consists of light-olive-gray and red sandstones, reddish-gray silty sandstone and red siltstone and silty claystone, arranged in well-developed thick fining-upward cycles.

Sedimentary units of Upper Devonian systems in the study area are the product of deposition in several environments identified as parts of a prograding coastline. Major facies comprising the Upper Devonian depositional system are shallow-shelf/littoral, chenier-plain/tidal-flat complex, tidal-flat/barrier complex, shelf-delta complex, and fining-upward alluvial complex.

The shallow-shelf/littoral facies is developed in the Trimmers Rock Formation, which underlies the Catskill Formation. These deposits consist of a sequence of thin- to medium-bedded and gray siltstone and olive-green to gray silty shale, interbedded with occasional thin layers of gray-green very fine grained sandstone layers. Crinoid columnals, pelecypods, brachiopod shells, and occasional bryozoan fragments are common in most of these beds. Except in two localities (Saxton and Port Matilda), the underlying Trimmers Rock sediments pass abruptly into nonmarine deposits without establishment of major nearshore sand bodies.

After the first establishment of nonmarine conditions, the sedimentary pattern of the Irish Valley Member of the Catskill Formation in the southern and central part of the study area is characterized by many (about 15-20) cycles consisting of

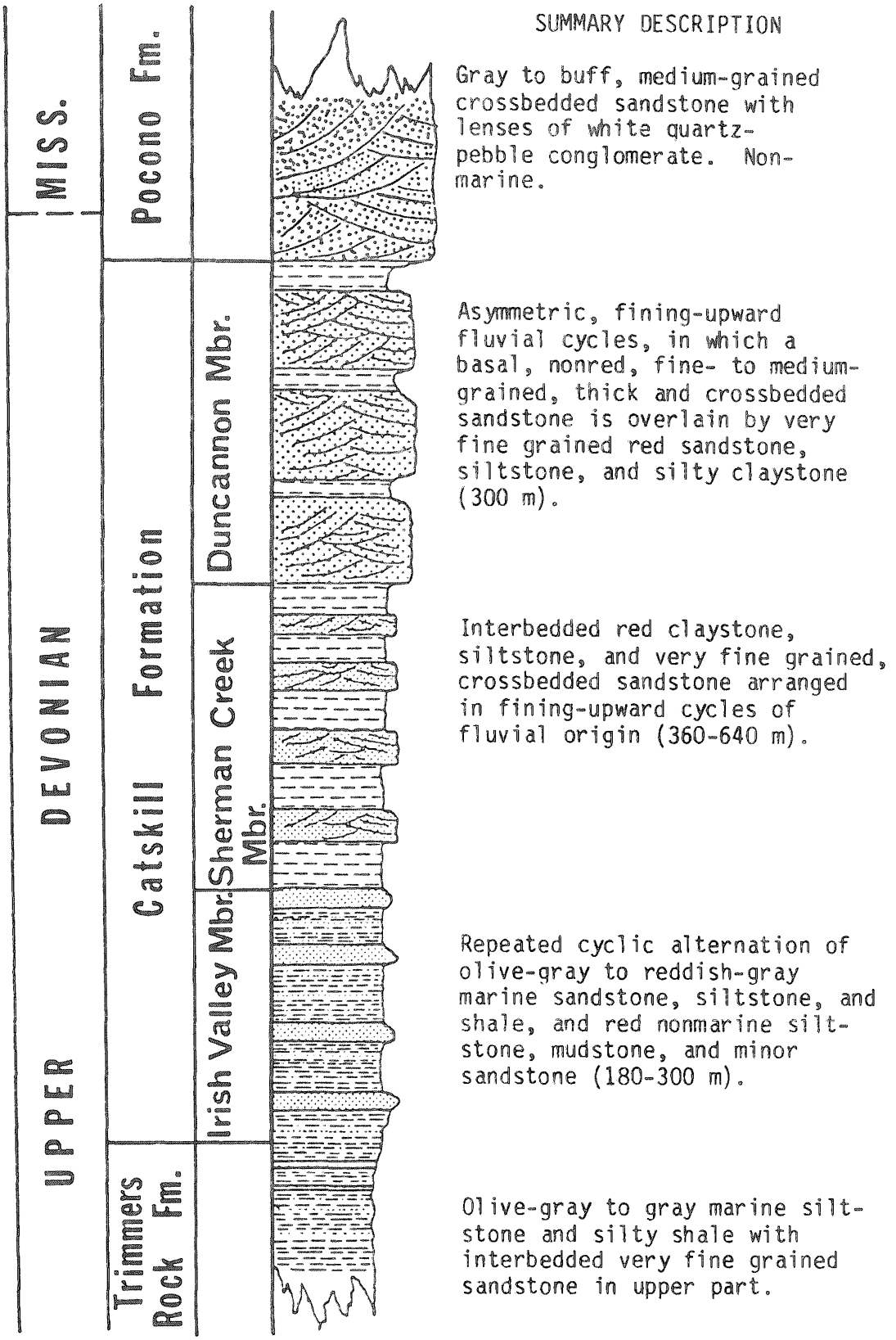

Figure 3. Generalized stratigraphic section of the Upper Devonian in central Pennsylvania (from Rahmanian, 1979).

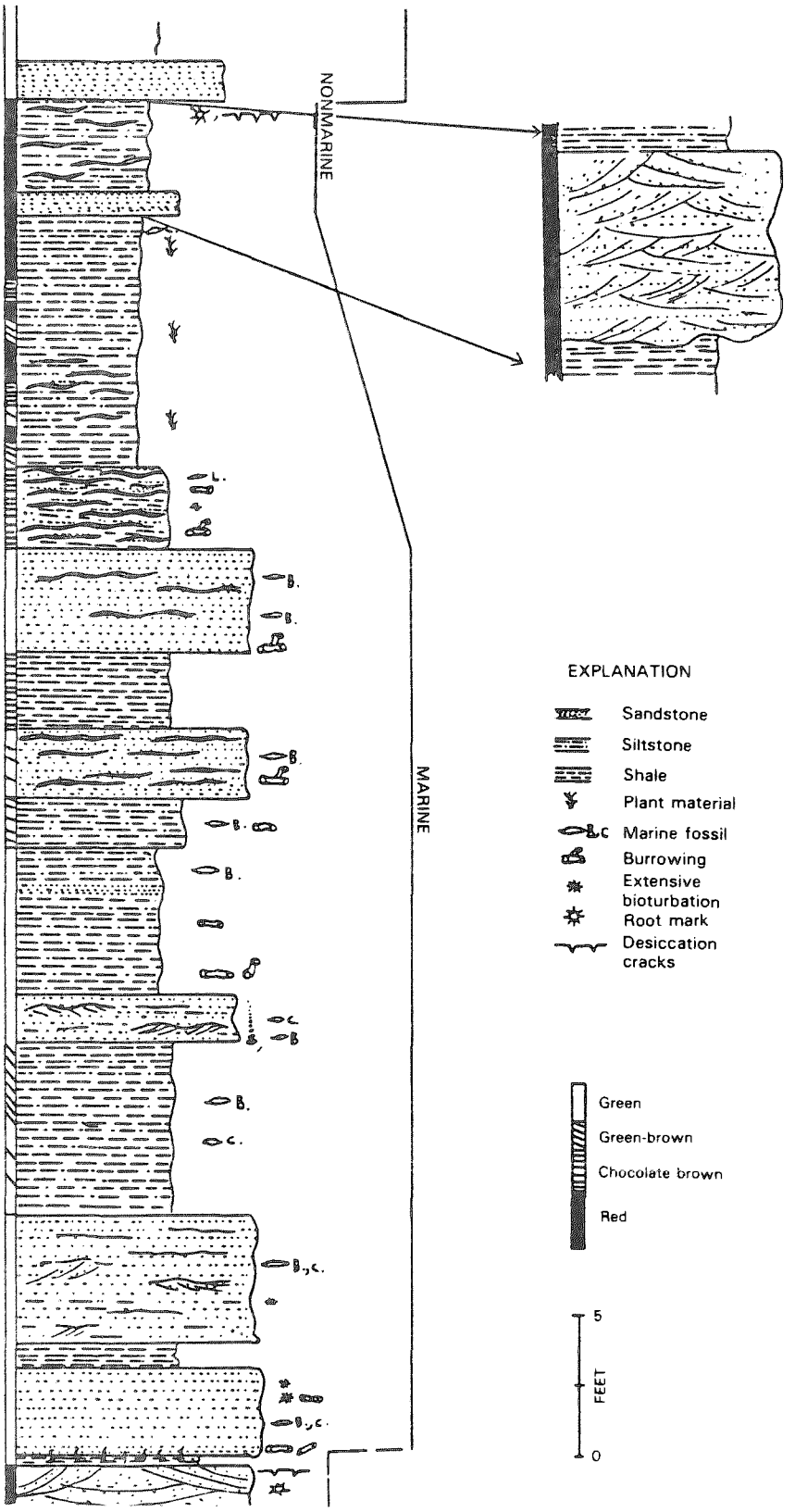

Figure 4. Generalized sequence of an Irish Valley motif from the Entriken section (from Rahmanian, 1979).

repeated alternations from marine sandstone and shale to nonmarine siltstone and silty sandstone which was produced by repeated lateral shifting of the shoreline. The thickness of each cycle varies from 5 to about 90 feet. These cycles begin with greenish-gray, fossiliferous, clean subparallel laminates overlain by bioturbated, fine-grained sandstone of variable thickness representing a marine transgression, and pass through a marine shoaling phase and an intertidal transitional phase, and finally grade into a nonmarine phase representing coastal-plain aggradation (Fig. 4). The marine shoaling phase of cycles commonly starts with gray-green to olive-green, fossiliferous shale and silty shale which grades upward to thin-bedded olive-green and chocolate-brown, fossiliferous and bioturbated shaly siltstone occasionally interlayered with thin layers of gray-green, very fine grained, fossiliferous, micro-cross-ripple-laminated sandstone. The shoreline of this marine shoaling phase is represented by usually thin (2-5 feet), olive-green, fine-grained, moderately sorted, subparallel to flaser and lenticular laminated, fossiliferous quartzitic sandstone. The transitional part of each cycle usually consists of interlayers of green, chocolate-brown, and red siltstone, shaly siltstone, and thin (1/2-1 foot) fine-grained, clean, well-sorted quartzitic sandstone.

Extensive bioturbation, diagnostic internal sedimentary structures such as herringbone cross-stratification, lenticular and flaser bedding and presence of composite rock types in the shallow marine-transitional part of most cycles attest to tidal origins of these deposits. Tidal sedimentation in some of the sections is further demonstrated by good development of relatively thick (5-20 feet), gray-green to chocolate-brown, medium to coarse and pebbly, fossiliferous cross-stratified quartzitic sandstone and conglomerate interpreted as tidal channels, and subtidal and intertidal sand bars.

The nonmarine part of cycles is dominantly red siltstone and shale which are characterized by the presence of rootlets and mudcracks. Fining-upward alluvial cycles of a few feet in thickness may be present on top of some cycles.

Upward-fining cyclicity of fluvial origin is the common characteristic of the other two members of the Catskill Formation (the Sherman Creek and Duncannon Members). An ideal cycle consists of a basal brownish-gray to red, fine- to very fine grained, micaceous, crossbedded sandstone with lenses of carbonate nodules and shale chips, and occasional plant fragments at its base. This sandstone occupies a channel or irregular erosional surface cut into the underlying cycle. This sand body grades upward to red to reddish-gray, very fine grained silty sandstone, red siltstone, and silty shale which represents the levee-overbank portion of a meandering-channel facies.

Facies assemblages and distribution of the Catskill Formation vary both towards the south and north laterally along depositional strike from the above description for the central parts of the area (Figs. 5 and 6). To the south, at the Saxton area, the first nonmarine deposition, marking the base of the Irish Valley Member, was established higher in the section, and consequently shallow marine sedimentation went on for a longer period of time relative to the adjacent area. Apparently this was in response to a reduction of the rate of sediment supply, which more or less prevented active coastal progradation and consequently resulted in more intensive marine reworking and a better development of shallow marine and nearshore sand bodies. In this area the sediments of the uppermost Trimmers Rock Formation and the Irish Valley Member are represented as tidal-flat and barrier-bay facies assemblages characterized by better developed and thicker marine sandbars and shoreface-foreshore sequences with associated tidal-channel sandstone bodies.

To the north (at Centre County) the well-developed cyclic sediments of the Irish Valley Member grade into a complex assemblage of tidal-influenced deltaic facies, comprising slope, prodelta, delta-front, and lower and upper delta plain facies (Figs. 5 and 6).

In summary, the available data on Upper Devonian deposits of the study area suggest that the depositional system of Late Devonian time in the south-central parts of Pennsylvania was a complex prograding delta-interdeltaic system (Fig. 7). The shoreline was fed by a tidally influenced delta at the northern part of the study area (at Centre County). Farther to the south and north of this depocenter occur well-developed cycles of marine-nonmarine origin in the Irish Valley Member, which point to development of a prograding, tidally influenced, muddy shoreline, consisting of a tidal-flat/chenier-plain complex, marginal to the delta. Available evidence suggests that sediments were supplied to these environments from the adjacent deltaic lobe by longshore currents and tidal currents rather than by local rivers crossing the coastal plain.

This shoreline shifted laterally several times in response to changes in position of the adjacent deltaic lobe. Further to the south, at the Saxton area, cyclic sediments are poorly developed. In this area, marine processes became dominant, as the rate of sediment supply through longshore currents from the north was reduced and a tidal-flat/barrier-bay complex formed the shoreline of this area (Fig. 7).

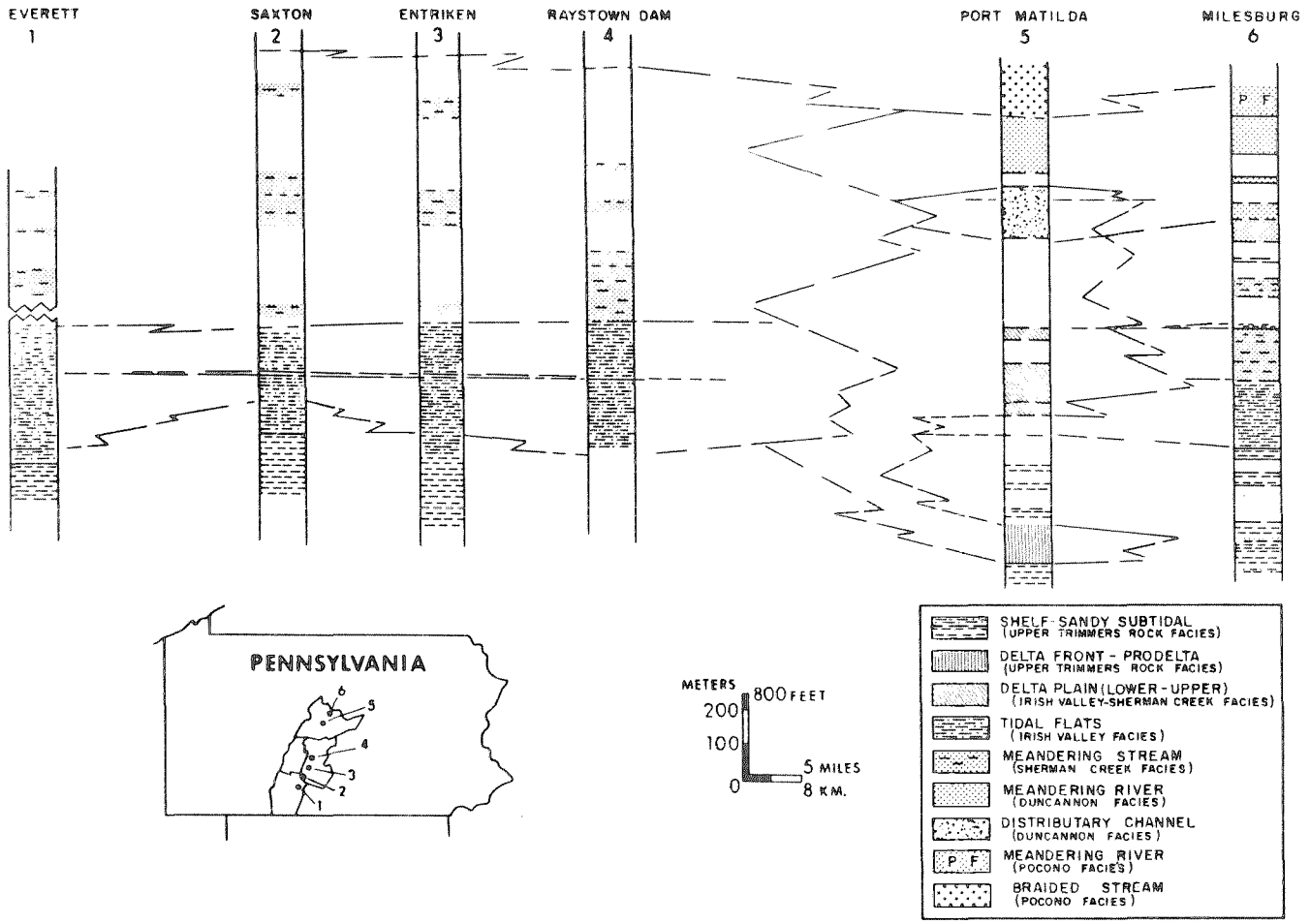

Figure 5. Correlation diagram of the major lithofacies in the Upper Trimmers Rock and Catskill Formations of central and south-central Pennsylvania and the inferred paleoenvironments (from Rahmanian, 1979).

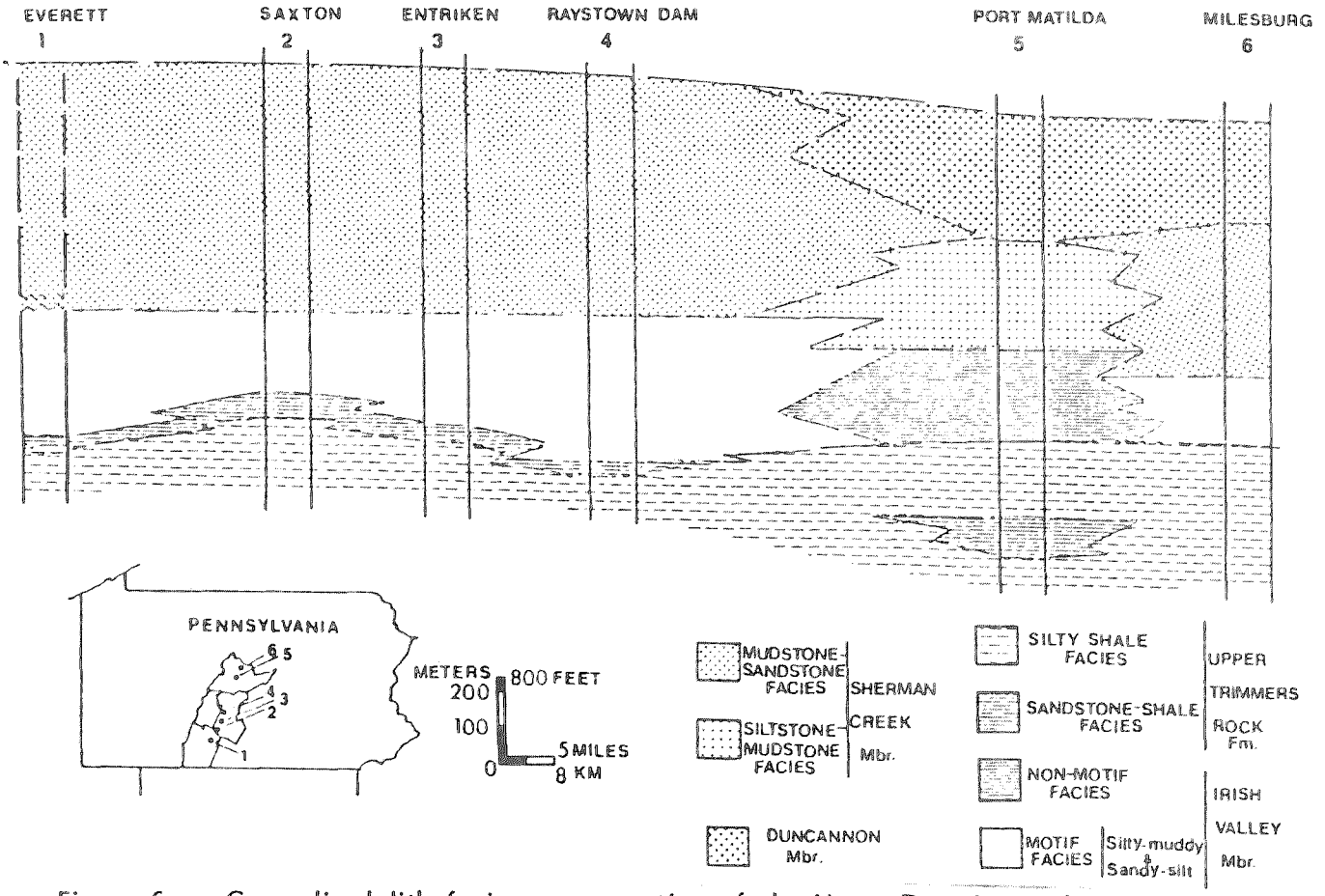

Figure 6. Generalized lithofacies cross section of the Upper Devonian rocks in central and south-central Pennsylvania (from Rahmanian, 1979).

At a given locality, for example along the Broadtop outcrop belt, the vertical succession of sedimentary facies indicates that the area, during the entire time of Irish Valley sedimentation, remained a part of an intradeltaic region, characterized by a coastal area largely composed of broad and extensive tidal flats. The lack of major sandstone units of fluvial or deltaic origin in the succession of these marine-nonmarine deposits indicates that the shoreline was not subjected to intermittent deltaic or intradeltaic sedimentation. In other words, neither the rivers from adjacent active sediment input systems nor a major river, heading directly from the southeastern source area, crossed this shoreline during Irish Valley time. This evidence leads to the important conclusion that the paleogeographic position of the major facies of the Catskill Formation (i.e., Irish Valley, Sherman Creek, and Duncannon) remained the same throughout the complete progradation history of the Upper Devonian across central Pennsylvania.

More specifically, the evidence suggests that the main river system in the north-central part of the area maintained a fixed longitudinal course without diversion or extensive lateral migration as it crossed the Upper Devonian basin across central Pennsylvania. The inferred longevity of the river system or confinement of its course suggests that structural elements possibly influenced its course during its westward journey across the Upper Devonian sedimentary basin. The river system was probably confined to a structurally low area which controlled its course and limited its lateral migration. A likely structural element which could have exerted such control on the course of this river system is the NW-SE-trending basement-

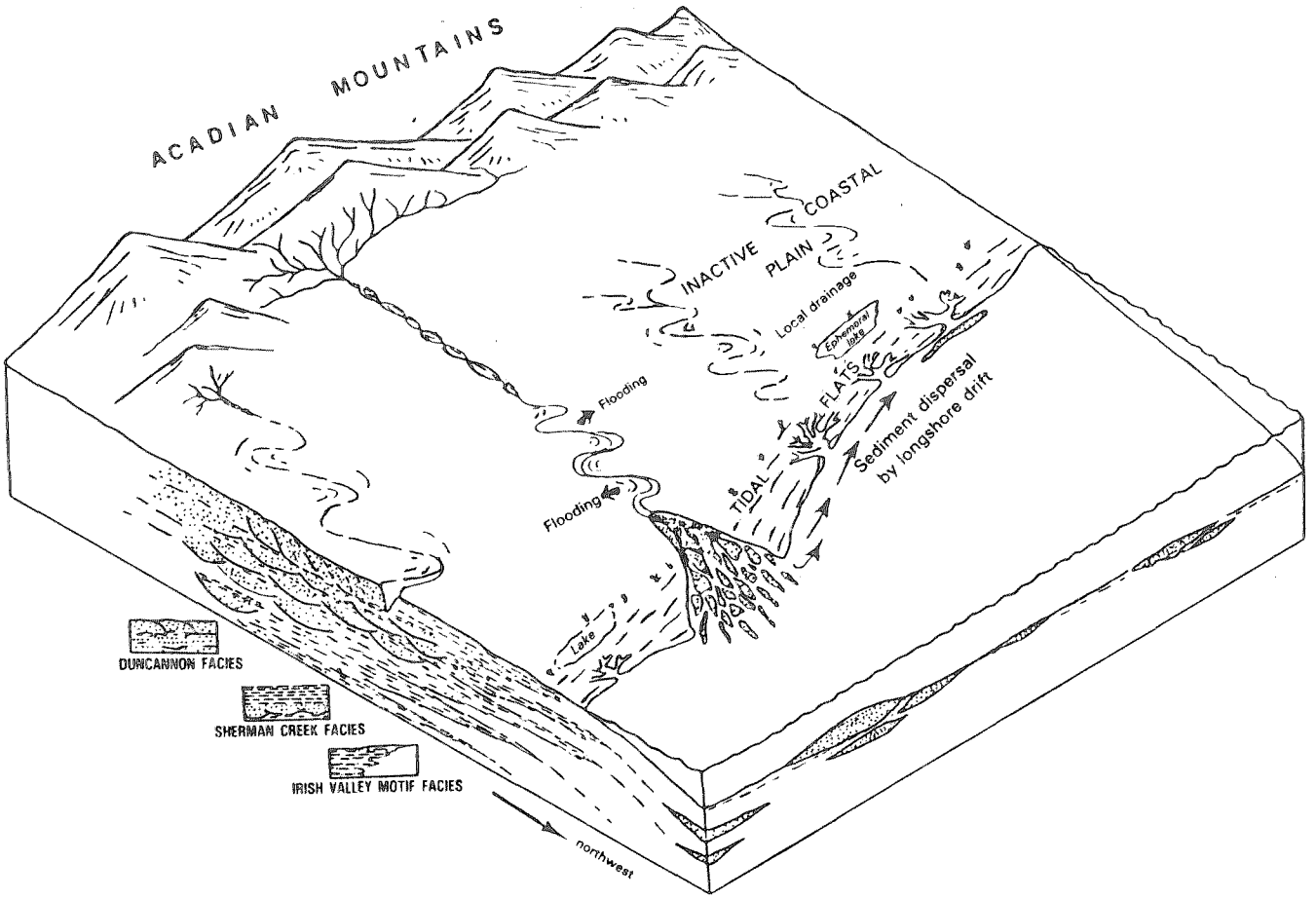

Figure 7. Sedimentation model of the Upper Devonian in central Pennsylvania (from Rahmanian, 1979).

controlled fault system mapped as the Tyrone-Mount Union lineament (Canich, 1977). This fault system extends almost perpendicular to the inferred depositional strike of the Devonian basin and separates the inferred sediment input area at Centre County in the north from its adjacent inactive coastal plain and marine embayments to the south.

The tidally dominated delta and interdelta shoreline model of Catskill sedimentation in central Pennsylvania was tested by two independent lines of evidence, namely paleocurrent analysis and petrography of sandstones.

Figure 8 illustrates the paleocurrent directions from crossbeds of the entire Irish Valley, Sherman Creek, and Duncannon Members at various localities. Figure 8 also illustrates the outline of the Devonian outcrop belts in the study area. Paleocurrent azimuths measured from the Sherman Creek and Duncannon Members are characteristically unidirectional and indicate progradation of nonmarine sequences in WNW to dominantly NW directions with respect to a NE-SW shoreline and a southeasterly source terrane. As mentioned in the preceding section, these sediment transport directions are in general agreement with regional paleodirectional measurements conducted by various workers on the Upper Devonian deposits of New York, Pennsylvania, and Maryland.

The paleocurrent azimuths from the crossbeds of the Irish Valley Member sandstones clearly indicate a NW-SE bipolar current direction (Fig. 8). A bipolar

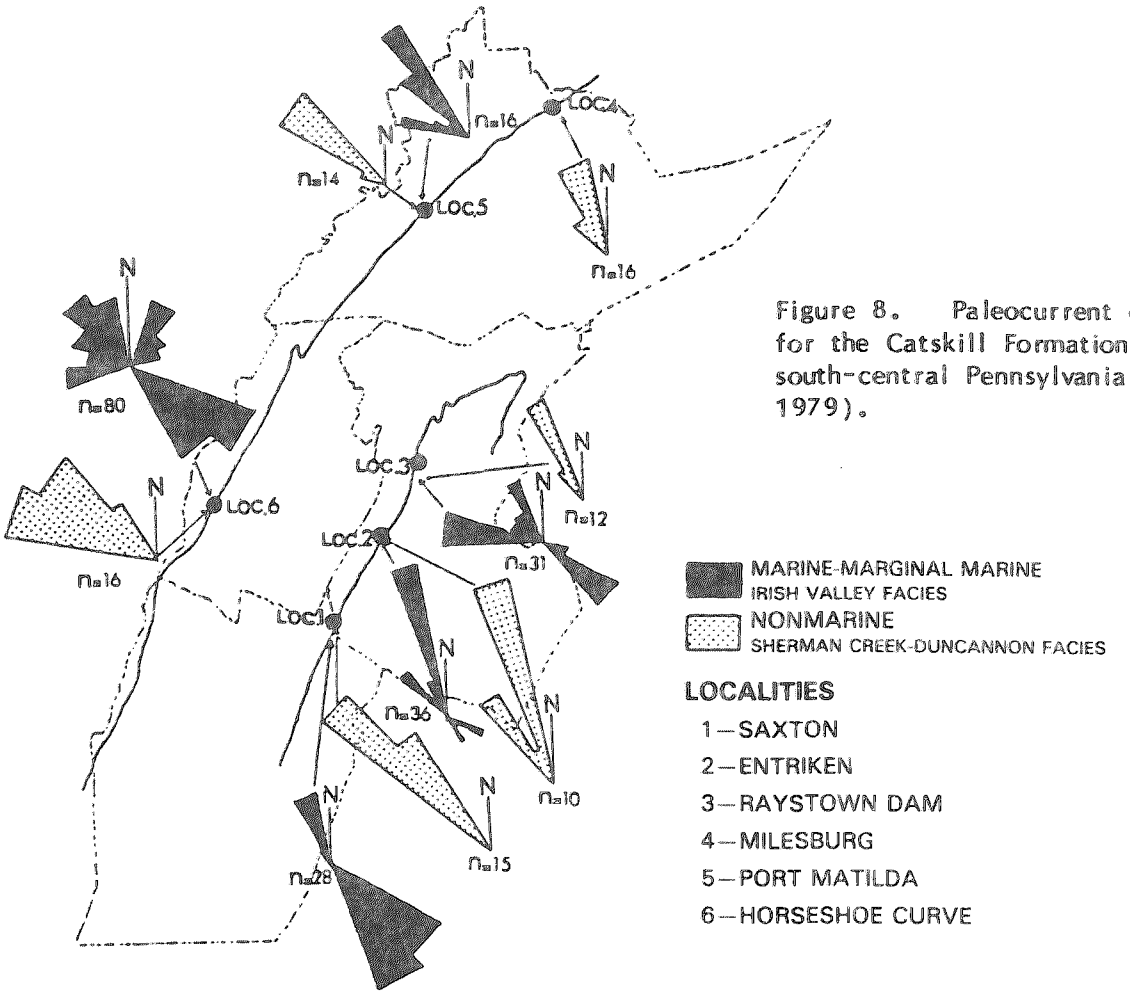

Figure 8. Paleocurrent directional data for the Catskill Formation in central and south-central Pennsylvania (from Rahmanian, 1979).

flow pattern inferred from crossbedding in this member is most satisfactorily accounted for by the ebb- and flood-current reversal typical of tidal environments. These paleodirectional data provide additional support for a tidal origin of the Irish Valley motif sequences. The relationship of the crossbed orientation in the Irish Valley sandstones (Fig. 8) with the inferred NE-SW shoreline trend indicates that the northwesterly and southeasterly oriented crossbeds are ebb- and flood-generated, respectively. Paleocurrent analysis of the Irish Valley sandstones (Fig. 8) suggests that in the Raystown Dam and Entriken areas the ebb currents have been the dominant constructional process in addition to a subordinate flood-current component, while the Saxton area appears to represent a flood-dominated shoreline with subordinate ebb-current components. These relationships are suggested by both the composite paleodirectional measurements of all the Irish Valley motif sandstones, and individual sandstone bodies which show a distinct unimodal, ebb- or flood-generated flow pattern. An example of such individual units is the thick conglomeratic sandstone unit at the Entriken section, which has distinct northwesterly oriented large-scale solitary sets generated by tidal-flood processes. Paleodirectional data at the Horseshoe Curve locality, while characterized by well-defined ebb and flood paleocurrent components, also show a distinct northeasterly oriented paleocurrent direction. This is interpreted to have been generated by tidal processes combined with a northeasterly long-shore movement of water. Similar influences of longshore movement of water have been inferred from the results of the paleodirectional measurements from the subtidal sandstone units of the uppermost

Trimmers Rock Formation at Saxton. Paleodirectional data of the Irish Valley Member at Port Matilda are exclusively from the sandstone units interpreted as distributary-mouth bars and show, predictably, a northwestward paleocurrent direction.

The petrographic analysis was based on 58 samples taken from sandstone units of the Trimmers Rock and Catskill Formations. These sandstone units are interpreted, based on field evidence, to represent sedimentation within five depositional environments, including shelf, subtidal/tidal-channel, beach, lower tidal flat, and fluvial. The mean values and standard deviations of the properties measured are given in Table 1. Examination of this table will show that these sandstones can be separated into three groups, namely marine shelf, shoreline (beach, tidal channel,

Table 1. Group means and standard deviations for each variable for the several paleoenvironments identified in the Catskill and Trimmers Rock Formations (size in phi; composition in percentage) (from Rahmanian, 1979).

Variables	Marine shelf		Beach		Subtidal-tidal channel		Tidal flat		Fluvial		Grand mean
	$\bar{x}$	S.D.	$\bar{x}$	S.D.	$\bar{x}$	S.D.	$\bar{x}$	S.D.	$\bar{x}$	S.D.	
1. Mean size a-axis	3.453	0.601	2.688	0.534	2.135	0.739	2.756	0.179	3.352	0.566	2.957
2. Standard deviation a-axis	0.400	0.070	0.386	0.087	0.748	0.367	0.369	0.042	0.420	0.070	0.466
3. Maximum size a-axis	2.570	0.674	1.954	0.612	0.173	1.373	1.900	0.268	2.518	0.499	1.911
4. Mean size b-axis	4.067	0.553	3.226	0.542	2.657	0.762	3.308	0.182	3.965	0.580	3.533
5. Standard deviation b-axis	0.432	0.083	0.388	0.087	0.761	0.348	0.396	0.041	0.424	0.087	0.480
6. Maximum size b-axis	3.187	0.582	2.364	0.615	0.689	1.345	2.410	0.348	3.159	0.564	2.470
7. Axial ratio (b/a)	0.676	0.031	0.709	0.034	0.715	0.030	0.699	0.014	0.678	0.03	0.692
8. Monocrystalline quartz	47.389	2.863	59.741	4.106	61.448	8.907	57.875	6.810	45.740	4.55	52.907
9. Polycrystalline quartz	5.331	2.581	6.515	3.195	13.105	8.346	4.207	1.486	4.683	2.110	6.633
10. Feldspar	2.556	0.999	3.221	1.520	2.240	1.421	3.749	2.364	3.44	2.011	3.039
11. Mica	4.248	3.122	1.036	0.874	1.061	0.988	0.498	0.471	3.713	1.901	2.459
12. Metamorphic rock fragment	18.083	3.940	5.702	2.705	6.847	5.128	12.625	7.181	17.964	4.289	13.241
13. Sedimentary rock fragment	0.194	0.265	0.740	1.391	0.333	0.536	1.581	1.178	0.760	0.814	0.672
14. Volcanic rock fragment	0.000	0.000	0.111	0.236	0.393	0.679	0.000	0.000	0.000	0.000	0.092
15. Detrital matrix	11.027	5.977	1.703	1.305	2.031	2.289	3.249	3.951	8.556	5.225	6.034
16. Authigenic matrix	1.278	1.154	1.038	1.060	0.515	0.970	2.375	1.148	0.648	0.621	1.052
17. Silica cement	8.557	3.411	12.260	5.195	7.056	1.873	9.709	3.098	6.926	2.122	8.500
18. Carbonate cement	0.027	0.095	7.370	5.630	4.030	5.957	3.710	4.941	0.000	0.000	2.425
19. Iron cement	0.833	1.789	0.037	0.110	0.787	1.752	0.209	0.590	7.315	3.912	2.626
20. Heavy minerals	0.471	0.480	0.517	0.912	0.151	0.229	0.206	0.171	0.258	0.293	0.315
21. P-M ratio (poly/mono)	0.112	0.053	0.108	0.047	0.224	0.154	0.076	0.034	0.102	0.041	0.124

tidal flat) and fluvial. The fluvial and marine shelf sandstones are quite similar in grain size (very fine grained), whereas the shoreline sandstones are all fine grained, a condition which suggests that the latter were not derived from the former. Because most of the fluvial samples were taken from the Sherman Creek, whose paleogeographic position was immediately upslope from the shoreline sediments of the Irish Valley, we conclude that these latter were delivered by longshore currents carrying sediments derived from coarser grained sediments of depocenters located near Port Matilda to the north or somewhere in Maryland to the south.

As expected, total quartz is higher and detrital matrix, mica, and metamorphic rock fragments lower in the shoreline sandstones when compared to the shelf and fluvial ones in which these components occur in about equal amounts. The higher energy and longer residence time in the nearshore environments probably accounts for the differences. Other important differences are found in carbonate and iron cements; carbonate cement, in the form of calcite, is much more abundant in the nearshore sandstones, very low in the shelf, and absent in the fluvial ones, relations which are probably a function of pH and permeability. Higher pH and permeability in the nearshore sandstone would favor the formation of calcite during diagenesis as would access of calcite-saturated seawater and opportunity for degassing of CO_2. In contrast, the lower pH in fluvial environments would likely favor calcite solution. In the shelf facies, higher matrix means lower permeability and therefore little space for cementation regardless of the availability of carbonate. The high iron content, in the form of hematite, in the fluvial sandstone, is explained by the fact that iron is generally insoluble in oxidizing environments.

The sandstones may be further separated by diagrams relating composition and texture. Figure 9 shows that the shoreline sandstones, in addition to being on average coarser grained, are also higher in quartz for a given grain size when compared to the fluvial and shelf sandstones. Figure 10 shows that the proportion of polycrystalline quartz relative to monocrystalline quartz is lowest, for a given grain size, in the shoreline sands, a feature to be expected in sediments where residence time is the longest so that differential abrasion and selective sorting are most pronounced.

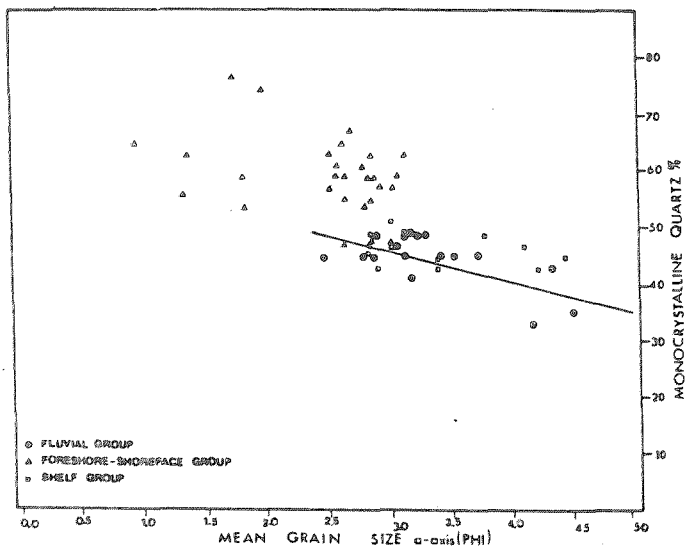

Figure 9. Plot of mean grain size of sandstones from the Catskill and Trimmers Rock Formations against monocrystalline quartz percentage (from Rahmanian, 1979).

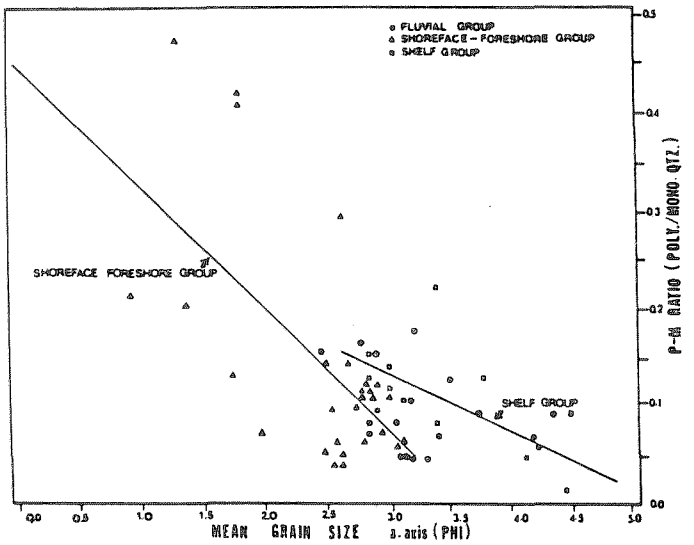

Figure 10. Plot of mean grain size of sandstones against P-M ratio (polycrystalline quartz/monocrystalline quartz) (from Rahmanian, 1979).

Our concept of Catskill sedimentation in central Pennsylvania is summarized in the idealized diagram presented in Figure 7. Reference to Figure 1 will show that the model incorporates as special cases the three suggested models which had been developed for specific areas in other parts of Pennsylvania. We therefore conclude that the differences in interpretation of Catskill sedimentation are largely related accidents of outcrop--each model valid for the area investigated but not for the whole region. The excellent exposures on Route 322 west of Port Matilda have allowed us to recognize facies in the upper Trimmers Rock and Catskill that had not been observed in this area.

Recent work by Smith and Rose (1985) has applied this model to the exploration for uranium in Pennsylvania, the results of which are summarized in this volume. They recognize another depocenter in northeastern Pennsylvania with characteristics similar to those found at Port Matilda, thus supporting the idea of Willard (1939), namely that there were multiple depocenters. Willard, based on biofacies analysis in the upper Trimmers Rock, concluded that there were three delta lobes, one of which (the Snyder Lobe), would, when projected westward, correspond to the inferred Port Matilda delta sequence.

SEDIMENTARY PROCESSES ON THE BASIN MARGIN OF THE LATE DEVONIAN CATSKILL SEA -- STORM- OR TIDE-DOMINATED?

by

Rudy Slingerland

Introduction

A central thesis of Rahmanian (1979) and Williams (this volume) is that the Upper Devonian Catskill shoreline in central Pennsylvania consisted of discrete deltas, each building onto a basin margin influenced by tide- and storm-driven flows. The assertion is made primarily from field observations given in the accompanying article and field guide. Proving the thesis is especially difficult in this case because there seems to be no modern counterpart to the Catskill depositional system. The facies sequences do not match modern river-dominated deltas, and so the specific coastal geomorphology is debated--were deltaic depocenters present, forming an irregular, embayed coastline or was the coastline muddy and relatively straight (see Williams, this volume, for a review)? Also, the submarine topography of epicontinental seas, and the Catskill Sea in particular, is poorly known. I have adopted Woodrow and Isley's (1983) term, basin margin, for the shallow edges of the Catskill Sea to emphasize its potential differences from modern continental shelves. Again for lack of modern counterparts, the occurrence of epicontinental tides in general, and Catskill tides in particular, is debated. Dennison (1985) and Woodrow and Isley (1983) ruled out tidal flows in the Catskill Sea on intuitive grounds because it was partly enclosed and comparatively shallow. Finally, on a basin margin as extensive in space and persistent in time as the Catskill, and which experienced numerous transgressions and regressions, it is entirely possible that both storm- and tide-driven flows were dominant at different times and places, depending upon the basin margin geometry. Certainly, this idea is suggested by the widely different process interpretations of Upper Devonian sedimentary facies in New York and Pennsylvania (Table 1).

Among the many questions raised above, two are both important and addressable now: 1) are significant tidal ranges even theoretically possible in the Catskill Sea, given our best estimates of basin shape, bathymetry, latitude, open ocean tidal ranges, and paleo-geophysical constants; and 2) how would those ranges vary at the coast as a function of basin margin widths, lengths, and depths? The purpose of this paper is to attempt to answer these questions by presenting the results of a numerical model simulating two-dimensional, shallow-water, long-wave propagation.

Methodology

To address the first question, a numerical hydrodynamic model simulating an M_2 co-oscillating tide was modified from Hess and White (1974) for the Catskill Sea (Slingerland, 1984, 1985, 1986). The model consists of the vertically integrated Navier-Stokes and continuity equations in which bed stresses are represented by the Chezy relationship where Manning's n equals 0.04 (gravel roughness). Basin planform was adopted from Heckel and Witzke (1979). Basin bathymetry was estimated from the facies maps of Heckel and Witzke (1979) using the basin margin-clinoform-basin floor scheme of Woodrow and Isley (1983). Forty-nine numerical experiments were conducted using a range of boundary and initial conditions. Solutions consisted of a vertically averaged flow velocity in the horizontal plane and water surface elevation

Table 1. Previous process interpretations for basin margin deposits in the Late Devonian Catskill Sea

Rock unit and investigator	Location	Specific bed type	Environment or mode of emplacement
West Falls Gp. (Woodrow and Isley, 1983)	Wellsburg, N.Y.	Hummocky cross-stratified fine sandstones	Wind-driven currents
Lock Haven Fm. (Woodrow and Isley, 1983)	Towanda, Pa.	Fossiliferous channelized sandstones	Flood discharges across delta platform from adjacent distributary
New Milford Fm. (Krajewski and Williams, 1971)	Susquehanna County, Pa.	Plane-parallel lam., flat-based sandstone pods in mudstone	Wave-swash on beaches or tidal flows
Irish Valley Mbr. of Catskill Fm. (Allen and Friend, 1968)	Newport and Girtys Notch, Pa.	Fining-upward shelly sandstones	Lateral accretion in tidal channels
Irish Valley Mbr. of Catskill Fm. (Walker, 1971)	do.	do.	Distributary fill or channel-mouth bars
Sonyea Gp. (Sutton and others, 1970)	Ithaca, N.Y.	Crossbedded fine sandstones with coquinite bases and wave-rippled tops	Storm, tidal, or wave-produced currents on a delta platform
Sonyea Gp. (Goldring and Bridges, 1973; Duke, 1985)	N.Y.	Sublittoral sand sheets with hummocky cross-strata	Hurricane-driven currents
Bioclastic carbonate units in Lock Haven Fm. and West Falls Gp. (Woodrow and others, 1981)	NE Pa.	Bidirectional trough and wedge crossbedded skeletal-fragment lime grainstone with lateral accretion bedding	Ebb-dominated tidal environment
Ashcraft unit (see above) (Bridge and Droser, 1985)	do.	do.	Laterally migrating sand bars adjacent to tidal channels
Sonyea Gp. (Goldring and Langenstrassen, 1979)	N.Y.	Sandy shell layers truncating bioturbated mudstones	Storm layers deposited rapidly under foul weather conditions
First Bradford Fm. (Murin and Donahue, 1984)	SW Pa.	Very fine to fine sandstone pods up to 10 m thick and oriented NE-SW	Inner to mid-shelf bar facies accumulated by current reworking
Upper Devonian hydrocarbon reservoir sandstones (Donaldson and others, 1984)	NW W. Va.	Herringbone crossbedded channel sandstones	Tidal flows

(with respect to mean water level) as functions of location within the basin, phase of the tide, and open ocean tidal range at the entrance to the basin. The results of one experiment, based on the present best estimates of basin geometry and Devonian open ocean tides, are presented in Figure 1.

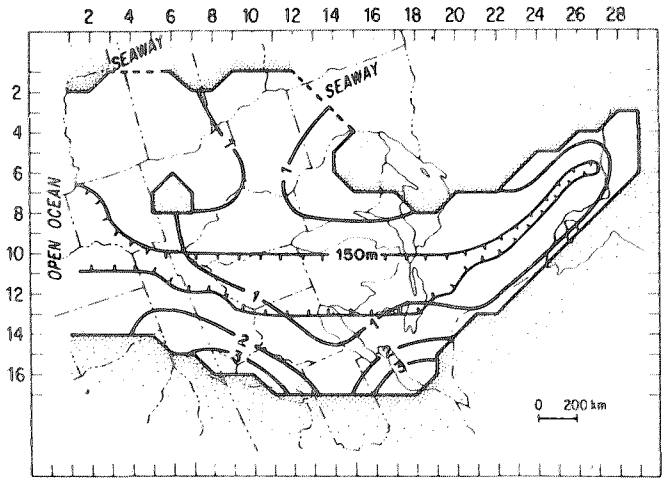

Figure 1. Paleotidal ranges (dark line in meters) in the Late Devonian Catskill Sea of eastern North America as predicted by the hydrodynamic model. Basin geometry is modified from Heckel and Witzke (1979) with paleonorth to the top and the center of the sea at approximately 10°S latitude. The 150 m bathymetric contour encompasses the Upper Devonian black shale facies; water depth decreases linearly landward from that contour. Open ocean tidal range at column 1 is 1 m, today's average ocean tidal range near the edge of the world's continental shelves. Tidal augmentation occurs along the Middle Atlantic States.

To address the second question, the same hydrodynamic model was modified to calculate resonance effects on generic margins of rectangular cross section and unit length alongshore (Slingerland, 1985). The forcing tide at the margin edge was a simple sinusoidally varying astronomical tide of constant amplitude equal to 0.45 m; the shore was a perfect reflector of the tidal wave. Thirty-eight numerical experiments were performed using various margin widths and friction factors. The results pertinent to this discussion are presented in Figure 2.

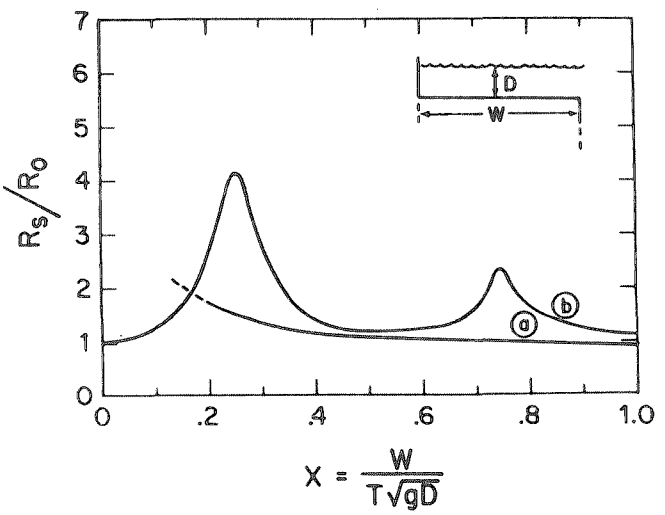

Figure 2. The relationship between dimensionless tidal range at the shore and dimensionless shelf width as predicted by the hydrodynamic model. The shelf is of unit alongshore length and uniform water depth D, equal to 20 m for curve (a) and 60 m for curve (b). Manning's n for both curves is 0.04. R_s (m) = computed tidal range at the shore, R_o (m) = given ocean tidal range at the margin edge (0.45 m), W = shelf width (m), T = M_2 tidal period = 44700 secs, and g = gravitational acceleration. Tidal augmentation due to resonance becomes important at some water depth between 20 and 60 m. Maximum augmentation occurs at quarter multiples of the tidal wavelength.

Discussion and Conclusions

Figure 1 depicts the modelled basin geometry and resulting co-range lines for the most probable boundary and initial conditions. Remarkably, the tides are augmented in this epicontinental sea by up to three times the ocean range with the highest values occurring along the Middle Atlantic States. Other experiments (Slingerland, 1986) have shown that the results are relatively insensitive to the bathymetry of the basin floor and to the open ocean tidal range, but are reduced as the entrance to the seaway is narrowed or the concavity of the southern (Devonian coordinates) shoreline is decreased. Thus, the answer to the first question is yes, mesotides (1-3.5 m range) are theoretically possible on the Catskill basin margin given our present best estimates of paleogeography.

The answer to the second question depends upon the causes of the augmentation. In general, augmentation of long waves is due to convergence and resonance. By convergence is meant a shoreward decrease in margin water depth or decrease in alongshore crest length of the tidal wave. For a frictionless, nonreflecting wave it is easy to show that if the wave energy is transmitted undiminished, then the amount of augmentation due to convergence is proportional to the quarter root of the convergence due to depth changes and the square root of the convergence due to crest length changes (Ippen, 1966, p. 502). Thus, a tidal wave traveling towards the Acadian Highlands across what is Pennsylvania today (Fig. 1) would have experienced approximately a threefold decrease in water depth and a one and one half-fold decrease in crest length, and therefore would have undergone a little greater than three-halves augmentation in height. That is approximately half the augumentation calculated in the model. This is only a first-order estimate because the actual tidal wave in the Catskill Sea propagated obliquely to the Acadian margin.

The other cause of augmentation is resonance, an oscillation of waters on the basin margin in phase with the forcing tides at the margin's edge. Figure 2 shows the amount of resonance augmentation predicted by the hydrodynamic model as a function of dimensionless margin width. Even at the high rates of frictional energy loss used in the model and a shallow depth (20 m), augmentation due to resonance occurs for dimensionless widths up to 0.9 (about 563 km for an M_2 tidal wave). For deeper waters (60 m), resonance augmentation occurs for all dimensionless widths up to 1 (about 1084 km) with two maxima at widths that are 1/4 and 3/4 multiples of the tidal wavelength.

The resonance portion of the augmentation seen in Figure 1 may be estimated from Figure 2. If the margin width through Pennsylvania is approximately 400 km (Fig. 1) and the average depth is 75 m, then the dimensionless width is 0.33 and K_S is greater than 2 times R_O. The two analyses taken together suggest that the predicted augmentation on the Catskill margin in Figure 1 is due about equally to convergence and resonance. Thus, decreasing the concavity of the shoreline in Figure 1 should reduce the augmentation by up to one-half. Increasing the dimensionless width of the basin margin (as in a transgression) from 0.33 while keeping the depth equal to 60 m would drastically decrease the resonance augmentation at first (Fig. 2), whereas if the depth were 20 m, increasing the dimensionless width would only slightly decrease the augmentation.

In conclusion, tidal flows could have played a more significant role in distributing sediment on the Catskill margin than previously recognized. Their contribution relative to storm-driven flows would have varied as a function of the local width, depth, and concavity of the shoreline, and therefore possibly with transgressions and regressions, an idea presently being considered by John S. Bridge (personal communication). A logical next step is to combine facies data like those in Table 1 with model results to determine the paleogeographic locations and ages in which each process was dominant.

REGIONAL DISTRIBUTION OF FACIES IN THE CATSKILL FORMATION AND THE CONTROLS ON RED-BED COPPER-URANIUM OCCURRENCES

by
Arthur W. Rose, Arthur T. Smith, and Christopher H. Gammons

Introduction

The studies of Rahmanian (1979) in central Pennsylvania as summarized by Williams in this volume clearly show the existence of several facies of Catskill sedimentation, and the existence of a large input center that remained in the vicinity of Port Matilda through Catskill time. Various other workers have identified facies, members, and other units in the Catskill over limited areas (Willard, 1939; Allen and Friend, 1968; Walker and Harms, 1971; Glaeser, 1974; Humphreys and Friedman, 1975; Epstein and others, 1974; Dyson, 1963, 1967), but a regional evaluation of facies has been lacking. As part of a regional study of red-bed copper-uranium occurrences, Smith (1983) and Smith and Rose (1985) have extended Rahmanian's work to furnish a regional correlation scheme and attempted to show how the groups of facies are interrelated within Pennsylvania. This paper summarizes this regional pattern, and also describes the relation of the copper-uranium occurrences to regional and local sedimentary characteristics.

Regional Distribution of Facies

Most previous work on the Catskill has concentrated on sedimentary facies within relatively limited areas of a few quadrangles. Stratigraphic units within these areas have been defined as members (Irish Valley, Sherman Creek, Duncannon, Clarks Ferry, Walcksville, Long Run, etc.), and correlated over distances of a few tens of kilometers. Over larger distances, especially east-west, these units seem to grade into each other, and correlation has not been attempted.

The approach of Smith and Rose (1985) was to define groups of facies, termed magnafacies, based on certain sequences of facies, and to correlate these magnafacies in widely spaced stratigraphic sections. Table 1 summarizes the characteristics used to define the facies. Associations of these 10 facies were then used to define four magnafacies, as illustrated on Figure 1. These magnafacies show consistent regional relations.

Magnafacies A generally forms a basal unit of the Catskill. It is composed dominantly of interbedded shale and fine sandstone, usually including both gray and red units, and is interpreted to have been deposited in an alternating marine to nonmarine tidal-flat environment. This magnafacies includes the Irish Valley Member in the field trip area, as well as the Towamensing and Beaverdam Run Members along the Lehigh River.

Magnafacies B is dominated by thick red shales accompanied by thin fine-grained sandstones, commonly in fining-upward cycles, and is interpreted as a low-energy fluvial deposit predominantly formed on relatively inactive parts of the coastal plain. Occasional thin sandstones interpreted as being of transgressive, tidal origin also occur in Magnafacies B. Magnafacies B is represented by the Sherman Creek Member in the field trip area, and by the Walcksville and Long Run Members in the Lehigh River area.

Table 1. Generalized criteria which define 10 facies associations in the Catskill Formation of Pennsylvania (after Smith and Rose, 1985).

Facies	Color[1]	Fossils[2]	Geometry	Grain size and lithology[3]	Sedimentary[4] structures	Commonly associated features
1	g	M and/or P	tabular	f-vf ss	massive beds, flasers, ripples, trough x-beds	--
2	g	M and/or P	lenticular	f-c ss ± quartz pebbles	do.	--
3	g	M and/or P	tabular	do.	do.	--
4	r or g	P	lenticular	f-vf ss	trough and planar x-beds, erosive basal contacts	fines up, basal cgl lag
5	g or r	P	do.	m-c ss	do.	cgl lag
6	g	P	do.	cgl	massive	facies 4, 5
7	g	M and/or P	lent./tabular	stst, mdst	bioturbated	thin, fss and facies 1, 2, 3
8	g	P	do.	f-c stst	bioturbated, root casts	do.
9	r	-	do.	stst, mdst	root casts	fines up and underlain by facies 4
10	g	P	do.	stst, mdst	--	facies 5

[1] g = gray; r = red (first letter is most common).
[2] M = marine; P = fossil plant material.
[3] f = fine; vf = very fine; c = coarse; m = medium; cgl = conglomerate; ss = sandstone; stst = siltstone; mdst = mudstone.
[4] x-beds = crossbeds.

Magnafacies C is composed dominantly of fine- to coarse-grained sandstone and conglomerate, usually gray, with minor shale. These thick sandstone units are interpreted as the product of large braided rivers carrying abundant coarse detritus from the uplifted source area to the east. Magnafacies C forms three northwest-trending lobes in Pennsylvania and southern New York (Figure 2A). These lobes are in the Harrisburg-Port Matilda zone, the Lehighton-Scranton zone, and southern New York. Part of the "Duncannon" Member visited in the Port Matilda section of the field trip belongs to Magnafacies C, as does the Clarks Ferry Member along the Lehigh River.

Magnafacies D is composed of thick fining-upward cycles with subequal amounts of gray or red sandstone and red shale. These sediments are inferred to have been deposited by meandering rivers and are thickest in the same areas that Magnafacies C is thick (Fig. 2B). Magnafacies D corresponds to the Duncannon Member in the sections along the Lehigh River, the lower Juniata Valley (Dyson, 1963, 1967), and the I-80 section of the field trip, and to part of the Duncannon section at Port Matilda.

The isopachs for Magnafacies C and D show a clear lobate zone extending northwest from the Lehigh River area, and a second thick lobe extending from Peters Mountain along the Susquehanna River northeast to the Port Matilda section visited on the field trip. A third area of thick sediment is suggested in southern New York state. Between these lobes, Magnafacies C disappears and Magnafacies D thins or disappears. This pattern is indicated on section A-A' on Figure 3. In general, the magnafacies tend to thin to the northwest, B and C most markedly (Fig. 3).

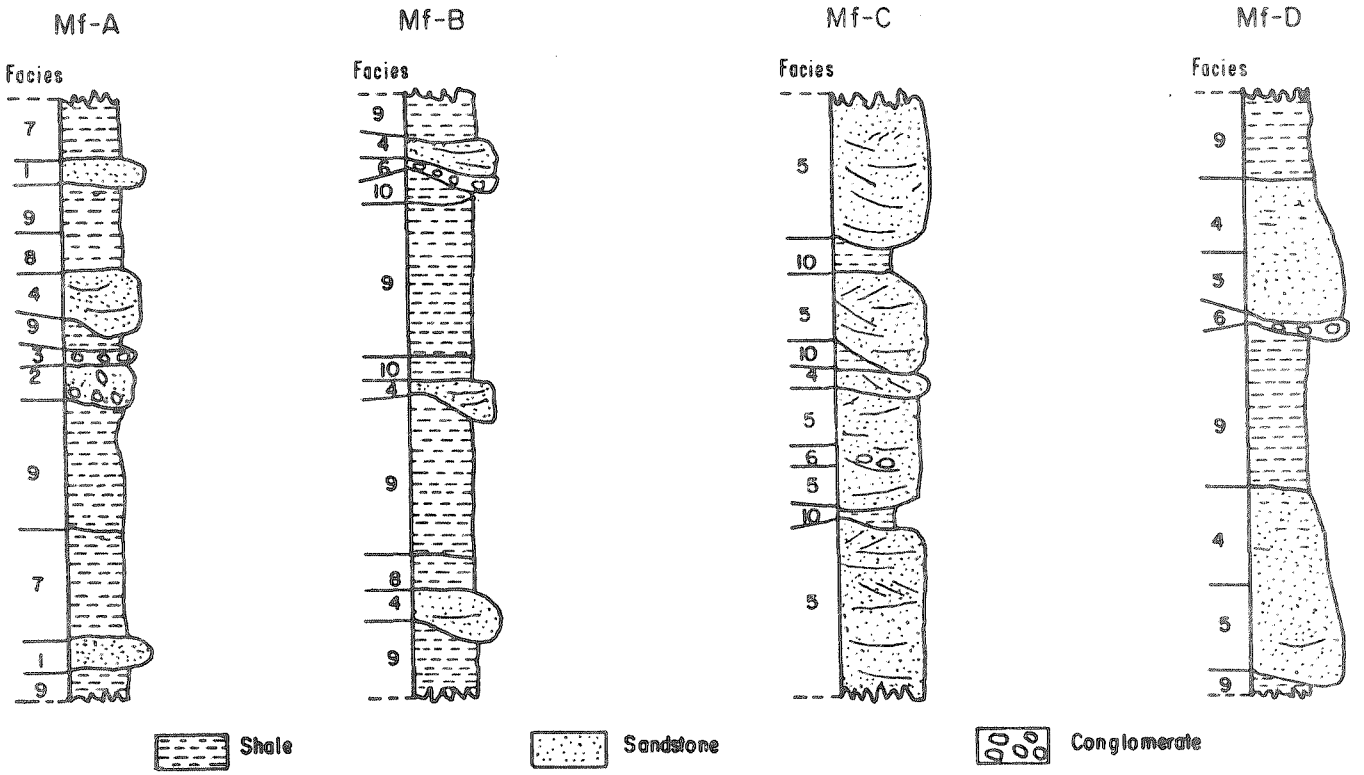

Figure 1. Idealized stratigraphic sections for four magnafacies (Mf) used in regional correlations of the Catskill Formation (Smith and Rose, 1985). See Table 1 for descriptions of component facies. Not to scale.

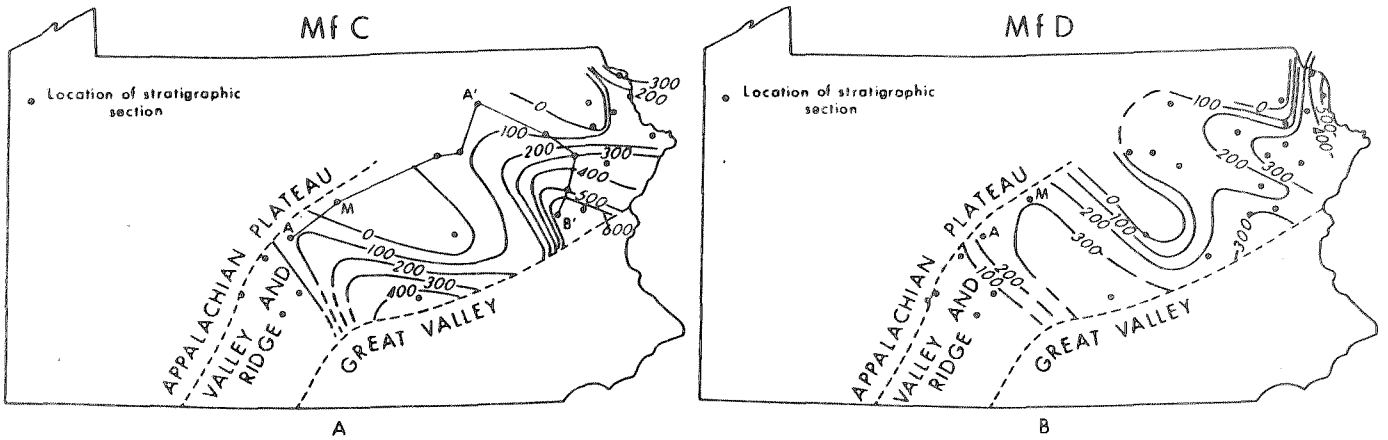

Figure 2. Isopach maps of Magnafacies C and D, in meters, showing lobes of thick sediment in the Port Matilda, Lehighton, and Southern New York areas. Sections A-A' and A'-B' are on Figure 3. Point A is the Port Matilda section and point M is the Milesburg (I-80) section. Modified from Smith and Rose (1985) as described in Appendix.

Given the coarse fluvial nature of most sediment in Magnafacies C and D, these lobes appear to be the loci of major river systems that crossed the alluvial plain from the source area to the east.

Red-Bed Copper-Uranium Occurrences

At least 80 small occurrences of copper/uranium are known in the Catskill Formation in Pennsylvania (Smith and Hoff, 1984; McCauley, 1961; Smith, 1980, 1983;

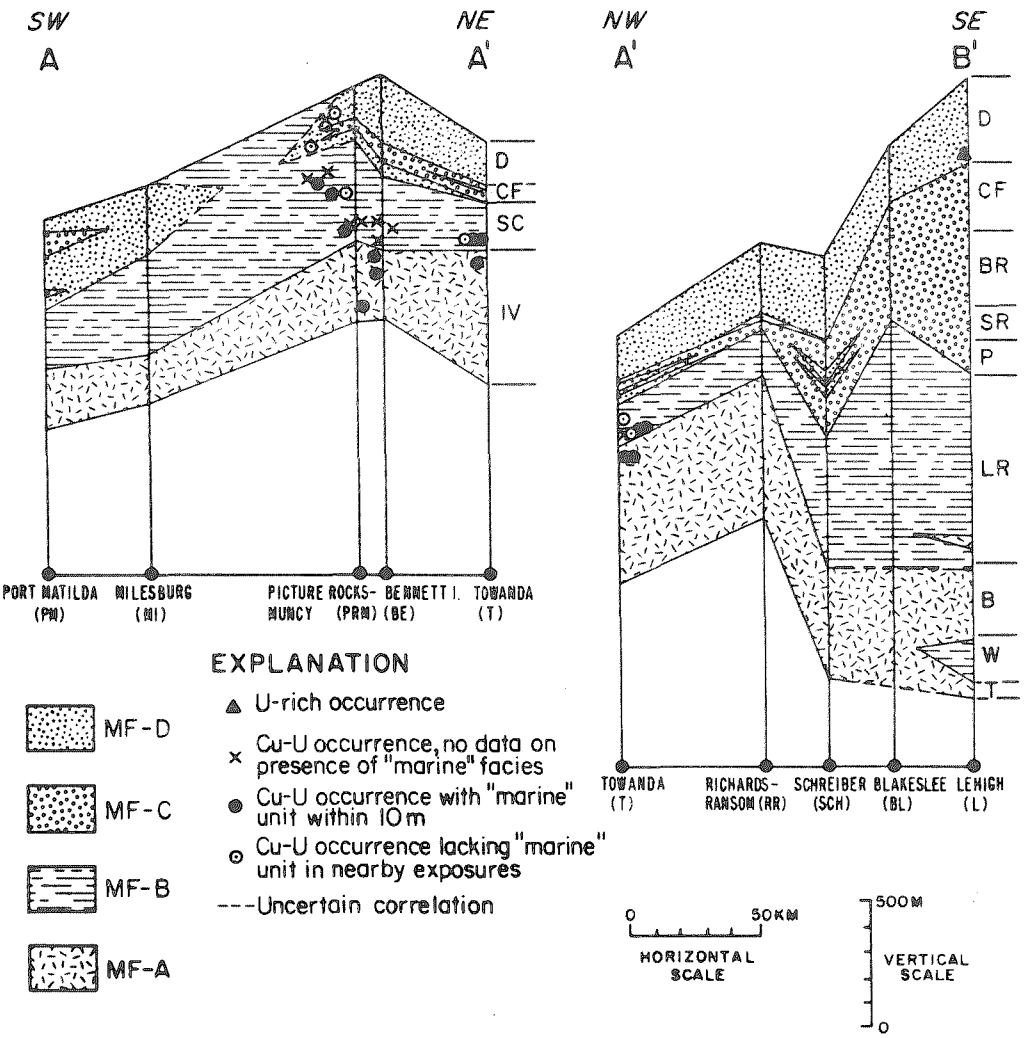

Figure 3. Regional cross sections showing distribution of magnafacies and Cu-U occurrences (modified from Smith and Rose, 1985, as described in the Appendix). Datum is Tioga bentonite +1500 m; nonpatterned area is marine Devonian. Abbreviations: IV, Irish Valley; SC, Sherman Creek; CF, Clarks Ferry; D, Duncannon; T, Towamensing Member; W, Walcksville Member; B, Beaverdam Run Member; LR, Long Run Member; P, Packerton Member; SR, Sawmill Run Member; BR, Berry Run Member. Slightly modified from Smith and Rose (1985).

Klemic, 1962; Sevon and others, 1978). These occurrences have the following general characteristics:

1. Mineralization is associated with and commonly replaces fossil plant material within gray or green facies of the Catskill Formation.

2. Mineralization is discontinuous but tends to be lensoid and stratiform. Typical mineralized zones are 1-50 cm in thickness and 1-10 m in length along bedding. Copper concentration is in the range of 0.05 to 0.3% Cu, and uranium contents are usually a few tens of parts per million. None of the presently known occurrences appear promising for economic development, though two produced small amounts of ore in the past.

3. The primary copper minerals appear to have been chalcocite and similar minerals, but partial to complete oxidation to bright-green malachite is common. Uranium occurs as uraninite at a few localities, but may be present in the organic matter at others. Many other minerals have been identified locally (Smith and Hoff, 1984).

4. Host rocks for mineralization are most commonly shales, but some are sandstones or conglomerates containing caliche pebbles and plant trash at the base of fining-upward cycles.

5. Features which suggest that the occurrences formed at low temperatures (<100°C) include orthorhombic chalcocite, exsolution of bornite from chalcopyrite on heating above 75°C, a wide range in $\delta^{34}S$ of sulfides, an apparent precompaction age relative to diagenetic minerals, fine grain sizes, and a general lack of evidence for elevated temperatures in the vicinity (McCauley, 1961; Smith, 1983; Rose and others, in press).

6. Sandstone beds with inferred original permeability higher than average for the Catskill are usually present within a few meters stratigraphically (Smith, 1983), and many occurrences are in zones of Magnafacies B containing nearby tongues of tidal sandstone.

7. Occurrences are most abundant within Magnafacies B, near the margins of large lobes of Magnafacies C and D (Fig. 4). A few occurrences are in the upper part of Magnafacies A and in Magnafacies D. None are in Magnafacies C, though this is the site of the uranium occurrences (no copper) near Jim Thorpe in eastern Pennsylvania.

Based on these characteristics, we infer that Cu and U were emplaced during diagenesis by pore fluids moving preferentially along the more permeable sand bodies in the Catskill. The copper and uranium were precipitated by the reducing effect of plant fragments and the accompanying bacterial sulfate reduction. Copper is not easily mobilized under oxidizing conditions except at acid pH, but in chloride-bearing waters at intermediate oxidation states it is very soluble as cuprous chloride complexes (Rose, 1976). The chloride may have been supplied to the pore waters by the occasional marine transgressions, or by evaporation of fresh waters in the relatively arid red-bed environment. Uranium is soluble under oxidizing conditions, including those under which cuprous chloride complexes are stable. Uranium mobility is accentuated at higher pH values, especially if dissolved carbonate is high, as is common in arid environments.

The source of the Cu appears to be the red beds themselves. Figure 5 shows that Cu content of pre-Catskill detritus, as indicated by the Cu content of marine rocks beneath the Catskill, was 20-25 ppm. No major change in composition of detrital material is expected for the subsequent nonmarine Catskill sediments, yet typical Cu contents of red beds are less than 5 ppm (Fig. 5). In contrast, green and gray Catskill sediments contain a wide range of Cu contents, up to hundreds of parts per million. A major redistribution of Cu has evidently occurred in the Catskill, leading to mobilization of copper out of the red units into some of the reduced (gray-green) units.

Data for Zn, Ni, and Co in the same samples show no differences between pre-Catskill and Catskill, and generally only small changes for Pb. These elements, unlike Cu and U, are not concentrated appreciably in the red-bed mineralization, and do not show depletion from the red beds.

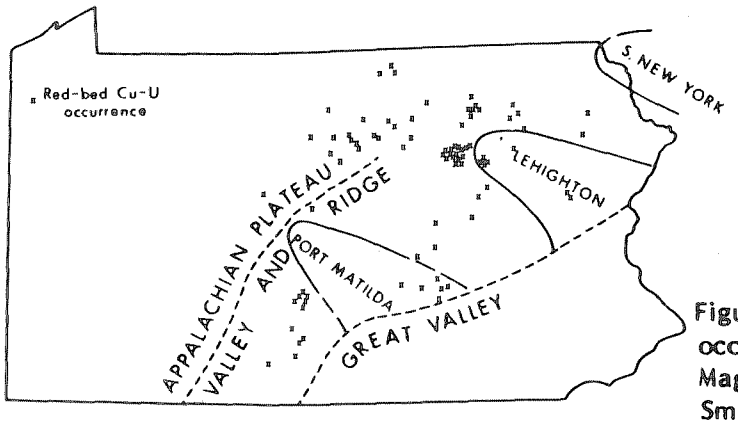

Figure 4. Location of red-bed copper-uranium occurrences relative to lobes of thick Magnafacies C. Modified from Smith and Rose (1985).

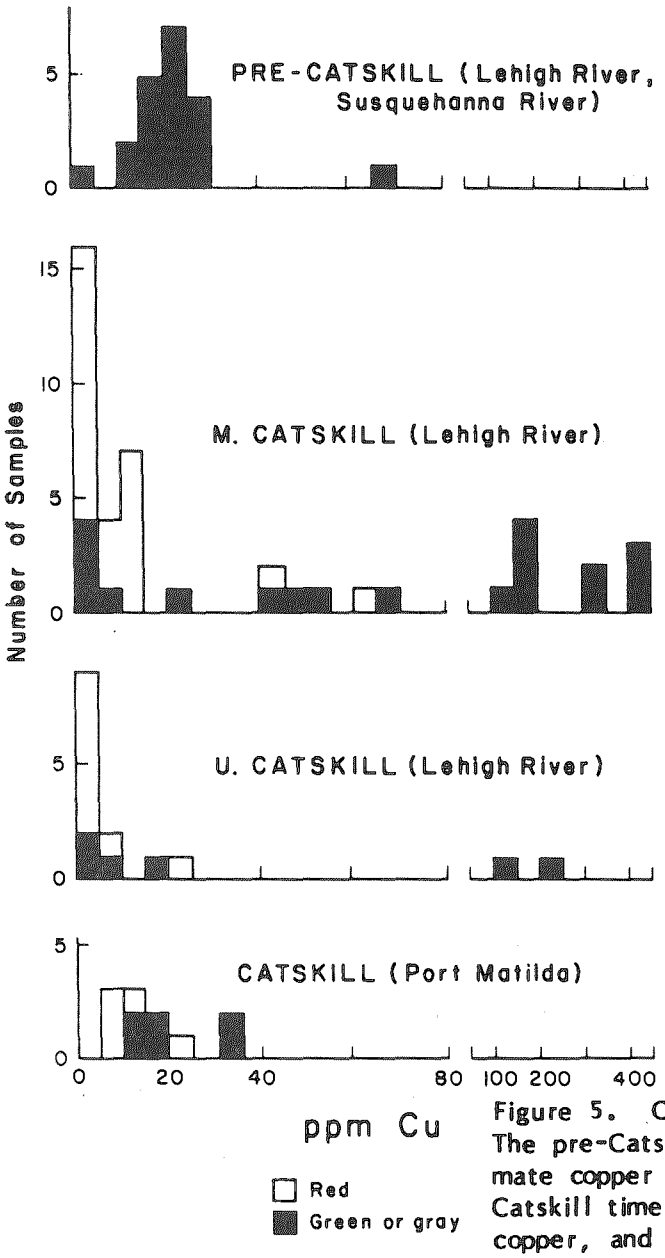

Figure 5. Copper content of Catskill and pre-Catskill rocks. The pre-Catskill rocks are inferred to indicate the approximate copper content of detritus entering the basin during Catskill time. The red beds have generally been depleted in copper, and green-gray beds have commonly been enriched.

Data for Cu content of samples from the Port Matilda section are also shown on Figure 5. Though the effects are not as extreme, the same tendency for depletion of Cu from red beds and enrichment in gray beds is noted.

One small copper occurrence has been found in the Port Matilda section, near the base of the exposures examined in the Irish Valley Member. It appears that Catskill sediments of Magnafacies B in the Port Matilda section may have lacked reduced zones or that chloride content remained low because of underflow of fresh groundwater down the alluvial plain beneath the river system at this point, thus leading to only rare accumulations of Cu.

Appendix

Data on thickness of Magnafacies C and D in addition to that reported by Smith and Rose (1985) and Smith (1983), and shown on Figure 2, are as follows:

Location of Section	Mf C	Mf D
Raystown Dam	0 m	< 50 m
Entriken	0	< 100
Horseshoe Curve/ New U.S. 22	0	< 50
Tyrone (Pa. 453)	0	< 100

These data demonstrate a rapid southwestward thinning of the Mf C and Mf D lobe at Port Matilda. Although exposures are poor, no more than one cycle of Mf D appears to exist at these localities.

In addition, a reexamination of the Port Matilda section indicates that an additional 56 m of the section fits the criteria for Mf C, with correspondingly less Mf D.

Stop localities for Field Trip #2, plotted on Radar Map of part of Central Pennsylvania (STAR-1 Imagery courtesy of INTERA Technologies Inc., September, 1984).

FIELD TRIP #2

FIELD GUIDE - CATSKILL SEDIMENTATION IN CENTRAL PENNSYLVANIA

E. G. Williams and Rudy Slingerland,
Field Leaders

Introduction

This field trip will attempt to illustrate the conclusion, presented by Rahmanian (1979) and Williams (this volume) that Catskill sedimentation in central Pennsylvania occurred in tide-dominated deltaic and interdeltaic environments, the latter exhibiting features of an open as well as a barred coastline. Specifically, the tide-dominated delta occupied an area extending approximately from Tyrone on the south to midway between Port Matilda and Milesburg on the north, a distance of about 30 miles. The rocks recording its existence are the sandstone-shale facies of the upper Trimmers Rock Formation, a noncyclic facies of the Irish Valley Member of the Catskill Formation, and a silty facies of the Sherman Creek Member of the Catskill Formation. Reference to Figure 1 shows that to the north, at Milesburg, the sandstone-shale facies of the Trimmers Rock Formation is absent and the motif or cyclic facies of the Irish Valley Member replaces the nonmotif facies of the Port Matilda section. Well-developed fining-upward cycles of red sandstone and mudstone of the Sherman Creek Member at Milesburg replace the finer grained noncyclic facies present at Port Matilda. In addition, but not shown on the diagram, important facies changes occur in both the Duncannon Member of the Catskill Formation and the Pocono Formation between Milesburg and Port Matilda, namely the fining-upward alluvial cycles become much thicker, fewer in number, and coarser grained at Port Matilda. Rahmanian and Williams interpret all the above facies changes, which also occur to the south of Tyrone, to be the result of the presence of a major depocenter whose axis was located at Port Matilda. There, a large braided river (represented by the Pocono Formation) supplied sediments to a delta consisting of anastomosing distributaries on the upper part (Duncannon Member) and tidally influenced channels, mud flats, shallow bays, and bars on the lower parts of the delta (Sherman Creek and Irish Valley Members). These graded seaward into storm-deposited shelf deposits (upper Trimmers Rock Formation). To the north and south of the delta existed broad muddy tidal flats, developed along both barred and open coastlines (motif facies of the Irish Valley Member), landward of which was a wide coastal plain crossed by low-gradient, meandering rivers (cyclic facies of the Sherman Creek and Duncannon Members).

The strategy of this trip will be to compare facies within and between the various members of the Trimmers Rock and Catskill Formations at the Milesburg and Port Matilda sections. The stops and the general facies and members seen at each are summarized in the following table:

Port Matilda transect (Route 322)

Stop	Description
1	Overview at Skytop.
2	Sandstone-shale facies and silty shale facies of upper Trimmers Rock Fm.
3	Nonmotif facies of Irish Valley Mbr., Catskill Fm.
4	Complex cycles of Duncannon Mbr., Catskill Fm.

Milesburg transect (Route I-80)

Stop	Description
5	Motif facies of Irish Valley Mbr., Catskill Fm. (Runville, Pa.)
6	Silty shale facies of upper Trimmers Rock Fm.
7	Cyclic mudstone-sandstone facies of Sherman Creek Fm.
8	Simple cycles of Duncannon Mbr., Catskill Fm.

The interval to be examined at each locality is noted on the appropriate stratigraphic section on Plate 1.

INC. MIL.	CUM. MIL.	DESCRIPTION
0.0	0.0	LEAVE parking lot of Holiday Inn, State College, Pa. Turn left (west) on Route 322 towards State College.
3.5	3.5	The red soils and scrub oak forests seen on both sides of the road are characteristic of the Upper Cambrian Gatesburg Formation, a cyclic orthoquartzite-dolomite on which very thick, kaolinitic, hematitic soils have developed during the late Tertiary. The soils are sandy and consequently the region underlain by the Gatesburg Formation is underdrained, producing a terrain called "The Barrens." The soils have been mined in the past as a source of iron ore and refractory clays; the iron mining town of Scotia, southwest of here, was founded at the turn of this century by Andrew Carnegie and named after his native Scotland.
2.85	6.35	Outcrop on right of Upper Cambrian Warrior Formation, the oldest exposed formation in the Nittany Valley. The small valley 100 m ahead (to the west) is a manifestation of the Birmingham thrust fault which brings the Warrior Formation in contact with the Bellefonte Dolomite, outcrops of which form the western valley wall.
1.25	7.60	Ahead, the road ascends Bald Eagle ridge, the westernmost ridge of the Appalachian Mountains in this area. Rocks exposed on the ascent are black silty shales and sandstones of the Upper Ordovician Reedsville Formation, a structurally thinned section of sandstones of the Bald Eagle Formation forming a secondary ridge, red sandstones, siltstones, and shale of the Juniata Formation of lesser resistance, and orthoquartzites of the Lower Silurian Tuscarora Formation forming the main ridge. The beds are vertical to slightly overturned.
0.85	8.45	**Stop 1:** Skytop Overlook. Discussant: E. G. Williams.

This locality sits on the crest of Bald Eagle Mountain overlooking Bald Eagle Valley and the Allegheny escarpment to the northwest. The valley separates the gently dipping upper Paleozoic rocks of the Allegheny Plateau to the west from the folded rocks of the Valley and Ridge to the east (see Gold, this volume, for details). Bald Eagle Mountain, which has an elevation of 2300 feet, is underlain by the Tuscarora Formation, a resistant orthoquartzite of Early Silurian age. The topmost and steepest slope of the escarpment is formed by the Pocono Formation, a low-rank graywacke, which has a quartz content of about 80 percent and is believed

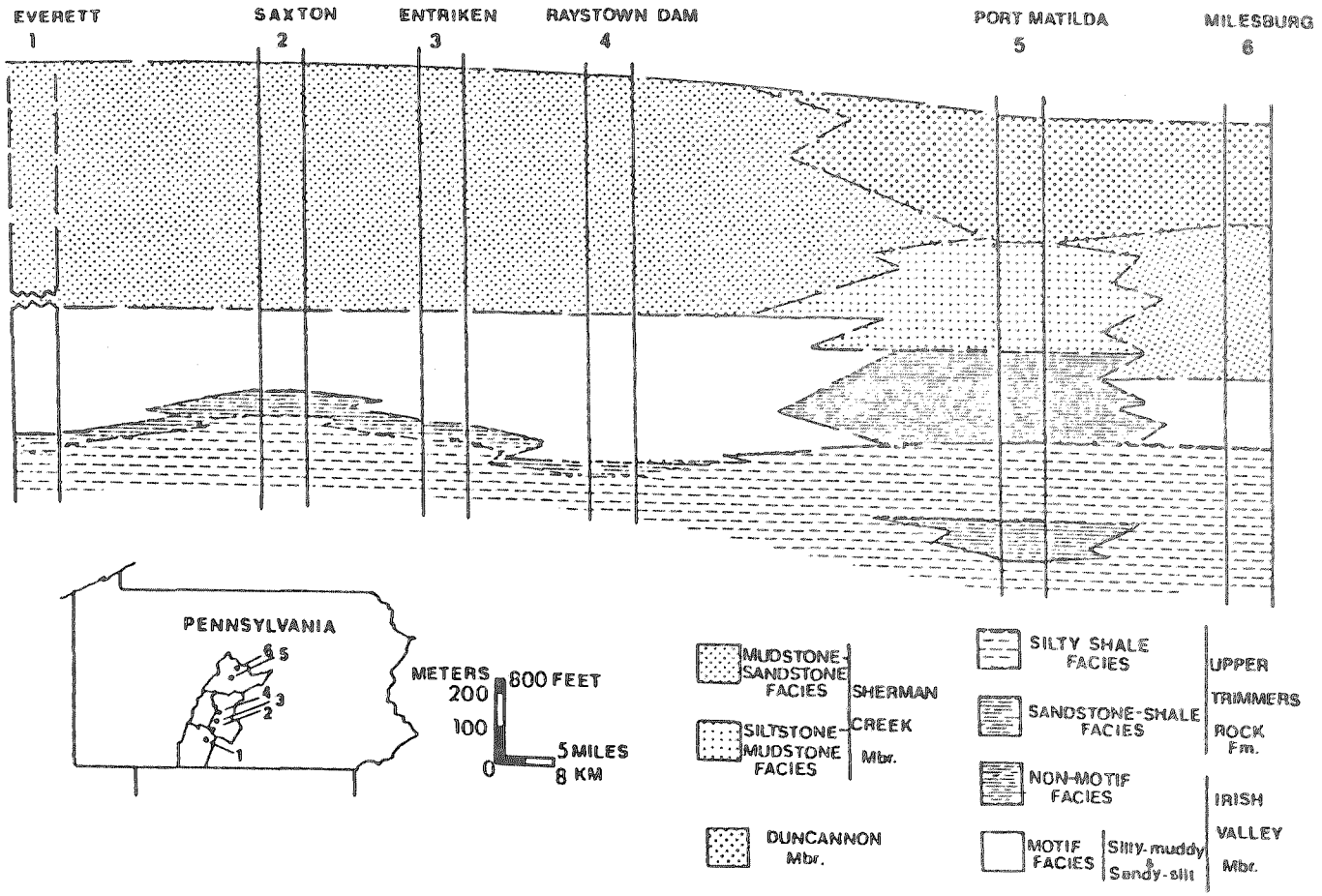

Figure 1. Generalized lithofacies cross section of the Upper Devonian rocks in central and south-central Pennsylvania (from Rahmanian, 1979).

to represent deposits of a braided river. The strike valley below the Pocono marks the top of the Catskill Formation, which is divided into three members, from bottom to top, the Irish Valley, Sherman Creek, and Duncannon. The several ridges below the steep slope of the escarpment are sandstones of the Duncannon Member, each 50 to 100 feet thick, inferred to be migrating alluvial channels which supplied sediment to the Catskill delta manifested in the ridges and strike valleys in the middle part of the escarpment. These constitute the Irish Valley Member. The ridges are distributary-mouth bars or tidal-sand ridges, and the strike valleys represent bay and tidal-flat muds. The several ridges in the lower part of the escarpment are underlain by shelf sandstones of the upper third of the Trimmers Rock Formation. All of the formations visible in the Allegheny escarpment intertongue and so, on a regional basis, are equivalent in age.

The gently undulating surface on the skyline is the Schooley peneplain of Johnson, an early Tertiary erosion surface. Based on measurements of porosity and bulk density of Pennsylvanian sandstones and reflectance of coals, an estimated 15,000 feet of denudation has occurred at the Allegheny escarpment since the Permian (Paxton, 1983).

LEAVE STOP 1 and proceed west on Route 322.

2.45	10.90	STOP SIGN; TURN LEFT on Route 220 South/322 West.

1.50	12.40	Outcrop on right of Upper Devonian Harrell Shale.
1.40	13.80	STOP LIGHT in Port Matilda; TURN RIGHT, continuing west on Route 322.
1.80	15.60	**Stop 2: Upper part of the Trimmers Rock Formation.** Outcrops are along a small gravel side-road. Discussants: E. G. Williams and R. Slingerland.

The rocks exposed at this locality comprise the silty shale and sandstone-shale facies of the upper part of the Trimmers Rock Formation. The sequence correlates with the exposure of the silty shale facies at Stop 6 (refer to Plate 1, section 7, 0-400 ft interval). A summary of the major lithologies and their environmental interpretations is presented in Figure 2. The lower 75 feet of the outcrop resembles the silty shale facies described at the Milesburg section. The sandstone-shale facies here displays entirely different sedimentary characteristics than have been observed at any of the other sections. It contains two different sandstone

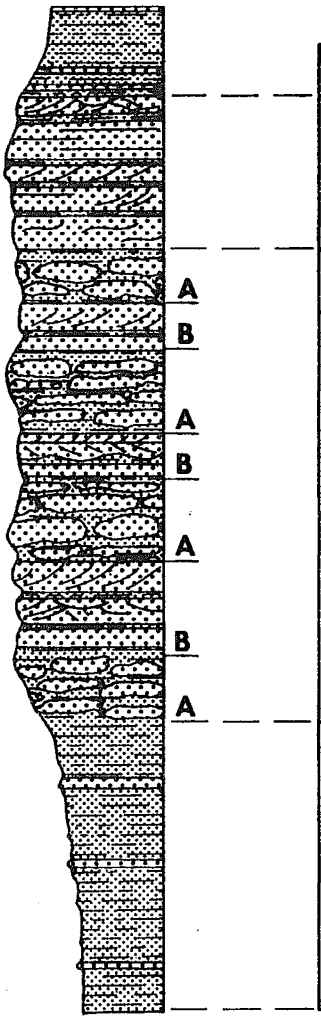

Facies	*Sedimentary structures*	*Interpretation*
Brown-gray fossiliferous fine-grained sandstone	Horizontal, flaser, lenticular, and large- and small-scale, planar and trough crossbedding	Tidal sand bar (low-tide terrace?)
Sandstone-shale facies A: Brown, massive to thickly bedded, fine- to very fine grained sandstone and siltstone B: Olive-green, fine-grained, fossiliferous, regularly bedded sandstone; silty shale and shale	– A: Abundant soft-sediment deformational structures; well-preserved horizontal lamination – B: Hummocky cross-strata; wavy, flaser, and rhythmic bedding; clay drapes on foresets; ripple lamination; bioturbated horizons common	Alternation of destructive (marine-influenced) and constructive (fluvial-influenced) phases of sedimentation in a storm-influenced prodelta and delta-front environment
Silty shale facies Gray olive-gray, fossiliferous silty shale to siltstone with thin sandstone layers interspersed	– Siltstones: Dominantly horizontally laminated – Sandstone: Small- to micro-scale cross-bedding, linear and interference ripples; hummocky cross-stratification	Shallow marine shelf

Sandstone Silty shale

Figure 2. Idealized vertical facies sequence of the uppermost Trimmers Rock Formation from pooled data at the Port Matilda section (modified from Rahmanian, 1979).

subfacies that occur together with interlayered siltstone and silty shale units in a semicyclic arrangement. These are called subfacies A and B (Fig. 3).

Subfacies A consists of chocolate-brown, thickly bedded and sometimes massive, very fine grained, micaceous sandstone and chocolate-brown and thinly bedded sandy siltstone, occurring in units 8-18 feet thick. A characteristic aspect of this facies is the large number of soft-sediment deformation features such as ball-and-pillow structures and convoluted laminations. Marine fossils are very rare and burrows and bioturbated sediments are absent.

Sandstone subfacies B, which alternates with subfacies A, consists of an alternation of light-gray sandstone and silty shale units which are devoid of any soft-sediment deformation features. The sandstone units have a higher quartz content and are coarser grained than those in subfacies A. Thicker beds are

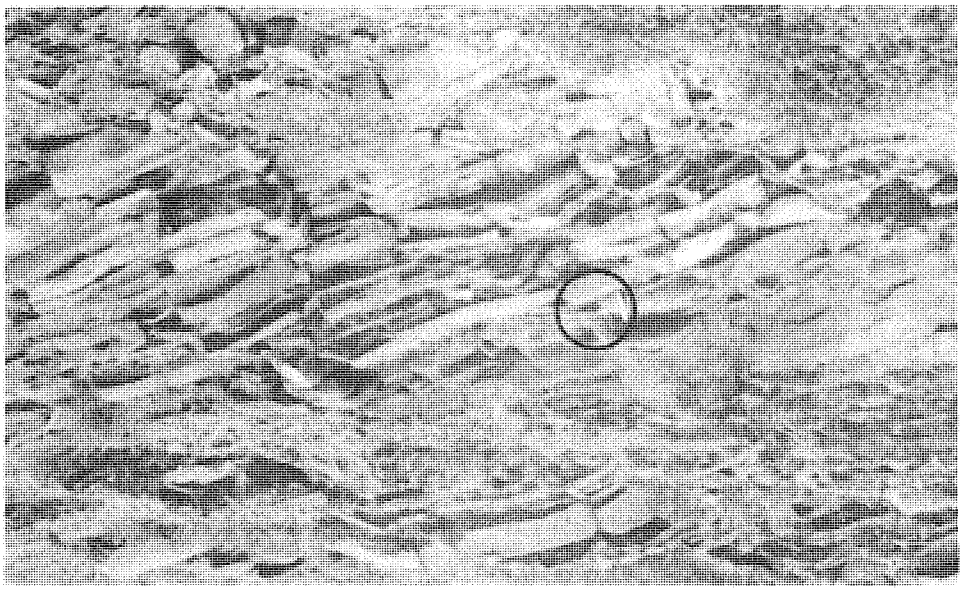

Figure 3. Alternation of sandstone subfacies A (above the hammer) and subfacies B (below) in the uppermost Trimmers Rock Formation at Stop 1.

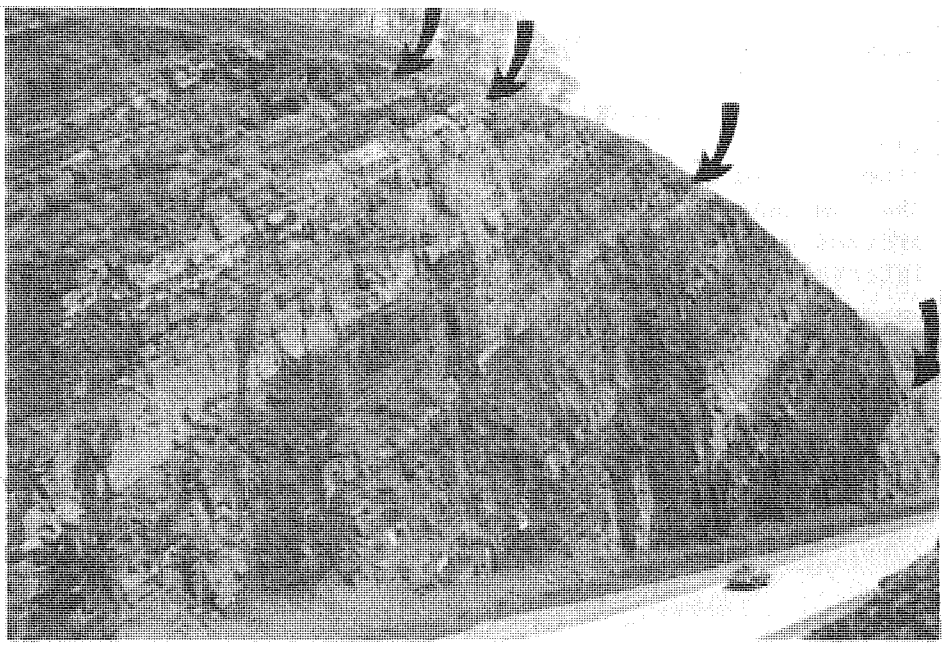

Figure 4. Exposures of the Irish Valley Member of the Catskill Formation at Stop 3. Arrows point to marine horizons. Note the anomalously high sand/shale ratio compared to Irish Valley sections to the north and south.

commonly both horizontally and cross-laminated; thinner beds exhibit rippled upper surfaces with clay drapes. Very thin beds exhibit flaser and lenticular bedding. Interbedded siltstones and shales are extensively burrowed. Marine fossils are abundant and scattered throughout this facies, but are most commonly found as brachiopod and coquina layers at the tops and bottoms of sandstone beds.

The overall characteristics of this facies are suggestive of a shallow marine prodelta-subtidal environment. The presence in subfacies B of flaser and lenticular bedding, hummocky cross-lamination, clean, well-sorted sandstones, clay drapes over rippled surfaces, extensive bioturbation, and abundant marine fossils points to deposition in a subtidal environment, characterized by alternation of storm-current bed-load sediment transport with deposition of the suspended load during slack water periods. Subfacies A displays features suggesting rapid sedimentation in a low-energy environment characterized by lower flow energies. The presence of ball-and-pillow structures, the absence of bioturbation structures and burrows, and the lack of marine fossils are taken together to mean sedimentation was rapid. Immature texture and composition of sandstones of this facies suggests little, if any, reworking by tides and waves. These features are suggestive of fluvially induced sedimentary processes in a prodelta, delta-front environment. It is suggested that these sediments were deposited basinward from the delta mouth in the absence of significant marine reworking. As soon as the rate of sediment supply was reduced, either as a result of lateral shift of the mouth or seasonal variations in river discharge, marine processes took over. During this phase of sedimentation, sediments were reworked and redistributed by waves and tidal currents into various types of shallow marine subtidal sandstone bodies, eventually producing subfacies B. Repeated alternation of the two subfacies might result from the process of delta switching.

LEAVE STOP 2 and proceed west on Route 322.

0.80 16.40 **Stop 3: Irish Valley Member of the Catskill Formation. Discussants: E. G. Williams and R. Slingerland.**

The rocks exposed at this locality (Fig. 4) are part of the nonmotif facies of the Irish Valley Member of the Catskill Formation and are correlated with those seen at Stop 5 (Plate 1, compare section 7, 1450-1700 ft, to section 6, 0-200 ft). There are two facies exposed; these are, from base to top: 1) green quartzitic sandstone-mudstone facies; and 2) interbedded red sandstone, siltstone, and mudstone facies.

The green quartzitic sandstone-mudstone facies in the lower part of the outcrop consists of a vertical alternation of thinly bedded olive-green mudstone and very fine grained quartzitic sandstone and siltstone. Wavy and lenticular bedding are the dominant sedimentary structures. Small brachiopods and bone fragments are present but uncommon. In the lowermost parts of the exposure occur two thin intervals of red, fissile, Lingula-bearing shale and siltstone.

The red facies consists of fine- to medium-grained, well-sorted sandstone beds interbedded with red, rooted and burrowed, laminated to massive mudstones and siltstones. Sandstones occur in two distinct groups of thickness--large (14-19 feet) and small (up to 4 feet). The larger units have relatively sharp and flat but generally interfingering basal contacts, with large-scale trough and planar crossbedding in the lower parts which grade upward to ripple and micro cross-lamination at the top. All measured crossbed dip directions are to the northwest (Williams, this volume, Fig. 8), but some inaccessible beds possess apparent dip

directions to the southwest. Two of the large sand bodies are completely cut by large channels trending approximately southwest-northeast, and filled with siltstone. At the tops of the sandstones and at other positions within the deposit occur thin, green, rippled sandstone and siltstone containing marine fossils.

The red mudstone and siltstone are arranged into coarsening-upward cycles, beginning with massive, burrowed mudstone which grades upward to interbedded red siltstone and sandstone beds. The top of the cycle may consist of very fine, rippled, green quartzitic sandstone, often with marine fossils.

The assemblage of facies of the Irish Valley at this section is believed to represent various subenvironments of a tidally influenced delta. The large sandstone bodies contain many features characteristic of large sand shoals reported from tidal channels of modern tidally influenced deltas. Large-scale trough and planar crossbedding in the lower parts and the presence of asymmetric (current), symmetric (wave), and linguoidal ripples with variable crest orientation near the upper parts of the sand bodies are evidence for their tidal origin. In addition, the large sandstone bodies interfinger at their bases with Lingula-bearing shale, show numerous internal pause planes of shale, are comprised of well-sorted and quartz-rich grains, and are tabular, not cigar-shaped. The red mudstones containing Lingula are thought to represent brackish-water lagoons and bays. Marsh sedimentation is inferred from red siltstones with abundant root traces. Thin, rippled, quartzitic, fossiliferous sandstones occurring at the tops of many of the sandstones represent marine transgressions, produced during periods when rates of sediment supply were low, a condition produced by lateral shifting of distributaries or variation in discharge, or produced by eustatic sea-level changes. Figure 5 is a diagram of the tidally influenced delta at Port Matilda.

The Sherman Creek Member occupies most of the strike valley to the west of this outcrop. The lack of resistance to erosion and the few small outcrops available lead to the conclusion that the principal lithologies are red mudstone and siltstone, which is in contrast to the greater abundance of sandstone in the corresponding section at Stop 7 in the Milesburg section.

LEAVE STOP 3 and proceed west on Route 322.

0.80 17.20 **Stop 4: Duncannon Member of the Catskill Formation.** Discussants: E. G. Williams, R. Slingerland, and A. W. Rose.

The rocks exposed at this locality (Fig. 6) are the fining-upward cycles of the Duncannon Member of the Catskill Formation. They resemble those described at Stop 8 of the Milesburg section (Plate 1; compare section 7, 2830-3320 ft to section 5, 2980-3250 ft), but they differ in that they are much thicker and contain relatively more sandstone and less red mudstone and shale. Several smaller cycles, each about 50 feet thick, occur low in the outcrop and are similar to those at Stop 8. Unique to this locality are the much thicker cycles commencing 200 stratigraphic feet above the base of the section. The first cycle is 133 feet in thickness, 126 feet of which is sandstone. Following an erosional base, the sandstone has a 3-foot-thick basal concentration of interformational conglomerate consisting of siltstone and shale clasts, calcareous nodules, carbonaceous wood and plant fragments, and scattered white quartzitic pebbles. Thin conglomeratic units of this composition rest on scoured surfaces at various levels throughout the sandstone body, breaking it up into a number of distinctive morphologic units which give the sandstone body a

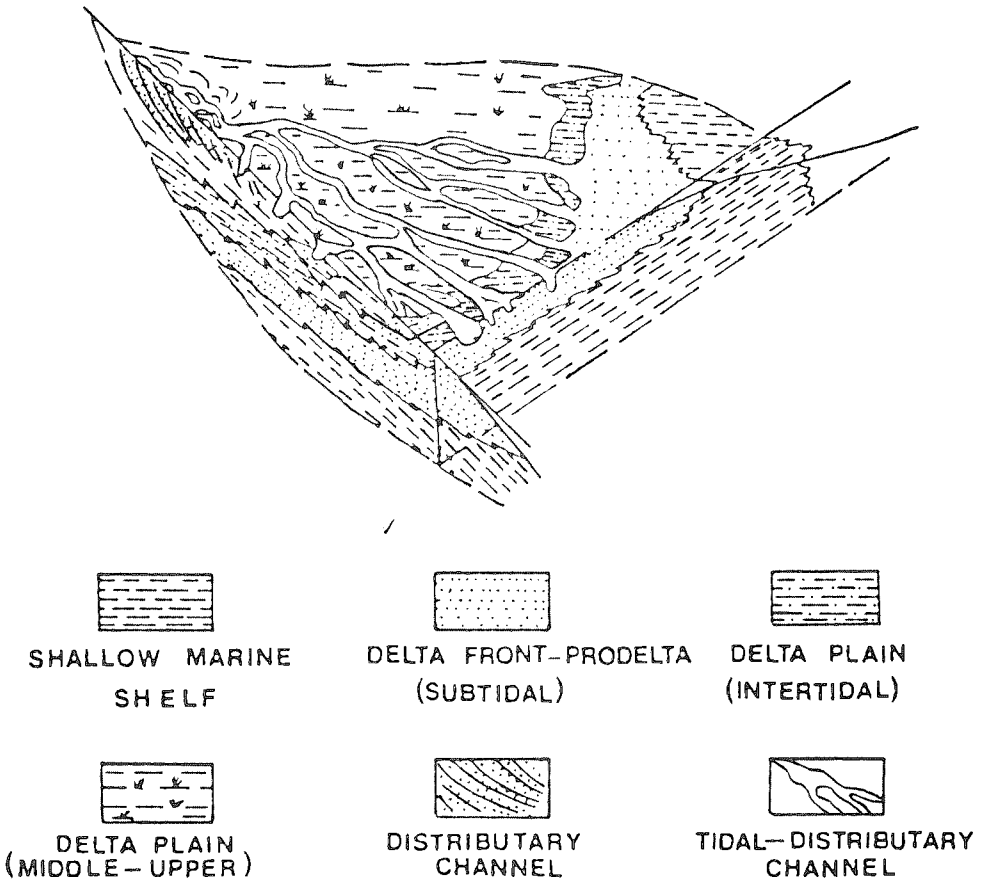

Figure 5. Paleogeographic model illustrating the various subenvironments and facies of the inferred tide-dominated delta at Port Matilda (from Rahmanian, 1979).

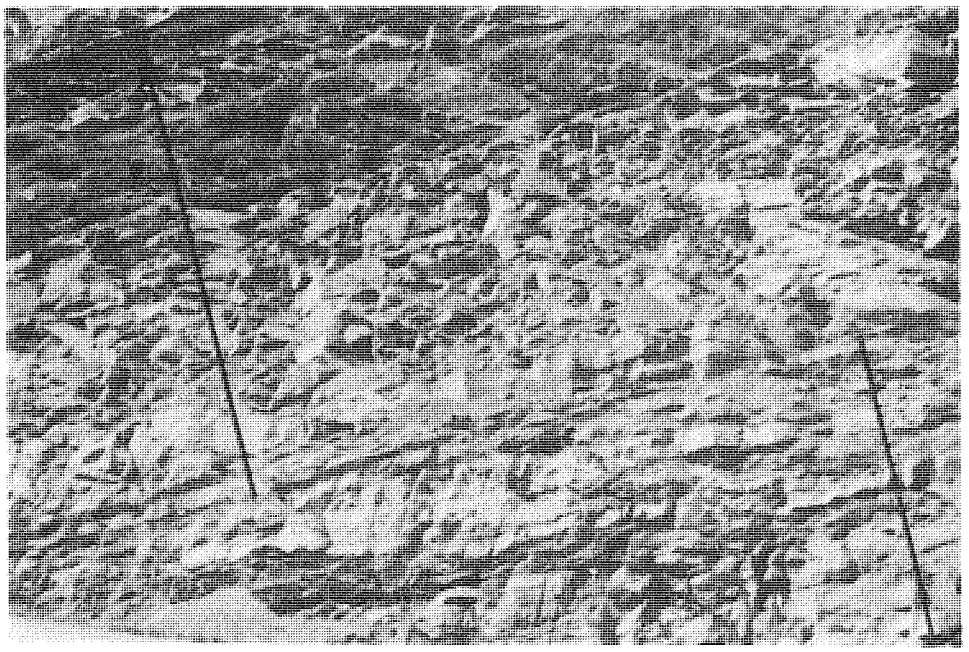

Figure 6. Exposures of the Duncannon Member of the Catskill Formation at Stop 4 containing a 133-foot-thick, fining-upward alluvial cycle denoted by the lines.

composite appearance. Individual sandstone units are green, fine- to medium-grained, micaceous and carbonaceous, and often complexly crossbedded. Measurements of trough and planar crossbedding gives a northwest transport direction (Williams, this volume, Fig. 8). The sandstone body fines upward and eventually grades into a 7-foot interval of red, thin interbeds of siltstone, shale, and claystone, containing many root traces and desiccation cracks. Associated with the rooted mudstone is a 1.5-foot-thick zone of numerous large and small, rounded calcareous nodules, which is interpreted to represent a partially preserved soil horizon. Directly above the soil is 4 feet of green, burrowed, fossiliferous siltstone and silty shale. The fossils are calcareous brachiopods. Stratigraphically above this locality to the west are several other Duncannon cycles of similar thickness and lithology.

The exceptionally thick sand bodies, within which are preserved a large number of lenticular sandstone units, and the scarcity of fine overbank deposits indicate rivers of moderate to low sinuosity whose channels were meandering to anastomosing. In this interpretation, the accretionary bedding so obvious in the outcrop was formed by lateral migration of mid-channel pebbly sand bars as in the Brownstones of southwestern England (Allen, 1983). The occurrence of thin transgressive deposits within the Duncannon would seem to indicate that the area of sedimentation was close to shore and may represent braided distributaries on the upper delta plain.

The origin of the various colors of the Catskill also will be considered at this locality. Facts relevant to this problem are:

1) Composition

	Red siltstone	Green-gray siltstone
Fe_2O_3	3.05%	3.23%
Fe^{3+}/Fe^{2+}	1.68%	0.72%
Grain size (ϕ)	3.84	4.12
Quartz %	24.65%	24.33%
Number of samples	20	19

2) The red color is produced by hematite, the green color by chlorite.

3) Red siltstones, although containing root traces, never have any carbonized remains of plant roots, stems, leaves, or spores, whereas the green and gray siltstones and fine sandstones in the fining-upward cycles generally contain abundant and various types of organic matter.

4) In situ calcareous nodules occur in red mudstones at the top of many cycles.

5) The red mudstones of the Irish Valley Member are brackish water in origin and were deposited in bays and lagoons.

6) Black and gray shale chips as well as deformed layers of black shale occur in many of the gray channel sandstones.

We interpret these facts to mean that sediments transported by the braided rivers of the Duncannon were initially gray and that the red mudstones and siltstones at the top of the cycles are overbank and levee deposits which have been oxidized in situ in an arid climate. Evidence for the latter interpretation comes from the calcareous nodules which are interpreted to be caliche deposits of a desert soil. The evidence for in situ oxidation of green muds to red ones is the occurrence of the black and red shale chips found in the gray channel sandstones.

We reason that these represent overbank muds which slumped into the adjacent rivers during channel migration and bank undercutting. Because the red fragments exhibit no reduction rims, we conclude that the black fragments were black when eroded. The absence of such deposits at the tops of the cycles suggests to us that all the dark sediment has been oxidized to red.

The red mudstones and shales of the Irish Valley Member have a different origin. Because they were deposited in lagoons and bays, it is unlikely that they could have been oxidized in place. We believe that the red mud and silt was transported from the red floodplains of the inactive coastal plains (Sherman Creek Member), where the red overbank sediments were being constantly eroded by meandering streams. Sedimentation was sufficiently rapid in delta-front environments that reduction did not occur even though the bays, with abundant fossils, may have been reducing.

LEAVE STOP 4 and proceed west on Route 322.

0.40	17.60	Rocks exposed on the right are the upper part of the Duncannon Member of the Catskill Formation.
0.40	18.00	Rocks exposed in this and the next large roadcut are sandstones of the Mississippian Pocono Formation. This sand body resembles those of the Duncannon in exhibiting multilateral sandstone bodies bounded by erosion surfaces and exhibiting trough and planar crossbedding. At the base of some channels are thin transported coals. No overbank shales have been observed. In comparison to the underlying sandstones of the Duncannon and to Pocono sandstones at the Milesburg section, the Pocono at this locality is much thicker, is coarser grained, and exhibits little or no overbank deposits. We interpret the Pocono at this locality to be a braided river, the principal river that supplied the delta located in the Port Matilda area.
2.1	20.1	Exposures on both sides of the road consist of the Loyalhanna Formation, a calcareous quartzite, which represents a transgressive shelf sand, and so marks the end of this major Upper Devonian Mississippian regressive sequence.
3.6	23.7	The road is descending along the southeastern dip-slope of the Philipsburg coal basin. The rocks exposed in various roadcuts from here to Black Moshannon State Park are in the Pottsville and Allegheny Groups of Pennsylvanian age.
1.6	25.3	TURN RIGHT directly before Dairy Queen.
0.2	25.5	TURN RIGHT on Route 504 East.
8.6	34.1	LUNCH STOP at Black Moshannon State Park.
		LEAVE LUNCH STOP continuing East on Route 504.

6.7	40.8	Edge of the Allegheny Escarpment with view of Appalachian Mountains to the southeast.
5.2	46.0	TURN LEFT on Route 220 North.
4.0	50.0	TURN LEFT on Route 144 North in town of Wingate.
2.9	52.9	Stop 5. Irish Valley Member of the Catskill Formation, Runville, Pa. Discussants: E. G. Williams and R. Slingerland.

The rocks exposed at this locality consist of alternating red, nonmarine sandstones, siltstones, and mudstones and marine gray and green sandstones and shales (Plate 1, section 6). These sequences are repeated several times and are very similar to those described by Walker and Harms (1971) in the Catskill of the Susquehanna Valley area, where they were called "motifs" to avoid the more rigid concept of cyclothem. They are characteristic of the Irish Valley Member of the Catskill Formation at this and other sections south of Port Matilda. Regionally, two types are recognized--a silty-muddy motif and a sandy-silty motif, but only the former occurs at Runville and adjacent localities. The lithology and environmental interpretations of a typical silty-muddy motif from this area are illustrated in Figure 7. Five subfacies can be recognized in these motifs, namely: 1) basal bioturbated sandstone, 2) green shale and silty shale, 3) green sandstone-mudstone, 4) red laminated siltstone, and 5) red massive mudstone and siltstone. The cycles vary in thickness from 5 to 65 feet and average about 15 feet. Each motif has an almost planar and sharp basal contact which separates the basal green marine sediments of the motif from the red mudstone of the underlying motif. Evidence suggests that each motif started with an initial transgressive event, now represented by the bioturbated basal sandstone and the overlying green fossiliferous silty shale facies. The presence of brachiopods and crinoidal debris and burrows of marine affinity implies a normal marine environment for this facies. Absence of thick and winnowed sand bodies in the transgressive phase reflects a rapid rate of transgression coupled with a high rate of mud and silt supply. In contrast, the sandy-silty motifs (best developed at Entriken and south) contain a basal quartzitic sandstone facies up to 4 m thick comprised of large solitary sets of bipolar, planar cross-strata, indicating reworking by tidal currents. The transgression was followed by a stage of very slow sedimentation through which extensive biological reworking of the deposited sediments, including the transgressive beaches, took place. Finally, marine deposition of mud gradually changed to deposition of thin, well-sorted sandstone with symmetric ripples (probably wave generated) as the sea shoaled. Above the shoaling phase occurs a fining-upward, regressive, tidal-flat sequence. The complexly bedded, thin quartzitic sandstone and the interbedded burrowed and flaser-bedded green siltstone and shales are interpreted to represent low- to mid-tidal-flat facies. The overlying red laminated siltstone and red massive mudstone are thought to occur in the high to supratidal range. The presence of root marks, desiccation and mud cracks, and carbonate nodules supports upper to supratidal-flat environments. The sandstone units which cut through the high-tide mudflat sediments may represent meandering tidal channels which drain the upper tidal flat and supratidal environments. However, the absence of such sand bodies in the underlying mid and lower tidal-flat deposits requires another interpretation, namely that they might represent small meandering streams which drained part of the coastal area. The scarcity, thinness, and fine grain size of these sandstone units suggest that only small and sluggish local streams drained this part of the coastal-plain area. This indirectly suggests that a coastal-fringe area, in the

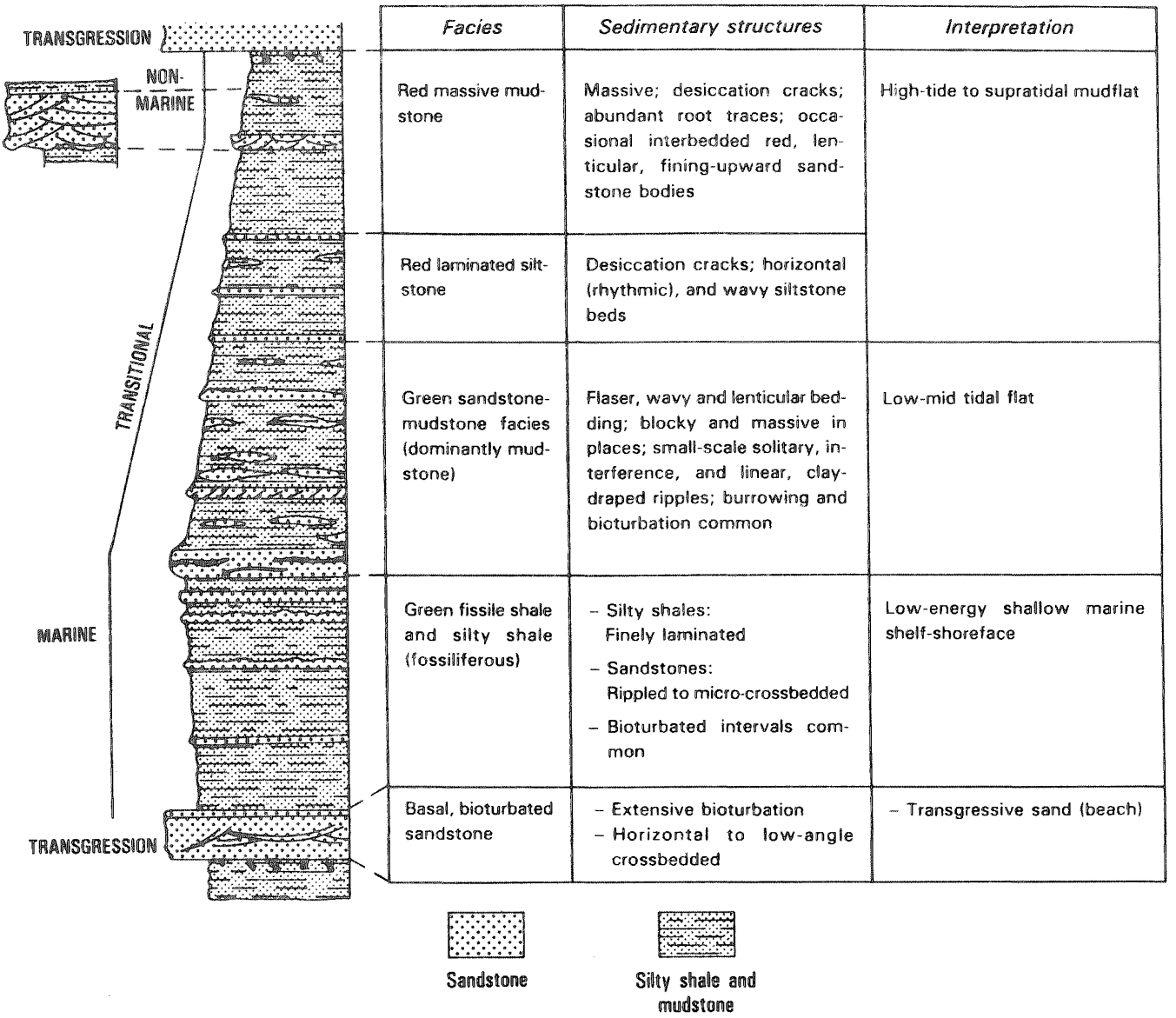

Facies	*Sedimentary structures*	*Interpretation*
Red massive mudstone	Massive; desiccation cracks; abundant root traces; occasional interbedded red, lenticular, fining-upward sandstone bodies	High-tide to supratidal mudflat
Red laminated siltstone	Desiccation cracks; horizontal (rhythmic), and wavy siltstone beds	
Green sandstone-mudstone facies (dominantly mudstone)	Flaser, wavy and lenticular bedding; blocky and massive in places; small-scale solitary, interference, and linear, clay-draped ripples; burrowing and bioturbation common	Low-mid tidal flat
Green fissile shale and silty shale (fossiliferous)	– Silty shales: Finely laminated – Sandstones: Rippled to micro-crossbedded – Bioturbated intervals common	Low-energy shallow marine shelf-shoreface
Basal, bioturbated sandstone	– Extensive bioturbation – Horizontal to low-angle crossbedded	– Transgressive sand (beach)

Figure 7. Idealized vertical facies sequence of the silty-muddy motif of the Irish Valley Member derived from pooled data from sections north and south of Port Matilda (modified from Rahmanian, 1979).

region of the development of the Irish Valley motifs, was flanked by an inactive alluvial plain.

The varying thickness and limited lateral extent of individual motifs leads to the conclusion that they were produced by variation in sediment supply, which resulted from lateral shifts in the position of the deltaic lobe or its distributaries located to the south near Port Matilda. Transgression occurred when the delta was diverted from a particular part of the shoreline, coupled with regional subsidence and compaction. Regression would occur when the delta or its distributaries shifted back to a closer position. Under this condition, increase in flux of sediments by longshore drift would have caused coastline progradation by depositional regression and seaward building of tidal flats.

LEAVE STOP 5; TURN AROUND and retrace path to Route 220.

3.0	55.9	TURN LEFT on Route 220 North.
3.0	58.9	TURN LEFT on entrance ramp for I-80 West towards DuBois.
2.1	61.0	Stop 6: Upper part of the Trimmers Rock Formation. Discussants: E. G. Williams and R. Slingerland.

The rocks exposed here are the silty shale and sandstone-shale facies of the upper part of the Trimmers Rock Formation (Plate 1, section 5, 0-400 ft). The lithologic characteristics and the environments are summarized in Figure 8. Sandstones are frequently hummocky cross-stratified with ripples on the upper surfaces, locally

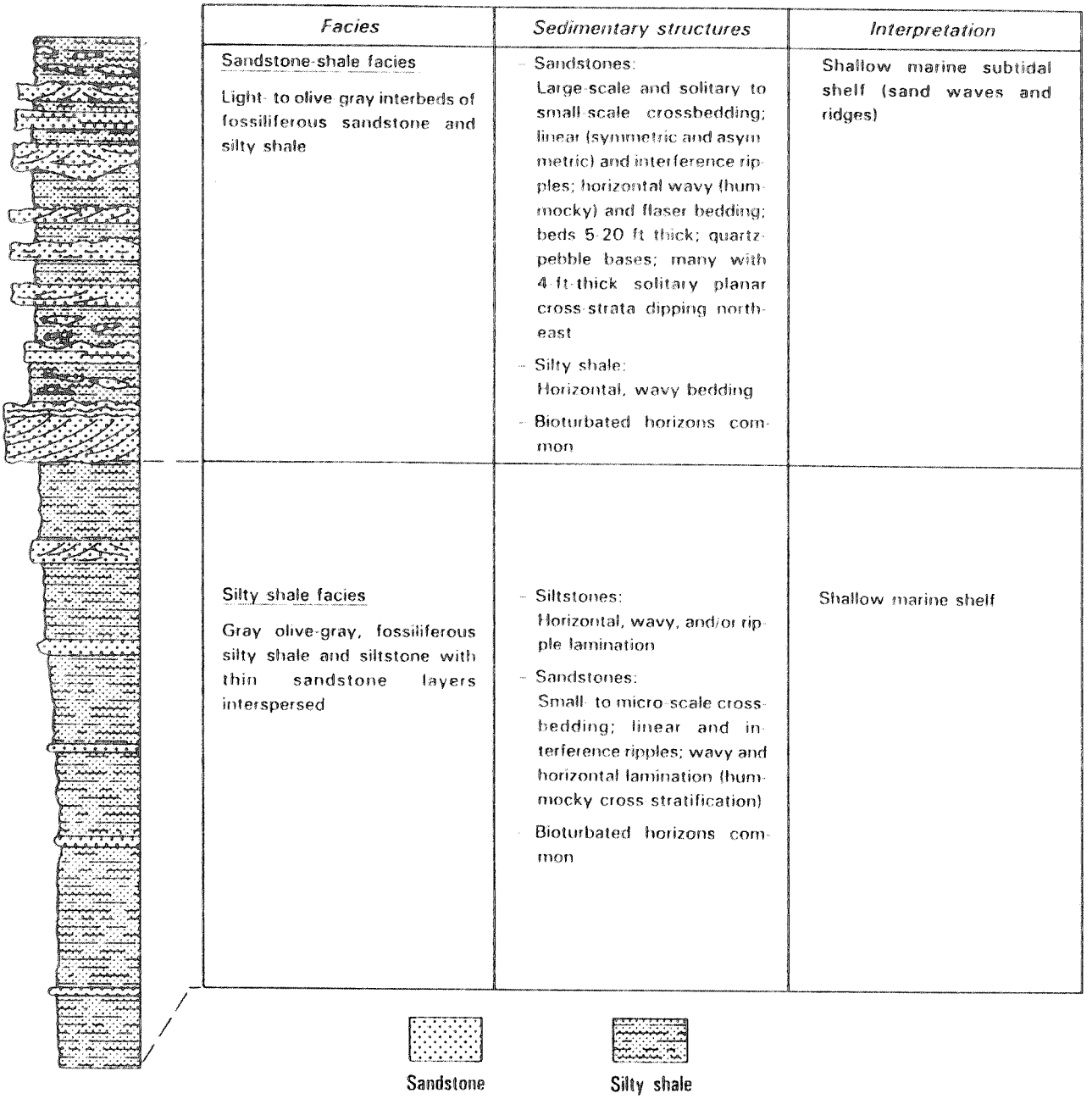

Figure 8. Idealized vertical facies sequence of the uppermost 250 to 500 feet of the Trimmers Rock Formation derived from pooled data from north and south of Port Matilda (modified from Rahmanian, 1979).

contain quartz pebbles, and have groove and flute casts along bottom contacts. Gray siltstone and shale beds are extensively bioturbated; burrows are usually solitary, oriented both parallel and perpendicular to bedding. Marine fossils occur throughout the interval. Brachiopods dominate but there are also pelecypods, crinoid columnals, bryozoan fragments and encrustations, fish plates, and plant fragments. Shells occur as solitary forms in shales and as coquina layers at the top of many sandstone beds. At most localities, the silty shale facies grades upward into a sandstone-shale facies which is illustrated in the upper half of Figure 8. Grain size, thickness, and the number of sandstone beds increase.

These facies are interpreted to have formed within a shallow marine shelf environment. The presence of hummocky cross-stratification and symmetric ripples in conjunction with small-scale crossbedding suggests a position above wave base in the shelf environment, where both waves and currents operate. Small-scale grain size variation found in the siltstone and silty shales indicates fluctuation in sediment supply and current velocity, which could be due to variation in tide- or storm-generated currents or both. Petrographically the sandstone beds resemble those of the alluvial sandstones of the Sherman Creek Member in terms of grain size and mineral composition.

LEAVE STOP 6 and proceed west on I-80.

1.4 62.4 Stop 7: Fining-upward alluvial cycles of the Sherman Creek Member. Discussants: E. G. Williams and R. Slingerland.

Rocks exposed at this locality (Fig. 9) are the fining-upward alluvial cycles of the Sherman Creek Member, consisting of interbeds of thick red mudstone, siltstone, and to a lesser degree red and green, fine- to very fine grained sandstone (Plate 1, section 5, 1720-2230 ft). The cycles start with dominantly red, lenticular to sigmoidally bedded sandstone units which usually possess basal erosional contacts and gradational tops. The basal sandstone units grade upward to a usually thick sequence of interbedded red siltstone with dominantly red mudstone at the top of the cycle. Cycles vary in thickness from 5 to more than 30 feet and average 20 feet. Small and large bone fragments and fish dermal plates occur together with basal interformational shale clasts. Crossbeds dip to the northwest (Williams, this volume, Fig. 8). The siltstone and mudstone units are usually massive with blocky and crumbly weathering, and contain small root traces and small calcareous nodules in the uppermost part of the cycles.

The inferred environments for the Sherman Creek cycles are those associated with shallow meandering rivers. The lower sandstone represents point-bar deposits; the laminated fine sandstone and siltstone units are interpreted as levee deposits. The red mudstones represent floodplain deposits as evidenced by desiccation cracks and calcareous concretions. Thin, lenticular sandstones interbedded with the red mudstones are thought to be crevasse deposits. The relative thinness of the basal sandstones and the small width of abandoned channels (8-40 feet) suggest that the rivers were relatively small. A few beds of green quartzitic sandstone and shale occur at irregular intervals throughout the Sherman Creek. These are similar to the marine part of the Irish Valley and are believed to have been deposited in a tidal-flat environment during a transgression.

The general paleogeographic setting for the fining-upward cycles of the Sherman Creek is that of the distal parts of a broad and inactive coastal-plain environment, bordered in the seaward direction by extensive tidal flats (Irish Valley motifs).

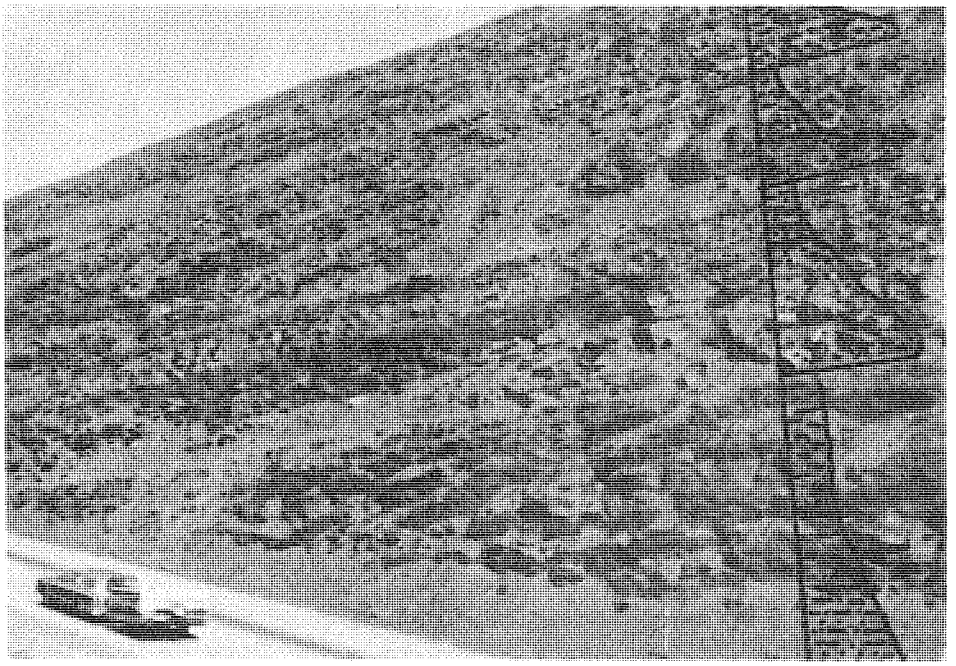

Figure 9. Exposures of the Sherman Creek Member of the Catskill Formation at Stop 7. Note the fining-upward cycles and the predominance of mudstone and siltstone.

The coastal plain had a very low gradient as indicated by the several marine transgressions within the alluvial sequence.

LEAVE STOP 7 and proceed west on I-80.

2.3 64.7 **Stop 8: Fining-upward cycles of the Duncannon Member of the Catskill Formation.** Discussants: E. G. Williams and R. Slingerland.

Rocks exposed at this locality (Fig. 10) are the fining-upward cycles of the Duncannon Member of the Catskill Formation. The cycles, which average about 50 feet in thickness, start with a sandstone unit which makes up approximately 60 percent of

Figure 10. Exposures of the Duncannon Member of the Catskill Formation at Stop 8 containing two fining-upward alluvial cycles.

the cycle, has an erosional base and gradational top, and grades upward into layers of finer sandstone, siltstone, and shale. Concentrations of drifted plant debris, shale pebbles, and calcareous nodules are usually found at the base. The lower half of the sandstone is usually green gray in color, grading upward to red as it becomes finer. The basal green sandstone is medium grained, poorly sorted, usually micaceous and carbonaceous, and thick to massively bedded at the base, and commonly shows an upward decrease in bed thickness. The red sandstone is fine grained and silty; it grades upward into red siltstones and shales of the upper parts of the cycle. Large-scale trough and planar crossbeds occur in the lower parts of the basal sandstone and exhibit northwestward dip directions. The red siltstones and mudstones commonly contain desiccation cracks and abundant calcareous nodules at the top of the cycle. These fine sediments make up less than 40 percent of the cycle.

In comparison to the underlying Sherman Creek cycles, those of the Duncannon contain thicker, coarser grained sandstones and thinner red overbank siltstones and mudstones, suggesting larger channels of lower sinuosity, as discussed at Stop 4.

LEAVE OUTCROP and proceed west on I-80.

1.8	66.5	Outcrops on right are the lower part of the Pocono Formation. All outcrops from this locality to the Snow Shoe interchange are in the Pocono Formation.
3.0	69.5	EXIT Route I-80, turn left at end of exit ramp, cross bridge, turn left and reenter I-80 heading east.
10.6	80.1	EXIT I-80 on Route 220 South towards Milesburg.
1.2	81.3	EXIT RIGHT on Route 150 South towards Milesburg.
3.4	84.7	STOP LIGHT in the center of Bellefonte, Pa. 100 m on the right is the Big Spring from which Bellefonte gets its water; for further information, see Parizek and White (this volume).
6.6	91.3	STOP LIGHT at junction of Routes 150 and 64. Continue south (straight) on Route 64 towards State College.
4.2	95.5	STOP LIGHT at corner of College Ave. and Atherton St. in State College; TURN LEFT on Atherton St.
1.5	97.0	Holiday Inn on right.

REFERENCES FOR FIELD TRIP 2

Allen, J. R. L., 1983, Studies in fluviatile sedimentation: bars, bar-complexes and sandstone sheets (low-sinuosity braided streams) in the Brownstones (L. Devonian), Welsh borders: Sedimentary Geology, v. 33, p. 237-293.

Allen, J. R. L., and Friend, P. F., 1968, Deposition of the Catskill facies, Appalachian region: with notes on some other Old Red Sandstone basins, in Klein, G. deV., ed., Late Paleozoic and Mesozoic continental sedimentation, northeastern North America: Geological Society of America Special Paper 106, p. 21-74.

Bridge, J. S., and Droser, M. L., 1985, Unusual marginal-marine lithofacies from the Upper Devonian Catskill clastic wedge, in Woodrow, D. L., and Sevon, W. D., eds., The Catskill delta: Geological Society of America Special Paper 201, p. 143-161.

Canich, M. R., 1977, A study of the Tyrone-Mount Union lineament by remote sensing techniques and field methods: University Park, Pennsylvania State University, Master's paper, 59 p.

Dennison, J. M., 1985, Catskill delta shallow marine strata, in Woodrow, D. L., and Sevon, W. D., eds., The Catskill delta: Geological Society of America Special Paper 201, p. 91-106.

Donaldson, A. C., Lewis, J. S., Mumcuoglu, Cetin, Boswell, Ray, Peace, Kenneth, and Jewell, Greg, 1984, Upper Devonian Catskill delta of West Virginia [abs.]: American Association of Petroleum Geologists Bulletin, v. 68, p. 1918-1919.

Duke, W., 1985, Hummocky cross-stratification, tropical hurricanes, and intense winter storms: Sedimentology, v. 32, p. 167-194.

Dyson, J. L., 1963, Geology and mineral resources of the northern half of the New Bloomfield quadrangle, Pennsylvania: Pennsylvania Geological Survey, 4th ser., Atlas 137ab, 63 p.

_____, 1967, Geology and mineral resources of the southern half of the New Bloomfield quadrangle, Pennsylvania: Pennsylvania Geological Survey, 4th ser., Atlas 137cd, 86 p.

Epstein, J. B., Sevon, W. D., and Glaeser, J. D., 1974, Geology and mineral resources of the Lehighton and Palmerton quadrangles, Carbon and Northampton Counties, Pennsylvania: Pennsylvania Geological Survey, 4th ser., Atlas 195cd, 460 p.

Glaeser, J. D., 1974, Upper Devonian stratigraphy and sedimentary environments in northeastern Pennsylvania: Pennsylvania Geological Survey, 4th ser., General Geology Report 63, 89 p.

Goldring, R., and Bridges, P., 1973, Sublittoral sheet sandstones: Journal of Sedimentary Petrology, v. 43, p. 736-747.

Goldring, R., and Langenstrassen, F., 1979, Open shelf and near-shore facies in the Devonian, in House, M. R., Scrutton, C. T., and Bassett, M. G., eds., The Devonian System: Paleontological Association, Special Papers in Paleontology, v. 23, p. 81-97.

Heckel, P. H., and Witzke, B. P., 1979, Devonian world paleogeography determined from distribution of carbonates and related lithic paleoclimatic indicators, in House, M. R., Scrutton, C. T., and Bassett, M. G., eds., The Devonian System: Paleontological Association, Special Papers in Paleontology, v. 23, p. 99-123.

Hess, K. W., and White, S. M., 1974, A numerical tidal model of Narragansett Bay: University of Rhode Island Marine Technical Report 20, 141 p.

Humphreys, Matthew, and Friedman, G. M., 1975, Late Devonian Catskill deltaic complex in north-central Pennsylvania, in Broussard, M. L., ed., Deltas--models for exploration: Houston Geological Society, p. 369-379.

Ippen, A. T., 1966, Estuary and coastline hydrodynamics: New York, McGraw-Hill, 744 p.

Klemic, Harry, 1962, Uranium occurrences in sedimentary rocks of Pennsylvania: U.S. Geological Survey Bulletin 1107-D, p. 243-288.

Krajewski, S. A., and Williams, E. G., 1971, Upper Devonian flagstones from northeastern Pennsylvania: Pennsylvania State University, College of Earth and Mineral Sciences Special Publication 3-71, 185 p.

McCauley, J. F., 1961, Uranium in Pennsylvania: Pennsylvania Geological Survey, 4th ser., Mineral Resource Report 43, 71 p.

Murin, T. M., and Donahue, Jack, 1984, Upper Devonian First Bradford Formation of southwestern Pennsylvania: environment of deposition and factors affecting gas production [abs.]: American Association of Petroleum Geologists Bulletin, v. 68, p. 1925.

Paxton, S. T., 1983, Relationship between Pennsylvanian-age lithic sandstones and mudrock diagenesis and coal rank in the central Appalachians: University Park, Pennsylvania State University, Ph.D. thesis, 503 p.

Rahmanian, V. D., 1979, Stratigraphy and sedimentology of the Upper Devonian Catskill and uppermost Trimmers Rock Formations in central Pennsylvania: University Park, Pennsylvania State University, Ph.D. thesis, 340 p.

Rose, A. W., 1976, The effect of cuprous chloride complexes in the origin of red-bed copper and related deposits: Economic Geology, v. 71, p. 1036-1048.

Rose, A. W., Smith, A. T., Lustwerk, R. L., Ohmoto, H., and Hoy, L. D., in press, Geochemical aspects of stratiform and redbed copper deposits in the Catskill Formation (Pennsylvania, USA) and Redstone area (Canada): Proceedings of Symposium on Copper Deposits, International Geological Congress, Moscow, Springer-Verlag.

Sevon, W. D., Rose, A. W., Smith, R. C., and Hoff, D. T., 1978, Uranium in Carbon, Lycoming, Sullivan, and Columbia Counties, Pennsylvania: Annual Field Conference of Pennsylvania Geologists, 43rd, Hazleton, Pa., 1978, Guidebook, 99 p.

Slingerland, Rudy, 1984, Numerical simulation of ocean tides in the Late Devonian Epeiric Sea of eastern North America [abs.]: Geological Society of America Abstracts with Programs, v. 16, p. 658.

_____, 1985, Numerical simulation of M_2 co-oscillating tides on very wide miocline shelves: Symposium on Modern and Ancient Clastic Tidal Deposits, Utrecht, Netherlands, in press.

_____, 1986, Numerical computation of co-oscillating paleotides in the Catskill Epeiric Sea of eastern North America: Sedimentology, in press.

Smith, A. T., 1980, Stratigraphic and sedimentologic controls for copper and uranium in red-beds of the Upper Devonian Catskill Formation in Pennsylvania: University Park, Pennsylvania State University, M.S. thesis, 216 p.

_____, 1983, Geology of the red-bed Cu-U occurrences in the Upper Devonian Catskill Formation, Pennsylvania: University Park, Pennsylvania State University, Ph.D. thesis, 240 p.

Smith, A. T., and Rose, A. W., 1985, Relation of red-bed copper-uranium occurrences to the regional sedimentology of the Catskill Formation in Pennsylvania, In Woodrow, D. L., and Sevon, W. D., eds., The Catskill delta: Geological Society of America Special Paper 201, p. 183-197.

Smith, R. C., II, and Hoff, D. T., 1984, Geology and mineralogy of copper-uranium occurrences in the Picture Rocks and Sonestown quadrangles, Lycoming and Sullivan Counties, Pennsylvania: Pennsylvania Geological Survey, Mineral Resource Report 80, 271 p.

Sutton, R. G., Bowen, Z. P., and McAlester, A. L., 1970, Marine shelf environments of the Upper Devonian Sonyea Group of New York: Geological Society of America Bulletin, v. 81, p. 2975-2992.

Walker, R. G., 1971, Nondeltaic depositional environments in the Catskill clastic wedge (Upper Devonian) of central Pennsylvania: Geological Society of America Bulletin, v. 82, p. 1305-1326.

Walker, R. G., and Harms, J. C., 1971, The "Catskill delta": a prograding muddy shoreline in central Pennsylvania: Journal of Geology, v. 79, p. 381-399.

Willard, Bradford, Swartz, F. M., and Cleaves, A. B., 1939, The Devonian of Pennsylvania: Pennsylvania Geological Survey, 4th ser., General Geology Report 19, 481 p.

Williams, E. G., this volume, Catskill sedimentation in central Pennsylvania.

Woodrow, D. L., Enos, P., Bottjer, R. J., and Minero, C., 1981, Bioclastic carbonate units in the Catskill clastic wedge, In Enos, P., ed., New York State Geological Association 53rd Annual Meeting, Binghamton, N.Y., Guidebook for field trips in southcentral New York: p. 201-229.

Woodrow, D. L., and Isley, A. M., 1983, Facies, topography, and sedimentary processes in the Catskill Sea (Devonian), New York and Pennsylvania: Geological Society of America Bulletin, v. 94, p. 459-470.

FIELD TRIP #3

APPLICATION OF QUATERNARY AND TERTIARY GEOLOGICAL FACTORS TO ENVIRONMENTAL PROBLEMS IN CENTRAL PENNSYLVANIA

by
Richard R. Parizek and William B. White

Introduction

Nittany and adjacent valleys near the western edge of the Valley and Ridge province are challenging but informative areas in which to study the evolution of drainages and erosion surfaces in the central Appalachians because rocks ranging in age from Late Cambrian to Pennsylvanian are exposed within less than 10 miles of each other, and the structural and topographic style changes from Valley and Ridge to the Allegheny Plateau setting.

Nittany Valley is the most distant valley from the Atlantic Ocean within the Ridge and Valley of Pennsylvania. Stream terraces and erosional surface remnants are more likely to be preserved in such an interior valley because more time is required for drainage networks to adjust headward in response to changes in sea level and tectonic uplift. Also, there is greater relief between stream valleys and uplands, and terrace remnants are likely to have greater vertical separation making them easier to identify when compared to valleys near the eastern margin of the province.

The northern edge of the province was overridden by continental glaciers of Kansan(?), Nebraskan, Illinoian and Wisconsinan age. Their deposits blanket older erosional surfaces and soil deposits that pre-date Pleistocene glaciation. The region was subjected to repeated climatic changes associated with the advance and retreat of continental glaciers that helped produce an array of periglacial deposits, landform, and erosional surfaces of variable age. These latter deposits and landforms, although posing challenges of their own, represent only minor alterations in the more regional landscape. These youngest deposits, together with erosional and constructional landforms are easier to date hence, help to set minimum ages for erosion surfaces and help estimate rates of erosion.

On the field trip, we bring up some of the old questions again. Given present knowledge of soils, landforms, drainage patterns, and their evolution, what can be said about the developmental history and time scale of development of the Nittany Valley.

Sevon's (1985) brief summary of previous work on Appalachian drainage covers the main concepts involved in the discussion of drainage and landscape development in Pennsylvania. He lists items important to these concepts which require further discussion. These include:

(1) The position of the drainage divide after the Alleghenian orogeny.
(2) The direction of initial drainage after this orogeny.
(3) The time of origin of southeastern drainage flow.
(4) The reality of peneplaination in Pennsylvania.
(5) The reality of Cretaceous transgression onto a peneplained surface.
(6) The reality of repeated uplift.
(7) The relation of transverse drainage to lithologic or structural weakness.
(8) The rate of denudation in the Appalachians and the age of the landscape.

Geologic Setting

Geology

Nittany, Penns and adjacent karst valleys are underlain by 6,000 - 8,000 feet of interbedded limestones and dolomites of Cambrian and Ordovician age (Figures 1 and 2) which were initially capped by 3200 feet of shales and ridge forming sandstones and many thousands of feet of younger strata Devonian through Pennsylvanian in age. These have been folded into gently plunging anticlines and synclines, and overturned to steeply dipping asymmetric folds displaying structural relief of 100 to several thousand feet, cut by numerous normal and thrust faults, weathered and eroded under climatic conditions varying from arid, tropical to subtropical to periglacial during the Pleistocene Epoch, to temperate-rainy at present where the mean annual precipitation approaches 38-43 inches. Elements of the present landsurface may reflect chemical weathering from Late Cretaceous to the present.

Rocks most resistant to erosion form ridge crests which surround canoe-shaped lowlands underlain by less resistant carbonate rocks and shale. Ridges surrounding Nittany, Penns and Kishacoquillas Valleys normally are double. The innermost ridge is underlain by the Bald Eagle or Oswego Sandstone, the higher and outer most ridge by the Tuscarora Quartzite (Stop 1). A saddle frequently is developed on the Juniata Formation which is largely composed of siltstone and shale. It lies between the Oswego and Tuscarora. Water gaps commonly are developed in the Oswego Sandstone or in the inner ridge and major drainages tend to cut through both ridges (Parizek et al., 1971). Minor sags and wind gaps reflecting narrow zones of weakness are repetitous in both ridges.

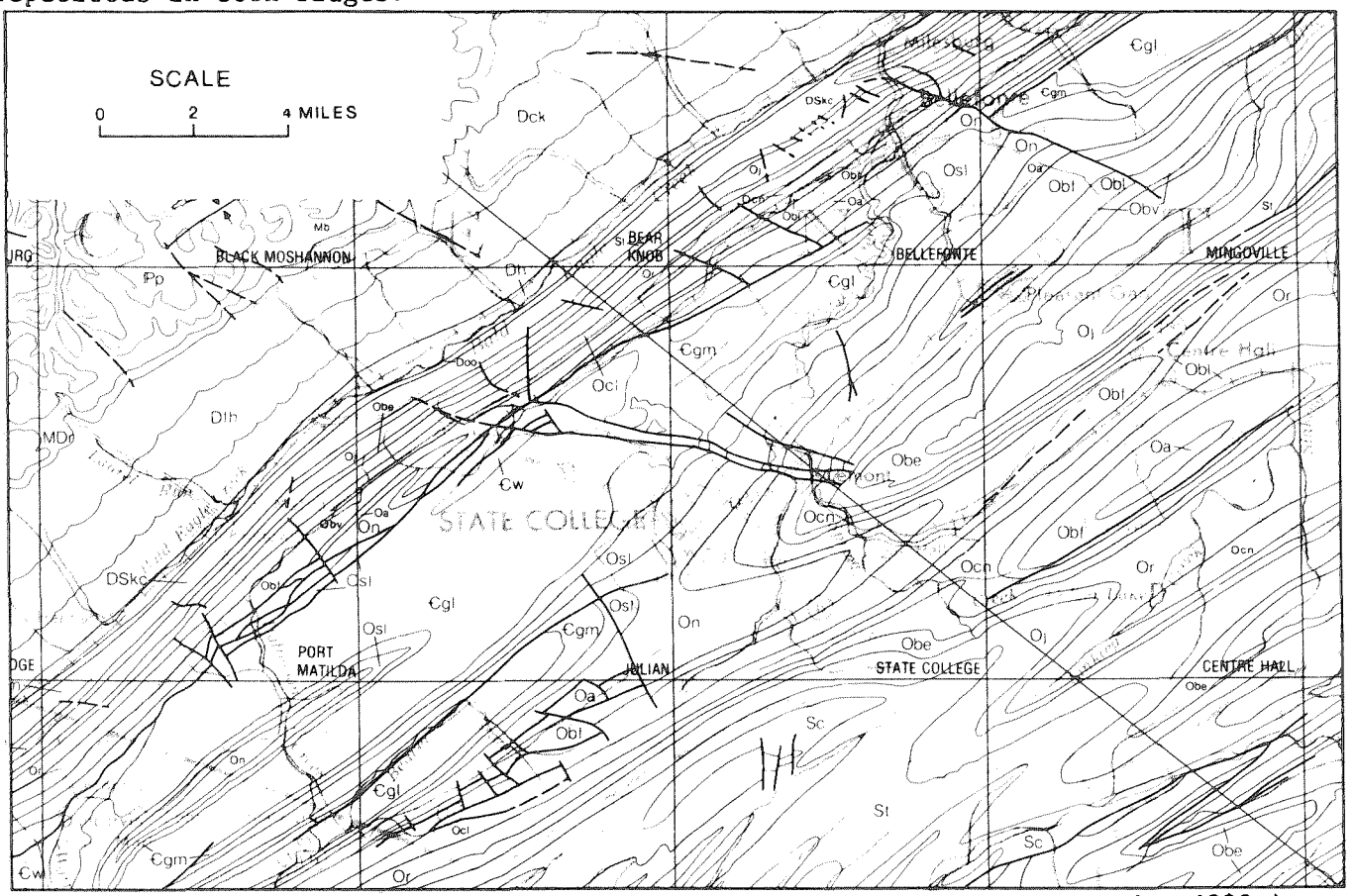

Figure 1. Geologic map of the Nittany Valley area (geology from Berg et al., 1980.)

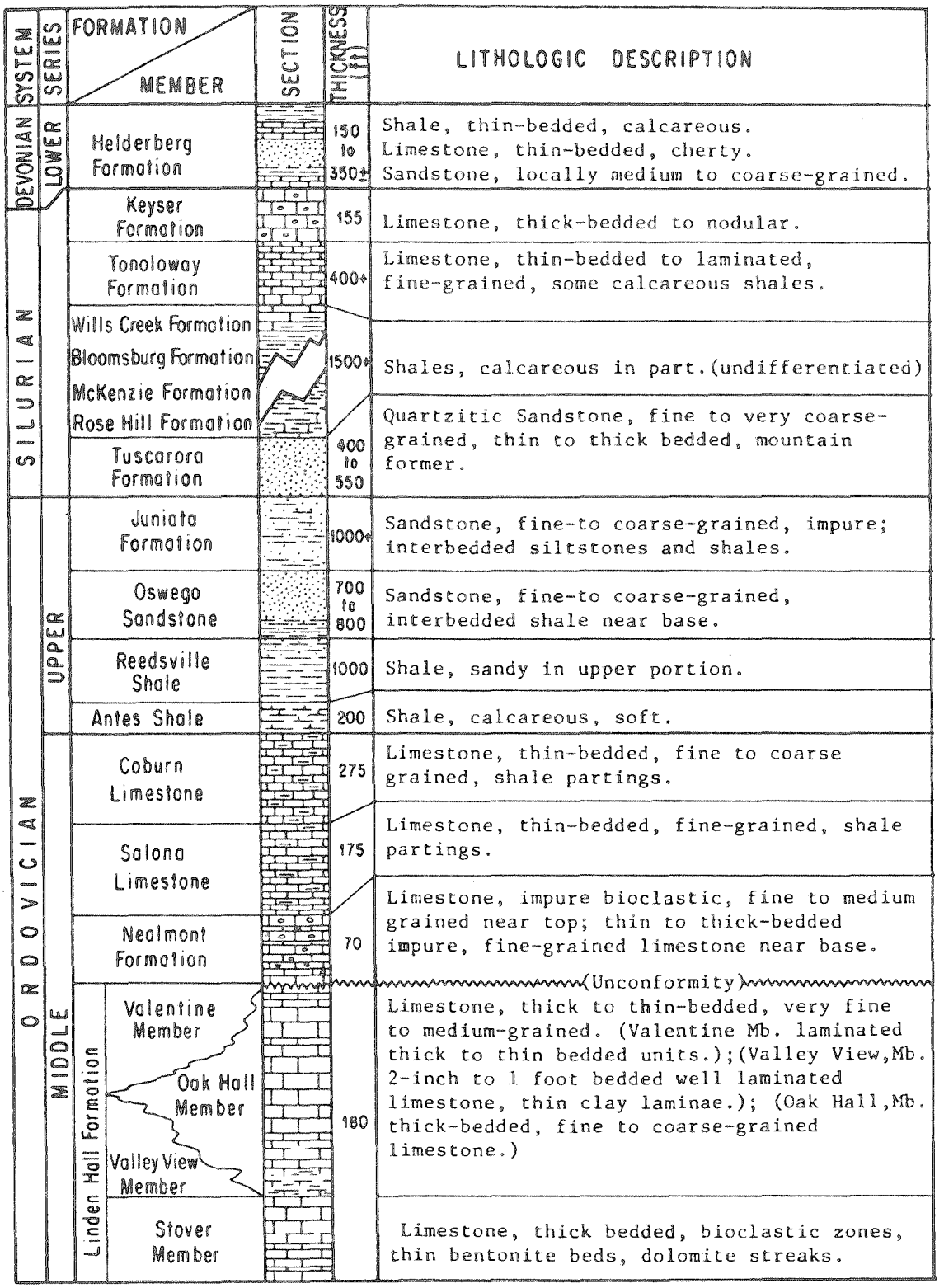

Figure 2. Stratigraphic section for Nittany Valley (from Parizek et al., 1971).

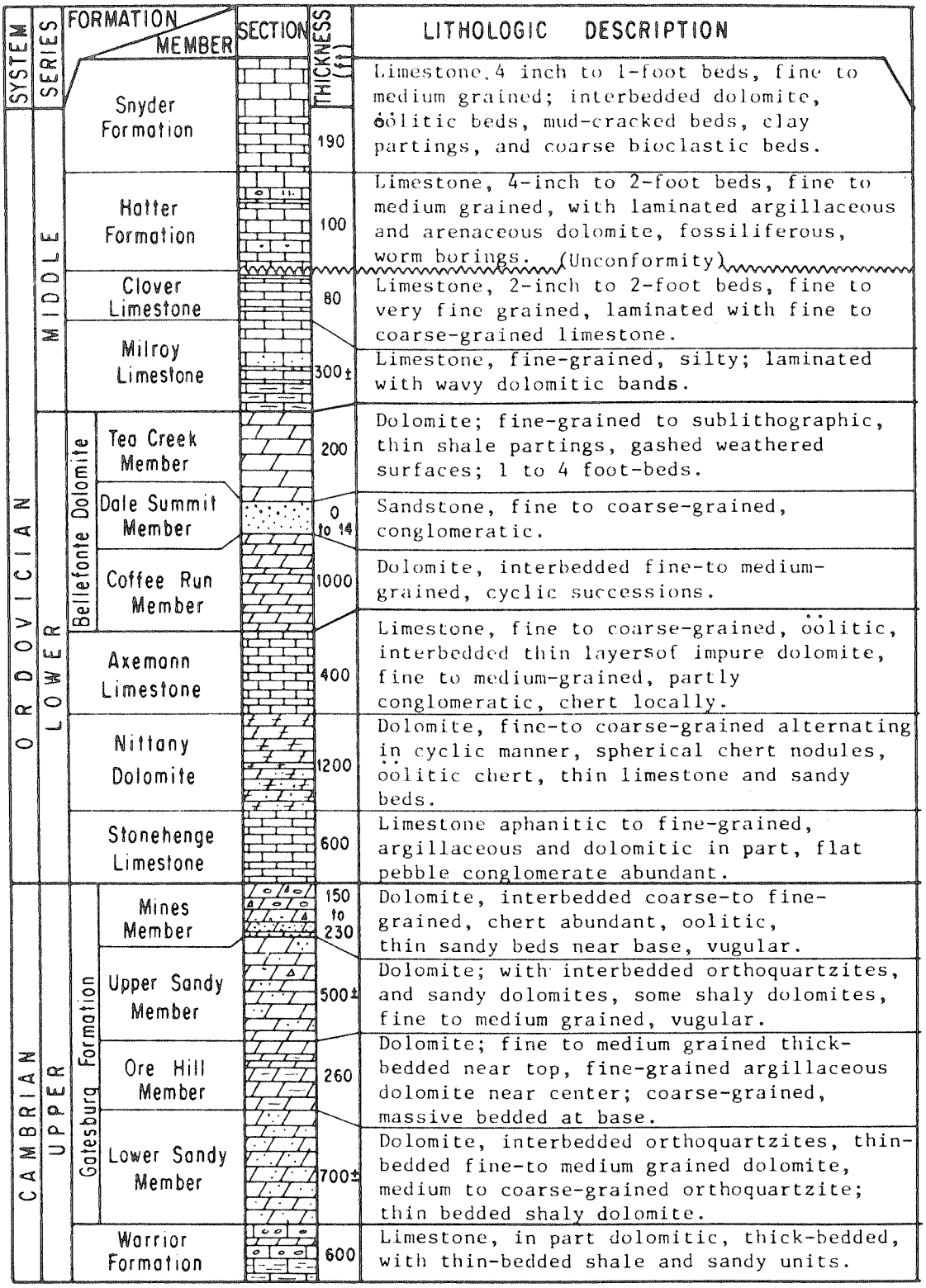

Figure 2. (continued)

Prominent Landscape Elements

The mountain ridges surrounding Nittany Valley display a nearly accordant elevation ranging from 2000 to 2400 feet which is lower than the sandstone capped eastern margin of the Appalachian Plateau located to the west (Stop 1). This surface was referred to as the Schooley Peneplain by Davis (1899). The relatively flat inner valley upland ranges from 800 to 1200 feet in elevation. It is underlain by carbonate rocks and some shales and is covered by residual soils (sapolite) of variable character and thickness (Figure 3). This surface was referred to as the Harrisburg Peneplain by Davis.

Spring Creek, Buffalo Run, Logan Branch, Slab Cabin Run, Nittany Creek, and Little Fishing Creek are the principal drainages for the northeastern portion of Nittany Valley. Bald Eagle Creek is the local base level for these streams which in turn, drains into the West Branch of the Susquehanna River near Lock Haven.

Halfmoon Creek, Spruce Creek, and Warriors Mark Run drain the southern portion of the valley via the Little Juniata River which joins the Susquehanna River at Amity Hall. The Juniata River cuts through Nittany Valley along one of the state's longest lineaments, the Mt. Union-Tyrone lineament which is the subject of a companion trip. The Juniata serves as a southern base level of erosion to Nittany Valley. Groundwater levels are controlled by elevations of the Juniata and by sandstone and shale beds truncated by the Juniata where it crosses Tussey Mountain.

These streams are incised into the valley upland to depths of 50 to 300 or more feet and often display steep cliffs. Valleys vary in width to just accomodate the width of tributary streams or they may be wide enough to support meanders and well developed alluvium. The floors of these valleys have been correlated with the Sommerville erosion surface by Davis and were believed to have been incised in response to regional uplift.

Floodplains display variable widths along these valleys having characteristics of both youth and maturity often only a short distance down the same valley. Changes in valley width occur where these rivers and creeks traverse bedrock units of varying resistance. Streams in narrow valley sections often are influent whereas they are often effluent along wider sections of the same valley. Many of the smaller tributaries to these streams are karst underdrained valleys that show varying stages of karst development. The fluvial origin of these underdrained valleys is obvious even where they lack floodplain deposits due to internal erosion and where their original fluvial profile has been disrupted by underlying karst processes.

The most prominent floodplains occur above shale and carbonate bedrock upvalley from more resistant bedrock that served as a temporary base level of erosion. Examples include the confluence of Spring and Slab Cabin Creek at Houserville (Stop 5), the flat at the 28th Division Shrine at Boalsburg upstream from where Spring Creek cuts across Nittany Mountain, a flat just above the Borough of State College (Water) Authority well field developed on Slab Cabin Run below Shingletown and elsewhere.

The time of incision of these valleys is hard to date but they existed in time to allow the development of at least one prominent stream terrace located just above the modern floodplain that predates the Sangamonian and alluvial-colluvial fan complexes of pre-Sangamonian and most likely, Woodfordian age.

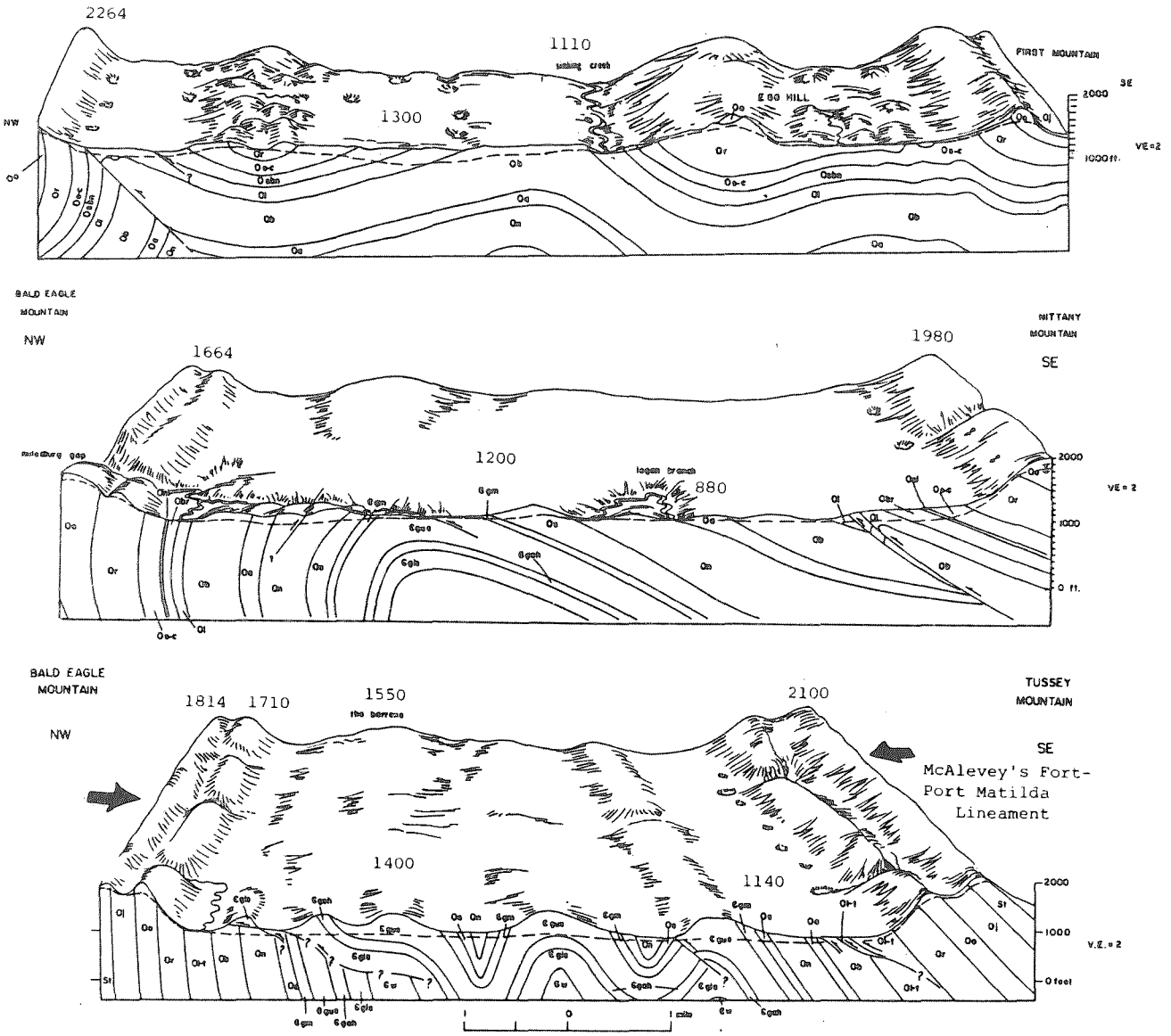

Figure 3. Geological cross-sections of Nittany Valley.

Karst Landforms

The carbonate rock-floored valleys of the Valley and Ridge Province are sculpted into a somewhat subdued karst topography. The three principal landforms are swallow holes and minor blind valleys, closed depressions, and caves. To these should be added a cutter and pinnacle topography etched onto the bedrock of certain formations but generally mantled by thick soils and not apparent unless the soil is removed. The cutter and pinnacle topography is, however, of great concern to those designing foundations for buildings, holding ponds, and other structures to be erected on the karst.

Although the solubilities of calcite and dolomite are nearly equal, the kinetics of calcite dissolution is much more rapid than the kinetics of dolomite dissolution. As a result, karst features are developed to a greater degree on the limestones than on the dolomites. Most of the limestone lithologically suited for

extensive karst development occurs in the Champlainian group near the top of the carbonate section. Because of the anticlinal valleys, the outcrop pattern generally has dolomite making up most of the center of the valley with the cavernous limestones occurring as parallel bands at the valley margins. As a result, closed depressions and caves are mainly located in these bands parallel with the mountain flanks. Sinkholes are both more sparse and more subdued in the dolomite portions of the valley and except on close inspection, Nittany and the other valleys do not look like karst to the casual observer.

Small surface streams arise in catchment basins of a few square miles on the flanks of the mountain ridges and flow out onto the carbonate valleys. With few exceptions, these allogenic streams sink at the contact with the Champlainian limestones later to resurge at the large karst springs. Sometimes the water merely disappears into its bed with a dry channel maintained down stream to be used in flood flow. Others have cut minor transverse valleys into the valley uplands and sink at the blind footwall of the incised valley. The depth of incision varies from a few feet to on the order of 100 feet. In some blind valleys streams flow into open cave entranes but mostly the water is simply lost in silt, collapse breccia, and debris. The allogenic mountain streams are an important source of recharge to the carbonate aquifer system accounting for more than 60 percent of recharge and only 20 percent of the area.

Closed depressions occur in a range of sizes from shallow swales a few feet deep to sinkholes many tens of feet in depth. Some are of solutional origin, a few represent cave roof collapses, and some are due to soil piping. The latter tend to be ephemeral features. There may be an abrupt collapse of the soil cover during spring thaws followed by the gradual slumping and infilling of the sink. In the more urbanized parts of the regions, soil piping sinks are a land use hazard and their development is exerbated by parking lot runoff, leaking water and sewer mains, and general disruption of overland flow (Parizek et. al., 1971; White et al., 1984). The permanent sinkholes are usually soil-mantled with little bedrock in evidence so that it is not easy to distinguish solution from collapse features. The largest of the closed depression features is Phantom Lake, nearly a mile in diameter but less than 100 feet deep. It is located two miles east of Pleasant Gap and is just off the field trip route. Water floods the sink by rising through sinkholes on the floor of the depression during periods of unusually high precipitation, thus the name. Although surface expression of closed depressions are sparse in most of the Valley, there is little surface drainage and the water falling onto the limestone surface infiltrates through the soil into the solution cavities beneath.

Determining Background

Prolonged sedimentation within the Appalachian geosyncline resulted in the accumulation of a thick sequence of rocks of variable resistance. These were deposited in marine and freshwater environments that reflect a major and prolonged marine transgression starting in the Cambrian and ending by Pennsylvanian and possibly Early Permian time with the deposition of largely freshwater, continental and nearshore marine deposits of Pennsylvanian age. More than 8,000 feet of limestone and dolomite were deposited in shallow Cambrian and Ordovician seas before influxes of clay, sand and conglomerate began to dominate sedimentation by Late Ordovician and Silurian time (Figure 2). With the exception of the accumulation of some limestone units in the Silurian and Devonian, Silurian through Pennsylvanian sedimentation was largely dominated by clastic rocks of variable resistance. These sedimentary rocks were folded and faulted during the Appalachian Orogeny in Permian

Time approximately 250 million years ago. The Nittany Anticlinorium arches from the eastern edge of the Appalachian Plateau nearly ten miles to the southeast. The Warrior Limestone is raised within this arch and represents the oldest rocks exposed in Nittany Valley. Numerous, small anticlines and synclines formed within this anticlinorium which have been subjected to more or less continuous and prolonged erosion to the present.

Ideas on the tectonic style of the Appalachians have changed since the first Pennsylvania Field Conference as new deep drilling data became available and the structural complexity more completely worked out. The mobile oil and gas test well drilled in Nittany Valley near Jacksonville (northeast of Bellefonte) together with the deep tests provided useful insight that lead to the "thinned skinned" tectonic model proposed by Gwinn (1964) and others (Figure 4). This tectonic setting together with the sequence of rocks deposited in the Appalachian geosyncline are important to the understanding of the erosional history of the Appalachians.

Global Plate Tectonic models also are new and shed light on the driving forces that are responsible for regional uplift and stress distribution that produced thrust and tear faults, zones of fracture concentration, and other planes of weakness that assisted weathering and erosion.

A well kept record of these erosional events is hidden in the many thousands of feet of sediment located in the Coastal Plain and continental shelf along with their elusive petroleum resource. Other clues to early history may be contained within the Triassic basin sedimentary record. However, lacking a well defined early tectonic and climatic history for the Appalachians, a detailed account of the early erosional history of this region may never be satisfactorily worked out.

Drainage

The Valley Upland Surface

The most pronounced feature of the Nittany Valley is the upland surface. In the interfluve areas between present day incised drainage, the valley uplands have very low relief. Near Centre Hall on the Penns Creek/Spring Creek divide, on the Penns Creek/Elk Creek divide in Brush Valley, and on the Spring Creek/Spruce Creek divide just west of Pine Grove Mills, the upland surface is nearly flat and truncates geologic structure. Remnants of the uplands can be seen in hill summits and upland flats in other parts of the valley. The uplands do have a measurable slope. In the Penns Valley area to the east, the upland flats are at elevations of nearly 1300 feet. In the area of State College, the uplands are at 1200 feet. Farther to the West, in the uplands bordering the Juniata River gorge the upland flats lie between 1000 and 1100 feet. In a certain vague sense, at least, the old valley floor surface (Harrisburg peneplain) slopes to the present location of the Juniata on the Tyrone lineament suggesting that the lineament may represent the location of very old east-trending drainage.

Incised Drainage

The conceptual difficulty with an old erosion surface dissected by younger drainage is that three out of the four major streams exit Nittany Valley though deep water gaps cut through quartzite in the bounding mountain ridges. If the paleodrainage required only a single exit along the Tyrone lineament, how did these other drainage lines initiate and what determines their location? These questions have perplexed Appalachian geomorphologists since the days of Henry Rogers.

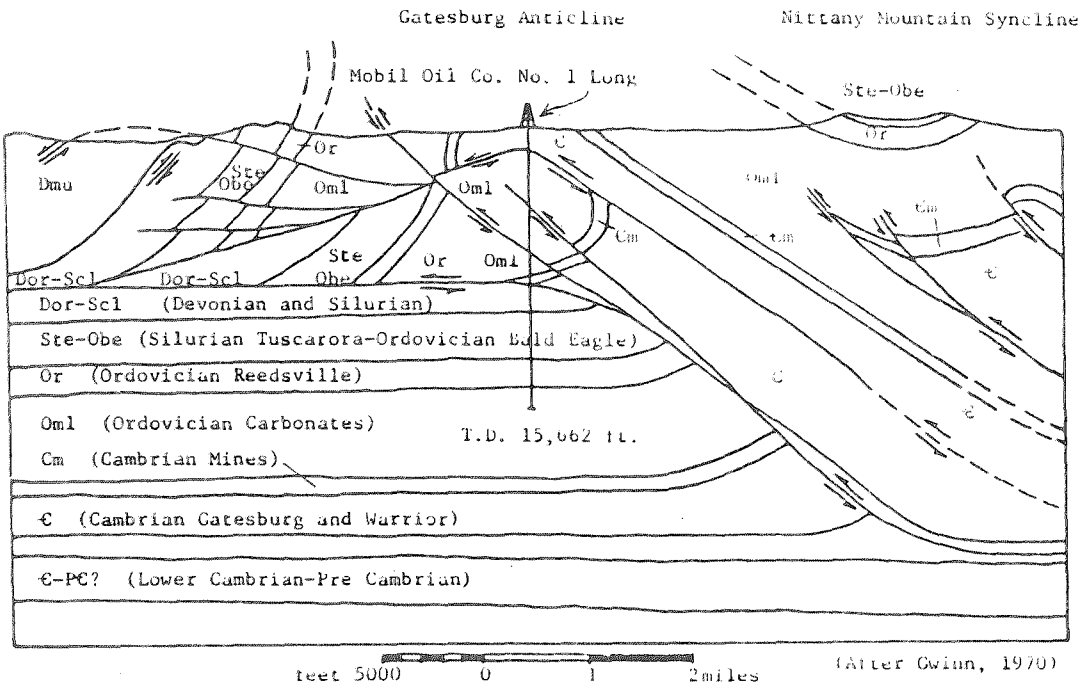

(a)

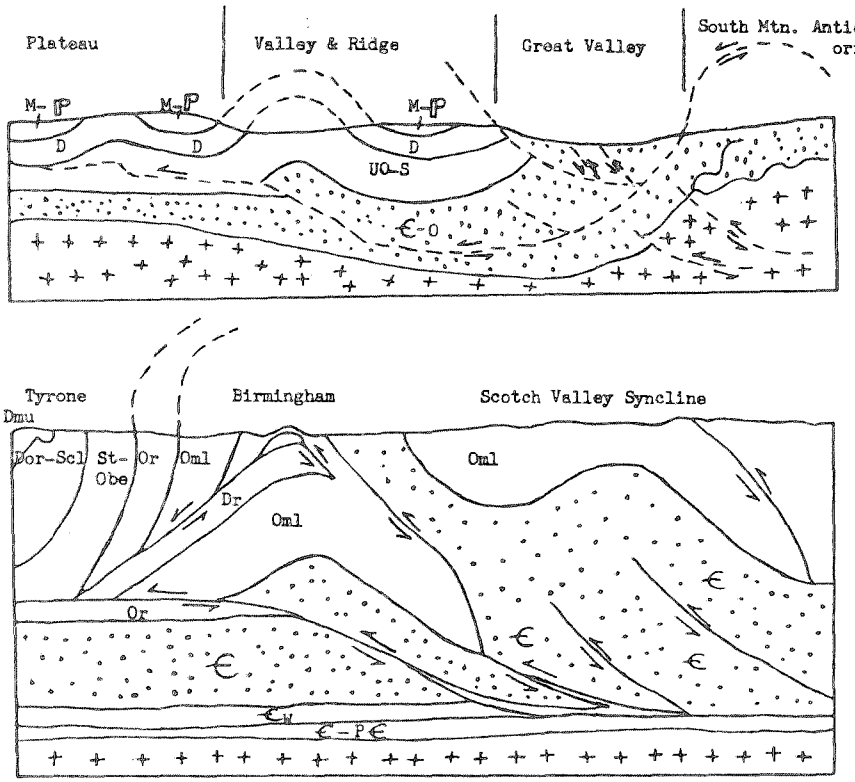

(b)

Dmu	Middle and Upper Devonian
Dor-Scl	Lower Orvonian & Post Tuscorora
St-obe	Tuscorora-Bald Eagle
Or	Reedsville
Oml	Middle & Lower Ordovician carbonates
€	Gatesburg
€w	Warrior
€-P€	Cambrian-PreCambrian

Figure 4. Geological cross-sections through Nittany Valley at Jacksonville: (a) (Gwinn, 1970) and (b) of the Birmingham "window" to regional structure (Gold, 1976).

Lattman and Parizek (1964) noted the rather repetitious spacing of smaller sags, wind and water gaps in ridge tops which they attributed to nearly vertical zones of fracture concentration revealed by fracture traces, lineaments, and minor reverse faults. It was possible to align some wind and watergaps with sinkholes, swallow holes, surface sags and depressions, springs, karst underdrained valleys oriented transverse to stratigraphic and structural strike, straight segments of cave passages, and transverse valleys with permanent streams. Such nearly vertical structures are required to fix the position of drainages in time and space as the

landsurface was eroded. The number of such alignments of drainage and the size of associated lineaments far exceeded the number of linear features known or inferred prior to the launching of LANDSAT (Gold, Parizek and Alexander, 1973, 1974).

Later Gold, Parizek, and Alexander (1973) proposed the concept of the "permancy of master streams" (major transverse drainages) when the number, magnitude and significance of lineament-related structures became apparent following more detailed study of LANDSAT and SKYLAB imagery and U-2 underflight photographs. Zones of fracture concentration revealed by lineaments and fracture traces were commonly associated with transverse drainages if not revealed by them, more productive well sites, foundation problems, etc. Vertical planes of structural weakness allow master streams to be let down across beds of variable resistance through geological time until these nearly vertical structural planes play out with depth or until streams are diverted through piracy. The fact that lineaments are straight in map view despite irregularities in topography, rock type or structure, demands that these planes are vertical to near vertical and may have depth influences approaching their length. Hence, master streams might be expected to remain fixed in map space as hundreds if not thousands of feet of rock are eroded.

This vertical plane master stream erosion model also works on the local tributary scale depending upon the size and length of the linear structural features and drainage area available to collect surface runoff. The number of lineaments in the 5 to 20 km or so length class as well as fracture trace class (< 1 km) far exceed the number used by transverse drainages of any size. See, for example, the lineaments map of Pennsylvania prepared by Kowalik and Gold (1976). Not enough water is available to establish major drainages along each lineament or minor drainages on fracture trace related structure. A stocastic process may have been involved in the evolution of transverse drainage networks where streams used some and not other zones of fracture concentration. The Tyrone-Mt. Union (Canich, 1976) and McAlevys Fort-Port Matilda lineaments (Hunter and Parizek, 1979) are both 45 km or longer in length, and yet only the Tyrone-Mt. Union lineament control major drainage, i.e., the Little Juniata River (Figure 5). The McAlevys Fort-Port Matilda lineament controls an underdrained karst valley of minor proportions by comparison (Hunter and Parizek, 1983) in Nittany Valley and a poorly developed watergap in Tussey Mountain. This watergap is confined to the inner ridge developed in the Oswego Sandstone. Only minor surface sags are developed in the Tuscarora Formation on both Tussey and Bald Eagle Mountains along this lineament. Its extension into Devonian to Pennsylvanian aged rocks is marked by a pronounced valley that extends into the Allegheny Plateau more or less parallel to Route 322. The lower reaches of Spring Creek and its well developed tributary, Logan Branch, on the other hand, and Nittany Creek all transect structure. Spring and Nittany Creeks cross Bald Eagle Mountain at Milesburg and Curtin Gaps. The surface expression of these lineament-related drainages are well developed (Figure 5) but both structures are short (15 miles) by comparison to the McAlevys Fort-Port Matilda lineament which is approximately 44 miles long.

The intensity of structures underlying lineaments vary with depth. Most likely some transverse drainages controlled by them abandoned their courses as the landsurface was lowered through time and more resistant rocks were encountered. Logan Branch may represent such a drainage that has lost its status. Its linear structural control is obvious between Gap Run along the western flank of Nittany Mountain where it cuts through the Oswego Sandstone. It extends across Nittany Valley, Bald Eagle Mountain and into the Allegheny escarpment to the west. Many other transverse drainages also extend up the Allegheny escarpment that define lineaments.

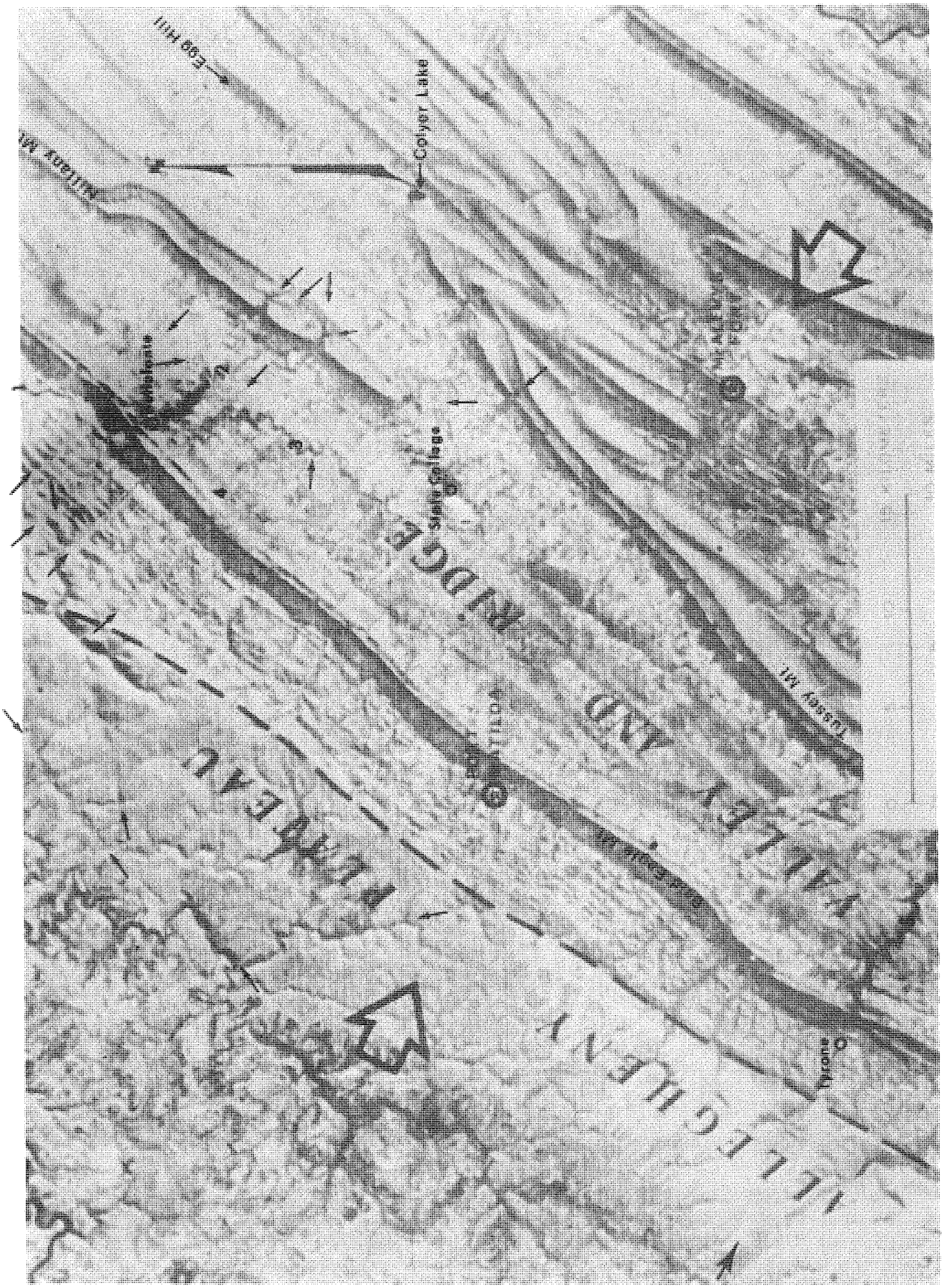

Figure 5. Selected lineaments in Nittany and adjacent valleys: 1, Bald Eagle Creek; 2, Logan Branch; 3, Spring Creek; 4, Buffalo Run; 5, Little Juniata River-Mt. Union-Tyrone lineament.

Logan Branch heads at 7 springs just below the village of Pleasant Gap and down slope from Gap Run that disappears in a swallow hole (Stop 8). Its zig-zag course across stratigraphic and structure strike within Nittany Valley is controlled by shorter fracture-trace related structures. Spring Creek near Lemont on the other hand, has only minor springs where it cuts across conduit prone limestones of Middle Ordovician-age. A water table map at the base of Nittany Mountain between Spring Creek and Logan Branch also reveals an interesting relationship. A water table trough extends 3.5 miles toward Spring Creek from the springs at the head of Logan Branch. The groundwater divide for this tributary groundwater basin is 3.5 miles from Logan Branch and only 1 mile from Spring Creek, the present master stream (Figure 6).

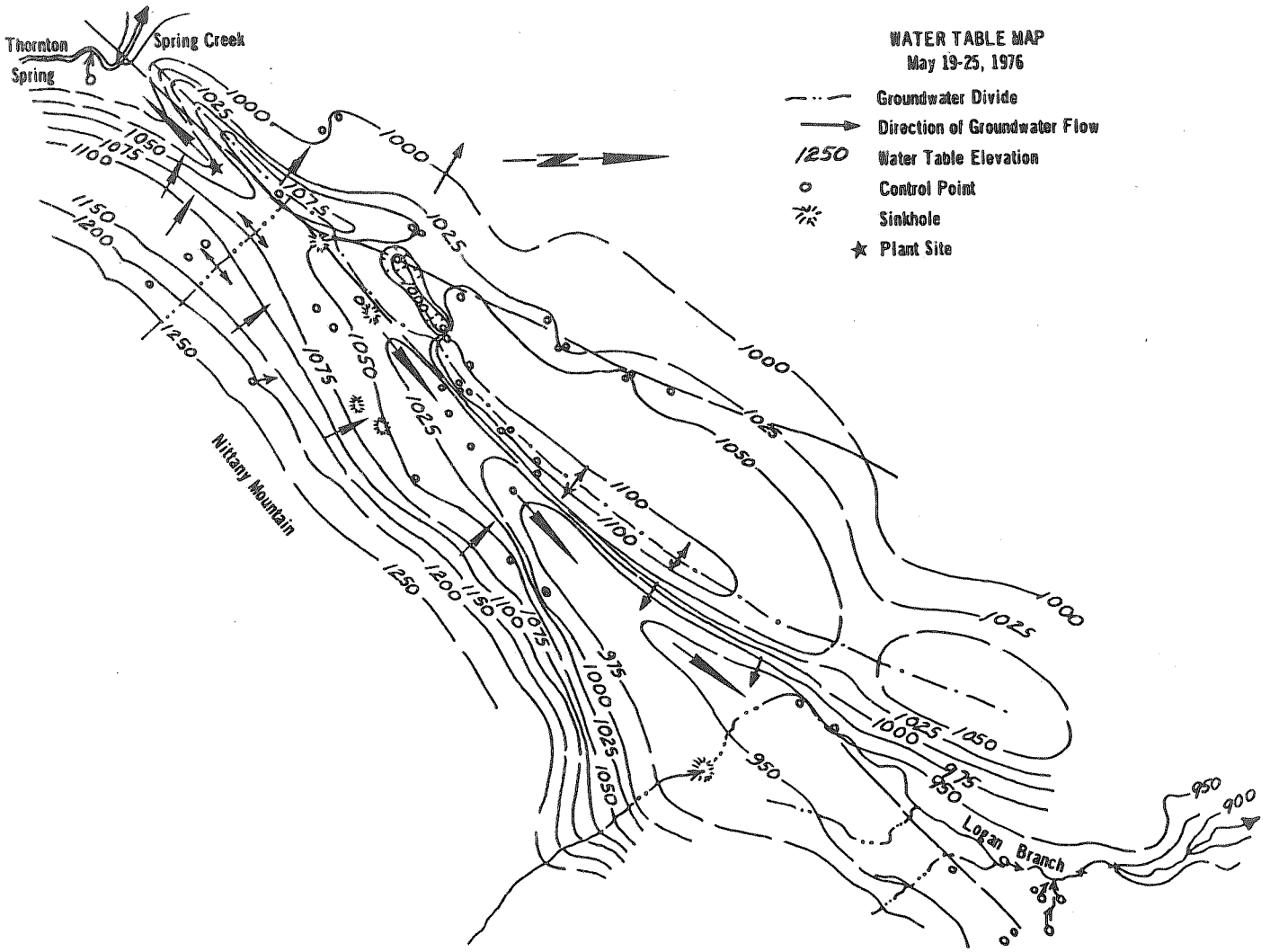

Figure 6. Water table configuration in the confluence between Logan Branch and Spring Creek.

These relationships suggest that Logan Branch was once the master stream and that its ancestral Nittany Mountain synclinal drainage and possibly Penns Valley drainage have long since been pirated by Spring Creek as it was able to erode through the plunging nose of Nittany Syncline. The groundwater basin along the western side of Nittany Mountain may still reflect the memory of Logan Branch's former more "glorious" status. Its groundwater basin to the northeast extends along

Route 64 beyond Zion for at least 7 miles. Details of the eastern segment of this groundwater flow system are obscured by an underground limestone mine that has resulted in a deep, localized cone of pumping depression. Marblehead Lime Company pumps up to 16,000 gpm to control groundwater flows during some periods of the year.

The relationship between stream valley location and limestone may be seen by reviewing various geologic and topographic maps of the area. Certain valleys appear to violate this generalization where they depart from limestone outcrop belts and cut across dolomitic strata. These cutoffs are almost always joint, zones of fracture concentration, or fault controlled. Valleys established across colluvium or alluvium at the base of ridges need not reflect these same structural and stratigraphical controls for short segments are consequent. These valleys segments have followed the consequent slope of Pleistocene colluvial-alluvial fans. Other valleys parallel the strike of limestone but are located in more resistant dolomite up dip (down stratigraphically) from the present limestone outcrop belt. This is accounted for by a space-temporal sequence of events illustrated in Figure 7.

When the drainage was first established, the land surface was higher as shown in Figure 7a. It was localized by differential solution along joints, bedding planes, more soluable beds and zones of fracture concentration within limestone. Integrated drainage developed directly above the limestone (Figure 7b) and down

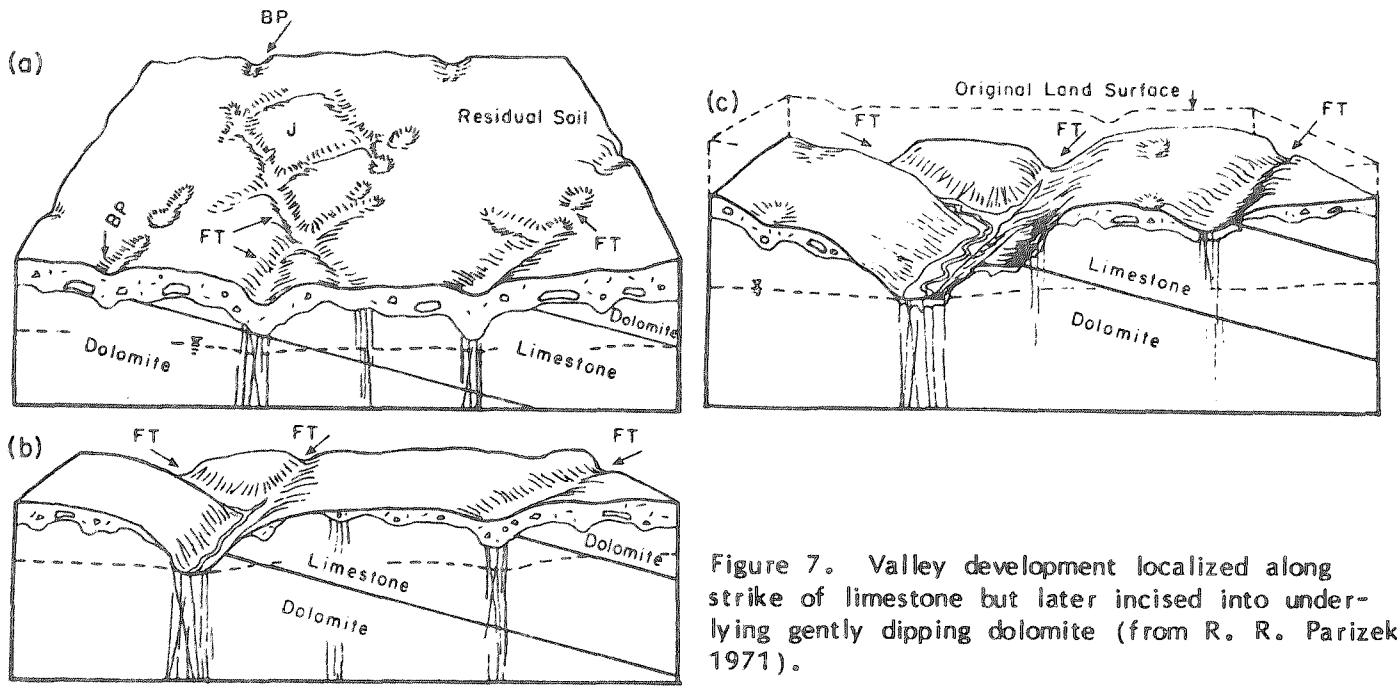

Figure 7. Valley development localized along strike of limestone but later incised into underlying gently dipping dolomite (from R. R. Parizek, 1971).

cutting and solution of land surface continued (Figure 7c) vertically along fracture zones, joints and faults which have fixed the channel position. The limestone outcrop belt continue to migrate in the down dip direction as the land surface was lowered. In time, the valleys may be incised completely into underlying dolomite and the initial limestone control valley location is no longer apparent. For larger drainages, valley widening is favored in the dip direction or toward the limestone valley wall.

It may be possible from these observations to estimate the amount of regional denudation which may have occurred since the valley position was fixed in plan view

(Figure 7c). This initial surface on which the drainage was established must have been graded to water gaps cut in resistant sandstone and quartzite which are responsible for maintaining local base levels for streams and groundwater. It can be shown that selected straight valley segments along Spring and other creeks are controlled by zones of fracture concentration revealed by lineament and fracture trace scale structures. The valleys show abrupt to nearly right angle turns at fracture trace intersections which produce an apparent meander pattern for this youthful, incised valley (Figure 8). From 50-90 percent of selected stream segments can be shown to be localized by these features in Nittany Valley. This is particularly evident along headwater tributaries where the control for valley location is still apparent. In adjacent uplands, solution along zones of fracture concentrations allows for subsidence of unconsolidated (residue) soils and produces lines of shallow depressions one to over ten feet deep (between HRB-Singer and the Kentucky Fried Chicken Restaurant on Route 322). Surface runoff concentrates in these depressions usually during the spring melt and after heavy rains. New tributary drainages are developed adjacent to valley walls as runoff becomes integrated. New straight valley segments are born in this manner where the water table stands near the land surface. To a lesser degree, master joint sets control the same process and together with zones of intersecting fracture concentrations and bedding plane openings, they produce irregular offsets in the new tributaries (Figure 8). Normal faults produce similar controls on drainage near State College (Parizek, 1971).

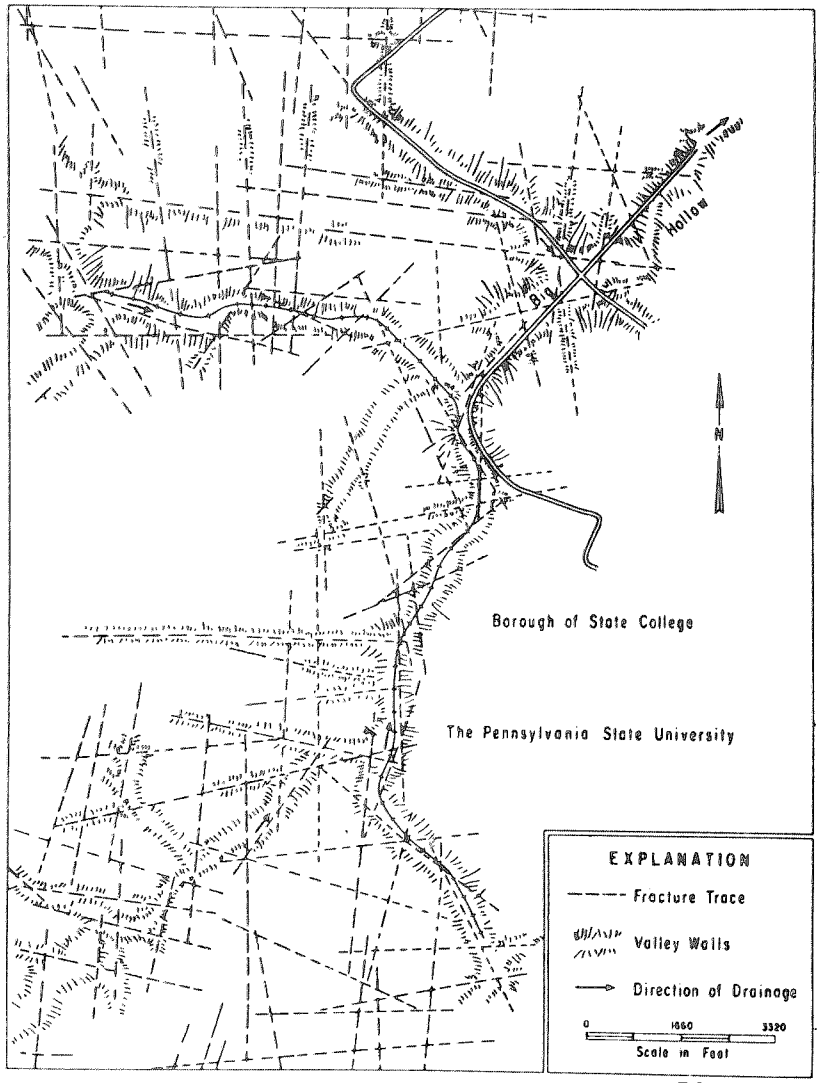

Figure 8. Valley development localized by zones of fracture concentration (from R. R. Parizek, 1971).

Subsurface Drainage

Many of the tributary valleys are underdrained and lack throughgoing surface streams. Sink holes are common along these valleys. Dolomite normally underlies uplands that have residual soil covers of varying thickness, 1 to 300 ft. Although these sediments may be depressed into solution zones in the top of bedrock, open sink holes are not common. Near surface cavities in limestones by contrast normally are larger and include both processes of solution and collapse. Internal drainage networks soon are established in limestone because of its increased solubility. Residual soil deposits are readily transported into sink and swallow holes and carried away along subsurface channel ways. Outcrops in limestone are more numerous when compared to outcrops observed for adjacent regions underlain by some dolomites. A topography may result where the limestone protrudes above adjacent, less soluble dolomite. This may be accounted for as follows. Once subsurface drainge is established within limestone, solution is concentrated in sink and swallow holes, and subsurface channel ways. Where the downcutting process is fast enough as at the heads of tributaries, undissolved masses of limestone remain only to be dissolved by direct precipitation and subsurface lateral solution. By contrast, solution openings along bedding planes and joints within dolomite are smaller and not as well interconnected. Their residual soils cover wide areas of bedrock. Surface water infiltration varies in topographically high and low areas according to detailed variations in soil characteristics and drainage. Surface runoff redistributes a greater proportion of precipitation to surface depressions where soil may be two to three times thicker than above adjacent topographically high areas. Percolating soil water rich in CO_2 tends to move through the entire soil profile attacking the top of bedrock more uniformly. The net effect is that the entire dolomitic landscape is lowered faster than some adjacent limestone areas now largely devoid of soil. Various examples of this erosion rate difference can be seen in central Pennsylvania. On the other hand, where slightly more resistant shale or sandstone is present (Salona-Coburn Formations, Upper Sandy Dolomite Member, Dale Summit Sandstone) or more dense dolomite (Tea Creek Member), these areas are marked by uplands of low relief (Parizek, 1971).

This seemingly anomalous weathering may be accounted for when one considers the role of the soil cover. Carbonation occurs in the soil in excess of what is possible in the atmosphere by at least an order of magnitude. Soil waters enriched in CO_2 are capable of dissolving more carbonate minerals than an equal volume of water which has fallen on exposed limestone. Once the soil has been washed into subsurface karst openings, solution lowering of bare rock surface will be slowed. Solution will continue along rapidly developing subsurface passageways developed around and below limestone pinnacles (Parizek, 1971).

Once the tributary drainages are established above limestone, the "cannibalistic process" of localized solution beneath the topographic low is speeded up. Surface water undersaturated with respect to $CaCO_3$ concentrates along the growing valleys at the expense of adjacent uplands. Permanent streams may be established for a time once valleys are deepened to the water table until subsurface solution zones may develop and underdrain these valleys. This further favors increased solution within the valley environment. The end result is to produce (1) an aquifer with major, regionally interconnected solution openings; (2) cavities and channel ways containing increased amounts of clay, sand, and gravel reworked from the initial unconsolidated overburden; (3) valley walls, floors, and adjacent uplands with discontinuous patches of residue soil cover, hence regions susceptible to rapid infiltration and to pollution; (4) regional groundwater underdrains producing 10-100 ft. of local relief on the free water surface; (5) sinking creeks,

hence major groundwater recharge areas capable of accepting million of gallons of water a day; (6) permanent surface drainages; and (7) conduits and more permeable aquifers where groundwater flow rates are rapid (Parizek, 1971).

Fragments of the conduit drainage system can be observed by examining the caves that occur widely in Nittany Valley. Some 90 caves are known in Centre County (Dayton and White, 1979) and additional caves are located in the same drainage basin in adjacent Clinton, Huntingdon, and Blair Counties. Caves, particularly Pennsylvania caves, are small and usually represent only tiny fragments of the present- or paleo-drainage system. The amount of cave passage explored in Nittany Valley is far too short to establish much of the paleodrainage or to establish the boundaries of the present-day groundwater basins.

Three sorts of caves are found. There are caves associated with the swallow holes where the mountain streams sink at the limestone contact. Noll Cave (Figure 9) is part of the floodwater inlet, now choked with sediment, at the sink of Gap Run (Stop 8). Stream sink caves are often used by the contemporary streams in their lower levels while higher levels represent abandoned channels or flood overflow routes. Sharer Cave and Veiled Lady Caves in Penns Valley are other examples. These caves often have high gradients consistent with the steep gradients of the mountain streams that feed them. The second sort of caves are found at spring mouths and allow the drainage system to be explored upstream into the subsurface. Few springs in Nittany Valley are explorable but the commercial Penns Cave is an

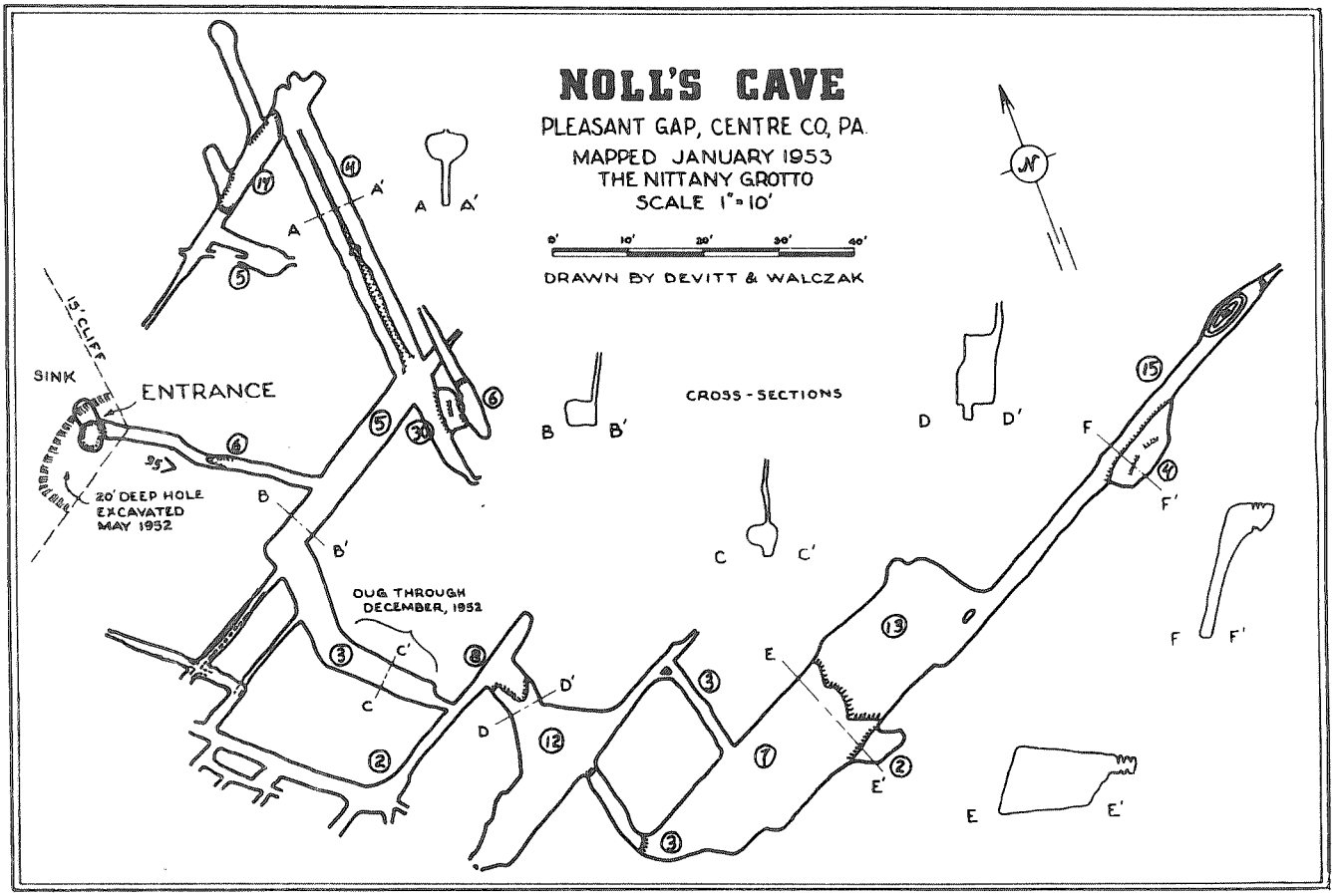

Figure 9. Noll Cave lies beneath a choke of sediments several hundred feet upstream for the swallow hole of Gap Run. High sediment loads carried by long-return period floods have a tendency to choke cave entrances in stream sink environments.

exception. The spring mouth at Penns Cave was not originally an explorable opening; the natural entrances are through sinkholes upstream along the master trunk channel. The third sort of caves are the fragments of old conduit now abandoned because of retreat of underground drainage to lower levels. These come in many sizes and shapes. Some are clearly related to present streams and can be thought of as a sort of underground terrance level. Others are related to the valley upland surface itself.

Figure 10 shows the distribution of caves and cave passage lengths for 75 caves in the Nittany Valley drainage. In a superficial way it appears that there is the greatest concentration of caves at the most probable elevation but there is more to it. The concentration of cave passage in the 800-850 foot interval occurs near the Juniata River and represents a major "terrace" 100-150 feet above the River. The cluster of caves and cave passage development between 900 and 950 feet are mostly in the lower reaches of the drainage system and are spaced about 100 feet above the present stream profile. The large cluster of caves between 1000 and 1100 feet is more problematic but could be related to the level developed near Houserville on the Spring Creek Drainage (Stop 5). Finally there is a large concentration of caves and cave passages near 1200 feet with fewer caves and less passage tapering off at higher elevations. These include some of the largest caves in the valley and also probably the oldest since they relate to the valley upland surface.

Stream alluvium derived from nearby mountain ranges becomes trapped in these growing sink holes and is deposited in caves, conduits, and other openings distant from swallow holes. Other sediment infiltrates from the valley floor through sinkholes and solutionally widened fractures. Conduit fillings range in texture from clay, silt, sand and gravel with pebbles up to 2 1/2 inches or more in diameter 2000 ft. or more from the nearest cave or solution opening. Assorted organic matter and clastic sediments may be present. Shale, quartzite, sandstone and chert pebbles to 2 1/2 inches in diameter have been recovered from gravel-filled conduits in the Bellefonte Dolomite and Middle Orodivician limestone at depths to 150 ft. below the water table. This is in an area where the water table has never been lower than at present. These caves and conduits formed at least 100 ft. below the water table. Runoff from mountain watersheds and watergaps may approach thousands of gallons a minute during periods of snowmelt. This water plunges into sink holes developed downslope from the Reedsville Shale and Salona-Coburn Formation and may cascade 30 to 150 ft. to the underlying water table. It is easy to see how groundwater flow velocities quickly mount to well above turbulent levels allowing transport of cobbles and boulders and how undersaturated groundwater becomes available well below the water table and distant from points of recharge. These factors favor concentrated and rapid solution of mountain base carbonates at the expense of adjacent carbonates. Some conduits transmit water only during wet-weather and extreme flood events. Others are well below the permanent water table.

The tendency for caves to maintain a horizontal longitudinal profile in spite of structure and lithology is accounted for mainly by the position of the water table. Once an integrated system of openings becomes established, it is capable of draining vast quantities of groundwater. Very low gradients are sufficient to convey all available groundwater to discharge areas even during peak periods of runoff. As the drainage net and groundwater basin becomes larger, conduits become better integrated and fewer in number.

Once these networks become established, chemically aggressive waters follow these avenues and dissolve strata within the region of water table fluctuation.

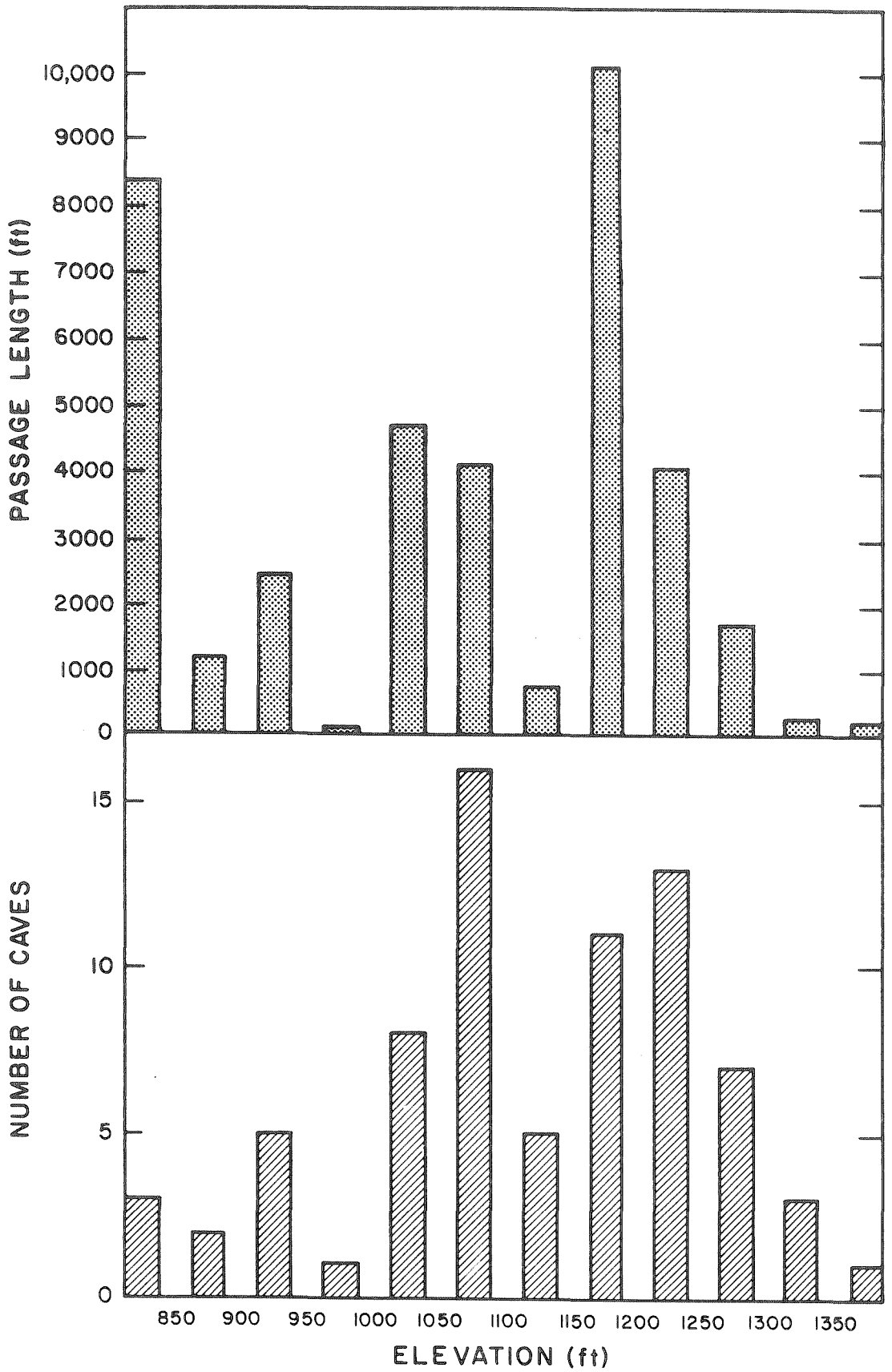

Figure 10. The distribution of passage length and number of caves in 50 foot elevation intervals through Nittany Valley. Data drawn from the Pennsylvania Cave Data Base maintained at the Pennsylvania State University by K. Wheeland.

Solution at greater depths below the water table is possible beneath regional recharge areas and where concentrated recharge occurs in swallow holes. Large solution openings may extend to greater depths below the water table (150 - 300 ft.) in these areas. Data from caliper logs indicate that cavities 1 to 5 ft. high can occur locally at depths of 500 ft. below ground level and 300 to 400 ft. below the water table.

The influence of water-table position on the solution process can be seen best at groundwater discharge areas. Springs most frequently emerge between bedrock valley walls and the contact with colluvial-alluvial valley fill sediments (Figure 11). These zones of groundwater discharge are usually at or slightly below the water table, are graded to the valley floor, and reflect zones of increased solution which extend beneath adjacent uplands at a gentle slope. Where valleys subsequently have been underdrained, these shallower conduits become abandoned. Here, younger and deeper conduit systems develop which are graded to underlying groundwater drains located beneath the valley floor. Wet weather springs occasionally mark the outlets

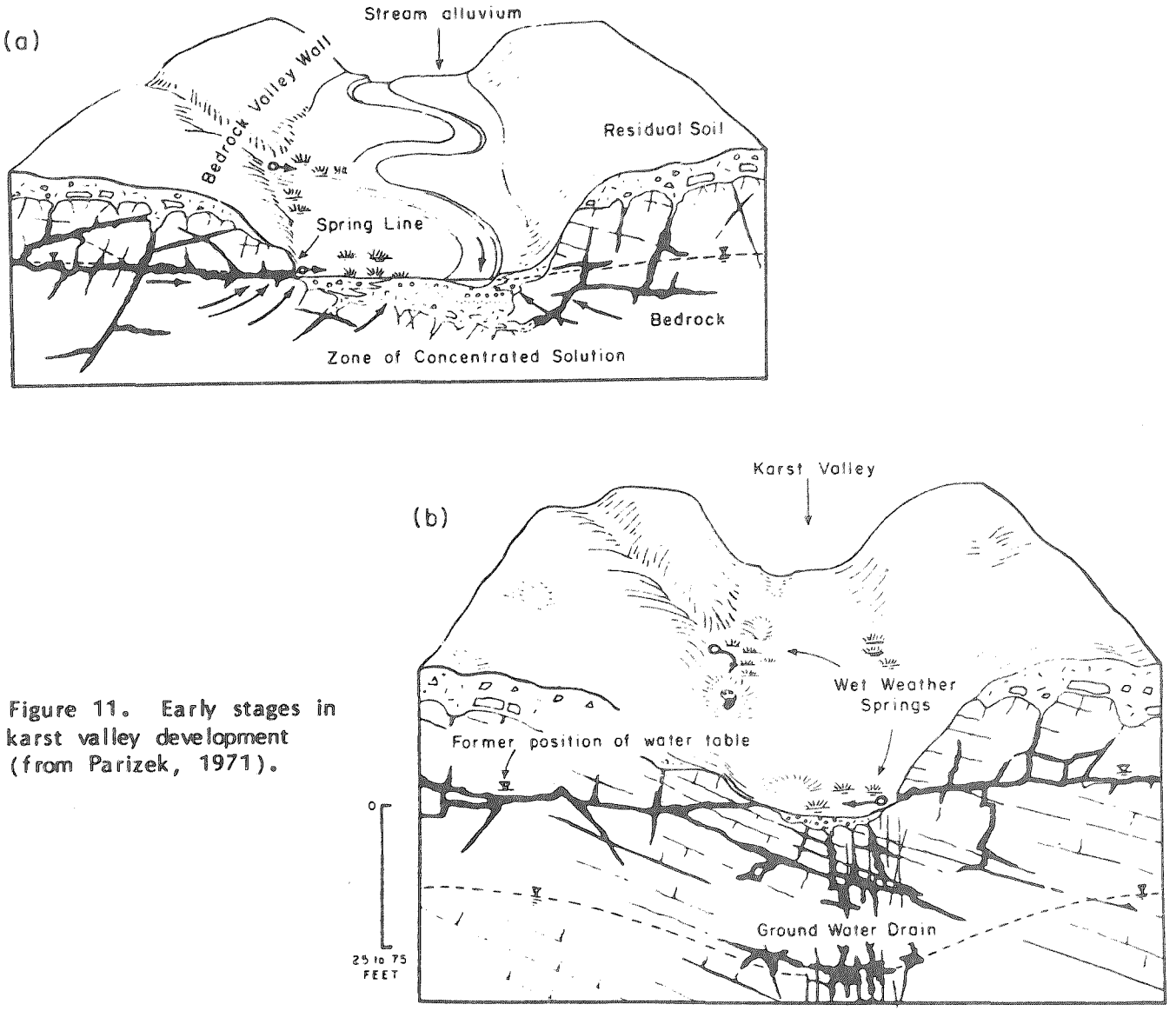

Figure 11. Early stages in karst valley development (from Parizek, 1971).

of these otherwise abandoned conduit systems. Where valleys are just now becoming underdrained (Stop 6) but still contain appreciable intermittent surface runoff, permanent and wet weather springs may still be present usually at the contact between the valley wall and less permeable valley fill sediments (Figure 11).

If cave levels, as indicated in a rough way by Figure 10, represent old terrace levels, some record of the chronology of the valley should be recorded in the caves. Although the cave sediments are complex sequences of sands, silts, and gravels, nothing equivalent to a stratigraphic section has been constructed. The depositional processes are chaotic and vary greatly from one part of a cave to the next. In spite of a rich sedimentary record, little use has so far been made of it.

Flowstone and dripstone deposits can be dated by $^{234}U/^{238}U$ and $^{230}Th/^{234}U$ disequilibrium with a time scale that extends to about 350,000 years BP (Thompson et al., 1975; Harmon et al., 1978). Most travertines are considerably younger than the caves in which they are deposited but dating of travertines from West Virginia caves show two clusters of dates: ages less than 6000 years BP and ages in the range of 70,000 to 200,000 years. These should represent post-Wisconsinian carbonate deposition and carbonate deposition during the Sangamon interglacial. It appears from these and other studies that carbonate deposition almost shuts down during the glacial advances. There is no uranium age data for Pennsylvania caves but visual inspections of dripstone deposits in some of the more highly decorated caves such as the commercial Lincoln Caverns reveals what appears to be two populations of travertine. There are underlying massive deposits overgrown with much smaller and somewhat differently colored deposits. It is suspected that the massive deposits are the Sangamon age material, largely because of a longer period available for growth and the small overgrown speleothems represent post-Wisconsinian deposition.

The clastic sediments in caves do contain minor amounts of magnetic minerals which provide a paleomagnetic signal. The iron oxides present are not strongly magnetic, they are few in number, and they are aligned only in a statistical sense because of turbulence and buffeting by sand and silt during deposition, but the magnetic signal can be measured. In a pioneering study of sediments in Mammoth Cave, Schmidt (1982) was able to follow the pattern of magnetic normals and magnetic reversals to 2 million years before present in the highest levels of the cave, thus confirming geomorphological evidence that the oldest part of the cave system are late Pliocene or very early Pleistocene age. Similar measurements have not been made in Pennsylvania caves but there is nothing inherently impossible in the hypothesis that the highest caves levels, those associated with the valley upland erosion surface, are of pre-Pleistocene age.

If the base level is fixed for a prolonged period, denudation dominated by dissolution within the vadose zone progresses and the land surface approaches the water table. Where this condition obtains, secondary porosity and permeability development tends to be limited with depth. Favorable aquifer characteristics are normally restricted to depths of 50-300 ft. below land surface and may be generally less than 150 ft. Where residual soils are available, the denudation process may continue somewhat uniformly almost to the water table.

Regions with extensive, shallow water tables and poorly drained lowlands reflect this condition. Examples may be seen near Chambersburg, Pennsylvania and Fredrick and Hagerstown, Maryland, and Martinsburg, West Virginia, and similar other regions where the landsurface has been eroded nearly to the local base level and the water table stands within a few feet to only several tens of feet below landsurface.

Here, deep internal drainage is restricted. Residual soils that must have existed previously similar to what are observed in Nittany and adjacent western Appalachian valleys have been largely eroded away to expose numerous bedrock outcrops. Aside from the shallow position of water table, reduced internal drainage hence, increased surface runoff and erosion, the general lack of a thick regolith in eastern carbonate valleys in the Ridge and Valley may also be due to their close proximity to master streams and regional base level. More time was available to permit erosion of residual soils approaching the eastern seaboard because these rivers would have been cut to base level for longer periods of time, and the water table would have been adjusted to baselevel earlier than for western interior basins.

Soils

The soils of the unglaciated Ridge and Valley show a strong association to landform (Figure 12, Table 1). Marchand et al. (1978) estimated that on average, soils formed on residum occupy approximately 67% of the Ridge and Valley. These occur on the more gently rolling valley floors and uplands while soils formed on colluvium occupy approximately 27% of the area. Colluvium occur on the lower one-half to three-fourths of the side slopes of major and secondary ridges (Stops 7 and 8). Colluvium also is widespread within the valley upland setting in Nittany Valley along intermittent drainage ways, and on the sides of smaller hills. The remaining 6% of the area is occupied by flvuial deposits including floodplain and terrace deposits (Ciolkosz et al., 1979). Aside from showing a strong association to landform, these soils are strongly related to parent material. For this reason, Ciolkosz et al. (1979) arranged Pennsylvania colluvial soils into four parent material-drainage groups and residual soils into seven classes (Table 1). They regard this sequential arrangement as a natural association of these soils in the landscape.

Residual Soil

The great bulk of unconsolidated overburden deposits that blankets carbonate bedrock in Nittany Valley is classified as residual having formed from prolonged physical and chemical weathering. These deposits have been documented to be at least 365 feet thick locally (just southwest of Gameland 176) and to vary with rock type and topographic setting. Bedrock outcrops are most abundant for the Bellefonte Dolomite, especially the Tea Creek Member which is a dense, crypto-crystalline dolomite. This unit is rather pure hence does not produce thick residual soil, nor does it favor internal or differential weathering of the top of bedrock. Its ridge forming character together with its low insoluable residue content and low permeability favors surface runoff and soil erosion.

The thickest residual soil deposits occur above the Gatesburg Formation especially the Mines Dolomite, and Upper and Lower Sandy Dolomite Members. These units yield higher proportions of insoluable residue when weathered, support a deep water table, are higher in bulk permeability and porosity than all other carbonate rocks in the region hence, promote internal drainage. Differential weathering is enhanced and detention storage is maximized by a myrid of well developed closed depressions.

Broad areas of the valley upland contain thick residual soils (sapolites or regolith) especially at interfluves. There is much evidence for their residual character (Stops 3 and 4).

Figure 12. Soil-landscape relations of Nittany Valley (A is northeast and B is southwest of State College) (from Ciolkosz et al., 1980).

(1) Bedding and lithologic variations in the soil can be matched with individual bedrock units from which they were derived.

(2) Structures in soil are relict and can be matched with similar structures in bedrock, i.e., mud cracks, ripple marks, spacing and relative abundance of insoluable residue, etc.

(3) Residual beds of chert, quartzitic sandstone, oolitic chert and sandstone can be matched with bedrock parent material.

(4) Rock fragments tend to be angular, nodular or irregular in shape not rounded, sorted or otherwise indicating that they have been transported by wind, water, gravity or ice.

(5) Soil units often can be correlated between drill holes or traced within trench excavations. These beds do not display bedforms or overall character of having been transported and deposited within fluvial, lacustrine or related environments.

Table 1 Major Soils of Central Pennsylvania Arranged According to Parent Material and Drainage.*

(Shallow) <20" to bedrock | (Moderately Deep) 20-40" to bedrock | (Deep >40" to consolidated bedrock)

Drainage Class and Depth to Mottling

Parent Material	(Well Drained >40")		Moderately Well Drained (20-40")	Somewhat Poorly Drained (10-20")	Poorly Drained 0-10"; some gleying)	Very Poorly Drained (0-10"; strong gleying)
Residual						
Gray and brown acid shale and siltstone	Weikert Lithic Dystrochrept; loamy-skeletal	Berks Typic Dystrochrept; loamy-skeletal	Bedington Typic Hapludult; fine-loamy Hartleton Typic Hapludult; loamy-skeletal	Blairton [Mod. deep------] Aquic Hapludult; fine-loamy Comly----------) Typic Fragiudalf; fine-loamy	Markes [Mod. deep] Typic Ochraqualf; loamy-skeletal Brinkerton Typic Fragiaqualf; fine-silty	
Gray and brown acid shale siltstone and some clay shale	Weikert Lithic Dystrochrept; loamy-skeletal	Gilpin Typic Hapludult fine-loamy	Rayne Typic Hapludult; fine-loamy	Wharton Aquic Hapludult; clayey	Cavode Aeric Ochraquult; clayey	Armagh Typic Ochraquult; clayey
Red acid shale and siltstone; dull red 4 chroma or less	Klinesville Lithic Dystrochrept; loamy-skeletal	Calvin Typic Dystrochrept; loamy-skeletal	Leck Kill Typic Hapludult; fine-loamy	Albrights----------) Aquic Fragiudalf; fine-loamy	Conyngham Unclassified	
Gray and brown acid sandstone	Ramsey Lithic Dystrochrept; loamy-skeletal	Dekalb Typic Dystrochrept; loamy-skeletal	Hazleton Typic Dystrochrept; loamy-skeletal Clymer Typic Hapludult; fine-loamy	Cookport----------) Aquic Fragiudult; fine-loamy	Nolo Typic Fragiaquult; fine-loamy	Lickdale Humic Haplaquept; fine-loamy
Red acid sandstone; dull red 4 chroma or less	Ramsey Lithic Dystrochrept; loamy-skeletal	Lehew Typic Dystrochrept; loamy-skeletal	Ungers Typic Hapludult; fine-loamy	Albrights----------) Aquic Fragiudalf; fine-loamy	Conyngham Unclassified	
Grayish brown sandstone (in some places a very sandy limestone)			Vanderlip Typic Quartzipsamment; coated Morrison Ultic Hapludalf; fine-loamy Leetonia Entic Haplorthod; sandy-skeletal, siliceous Gatesburg Entic Haplorthod; sandy, siliceous			
Very cherty limestone			Elliber Typic Hapludult; loamy-skeletal	Kreamer Aquic Hapludult; clayey	Evendale----------) Aeric Ochraquult; clayey	
Cherty limestone			Hublersburg Typic Hapludult; clayey			
Relatively pure limestone	Oqequon Lithic Hapludalf; clayey		Hagerstown Typic Hapludalf; clayey**	Clarksburg Typic Fragiudalf; fine-loamy	Penlaw Aquic Fragiudalf; fine-silty	Thorndale Typic Fragiaqualf; fine-silty

Parent Material	(Shallow) <20" to bedrock	(Moderately Deep) 20-40" to bedrock	(Deep >40" to consolidated bedrock)				
	Drainage Class and Depth to Mottling						
	(Well Drained >40")		Moderately Well Drained (20-40")	Somewhat Poorly Drained (10-20")	Poorly Drained (0-10"; some gleying)	Very Poorly Drained (0-10"; strong gleying)	
Residual (cont'd.)							
Thin bedded limestone and calcareous shale		Ryder Ultic Hapludalf; fine-loamy	Duffield Ultic Hapludalf; fine-loamy Edom Typic Hapludalf; clayey**, illitic Frankstown Typic Hapludult; fine-loamy	Clarksburg Typic Fragiudalf; fine-loamy	Penlaw Aquic Fragiudalf; fine-silty	Thorndale Typic Fragiaqualf; fine-silty	
Colluvium							
Brown and gray acid shale, siltstone and fine grain sandstone			Shelocta Typic Hapludult; fine-loamy	Ernest Aquic Fragiudult; fine-loamy		Brinkerton Typic Fragiaqualf; fine-silty	
Red acid shale, siltstone and fine grain sandstone; dull red chroma 4 or less			Meckesville Typic Fragiudult; fine-loamy	Albrights Aquic Fragiudalf; fine-loamy		Conyngham Unclassified	
Gray and brown acid sandstone and shale			Laidig Typic Fragiudult; fine-loamy	Buchanan Aquic Fragiudult; fine-loamy		Andover Typic Fragiaquult; fine-loamy	
Brown and gray limestone, shale and sandstone			Murrill Typic Hapludult; fine-loamy	Clarksburg Typic Fragiudalf; fine-loamy	Penlaw Aquic Fragiudalf; fine-silty	Thorndale Typic Fragiaqualf; fine-silty	
Very cherty limestone and shale			Mertz Typic Hapludult; loamy-skeletal	Kreamer Aquic Hapludult; clayey	Evendale Aeric Ochraquult; clayey		
Recent Alluvium (Floodplains)							
Alluvium from acid gray and brown shale, siltstone and sandstone uplands.			Pope Fluventic Dystrochrept; coarse-loamy	Philo Fluvaquentic Dystrochrept; coarse-loamy	Stendal Aeric Fluvaquent; fine-silty	Atkins Typic Fluvaquent; fine-loamy	Elkins Humaqueptic Fluvaquent; fine-silty
Alluvium from acid red shale, siltstone and sandstone uplands; dull red chroma 4 or less			Barbour; Linden Fluventic Dystrochrept; coarse-loamy	Basher Fluvaquentic Dystrochrept; coarse-loamy		Holly Typic Fluvaquent; fine-loamy	Papakating Mollic Fluvaquent; fine-silty
Alluvium from limestone, shale and siltstone upland			Nolin Dystric Fluventic Eutrochrept; fine-silty	Lindside Fluvaquentic Eutrochrept; fine-silty	Newark Aeric Fluvaquent; fine-silty	Melvin Typic Fluvaquent; fine-silty	Dunning Fluvaquentic Haplaquoll; clayey**
Old Alluvium (Terraces) and Lacustrine							
Gray and brown acid shale siltstone and sandstone			Allegheny Typic Hapludult; fine-loamy	Monongahela Typic Fragiudult; fine-loamy	Tyler-Aeric Fragiaquult; fine-silty Tygart - Aeric Ochraquult; clayey	Purdy Typic Ochraquult; clayey	

* Almost all soils are also mixed, mesic.

** These soils are classified in the fine family but for the purpose of this table clayey will be used. In Pennsylvania most pedons are skeletal.

(6) The mineralogy, texture and character of float, etc. within the overburden can be traced along stratigraphic strike and correlated with underlying bedrock units from which it was derived. Foreign rock fragments are absent.

(7) The contact between the regolith and underlying bedrock can be gradational characteristic of a sapolite.

(8) Distinctive soil units occupy distinctive positions on the landscape, i.e., sandy soils overlie the Upper Sandy Dolomite Member of the Gatesburg Formation, thick kaolinite deposits occur above and along the Lower Sandy Dolomite Member, irregular masses of oolitic chert follows the Mines Dolomite Member of the Gatesburg, some soil units show distinctive color above the Trenton series of carbonates, etc.

Figures 13 and 14 show residual soil thickness at two sites near State College. Both are underlain by the somewhat sandy Gatesburg Formation. The maximum thickness of residual soil observed was in coreboring GM-6. Split spoon samples were collected at 2.5 foot intervals to a depth of 162.5 feet before the first bedrock was encountered. Much of the Gameland 176 contains in excess of 100 feet of residual soil. Residual soils at the Agronomy-Forestry Waste Water Treatment area exceed 60 feet in thickness but thin along the upland edges of tributary valleys where more extensive surface erosion has occurred. Bedrock outcrops are restricted to valley walls and valley bottoms where residual soils have been totally removed.

Even greater thicknesses of soil were noted in test wells drilled above the Lower Sandy Dolomite Member of the Gatesburg Formation. Two air rotary holes drilled on the Stevenson Property by the Borough of State College (Water) Authority penetrated regolith to depths in excess of 365 feet before any resistant bedrock was encountered. This is the thickest residual soils documented in Nittany Valley. It occurs above inclined beds of the Lower Sandy Dolomite Member where bedrock dips may exceed 15 to 20°. Beds are not vertical to near vertical as observed at Stop 2.

Variations in soil thickness within a given area are related to rock characteristics, presence of systematic and non-systematic joints, their intersections, zones of fracture concentration, faults, and bedding plane partings and the amount of post dissolution erosion. Usually, soil thickness is a maximum below surface sags and depressions where internal drainage dominates over surface runoff. For example, soils may be 60 to 100 feet thick below closed surface depressions and only 5 to 20 or so feet thick above immediately adjacent topographic highs. The surface topography of internally drained uplands strongly mimics the bedrock surface topography underlying residual soil deposits.

Subsidence depressions can persist for very long periods of time, both at the landsurface and bedrock surface. Topographic evidence for the former can be eliminated if the rate of surface erosion exceeds the rate carbonate rock dissolution at the soil-bedrock contract. In time, topographic irregularities related to differential weathering of bedrock are truncated by surface erosion and eliminated. Where topographic evidence for former closed surface depressions have been lost, sites of maximum dissolution can still be observed by (1) mapping the configuration of the top of bedrock, (2) mapping letdown structures within the soil overburden revealed by lithologic variations inhereted from the bedrock, i.e., silt, sand and claybeds, chert horizons, etc., and (3) mapping sinkhole fills, etc.

Where lithologic variations are distinct within soil overburden deposits, beds mapped within topographic lows within the bedrock surface will rise in elevation approaching bedrock highs or may be exposed and truncated at the land surface. In extreme cases of soil collapse, evidence for relict bedding may be eliminated during this inversion process.

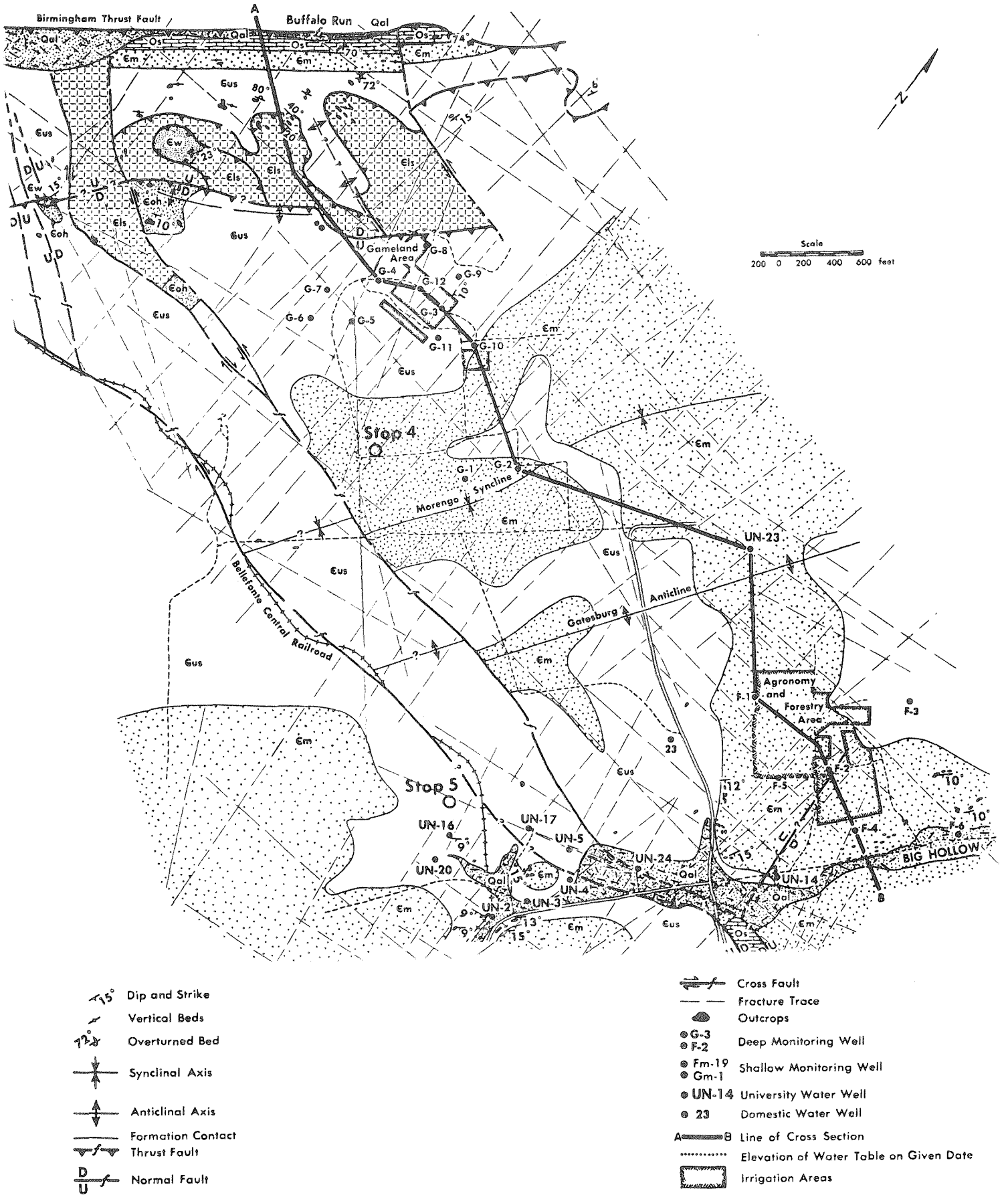

- Dip and Strike
- Vertical Beds
- Overturned Bed
- Synclinal Axis
- Anticlinal Axis
- Formation Contact
- Thrust Fault
- Normal Fault
- Cross Fault
- Fracture Trace
- Outcrops
- G-3, F-2 — Deep Monitoring Well
- Fm-19, Gm-1 — Shallow Monitoring Well
- UN-14 — University Water Well
- 23 — Domestic Water Well
- A—B — Line of Cross Section
- Elevation of Water Table on Given Date
- Irrigation Areas

Figure 13. Geologic map of Penn State's Living Filter Project area (from Parizek et al., 1967).

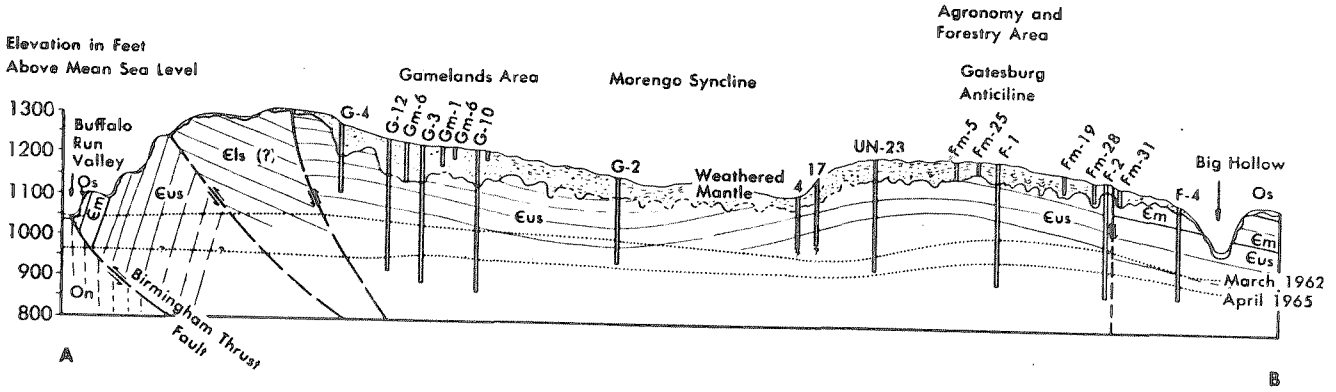

STRATIGRAPHIC AND SOIL SUMMARY

Age			Description	Soil Series	Texture
Recent		Qal Quaternary Alluvium	Mixture of clay, sand, chert, and quartzite cobbles and boulders 1 to 30 feet	Araby, Huntingdon	Coarse to Medium
Lower Ords.		On Nittany Dolomite	Thick bedded, coarsely crystalline dolomite, fine to coarse, chert nodules. 1209 ± feet.	Hagerstown- Hublersburg	Medium to Fine
		Os Stonehenge Limestone	Fine-grained limestone, some dolomite beds, edgewise conglomerate. 360 to 702 feet.	Hagerstown- Hublersburg	Medium to Fine
Upper Cambrian	Gatesburg Formation	Em Mines Dolomite Member	Massive dolomite, beds of oolitic chert, sand stringers. 130 to 230 feet.	Hublersburg- Hagerstown	Medium to Fine
		Eus Upper Sandy Member	Recurring beds of dolomite, sandstone, and quartzite. 650 to 700 ± feet.	Morrison, Gatesburg	Coarse
		Eoh Ore Hill Member	Massive dolomite, beds of platy dolomite. 250 feet.	Hublersburg- Hagerstown	Medium to Fine
		Els Lower Sandy Member	Recurring beds of dolomite, sandstone, and quartzite less abundant. 300 feet.	Morrison, Gatesburg	Coarse
		Ew Warrior Limestone	Limestone interbedded with some dolomite, thin shale units. 600 feet.	Hagerstown- Hublersburg	Medium to Fine

Figure 14. Geologic cross-section through Penn State's Living Filter Project area (from Parizek et al., 1967).

The significance of zones of fracture concentration revealed by fracture traces and lineaments in differential weathering of carbonate bedrock is dramatically shown in figure 15. Foundation borings were made for the East Halls dormitory complex on the Penn State University Campus. Borings and later buildings were located above two fracture trace-related structures and their intersection within the Stonehenge Limestone and overlying Nittany Dolomite. Physical and chemical weathering of the Nittany Dolomite were enhanced along these zones of fracture concentration. Depths to bedrock were 25, 50 to 75 feet on the structures and < 5 to 25 feet or so at immediately adjacent sites located off these structures. The cumulative thickness of weathering products is obvious and must include the insoluble residue derived from a significant volume of carbonate bedrock. The insoluble residue content of the Nittany Dolomite is lower than that measured for the Mines and Upper Sandy Dolomite Members of the Gatesburg Formation. Hence, its residual soils represent the remnants of weathering products resulting from the removal of several thousands of feet of carbonate bedrock that have accumulated slowly over millions of years.

High angle faults observed in the Gameland 176 area also localize thick residual soils that exceed 100 feet, surface sags and depressions and perched ponds all indicators of differential weathering of the underlying bedrock surface.

Kaolinitic Soils from Barrens

Feldspathic shales, siltstones and sandstones within the Gatesburg Formation have been identified by R. Pollock (personal communication). These beds were penetrated by drill cores as part of the Living Filter site characterization efforts. Fine-grained shale, siltstone, and silty dolomite beds are present at various depths within the Upper Sandy Dolomite Member. These greenish beds were

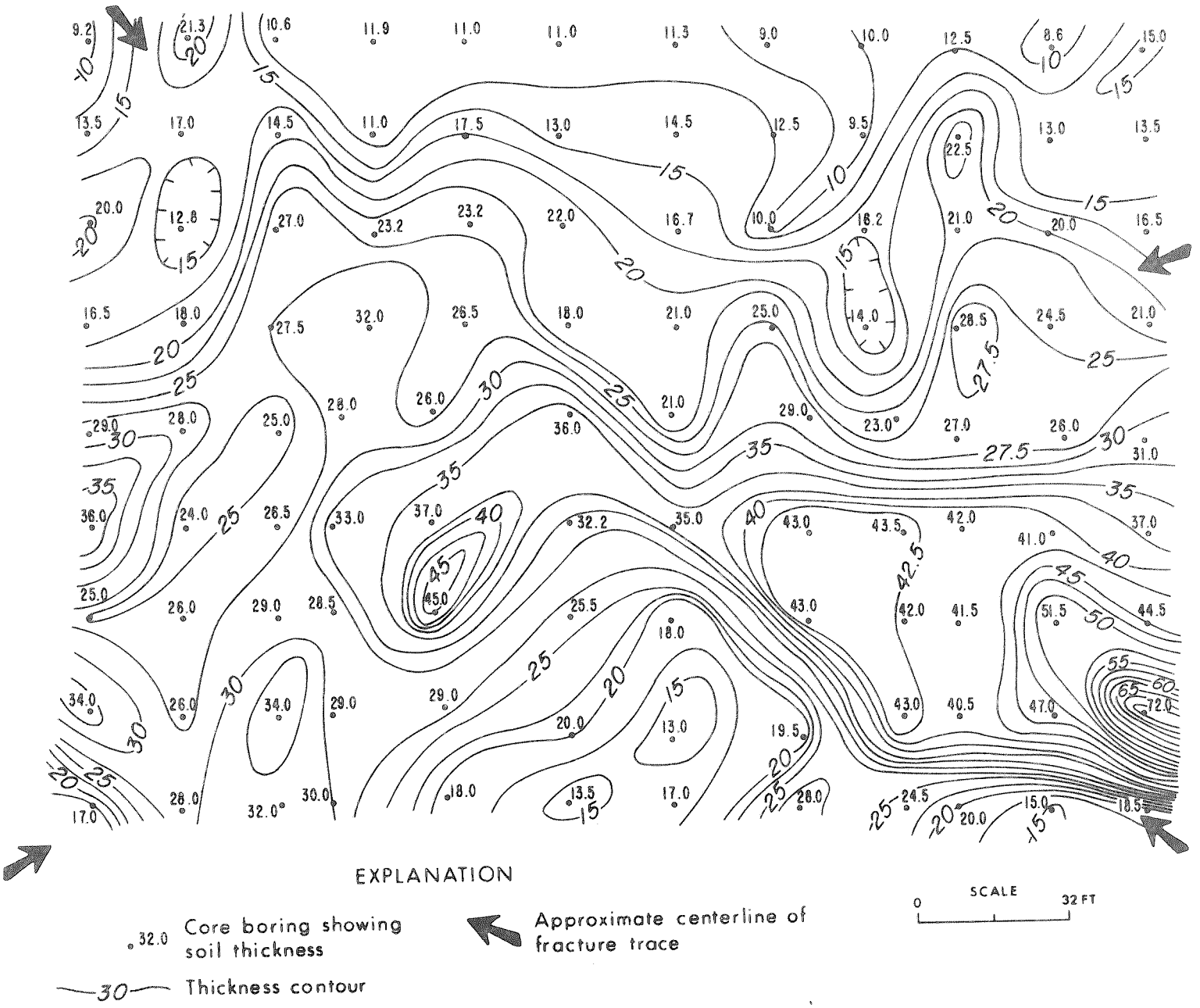

Figure 15. Thickness of residual soil developed below a fracture trace intersection in the Nittany Dolomite, East Halls Cafeteria, Penn State University.

described as being composed mainly of clay and quartz based on a binocular level of inspection. Later, Pollock showed them to be rich in feldspar, the parent material for kaolinite observed in the Barrens. The problem was how to form the thick kaolinite clay deposits (Stop 2) given the predominantly dolomitic and quartz sand nature of the Upper and Lower Sandy Dolomite Members of the Gatesburg. R. Pollock reports that some of these clay deposits are nearly pure kaolinite and highly refractory. Following carbonate dissolution and chemical alteration of feldspar, quartz had to be leached from the clay. This would be possible under a prolonged tropical to subtropical climate where silica is more soluable than at present. E. G. Williams and R. Pollock both identified the mineral bauxite associated with these kaolinite deposits which offers further evidence for a tropical to subtropical paleoclimate in Nittany Valley.

Evidence for Late Paleocene through Early Eocene bauxitization in the southeastern states and Arkansas under a humid tropical climate helps to explain the sparse occurrences of bauxite in the Barrens which is located more than 500 miles to the north. Barrens deposits may have formed under a more temperate zonal climate that extended to the north into Pennsylvania.

Pollock offered an explanation of how kaolinite deposits might have become so thick in the Barrens regions lacking outcrops or cores showing thick feldspathic sands in the underlying Lower Sandy Dolomite Member. To the west of the Birmingham thrust fault, beds are vertical to near vertical or steeply dipping (west of Stop 2). Selective weathering along bedding planes and along beds with high feldspar content would produce long narrow beds of kaolinite. These deposits would accumulate as vertical weathering continued. Thick, near vertical beds of kaolinite would result that display relict bedding. Where original bedrock had more gentle dips, kaolinite deposits would be let down over a wider area and subjected to differential erosion. Alternatively, thick irregular beds of feldspathic sand may have been present in the Gatesburg that have been altered to kaolinite deposits observed although silty and sandy dolomite beds are known to occur in the Lower Sandy Member, no irregular feldspathic sandstone bodies have been observed to date that might account for irregular occurrences of Barren's kaolinite.

It is unlikely that Barrens' kaolinite deposits are of primary marine origin. Marine environments are alkaline, there is no leaching, and water contains a good deal of dissolved calcium. According to Grim (1953) these environmental conditions favor the formation of montmorillonite, illite or chlorite clay minerals rather than kaolinite. Millot (1942) indicated that Ca^{++} tends to block the formation of kaolinite. To produce kaolinite from a dolomite parent material, carbonate minerals must first be leached. The pH of the geochemical environment had to be in the 5 to 9 range where silica becomes more soluable in order to remove quartz.

Grim (1953) indicates that primary kaolinite, if deposited in a marine environment, is likely to persist because diagenetic alteration of kaolinite is slow. Relict bedding observed at Stop 2 is more indicative of a weathering alteration mechanism of kaolinite formation rather than primary deposition. The pod-like character of Barrens kaolinite deposits also does not support a primary deposition model for this kaolinite. Dark gray dolomite units in the Gatesburg Formation are interpreted as having been deposited in an off-shore environment. Individual beds may be traced for a considerable distance when compared to beach sands and lagoonal facies. Clay deposited in an offshore marine environment most-likely would produce sheet-like deposits rather than the discontinuous, lense-like deposits observed. Sands and shales in the Gatesburg on the other hand, are lense-like and are the most probable source of feldspars that gave rise to these kaolinite deposits.

There is no evidence to support a hydrothermal origin for the Barrens kaolinite as are sometimes found as an aureole around metalliferous deposits. Elsewhere, a supergene origin for kaolinite has been found associated with metalliferous sulfide ore bodies. Grim (1953) reports that such clays are developed during the downward movement of acidic water produced by the oxidation of the sulfides. Lead and zinc have been mined in the Milesburg Gap area near Bellefonte (Stop 7) and near Birmingham, Pennsylvania, but such deposits if responsible for Barrens kaolinite, have long since been eroded.

A soil weathering mechanism offers the best explanation for the origin of Barrens kaolinite and immediately adjacent beds of iron ore. Under long periods of

continued weathering in a hot wet environment, organic acids and a neutral or slightly alkaline environment ideal for lateritic alteration might develop that allow for magnesium removal, silica to be carried away, and iron and alumina to be concentrated at or near the surface. In weathering calcareous sediments, there is substantially no alteration of silicates until the carbonate is completely broken down and calcium removed from the environment by deep leaching. After calcium is removed, development of a zone of aluminum and iron concentration are possible (Grim, 1953).

Alluvial Soils

Baxter (1983) mapped two prominent, longitudinally continuous terrace levels along Beech, Fishing and Bald Eagle Creeks and West Branch of the Susquehanna River Valley. Flood plain alluvium comprises the lower level and intermediate terrace alluvium, the higher level. He also mapped a discontinuous terrace alluvium between and above these two main levels.

Depending upon where the pre-Wisconsinan glacial boarder is mapped below Lock Haven (figure 16) several origins are possible for these terrace remnants. If ice

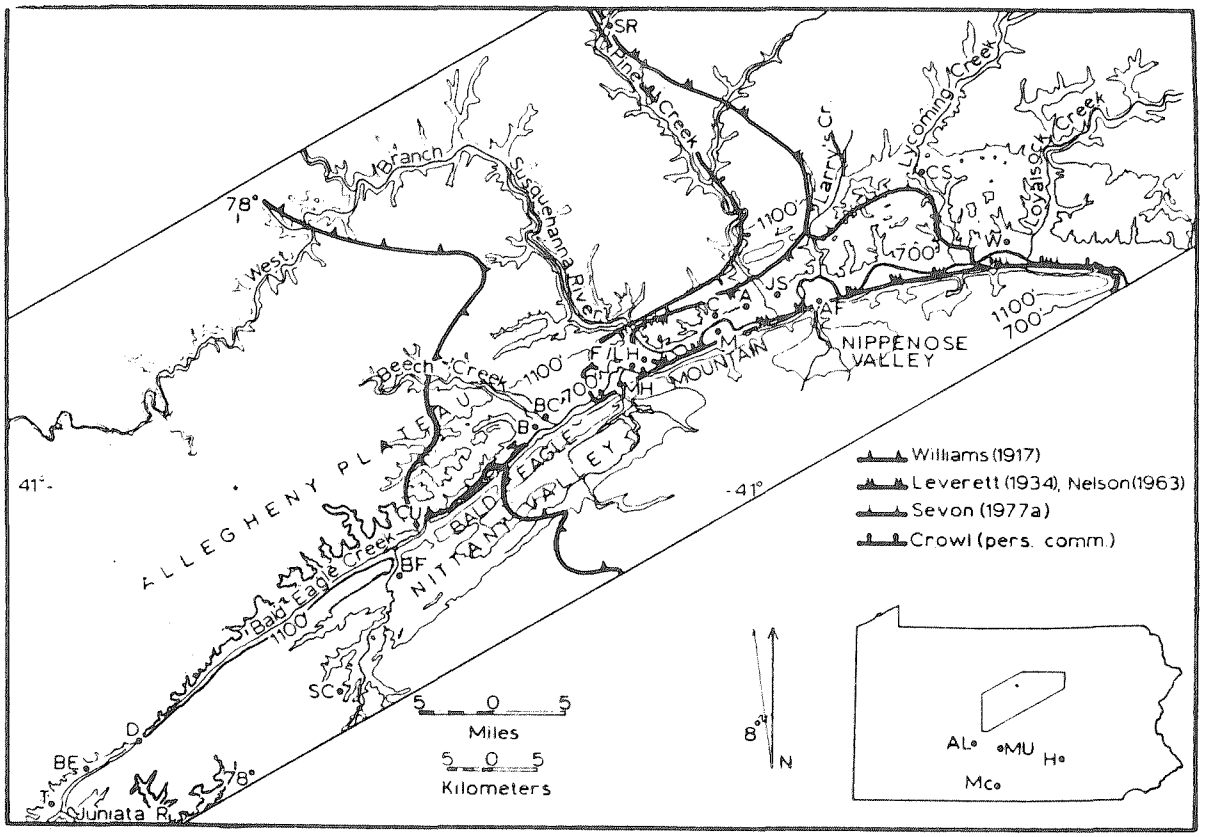

Figure 16. Proposed positions for a pre-Wisconsinan glacial border within the West Branch and Bald Eagle Creeks near Lock Haven (from Baxter, 1983). The 1,100 ft contour shows extent of Lake Lesley (Williams, 1895, 1917, 1920). 700 ft contour shows extent of the lower elevation proglacial lake (Leverett, 1934; Bucek, 1975, 1980; Sevon, 1977a). Location abbreviations are: A-Avis; AF-Antes Fort; AL-Altoona; B-Blanchard; BC-Beech Creek; BE-Bald Eagle; BF-Bellefonte; C-Charlton; CS-Cogan Station; CU-Curtin; D-Dix; F/LH-Flemington/Lock Haven; H-Harrisburg; JS-Jersey Shore; M-McElhattan; MC-Mercersburg; MH-Mill Hall; MU-Mount Union; SC-State College; SR-Slate Run; W-Williamsport.

stood near Jersey Shore, then alluvial terraces were colluviated producing diamictons that were graded to a temporary base level in the West Branch. However, Baxter (1983) rejects this "nonglacial" model as well as a model that proposed a glacial advance up Bald Eagle Valley to Blanchard to explain extensive diamicton deposits to this point. This would require the presence of a proglacial lake within Bald Eagle Valley controlled by a spillway elevation of approximately 1110 feet above sea level at Dix (8 miles west of Stop 1) as proposed by Williams (1917) or a small or short lived lake if meltwater followed the present valley through subglacial and englacial channels in the ice marginal to the end of Bald Eagle Mountain (Bucek, 1975; Baxter, 1983). Baxter (1983) rejects this more extensive glacial model on the best available data. Rather he presents evidence that a pre-Wisconsinan glacier advanced to the vicinity near Lock Haven (Figure 16) and solves the proglacial lake problem by (1) allowing the upper West Branch of the Susquehanna River, Bald Eagle Creek, and Fishing Creek to drain subglacially and englacially around the east end of Bald Eagle Mountain for a distance of 40 miles or (2) the streams to dam for only a short time to preclude significant accumulation of lacustrine deposits within Nittany and Bald Eagle Valleys to an elevation of approximately 1110 feet above sea level. This elevation would allow a lake to extend nearly to State College.

A lower lake level would help to some extent because no lacustrine sediments are known within Nittany Valley to this or even lower levels. The col at Dix is rather narrow but the col could contain Wisconsinan colluvial fill derived from Bald Eagle Mountain. A 10 to 30 foot thickness of colluvium is possible which would result in a 1100 to 1080 foot lake level.

Baxter (1983) uses the retreating ice to help aggrade these valleys with fluvial sediments to the reconstructed terrace longitudinal profiles. He regards the intermediate and upper terraces in Fishing Creek (below Lamar) as old alluvium because this valley was isolated from continental glaciation by Bald Eagle Mountain. He states that these terraces are found only in terrace position along these stream, their reconstructed longitudinal terrace profiles are smooth and parallel to the present stream profile and Beech Creek and Bald Eagle Creek terraces contain clasts derived from the Allegheny Plateau and Bald Eagle Mountain.

Baxter (1983) postulates that the intermediate terrace level resulted from the rapid influx of colluvium into these drainages as an Illinoinan glacier retreated from its position at Lock Haven. Incision followed shortly after to produce the intermediate terraces.

Deep weathering followed during the Sangamonian and this was followed by Early Wisconsinan glaciation to the vicinity of Loyalsock Creek near Williamsport (Bucek, 1975). This Early Wisconsinan ice dammed the West Branch at Williamsport to produce proglacial Lake Lesley II which was less extensive than Lake Lesley I proposed by Williams earlier. According to Baxter (1983), glacial outwash near Williamsport allowed the aggradation of the Susquehanna River and the development of the lower alluvial terrace levels at Lock Haven, along Fishing Creek and near Beaver Creek.

The terrace noted at Houserville (Stop 5) most likely correlates with the intermediate terraces of Baxter (1983) lower in the Bald Eagle and Susquehanna drainage system judging from its well developed weathering profile. This terrace does not owe its origin to younger fan alluvium associated with Late Wisconsinan glaciation because no such fans impinge on Spring Creek between Houserville and Milesburg Gap where Spring Creek joins Bald Eagle Creek. Its mapped extent is shown in figure 17.

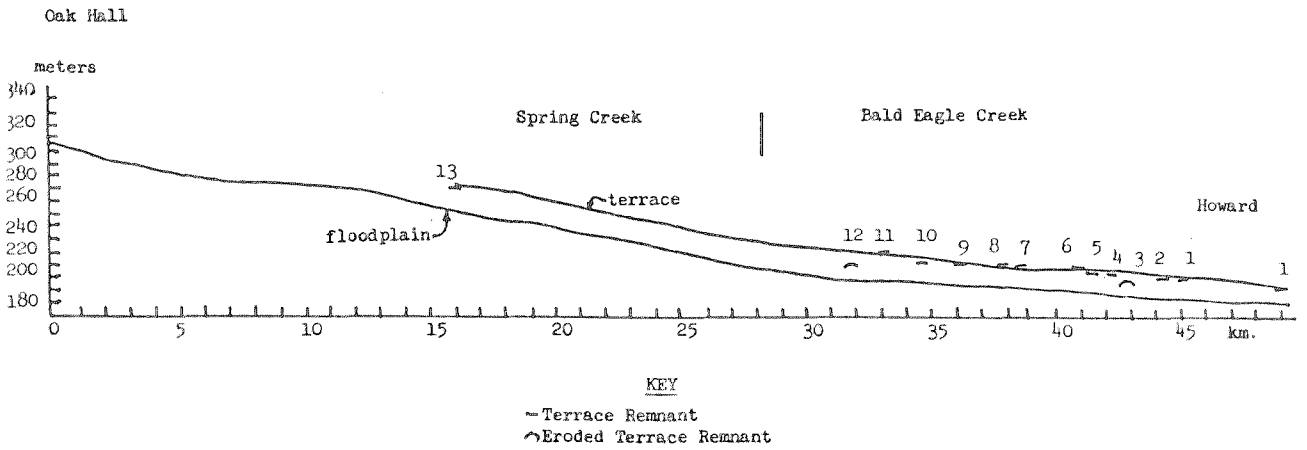

Figure 17. Floodplain and terrace longitudinal profiles along Spring and Bald Eagle Creeks to Howard, Pennsylvania (from Kashatus, 1984).

The presence of a buried soil profile below Spring Creek alluvium is of interest. This soil underlies recent alluvium by a depth of 4 to 8 feet. It is not known if this buried surface correlates with charcoal dated nearby by Bilzi and Ciolkoz (1977) at 200 Y.B.P. A problem remains; when was this soil developed?

Sewer main construction encountered bedrock at depths of 6 to 12 feet near the confluence of Spring and Slab Cabin Creeks. No deep bedrock channel stage was recognized below this alluvium that would allow this buried surface to be elevated for a long enough period to produce the soil profile observed. How might such a soil profile develop below the active flood plain level? Spring Creek is influent near Stop 5. The water table stands 12 feet below the level of Spring Creek at present but it is not clear how this might have allowed the development of a soil profile in a flood prone setting.

A cattle underpass was constructed under the State College Bypass just across Spring Creek (Stop 5). Trench walls at this site revealed the presence of cyclic sediments resembling varves to a depth of more than 6 feet. Is this the long sought after evidence for Lake Lesley I? Unfortunately, this deposit may have been produced by iron ore washing activities during the last century. Extensive excavations for iron ore have been covered over just beyond the bypass and below the Mountainview Hospital. These finely laminated deposits noted on Spring Creek flood plain by the cattle underpass may be related to orewashing activities rather than a proglacial lake. This surface was flooded during Agnes (June, 1972) but there is no chance that these cyclic sediments record a past frequent flooding history similar to Agnes. Biological processes destroyed bedding in Agnes overbank sediments shortly after they were deposited. These cyclic deposits observed had to have been protected from such biologic activity.

The buried soil observed may be of Early Wisconsinan age and does not appear to have been caused by iron mining activities. The soil underlies a distinct flood plain surface and alluvium, not man-made land.

No evidence has been found in the region to support the suggestion that significant quantities of the overburden was deposited by rivers or a marine transgression sometime in the distant past. The Cretaceous outlier located near Chambersburg, Pennsylvania appears to be a unique occurrence. It was an isolated lignite deposit not part of a marine transgression.

Colluvial Soils

Mountain slope colluvium and alluvial fan complexes are well developed opposite water gaps and along the lower slopes of Bald Eagle, Nittany and Tussey Mountains (Figure 18). These deposits overlie residual soils and are distinctive. They tend to thin out in an irregular manner as they are traced out onto residual soils of the valley upland. They may thicken significantly where they were deposited in sink and swallow holes, and closed surface depressions reflecting paleokarst landforms formed during interglacials when processes of colluviation were largely inactive.

In the Barrens region, for example, residual soils have been reworked and transported up to a mile or more along intermittent drainage ways. Distinctive pebbles, cobbles and boulders of chert, quartzitic sandstone, and oolitic chert may be traced down slope across younger bedrock units that are located 2,000 feet or more higher in the stratigraphic section. These deposits were worked for iron ore in the early days having been excavated to depths of 20 to 30 or more feet in open pits and shafts. Such deposits were termed "wash ore" and are lag concentrates of iron oxides, sandstone, chert and other impurities. These deposits show a sharp contact with underlying residual soils, have distinctive color and a gravelly texture when compared with underlying residual soils.

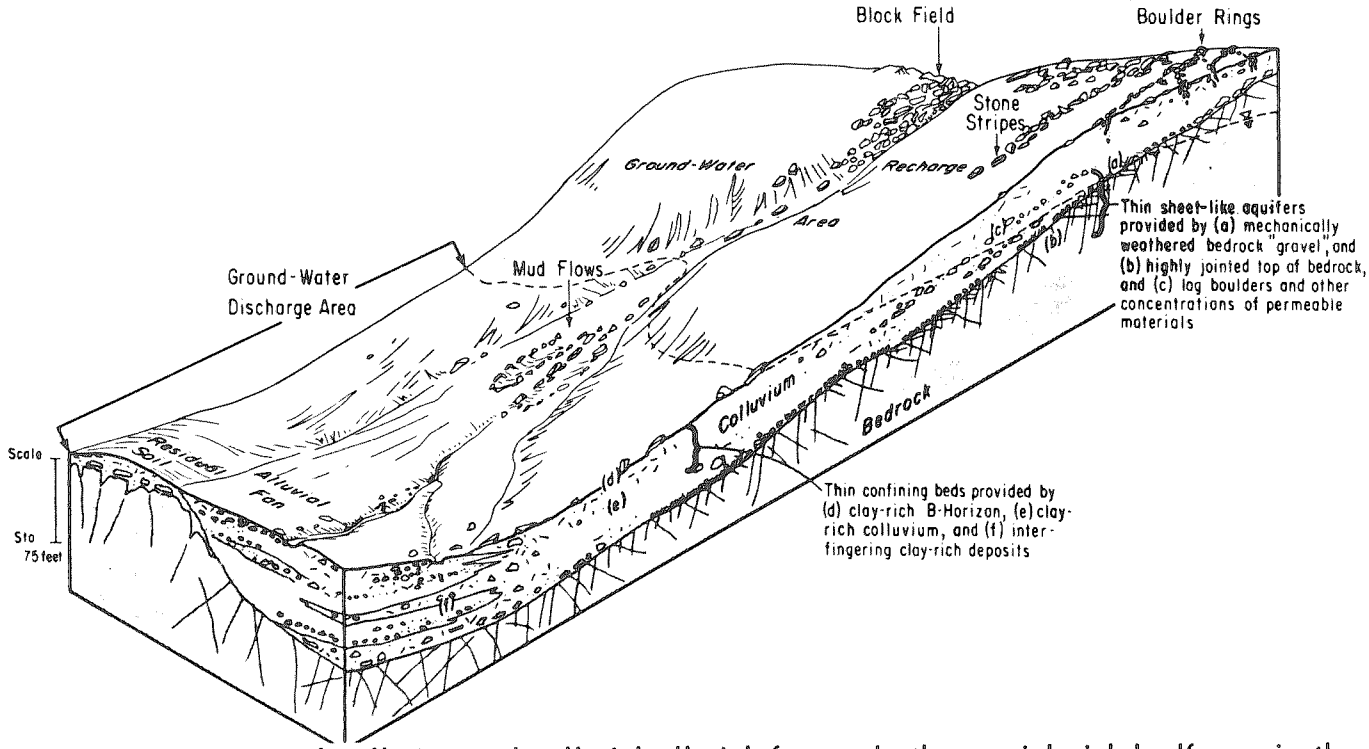

Figure 18. Nature of colluvium and colluvial-alluvial fans and other periglacial landforms in the Ridge and Valley (from Parizek, 1971).

Where the Gatesburg Formation stands in topographic relief above adjacent bedrock units, colluvium may appear as a blanket of surficial sediments of variable thickness (2 to 8 or more feet). In an area in Huntingdon County, southeast of Stop 2, characteristic swell and swail topography post dates this colluvium. Differential dissolution of bedrock has resulted in the development of closed surface depressions with 5 to 10 or more feet of relief. These depressions may be 50 or more feet wide and elongate parallel to regional joint sets. The surficial landform is younger than the thin vaneer of colluvium indicating that regional carbonate rock dissolution has been appreciable since the colluvium was deposited.

Soil characterization studies by Penn State Agronomists are helpful in distinguishing colluvium. Soils of the Meckesville and Laidig groups (Table 1) have a large component of sandstone material in their colluvium; hence, have medium to coarse textures. Soils of the Murrill group are associated with the Laidig and Meckesville groups but are located farther downslope where colluvium extends out over limestone bedrock. The Murrill soils have a significant quantity of limestone residuum mixed into them which accounts for their higher clay contents and fewer rock fragments (Ciolkosz et al., 1979).

The Mertz groups of soils is associated with low ridges and mantles limestone and shale bedrock. They are generally located on the upper side slopes of these ridges and have been less influenced by underlying limestone and shale than the Kreamer and Evendale soils located farther downslope. This makes the Mertz soil slightly coarser textured than the Kreamer and Evendale soils.

Ciolkosz et al. (1979) suggest that the colluvial material was moved and deposited in thinner sheets or flows on the lower ridges than on the higher major ridges. All contain rock fragments derived from up slope bedrock and older colluvium. The fragments are sandstone with some shale in the soils of the Laidig, Meckesville, and Murrill groups and chert in the soils of the Mertz group. The authors characterize rock fragments as follows:

(1) Fragments of chert are usually < 7.5 cm in diameter and equidimensional while sandstone fragments are flat and variable in size,
(2) high concentrations of large sandstone fragments may form pavements on the surfaces of the soils of the Laidig and Meckesville groups, and
(3) the soils of the Murrill group generally have fewer coarse fragments than soils of the Laidig and Meckesville group.

Ciolkosz et al. (1979) report that colluvial soils show a general trend of less thorough leaching from the well-drained to the more poorly drained members of the colluvial soil sequences. This trend has been noted for other soils with fragipans (Peterson et al., 1970) as well as for soils without fragipans (Ranney et al., 1974) Ranney et al. (1974) points out that percent base saturation is a more sensitive indicator of leaching than pH.

Soils of the Laidig and Meckesville groups and the Clarksburg soil have fragipans, though the Murrill soil and Mertz group soils do not (Ciolkosz et al., 1979). The fragipan horizon in the Meckesville and Laidig soils are deeper in the profile than their more poorly drained associates. Ciolkosz et al. (1971) indicates that there is a general trend of increasing fragipan development progressing from well-drained to somewhat poorly drained soils. Fragipans display a firmness, brittleness, and mottling reflecting poor drainage. These soils also show a coarse prismatic structure and higher bulk density than other soils.

Mertz, Kreamer, Evendale, and Murrill soils lack a fragipan, and the Clarksburg, Laidig and Buchanan soils have fragipans. The lack of a fragipan appears to be related to their high clay content hence fine texture, and limestone influence (Ciolkosz et al., 1973).

Although colluvial soils show major textural variations both vertically and laterally, argillic horizon development has altered the texture of the upper meter of the soil by depleting the A and enriching the B horizon with clay (Ciolkosz et al., 1979). They indicate that this clay migration has not obscured the original

textural heterogeneity of the parent material. For example, argillic horizon development is weak to moderate in soils of the Laidig and Meckesville groups and moderate in soils of the Murrill and Mertz groups. The alluviation of clay (< 0.002 mm) from the upper horizons and deposition in the B horizon, presence of clay skins on ped faces and in soil pores all indicate that these colluvial slopes have remained static for a prolonged period and allowed the development of distinct soil profiles.

Further evidence for soil profile development in the distinctive relationship of decreasing expandable-layer silicates (mainly vermiculite) and increasing illite content with depth. Johnson et al. (1963) indicate that this is a useful weathering index for Pennsylvania soils. Illite tends to be converted to illite weathering products or vermiculite and other expandable silicates. The ratio of expandable to nonexpandable materials is used as a weathering index. It is most intense near the surface and decreases to a relatively constant level in the middle and lower parts of the profile. Weathering ratio data also indicate that as soils become more poorly drained, there is a decrease intensity of weathering paralleling the trend of higher base saturation resulting from less thorough leaching.

Time is required for fragipan formation, significant leaching, and clay mineral weathering. Soils with argillic horizon are found on stable landscapes that are known to date back to many thousands of year (Soil Survey Staff, 1975). Ciolkosz et al. (1979) indicate that fragipans in soils also indicate landscape stability. Nearly all transported soils developed on glacial drift of suitable texture have fragipans where as they are absent in recent floodplain soils. Bilzi and Ciolkosz (1977) studied soil development in four floodplain soils ranging in age from 200 to 2000 years BP including the Nolin soil on Spring Creek near Houserville, Pennsylvania (Stop 5).

Soil formed in these alluvial deposits lack a fragipan or an argillic horizon. Both time and landscape stability are required for these to be present. Leaching of soils extensively enough to form ultisoils also requires time and stability as does the observed clay mineral weathering index properties noted. The regular decrease of the lwp: Illite ratio with depth, and its close similarity to that noted for Wisconsinan age till soils of similar drainage and texture indicates that these soils probably date back to Wisconsinan time (Ciolkosz et al., 1979).

Aside from these lines of evidence, other observations support evidence for stability of colluvial slopes and alluvial-colluvial fan complexes. The largest trees show an upright growth position as do stumps related to past timber cutting activities. Railroad and road cuts have remained stable for 100 or more years with some notable exceptions where cuts were placed above shale within groundwater discharge areas (Parizek, 1971). Building, railroads and other structures are rather stable despite the fact that often, no special foundation design precautions were taken. Exposed surfaces of boulders derived from the Oswego and Tuscarora Formations show a weathered, sandy, dull surface character indicating that they have remained upright for a prolonged period compared with their fresher, smoother, and brighter colored undersides. Lichens and lichen rings etched into sandstone surfaces also are evidence of slope stability.

The association of colluvium with other periglacial features such as patterned ground (Walters, 1978; Clark, 1968; Parizek, 1971) boulder fields, grezes litees and involutions (Marchand, 1978) flow lobes and store stripes (Parizek, 1971) and the similarity in soil development between these soils of colluvial deposits and

Wisconsinan glacial till deposits also indicates Wisconsinan periglacial movement and deposition (Parizek, 1971; Marchand et al., 1978; Ciolkosz et al., 1979).

Most likely the last active period of colluviation occurred during the Woodfordian because soils have an appearance not unlike soils developed on Woodfordian tills. In glaciated regions to the northeast of Nittany Valley, Woodfordian till was colluviated and has since been stable long enough to allow profile development.

At least one other major episode of colluvium development is commonly recognized. Where exposures are deep enough and colluvial deposits are well developed, a truncated paleosol of variable thickness sometimes can be observed. This soil has a distinct "Allenwood character". It contains an abundance of clay films and coating on pebbles and cobbles, abundant iron enrichment as coatings on rock fragments and mixed with matrix fines. Distinct weathering rhins on cobbles and pebbles also are noted. The brightness of color and overall appearance of these buried soil deposits strongly suggests that they are truncated paleosols of at least Sangamonian age if not Altonian age. These older colluvial deposits often are thicker than the younger Wisconsinan colluvium that covers them suggesting that residual soil deposits developed before Illinoian glaciation probably were thicker than the soils available for movement during the Wisconsinan or that the Illinoian periglacial climate was more severe and persistant. Illinoian glaciation was more extensive in northeastern Pennsylvania than Wisconsinan glaciation. It would be reasonable to expect more extensive development of colluvial deposits in proglacial settings such as Nittany Valley because of its closer proximity to the Illinoian glacial border than to the Wisconsinan borders.

Older colluvium often shows a sharp contact with younger, dull colluvium that overlies and truncates the paleosol. Elswhere, bright "Allenwood type" soil deposits are included in overlying younger colluvium either as iron coated rock fragments, and rock fragments with weathering rhins (Stop 7). Masses of weathered colluvium also can be contorted or balled up into younger colluvium suggesting that mass movement of soil involved structural development and flow as well as downslope creep of individual rock particles.

Where colluvium overlies the Reedsville and other shales, shale chip gravel deposits sometimes are well developed. They have all the appearances of grezes litees but are usually overlain by more typical sand, silt, clay boulder enriched colluvium. Greze litee requires a periglacial climatic regime. It is interesting to speculate on the timing of these deposits. Greze litee would have to be derived from shale outcrops exposed upslope before more coarse textured sandstone float and matrix fines moved downslope and buried these shale chip deposits. This suggests that the greze litee environment may occur slightly earlier than the environment favoring colluvial development or time was required for colluvium to overwhelm shale exposures that may have stood slightly higher in elevation than adjacent shale surfaces.

The irregular thickness of colluvium noted below water gaps and mountain slopes and below the Salona-Coburn or Reedsville contact, or shales stratigraphically below but upslope from the Old Port Formation indicate that sink and swallow holes existed in these settings before colluvium development. Depressions 20 to 150 feet or more deep and of variable size revealed by water well records had to be filled with colluvium and alluvial deposits before the transport slope was established that allowed for continued downslope movement of colluvium. Post-glacial dissolution of

limestone and inwash and collapse of colluvium into paleokarst channels and voids has occurred since the retreat of the last glacier. Sink- and swallow-hole development is extensive in some cases despite the relative brief period that has elapsed since the retreat of the last glacier 18,000 to 12,000 yrs BP. Some existing sink and swallow holes are 30 to 50 or more feet deep and up to 100 to 300 feet or more in diameter suggesting that some paleokarst sink filling debris must have been flushed into underlying conduits rather than having formed soley as a result of post-Woodfordian limestone dissolution.

Boulder fields and thick colluvium also have been observed draped into karst depressions high on the western flank of Bald Eagle Mountain where the surface watershed area is limited. The McAlevy's Fort-Port Matilda lineament cuts across this portion of the mountain. Sinkholes formed in this setting in post-Woodfordian time most likely were formed by lateral flow of groundwater moving parallel to stratigraphic strike from a larger watershed rather than just from immediate upslope.

Aside from sinkhole collapse, many colluvial-alluvial fan complexes opposite water gaps and blanket type deposits between gaps show gullie development and only minor evidence of stream erosion. Although some of this erosion post dates clear cutting of mountain slopes during the peak of iron mining and early attempts at cultivation of steep mountain slopes, most of this erosion appears to predate European settlement.

Evolution of Nittany Valley

A modified version of Davis' (1889) model for the evolution of Appalachian topography illustrating Nittany Valley is presented in figure 19 (Gardner, 1983). Ciciarelli (1971) elaborated on certain aspects of the initial stages of the model in Sugar Valley. According to Gardner (1983), Ciciarelli's model can be segmented into four convenient stages. The model starts with an initial surface of Tuscarora Sandstone that is folded into anticlines and synclines where anticlines are structurally and topographically the highest point on the land surface. First order consequent streams (streams without tributaries) develop along the flanks of anticlines and drain into larger, consequent streams in synclines. Synclines act as focal points for collection of drainage. Consequent synclinal streams drain to the northeast, down the structural plunge. The Tuscarora is breached by first order streams at the structural culmination along the crest of each anticline. Ciciarelli (1971) has shown that breaching initially occurs at the structural culmination as a result of increased fracture density in that area. The Tuscarora is mechanically weakened and more susceptible to erosional processes. Cliffs form in the Tuscarora and erode headward, exposing the less resistant Juniata. Small drainage basins with subsequent streams develop as the valleys expand in less resistant rock.

In the second stage individual basins are separated by cols of Tuscarora. Drainage divides migrate headward and basins coalesce. As downcutting continues, the Oswego is exposed along the topographically high anticlinal crest and the characteristic double inner and outer ridge takes shape. During the third stage the drainage line which has an exist gap at the lowest base level (furthest down the plunge of each anticline) captures drainage from other subsequent basins. As the Tuscarora and Oswego cliffs erode headward, anticlinal valleys continually gain surface area at the expense of consistantly shrinking synclines. Cambro-Ordovician carbonates are exposed in the anticlinal core. Since carbonates are less resistant than the sandstones, a process of topographic inversion takes place. The limestone

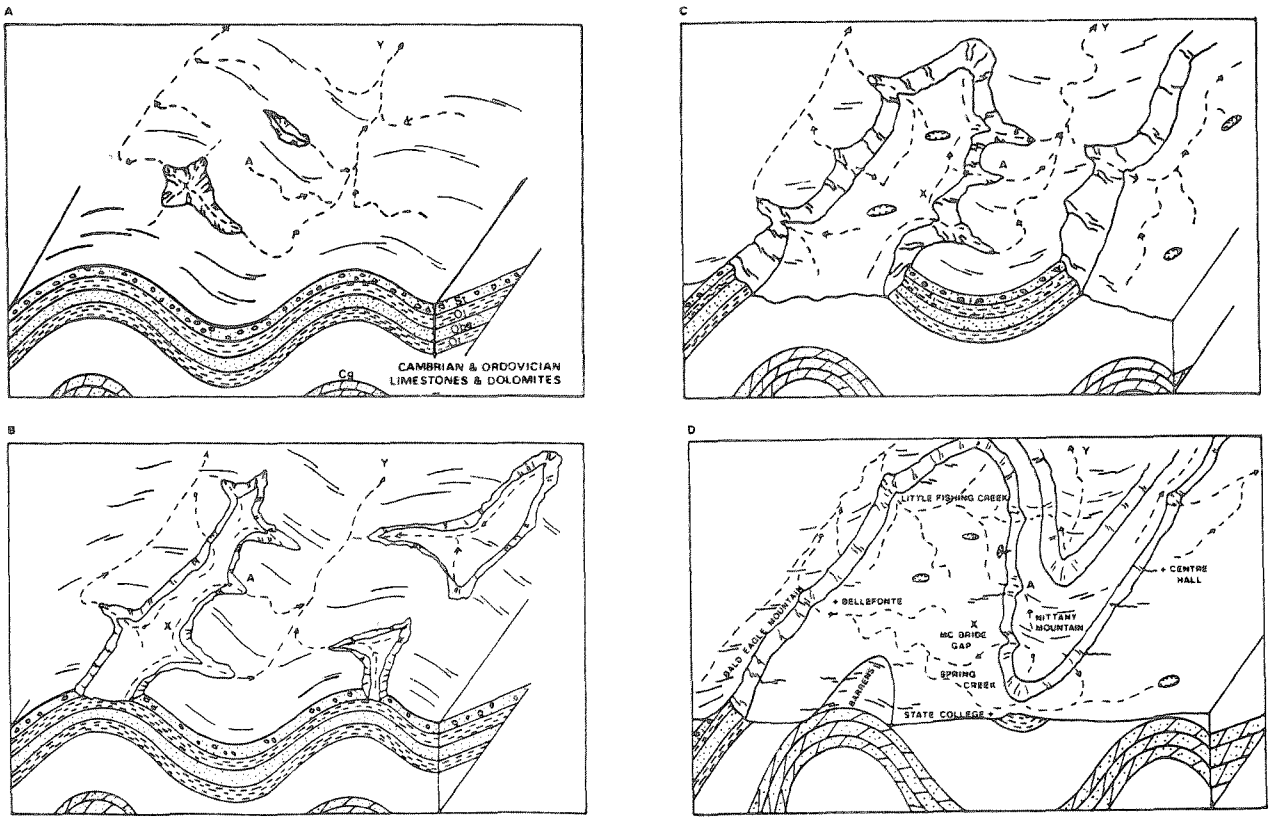

Figure 19. Four stage (a, b, c and d) model for the geomorphic evidence of Nittany Valley. Y is a major synclinal, consequent stream. X is a developing anticlinal subsequent stream. A is a fixed reference point showing the capture of the synclinal stream in part C (from Gardner, 1983).

surface is lowered faster than the adjacent sandstones: the originally higher anticlines become topographic lows while the lower synclines become topographic highs. With continued topographic inversion drainage is diverted from the synclinal axes and an integrated drainage pattern is established in the newly formed anticlinal valley.

During stage four, major drainage lines in Nittany Valley assume their modern configuration. The present surface takes shape and topographic inversion reaches its culmination.

Gardner (1983) points out an interesting complication to this model arising from the fact that downcutting may not have been continuous during all stages of topographic development. According to Davis, the ideal cycle of erosion and peneplaination begins with rapid uplift of a land mass. It is followed by a long period of tectonic quiesence. During the period of stability the landscape progresses through a sequence of stages; youth, maturity, and old age. As the region under consideration passes from one stage to another, its characteristic features gradually change as once mountainous areas have been worn down by erosion. In the end, at old age a flat, featureless plain, or peneplain, develops at the regional base level.

It has been suggested that three major episodes of peneplaination are preserved in the Appalachian Mountains. From oldest to youngest, they are the Schooley,

Harrisburg and Sommerville Surfaces. The evolution of those peneplains from initial Appalachian folds is depicted in Figure 20. The Schooley Surface is reported to be either Cretaceous (Davis, 1889) or early Tertiary (Johnson, 1931) in age, but data are equivocal. It is one of the most complete cycles, effectively beveling the folded sedimentary rocks in Pennsylvania and adjoining areas. One of the most striking attributes of the physiography of the Nittany Valley area, the accordant summits of the Tuscarora Ridges, is thought to have resulted from Schooley peneplaination. Superposition of major drainage lines from the Schooley Surface has been suggested as a mechanism for transverse Appalachian drainage, where streams cut across the stratigraphic and structural strike.

After Schooley peneplaination the area was subjected to renewed uplift and stream downcutting. Valleys were opened in less resistant rock types. Another pose in downcutting resulted in the formation of the Harrisburg peneplain in middle Tertiary time. Thus, the Harrisburg Surface has been termed a partial peneplain. The wide expanse of Nittany, Penns, and adjacent valleys marks the Harrisburg surface. Development of the Sommerville Surface is marked by incised valleys of major drainage lines in Nittany Valley. Further southeast, it is more fully developed on carbonate rocks of the Great Valley. Incision is thought to have occurred in latest Tertiary or Quarternary time.

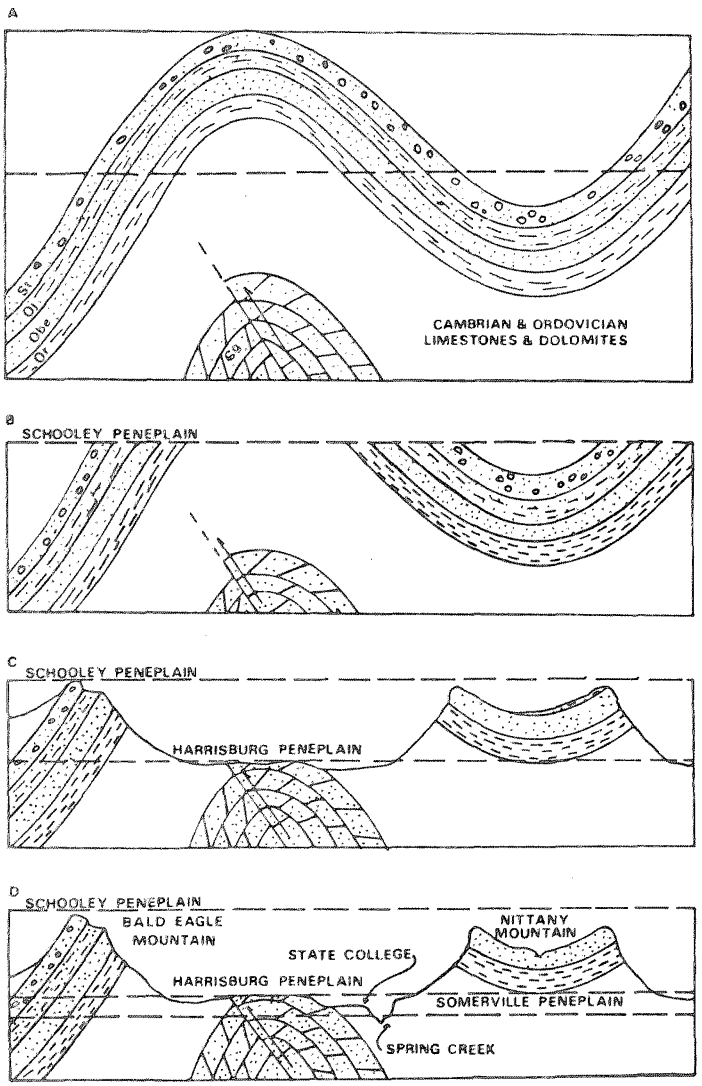

Figure 20. Evolution of the peneplain surfaces of Davis in the Nittany Valley (from T. Gardner, 1983).

Hack (1960) proposed an alternative model for the evolution of Appalachian topography. His theory of dynamic equlibrium maintains that "... the landscape and the processes molding it are considered a part of an open system in a steady state of balance in which every slope and every form are adjusted to every other. Changes in topographic form take place as equlibrium conditions change, but it is not necessary to assume that the kind of evolutionary changes envisioned by Davis ever occur." Differences in topography are thus explainable in terms of differences in the erodibility of bedrock (Ashley, 1935). Using this model, Gardner (1983) shows how the multi-level landscape of Nittany Valley is attributed to differences in bedrock erodibility rather than peneplaination. The Tuscarora and Oswego stand as ridges above the valley floor because they are more resistant. Furthermore, accordant summits of the Tuscarora ridges are a result of the nearly uniform resistance and thickness of that formation. Water gaps are located along zones of structural weakness.

Using the inversion model concept shown in Figure 20, it is interesting to speculate on how the more recent details of landscape evolution might have taken shape through time. If similar relative relief is maintained between more resistant sandstone and shale beds and carbonate rocks to what is observed at present, then the present erosional surface can be incrementally projected upward in space with some degree of confidence at least until the synclinal roots of the next overlying, more resistant clastic sandstone unit is encountered. This exercise is revealing because it shows how drainage divides developed along resistant ridges migrated downdip as the landsurface was lowered. The development of valleys above beds of low resistance and the characteristic trellis pattern emerges. However, a mechanism is required to initiate and maintain transverse valleys, the same problem faced by earlier workers. The answer to this problem was made possible with satellite images and plate tectonics theory.

Some information of carbonate rock removal can be obtained by examination of insoluble residues that remain as residual soils. Interfluves between major drainages are good places to search for thick residual soils especially above bedrock that is deeply underdrained. If the infiltration rate is rapid enough, overland flow and surface erosion are minimized. However, a fine-textured karst is more favorable than a coarse-textured karst because internal soil erosion will be less for the former case. A silty to sandy carbonate bedrock has an added advantage. Clay, silt, and sand tend to bulkup within solution openings thereby reducing the amount of internal soil erosion. Further, as the sand content increases within carbonate rock, secondary porosity and most likely primary porosity also increases (Parizek et. al., 1971). Beds with greater intergranular permeability and porosity for whatever reason, tend to enhance deep dissolution of carbonate bedrock and differential weathering of its surface. This is apparent by studying cores obtained from the Mines and Upper Sandy Dolomite Members of the Gatesburg Formation. As the sand content increases within dolomite, weathering and cavity development increase. Conduits and cavities are best developed in sandy units, and are rarely observed within purer beds of dolomite located either above or below the water table.

Core samples were selected to represent the lithologic variations noted for the Mines Dolomite and Upper Sandy Dolomite Members of the Gatesburg Formation. These were drilled as part of site characterization efforts for Penn State's Living Filter Project (Parizek, 1963, 1974). Samples were crushed to a workable size and 50 gram samples treated with (1:4) HCl for 24 hours, checked for carbonate and retreated one or more additional times as needed. Final residues were rinsed to remove salts and

allowed to stand in water for 24 hours. Samples were oven dried and weighed when dry and cold to obtain the weight percent of the original sample that is insoluble residue (Table 2).

Table 2. Insoluble residue for selected cores taken from the Mines Dolomite and Upper Sandy Dolomite Members, Gatesburg Formation.

Well Number	No. of Samples	Wt. Percent of Insoluble Residue	Depth Internal Sampled and Total Thickness, Ft.
F-1	37	3.79	148.2 to 215 (66.80)
F-2	30	4.46	149 to 204 (55)
F-3	31	3.43	95 to 154 (59)
F-4	21	7.54	167 to 198 (31)
F-5	48	4.86	121 to 183 (62)
F-6	14	19.51	28 to 41 (13)
Totals	181	7.27	286.8 Ft.
Outcrop	16	10.25	Elevation 1066 to 1121 (55 Ft.)

To get an idea of the amount of carbonate rock removed, consider a specific soil column of depth 162 feet to bedrock. Given 7.27% as the average insoluble residue, a bulk density of soil of 1.76 g cm^{-3}, and a density of dolomite bedrock of 2.85 g cm^{-3}, simple mass balance considerations demand that roughly 1400 feet of dolomite must be dissolved to produce the 162 feet of residual soil. This is a minimum figure since removal of soil by solution of some of the components or by piping into solution cavities in the bedrock would demand an even larger bedrock thickness.

The rate of dissolution (karst denudation) of carbonate rock terrains in many parts of the world has been an on-going preoccupation of karst geomorphologists (e.g., Smith and Atkinson, 1976; Jennings, 1981; White, 1984). Factors that enter the denudation rate are temperature, precipitation, and carbon dioxide production in the soil (which in turn is a complicated function of soil character and plant cover). At present, Centre County receives about 40 inches of annual rainfall of which about half is lost to evapotranspiration. Using typical present day data in combination with the denudation rate curve given by White (1984) the rate of removal of carbonate rock is calculated to be 30 mm ka^{-1}. Continuing this exercise in the combination of crude but not totally impossible numbers, the time required for the removal of the 1400 feet of carbonate rock represented by the residual soils is 14

Ma. This would place the oldest surface for which there is any record in the residual soils at mid-Miocene, a result which is at least consistant with geomorphic arguments for the ages of the valley erosion surfaces.

One other result comes out of this number-juggling. There is at present only about 300 feet of relief in the valley uplands. Taken as a proportion of the 14 Ma that they valley floor has been deflating, the oldest cave fragments in the valley uplands cannot exceed 3 Ma, a figure in good agreement with the late Pliocene to early Pleistocene ages proposed for many of the older caves in the Appalachian Highlands.

Evidence of the climatic history of the Appalachians is hidden in the coastal plain and continental shelf sedimentary record, in the geochemical character of residual soils, cave fillings, pollen records of bogs, and in deposits and landforms formed under former climatic conditions. Knowledge of past climates is important to the interpretation of past rates of erosion and sedimentation and landform development.

Sevon (1985) reviewed the evidence for climatic change within the Appalachian region from Late Paleozoic to Recent. Highlights are included here as background.

By Permian time the climate gradually changed from temporate during Carboniferous coal deposition to arid (Schwarzback, 1961). The Triassic is believed to have been arid as well. Hay and others (1982) suggest that local topography may have had a significant influence on basin climatic conditions. They postulate that the average elevation of the Appalachian during Triassic time was about 2 km above base level and sea level may have been 60 m lower than at present. This is in agreement with Hallam (1984). Sevon (1985) believes that much of the Appalachian area was at least semi-arid and because of the general proximity of North America to the equator and its considerable distance from the sea at this time.

Sevon (1985) suggests that arid conditions probably extended into Early Jurassic time as the world climatic trends during the period indicate continued warm temperatures and increased moisture. He further states that some of this humidity may have been due to the Atlantic Ocean that was open during much of the Jurassic. He cites the Cost No. B-3 offshore well and geophysical data that indicate up to a 9 km thick pile of Jurassic sediments were eroded from the Appalachians during this time. Marine coals encountered in this same core suggests that at least coastal areas may have been humid by Late Jurassic (Scholle, 1980). According to Scholle (1977) the COST No. B-2 and COST No. B-3 (Scholle, 1980) sediment records indicate that there was a gradual but definite decrease in clastic input to the eastern seaboard throughout the Cretaceous. This suggests a continued change to a more humid climate, increased vegetation and reduced erosion of coarse clastics. The presence of carbonate sediments rated in the COST wells is offered as further evidence that the landscape was lowered and being eroded at a slower rate than during the Jurassic.

Sevon (1985) indicates that by Late Cretaceous, maximum marine transgression had occurred and climatic moderation spread world wide. Vegetation flourished in both polar regions. Pennsylvania may have been subtropical along with much of the rest of the world. Tropical conditions would have been ideal for intense chemical weathering and slow changes in relief. Such conditions would favor the double plaination surfaces proposed by Budel (1982) and coal swamp in the Great Valley (Pierce, 1965). This would be the time of intense chemical weathering in the Piedmont (Cleaves and Costa, 1979).

Sevon (1985) indicates that the Tertiary climate is known mainly from the Eocene flora of the southeastern states along with some correlations with isolated Eocene floras farther north and the presumed requirements for the formation of the secondary mineral deposits associated with the Harrisburg surface. There were fluctuations of cooling and warming during the Paleocene and Eocene, but overall the trend was one of warming to the Middle Eocene and then gradual cooling to the end of the Eocene (Wolfe, 1978). Bauxitization in the southeastern states and Arkansas occurred in Late Paleocene through Early Eocene (Gordon and others, 1958; Overstreet, 1964) in a humid tropical climate. The climate moderated farther north, but warm humid conditions were present as far north as Vermont where deep weathering produced clay deposits and iron and manganese ores in association with the Brandon lignite (Burt, 1928) on the regional equivalent of the Harrsiburg surface. A cooling trend occurred from the Middle Eocene into the Oligocene (Sevon, 1985).

Sevon (1985) comments on the work of Olsson et. al. (1980) who report that a major lowering of sea level occurred in the Early Oligocene which they postulate correlates with development of glacial ice in the Antarctic as well as general worldwide decline in temperature. There were fluctuations in temperature and moisture during the Oligocene, Miocene, and Pliocene, but in general the overall trend was that of climatic cooling which culminated in the Quaternary with Pleistocene continental glaciation (Blackwelder, 1981; Donnelly, 1982).

The Miocene and Pliocene climatic record is less clear for the Atlantic coastal region. Both arid in the southeast and subtropical conditions as far north as New Jersey have been proposed (Sevon, 1985). By the Pleistocene, colder climates prevailed when at least three major glaciations occurred and possibly a fourth. Watts (1979; 1983) indicate that a tundra vegetation existed up to 100 km beyond the ice boarder about 18,000 years ago. This is when most of the recent periglacial landforms and deposits were formed beyond the Woodfordian glacial border.

We are not in disagreement with Sevon's (1985) summary of the most probable age of the valley upland surface in Nittany and adjacent valleys. He indicates that prolonged physical and chemical weathering during a humid subtropical climate that persisted through Late Cretaceous, Paleocene and Early Eocene produced carbonate valley surfaces of low relief bordered by resistant moutain uplands. This he postulates was the time of thick saprolite development, the formation of thick clay deposits throughout the east coast (Burt, 1928; Potter, 1982; Bridge, 1950) and secondary mineral deposits of iron. Such a climate we believe would help account for the limited amounts of bauxite, thick kaolinite clay and iron deposit observed in the Barrens near State College.

Sevon states that the development of the Harrisburg surface may have occurred over a period that may have been as long as 45 m.y. Our own insoluble residue thickness data and estimated rate of carbonate rock dissolution data suggests a conservative age for the valley upland of 14 million years assuming no solution removal or erosional losses of this residum which cannot be the case.

Olsson et. al. (1980) suggestion of an early Oligocene lowering of sea level may have helped to initiate incision of the Susquehanna, Potomac and Delaware Rivers and their tributaries. We are not aware of any evidence for a mid-Tertiary regional uplift in the Appalachian region that may have initiated this incision.

Pre-Sangamonian soil terrace levels just above the modern flood plain level for local streams incised in the valley upland suggest that these valleys were deeply

incised by mid-Tertiary time if not during or just before the onset of Pleistocene glaciation about 350,000 years ago.

This review of climatic data for the eastern U.S. is helpful to the present discussion. Subtropical conditions during Late Cretaceous at least through Middle Eocene are indicated by more than one line of evidence; vegetation, soil development, lignite beds and occurrence of mineral deposits. The thick kaolinite clay deposits in the Barrens region most likely reflect such a time of intense chemical weathering.

Concluding Remarks

The mechanism of carbonate rock denudation includes attack at the soil-rock contact as well as internal dissolution within the rock mass itself. This process produces residual soil that is inverted from is normal stratigraphic sequence. Insoluble residue just released is added to the regoliths from the bottom up with the oldest soil being present at the top. Hence, we are looking at the residuum of rock that has long since been dissolved away, often under climatic conditions vastly different than at present. Residual soils documented to be > 100 to 365 feet thick, may be weathering products that have been accumulating since Early to Late Tertiary if not longer. This is suggested by the great thickness of regolith present, the slow rate of carbonate rock dissolution, say about 40 mm/1,000 years, and the fact that some insoluable residue has dissolved or been eroded away during this period.

The presence of bauxite, thick kaolinite clay and iron ore deposits associated with these residual soils suggests a more humid and tropical climate favorable to laterite production. The Sangamon interglacial also has produced a soil profile far more extensively developed when compared with soils developed on Wisconsinan glacial and periglacial deposits but it is unlikely that this weathering interval contributed much to the overall development of thick residual soils observed in the Barrens region. Colluvium with a buried Sangamon paleosol underlie colluvium most likely of Woodfordian age. These inturn overlie thick residual soils along the lower flanks of mountain slopes which predate Illinoian glaciation and the Pleistocene.

These thick residual soils demand favorable conditions for their preservation: (1) remoteness from the coast, (2) separation from ultimate baselevel by a number of local baselevels provided by resistant sandstones, (3) location on interflues between drainages that have maintained their basic position on the landscape for prolonged periods of time, (4) master streams fixed along vertical planes of weakness for prolonged periods, (5) a deep regional water table and (6) karst conditions that favor internal drainage.

Aside from local pyricies, master streams must have occupied nearly their same water gap portions as hundreds if not thousands of feet of carbonate rock have been removed since the breaching of the Nittany anticlinorium.

Lovers of Nittany Valley will be pleased to learn that the Valley has widened through geologic time as surface water divides migrated in the down dip direction, i.e., Bald Eagle Mountain has remained nearly in its present position for a longer period controlled by its near vertical bedrock dips, Nittany Mountain has grown narrower and Tussey Mountain has migrated eastward. Nothing for the distant forseeable geolgoical future should change this condition because carbonate rocks

under lie Nittany and Penns Valleys for depths well in excess of several thousand feet or well below sea level. These rocks will be deeply eroded only if the Appalachian Mountains are uplift above present base level.

In the meantime, several mechanism are in operation. The valley upland can be lowered to the local base level controlled by the elevation of sandstones in Milesburg and Curtin Gaps, Jacksonville-Howard Gap, the Gap near Lock Haven, and Water Street. Ultimately this would produce a low relief karst plain, bordered by moutains. In the mean time, Spring and Bald Eagle Creeks, the Juniata River, etc., will continue to downcut as Pleistocene-aged sediments continue to be removed from storage and rapids on the Susquehanna River are slowly eroded away. Continued down cutting of the local drainage network should help to maintain relief between these incised streams, the valley upland and mountain ridges, and a deep water table and internal drainage. Sea level changes resulting from ice cap retreat or renewed glaciation would have little influence on Nittany Valley.

Record of such future events will be recorded in residual and transported soil deposits that are more likely to be preserved within deep karst depressions developed in the top of carbonate bedrock in a manner similar to the present soils that are preserved in the region.

Table 3. Summary of geological events and possible ages

Time and Climate	Features
Holocene (warming trend)	Accelerate sinkhole development due to storm runoff and construction activities 0 to 50 YBP.
	Accelerate sheet and guille erosion, extensive charcoal production and farming 100 to 220 YBP; cyclic sedimentation due to ore washing.
	C14 200 to 2,000 YBP on flood plain deposits.
	Cave travertines $\leq$6,000 YBP.
	Soil development on colluvium 15,000 to present.
Woodfordian Glaciation (cold)	Extensive colluvium and colluvial-alluvial fan complex development on mountain slopes, water gaps and valley upland surfaces; stone stripes, boulder fields, sorted polygons, formed.
(warming trend)	Tundra vegetation to 100 km beyond glacial boarder. Formation of Bear Meadows. Buried soil on Spring Creek(?)
Altonian Glaciation (cold)	Colluvium development (?) and related periglacial landforms and deposits; accelerated erosion.
Sangomonian (warmer than present)	Extensive development of soil on colluvium and alluvium and sapolite ("Allenwood" in character).
	Terrace development along major drainages;
	Accelerated development of cave networks graded to terrace levels.
	Extensive development of speleothems 70,000 to 200,000 YBP.

Table 3. (Continued)

Time and Climate	Features
Illinoian Glaciation (cold)	Extensive colluviation of valleys, mountain slopes and water gaps. Start of development of diamictions. Lake Lesley I; elevation ~ 1110 ft. Cave passage development graded to valley fill.
Early Pleistocene (cooling trend with interglacials)	Deposits and landforms not documented. 800 to 850 ft. elev. cave passages. 900 to 950 ft. elev. cave passages. 1000 to 1100 ft. elev. cave passages. 1200 ft. elev. few remnant cave passages, most likely less than 3 MYBP.
Late Pliocene-Early Pleistocene (cooling trend)	Magnetic reversal in Mammoth Cave, Kentucky.
Mid-Miocene (minimum age)	165 feet of residual soil development in Barrens region, at least 14 MYBP. 365 feet of sapolite even older.
Oliogocene-Pliocene(?) (cooling trend mid-Eocene to Oliogocene)	Incision of master streams; Bald Eagle, Spring and other creeks; start of extensive soil erosion within the Great Valley (?).
Early Oliogocene Late Eocene (cooling trend)	Drop in sea level, ice cap in Antartica.
Early Eocene (warming trend, tropical to subtropical)	Bauxite formation in Ankansas, warm and humid.
Late Paleocene to Early Eucene	
Late Cretaceous (Subtropical to tropical)	Maximum marine transgression; formation of thick sapolite, kaolonite, bauxite, iron ore deposits. Development of Little Juniata River (?); lignite outlier near Chambersburg, PA.
Jurassic	Extensive erosion of Appalachian Mountains; up to 9 km thick sediment wedge on the continental shelf and slope.

Table 3. (Continued)

Time and Climate	Features
Early Jurassic (Arid to semi-arid)	
Triassic (Arid to semi-arid)	Rifting; development of valleys.
Permian	Appalachian Orogeny; extensive folding and faulting of the Ridge and VAlley region.
Early Permian	Possible deposition of terrestrial sediments.
Pennsylvanian (Temperate)	Deposition of coal measures of marine, brackish and fresh water origin.
Cambrian-Pennsylvanian	Development of Appalachian geosyncline.

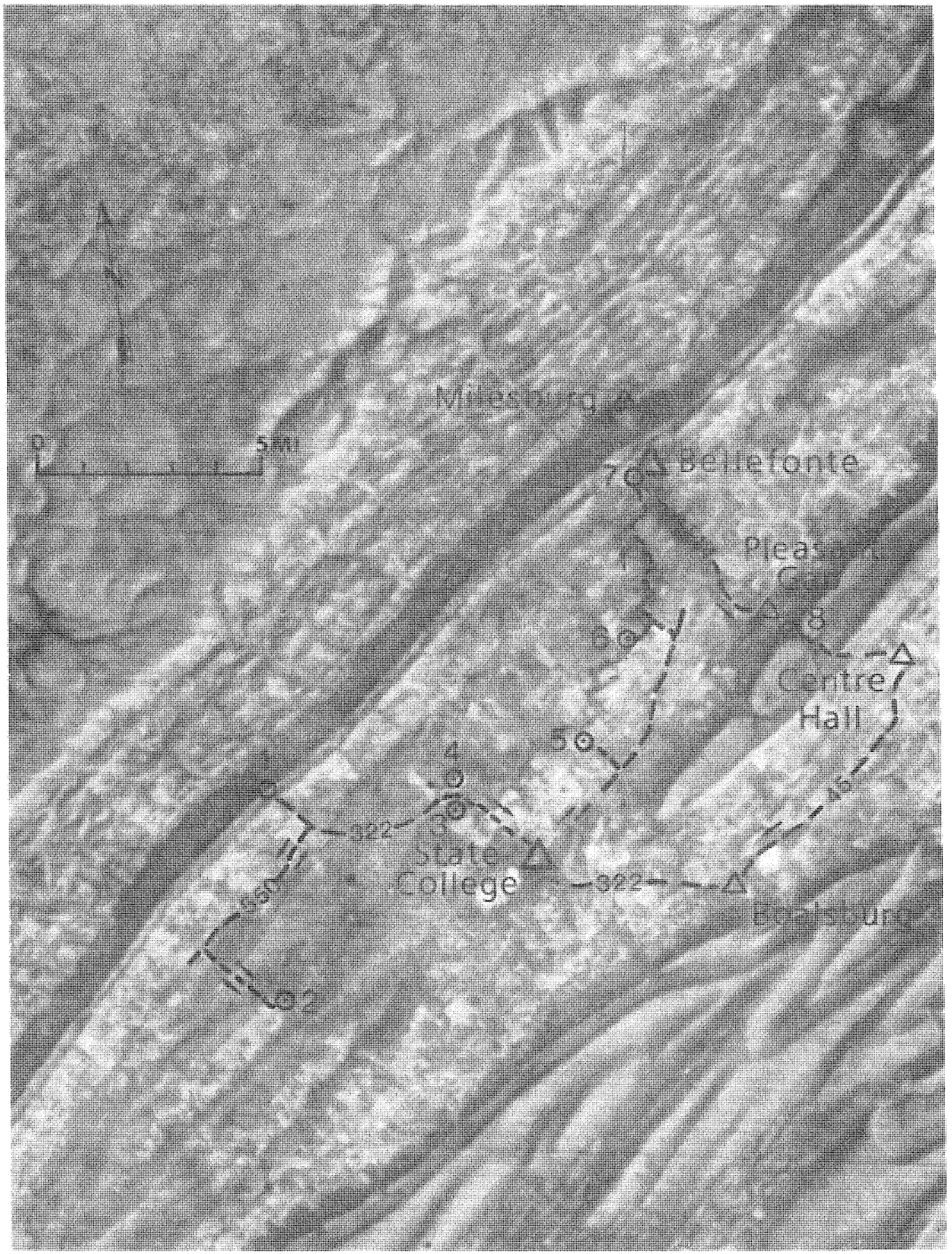

Stop localities for Field Trip #3, plotted on Landsat Image of part of Central Pennsylvania (scene E 1243-15253, band 7, of March 23, 1973).

FIELD TRIP #3

FIELD GUIDE - ON THE SOILS AND GEOMORPHIC EVOLUTION OF NITTANY VALLEY

R. R. Parizek and W. B. White
Field Leaders

0.0 Holiday Inn. Turn left and follow Atherton Street, Route 322 to the northwest.

0.6 Westerly Parkway. These shallow tributary valleys to the Spring Creek drainage are all underdrained even before the installation of streets and storm drains. The storm drain systems in this part of State College are discontinuous. They drain into sinkholes. Natural conduit systems are used as an essential part of the storm drain. The water ultimately resurges as springs in Walnut Spring Park and in Thompson Spring on the eastern side of State College.

1.5 College Avenue. Cross Route 26 and continue west on Route 322.

2.7 Big Hollow. The main underdrained tributary of the State College area. Water table maps indicate a groundwater trough paralleling Big Hollow some 100 feet below the valley bottom.

4.2 Park Forest Village. We are here crossing the northern end of Gatesburg Ridge, underlain by the Gatesburg dolomite with thick, low-organic-content residual soils. The site of the former State College land fill lies on these residual soils just to the right of the Highway. The stands of oak that shade the Park Forest Village housing development are typical of the plant cover supported by the Gatesburg soils.

5.3 Cross State College By-Pass.

7.5 Matternville. Cross Route 550 and continue up Bald Eagle Ridge on Route 322. The rocks exposed are first the Oswego or Bald Eagle sandstone and then the red Juniata shales and siltstones.

8.3 Skytop. STOP 1.

From this vantage point one sees the transition from the Valley and Ridge Province to the Allegheny Plateau Province. The bedrock under foot is the Silurian Tuscarora sandstone. The lower Devonian Helderberg limestones and Oriskany sandstone crop out near the base of the ridge. Bald Eagle Creek flows on a valley of Devonian shales. The foreridges of the Allegheny front are the Catskill red shale and the Pocono sandstone. The top of the escarpment is supported by the Pennsylvanian Pottsville sandstone.

The escarpment itself is a major geomorphic feature that can be traced, at continuously rising elevation southward through Maryland and West Virginia to become the Cumberland Escarpment of Tennessee.

From Skytop, return eastward on Route 322.

9.1 Intersection with route 550. Turn right onto Route 550.

11.6 Turn left onto dirt road that crosses the valley toward Gatesburg Ridge.

12.7 Clay pits and related mining activity in Gatesburg residual soils. [STOP 2].
Return along same route.

13.8 Route 550. Turn right.

16.3 Route 322 intersection. Turn right, eastward.

18.2 Leave Route 322 and continue straight ahead onto the State College By-Pass.

The By-Pass is cut through the Gatesburg Ridge. Residual soils are exposed where construction work is underway on a new interchange.

22.6 Exit the By-Pass onto Park Avenue Extension (Pennsylvania State University Exit).

The lands along Park Avenue are part of the University farms underlain mainly by Ordovician dolomites.

23.8 Traffic light. Turn right onto Fox Hollow Road.

24.6 Turn left onto blacktop road just past National Guard Armory and before crossing under the By-Pass.

25.2 Turn right onto gravel road just past the fire school.

25.3 Take left fork of gravel road.

25.4 Farm gate on right. Barrow pit exposing residual soils is on the hillside beyond [STOP 3].

The bulk of the soil exposed at this location is residual from the Gatesburg formation. Relict bedding structures are visable. Late Pleistocene soils are visible as a thin veneer capping the sequence.

Backtrack to Fox Hollow Road.

25.5 Turn left on blacktop road. The University water supply is obtained from wells drilled in the Gatesburg aquifer along this hollow and its tributaries. In general, the Gatesburg is a productive aquifer in the State College Region because of its high primary permeability through sandy units and vuggy openings.

26.1 Fox Hollow Road. Turn left.

27.1 Turn left into Toftrees Development. Follow the main street, Toftrees Avenue.

27.4 Turn right onto gravel lane which leads immediately to the gate at State Gamelands site [STOP 4].

This site is one of two used for disposing of sewage plant effluent by the Living Filter concept. The Gatesburg soils are thick, the water table is some 200 feet below the land surface. The shallow depressions are slump features in the soils which hold perched ponds of water.

Backtrack.

27.6 Fox Hollow Road. Turn right.

29.5 Traffic light at Park Avenue Extension. Turn left.

30.3 Turn right onto State College By-Pass.

View of Nittany Mountain is good from the By-Pass. The nose of Nittany Mountain is the steep outer slope formed by the northeast-plunging syncline.

31.6 Traffic light at intersection with Route 26, Benner Pike. Turn left.

32.3 Traffic light. Turn left onto Houserville Road.

32.8 Turn left into Spring Creek Park.

32.9 Spring Creek Park. LUNCH. [STOP 5].

Spring Creek here flows on a narrow flood plain not far below the valley uplands. A terrace level thought to be Sangamon age lies only a short distance above the Creek. A buried soil can be observed here.

Return to Benner Pike.

33.5 Traffic light at Benner Pike. Turn left.

34.4 Y-intersection at Nittany Mall shopping center. Keep left on Route 150.

The Nittany Mall provides an interesting example of environmental problems with land development in karst areas. The large extent of roof and parking lot concentrates the runoff and enhances sinkhole development at the margins of the area. Much of the runoff is concentrated in a sinkhole visable in the arms of the Y of the highway intersection. Other sinkholes parallel the flank of Nittany Mountain. Many of these are filled with trash. The sinkholes provide pathways for the injection of solid wastes into the conduit system carrying groundwater below.

Benner Pike crosses the valley uplands diagonally between the Nittany Mall and Bellefonte. Here the Gatesburg Ridge is not prominent and there is a uniform upland surface, mostly on the Ordovician dolomites spanning the valley between Nittany Mountain and Bald Eagle Ridge.

38.2 Turn left on black top road to Fisherman's Paradise.

38.8 T-intersection. Turn left.

39.4 Parking area at Fisherman's Paradise [STOP 6].

Spring Creek has here downcut into a deep gorge below the flood plain at Spring Creek Park. The creek provides a pronounced trough toward which groundwater discharges as a series of springs emerging from the carbonates along the banks of the creek. Benner Spring is one of the larger.

Return down Spring Creek.

40.0 Continue straight at the intersection.

The floor of the Spring Creek gorge has bits of floodplain here and there as the valley widens and narrows. This suggests a stable location of the creek for some time, presumably due to the damming of the creek by the resistant Tuscarora quartzite which the stream must cross at Milesburg Gap. The creek is spring-fed and thus maintains a stable flow throughout the year.

41.7 Intersection. Turn right.

42.1 Intersection with Route 550. Turn right.

42.9 Intersection with Route 150 in Bellefonte. Turn left.

43.3 Big Spring rise pool behind the wall on the left. Big Spring is the largest carbonate spring in the valley with an estimated discharge of 30 cfs. The water has unusually low hardness for a carbonate spring, 130 ppm as $CaCO_3$. The spring provides the water supply for Bellefonte and for the Corning Glass Works near the Nittany Mall.

43.4 Traffic light at High Street. Continue straight ahead.

Beyond the High Street intersection, Spring Creek flows in an artificial channel just to the left of the roadway. Comparison of the flow seen here with the flow in Spring Creek gorge gives some impression of the contribution of Big Spring and Logan Branch to the overall runoff from the valley.

43.8 Intersection. Continue straight ahead.

44.9 Entering Milesburg Gap through Bald Eagle Ridge. There are only six feet or so of alluvial sediment overlying bedrock in the stream channel. Steeply dipping beds of Bald Eagle sandstone and Tuscarora quartzite plunge below stream level and form a dam which resists downcutting of the stream behind it.

45.3 Fill bank exposing colluvial soils. Pull off on right [STOP 7].

Return through Milesburg Gap.

46.7 Intersection with Rt. 144. Keep right on Route 150.

47.2 High Street intersection. Straight ahead.

47.4 Intersection. Turn left to Route 144.

47.5 Intersection. Continue straight ahead on Route 144.

48.3 Cerro metal plant. The cut to the left of the road is one of the best exposures of the Gatesburg dolomite. The characteristic sandy beds and vuggy texture are clearly visable here.

49.3 Axemann Spring to left of road in stone springhouse. This has been a water supply spring in the past and may be used again.

Route 144 follows the valley of Logan Branch which here appears to have a meandering course. Close examination of the stream pattern on topographic maps or air photographs reveals that the stream is flowing diagonal to the regional fracture system and thus pursues a zig-zag course with individual straight valley segments oriented along fracture traces.

Like the other tributaries to Spring Creek, Logan Branch is spring-fed. The source of the Branch is a group of springs west of Pleasant Gap.

51.7 Traffic light at intersection with Route 26 in Pleasant Gap. Turn left on Route 26.

52.2 Traffic light. Turn right on Harrison Road.

52.5 Hildas Beauty Parlor pull-off on left [STOP 8].

Gap Run sinks in its bed behind the Beauty Parlor. Like most other swallow holes in the valley, Gap Run sinks into the Champlainian limestone. There is no stream channel downstream from the swallow hole. This implies that all sediment transported from the mountain flanks must be carried by the conduit system. It also has implications for the behavior of large floods that overwhelm the swallow hole.

Continue up Harrison Road toward Nittany Mountain.

52.8 Intersection with Route 144. Turn left up the gap.

In spite of the unreliability of the supply, mountain streams continue to be prized as water supplies because of low hardness and good chemical quality. The pipes seen along the highway are part of the collector system for the Pleasant Gap Water Company. The actual collectors are in the small tributary valleys away from the influence of the highway.

Much of this roadway was washed out in the Hurricane Agnes storm of 1972. The concrete retaining walls and new fill structures were emplaced at that time.

55.1 Nittany Mountain summit. There is an excellent view into Penns Valley in an interfluve area between the Spring Creek drainage to the west and the Penns Creek drainage to the east. The valley floor is beveled across folded carbonate rocks and represents the Harrisburg surface at about 1300 feet elevation. The excellent preservation of the surface is due partly to its location in an interfluve area and partly to karstic drainage so that there is no dissection of the valley uplands.

56.3 Borough of Centre Hall. There is a typical large sinkhole in the Champlainian limestone to the left of the highway at the foot of the mountain.

57.7 Traffic light. Intersection with Route 45 in Old Fort. Turn right onto Route 45.

Somewhere along the highway is the subsurface divide. To the east, underground flow is to the Penns Cave Rising or to the Spring Mills spring

some five miles away. To the west the drainage rises in the Linden Hall springs. A few miles west of Old Fort the trace of a westward-trending dry valley appears.

62.6 Upper Linden Hall Springs to the right. These have shallow rise pools in the valley floor with no enterable conduits. The discharge from the springs is part of the Spring Creek drainage.

65.1 Intersection with Route 322 in Boalsburg. Turn right and follow Route 322 back to State College.

68.0 Holiday Inn on left. End of field trip.

REFERENCES FOR FIELD TRIP 3

Ashley, G. H., 1935, Studies in Appalachian mountain sculpture: Geological Society of America Bulletin, v. 46, p. 1395-1436.

Baxter, J. E., 1983, The Quaternary geology of the West Branch of the Susquehanna River valley near Lock Haven, Pennsylvania: University Park, Pennsylvania State University, M.S. thesis, 135 p.

Berg, T. M., Edmunds, W. E., Geyer, A. R., and others, compilers, 1980, Geologic map of Pennsylvania: Pennsylvania Geological Survey, 4th ser., Map 1, scale 1:250,000, 3 sheets.

Bilzi, A. F., and Ciolkosz, E. J., 1977, Time as a factor in the genesis of four soils developed in Recent alluvium in Pennsylvania: Soil Science Society of America Journal, v. 41, no. 1, p. 122-127.

Blackwelder, B. W., 1981, Stratigraphy of Upper Pliocene and Lower Pleistocene marine and estuarine deposits of northeastern North Carolina and southwestern Virginia: U.S. Geological Survey Bulletin 1502-B, 16 p.

Bridge, J., 1950, Bauxite deposits of the southeastern United States, In Snyder, F. G., ed., Symposium on mineral resources of the southeastern United States: Knoxville, Tennessee University Press, p. 170-201.

Bucek, M. F., 1975, Pleistocene geology and history of the West Branch of the Susquehanna River valley near Williamsport, Pennsylvania: University Park, Pennsylvania State University, Ph.D. thesis, 197 p.

Budel, J., 1982, Climatic geomorphology: Princeton, New Jersey, Princeton University Press, 443 p.

Burt, F. A., 1928, The origin of the Bennington kaolins: Report of the State Geologist of Vermont 1927-1928, v. 16, p. 65-84.

Canich, M. R., 1976, A study of the Tyrone-Mount Union lineament by remote sensing techniques and field methods: University Park, Pennsylvania State University, M.S. thesis.

Ciciarelli, J. A., 1971, Geomorphic evolution of anticlinal valleys in central Pennsylvania: University Park, Pennsylvania State University, Ph.D. thesis, 98 p.

Ciolkosz, E. J., Petersen, G. W., and Cunningham, R. L., 1980, Soils of Nittany Valley, In Ciolkosz, E. J., and others, Soils and geology of Nittany Valley: Pennsylvania State University Agronomy Series 64, p. 24-52.

Ciolkosz, E. J., Petersen, G. W., Cunningham, R. L., and Matelski, R. P., 1979, Soils developed from colluvium in the Ridge and Valley area of Pennsylvania: Soil Science, v. 128, no. 3, p. 153-162.

Clark, G. M., 1968, Sorted patterned ground, New Appalachian localities south of the glacial border: Science, v. 161, p. 255-256.

Cleaves, E. T., and Costa, J. E., 1979, Equilibrium, cyclicity, and problems of scale--Maryland's Piedmont landscape: Maryland Geological Survey Information Circular 29, 32 p.

Craig, R., 1978, A simulation model of landform evolution: University Park, Pennsylvania State University, Ph.D. thesis, 536 p.

Davis, W. M., 1889, The rivers and valleys of Pennsylvania: The National Geographic Magazine, v. 1, no. 3, p. 183-253.

Davies, W. E., 1960, Origin of caves in folded limestone: National Speleological Society Bulletin, v. 22, pt. 1, p. 5-18.

Dayton, G. O., and White, W. B., 1979, The caves of Centre County, Pa.: Mid-Appalachian Region, National Speleological Society Bulletin 11, 126 p.

Donelly, T. W., 1982, Worldwide continental denudation and climatic deterioration during the late Tertiary: Evidence from deep-sea sediments: Geology, v. 10, p. 451-454.

Epstein, J. B., 1966, Structural control of wind gaps and water gaps and of stream capture in the Stroudsburg area, Pennsylvania and New Jersey: U.S. Geological Survey Professional Paper 550-B, p. B80-B86.

Fenneman, N. M., 1938, Physiography of eastern United States: New York, McGraw-Hill, 714 p.

Gardner, T. W., 1980, Geomorphology of Nittany Valley, in Ciolkosz, E. J., and others, Soils and geology of Nittany Valley: Pennsylvania State University Agronomy Series 64, p. 52-75.

Gold, D. P., and Parizek, R. R., 1976, Field guide to lineaments and fractures in central Pennsylvania: University of Delaware, International Conference on the New Basement Tectonics, 2nd, 75 p.

Gold, D. P., Parizek, R. R., and Alexander, S. S., 1973, Analysis and applications of ERTS-1 data for regional geological mapping, in Freden, S. C., and others, eds., Symposium on Significant Results Obtained from the Earth Resources Technology Satellite-1: NASA SP-327, VIA, p. 231-246.

_____, 1974, Application of remote sensing to natural resource and environmental problems in Pennsylvania: Earth and Mineral Sciences, v. 43, no. 7, p. 49-53.

Gordon, M., Jr., Tracey, J. I., Jr., and Ellis, M. W., 1958, Geology of the Arkansas bauxite region: U.S. Geological Survey Professional Paper 299, 268 p.

Grim, R. E., 1953, Clay mineralogy: New York, McGraw-Hill, 384 p.

Gwinn, V. E., 1964, Thin-skinned tectonics in the Plateaus of northwestern Valley and Ridge province of the central Appalachians: Geological Society of America Bulletin, v. 75, p. 127-149.

_____, 1970, Kinematic patterns and estimates of lateral shortening, Valley and Ridge and Great Valley provinces, central Appalachians, south-central Pennsylvania, in Fisher, G. W., and others, eds., Studies of Appalachian geology: central and southern: New York, Interscience Publishers, Division of John Wiley and Sons, p. 127-146.

_____, 1964, Thin-skinned tectonics in the Plateaus of northwestern Valley and Ridge province of the central Appalachians: Geological Society of America Bulletin, v. 75, p. 127-149.

Hack, J. T., 1960, Interpretation of erosional topography in humid temperate regions: American Journal of Science, v. 258-A, p. 80-97.

_____, 1979, Rock control and tectonism--their importance in shaping the Appalachian highlands: U.S. Geological Survey Professional Paper 1126-B, p. B1-B17.

_____, 1982, Physiographic divisions and differential uplift in the Piedmont and Blue Ridge: U.S. Geological Survey Professional Paper 1265, 49 p.

Hallam, A., 1984, Pre-Quaternary sea-level changes, in Wetherill, G. W., and others, eds., Annual review of earth and planetary sciences: Palo Alto, California, Annual Reviews, Inc., v. 12, p. 205-243.

Harmon, R. S., Thompson, P., Schwarcz, H. P., and Ford, D. C., 1978, Late Pleistocene paleoclimates of North America as inferred from stable isotope studies of speleothems: Quaternary Research, v. 9, p. 54-70.

Hay, W. W., Behensky, J. F., Jr., Barron, E. J., and Sloan, J. L., II, 1982, Late Triassic-Liassic paleoclimatology of the proto-central North Atlantic rift system: Palaeogeography, Palaeoclimatology, Palaeoecology, v. 40, p. 13-30.

Hunter, P. M., and Parizek, R. R., 1979, A structurally disturbed zone in central Pennsylvania, surface expression of a domain boundary: University of Maryland, International Conference on the New Basement Tectonics, 2nd, Contribution 7.

Jennings, J. N., 1983, Karst landforms: American Scientist, v. 71, p. 578-586.

Johnson, D., 1931, A theory of Appalachian geomorphic evolution: Journal of Geology, v. 39, p. 497-508.

Johnson, L. J., Matelski, R. P., and Engle, C. F., 1963, Clay mineral characterization of modal soil profiles in several Pennsylvanian counties: Soil Science Society of America Proceedings, v. 27, p. 568-572.

Kashatus, G. P., 1984, A field study of alluvial terraces along a portion of Bald Eagle and Spring Creek in Centre County, PA: University Park, Pennsylvania State University, Honors Senior thesis, 29 p.

Kowalik, W. S., and Gold, D. P., 1976, The use of Landsat-1 imagery in mapping lineaments in Pennsylvania: International Conference on New Basement Tectonics, 1st, Proceedings, Utah Geological Association Publication 5, p. 236-249.

Lattman, L. H., and Parizek, R. R., 1964, Relationship between fracture traces and the occurrence of ground water in carbonate rocks: Journal of Hydrology, v. 2, p. 73-91.

Leverett, Frank, 1934, Glacial deposits outside the Wisconsin terminal moraine in Pennsylvania: Pennsylvania Geological Survey, 4th ser., General Geology Report 7, 123 p.

Mackin, J. H., 1938, The origin of Appalachian drainage--a reply: American Journal of Science, v. 236, p. 17-53.

Marchand, D. E., 1978, Quaternary deposits and Quaternary history of central Pennsylvania, In Marchand, D. E., and others, Quaternary deposits and soils of the central Susquehanna Valley of Pennsylvania: Pennsylvania State University Agronomy Series 52, 89 p.

Meyerhoff, H. A., 1972, Postorogenic development of the Appalachians: Geological Society of America Bulletin, v. 83, p. 1709-1728.

Meyerhoff, H. A., and Olmsted, E. W., 1936, The origins of Appalachian drainage: American Journal of Science, v. 232, p. 21-42.

Mittot, G., 1942, Relations entre la constitution et da genese des roches sedimentairies argileuses: Nancy, France, Geol. Applig. et Prosp. Mines, v. 2.

Nelson, J. G., 1963, Pre-Illinoian glaciation in central Pennsylvania: Canadian Geographer, v. 7, no. 3, p. 145-147.

Nickelsen, R. R., 1963, Tectonics and Cambrian-Ordovician stratigraphy, central Pennsylvania: Pittsburgh Geological Society and Appalachian Geological Society, Guidebook, 129 p.

Olsson, R. K., Miller, K. G., and Ungrady, T. E., 1980, Late Oligocene transgression of Middle Atlantic coastal plain: Geology, v. 8, p. 549-554.

Overstreet, E. F., 1964, Geology of the southeastern bauxite deposits: U.S. Geological Survey Bulletin 1199-A, 19 p.

Parizek, R. R., 1971, Hydrogeologic framework of folded and faulted carbonates, In Hydrogeology and geochemistry of folded and faulted carbonate rocks of the central Appalachian type and related land use problems: Pennsylvania State University, Mineral Conservation Series, Circular 82, p. 9-20, 28-64.

_____, 1971, Impact of highways on the hydrogeologic environment, In Coates, D. R., ed., Environmental geomorphology: Binghamton, State University of New York, Annual Geomorphology Symposia Series, 1st, Binghamton, N. Y., 1970, p. 150-159.

_____, 1974, Suitability of Pennsylvania State Gameland 176 for the expansion of sewage effluent by spray irrigation: Pennsylvania State University, Office of Maintenance and Operations, 400 p.

_____, 1975, On the nature and significance of fracture traces and lineaments in carbonate and other terranes, In Karst hydrology and water resources; v. 1, Karst hydrology: Ft. Collins, Colorado, Water Resources Publications, Proceedings of the U.S.-Yugoslavian Symposium, Dubrovnik, June 2-7, 1975.

Parizek, R. R., Kardos, L. T., Sopper, W. E., and others, 1967, Waste water renovation and conservation: Pennsylvania State University Studies 23, 71 p.

Petersen, G. W., Ranney, R. W., Cunningham, R. L., and Matelski, R. P., 1970, Fragipans in Pennsylvania soils: A statistical study of laboratory data: Soil Science Society of America Proceedings, v. 34, p. 311-722.

Pierce, K. L., 1965, Geomorphic significance of a Cretaceous deposit in the Great Valley of southern Pennsylvania: U.S. Geological Survey Professional Paper 525-C, p. C152-C156.

Potter, N., Jr., ed., 1982, Geology in the South Mountain area, Pennsylvania: Annual Field Trip, 1st, Harrisburg Area Geological Society, Guidebook, 37 p.

Ranney, R. W., Ciolkosz, E. J., Petersen, G. W., and others, 1974, The pH base-saturation relationships in B and C horizons of Pennsylvania soils: Soil Science, v. 118, p. 247-253.

Rogers, H. D., 1858, The geology of Pennsylvania: Philadelphia, J. B. Lippincott & Co., v. 2, 1045 p.

Schmidt, V. A., 1982, Magnetostratigraphy of sediments in Mammoth Cave, Kentucky: Science, v. 217, p. 827-829.

Scholle, P. A., ed., 1977, Geological studies on the COST No. B-2 well, U.S. Mid-Atlantic outer continental shelf area: U.S. Geological Survey Circular 750, 71 p.

_____, 1980, Geological studies of the COST No. B-3 well, United States mid-Atlantic continental slope area: U.S. Geological Survey Circular 833, 132 p.

Schwarzbach, M., 1961, The climatic history of Europe and North America, In Nairn, A. E. M., ed., Descriptive paleoclimatology: New York, Interscience Publishers, p. 255-291.

Sevon, W. D., 1977, Surficial geology of the Linden and Williamsport quadrangles, Lycoming County, Pennsylvania: Pennsylvania Geological Survey, 4th ser., Atlas 134ab, Plate 2, scale 1:24,000.

_____, 1985, Pennsylvania's polygenetic landscape: Annual Field Trip, 4th, Harrisburg Area Geological Society, Guidebook, 55 p.

Sevon, W. D., Potter, N., Jr., and Crowl, G. H., 1983, Appalachian peneplains, an historical review: Earth Sciences History, v. 2, p. 156-164.

Smith, D. I., and Atkinson, T. C., 1976, Process, landforms and climate in limestone regions, In Derbyshire, E., ed., Geomorphology and climate: London, John Wiley, p. 367-409.

Soil Survey Staff, 1975, Soil taxonomy, U.S.D.S. Agriculture Handbook No. 436: Washington, D. C., U.S. Government Printing Office.

Strahler, A. N., 1944, Regional superposition on the Schooley peneplane: American Journal of Science, v. 242, p. 563-567.

_____, 1945, Hypotheses of stream development in the folded Appalachians of Pennsylvania: Geological Society of America Bulletin, v. 56, p. 45-88.

Swinnerton, A. C., 1942, Origin of limestone caverns: Geological Society of America Bulletin, v. 43, p. 663-693.

Theisen, J. P., 1983, Is there a fault in our gap?: Pennsylvania Geology, v. 14, no. 3, p. 5-11.

Thompson, H. D., 1939, Drainage evolution in the southern Appalachians: Geological Society of America Bulletin, v. 50, p. 1323-1356.

_____, 1949, Drainage evolution in the Appalachians of Pennsylvania: New York Academy of Science, Annals, v. 52, p. 31-63.

Thompson, P., Ford, D. C., and Schwarcz, H. P., 1975, U^{234}/U^{238} ratios in limestone cave seepage waters and speleothem from West Virginia: Geochimica et Cosmochimica Acta, v. 39, p. 661-669.

Walters, J. C., 1978, Polygonal patterned ground in central New Jersey: Quaternary Research, v. 10, p. 42-54.

Watts, W. A., 1979, Late Quaternary vegetation of central Appalachia and the New Jersey coastal plain: Ecological Monographs, v. 49, p. 427-469.

_____, 1983, Vegetational history of the eastern United States 25,000 to 10,000 years ago, In Porter, S. C., ed., The Late Pleistocene, v. 1, In the collection Late Quaternary environments of the United States: Minneapolis, University of Minnesota Press, p. 294-310.

Williams, E. H., Jr., 1917, Pennsylvania glaciation--first phase: Woodstock, Vt., 101 p.

White, E. L., Aron, G., and White, W. B., 1984, The influence of urbanization on sinkhole development in central Pennsylvania, In Beck, B. F., ed., Sinkholes: Their geology, engineering, and environmental impact: Rotterdam, A. A. Balkema, p. 275-281.

White, W. B., 1960, Terminations of passages in Appalachian caves as evidence for a shallow phreatic origin: National Speleological Society Bulletin, v. 22, pt. 1, p. 43-53.

_____, 1984, Rate processes: Chemical kinetics and karst landform development, In LaFleur, R. G., ed., Groundwater as a geomorphic agent: London, Allen and Unwin, p. 227-248.

Wolfe, J. A., 1978, A paleobotanical interpretation of Tertiary climates in the northern hemisphere: American Science, v. 66, p. 694-703.

FIELD TRIP #4

STRUCTURAL FEATURES IN THE TYRONE - MT. UNION LINEAMENT, ACROSS THE NITTANY ANTICLINORIUM IN CENTRAL PENNSYLVANIA

by
M. R. Canich and D. P. Gold

Introduction

An alignment of stream and river valleys, wind and water gaps, and tonal variations on LANDSAT-1 imagery is apparent for approximately 150 km (90 miles) through central Pennsylvania. This linear feature, known as the Tyrone-Mount Union lineament (Gold et al., 1974), extends from the Blue Ridge physiographic province northwestward across the Appalachian fold mountain belt and into the Allegheny Plateau. The absence of mega- and macro-scopic scale faults in this region is difficult to reconcile with this major transgressive geomorphic feature. In a field study, Canich (1976) compared the structures and stratigraphic relationships on sections (see Fig. 1b) straddling the lineament, and examined the bedrock conditions within the lineament zone. It soon became apparent that at least in the Tyrone - Petersburg part of the lineament there is no major fault, but rather a zone about 1 km wide of anomalous fracture concentration.

The study area encompasses a 9 km (5.5 mile) wide and 16 km (10 mile) long swath, centered on the Little Juniata River between Tyrone and Petersburg, in Blair and Huntingdon Counties (Fig. 1a). A number of active quarries are located within the valley expression of the lineament, and a serviceable country road network provides access to most of the area. The lineament crosses the Sinking Valley anticline, a southwest plunging anticlinal domain of the Nittany Anticlinorium in the westernmost first-order anticline of the Valley and Ridge Physiographic Province of central Pennsylvania. Although a linear base metal mineral trend has been recognized in the Juniata River valley (Smith et al., 1971), it was not until LANDSAT-1 imagery became available (1972) that the feature was mapped and named the Tyrone - Mt. Union lineament (Gold et al., 1974). The area around the northern segment of this lineament has been the focus of geological investigations for some time. Although the various geological maps differ only in detail, interpretations of their subsurface significance differ greatly.

The history of work in this area dates back to the mapping of Rogers (1858), followed by Platt (1881), Lesley (1885), Butts (1918), and Butts et al. (1939). These were regional studies, conducted by The Pennsylvania Geological Survey. More recently, detailed studies of an area where a window exposes late Ordovician to Early Silurian units near Birmingham, have been made by Zeller (1949), Fox (1950), Moebs and Hoy (1959), and Schmiermund and Palmer (1973). Besides the above reports, in which cross-sections are presented by all except Rogers (1858) and Butts (1918), subsurface interpretations have been published by Stose (in Butts et al., 1939) and Gwinn (1964 and 1970). Each cross-section exhibits a different subsurface configuration and presupposes a different kinematic and dynamic model for the Nittany Arch.

It is apparent that the subsurface interpretations of geology near this lineament are ambiguous. This study was intended to test whether the structural complexity is related to the presence of the lineament. The results of some of the fracture studies are summarized in this paper.

Stratigraphy

Stratigraphic units from Cambrian to Silurian age are exposed. The oldest, the Pleasant Hill Limestone, is located near Huntingdon Furnace; the youngest unit, the Wills Creek Formation, is located in the eastern part of the study area near Petersburg (see Fig. 1a). The stratigraphic column shown in Fig. 2 does not distinguish the Lower Ordovician Larke Dolomite, as noted by Butts et al. (1939) and Donaldson (1959), nor is it mapped as a separate unit on the geologic map (Fig. 1a). Donaldson, who has developed detailed sections near Honest Hollow and Spruce Creek along the Little Juniata River, has shown that the Larke Dolomite intertongues with the Stonehenge Limestone. Discriminating the tongues of the Larke Dolomite from the Mines member of the Gatesburg Formation, below the Stonehenge Limestone, and the Nittany Dolomite, above, is difficult and only of academic interest. Because its precise position has little bearing on this paper it has been mapped with the dominant adjacent dolomite unit: either with the overlying Nittany Dolomite or the underlying Mines member of the Gatesburg Formation.

Fracture Studies

Fractures are apparent on LANDSAT-1 imagery, low altitude aerial photography, and in field outcrops. These are referred to as mega-, macro-, and meso-scopic scale fractures, respectively. The worldwide pervasiveness of fractures has been demonstrated by the compliation of Gay (1973). The orthogonal fracture patterns, which he referred to a "pairsets", are thought to be genetically related to basement fractures.

In order to determine the bedrock nature of a lineament, mesoscopic and macroscopic features along the Tyrone - Mount Union lineament were mapped and analyzed. Field data were obtained from road and railroad cuts, quarries, and natural outcrops. Each outcrop was investigated for composition, stratigraphic position, bedding thickness, location with respect to second-order folds, and various structural elements of interest, such as bedding and joint orientations, joint density, fault planes with associated slickenlines, sense of movement on slickenlines, and attitude of fold axes and axial planes. Station numbers were assigned to the outcrops, the formations exposed at each station were identified, and the structural elements present were measured according to the criteria listed in Table 1.

It can be seen from the table that the measurement of joint density imposed some special requirements not inherent to the other data collected. Because joint density varies with bedding thickness and lithology, measurements were made only in areas of similar lithologies, and where two or more roughly orthogonal cuts were available for a 3-dimensional determination of joint spacing.

For frequency determination, the joints were described as being systematic or non-systematic, according to a modified version of joint description developed by Hodgson (1961). Although this terminology is useful in describing joint frequencies, it was not practical in the joint orientation studies here because the systematic joints varied greatly in definition and frequency. Thus for orientation data, a three-fold classification was used, where joints were referred to as dominant, subordinate, and rare. This ordinal quality scale can be equated to the systematic and non-systematic terminology by considering the dominant and subordinate joints as the former and the rare

Figure 1B

STRUCTURE SECTIONS AA' & BB'
For Geologic Map (Plate 2)
by M.B. CANICH 1976

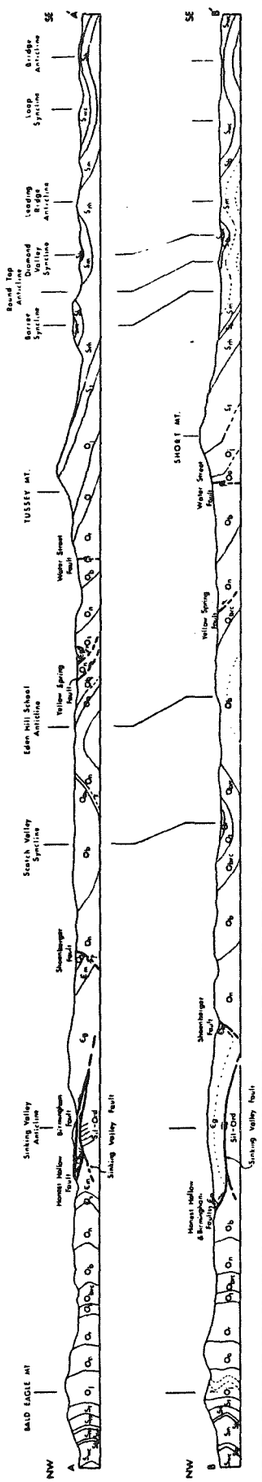

Map of the Geology surrounding a segment of the Tyrone - Mt. Union Lineament

Huntingdon and Blair Counties, Pa.

MAP SOURCES: Geology by Michael B. Canich, 1976, modified after Butts et al (1934), consultations with M.D. Kroen & J. Way

Figure 1.A

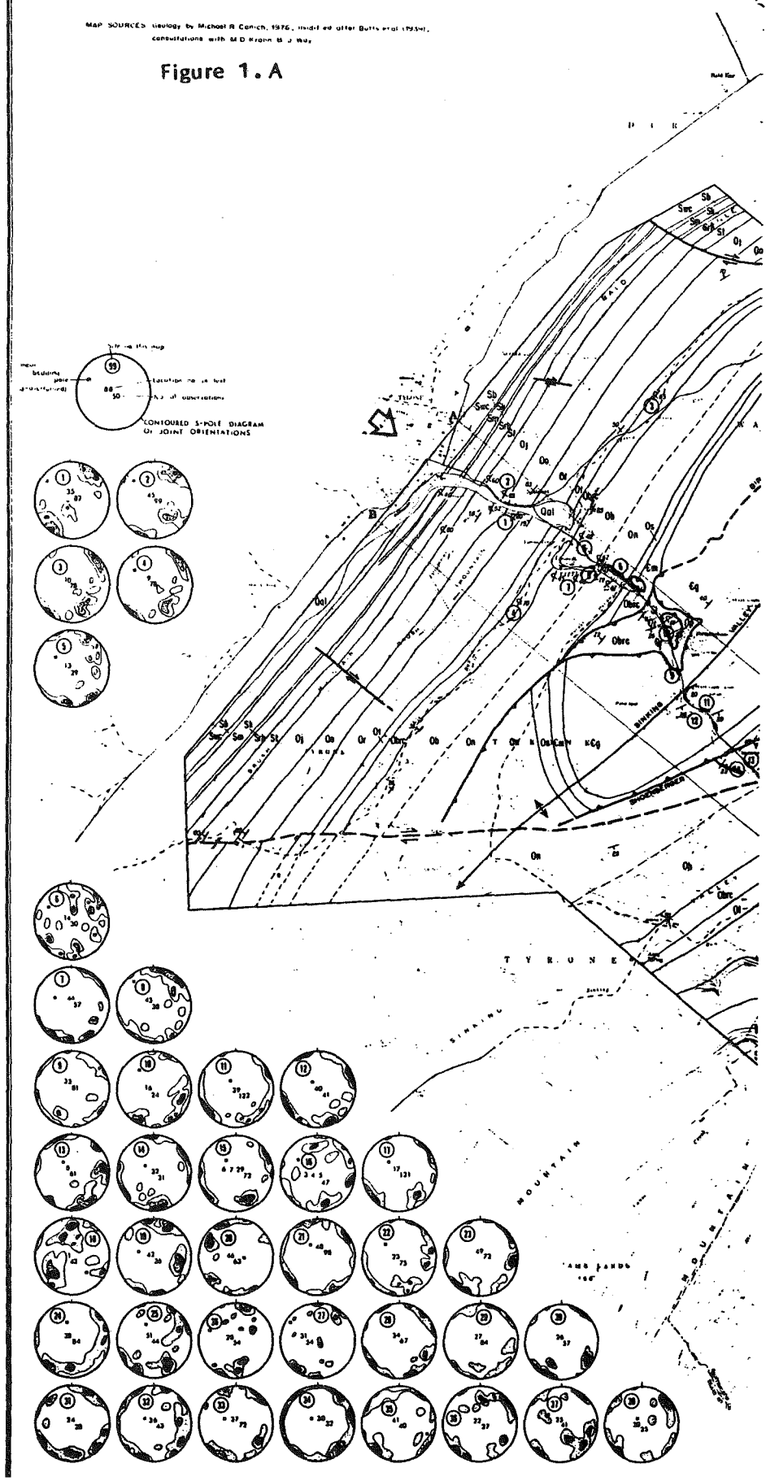

LEGEND

- Strike and Dip of Bedding
- Strike and Dip of Overturned Bedding
- Geologic Contact, dashed where inferred, dotted where concealed
- Fault (U / D)
- Thrust Fault, barbs on hanging wall
- Taar Fault showing sense of motion
- Probable photo geologic fault
- Axis of Anticline
- Axis of Syncline
- Segment of the Tyrone-Mt Union Lineament

SILURIAN
- Qal Alluvium
- Swc Wills Creek Formation (calcareous shales)
- Sb Bloomsburg Formation (red shales)
- Sm Mifflintown Formation (shales and interbedded thin bedded limestones)
- Sk Keefer Formation (calcareous sandstone, some oolitic hematite)
- Sr Rose Hill Formation (argillaceous shale)
- St Tuscarora Formation (quartzitic sandstone)

ORDOVICIAN
- Oj Juniata Formation (red sandstone, siltstone and shales)
- Oo Oswego Sandstone (sandstone, some cross bedding)
- Ou Undifferentiated
- Or Reedsville Shale (shale, some layers calcareous)
- Ot Trenton Group (dark limestone)
- Obrc Black River Chazy Group (light bluish gray limestone)
- Ob Bellefonte Dolomite (dolomite, cyclic light and dark layers)
- Oa Axemann Limestone (limestone, partly oolitic)
- On Nittany Dolomite (dolomite, chert nodules and anlitic chert)
- Os Stonehenge Limestone (limestone, argillaceous and dolomitic in part)

CAMBRIAN
- Cm Mines Member (dolomite, abundant chert and siliceous oolites)
- Cg Gatesburg Formation / Upper Sandy, Ore Hill, Lower Sandy Members (dolomite with interbedded orthoquartzites and sandy dolomite)
- Cw Warrior Formation (limestone, in part dolomitic)
- Cph Pleasant Hill Formation (argillaceous limestone)

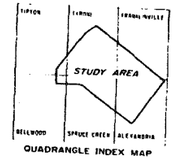

QUADRANGLE INDEX MAP

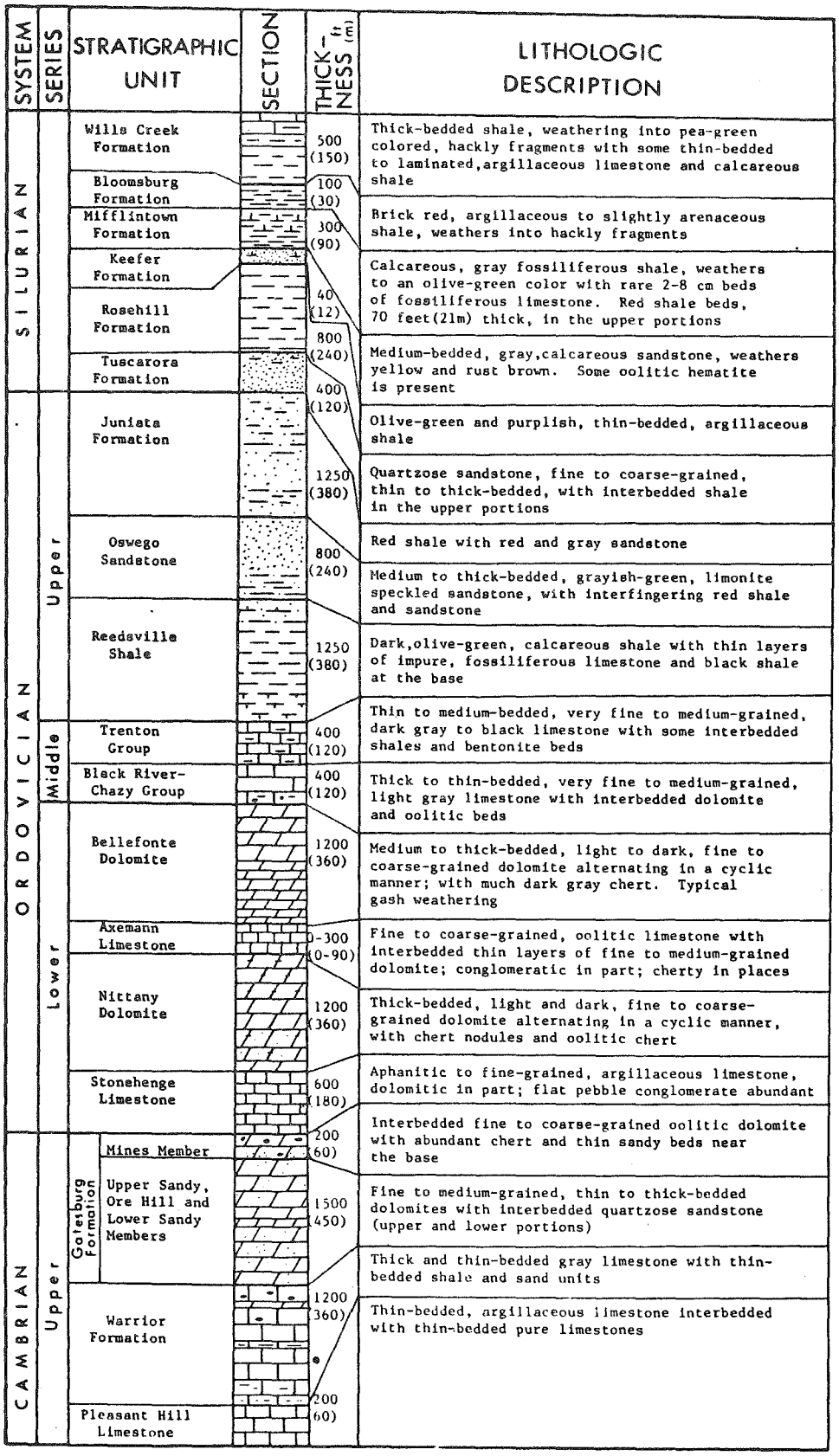

Figure 2. Stratigraphic column of the Tyrone area.

Table 1. Criteria for Measurement of Structural Elements

Structural Element	Parameters	Restrictions on Measurement
Joint	Orientation	None
	Dominance or type	None
	Density	Only in similar lithologies where orthogonal faces could be sampled
Fault	Orientation	None
	Direction of motion	None
	Sense of motion	None
	New movement	None
Fold	Orientation of axial line	None
	Orientation of axial plane	None
	Order	None
	Sense of rotation	None
Bedding	Orientation	One reading for each cell at each sample site

joints as the latter. The number of joint orientations was determined by an intergraded count of frequency from the entire outcrop. This value was then applied to the local setting in order to filter out, where necessary, localized joint sets induced by blasting. By contrast, the dominance quality was determined by inspection of the entire outcrop to compensate for very localized zones of high joint density.

The selection of joints to be measured was as random as possible, considering the bias of outcrop availability. Sample points were located at equal intervals along the outcrop and all joints present at each site were measured. The presence, attitude, and sense of calcite-or quartz-filled joints and tension cracks or gashes were also noted.

As shown in Table 1, the attitudes of faults and associated slickenlines were measured. If the sense of motion could be determined by inspection of the jogged slickenlines, the direction of motion of the hanging wall was given by an arrow symbol in the stereographic plots. For many faults the sense of motion and the net slip were not apparent, but both parameters were readily observable for wedge faults (described by Cloos, 1964) on the mesoscopic scale. For these, the sense of motion and amount of slip

were determined from slickenlines and the geometry of the competent beds comprising the wedge (Fig. 3, Gold and Pohn, this volume). Consistent with Cloos' observation, wedge faults were found to occur preferentially in the cores of anticlines. The attitudes of the axial planes and axial lines were measured for these anticlines as well as for all other folds observed. To determine the geometric compatibility of the different orders of folds, the scale and sense of folds were noted.

Six 1:24,000 7.5 minute USGS quadrangle maps were compiled for a topographic base map and the Tyrone quadrangle geologic map by Butts et al. (1939), on a scale of 1:65,000, was enlarged to 1:24,000 to give a general geologic reference base. Low altitude aerial photographs (1:20,000), U-2 photographs (1:135,000) and LANDSAT-1 imagery (1:230,000) were used in conjunction with the field work. Positional data from all scales were plotted on the 1:24,000 topographic map to produce a fracture trace and lineament map and a detailed geological map (Fig. 1a), and cross section profiles of the structure and geology either side of the Tyrone - Mount Union lineament were drawn (Fig. 1b).

The fracture trace map was developed from linear features mapped on stereo-pairs of low altitude aerial photographs (1:20,000), using conventional photo-geologic techniques. The megascopic data were mapped on monoscopic orthoimages, with a time limit set for each map section. The LANDSAT image was enlarged and cropped, yielding a 1:230,000 image of central Pennsylvania, encompassing the Nittany Anticlinorium and portion of the Allegheny Plateau and the Broadtop Synclinorium.

Results

Joints

The S-pole diagram (Fig. 3) contains all of the joint orientations measured. It exhibits a point maximum of 045° and a subsidiary peaked cluster at 130°. These maxima correspond respectively, to a subvertical plane set centered on 130° strike, and a predominantly northwest dipping set striking about 045°. The former joint set is generally dominant in expression

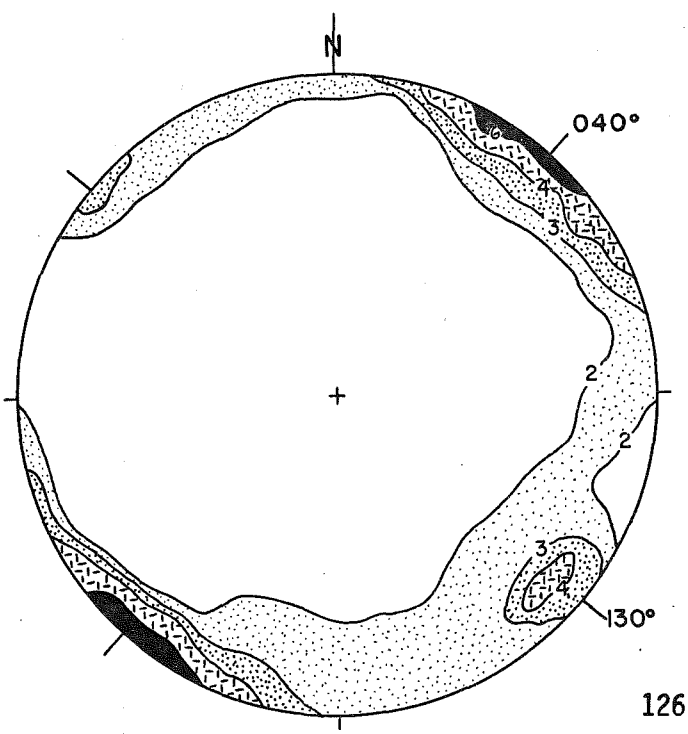

Figure 3. Synoptic S-pole diagram of 2316 joint attitudes, contoured at 2, 3, 4, and 6% per 1% area. Planes associated with the peak concentrations are inclined at 045° and 130°.

and frequency in the field. However, this does not imply that it is the dominant joint or joint set at each outcrop. Variations are apparent in the individually contoured S-pole diagrams for some of the locations shown in Figure 1a. These diagrams reveal how joint orientations vary with location on the second and third order folds present, as well as across the lineament. It was also noted during this study that joint density decreases with an increase in bedding thickness; thus comparisons are valid only between units of similar thickness and lithology.

The pole representing the mean bedding plane for an outcrop is included on the individual contoured joint diagrams in Fig. 1a. The strike orientation is nearly constant within most of the outcrops but the dip angle varies. Therefore, the mean bedding plane was determined by finding the arithmetic average of dip angles and using the approximate strike orientation. In view of the contorted nature of the beds, this pole could not be included for some localities. The geometry of the joints with respect to an assumed horizontal bedding attitude before folding was determined by rotating measured joint orientations about the bedding strike and through the dip angle of the beds to a horizontal attitude. Because joints in flat-lying strata are commonly parallel and perpendicular to the bedding planes (De Sitter, 1956), those sets parallel or orthogonal to bedding planes were interpreted as joints inherited from pre-Alleghenian orogenic events, and the others were interpreted as superimposed. This assumption, however, cannot be used to unambiguously sort out pre- or post-folding joint sets nearly perpendicular to bedding strike (i.e., the axis of rotation). Determination of the age of origin for each joint set should be made in an area of through-going joints, oblique to the bedding strike. For example, nearly vertical joints oriented at 130° are observed in most outcrops regardless of the bedding attitude. From geometric considerations, the age of this joint set is ambiguous for outcrops with a bedding strike of 040° but definitely is post-folding for other bedding orientations.

Faults

High angle faults with small displacements are ubiquitous throughout the study area, and some appear to form conjugate sets. A synoptic, contoured S-pole diagram of 159 of these fault orientations yielded maxima with strikes of 110° and approximately 140° (Fig. 4a). In conjugate sets of faults, the σ_2 axis (intermediate principal stress axis) is defined by the attitude of the line of intersection, and the position of the maximum principal stress axis, σ_1, coincides geometrically with the perpendicular bisector of the acute dihedral angle between the fault planes, shown in Fig. 4a as the line X - Y, the bisector of the obtuse dihedral angle between poles to the fault planes. The plunge of the slickenlines associated with these faults forms a broad girdle about the 120° plane, and most of the slickenlines plunge to the southeast and northwest at moderate angles (Fig. 4b).

The polarity of slickenlines on the fault planes from a few well exposed localities along the lineament are portrayed in Figs. 5a and 5b. The stereographic plots show not only the plunge of the slickenlines, but also a short segment of the fault plane through it and the sense of motion of the hanging-wall block. The sampling locations are, Tyrone Gap (Locations 1 and 2), a roadcut near Union Furnace (Location 17), and two Locations (30 and 31) in an

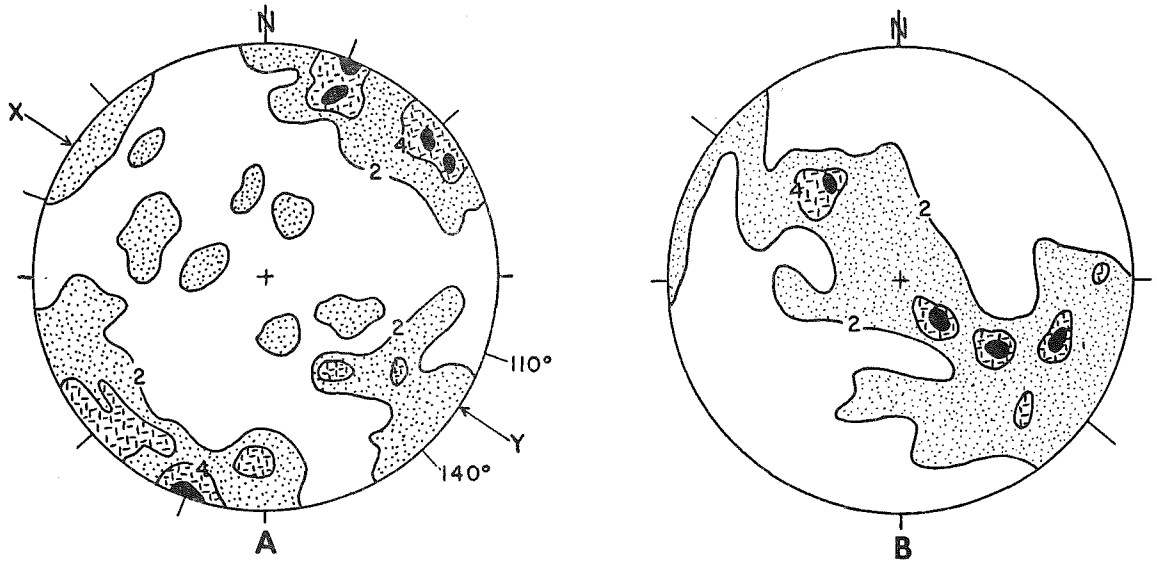

Figure 4a. Synoptic S-pole diagram of 159 fault planes, contoured at 2, 4, and 6% intervals per 1% area. The pole maxima represent strike directions of 110° and 140°, respectively. Line X-Y is the perpendicular bisector of the acute dihedral angle between the dominant fault attitudes.

Figure 4b. Orientation diagram of 136 slickenlines, contoured at 2, 4, and 6% per 1% area.

area 150 m (500 ft) east of the railroad tunnel in Spruce Creek Gap (see Fig. 1a). The data from Tyrone Gap are plotted in Fig. 5a and those from locations 17, 30, and 31 are plotted in Fig. 5b.

At Tyrone Gap, the general trend of motion to the northwest and southeast differs from the north-south motions recorded in the west limb of the Scotch Valley syncline near Union Furnace (Location 17 and Diagram 17 on Fig. 1a). Most of this difference can be reconciled if the beds are rotated to a horizontal attitude; the difference may also be attributed to redistribution of stresses in the nose of the syncline. The former solution is favored because, by rotating the bedding attitudes at Location 17 back to horizontal through the dip angle the slickenlines correspondingly rotate to a shallow northwest-southeast plunging orientation. This orientation is consistent with those measured in Tyrone Gap (Fig. 5a), as well as with the overall trend in the synoptic slickenline diagram (Fig. 4b).

The interpretation of fault type from slickenline polarity requires a knowledge of fault chronology, because the slickenlines generally represent only the latest movement(s). The initial attitude of the fault plane must also be known because it may have changed as a result of folding events. For example many conjugate faults exposed in the Tyrone Gap section exhibit non-unique slickenline directions in their surfaces. Most of these fault sets, developed in the sandstone planes and shale beds of the Bald Eagle Formation, have a subhorizontal line of intersection oriented about 140°. Other fault planes in the same outcrop contain two sets of slickenlines, with a subhorizontal set superimposed on a steeply plunging set.

In a conjugate set near Station 12 on Figure 2 (p. 169), Gold and Pohn, this volume (STOP #2), the slickenlines on one fault are subparallel to the nearly vert-

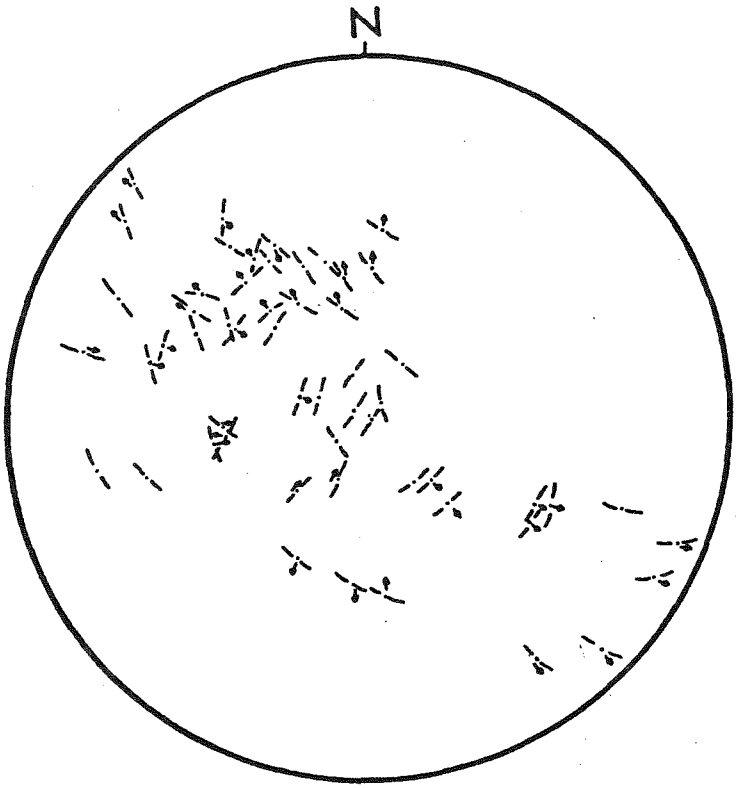

Figure 5a. Stereographic plot of slickenline polarity in Tyrone Gap. Fifty-seven observations are plotted. A segment of the fault plane (—·—) and the sense of motion of the hanging wall (—➔) are shown.

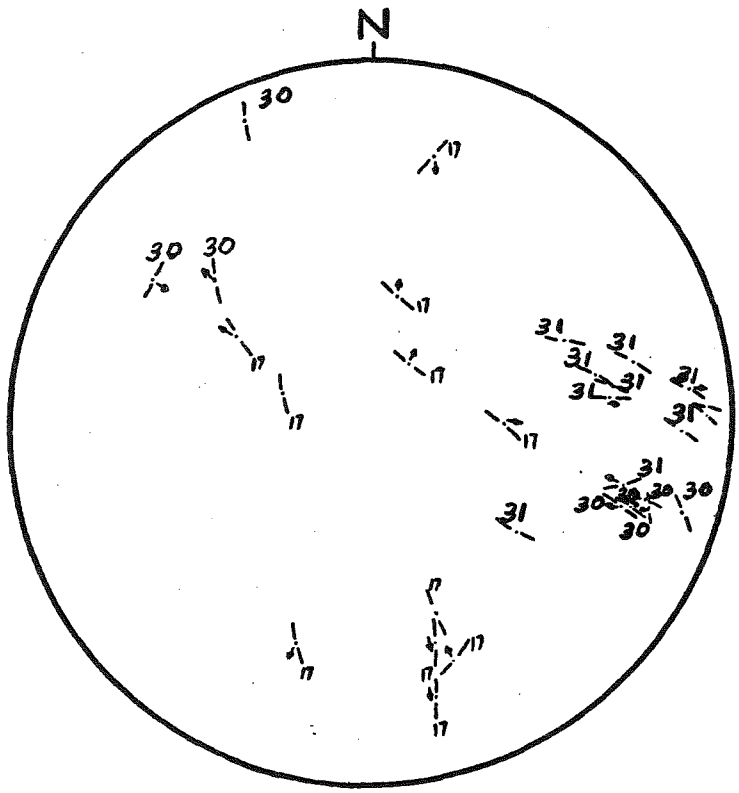

Figure 5b. Stereographic plot of slickenline polarity at Locations 17, 30, and 31. A segment of the fault plane (—·—) and the sense of motion of the hanging wall (—➔) are shown.

ical bedding surface (indicating a dip-slip movement), whereas the subhorizontal striae on the other fault indicate that it is essentially strike-slip in nature. This variation in slickenline attitude may have resulted from a southeast-northwest directed stress acting intermittently on a fault plane while the beds were being rotated during the development of the Nittany anticlinorium. It may also be the result of rotation of the stress field, producing early dip-slip faults and later strike-slip faults, both with small displacements. The former hypothesis is favored, mainly because (a) dip separations on either side of the lineament are not apparent from the detailed lithologic mapping, and (b) many mesoscopic right and left strike-slip faults with compensating displacements were mapped in the lineament zone. Thus the dip-slip fault that is nearly perpendicular to the bedding surface probably developed as a strike-slip fault prior to folding, when the beds were subhorizontal. Reactivation of the conjugate fault plane after the folding episode, by similar compressive stresses, would account for its current, in situ dip-slip normal mode.

About 3.5 km (2 miles) northwest from STOP # 5, in the area 150 m (500 ft) east of the railroad tunnel in Spruce Creek Gap (Sites 30 and 31 in Fig. 1a), the plunge directions of slip lines vary by at least 20° from one side of the gap to the other, a distance of approximately 180 m (600 ft).

Mesoscopic scale folds are ubiquitous, and seem to occur preferentially where competent and relatively incompetent units are interbedded, such as the Bald Eagle Sandstone in Tyrone Gap and the Mifflintown Formation near Barree. Where the competent unit is dominant, folds tend to be larger, from 3 to over 30 m (10 to over 100 ft), than in the areas where the incompetent unit is dominant, where the folds range from 0.03 to 3 m (0.1 to 10 ft). All of the fold axes measured are compatible with a northwest direction of transport, which is consistent with the orientations of slickenlines and fault planes and the general geometry of the Nittany Anticlinorium. Not all of the minor folds are consistent in drag sense with their location on higher order folds. These minor folds may be disharmonic, with scale-related decoupling between the third and higher-order folds, i.e., where a decollement in the stratigraphic section separates folds of different scale and style (Nickelsen 1963). For example, a fourth-order kink fold in Tyrone Gap is incompatible in drag sense with its location in the west limb of a first-order anticline, the Nittany Anticlinorium. Slickenlines on the bedding surface perpendicular to the fold axis suggest a flexural slip mechanism for these kink folds. A nearly vertical fault plane, obliquely transecting the fold, contains subhorizontal slickenlines. These relationships suggest that an early flexural slip-folding event preceded the transgressive strike-slip faults of small displacement.

The entire study area, 9 by 16 km (5.5 by 10 miles), was covered by photogeologic studies at different scales. A strip 3.2 km (2 miles) wide, centered on the Tyrone - Mount Union lineament, was mapped in detail in the field. With the improved data base (aerial photographs and satellite imagery) the author was able to extend coverage of units into areas of limited or poor exposure. These mapping methods proved to be complementary and enabled the author not only to extend in detail the geological and structural mapping of Butts et al. (1939) with additional faults and folds, but also to correct the positions of subsequently mapped faults and lithologic contacts. This new data base has spurred new interpretations and necessitated a reinterpretation of the earlier data.

The following list of observations and interpretations are considered to be the more important contributions of this paper:

1. The trace of the Shoenberger fault, which Butts et al. (1939) showed to terminate in the Nittany Formation, is seen on LANDSAT imagery to extend into a N 80° E trending lineament that passes through Brush Mountain at Skelp Gap. This lineament probably represents the trace of a fault, because right lateral displacements of the Middle Ordovician section are apparent near Skelp. This movement is compatible with the reverse sense proposed by Butts et al. (1939) for the Shoenberger fault. Indeed, the latter fault may terminate on the former.

2. The reversal of dips in beds of the Juniata Formation exposed in Plummer Hollow, south of Tyrone Gap (Fig. 1a), probably reflects the presence of a third-order fold confined to this formation. This fold does not project across Tyrone Gap to the north (Fig. 1a). Its presence would account not only for increase in the thickness of this formation south of the river, but also for the development of the strike valley in Plummer Hollow.

3. Mesoscopic scale strike faults that duplicate beds occur singly or in conjugate pairs in the Tyrone Gap exposures (Krohn 1976). Although their present attitude requires them to be classified as normal dip-slip faults, they have been interpreted as pre-folding compressive or wedge faults (Cloos 1964). On some of the faults, superimposed slickenlines attest to a late strike-slip movement, consistent with the motions on mesoscopic dip and oblique faults that cut the earlier "wedge" faults. The late strike-slip faults also occur in conjugate sets, in which adjacent faults may exhibit right and left lateral displacements, respectively. The apparent lack of offset across the lineament in Tyrone Gap indicates that the mesoscopic scale strike-slip displacements are compensatory.

4. The area around Birmingham (STOPS # 3 and 4) has long been recognized for its structural complexity (Butts et al. 1939; Fox 1950), with anomalous thinning in overturned beds of the Upper Ordovician and Lower Silurian formations in a local fenster called the Birmingham window (see Figures 5 to 12, Gold et al., this volume). The Knarr window, 2.4 km (1.5 miles) to the northeast, exposes Ordovician rocks within Cambrian formations. Detailed mapping of the Birmingham window by Moebs and Hoy (1959) (see Figs. 9 and 10, Gold et al., this volume), Schmiermund and Palmer (1973) (Fig. 12a, Gold et al., this volume) and Canich (1976) (Fig. 1a) show the juxtaposition of overturned Reedsville, Bald Eagle, Juniata, and Tuscarora beds against upright Black River-Chazy Group beds south of the river. Cross sections drawn by Moebs and Hoy (1959) (Figs. 9 and 10, Gold et al., this volume) from drill core data imply varying thickness or attitude of the Upper Ordovician Juniata and Reedsville units beneath the Sinking Valley fault, even though no mention was made of these variations in their text. The subsurface configuration shown here (Fig. 1b) is inferred from an analysis of the drill data presented by Moebs and Hoy (1959) and projections of the outcrop mapping done by Canich (1976). The "surprising difference in the beds exposed" (Fox 1950) and the absence elsewhere of any of

the units exposed in the Birmingham window, even though equivalent and lower topography is developed on the southwest side of the river, suggest the presence of a ramp in the thrust plate coincident with the river. A fault of sufficient displacement to fit the observed geometry is inconsistent with the outcrop pattern of the Birmingham and Honest Hollow faults.

5. A thrust fault of undetermined displacement is exposed in the north wall of Warner's Main Quarry at Union Furnace, and is expressed as a fracture trace on aerial photographs (1:20,000). Its reverse sense of motion is compatible with the compressional regime in the core of the Scotch Valley syncline above the intrados surface.

6. The Water Street fault (Butts et al., 1939), a high angle fault with a downthrown east side, may be genetically associated with a fracture zone and anomalous bedding orientations along the Little Juniata River in Spruce Creek Gap (Fig. 1a, and Fig. 14, Gold et al., this volume). Farther east, a low angle thrust fault (Location A in Fig. 14 (p. 188), this volume), gently inclined to the northwest, has a measured stratigraphic separation of 30 m (100 ft). This antithetic fault zone has strata rotated counter-clockwise on a thrust slice between the main fault (lower) and an associated splay fault (upper). An increase in the dips of beds close to the Water Street fault suggests that the local thrust fault (A) may have formed in response to flexures induced by movement of the Water Street fault (see cross section in Fig. 14 in Gold et al., this volume).

The acute downstream junction of Spruce Creek with the Little Juniata River and the diversion of the river around a spur of Bald Eagle Sandstone are anomalous. High level gravels preserved on this spur above the railroad tunnel (Butts et al., 1939) indicate that the river in Spruce Creek Gap at one time followed a more linear course, subparallel to the Tyrone-Mt. Union lineament. The saddle 0.5 km (0.31 mile) east of the village of Spruce Creek (Fig. 1a), which is part of the Spruce Creek Gap, is at the same elevation as the gravel deposits on the opposite spur, and may represent the fossil course of Spruce Creek. The abrupt change in the Little Juniata River course probably is a result of capture along the fossil Spruce Creek drainage, which is controlled by a fracture zone through the sandstone ridge (see Fig. 14 (p. 188), Gold et al., this volume). Structural evidence for a fault in Spruce Creek Gap is seen (a) in the alignment of highly fractured rocks on the northern tip of the Bald Eagle spur, with disturbed beds exhibiting highly variable slip line orientations 150 m (500 ft) to the east of the Spruce Creek Gap railroad tunnel; (b) a slight offset in the projection of geologic contacts across the river; and (c) a variation in bedding attitude in the Bald Eagle Sandstone, from 70° to 85° on the spur to 15° to 25° S on the north side of the river. The authors interpret these data to indicate that a fault, the Spruce Creek Gap fault (Fig. 14 (p. 188), Gold et al., this volume), intersects the Water Street fault near Spruce Creek and exerts structural control over the present diversion of the Little Juniata River.

Other manifestations of the Water Street fault may be seen in the steep dip of the Tuscarora beds exposed in the ganister quarry on Short Mountain, 1.1 km (0.7 mile) northeast of Water Street (Fig. 1a, Location 26). Elsewhere, along Short and Tussy Mountains these beds have a dip of 15° to 20° S. Drag flexures associated with eastside downward movement (Fig. 14 (p. 188), Gold et al., this volume) on the fault plane would account for the anomalous dips in the vicinity of the fault.

7. Field follow-up studies on two fracture traces mapped on aerial photographs showed them to be underlain by highly jointed zones up to 45 m (150 ft) wide. The mesoscopic fractures in one of these zones, exposed in the railroad cut between Spruce Creek and Union Furnace (see Fig. 1a), are seen to dip approximately 60° SE. However, a vertical dip is implied by the essentially linear trace of this zone, which suggest an en echelon disposition of the inclined mesoscopic fractures in a vertical macroscopic fracture zone. The other fracture trace is located on the western limb of the Barree syncline, where the Keefer formation is offset by a fault with a vertical throw of approximately 6 m (20 feet). This fault zone is exposed only in an abandoned mine pit, and no fracture density studies were attempted.

8. A curve in the trace of Bald Eagle Mountain (Fox, 1950) is evident on the LANDSAT imagery as a sharply bounded segment from Tyrone Gap to south of the village of Bald Eagle. This salient may represent the movement of a small thrust plate bounded by tear zones (Gwinn, 1964; Kowalik, 1975), expressed as lineaments on the LANDSAT images. (The northernmost of these two lineaments is outside the study area, and therefore not plotted on Fig. 1a.) These boundaries are envisaged as diffused zones of structural decoupling, i.e., the domain boundary concept of Gold and Parizek (1976), rather than as discrete tear faults.

9. Landslides which developed during and after construction of the Route 220 Bypass near Tyrone appear to be related to lineaments. Two slumps flanking Tyrone Gap, and another 8 km (5 miles) to the north, near Bald Eagle, are on lineaments mapped by Krohn (1976) and Kowalik (1975). An increase in pore pressure along the lineament near Bald Eagle was monitored in a drill hole in the road bed during the spring of 1975. Local slumps occurred high in the road cut, and "quick" conditions developed near the base, disrupting the road bed for approximately 100 m (300 ft) and delaying the opening of this section of highway (Gold and Krohn, in Gold and Parizek, 1976). These observations support the concept that some lineaments and fracture traces are the surface expression of secondary structural zones of increased porosity and permeability (Gold and Parizek, 1976).

10. A discordance of 15° in the strike of the Tuscarora and Bald Eagle beds with the ridge crest trend of Brush and Bald Eagle mountains between Skelp Gap and Vail Gap (John Way and M. Dennis Krohn, pers. comm.) is largely accommodated by right lateral offsets of small displacement (Krohn, 1976). Some larger faults with the

same right lateral sense of displacement have been mapped (see Fig. 1a), e.g., the fault mapped by Butts et al. (1939) east of Vail. The reason for the pattern of small displacement faults in the competent beds is not known, but they appear to be more common in the vicinity of lineaments, particularly the Tyrone - Mount Union lineament.

11. The only outcrops of the Axemann Limestone in the study area are between Union Furnace and Spruce Creek, in the core of the Eden Hill School Anticline (Fig. 1a). The general absence of this unit in the southwestern portion of the Nittany Anticlinorium was attributed by Butts et al. (1939) to sedimentary processes (non-deposition or a facies change to dolomite).

Discussion

The Tyrone - Mount Union lineament is a cross-strike topographic feature that appears to be the locus of structural and topographic anomalies such as a high density of mesoscopic scale faults and fractures, truncation of tectonic windows, termination of folds, and juxtaposition of beds of contrasting attitude and thickness. Gold and Parizek (1976) suggested, from gravity and seismic data, that this lineament is underlain by a fracture zone that acts as a domain boundary, separating blocks of different strain (structural style) even though stresses in each may have been similar. Conceptually, this zone would act as a buffer, enabling folds of different magnitude and style to develop in neighboring blocks, or attenuating fold forms across from one block to another. For example, the Scotch Valley syncline extends at least 16 km (10 miles) south of its intersection with the Tyrone - Mount Union lineament, but it terminates just north of its intersection with the lineament, as does the Eden Hill School anticline. Many third- and fourth-order folds in the Silurian shales near Alexandria do not extend north of the southern branch of this lineament. The Shoenberger and Birmingham faults also appear to terminate in the vicinity of the lineament (see Fig. 1a). The former extends from Skelp Gap eastward for 6.5 km (4 miles) and dies out about 1.6 km (1.0 mile) north of the lineament, whereas the latter extends approximately 48 km (30 miles) to the north in Nittany Valley and terminates in Sinking Valley anticline 2.3 km (1.5 mile) south of the lineament.

Estimates of northwestward lateral shortening in the Appalachian fold belt during the Alleghenian orogeny range from 32 km (20 miles) by Chamberlain (1910) to 80 km (50 miles) by Gwinn (1970). Manifestations of the northwest transport direction are seen in the map area by (a) a northwest-southeast girdle of slickenlines in the synoptic orientation diagram (Fig. 4b); (b) fold axes coincident with the pole of the slickenline girdle; (c) a strike of 110° to 140° for the slickenline plunges of most faults (Fig. 4a); and (d) the northwest-southeast compression implied by the geometry of the Nittany Anticlinorium. Greater foreshortening north of the lineament than south of it is indicated by the pattern of the Water Street and Yellow Springs faults.

These faults extend individually for some distance to the south of the lineament. However, to the north they converge with a number of smaller faults, associated with another thrust and a high angle reverse fault shown in cross-section A-A' on Figure 1b.

Other indicators of differential foreshortening are the salient in Bald Eagle mountain north of the Tyrone - Mount Union lineament and the Round Top and Leading Ridge anticlines south of the lineament and east of Tussey mountain. Additional folds in these second-order anticlines expose more Tuscarora ridges on the north side, and imply greater crustal foreshortening, than on the south side of the lineament. Much of the differential foreshortening on the north side may have been taken up in the Scotch Valley syncline to the southwest. The misalignment of structural features caused by differential foreshortening across part of the lineament has led to the domain boundary or strain boundary concept, a zone along which local foreshortened segments or displacements in the cover rocks compensate over a longer distance. This subvertical zone of superimposed structural discontinuities is interpreted as a decoupling zone to Alleghenian deformation as well as the locus of late deformations, such as small displacement right and left lateral strike-slip faults.

The formation of wedge faults and kink folds early in the deformation process has been noted by Cloos (1964) and Faill (1973). The curved fault surfaces and superimposed sets of slickenlines of mesoscopic wedge faults attest to their early formation. Such faults are particularly abundant in Silurian shales. Compressional slip motions are indicated by wedge faults, and by the bedding slip lines in the kink folds. The Sinking Valley, Birmingham, and Honest Hollow faults, and some kink bands which have a sense of rotation incompatible with their location on lower order folds and/or have anomalous plunges, are examples of structures formed early and geometrically altered as deformation continued.

Evidence for the additional motion of the crustal block north of the lineament was mentioned earlier. The mechanism causing this differential motion includes participation of the Birmingham fault in the formation of the Nittany Anticlinorium. The salient in Bald Eagle mountain could have been a result of the overriding thrust plate of the Birmingham fault, north of the lineament, moving farther to the northwest than in the adjacent areas due to basement "uncoupling."

Another possible model (Kowalik & Gold, 1976; Gold, 1980) involves a ramp in the Sinking Valley fault with differential movement of thrust plates. This model is preferred because a ramp in the Sinking Valley fault is implied by the stratigraphic offset and structural anomalies present in the Birmingham window area. This differential motion was followed by continued folding, evident in the present geometry of the Nittany Anticlinorium. The late formation of the high angle and/or westerly dipping faults is indicated by the apparent truncation of the Birmingham fault by the Shoenberger fault in the Sinking Valley anticline.

It is concluded that the Tyrone - Mount Union lineament originated not later than late Paleozoic time, and the presence of a dominant pervasive joint set parallel to it infers a continuation of influence of the lineament until at least the termination of the Alleghenian orogeny. The 130° joint orientation (parallel to the lineament) was noted in each outcrop, with joints ranging in number from one or two to many per outcrop (sufficient to apply a quality of "subordinate" to it), regardless of the orientation of the rotation axis (strike of beds). Therefore, in the areas where the strike of the beds is presently neither parallel nor perpendicular to 130°, vertical joints, particularly those oriented at 130°, must be superimposed after folding (i.e.,

in the post-Alleghenian orogeny) because it is unlikely that this unique geometry would be preserved through folding rotations. Post-tectonic joints may be very young, and may even be forming today as a result of earth tides (Blanchet, 1957; Gold et al., 1973) causing various size blocks, determined by the location of lineaments, to react with a slightly different amount of vertical motion. Such diurnal motions might activate fractures in fossil fracture zones (dormant lineaments) and thus enhance degradation processes and topographic expression of lineaments relative to other structures in the area.

Although the morphological expression of the Tyrone - Mount Union lineament is confined to a narrow belt between 0.5 to 2 km (0.35 to 1.2 miles) wide, its structural manifestations may be more extensive. However, its limits cannot be determined unambiguously from the data currently available. Not only do the two segments of the lineament overlap en echelon between Alexandria and Barree, but the short lineaments and fracture traces which occur throughout the area, influence the local joint density. In addition, some segments bounded by fracture zones within the major lineament are essentially free of deformation effects. It can be seen, therefore that the size of the sample area is important. It is apparent from the data and these discussions that the nature of the surficial bedrock character of this lineament is difficult to establish for three major reasons: 1) the lack of continuous exposure across the lineament; 2) the size of the feature; and 3) a lack of experience with similar features.

The key question, and an even more difficult problem on which to gather data, is the subsurface nature and extent of the lineament. However localization of base metals and geophysical data permit some inferences regarding its nature at depth. The localization of five base metal sulfide occurrences and one formerly productive lead-zinc mine (the Keystone Mine near Birmingham, circa 1795) (Smith et al., 1971; Smith, 1977) along the Tyrone-Mt. Union lineament, suggests the migration of ore fluids in a zone of increased porosity and permeability. The Bouguer anomaly gravity map of Pennsylvania, compiled by P. M. Lavin (reproduced as Fig. 1a, Gold and Pohn, this volume, from Parrish and Lavin, 1982) shows a truncation of the regional anomalies coinciding with the Tyrone-Mt. Union lineament. A steep gradient near and perpendicular to the lineament implies an involvement of the basement rocks in its location and expression. Disturbed contour patterns in the aeromagnetic maps (see Fig. 1b, Gold and Pohn, this volume) are interpreted to represent changes in the basement topography coincident with the Tyrone-Mt. Union lineament. A structural link from the basement structure through the Paleozoic cover rocks to the surface is suggested not only by the attenuation of seismic waves across this zone (Alexander and Abriel, 1976), but also by evidence that the lineament is the locus of current micro-seismic activity (S. S. Alexander, pers. comm., 1976).

Summary and Conclusions

Field data combined with investigation of the geologic map (Fig. 1a), supports the domain boundary hypothesis for the Tyrone - Mount Union lineament. Stratigraphic offsets and structural anomalies exist along the lineament, and the authors believe these are genetically linked to an underlying fracture zone. Thus, the lineament is thought to represent the surface expression of basement fractures modified in various ways through the stratigraphic column and through time.

A model of the lineament requires that it (a) be a zone of fractures but not a fault, (b) be controlled by a feature in Precambrian rocks of the "basement" beneath 3000 to 4000 m (10,000 to 13,000 ft) of sediments, and (c) be currently active (at least seismically). This model is consistent with constraints on other lineaments mapped in Pennsylvania which transgress the metamorphosed Precambrian and Paleozoic rocks of the Piedmont, Mesozoic sediments in the Triassic Basin, Paleozoic strata in the Appalachian fold belt, and recent sediments of the Coastal Plain (Gold et al., 1973). The model accommodates a fracture zone through the Nittany Anticlinorium that locally influenced the "Valley and Ridge" deformation during the Alleghenian orogeny (Root, 1974). The sequence of events during late Paleozoic Alleghenian deformation is envisaged as (a) initial compression and lateral shortening in a northwesterly direction with the development of wedge faults and kink folds, followed by (b) the main episode of folding and thrusting and development or reactivation of a decoupling zone with local differential displacement, and (c) contemporaneous development of high angle faults with downthrown east sides along with low angle westerly-dipping thrust faults during the late folding stage, and, finally, (d) development of late strike-slip faults of small displacement in the lineament fracture zone.

The observations discussed here lead to the following conclusions:

1. The dominant joints in the region (130° and 045°) are related geometrically to the Tyrone - Mount Union lineament.

2. There is a general increase in fracture density as one approaches the lineament.

3. The joint density is influenced by lithology and bedding thickness, and by proximity to fracture traces.

4. The $\sigma_1 - \sigma_2$ plane trends approximately 320° and has been constant throughout the Alleghenian orogeny.

5. The Tyrone - Mount Union lineament is linked to a basement fracture, acted as a domain boundary during the Alleghenian orogeny, and may still be a slightly active stress relief zone.

THE NATURE OF CROSS-STRIKE AND STRIKE-PARALLEL STRUCTURES IN CENTRAL PENNSYLVANIA

by
D. P. Gold and H. A. Pohn

Introduction

This field trip will emphasize the similarity of structural features at different scales and the sequence in development of structures, as well as introduce a conceptual model for the strike-parallel zones of disturbed strata, and the cross-strike zones of near vertical fracture concentration.

It is surprising how many structures (features) of similar form and style occur over such a wide range in scale. Structural features seen in outcrop, such as snake-head folds, concentric and box folds, wedge and ramp faults, commonly mimic 2nd and 3rd order structures on the quadrangle map, and even 1st order structures evident in seismic reflection profiles.

Using superposition and cross-cutting criteria, it is apparent that the main episode of faulting (with associated minor folds and faults in disturbed zones) predates the development of the major folds in this portion of the Appalachian Fold Belt. This early event involved layer parallel shortening phenomena such as wedge faults, ramp and snake-head folds, concentric folds, kink bands and box folds. Many of these faults have been rotated or folded by the later folding event. In some of these the dip direction has been reversed by rotation associated with the growth of the major folds. The general sequence is (1) early wedge faults and other layer parallel shortening structures, followed sequentially by (2) splay faults, probably off a deep decollement, with the development of disturbed zones that initiated (3) the growth of the major folds with associate uplimb thrusts, and (4) by a late stage with extensional faults.

The concept of "disturbed zones" involves a splay fault model in which the deformation features (i.e. the amount of strain) varies with depth. This is, in a sense, a deformation facies of splay faults, with a deminution of strains (displacements) upward from the decollement. According to Harris and Milici (1977) the "lower broken zone, which overlies the detachment fault and is generally bound above by a lesser thrust fault, is composed of a series of strata that are separated into disconnected irregularly shaped masses and elongate slabs by faults spaced from a few to about 10 feet apart. Subhorizontal faults and splay thrusts, rotational normal faults, and antithetic normal faults are common features of this zone. Differential movement within the decollement zone has resulted in internal distortion, so that thrust faults that are interpreted to be horizontal when first formed are warped and commonly offset by later faults."

"The upper fractured zone is much less internally deformed; however it shows a gradual upward change in structural style. The lower part of this

zone is dominated by splay thrusting that has a relatively large magnitude of throw. This gives way upward to splay thrusts that have low magnitude of throw alternating laterally and vertically with areas of normal faults and normal shear faults. The upper fracture zone grades vertically into relatively undeformed strata" (Harris and Milici, 1977, p. 11).

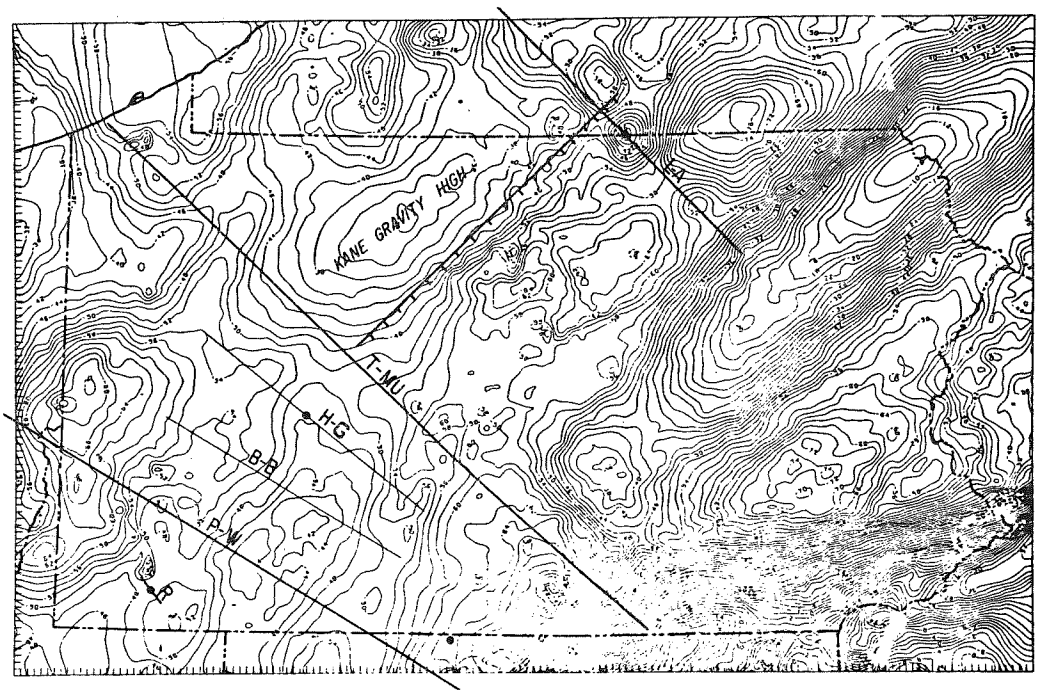

Figure 1a. Simple Bouguer Anomaly map of Pennsylvania, showing the location of kimberlites (solid dots) and cross-strike lineaments. L-A = Lawrenceville-Attica; T-MU = Tyrone-Mt. Union; H-G = Home-Gallitzin; B-B = Blairsville-Broadtop; P-W = Pittsburgh-Washington; R = Roen's transcurrent feature. (After Parrish and Lavin, 1982.)

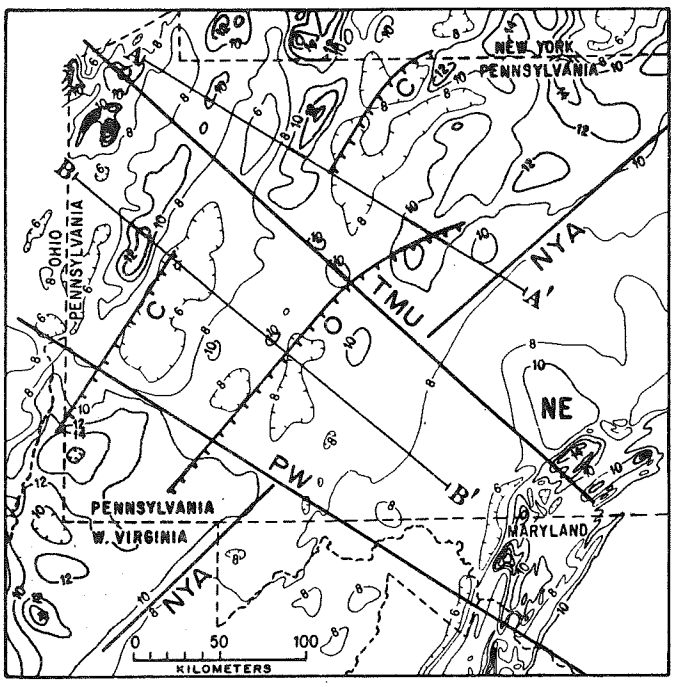

Figure 1b. Aeromagnetic map of western Pennsylvania, contoured in hundreds of gammas. The shaded areas are the magnetic highs. Symbols, as above, and NY-A = New York-Alabama magnetic lineament. Upper Cambrian (C) and Lower Ordovician (O) growth faults are indicated by the hachured lines. (After Lavin et al., 1982.)

The large cross-strike fracture zones are viewed conceptually as zones of fracture concentration (rather than a discrete break) that act as domain boundaries or strain discontinuities through long periods of geologic time. The increase in surface area, porosity and permeability of the rocks in these zones ensures they are eroded more readily than the surrounding rocks, and hence are manifest topographically as depressions across the regional structural grain. They may be the surface expression of the boundaries between crustal blocks (Lavin et al., 1982) that are kept active by differential movement in response to earth body tides. It has been suggested they are upward projections of intermittently active basement faults now largely buried by younger sedimentary rocks, or the trace of a paleo-transform fault (Parrish and Lavin, 1982). That they are deep-seated is evidenced by the magnetic and gravity discontinuities (see Figures 1a and b).

Narrower zones of fracture concentration, from 10 to 50 feet across and up to one mile in length, have been termed fracture traces (Lattman, 1958). The third dimension of some of these fracture traces can be seen along the Tyrone bypass. In this region the fracture traces have a preferred orientation at about 095° and 170°, i.e., conjugate directions about the 140° trend for the Tyrone-Mt. Union lineament. The relationship between joints (mesoscopic scale), fracture traces mapped on aerial photographs (macroscopic scale) and lineaments mapped from LANDSAT images (macro- and megascopic scale) in the Tyrone-Mt. Union area may be linked in orientation and scale through a 2nd order shear model. These geometric relationships are depicted below in Figure 2, along with the directions of the dominant and pervasive joints in this area (see Figure 3, Canich and Gold, this volume). The pervasive 140° striking joints represent the mesoscopic scale of cross-strike fractures.

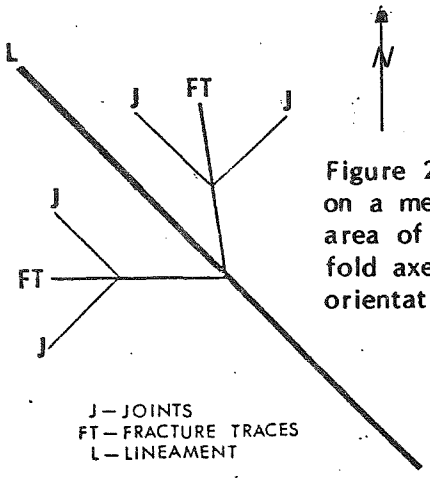

Figure 2. Geometric relationship between "fracture forms" mapped on a meso-, macro-, and megascopic scale in the Tyrone-Mt. Union area of central Pennsylvania. The strike-parallel lineaments and fold axes trends (northeast) have been omitted from this size-orientation summary diagram. (After Canich, 1976.)

Definitions and Terms

Antithetic thrust - A thrust fault (usually a splay) whose fault plane rises in a direction opposite to that of tectonic transport. In Pennsylvania, this direction ranges from north to west-northwest. Many (most?) antithetic thrusts may be leading edges of intercutaneous wedges.

Blind thrust - A thrust fault which does not reach the ground surface; generally dies out upward in a fold.

Concentric fold - A fold in which the strata have not changed their original thickness during deformation (AGI Glossary, 1973, p. 146).

Decollement - Bed-parallel detachment structure of strata due to deformation, resulting in independent styles of deformation in the rocks above and below (AGI Glossary, 1973, p. 182).

Disturbed zone - A zone of tightly folded and thrust-faulted beds in either the hanging wall or the footwall rocks adjacent to a thrust fault, or in a zone between a closely spaced pair of series of approximately parallel thrust faults (Figure 3). In contrast to the intense deformation within a disturbed zone, the beds adjacent to the zone are relatively undeformed. Disturbed zones range in size from tens to hundreds of meters thick and commonly may be traced for a few kilometers to tens of kilometers along their strikes. They are distinguished from a horse block or a duplex (Figure 4) because neither the horse blocks nor the duplexes need to be intensely folded or faulted in the fault-bounded zone.

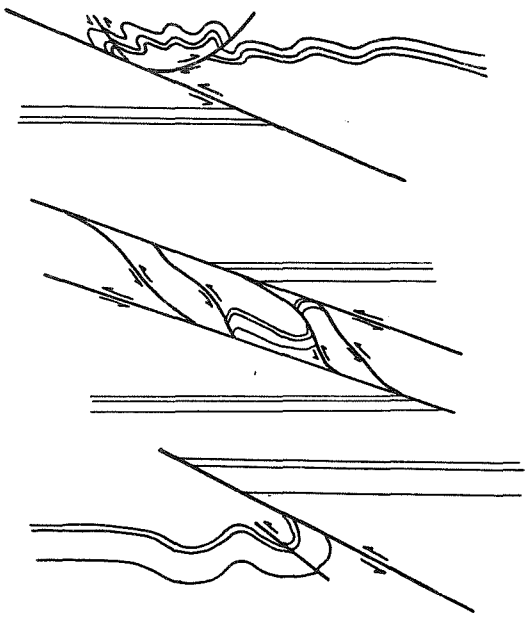

Figure 3. Characteristics of some disturbed zones. (A) Development of antithetic faults in the hanging wall. (B) Deformation between two subparallel thrust faults. (C) Development of footwall splays.

Figure 4. Isometric diagram to illustrate some thrust fault terminology.

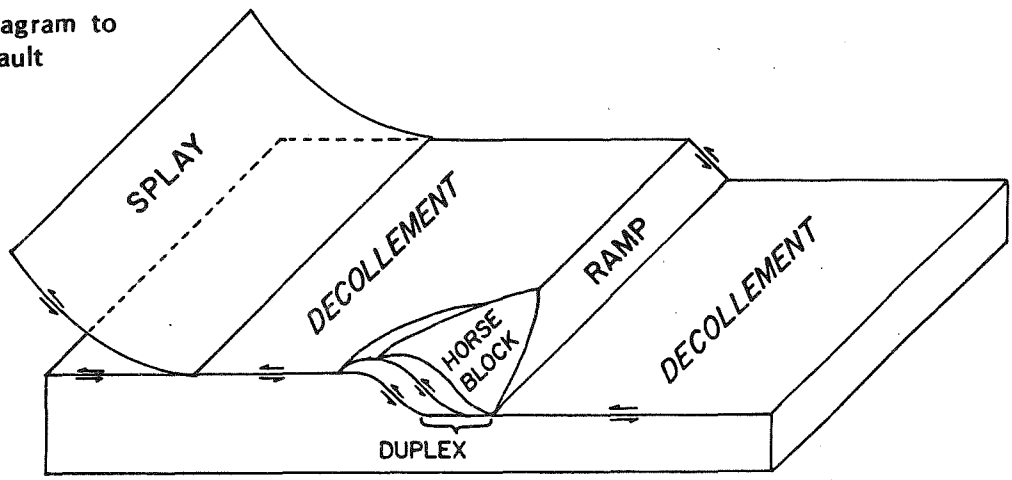

The thrust faults bounding disturbed zones may be either bed-parallel or bed-oblique. Although similar in appearance to drag folds, bed-parallel disturbed zones may be differentiated from drag folds in that disturbed zones are (1) not restricted to the limbs of a host fold, (2) generally contain more intense deformation than drag folds, and (3) may show opposite senses of rotation of axial planes of folds within the fault block.

Duplex - An imbricate thrust system where each splay or subsidiary thrust joins two common thrusts, an upper roof thrust and a lower floor thrust (Charlesworth and Gagnon, 1985).

Intercutaneous wedge - A boomerang shaped detached wedge associated with, and stacked above the ramp to form an anticline in the covering rocks. The successive stages of wedge development are illustrated in Figure 5.

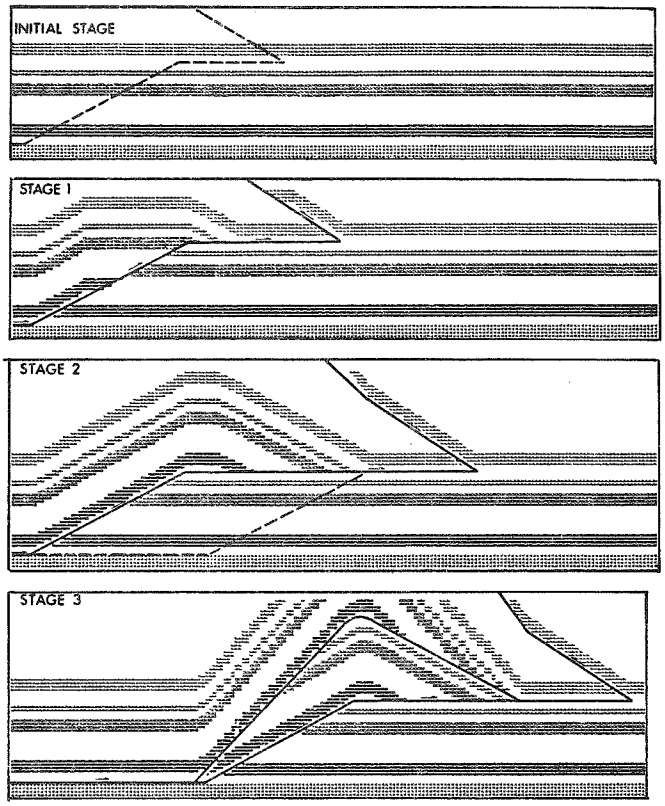

Figure 5. Synthetic models showing four stages in the development of an intercutaneous wedge. Note the widening of the highest flat of the lower thrust, which leads in stage 3 to collapse of the footwall ramp and incorporation of a horse in the active wedge. The dimensions of the horse and the displacement along the new segment of the lower thrust are such as to produce an anticlinal stack, where the axial traces of the anticlines above and below the thrust are continuous. For the sake of clarity, the upper stratigraphic horizons have been omitted. Dashed lines represent incipient thrusts. (After Charlesworth and Gagnon, 1985.)

Kink fold - A chevron fold with a narrow hinge and long planar limbs.

Ramp - An inclined thrust fault that connects two decollements at different stratigraphic levels. "Decollements tend to form as subhorizontal features over great distances only in incompetent zones and shift abruptly upward along short diagonal ramps through more competent zones into other incompetent zones" (Harris and Milici, 1977, p. 5).

Snake-head fold - A synclinal flexure and partial anticline over a ramp fault, where the hanging wall layers (beds) wedge out just beyond the top of the ramp (see stages 1 and 2 in Figure 5).

Stacked anticlines - A structural configuration in which an anticline is thrust up over an adjacent anticline along a splay fault, resulting in no real synclinal axis, only adjacent anticlines separated by a fault.

Splay fault - A thrust fault which rises from a decollement and continues to rise through the stratigraphic column until it penetrates the surface or dies out in the core of a fold.

Synthetic thrust - A thrust fault (usually a splay) whose fault plane rises in the direction of tectonic transport. In Pennsylvania this direction ranges from south to east-southeast.

REGIONAL JOINT EVOLUTION IN THE VALLEY AND RIDGE PROVINCE OF PENNSYLVANIA IN RELATION TO THE ALLEGHANY OROGENY

by
Nebil Orkan and Barry Voight

Introduction

For this conference we present some results of analysis of regional jointing in, primarily, the Valley and Ridge Province of Pennsylvania. The study was initiated in order to describe the geometry, physical features, and sequence of development of joint sets, to establish which patterns are regional in extent, to note geometric relationships between joint sets and local and regional structures, and to provide some insights on the orogenic evolution of the central Appalachians.

Wood, Arndt and Carter (1969) examined joints in the western part of the Anthracite region in eastern Pennsylvania, and summarized the sparse literature on joints in the Valley and Ridge Province. Studies of regional fracture patterns in nearby areas include those of Nickelsen and Hough (1967) in Pennsylvania, Parker (1942) and Engelder and Geiser (1980) in New York, and Ver Steeg (1942, 1944) in Ohio. One of our original objectives was to compare joint systems within the Valley and Ridge and to examine their relationships to those of the Allegheny Plateau in Pennsylvania and adjacent New York. Although correlations of this type had been locally attempted (e.g., Nickelsen, 1974, Fig. 3; 1979; Faill, 1979) and were successful in demonstrating that certain fracture sets could cross such major structural boundaries as the Allegheny Structural Front, no detailed regional study had yet been conducted. Furthermore, though mineral fillings are rarely present in the Allegheny Plateau (Nickelsen and Hough, 1967, p. 616; Engelder and Geiser, 1980, p. 6333), as characteristic features of fracture sets in the Valley and Ridge they open further avenues for research. We hoped to be able to utilize fluid inclusion studies on vein minerals enclosed within fractures in order to establish some conditions of temperature and pressure associated with fracture formation, and hence, with various phases of orogeny. We thank Kirby Young for proofreading this manuscript. Kirby, who found parts of the paper "understandable but confusing", therefore must share the responsibility for all errors of fact or interpretation presented.

Fracture Geometry

Field Methods

In the summer of 1979 and 1980 fractures were studied at 48 stations, mainly in the Pennsylvania Valley and Ridge Province (Fig. 1). A few stations were located in the Great Valley, which in southern Pennsylvania is intimately connected to the Valley and Ridge (e.g., Root, 1971, Fig. 29-30). In station selection, priority was given to locations displaying both adequate fracture development and fracture fillings suitable for fluid inclusion analysis. Stations were concentrated at several stratigraphic levels in order to examine the role of depth in regional comparisons of fracture development and fluid inclusion data. Ordovician limestones, lower Devonian limestones, and the Llewellyn Formation sandstones seemed especially suitable because of regional continuity and adequacy of exposure. Stations were mainly grouped near four transects crossing the regional structural trend, as denoted by traces of major anticlines.

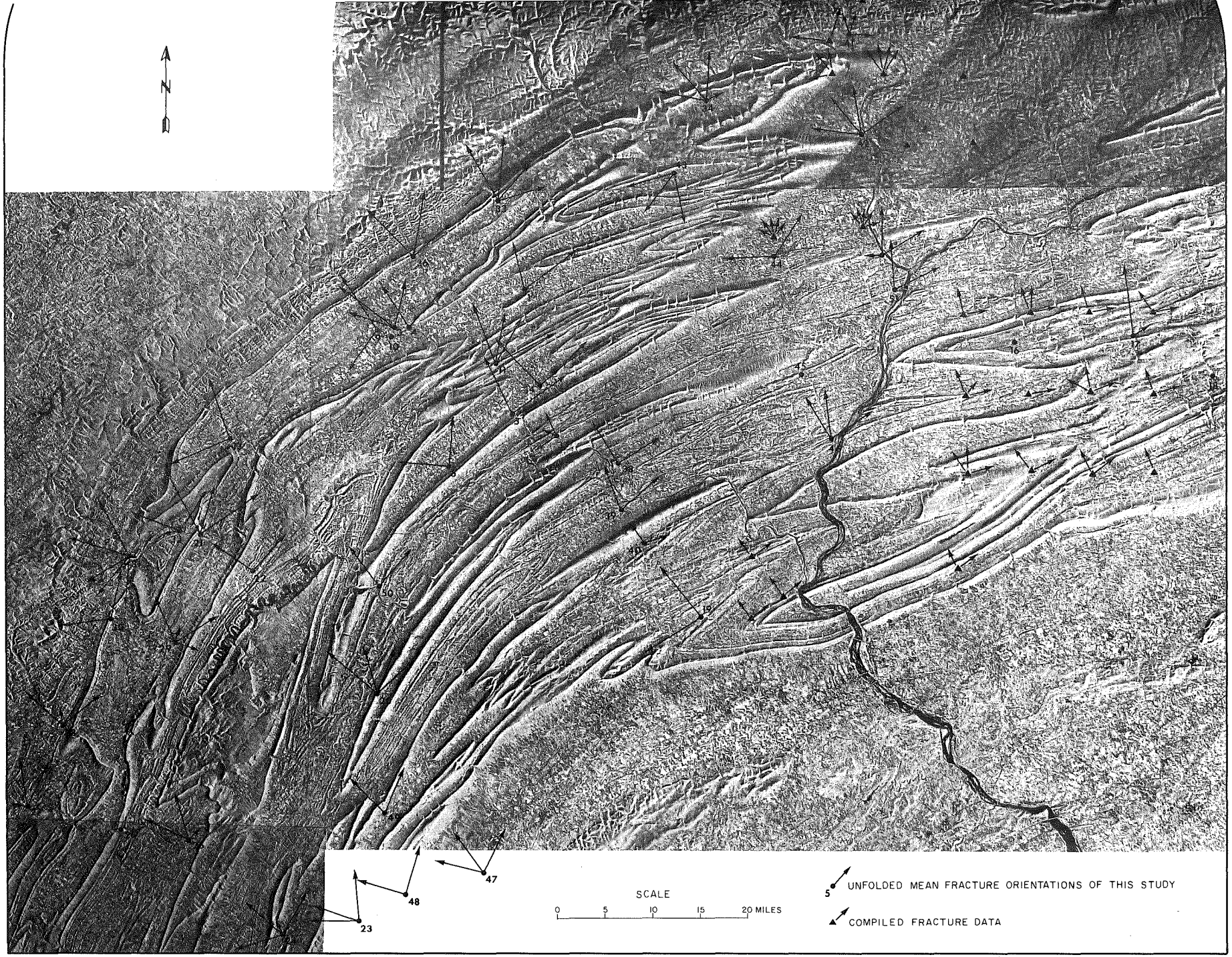

Figure 1. Map of joint strikes, Valley and Ridge Province: data rotated about bedding strike. (Base is synthetic aperture radar image mosaic.)

At each station, 16 to 70 fracture orientations were measured by Brunton compass. Mean orientations of fracture sets were determined graphically from computer contoured (line printer output) equal area nets (Jeren and Mashey, 1970). Cross-cutting relations were recorded in order to establish relative ages (cf. Grout and Verbeek, 1983, Fig. 15A).

Data Presentation

Fracture data are grouped by stations. Mean orientations of fracture sets, relative ages, vein mineral sample numbers, bedding orientations, and unfolded mean orientations of fracture sets are summarized in Orkan and Voight (manuscript in prep.). In Figure 1 we present a simplified view of regional trends, using as a base an airborne radar map. To reduce the influence of folding, bedding planes were rotated to horizontal; the resultant rotated strike orientations of fracture sets are given in Figure 1. Plunge angles of major folds in the Valley and Ridge are typically small, and rotating fractures about the strike of bedding at individual stations was considered reasonable as a first-approximation approach to analyze local fracture patterns.

Finally, because our sampling localities comprised rather small areas, we have supplemented our data with information reported in the literature. These data, usually taken over quadrangle-sized regions, generally compare favorably with our measurements; this suggests that our trends and observations may often be extrapolated with some confidence over a larger region. Furthermore, the results of our vein mineral studies may be justifiably considered in terms of regional application.

Some Results

1. Although low to moderate angle (<60° dip) fracture sets are locally abundant, most fracture sets generally are nearly perpendicular to bedding planes. The unfolded fracture orientations demonstrate this relation, for in unfolded positions the joints tend to be subvertical, with the great majority dipping more steeply than 80°. This relationship suggests (but does not require) that in many cases the fractures are pre-folding in age. A strong role is indicated for bedding in the transmission of causative stresses associated with fracturing.

2. At virtually all stations at least two systematic fracture sets are evident. At most stations one set is highly oblique to the regional structural trend, and another set either is parallel to regional fold structure or is slightly oblique to it. The terms "transverse" and "longitudinal" may be applied to these sets. In some respects, these are similar to the "fundamental joint system" defined by Nickelsen & Hough (1967), comprised of an approximately orthogonal systematic and nonsystematic set of joints. We comment further on joint terminology in a later section of this paper.

3. At some stations, joint sets additional to the transverse and longitudinal sets are present, and certain regions within the study area appear to be characterized by exceptionally complicated fracture relationships. Examples of such regions include the Williamsport area in the north, and territory near Bedford and Altoona in the southwest, where complex systems of joints are present. These are interpreted in terms of overprinting of simple systems, systems which may occur without complication in adjacent areas.

Other causes of complicated patterns include the influence of local structures. In the area of this field conference this is demonstrable near the

Tyrone-Mt. Union lineament. Northwest of Birmingham in a homoclinal sequence (Stops 3, 4, Trip 4) the fracture pattern is quite regular, with a pole concentration oriented at 040° and 130°. Southeast of this point numerous faults slice across the folded terrane and the fracture pattern displays marked local variations about a persistent 040° set (cf. Canich, 1976; Canich and Gold, this guidebook).

4. Shear fractures are present locally, but we interpret the regional joint sets as quasi-vertical extension fractures (Mode I cracks in the jargon of Fracture Mechanics), in agreement with the interpretations of Nickelsen and Hough (1967), Nickelsen (1979), and Engelder and Geiser (1980). Vertical joints propagate perpendicular to the least principal stress at the time of deformation, thus permitting inferences regarding orogenic stress fields.

5. Transverse fracture sets maintain systematic orientations over large areas of the Valley and Ridge and adjacent Allegheny Plateau. Figure 2 compares the patterns of systematic shale fractures in the Allegheny Plateau from Nickelsen and Hough (1967, Plate 3) and Geiser and Engelder (1983, Fig. 6A), and the transverse fracture sets in the Valley and Ridge from this study. Nickelsen and Hough found five different sets of systematic shale joints labeled A, B, C, D, and E on Figure 2. All of the sets can be traced into the Valley and Ridge. It is emphasized that correlation requires consideration of other criteria in addition to geometry, such as relative age and sequence of development; discussion of such issues is postponed to a later section of this report.

The best documented set on the plateau is A, which extends northeast along the Allegheny Structural Front for a distance of 140 miles, and northwest from the Front, into New York State for a comparable distance. This set is widespread in the Valley and Ridge, which it completely crosses, and is recognized at some localities in the Great Valley (e.g., Station 47). Along bedding strike, it can be traced over a hundred mile stretch from Chambersburg to east of Harrisburg.

In the Plateau, the north-northwest striking D joint set appears in the vicinity of Lock Haven; its occurrence seems widespread to the north in New York State, and to the east in Pennsylvania and New York. Set D extends into the Valley and Ridge, where it is particularly evident at stations in the vicinity of Lock Haven and Williamsport (e.g., stations 41-43), and in the Anthracite region.

Also occurring near Williamsport is the north-northeast striking set E (Nickelsen and Hough, 1967), which occupies extensive territory to the east and north, at least as far north as Syracuse (data of Engelder and Geiser, 1980). Overprinting of the three sets A, D, and E seem to account for much of the complexity of the joint fabric between Williamsport and Harrisburg. Most stations show two intersecting sets, typically A-D intersections along the "join" Williamsport-Harrisburg, and typically D-E intersections further to the east. Station data often mirrors the trends of much larger regions; thus station 42 reflects the pattern of the Montoursville South quadrangle (Faill 1979), which displays a dominant D set and subordinate A set. Similarly, station 41 displays the prominant E trend documented in the Montoursville North, Huntersville, and the northern quarter of the Montoursville south quadrangle (Faill, 1979; Wells and Bucek, 1980). A, D, and E trends can also be discerned in data from the Western Middle Field of the Anthracite region (Fig. 2; Wood et al., 1969).

South of Williamsport we also recognize a distinctive northeast-trending set of joints that cuts obliquely across structural grain. Elsewhere in the Valley and Ridge fractures of similar trend are aligned with the grain, and hence, as strike

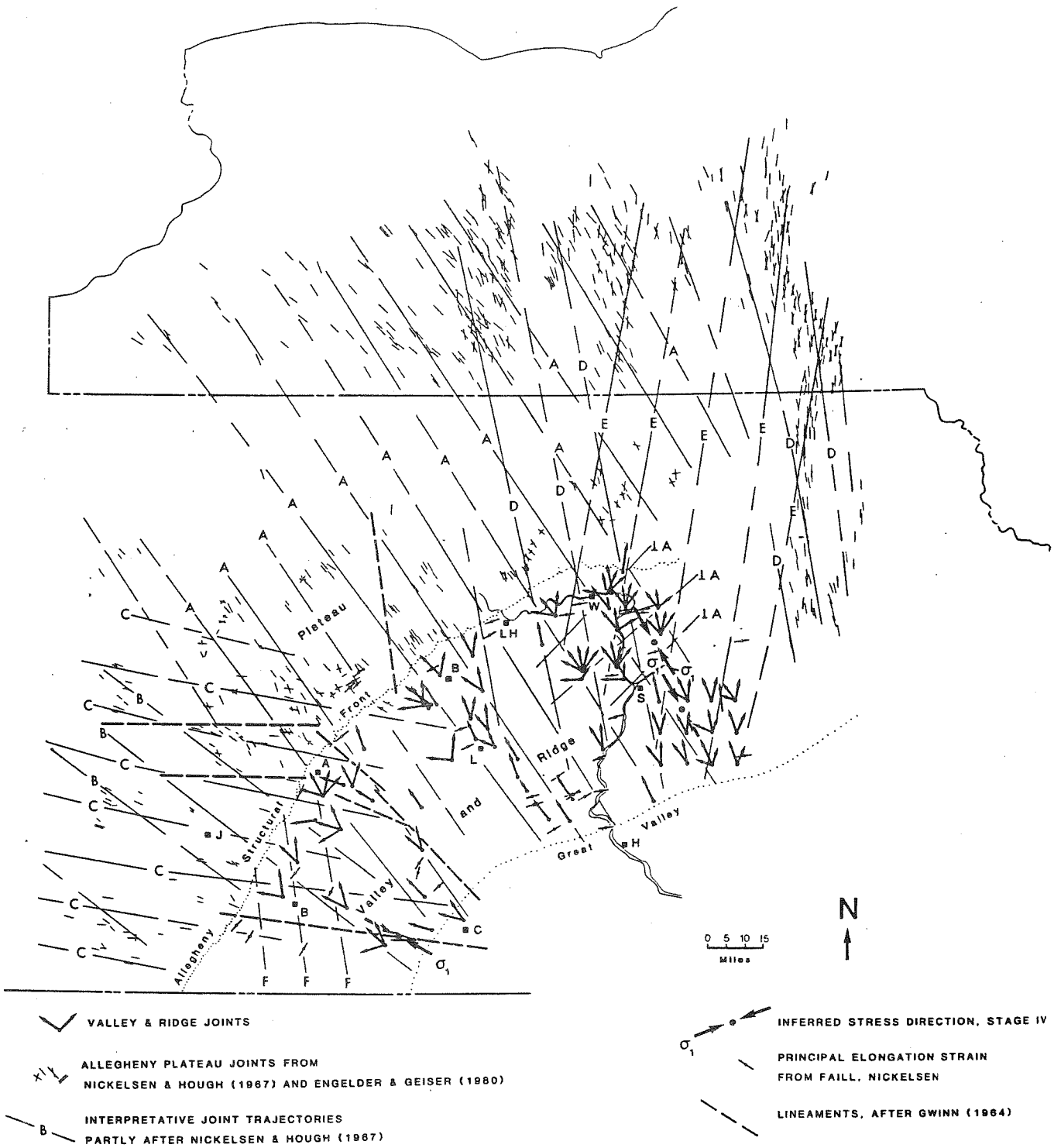

Figure 2. Strike of major transverse joint sets in the central Appalachian foreland, with interpreted trajectories of systematic sets. Supplementary data mainly from Nickelsen and Hough (1967), Wood et al. (1969), and Engelder and Geiser (1980).

joints, could be interpreted as part of the folding process. But the data near Williamsport reveal the independence of this set to existing fold structure; we interpret these elements as a "⊥A set", that is, an orthogonal set to A and perhaps part of the "fundamental joint system" of A in the sense of Nickelsen and Hough.

South of Tyrone along the Allegheny Front, the A set diminishes and is replaced mainly by, the west-northwest-striking C set, which becomes the dominant set southwards to at least the Maryland line. The C set can be traced across the Valley and Ridge to the Great Valley and South Mountain; many stations in the Valley and Ridge show intersections of sets A and C.

In addition, a B set of orientation intermediate between A and C seems to occur on the Plateau, between Johnstown and areas northwest of Altoona. Nickelsen and Hough (1967) were uncertain whether the B set was distinct from A or whether it represented a slight change in A orientation. We have similar uncertainty, though the data of station 24 simulates an A-B intersection and suggests that B may be a distinct set associated with local stress reorientation. It appears restricted on a regional basis.

In the vicinity of Bedford we recognize still another joint set of north-northwest trend, here called set F which intersects the C set at stations 25, 27, and 28. Its orientation is similar to that of set D near Williamsport, and the two sets may be somehow related although the two regions seem spatially distinct. Its orientation is nearly identical to that of north-northwest systematic joints in coal in the Windber quadrangle south of Johnstown (Nickelsen and Hough, 1967, plate 2). The attitude of these coal joints seem abnormal when compared to the regional patterns of coal joints on the plateau, but perhaps represents a more local northerly-trending variation of joint set II of Nickelsen and Hough (1967, plate 3); these coal joints seem genetically related to the shale-sandstone A set. We found no A-F intersections, though our data set is small, but it is conceivable that set F represents a distinct local reorientation of the "set A stress pattern" in the southwest Valley and Ridge of Pennsylvania.

Bear Valley: Some Observations

In a painstaking study carried out in the finest of Cloos traditions, Nickelsen (1979) recognized at Bear Valley (Fig. 1, Station 16) the following sequence of structural events:

(I) Extension jointing in coals at azimuth 050-070, prior to the Alleghany orogeny.

(II) Extension jointing in sandstone and ironstones as the first Alleghany event; the initiation of layer parallel shortening.

(III) Spaced (pressure solution) cleavage in shales and small wavelength intrabed folding in ironstones, offsetting earlier stage II joints.

(IV) Conjugate wrench faults, and (probably slightly later) wedge thrusts. Slickenlines on wrench faults parallel fault-bed intersections, proving pre-fold relations.

(V) Buckling leading to large wavelength finite amplitude folding.

(VI) Stretching in the outer arc of folded sandstones, creating strike grabens and transverse grabens, some following earlier wrench faults; upthrusts in fold cores.

(VII) Wrench faults associated locally with major topographic gaps and lineaments (Nickelsen, 1983).

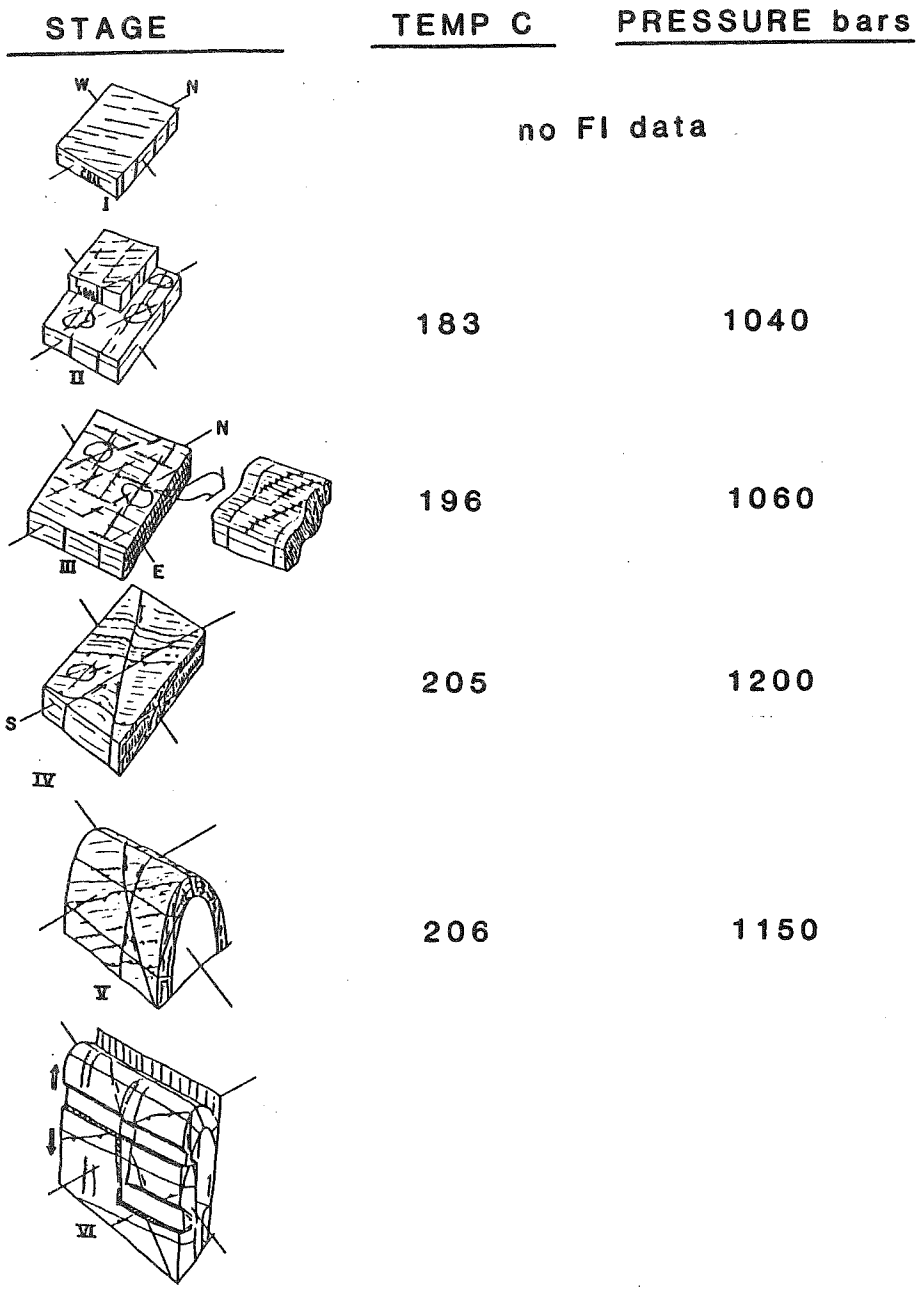

Figure 3. Evolution of structural stages at Bear Valley Mine (after Nickelsen, 1979) with temperature and pressures established by this study.

Because all structural stages are superimposed at one locality, progressive deformation and relative timing of various phases could be proven. The major fold trend is 072°, with mean cleavage-bedding intersections about 065-078°. The mean acute bisector of the conjugate wrench system is about 330° and for the thrust system about 340°; these may be taken as estimates of the maximum compression azimuth during the later stages of layer parallel shortening. Two different sets of stage II extension joints were reported at Bear Valley. Some stage II joints are perpendicular to rock cleavage and are partly contemporaneous with cleavage (hence, they might be considered as stage III joints) whereas others are intersected by cleavage at oblique angles, and have been offset by cleavage related pressure solution.

Joint sets A, D and E seem represented in the regional compilation of Wood et al. (1969), which suggests the dominance of a NNW D set throughout the Western Middle Field, the presence of E, and A in the southwest quarter of their area of investigation (Fig. 2). At Bear Valley the D set orientation lies approximately perpendicular to the major fold trend, whereas the earlier-developed stage IV wrench fault bisector closely approximates the A trend.

Geiser and Engelder (1983) recognize this relationship (Nickelsen, 1979, Fig. 4) and suggest that the system of structures at Bear Valley "correlates almost precisely" with their set Ib joints and their Lackawanna phase of deformation, the earliest of two major deformations recognized by them. Some aspects of this interpretation raise problems. Set Ib in western New York includes elements that seem to correlate geometrically, by interpreted gradual azimuth change, with both sets A and D in Pennsylvania; yet the precise parallelism of especially set A and the various localities in Pennsylvania where A and D intersect in both the Plateau (Nickelsen and Hough, 1967, p. 618) and Valley and Ridge (Fig. 1, e.g. near Williamsport) suggest that sets A and D are distinct structural elements.

Comments on Origin of Joints and a Proposed Classification

The discussion of Bear Valley structure provides background for a classification of fractures, particularly for those produced as Alleghanian structures in the Valley and Ridge. This classification is intended to provide a framework for interpretation of local and regional joint patterns. For jointing transverse to structural grain, the following categories are considered.

Event	Stage	Geometry							
		A	B	C	D	E	F	Horizontal	Other, including 1 A, etc.
Initial Coal Deformation	I								x
Layer-Parallel Shortening	II	x	x	x	x	x	x		x
	III	x	x	x	x	x	x		x
	IV	x	x	x	x	x	x		x
Finite-Amplitude Buckling	V	x		x	x			x	
	VI	x			x			x	
Local Wrenching	VII								
Post-orogenic Denudation	VIII	x							

FIELD TRIP PARTICIPANTS MAY WISH TO ATTEMPT TO FILL IN THE x's AT VARIOUS EXCURSION STOPS.

The classification recognizes that orogenic regional jointing of most rocks begins with layer-parallel shortening, but stipulates that jointing continues as orogeny proceeds. In early parts of the layer-parallel shortening, vertical extension fracturing is the principal structural element created. Extension fracturing however continues through stages III and IV, where fractures are contemporaneous with additional LPS structural elements such as cleavage and wedge faults. The attitudes of joints may change from vertical to horizontal where stress reorientation occurs, e.g. in the transition from wrench to wedge faulting in stage IV by exchange of σ_2 and σ_3 stress axes (cf. Voight, 1976, p. 349-50; Nickelsen, 1979, p. 234). Folding is encouraged by vertical σ_3, the direction of easiest relief, and by horizontal fractures which reduce critical buckling stress via a decrease in mean layer thickness of the multilayer. Horizontal fracturing may also encourage decollement propagation. Jointing continues through stage V and VI in association with the buckling process, and both transverse and longitudinal sets may develop. Regional layer-parallel stress components are overprinted with stress components generated in buckling, and the resultant stresses-at-points control fracture generation and propagation. Stage VI is dominated by vertical extension, resulting in layer-parallel extension in rotated steeply dipping beds. Extension fractures form on fold limbs in longitudinal position, bisecting strike-grabens, and in transverse position, bisecting transverse-grabens formed by axial stretching. Extension fractures may also develop in association with late wrench faults having horizontal slickenlines cutting fault-bed interactions at angles approaching 90° (Nickelsen, 1983).

Finally, extension jointing may occur because of changes in stress associated with denudation. Elastic and thermoelastic stress components are generated by denudation; these stress changes are superposed upon the existing tectonically-influenced stress components to control the attitude of fracture propagation (Voight and St. Pierre, 1974). Removal of overburden occurred during and following orogeny, being of more importance in some areas than in others. Engelder and Geiser (1980, p. 6333) alluded to some role of load removal in the formation of joints in New York State.

Temporal and spatial relations need to be independently considered. The initiation of Stage IIA fractures, for example, is presumed to have passed as a "tectonic front", from southeast to northwest. The oldest IIA joint in the central Valley and Ridge are therefore older than the first-formed IIA joints at the Alleghany Structural Front, and these in turn are older than similar joints in northwest Pennsylvania. At any given locality, joints of A orientation may be comprised of fractures produced in several stages by progressive deformation; Stage IIIA and VA joints may exist with similar attitudes adjacent to IIA joints in the same outcrop. Relative ages as deduced by examination of the relation of, say, individual A joints to tectonic elements (e.g. cleavage) may thus differ at a given outcrop, providing challenges for interpretation. Whereas elements of a given stage may not necessarily be presumed to be age equivalent everywhere, elements of different stages may be contemporaneous at different spatial locations. Thus, a IVD joint set in the Valley and Ridge may form contemporaneously with a IIID joint set at the Allegheny Front, and with a IID joint set in the Allegheny Plateau.

Fluid Inclusion Analysis of Vein Minerals

Laboratory Methods

Laboratory work was an especially prolonged and painful process; we here minimize the reader's pain by making its description brief.

Prepared samples were examined by petrographic microscope, and domains containing inclusions suitable for thermal analysis were identified in each sample. Small chips were then subjected to analysis in a thermal stage, following procedures described by Roedder (1979). A crushing stage was used to identify condensed gases in inclusions (Roedder, 1970).

Fluid inclusions were investigated at Penn State on Chaix-Meca and U.S. Geological Survey Gas Flow heating and freezing stages. Both instruments have been described elsewhere (Woods et al., 1981; Hollister et al., 1981).

Terminology for Fluid Inclusion Analysis

The following definitions are adhered to:

Primary Inclusion: An inclusion which formed during the crystal's growth.

Secondary Inclusion: An inclusion which formed as a result of the healing process of a later rupture in the crystal.

Homogenization Temperature T_h: The temperature at which liquid and vapor phases in an inclusion become a single phase due to heating in the absence of a solid phase. Also called the filling temperature.

Trapping Temperature T_t and Trapping Pressure P_t: The temperature and pressure at which the fluid inclusion originally formed.

Freezing Temperature T_f: The temperature at which the first solid phase, not present at room temperature, crystallizes in an inclusion due to cooling. In actual practice, freezing temperature is determined as the final melting temperature of a solid inclusion crystal produced by over-cooling in a laboratory (Roedder, 1962).

Solubility Limit: The solubility of a given substance in an inclusion fluid at the T_t, and P_t conditions.

Composition and PVT Determination

Data needed in order to determine trapping conditions T_t, P_t from fluid inclusion analysis are the chemical composition of the inclusion fluids, and the phase relationships and P-V-T-X properties for the fluid of that composition (Roedder and Bodnar, 1980).

Temperature data for phase changes were the only data directly recorded during the laboratory study. For the conventional H_2O-NaCl system inclusions, P-V-T diagrams, and composition determination charts from freezing temperatures were readily available and were employed in this study. For CO_2-CH_4 system inclusions, P-V-T diagrams were constructed using experimentally measured compressibility factors, and a procedure was developed to calculate the composition of the inclusion fluid.

Trapping Temperature

The methods used to estimate trapping temperatures (T_t) are summarized in Table 1.

Table 1. A brief summary for trapping temperature (T_t) estimation methods used in this study. (1) $T_{p.c.}$ (pressure effect correction) based on estimated depth from T_t and temperature gradient=35°/km.

Group	Characteristics	Tt Calculation
Group 4	Coevally trapped CH_4-rich and aqueous (aq.) inclusions	$T_t = T_{sol}(CH_4) = T_h(H_2O)$
Group 1	Aq. inclusions, dissolved gases at solubility limit	$T_t = T_{sol}(CH_4) = T_h(H_2O)$
Group 2	Aq. inclusions, some gases	$T_t = 1/4\ [3T_t(min) + T_t(max)]$ $T_t(min) = T_h$ $T_t(max) = T_h + T_{p.c.}$ (1)
Group 3	Aq. inclusions, negligible gases	$T_t = T_h + T_{p.c.}$

Group 4: Samples in this group contain coeval methane-rich and water-rich inclusions. Crystallization occurred in an environment containing immiscible fluids, with the main components water (with minor sodium chloride), and methane (with minor carbon dioxide). The methane proportion of such an immiscible fluid mixture at trapping conditions must have exceeded the solubility limit of methane in water in order to have permitted a discrete methane-rich immiscible phase. Likewise, the quantity of methane in the coexisting water-rich phase must have been at its solubility limit under the trapping P,T conditions. In this instance, $T_t=T_{sol}=T_h$ and no pressure-effect correction is necessary in order to estimate T_t from homogenization temperature.

Group 1: All the inclusion fluid is interpreted similarly to the water-rich inclusions in the samples of group 4. Samples of both groups should have very similar gas contents. Because dissolved methane is presumed at or near the solubility limit, no pressure-effect correction is required for these samples: $T_t=T_{sol}=T_h$.

The error produced by treating such an inclusion as a conventional aqueous fluid is substantial and leads to a gross overestimation of T_t. For sample 55 the overestimation of trapping temperature is by as much as 90°C.

Group 2 Inclusion fluids in these samples are interpreted as aqueous with the methane proportion below the solubility limit at trapping P,T conditions. Because neither the methane content nor the salinity of the aqueous solution is known, it is not possible to select a unique P-V-T diagram for pressure-effect correction of filling temperatures, though limits can be specified. In this paper, a rough approximation for regional interpretations of T_t for inclusions in this class is given by: $T_t=1/4\ [3T_t(min)+T_t(max)]$

Group 3: No condensed gases were detected by crushing stage tests, and pressure-effect corrections for T_h are of the conventional type for aqueous solutions. P-V-T relations for 10 mol% NaCl equivalent salinity are used for samples for which freezing temperature was not determined.

An example of pressure-effect correction follows, based on group 3 sample 88 for which T_h=161°C. For this example fluid pressure is assumed to be hydrostatic, with complete saturation of ground to the earth's surface. Assumed gradient G is 35°C and surface temperature is 20°C. Solution is by trial and error.

For trial (1) let estimated T_t=161°C.

$$\text{Estimated overburden depth } Z = \frac{T_t - T_{surface}}{G}$$

$$= \frac{161°C - 20°C}{35.0°/km} = \frac{141°C}{35.0°C/km} = 4.03 \text{ km.}$$

Fluid pressure is then $P_t=Z_w$ x Hydrostatic pressure gradient (100bars/km) P_t=4.03km x 100 bars/km = 403 bars, leading to a revised estimate, T_t-193°C.

$$\text{For trial (2), } Z = \frac{193.0°C - 20.0°C}{35.0°C/km} = 4.94 \text{ km,}$$

P_t=494 bars, and revised T_t= 199°C. The trials continue because the fluid pressure-overburden ratio must be assumed, no unique determination of T_t is possible with this procedure.

Trapping Pressure

Determination of P_t is essential to approximate the pressure effect correction $T_{p.c.}$ for the samples of group 2, and 3.

Group 4: Samples that contain coexisting primary water-rich and methane-rich inclusions are especially valuable because they permit the unambiguous determination of <u>both</u> trapping temperature and pressure. In this study 17 samples fall in this category, some of which are listed in Table 2.

The two types of inclusions are considered separately. First, water-rich inclusions saturated with soluble methane are considered. As previously discussed such inclusions yield filling temperatures that are identical to trapping temperatures; with a pressure effect lacking, trapping conditions are represented by a vertical path passing through $T=T_h=T_t$ in a P-T space. Next, coexisting methane-rich inclusions are examined. The filling temperature associated with sub-zero phase separation of methane defines a P_t-T_t path along the isodensity line defined by $T_h(CH_4)$ in the appropriate CH_4 or CH_4-CO_2 P-V-T diagram. The intersection of these two paths in P-T space uniquely defines P_t, T_t the conditions of entrapment.

Group 2, and 3: Trapping pressure P_t cannot be determined uniquely for samples of these groups. In order to estimate P_t, overburden depth Z is assumed. In this study Z was estimated by

$$Z = \frac{T_t - T_{surface}}{G(\text{temperature gradient})}$$

using an assumed surface temperature of 20°C and a normal temperature gradient of 35°C/km. (Paleo-temperature gradient for Pennsylvanian rocks was found to be less than 37°C/km at station 16). Then, P_t can be estimated by,

$$P_t = Z \lambda \gamma$$

where λ is fluid pressure ratio and γ is specific weight (γ =2.4 g/m^3 for saturated condition). Estimates of P_t depend on assumed values of G and λ. Lithostatic (λ =1.0) and hydrostatic (λ =0.4) conditions were taken as upper and lower limits of the fluid ratio, and the corresponding estimates of P_t were given as P_t(max) and P_t(min).

Paleotemperatures and Pressures During the Alleghany Orogeny

We begin discussion with station 16, the Bear Valley Strip Mine, perhaps the best exposure to demonstrate the sequence of structural stages of the Alleghany Orogeny (Nickelsen, 1979).

Paleotemperature and pressure data were determined in this study for stages II through V from quartz mineral fillings in tension joints and tension gashes related to the appropriate structural features.

Samples for stage II extension joints were collected from ironstone carbonate concretions. A sample from a small longitudinal extension joint, parallel to a small-scale fold axis, is interpreted as stage III because it is cut by a wrench fault (stage IV). In the classification presented here, this fracture may be classified as set III$\perp$A because of its azimuth. Stage IV samples are from north-northwest trending quartz-filled tension gashes clearly related to wrench faults (hence, set IVA). Stage V samples were collected from longitudinal extension joints parallel to the major fold axis, on the outer arc of the whale-back anticline (set V$\perp$D).

All samples analyzed from Bear Valley were categorized in "Group 4", as they are characterized by CH_4-rich inclusions trapped coevally with H_2O-rich inclusions. CH_4-rich and H_2O-rich inclusion pairs from individual samples permitted the determination of paleotemperatures and paleofluid pressures at the time of mineral precipitation. Results are summarized in Table 2.

CH_4-rich inclusions in the Bear Valley samples mainly comprise a mixture of CH_4 and CO_2. Although the samples represent different stages of the Alleghany Orogeny, the inclusion chemistries of mixed CH_4-CO2 inclusions remained approximately uniform throughout these stages. Inclusion composition is estimated at 85 mol%CH_4, and 15mol% CO_2. Mean freezing temperature T_fCO_2 shows a range in between -76.5 to -77.5°C which correspond to composition of 14.5 and 15.2mol% CO_2, respectively, in the CH_4-CO_2 system.

Table 2. Fluid inclusion data of group 4 samples in stations 16, and 17. (1) Station 17 sample.

Stage of the Alleghany Orogeny	Sample Numbers	CH_4-Rich Inclusions			H_2O-Rich Inclusions	Trapping Conditions	
		$T_e(CO_2)$	$T_h(CH_4-CO_2)$	Estimated Fluid Composition	$T_h(H_2O)$	P_t	T_t
II	57a,b,d	-77.5°C	-80.5°C	14.5%CO_2 + 85.5%CH_4	+183°C	1030 bars	183°C
	57c	No CO_2	-91.0°C	100%CH_4	+183°C	1000 bars	183°C
III	59a,b,c	-77.0°C	-78.0°C	14.8%CO_2 + 85.2%CH_4	+196°C	1030 bars	196°C
IV	55a,b	-76.5°C	-87.0°C	15.2%CO_2 + 84.8%CH_4	+206°C	1235 bars	206°C
	56a,b	-77.0°C	-87.0°C	14.8%CO_2 + 85.2%CH_4	+203°C	1220 bars	203°C
V	60a,b,c	-76.5°C	-81.0°C	15.2%CO_2 + 84.8%CH_4	+206°C	1140 bars	206°C
V	61(1)a,b	-76.0°C	-80.0°C	15.5%CO_2 + 84.5%CH_4	+212°C	1170 bars	212°C

Relatively pure-CH_4 inclusions were also detected in stage II samples. Although homogenization temperatures T_h were different by 10°C for pure-CH_4 and CH_4-CO_2 inclusions, practically identical entrapment P, T conditions (1000 bars, 183°C for pure-CH_4 inclusions, and 1030 bars, 183°C for mixed CH_4-CO_2 inclusions were estimated using the appropriate P-V-T diagrams.

Figure 3 summarizes the estimated temperatures and fluid-pressures for Bear Valley. In general, T and P seem to progressively increase at this locality with stage of Alleghanian deformation (Orkan and Voight, 1983). Highest T and P occur for stages IV and V.

Overburden depth is estimated from the relation

$$Z = \sigma_v / \gamma,$$

where σ_v is total pressure and γ is specific weight. Since the fluid pressure ratio is by definition $\lambda = P / \sigma_v$, overburden depth can be written as

$$Z = P / \lambda \gamma.$$

Assuming the lithostatic conditions for fluid pressure (λ=1), and taking P =1150 bars (kg/cm^2), and γ = 2.4 g/cm^3

$$Z = \frac{1150 \times 1000 \text{ g/cm}^2}{1 \times 2.4 \text{ g/cm}^3} = 479166 \text{ cm} = 4.8 \text{ km}.$$

The geothermal gradient (G) implied by this depth is given by

$$G = \frac{205 - 20}{4.8} = 37^\circ \text{ C/km},$$

assuming 20°C as a reasonable estimate for ground surface temperature.

Estimates of depth and temperature gradient depend on the assumed values of λ. For the compressional regime, moderate to high values of appear justified ($\lambda >> 0.4$). The sensitivity of the analysis to assumed values of can be examined by considering the moderately high value $\lambda = 0.70$; for this case

$$Z = \frac{1150}{0.70 \times 2.4} = 6.8 \text{ km},$$

and

$$G = \frac{205-20}{6.8} = 25^\circ \text{ C/km}.$$

These estimated burial depths of 5 to 7 km (implying values in the range of 0.7-1.0) compare well with Paxton's (1983) estimate of 6-7 km for the Semi-Anthracite region, using mudrock and sandstone bulk-density and porosities. The maximum temperature, T=205°C, is in excellent agreement with estimates of maximum temperatures using "Level of Organic Metamorphism" (LOM) converted from vitrinite reflectance (see Hood, et al., 1975).

A maximum heating temperature for the coals in the Bear Valley Strip Mine is estimated as 206°C based on LOM=16 (converted from Hower (1978) reflectance data) and 50 M.Y. effective heating time. Using the LOM approach, Levine (1983) suggested a maximum temperature of 185°C for the western edge of the Western-Middle Coal Field based on 2.5% vitrinite reflectance. For the Bear Valley location, however, the temperature estimate would be about 200°C, since it falls approximately on the 3% vitrinite reflectance contour (Levine, 1983, Fig. 25).

Other data in Pennsylvanian age rocks were recorded for stations 17 and 18, east of Bear Valley. Sample 61 from a set D fracture at station 17 was categorized in "Group 4", and paleotemperature and paleopressure were determined from coevally trapped CH_4-rich and H_2O-rich inclusions pairs in the sample. Locally, set D has concurrent mineral filling with a longitudinal fracture set parallel to the local 3rd-order fold axis. Thus, the set may have been formed or reactivated during the stage V (large scale folding), rather than stage II; we regard it as a VD set. Entrapment P, T conditions are estimated as 1170 bars, and 212°C. These P, T estimates are similar to but slightly higher than stage V conditions proposed for Bear Valley, 20 km west.

In order to estimate a paleotemperature and a paleopressure at station 18, a pressure correction was applied to measured homogenization temperatures. Paleotemperature was estimated as 222°C for the sample 64 which was collected from a stage V bedding fault filling. P, T estimates for two other samples were collected from longitudinal fracture sets which are interrelated to large folding (V D). Assuming the intermediate pressure condition $\lambda = 0.7$, paleotemperature was estimated at 232°C.

An additional paleotemperature datum was gathered from fold related (V D) extension fractures at station 51 in the Irish Creek member of the Catskill formation. It bears coevally trapped CH_4-rich and H_2O-rich inclusions. A paleotemperature of 236°C was estimated for the Irish Creek member. Normalized to the Llewellyn formation using a normal temperature gradient of 30°C/km,

$$\text{Normalized } T_t = 236^\circ\text{C} - \left(\frac{30^\circ \text{ C}}{\text{km}} \times 1.5 \text{ km}\right) = 191^\circ\text{C}$$

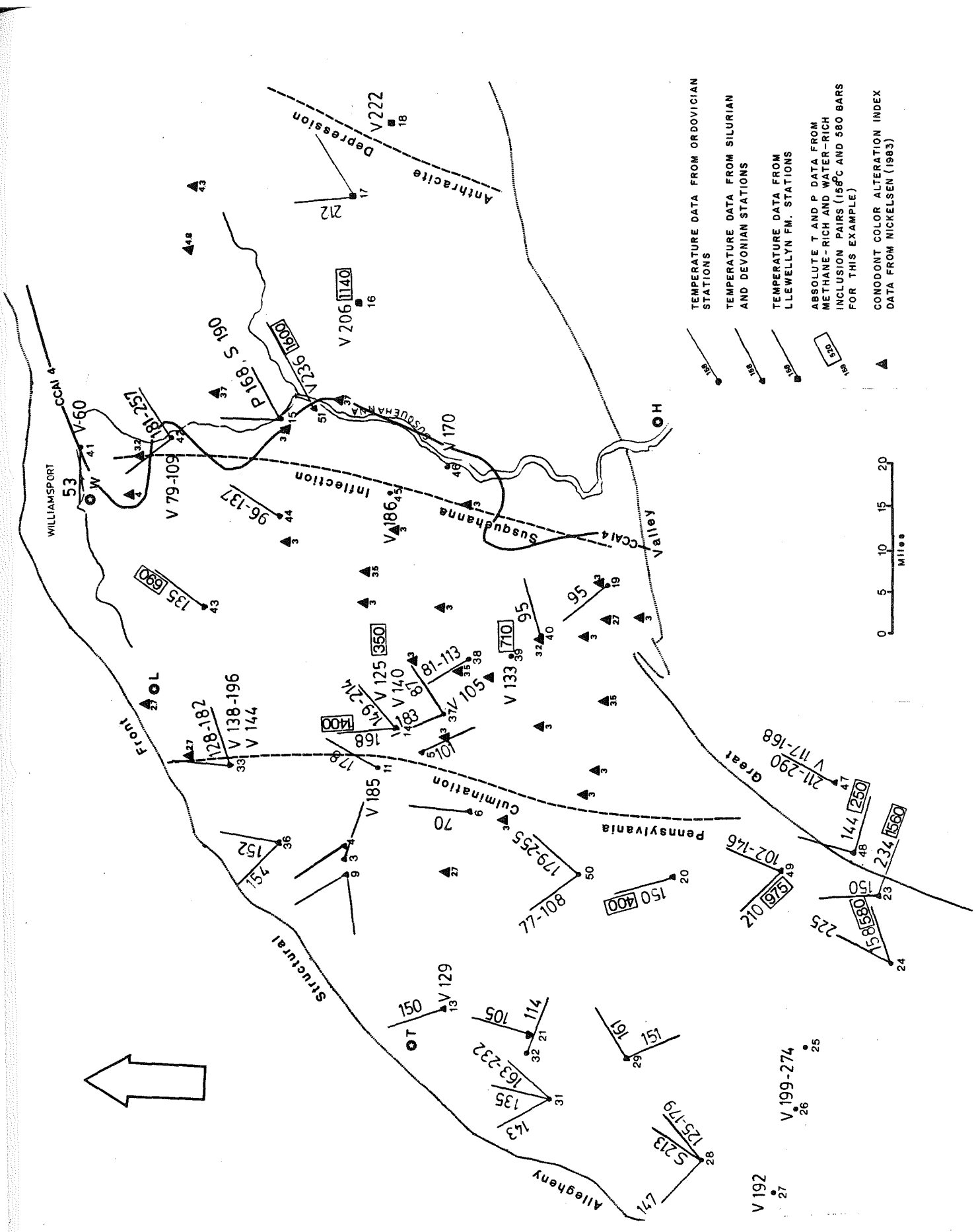

Figure 4. Temperature and pressure data from fluid inclusion analysis, Valley and Ridge Province. Color alteration index numbers from conodonts by Harris et al., 1978 (cf. Nickelsen, 1983b).

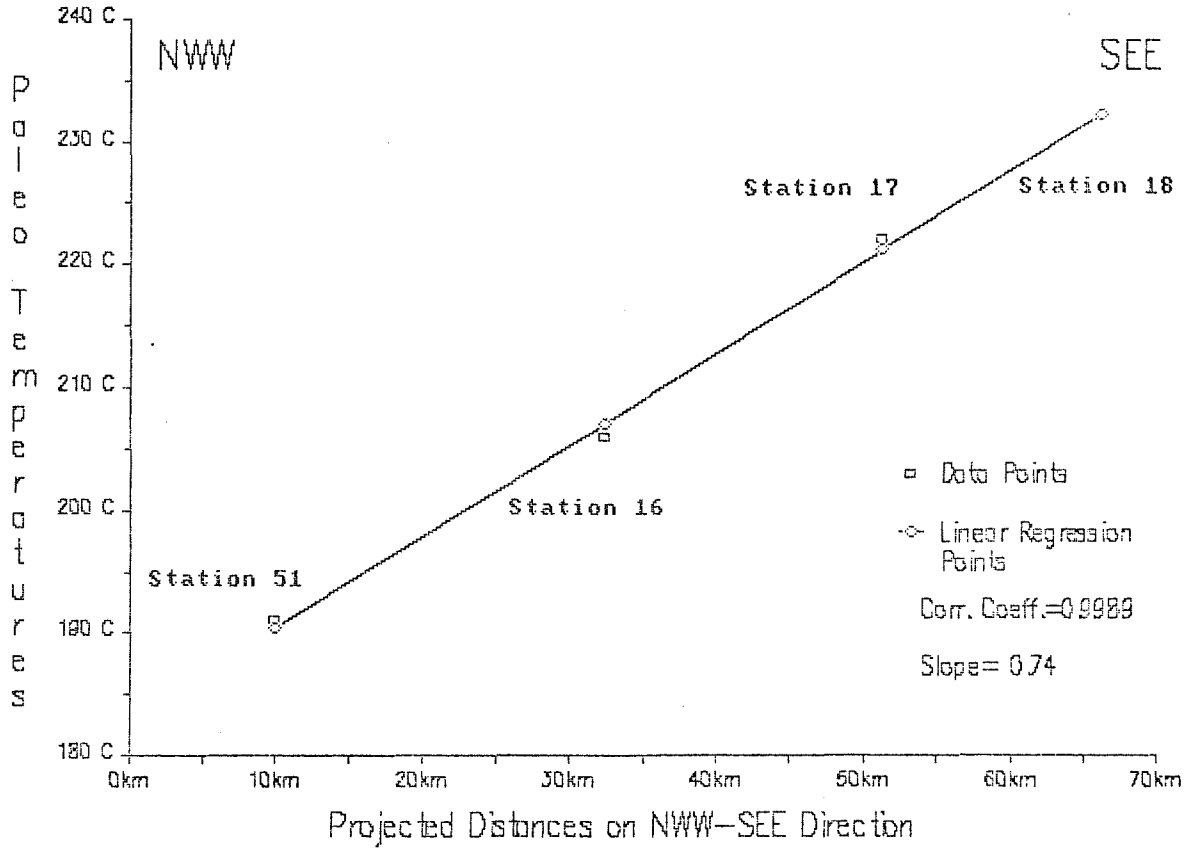

Figure 5. Fluid inclusion paleotemperatures along an ESE traverse in the vicinity of the Western Middle Coal Field. Data normalized to the Llewellyn Formation.

Data from the Pennsylvanian rocks were projected on a WNW-ESE traverse line and plotted against fold related (Stage V) paleotemperature estimates (Fig. 5). Linear regression analysis yields

$$T_t = 183 + 0.74 \times \text{Distance}$$

with a correlation coefficient of 0.999.

The increase of paleotemperature is 0.74°C/km. Using the paleotemperature estimate of G=30°C/km, the local horizontal temperature gradient corresponds to an increase in overburden depth of

$$\frac{1000\text{m}}{30°\text{C}} \times 0.74°\text{C/km} = 24.7\text{m/km}$$

that is, 24.7 m for each km of horizontal distance in SEE direction.

Paxton (1983) estimated a change of overburden depth as 27m/km (Slope of 1.5°) across the Northern Anthracite Field in NW-SE direction. If one accounts for this difference in section orientation, the estimates are remarkably similar.

An easterly increase in magnitude of P, T conditions resembles the regional increase in coal rank from west to east in the Pennsylvania Anthracite region (Hower,

1978). Hower suggested that a geothermal gradient of approximately 79°C/km was needed for the same region if the overburden depth was constant for Pennsylvanian rocks throughout Pennsylvania. On the other hand, Orkan and Voight (1983) argued that the geothermal gradient had to be lower than 37°C/km. Abnormal high geothermal gradient seem unlikely to be the cause of these high paleotemperatures. Increasing paleotemperatures in Pennsylvanian rocks are better interpreted as a result of thickening overburden in the same direction.

Interpretation of Overburden Estimates

The magnitude of overburden required by the paleopressure data and the restricted available time suggested by comparison of the age of the youngest exposed deformed sediments, and age estimates for the Alleghanian Orogeny, preclude the development of this much overburden through ordinary sedimentary processes. In our interpretation the bulk of the overburden was tectonically produced, e.g. by the emplacement of a stack of thrust slices or an olistostrome over the anthracite region. A similar conclusion has been considered by Levine (1984) in his Penn State Ph.D. study on coal reflectance. The emplacement of the allochthonous slices and an associated sediment wedge must have been accomplished in association with layer-parallel shortening in subjacent rocks. The data of Figure 3 show that high temperatures and pressures were already present during the layer-parallel event, and increased with time. The progressive increase in T, P noted at Bear Valley may be reasonably interpreted in terms of an advancing superjacent allochthonous wedge.

In our interpretation the approximate western boundary of the thrust sheet -- which we informally refer to as the "Anthracite Nappe" -- is aligned in a north-south direction just west of the Susquehanna River. We believe that the boundary of the nappe is marked approximately in this region by the CAI 4 contour of Harris et al., 1978 (Fig. 4), which simulates a boundary between low-temperature terrane to the west and higher temperature terrane to the east. The regional extent of the nappe is unclear, but CAI contours suggest that it may have swung eastward or northeastward from Williamsport. The nappe boundary is perhaps reflected in a sharp eastward gradient in coal rank that occurs north of Harrisburg (see Levine, 1983, Fig. 24).

The Pennsylvania Culmination (Nickelsen, 1963) connects high points on individual folds across the salient; to the east, the folds plunge into the anthracite coal basin of eastern Pennsylvania, a deep basin which has been referred to as the Anthracite Depression (Nickelsen, 1963). Reasons for the culmination have been poorly understood, and some authors have considered it a product of Triassic basin uplift transverse to Alleghanian folding (Gwinn, 1970). We observe that the line of inflection separating the Pennsylvania Culmination from its adjacent depression is aligned approximately north-south near the Susquehanna River. This feature, the Susquehanna Inflection, closely coincides with the inferred western boundary of the Anthracite Nappe. We propose that the culmination may be reasonably interpreted as a forebulge effect in front of the advancing nappe, which was buckled and severely compressed during orogeny.

Speculations on the "Big Picture"

Regional relationships during the Alleghanian Orogeny are depicted on a non-palinspastic base in Figure 6. Approximate boundaries of tectonic zones are indicated by A to E, which represent regions characterized by distinct joint sets of similar designation, following the Nickelsen and Hough (1967) terminology. The uniformity of joint sets in individual zones requires relatively uniform causative

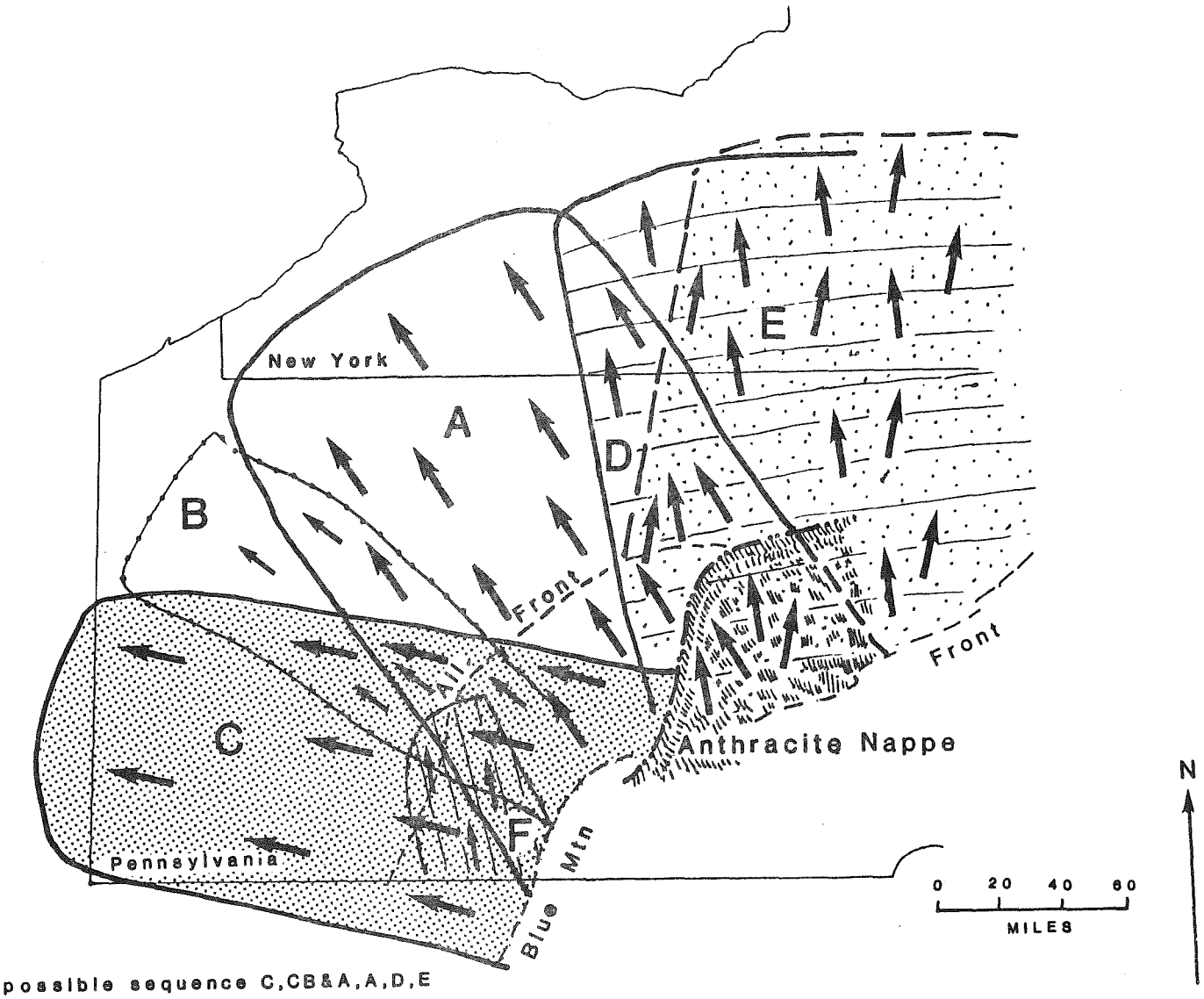

Figure 6. Kinematic interpretation of Alleghany Orogeny in the central Appalachian foreland.

stress directions, implying regularity in the boundary conditions associated with thin-skin loading and displacement patterns.

In our interpretation, progressive deformation began as a WNW compression, aligned in perpendicular fashion to the Allegheny Front and related decollement along a 220 mile stretch from Altoona to White Sulfur Springs. With continued compression, propagation of a decollement occurred in central Pennsylvania to the WNW, with stress trajectories maintaining unusual regularity in producing the A joint set. The B set appears to be related to stress reorientation at the change in strike of the Allegheny Structural Front near Tyrone. East of the Susquehanna the A set developed in Pennsylvanian age rocks under large overburden, suggesting the presence of a superjacent Anthracite Nappe. Stress orientation in the central Appalachian foreland apparently then shifted further toward north (set D; and perhaps F) and then to the NNE (Set E).

Tectonic overprinting, involving the A set followed by more northerly-directed compression, has been documented by the Bear Valley studies

(Nickelsen, 1979) and further supported by the New York State studies of Engelder and Geiser (1980). The latter authors preferred the concept of two separate (WNW and N directions) events because of the distinctiveness of two structural trends and the assumption of rapid response of an orogen to stress loading (Geiser and Engelder, 1983, p. 170). On the other hand, our work suggests that the P, T conditions at Bear Valley sustained insignificant change between phases IV and V (Fig. 3), associated with these two trends (A and D). We also recognize four distinct trends (C, A, D, G) rather than two. The matter remains open for debate, but our present view tends to support a relatively continuous event in which, in Pennsylvania, the stress field rotated almost 90° clockwise.

Alleghanian structures display distinct incremental changes in orientation, rather than a continuous range of orientations, and this feature of the deformation pattern requires explanation. We interpret this phenomenon as a reflection of incremental kinematic adjustments of distinct riser-decollement systems. The lateral boundary conditions of separate decollement plates constrained the kinematic alternatives at the western edge of an orogenic core structure, a core structure that applied compression in Pennsylvania in a relatively continuous clockwise fashion throughout the Alleghanian Orogeny. This change in compression direction may in turn reflect the geometry of a corner of the plate tectonic indenter impressed in a plastic foreland.

Stop localities for Field Trip #4, plotted on Radar Map of part of Central Pennsylvania (STAR-1

FIELD TRIP #4

FIELD GUIDE - CROSS-STRIKE AND STRIKE-PARALLEL DEFORMATION ZONES IN CENTRAL PENNSYLVANIA

Prepared by D. P. Gold and H. A. Pohn
Field Leaders: D. P. Gold, A. L. Guber, B. Voight, H. Pohn, and M. R. Canich

Miles	Interval	
0.0	0.0	Leave Holiday Inn and turn left onto Rte 322.
1.8	1.8	University Park Campus - Nittany Lion Inn on left.
7.25	5.45	Carsons Corner - intersection with Rte 550. Continue on Rte 322.
7.5	0.25	Note exposure of Reedsville Shale in quarry to left (south) of road.
7.6	0.1	The 500 foot road-cut to the right exposes a gradational contact from dominantly shale (Reedsville) to dominantly quartzite beds (50 cm to 2 cm thick) intercalated with thin (up to 50 cm) shale beds of the Bald Eagle (equivalent to Oswego) Formation. The contact is taken as the same marine fossil bed seen at STOP #2. The general bedding attitude of 080°/78°S is not compatible with the ridge crest trend of 060°, and probably represents rotational strain associated with an unusual density of fractures (140°/vert) and faults (000°/80°W) in the Sky Top wind gap. The rusty appearance of these outcrops is due to limonite staining and encrustations from sulfides in these fractures. Slickenslides plunge 30°/320°.
7.75	0.15	The next road-cut to the right exposes steeply dipping (080°/vert) red greywackes and shales of the Juniata Formation.
8.0	0.25	STOP #1. SKYTOP OVERLOOK, on crest of Bald Eagle Mountain. Park vehicles on right hand side and walk 50 yards northwestward to edge of embankment. The steeply dipping Juniata beds across the road to the southeast can be contrasted with the overturned (085°/60°) beds of Tuscarora Quartzite in the small excavation behind us. The view from this Tuscarora ridge reveals the Schooley Peneplain surface on the western horizon (see Figure 1) at a higher elevation (2400 ft) than where we are standing (1520 ft). In fact, the drainage divide is farther west where some of the highest elevations of the Pennsylvanian Appalachian Belt are preserved.

THEME:

- The Catskill Delta; axis of the central lobe.
- The Allegheny Front; boundary between the Valley and Ridge and Allegheny Plateau Provinces.
- Northwesterly trending fracture control of tributary valleys.

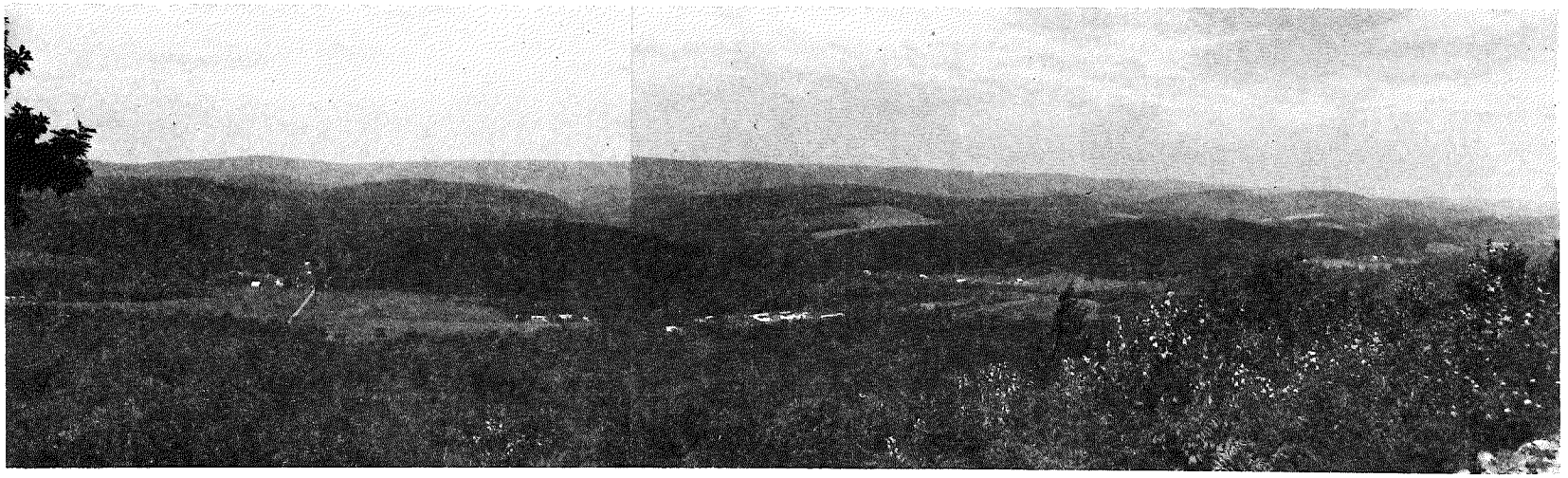

(a)

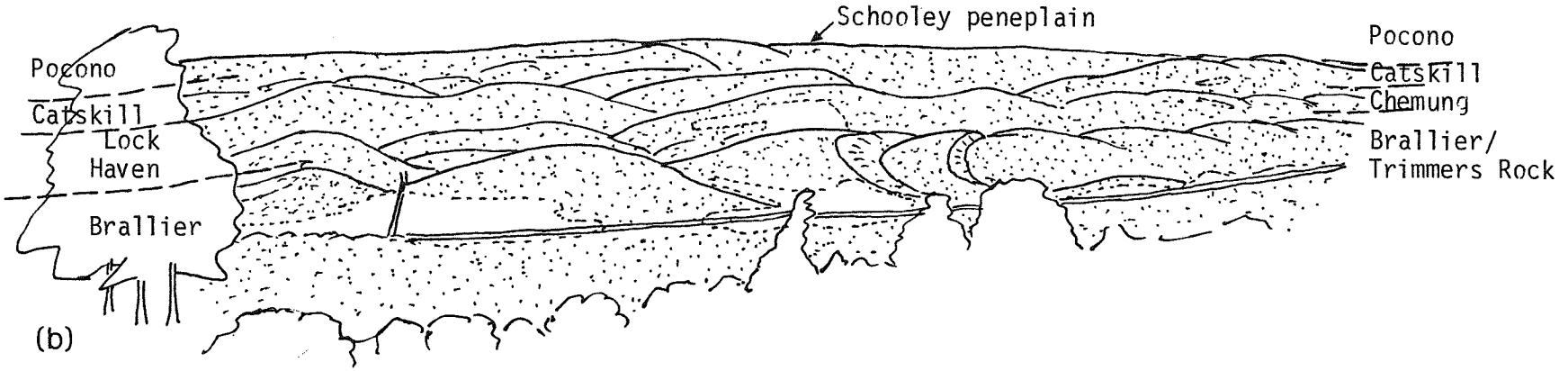

Figure 1. View from Skytop overlook along the axis of the Catskill Delta through progressively the Trimmers Rock/-Brallier Formations (Dbt), the Lock Haven Formation (Dlh) and Catskill Formation (Dck) to the skyline ridge of the Pocono Formation (Mp-Mb) capped locally by the Burgoon Sandstone. The Appalachian Front is defined physiographically as the escarpment, but structurally as the Bald Eagle Valley (foreground), where steeply dipping and overturned beds characteristic of the Valley and Ridge province give way to gently dipping strata of the Allegheny Plateau province (skyline). (a) Panoramic photograph, and (b) annotated sketch.

NARRATIVE: SKYTOP OVERLOOK

We are standing on the axis of the central lobe of a Devonian drainage/depositional system known as the Catskill Delta. The successive delta lobes that prograded westward from a point near to our current position, are preserved as a step-like ridge on the far side of Bald Eagle Valley (see Figure 1). The valley floor is underlain by shales of the Brallier (Trimmers Rock) Formation, which represents deep water deposition. This shale intertongues with and grades upward into Trimmers Rock shales and siltstones that are expressed topographically as the lowest ridges on the western side of Bald Eagle Valley, and represent a continental slope setting. The next lateral series (with open fields) and the low ridges beyond underlie the shelf setting deposits of the Lock Haven Formation. The next lateral ridges are underlain by the Sherman Creek and Duncannon Members of the Catskill Formation, and represent the meandering stream facies of the delta. The upper ridges and skyline are underlain by the braided stream alluvial deposits represented by the Pocono Formation and Burgoon Sandstone.

The influence of lithology on topography is reflected in the overall geometry of the delta. Not only do the beds in this prograding delta complex attain their maximum thickness along the axis and diminish laterally, but the ridges also can be seen to diminish in size in the view to the north.

Note the periodicity and orientation of the tributary valleys. Most of these are controlled by zones of increased fracture density that trend 140°. Some of these extend to water and wind gaps in the Valley and Ridge Province. Does the structural relief of some 15,000 to 20,000 feet between us and the Plateau account for their contrasting styles of deformation?

* * *

Miles	Interval	
		Return to vehicles and continue on Rte 322 W.
8.1	0.1	Note the overturned beds of Tuscarora Quartzite in the road-cuts to the left. Although the dip of these beds may be modified by soil creep (40° and as low as 15°SE), the general strike of 060° is similar to the regional ridge axis.
10.35	2.25	Turn left at intersection with Rte 220S, into Bald Eagle Valley.
10.6	0.25	The hills to the west (right) are underlain by Upper Devonian rocks (Brallier/Trimmers Rock Formation)
10.9	0.3	dipping gently to the northwest. The hills to the left (east) are underlain by Ridgeley Sandstone (Oriskany Group). These rocks have a proven potential for oil and gas farther west.
		Note shallow dips in the quarry to the right.
11.4	0.5	Brallier shales and siltstones in road-cut.
11.8	0.4	Note the well developed joints (135°/vert) in Brallier shale and siltstone (bedding attitude 035°/30°NW).
13.15	1.35	Traffic light in village of Port Matilda.
13.5	0.35	Long road-cut in Brallier Shale (bedding 020°/30° to 40°NW; joints 140°/80°SW to vert).

Miles	Interval	
20.9	7.4	Note the gap in the ridge to the left (east): this marks the trace of an oblique fault.
21.9	1.0	Traffic light near Bald Eagle. Turn left onto Rte 220 bypass.
22.5	0.6	Bridge over Bald Eagle Creek.
22.7	0.2	Note scar of landslide in the northbound road-cut to the left. This marks the trace of a lineament mapped on Landsat imagery as trending 140°. The Ridgeley Sandstone (Upper Lower Devonian - formerly Oriskany Group) at the base of the scar was in a quick condition, and drill holes through a heaved portion of the road bed adjacent to the toe, had a hydraulic head of more than 5 feet. The black top section of road indicates the area affected by the landslide shortly before the opening of the bypass during the Spring, 1975. The dark shales (Marcellus Formation - Middle Devonian), that are exposed in the road-cut to the southwest, directly overlie the Ridgeley Sandstone in this area. A northeast trending fault with a right lateral separation duplicates this section farther along the road, where grey shales and limestone beds of the Shriver Formation are exposed in a nearly vertical
23.0 to 23.15	0.3	attitude beneath locally highly fossiliferous Ridgeley sandstone beds.
26.2	3.2	Turn right on Tyrone exit. Note the overturned (030°/80-55°SE) red and green shale beds of the Bloomsburg Formation (intertongues with the Wills Creek Formation) on the left (eastern) side of the highway.
26.45	0.25	Turn left on Rte 453E at interchange.
26.7	0.25	For the next 0.35 mile red shales, siltstones and sandstones of the Juniata Formation (Upper Ordovician) are exposed in the road-cut to the left (northeast). Note how the attitude of the beds steepen from about 60°SE (overturned) to vertical at the southeastern end of the road-cut.
26.95.	0.25	Turn right and cross bridge.
27.05	0.1	Stop near railroad line and walk southeast for 0.3 mile to the railroad cut 40 yards beyond the signal box, to Station #1. Busses can back down the side road and park near the signal box. CAUTION - this is a busy railway route. PLEASE keep clear of the tracks!

STOP #2. BONTA FARM RAILROAD CUT.

From Station #1 follow the schematic cross-section guide (Figure 2) for 300 feet to the northwest.

THEME:

- Close look at the rocks of the Upper Reedsville and Bald Eagle Formations.
- Early "layer parallel shortening" features such as wedge faults, snake-head folds in individual beds, concentric folds, kink bands and some associated box folds, rotated strike-slip faults.
- Late extensional (normal) faults.
- Pervasive 140° fractures (faults and joints) and conjugate sets about this axis.

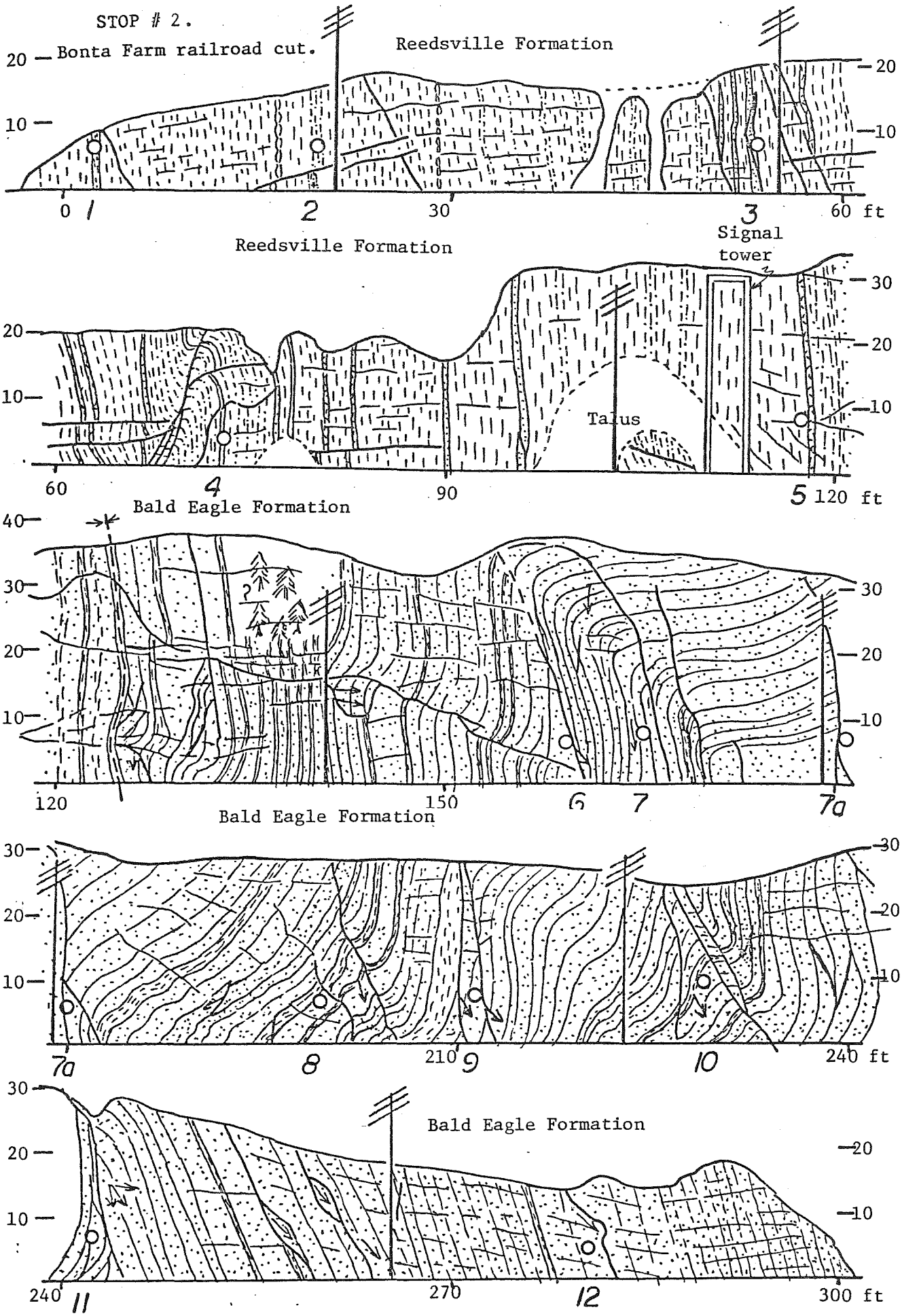

Figure 2. Schematic cross-section of railroad cut.

NARRATIVE: THE BONTA FARM RAILROAD CUT.

These outcrops are located on the south side of the Tyrone Gap, in the northwest limb of the Sinking Valley-Nittany anticlinorium. The Tyrone-Mt. Union lineament passes through the gap and extends northwestward into the Allegheny Plateau. The shale unit intercalated with thin sandstone and limestone beds is part of the Reedsville Formation. The contact with the Bald Eagle Formation, farther along the cut, is gradational, but a change in structural style is apparent in the greater abundance of 3rd and 4th order folds in the latter. Many of the minor folds are disharmonic in sense with the Sinking Valley (Nittany) anticline, suggesting their development prior to the main folding episode. Although folds of different scale may be decoupled in the same event, the presence of bedding plane slickenlines, perpendicular to the minor fold axes, suggest an early flexural-slip folding process. Mesoscopic scale wedge faults that locally duplicate beds, also are related to this early compressional event.

A number of structural features that are common in the Valley and Ridge province in Pennsylvania, are exposed in this outcrop. Perhaps the most conspicuous are the wedge faults, a pre-folding, layer parallel contraction fault (Norris, 1958; Cloos, 1964; Berger et al., 1979), that can be seen at virtually every outcrop on the field trip (e.g., near Station #11). That they preceed folding is well illustrated here, where wedge faults can be seen to curve around fold hinges. We believe that the wedge faults promote the instatiliby that focusses the growth of anticlines. Certainly, most of the early and smaller anticlines are cored by wedge faults, and we suspect that most of the larger (3rd and 2nd order) may be as well. Wedge faults commonly produce zones of high fracture porosity in brittle units, and are believed (Pohn) to be the brittle rock equivalent of disturbed zones in the more ductile rocks (Pohn and Purdy, in preparation).

A second common feature here is the presence of strike-slip slickenlines. Some of these have been flagged with dayglow orange tape. The strike-slip refers to movement sub-parallel to the bedding surface before rotation into the first order anticline. Slickenlines on the dip fault through the folds at Station #7 give a relative sense of timing. The minor folds here formed prior to the fault movement, because the slickenlines on the fault maintain a constant orientation through the hinge zone of the fold. In turn the strike-slip slickenlines must predate, or be contemporaneous with the deformational event that produced the Nittany anticlinorium, i.e., the beds have been rotated to a vertical attitude after (or during) the strike-slip movements. This same sequence is apparent elsewhere in this region. The presence of two or more directions of slickenlines on a fault surface suggests that the strike-slip movements were contemporaneous with the growth of the Nittany anticline. This supposition is confirmed where an age sequence of slickenlines from early (steep) to late (shallow) can be determined, as at Station #11.

Other features apparent in these rocks include conjugate fault sets, several compressional faults of unknown displacement, and several extensional faults of small displacement (e.g., at Station 7a).

lensc

* * *

Miles	Interval	
27.75	0.7	Retrace route, cross bridge and turn right onto Rte 453E at intersection.
28.05	0.3	Intersection with Rte 550. Cross bridge to right on Rte 453E.
28.5	0.45	Cross bridge. Note quarry on left, developed in Middle and Upper Ordovician carbonates, from the Coburn Limestone in the northwest to the Bellefonte Dolomites in the southeast. Also note the thick (1200 ft) section of Bellefonte Dolomite in the road-cuts up the hill to the southeast.
28.7	0.2	Ridge crest in cyclically bedded dolomites of the Bellefonte Formation.
28.9	0.2	Contact with the Nittany Formation near road intersection. Note the well-developed cycles of light and dark gray dolomite in beds 50 cm to 2 m thick. Locally developed sandy layers are quarried for skid resistant aggregate.
29.15	0.25	Bridge to right.
29.2	0.05	Stonehenge Limestone in road-cut to left.
29.75	0.55*	Turn right, cross bridge and drive through railroad underpass.
29.93	0.18	Turn right on dirt road and park at top of underpass.

*If busses are used, leave them about 60 yds northwest of the Birmingham turnoff on the lefthand side of the road, and walk across the bridge and southeast along the railroad to the Birmingham Thrust Fault.

STOP #3. THE BIRMINGHAM THRUST FAULT.

Leave vehicles on road adjacent to the railway lines, and walk 600 yards to the southeast along the railway line to Station #1. The Birmingham thrust fault is exposed in the railroad embankment, where cherty dolomite of the basal Gatesburg Formation(?) overlies Middle Ordovician limestone along a well defined low angle thrust plane. Follow schematic cross-section guide (Figure 13) for 1700 feet from stations 1 to 16.

CAUTION: This is a busy railway route. Please keep to the inside track, and watch out for trains.

THEME:

- Close look at early "layer parallel shortening" features in the Ore Hill Member of the Gatesburg Formation.
- Depositional cycles in the Ore Hill dolomite beds.
- Deformation associated with a low angle thrust fault.
- Difference in lithology of the autochthonous block either side of the river, i.e., across the Tyrone-Mt. Union lineament.
- The stratigraphic identity of the sheared hanging wall unit.

NARRATIVE: THE BIRMINGHAM THRUST FAULT.

The Birmingham "thrust" zone is composed of a number of planar and lensoid fault planes in both the hanging wall (Gatesburg dolomites and

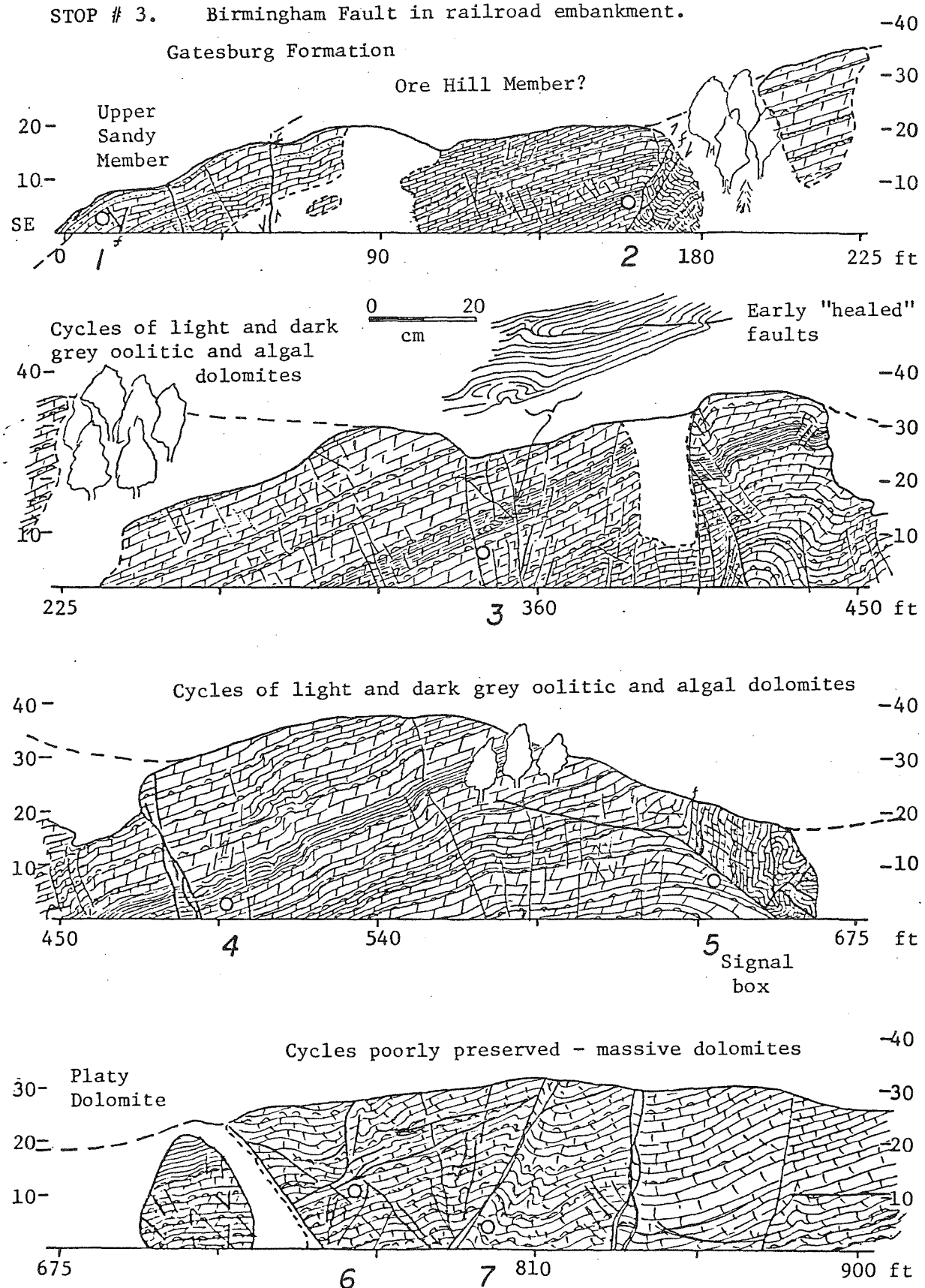

Figure 3. Schematic cross-section of railroad cut south of Birmingham. This section is drawn Warrior Limestone) overlying Middle Ordovician Limestones.

STOP # 3. (continued)

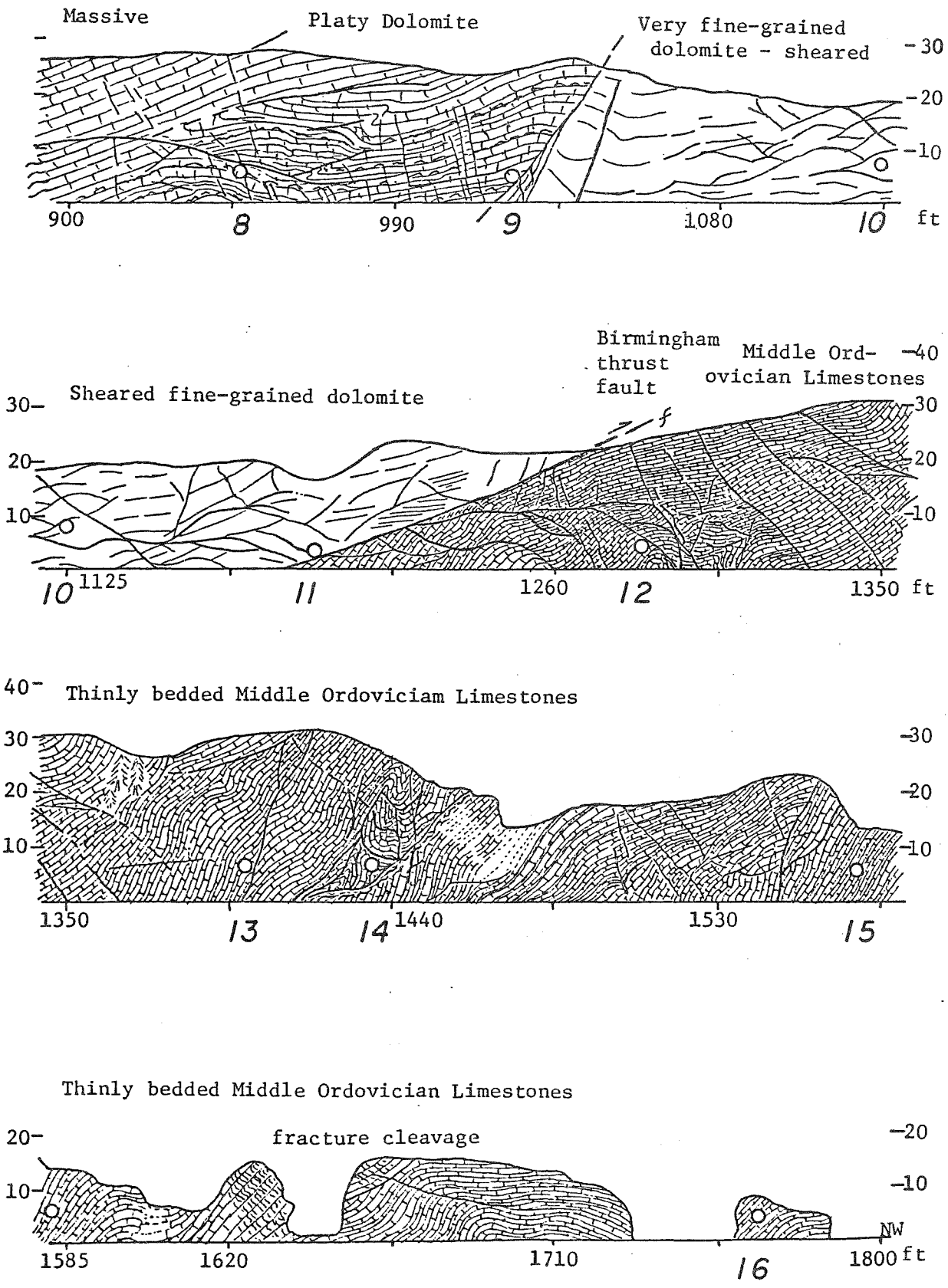

from southeast to northwest, and shows members of the Gatesburg Formation (possibly also Upper

sandstones) and footwall rocks (Middle Ordovician to Silurian at these localities). A discrete thrust plane is exposed above the abandoned quarry at STOP #4, where Gatesburg rocks overlie sheared Black River and Chazy group limestone, and in the railroad cut at STOP #3 (at Station #11 of Figure 3), where sheared cherty dolomites and calcareous sandstones of the Gatesburg Formation or possibly Warrior Formation (Butts, 1918) overlie Middle Ordovician limestones.

STOP #3 (see Figure 3) is one of the locations visited on the First Field Conference of Pennsylvania Geologists during May, 1931. Although Butts (1918, p. 530) states that "The overthrust mass is Warrior limestone and the overridden beds are Carlim limestone", he records the hanging wall rocks as either Warrior limestone or Basal Gatesburg Formation in his later publication (Butts, et al., 1939). The highly sheared, recrystalline(?) and reconstituted nature of the immediate hanging wall rocks precludes a precise stratigraphic identification. Lensoid masses of fine-grained dolomite, quartzite, and cherty limestone have been identified in this rock in which no primary structures are preserved. It is bound about 150 feet to the southeast (Figure 3, Station #9) by a high angle fault that juxtaposes typical Ore Hill Member lithologies (Gatesburg Formation), that are relatively undeformed and dip at about 15° to the southeast (see Figure 3).

It is a matter of conjecture whether or not the Birmingham Fault, which can be traced from about 2 miles to the southwest intermittently to beyond Sky Top (STOP 1), is the major thrust fault in the region or just a minor splay off the deeper Sinking Valley fault. Unfortunately the simple anticlinal form (Figures 5, 8, 10) of the southern end of Sinking Valley is complicated here by faults, some of which are inferred from drill cores (see Figures 9 and 10). The Sinking Valley fault and its splays are arched along an axis plunging southwest, which is nearly coincident with the axis of the Sinking Valley anticline. The northwest limb is displaced about 2 miles. This thrust fault has no apparent surface expression except at the two fensters (windows) near Birmingham, where Ordovician and Silurian rocks are exposed beneath Cambrian dolomites and sandstones. The Sinking Valley fault dips northwestward from the fensters at Birmingham under Brush Mountain, and presumably continues under the Allegheny Plateau.

If the Honest Hollow and Birmingham faults are splay faults off the Sinking Valley thrust fault, then they represent the bounding faults of the Birmingham "window" slice (see Figures 5c and 10b). More drill-holes are needed to determine the relationship of the Shoenberger fault to the Sinking Valley fault system.

In the railroad cut at STOP #3, numerous intraformational antithetic and synthetic thrust faults of unknown displacement, and several extensional faults of small displacement are well exposed in the hanging wall rocks (Ore Hill, and Lower Sandy(?) members of the Gatesburg Formation). In addition, there are a number of "healed" fault planes that reflect an earlier deformational event (possible early Alleghenian in age, or even from an earlier orogeny (Acadian?)).

The footwall is composed of meters to tens of meters sized horse blocks (e.g., Station #12) with a complex relationship to the main thrust

fault. Although most of the larger faults are synthetic, small antithetic faults are present. Extension faults of small displacement are common; the early "healed" faults are rare.

One of the most complex structures in the footwall units is located 240 feet (about 75 m) along the railroad cut (Station #14) northwest of the main exposure of the thrust plane at Station #11. This structure is a totally isolated block, bounded by a folded fault. The beds within the block exhibit a nearly 180° clockwise rotation.

Some of the features to note in your traverse through this railroad cut include:

(a) the conglomerate and sandy beds near Station #1.
(b) the thinly bedded and cyclical nature of the Ore Hill Member on a scale of 1-2 meters, starting with a limey algal unit and grading upward through dark gray oolitic dolomite to platy gray and buff dolomite. These are well developed between Stations #2-7.
(c) the well developed algal heads at Station #4.
(d) the healed faults, representing early layer parallel shortening on a scale of decimeters, near Station #3.
(e) the antithetic splay fault and complex deformed zone behind the signal box, near Station #5.
(f) the Birmingham fault at Station #11. Lensoid and curviplanar splay faults can be seen in the hanging well rocks between Stations #9 to 11, and curved "under-splay" faults occur in the footwall between Stations #11 and 12.
(g) the folded faults in the disturbed zone near Station #14. Clockwise rotation of the beds is apparent between the main breccia (shear) zone and at the fault dipping to the southeast.

* * *

Miles	Interval	
30.1	0.1	Return to vehicles and retrace route through the underpass, across the bridge to junction with Rte 453 and turn left towards Tyrone.
31.85	1.75	Junction with Rte 550.
32.65	0.8	Rte 220 - overpass.
32.8	0.15	Right turn on Rte 453N (Main Street in Tyrone) and follow
34.0	1.2	453N to Y intersection. Leave 453N on righhand fork for
34.25	0.25	Tyrone City Park.
34.3	0.05	Turn left at gate into park for LUNCH LUNCH STOP - Tyrone City Park.
34.6	0.3	Return to junction with 453E, and retrace route to Birmingham.
35.95	1.35	Rte 220 - overpass.
36.75	10.8	Junction with Rte 550.
38.65	1.8	Birmingham turnoff. Park vehicles on left side of road about 20 yds northwest of the turnoff to Birmingham. STOP #4. THE BIRMINGHAM WINDOW. Walk back along the road some 250 yds northwestward to Station #1. Follow schematic cross-section guide

(Figure 4) back southeastward towards the vehicles and along the Birmingham road some 30 yds to Station #3 in sheared Bald Eagle quartzite(?). Continue walking along Rte 453 for about 200 ft to the southeast and enter abandoned shale quarry near road sign; follow path to Reedsville Shale outcrop at Station #4, and around the quarry wall to the south to the spring (at Station #5) in Ordovician limestone.

THEME:

- The Birmingham Window, with overturned(?) beds of Tuscarora Quartzite, Juniata Shales, and highly fractured and sheared Bald Eagle Quartzite, exposed in the road-cut, and a reduction of thickness of the Upper Ordovician - Lower Silurian section.
- Contrasting lithology and attitude of the rocks exposed within the window on either side of the Tyrone-Mt. Union lineament.
- The irregular nature of the contact and inverted stratigraphy between the Reedsville (Antes?) Shale and overlying Ordovician carbonates. Is this a series of small displacement splay faults, only 10's of meters apart, on the overturned limb of a northwestward verging fold, or a sedimentary contact with overturned Middle Ordovician carbonate units that have been dragged and attenuated beneath the Birmingham thrust fault?

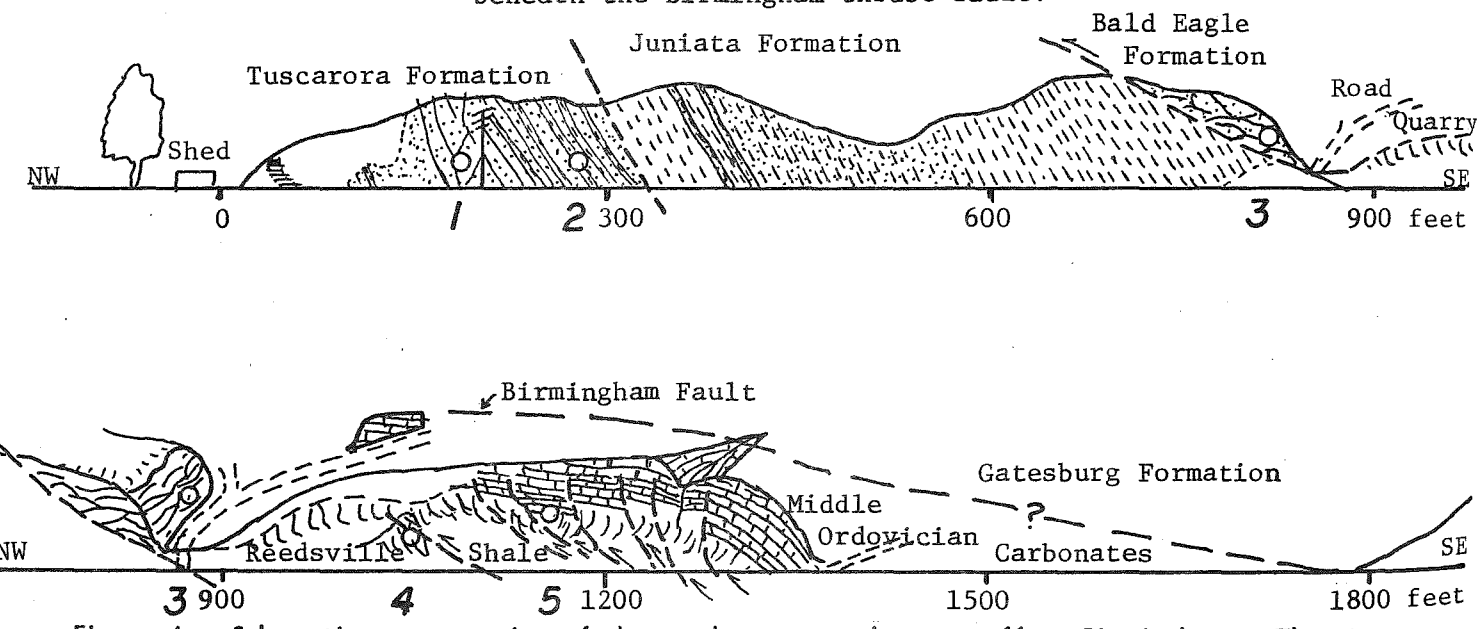

Figure 4. Schematic cross-section of the road-cut near the turn-off at Birmingham. The Upper Ordovician and Silurian formations are overturned and thinner than in the Tyrone Gap. Part of this reduction in thickness is attributed to splay faults beneath the Birmingham fault.

NARRATIVE: THE BIRMINGHAM WINDOW.

Although faults in the Birmingham area were noted by Rogers in the First Pennsylvania Geological Survey Report of 1858, it was not until 1918 that Butts reported on the anomalous outlier and thrust fault (Field trip Stop #3) in the Birmingham area. The "Birmingham Thrust Fault Structure" was visited during the afternoon of Saturday May 30, 1931,

following an early start (6:30 A.M.) from State College to take the 8:10 A.M. train from Altoona to Gallitzin, with a walk back to Altoona. In keeping with the times, most of the First Field Conference of Pennsylvania Geologists Guidebook was devoted to stratigraphic descriptions, e.g., of the Bellefonte Quadrangle (F.W. Swartz), and the Geologic Sections of Blair and Huntingdon Counties (C. Butts). No doubt the thrust fault and locally overturned formations near Birmingham were visited and discussed by Charles Butts on this field trip, but neither maps nor cross-sections of the Birmingham Window were published until 1939 in his Report on the Tyrone Quadrangle.

The outcrops of overturned(?) Tuscarora Quartzite (Lower Silurian) Upper and Middle Ordovician Juniata, Bald Eagle and Reedsville Formations, and sheared carbonates of Middle Ordovician age in the road-cuts along Rte 453 (see Figure 4) and for a restricted area around Birmingham, probably has challenged more minds over the past 50 years than any other structure in central Pennsylvania. This window or fenster is bordered to the northwest by Upper Cambrian Mines Dolomite and Lower Ordovician Bellefonte Dolomite across the Honest Valley fault, and to the southeast by gently dipping Upper Cambrian Gatesburg Dolomite above the Birmingham Thrust fault. This latter fault, which dips at 15° to the southeast in the railroad-cut across the river to the south (Stop #3), represents a vertical stratigraphic separation of some 10,000 feet. One locality to be revisited on the Golden Anniversary Field Trip is the road-cut with its overturned(?) and tectonically thinned section, which has been interpreted either as part of a second (lower) plate beneath the Sinking Valley Fault and the overlying Ordovician carbonates (Black River and Chazy Groups), or as a "dragged" slice from a syncline to the southeast beneath the Birmingham fault. While the mapped configuration of windows (fensters) exposed in this area have changed but little through the past 50 years, there has been a considerable variation in the interpretation of the sub-surface geology. The evolution in the interpretation is summarized in Figure 5 to 12.

Later mapping (Butts et al., 1939) revealed the presence of two fensters, now known as the Birmingham and Knarr windows (see Figure 5a). The appearance of two models, an overthrust truncated fold by Butts (Figure 5b), and thrust-slice decken by Stose (Figure 5c) in the same publication (Butts et al., 1939) illustrates the uncertainty of subsurface structural projections from the same surface data. In Butt's model (Figure 5b), the Gatesburg Formation is thrust from the southeast over an inverted sequence of Black River-Chazy group limestones (Obrc), Reedsville Shale (Or), Bald Eagle (Os or Obe), Juniata Formation (Oj), and Tuscarora Quartzite (St) that have "been strangely preserved and faulted downward on the northwest side". "This interpretation involves the complete crushing out of the southeast limb of an overturned anticline between Tyrone and Birmingham and the survival of a fragment of the overturned northwest limb of a second anticline lying southeast of Birmingham." (Butts et al., 1939, p. 77-78). The Stose interpretation (in Butts et al., 1939) involves 3 southeasterly dipping splay faults, with the overturned sections as a horse in a duplex system (see Figure 5c).

Zeller (1949) remapped the area (Figure 6a) and examined two models. In his overthrust-fault model (Figure 6b) an early thrust fault

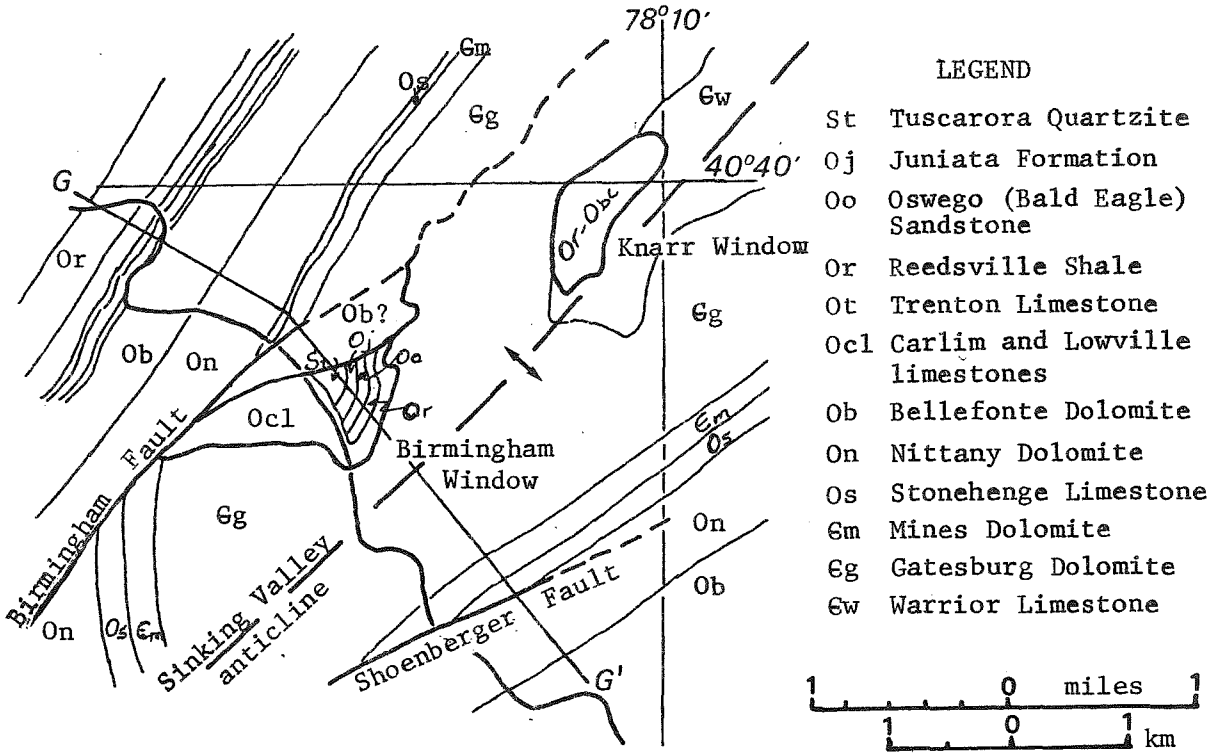

Figure 5a. Geological map of the Birmingham area, showing the locations of the Birmingham and Knarr windows. (After Butts et al., 1939.)

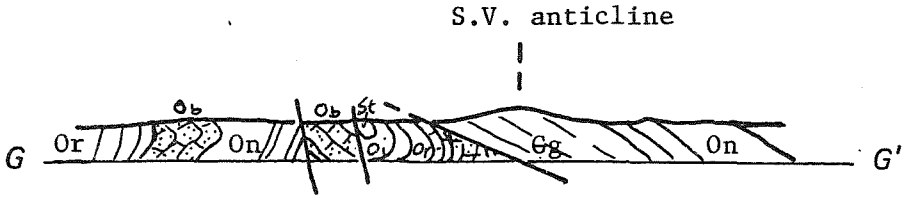

Figure 5b. Structural interpretation along line G-G' by Butts.

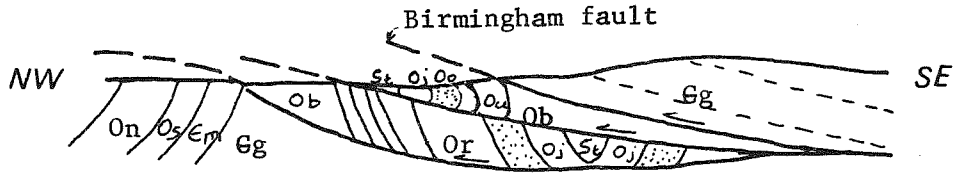

Figure 5c. Structural interpretation along portion of line G-G' by G. W. Stose (in Butts et al., 1939).

displaces overturned anticlines northwestward, preserving the synclines beneath. A second low angle thrust fault (Curly Fault) is inferred for the contact between the Reedsville Shale and the overturned Middle Ordovician limestones above it. This fault is largely concealed by a blanket of the Gatesburg Formation transported on the later and shallower Birmingham thrust fault (Figure 6b). In the graben model, the overturned section is preserved in a graben (Figure 7a) that formed as a result of crustal extension on a fold system overturned to the northwest. Early (Curly) and late (Birmingham) thrust faults (Figure 7b), associated with compressional regimes, truncated the folds and the graben (Figure 7c).

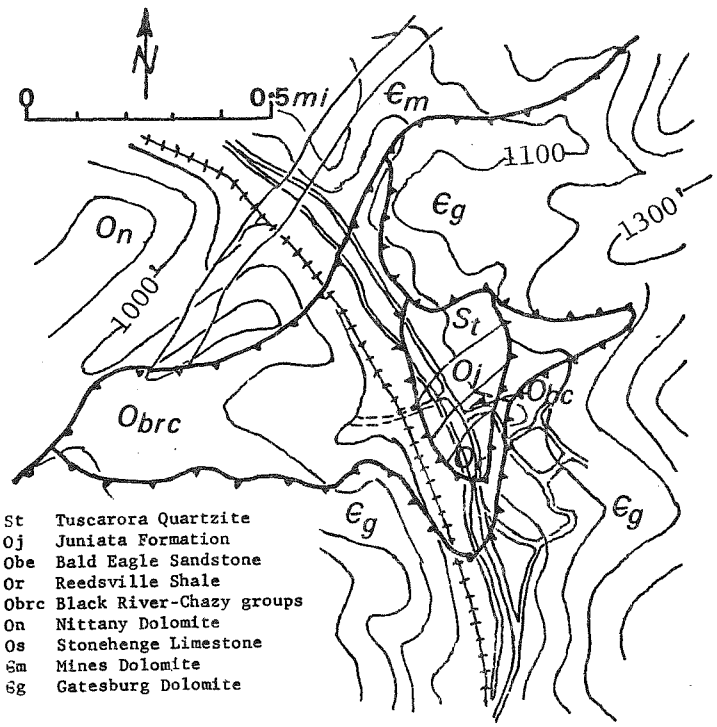

Figure 6a. Geological map of the Birmingham area. (After Zeller, 1949.)

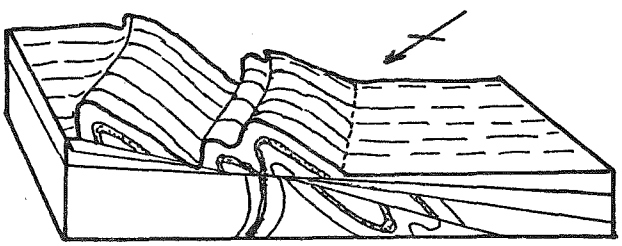

Figure 6b. Isometric diagram depicting the Overthrust Model, in which overturned folds are carried northwestward on an early thrust fault (e) that subsequently was overridden by the Curly (C) then Birmingham (B) faults.

Stage 1. Graben development on early overturned folds of the Nittany Anticlinorium.

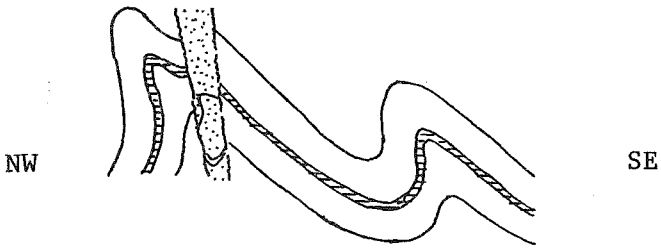

Stage 2. Displacement of the graben on the Curly Fault.

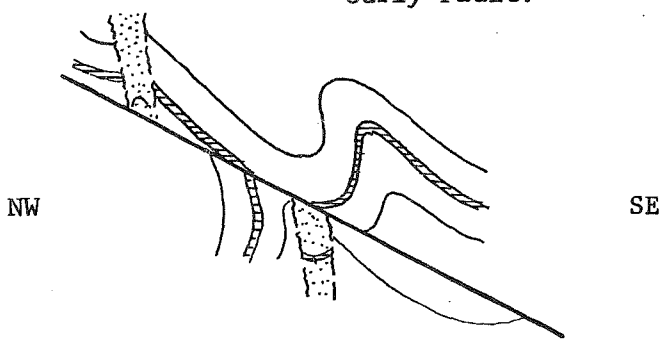

Stage 3. Displacement of the graben on the Birmingham Fault.

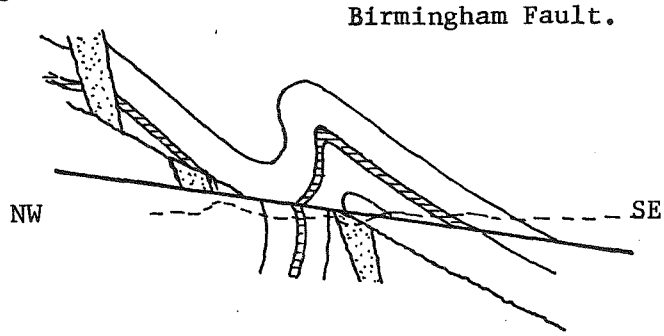

Figure 7. Schematic cross-sections depicting the Graben Model. The present erosion surface is shown as a dashed line. (After Zeller, 1949.)

The "graben, overridden by thrust sheet" hypothesis was refined by Fox (1950), who used Zeller's map (Figure 8a) to develop cross-sections through the Birmingham (Figure 8b) and Knarr (Figure 8c) windows. Although it was not well received at the time because of the necessity of a sequence of compression-extension-compression regimes, this model deserves rethinking, recognizing the role of imbricate uplimb thrust faults during the growth of anticlines, with down-dropped hinge or core zones (Gwinn, 1964). All explanations, except the graben models, require that the younger outlier rocks be thrust from the overturned limb of an anticline 4 to 5 miles to the southeast, a distance that is difficult to reconcile with the limited southward extension (2 miles) of the Birmingham fault.

The presence of a deeper thrust fault (the Sinking Valley fault) was demonstrated in a minerals exploration drilling program by the New Jersey

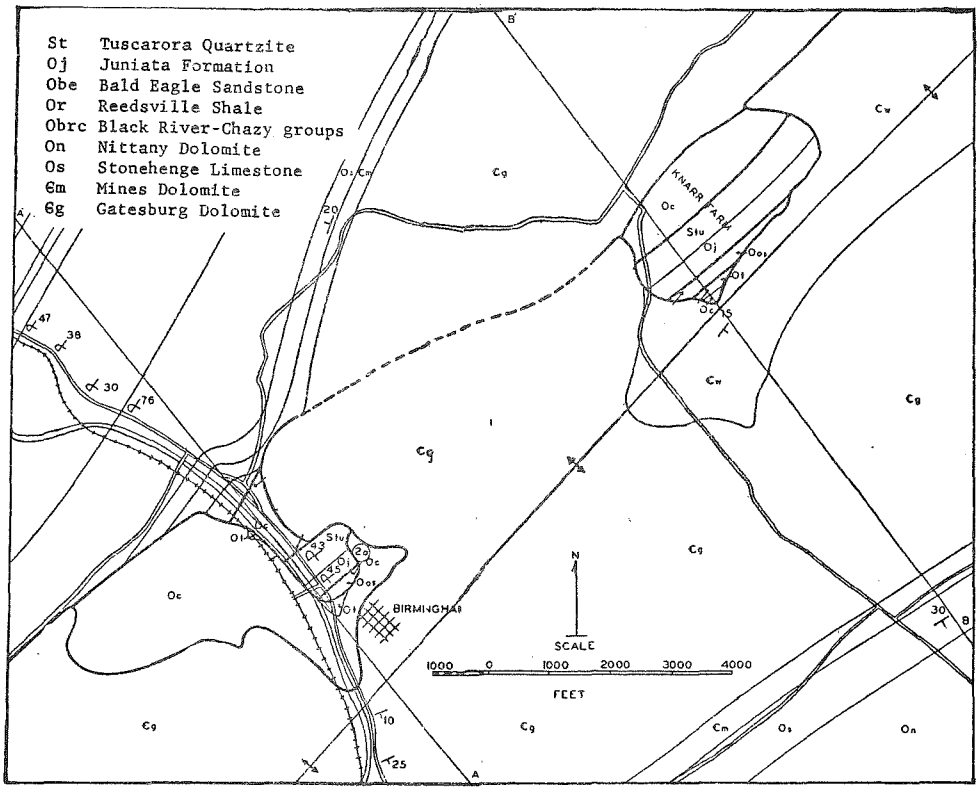

Figure 8a. Geological map of the Birmingham and Knarr windows (After Fox, 1950.)

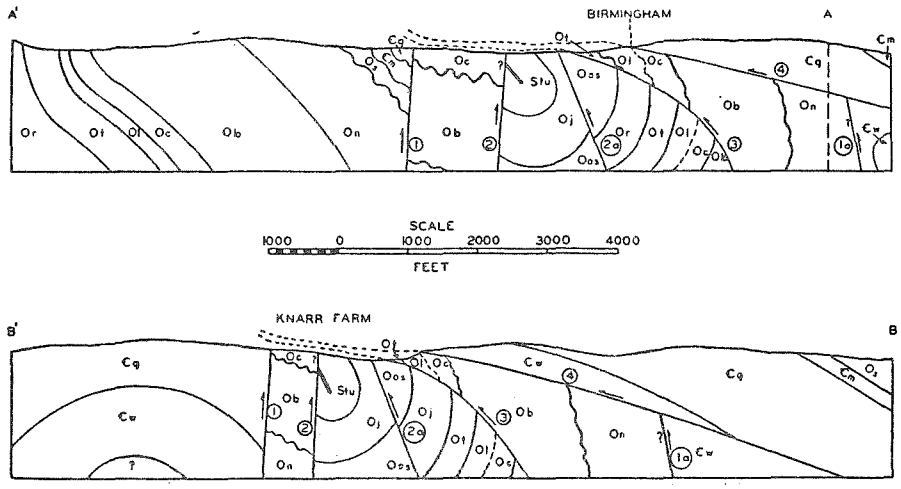

Figure 8b. Structural interpretations along lines A'-A (top) and B'-B (bottom), showing a steep concave thrust and part of a syncline preserved in a "graben" beneath the Birmingham fault. (After Fox, 1950.)

Zinc Company (Moebs and Hoy, 1959). The drill data are summarized in maps (Figures 9a and b), and cross-sections (Figures 9c to f). The suboutcrop of the Sinking Valley fault, which is exposed in the Birmingham and Knarr windows, is shown to be inclined to the south and west beneath some 350 to 1100 feet to cover (Figure 9b). This map shows the suboutcrop position of Reedsville Shale (350 to 900 feet below the surface) and Juniata Formation (400 to 1100 feet deep) that were

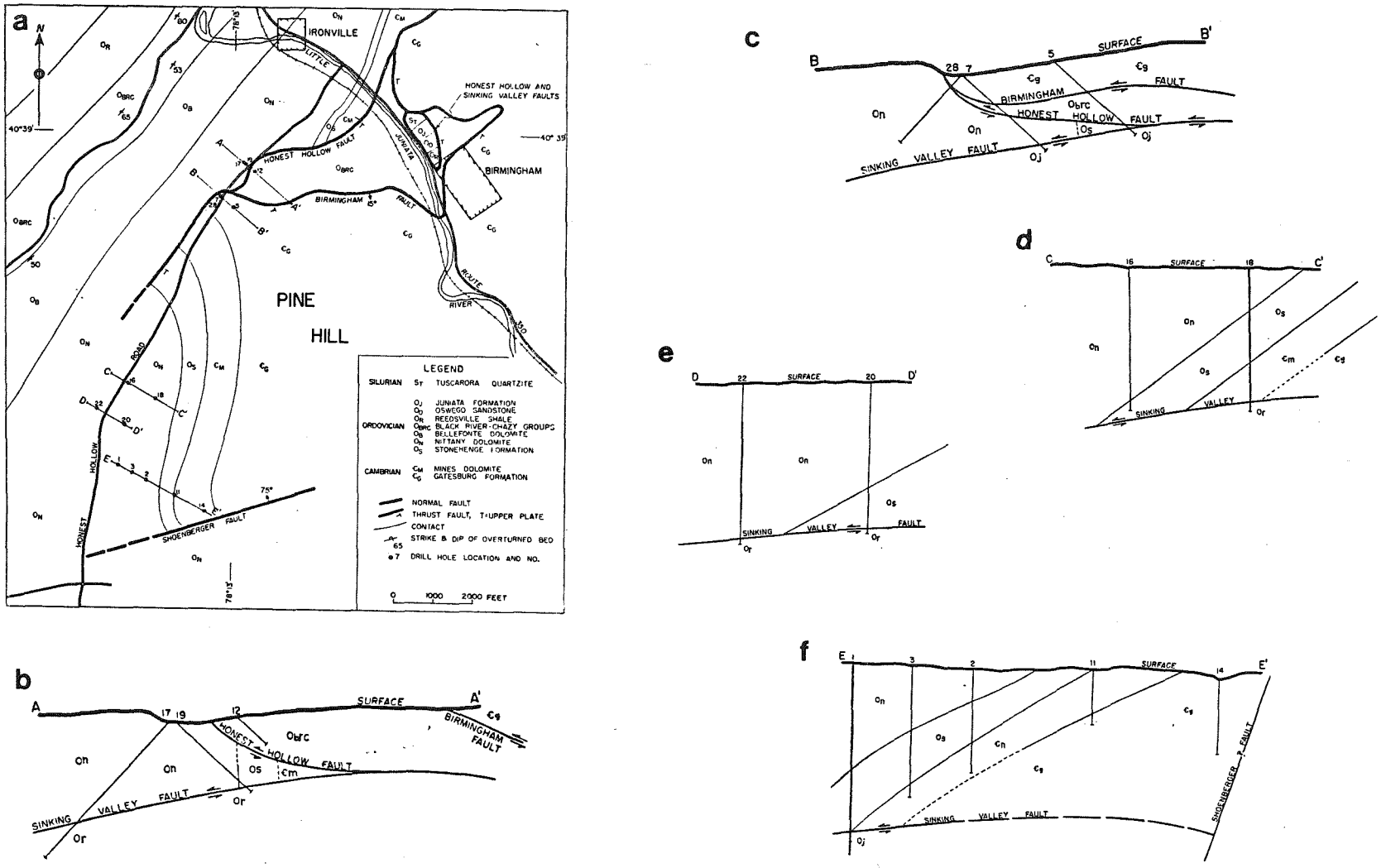

Figure 9. Geological map and cross-sections of Sinking Valley, with diamond drill-hole locations (9a) and structural interpretations (9b, c, d, e, f) respectively for drill-sections A-A', B-B', C-C', D-D', and E-E'. Note the expanded scale for sections A-A' and B-B'. (After Moebs and Hoy, 1959.)

intersected beneath the regional low angle thrust fault. Refinements to the map by Zeller (1949) are included in Figure 9a. Their composite sections (see Figure 10b) through Birmingham and parts of Sinking Valley (Figure 10a) show this fault to be convex upward, with the Birmingham and Honest Valley as splay faults.

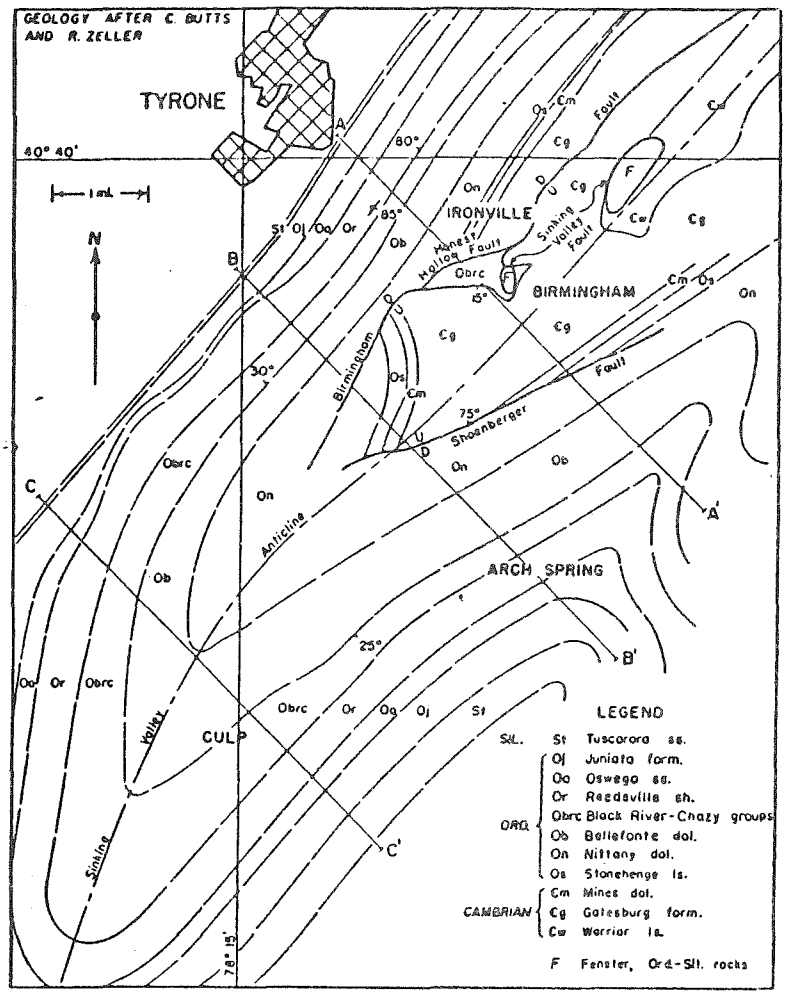

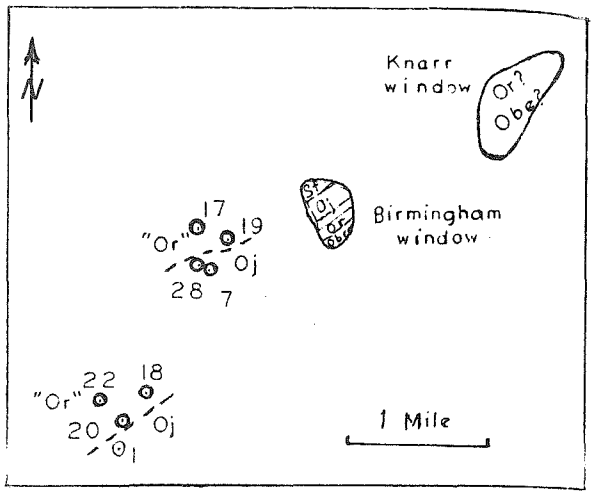

Figure 10c. Outcrop and sub-outcrop map of the formations beneath the Sinking Valley fault. This map was generated from the drill data presented by Moebs and Hoy (1959), and redrawn by Swartz (1966).

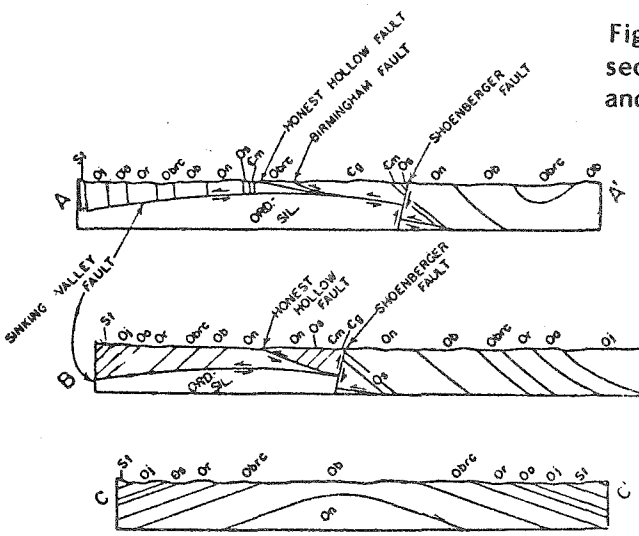

Figure 10a and b. Geological map (10a) and cross-sections (10b) through Sinking Valley. (After Moebs and Hoy, 1959.)

The introduction of thin skinned tectonics concepts in the Appalachian fold belt has yielded other plausable explanations for the limited aerial extent and large displacements, and the arched nature of some thrust faults. The deformation cycle is initiated by ramping on a decollement with the development of a duplex splay, followed by arching over the ramp and the synchronous development of uplimb thrust faults on the flanks of the growing anticline in which the core or hinge zones may be depressed relative to the limbs (Gwinn, 1964; 1970). The role of synthetic and antithetic uplimb faults or imbricate thrust faults on the flanks of anticlines, and their relationship to deeper ramp faults, was recognized by Gwinn (1964) as a possible configuration for the Birmingham window. He shows (Figure 11a and 11b) the Sinking Valley fault as an up-arched structure that developed with the growth of the Nittany Arch over a ramped decollement at depth, and a convergence of the Sinking Valley fault with the decollement to the northwest. A similar mechanism involving stepped ramps has been proposed by Charlesworth and Gagnon (1985) for the development of intercutaneous wedges (see Fig. 5, Gold and Pohn, this volume) that are bounded by folded thrust faults beneath an anticlinal structure.

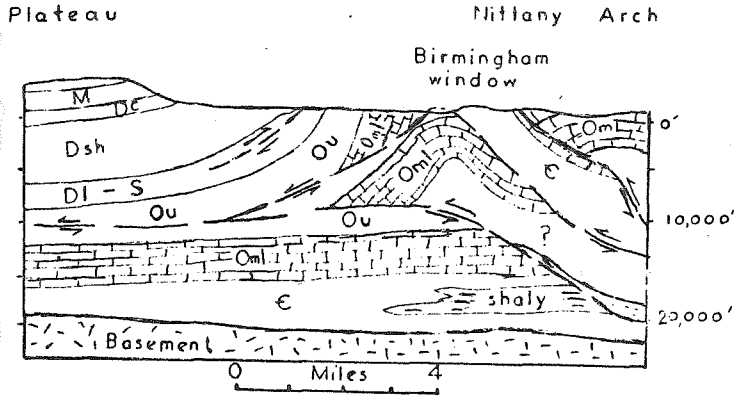

Figure 11a. (After Gwinn, 1964.)

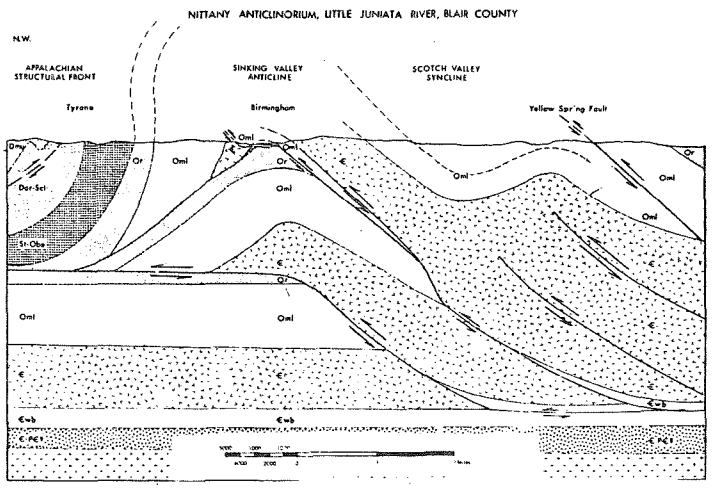

Figure 11b. (After Gwinn, 1970.)

Figure 11c. (After Swartz, 1966.)

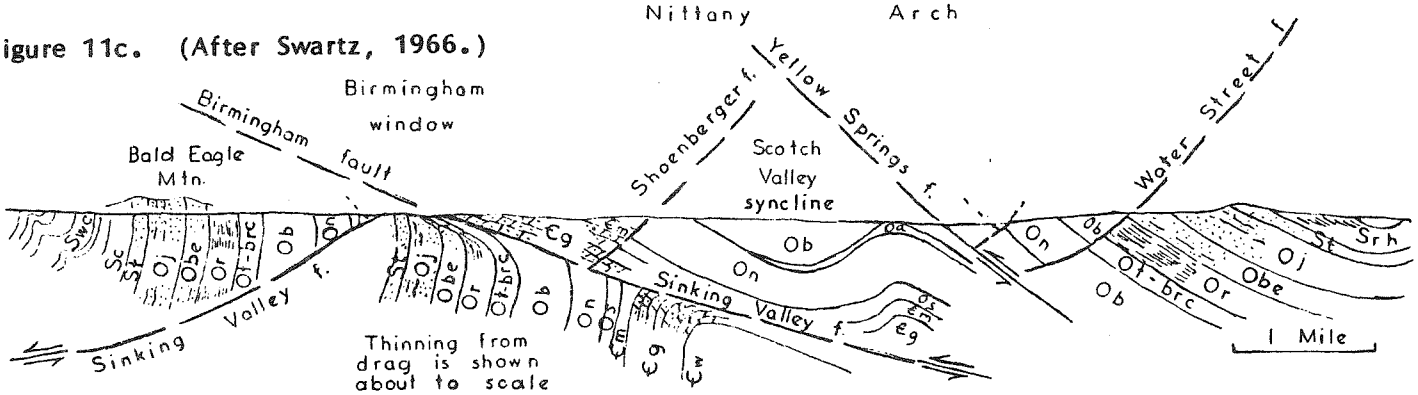

Figure 11. Structural interpretations of the Birmingham window involving "thin-skinned tectonics" concepts. Note the folded nature of the Sinking Valley fault, and the appearance of antithetic and synthetic faults as well as chisel and wedge faults in the cross-sections. Gwinn's models require a ramp, with stacked thrust wedges beneath an anticline. The findings of Gwinn (1964, 1970) that most Appalachian anticlines with anti- and synthetic faults on the limbs have developed over decollement ramps, has led to the recognition of an Eastern Overthrust Belt.

A comparison in thickness of formations in the Tyrone Gap and Birmingham window indicates reductions in the order of 65% (400 to 500 feet from 1200 to 1400 feet) for the Juniata beds, and more than 90% for the Bald Eagle Quartzite (50 from 650 feet) and Reedsville Shale (down to about 100 from 1100 feet) (Swartz, 1966). Despite the reduction in thickness of these units, the Tuscarora and Juniata Formations show relatively little internal deformation, whereas the Bald Eagle and Reedsville rocks are highly sheared. Blocks of sheared and fractured limestone are preserved locally in the abandoned quarry overlying the strongly overturned Reedsville Shale. In the far wall of this same quarry southeast of the Birmingham turnoff, the contact on the mesoscopic scale is irregular with local indentations of sheared shale into fracture limestone. Thin carbonate veins, probably healed features on a mesoscopic and microscopic scale, are ubiquitous in the sheared carbonates, and renders precise stratigraphic correlation uncertain. "The rock appears to represent the Middle Ordovician Trentonian, Black Riverian and Chazyan limestones which in neighboring belts of outcrop are about 1200 feet thick below the Reedsville Shale..." (Swartz, 1966). Swartz (1966) accommodated these features as an attenuated drag beneath the Birmingham fault (see Figure 11c). Rather than invoking a second thrust fault, Swartz (1966) has utilized some "thin-skinned tectonic" concepts to accommodate the northwest dip to the Sinking Valley fault by curving it into the Birmingham fault as a downward splay at the fenster (Figure 11c). He also suggests that in both the Birmingham and Knarr windows "the Sinking Valley fault is presumed to be locally close to and not generally out of parallel with the Birmingham fault." This he shows (Figure 11c) as a northwest dipping fault that transgresses Upper Ordovician and Lower Silurian beds. The present authors interpret the situation as a tectonically modified sedimentary contact on a series of closely spaced splay faults (Figure 4).

It is unlikely that the final chapter on the Birmingham fenster will be written without additional deep drilling and detailed subsurface seismic profiling data. As recently as 1973 Ronald Schmiermund and Carl Palmer mapped in detail the underground entries of the mines on Pine Hill (reproduced in Smith, 1977) and they presented a geological map of the Birmingham area as part of the class project in Field Methods in the Department of Geosciences at The Pennsylvania State University. Part of the map, reproduced as Figure 12a, shows the Birmingham outlier as two discrete windows, with three small klippe of Gatesburg Dolomite to the northwest, straddling the Honest Valley fault. The implication of these data are that the Birmingham fault must be close to the present topographic surface and postdate the Honest Hollow fault. One way to resolve the time-space problem is to have the Sinking Valley fault as an antithetic uplimb thrust to the northwest and as a synthetic thrust to the southeast. The Middle Ordovician carbonates (Obrc) and underlying inverted section may represent intercutaneous wedges associated with a southeasterly dipping ramp fault.

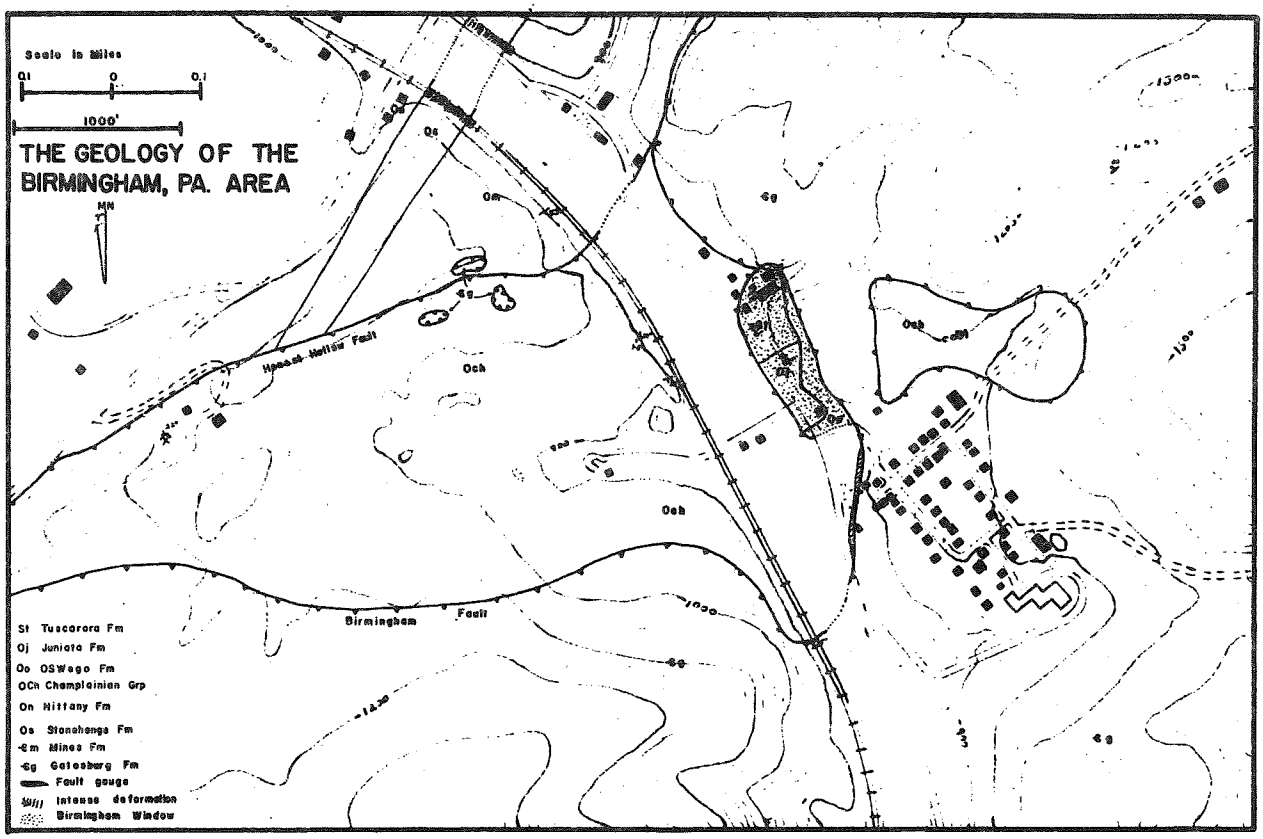

Figure 12a. Geological map of the Birmingham area by Schmiermund and Palmer, 1973. Note the three klippe straddling the Honest Hollow fault.

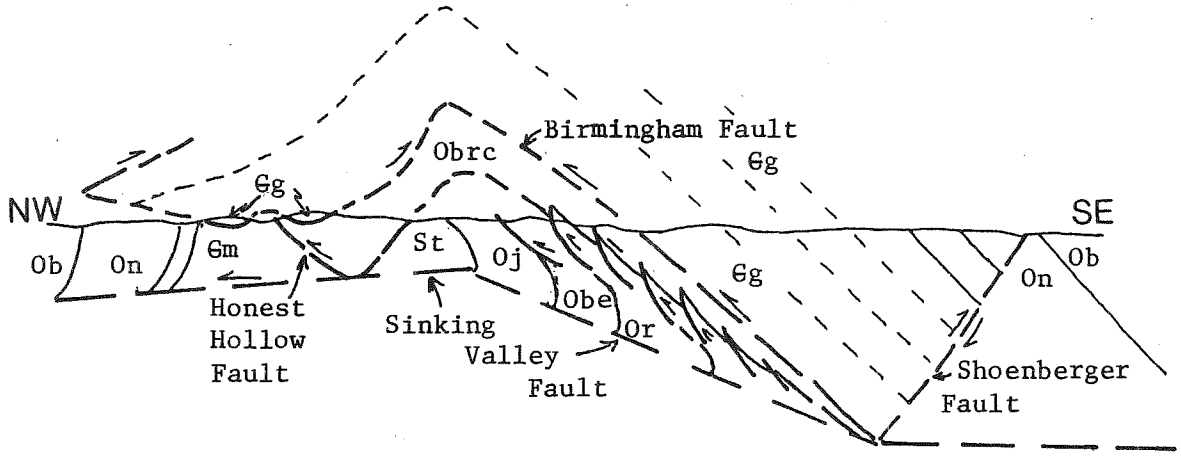

Figure 12b. Cross-section cartoon depicting the klippe of Schmiermund and Palmer (above map), and the Birmingham window as an intercutaneous wedge that is ramped on the Sinking Valley Fault. A notable departure from the model of Charlesworth and Gagnon (1985) (see Fig. 5, in Gold and Pohn, this volume) is the steep inclination to most of the beds.

* * *

Miles	Interval	
38.65		Return to vehicles and continue southeastwards on Rte 453S.
38.85	0.2	Grier School on left is built on allochthonous Gatesburg beds.

Miles	Interval	
39.25	0.4	Note the cycles in the Gatesburg dolomite in the road-cut near the ridge crest. (Bedding, 070°/15°SE; main fractures, 140°/vert).
	0.35	Note drill-holes on left (for paleomagnetic measurements).
39.75	0.15	End of road-cut.
39.95	0.2	Road crosses the traces of the Shoenberger fault, which trends northeastward along the valley near the sign to Delta Quarry. This contact marks the closure of the Cambrian rocks in the core of the Sinking Valley anticline.
40.0	0.05	Note the cyclical nature of dark (subtidal) and light (supra-tidal) dolomites of the Nittany Formation and southeasterly dips (045°/32°SE) over the next 0.3 mile.
40.35	0.35	Bellefonte dolomites exposed in road-cuts.
40.6	0.25	Bridge across Juniata River, with a very fine-grained dolomite (Tea Creek Member of uppermost Bellefonte Formation) on southeast side.
	0.1	Middle Ordovician limestones (Chazy Stage).
	0.1	Loysburg Formation.
41.1	0.1	Ridge crest - Black River Stage.
	0.1	Thinly bedded limestones of Salona and Coburn Formations.
	0.1	End of road-cut near axis of Scotch Valley syncline.
41.7	0.4	Arch Spring turn-off to right - remain on Rte 453S.
44.35	2.65	Junction with Rte 45 - remain on Rte 453S to Water Street.
	0.3	Gently southeasterly dipping beds of Bellefonte Dolomite exposed in road-cuts for next 0.2 mile.
	0.4	Cross trace of Water Street fault near triangular intersection: overturned Reedsville Shale exposed on hillslope to left.
45.1	0.05	Triangular intersection. Turn left to join Rte 22E after 0.05 mile. The road-cut to the left successively exposes:
	0.05	Overturned Bald Eagle Sandstone (010°/73°W) to upright eastward;
	0.1	Red shale and sandstone of the Juniata Formation in beds 5-90 cm thick. Note easterly dipping extension faults;
	0.4	Scree slope of white Tuscarora Quartzite across river to southwest.
	0.1	Upright and gently easterly dipping beds (030°/17°E) of interbedded shale and quartzite of the Tuscarora Formation, conformably over Juniata Red beds.
45.85	0.05	Turn left on road to Alexandria.
	0.3	Railway line. Old Ganister Plant on left; the beehive like tops of the kilns can be seen through the trees.
46.95	0.8	Left at first intersection beyond Mead Products Plant.
	0.8	Red shales and siltstones of the Bloomsburg (Lower Wells
	0.4	Creek) Formation. A bedding attitude of 040°/70°SE
	0.25	reflects the southeastern limb of the Round Top anticline. The prominent joints (140°/80°S to vertical) are similar in attitude to the Tyrone-Mt. Union lineament.
48.8	0.4	Turn right 20 yards southwest of railway crossing, and
49.0	0.2	park 0.2 mile to the southeast, in the field. Walk 300 yards along the railroad tracks to the southeast to the cuts excavated into the low hill that forms the axis of the Round Top anticline.

STOP #5. BARREE SOUTHEAST RAILROAD CUT.

Follow the schematic cross-section (Figure 13) in a traverse starting at Station #1 in thinly bedded shale and limestone of the McKenzie Member (Upper Mifflintown Formation), through the Rochester Shale Member (Stations #7 and #9) and into the underlying Keefer Formation (Station #10) at the northwest end of the cut. In an earlier stratigraphic nomenclature these rocks were considered to be part of the Clinton Group.

CAUTION: This is a busy railroad. Please watch for trains.

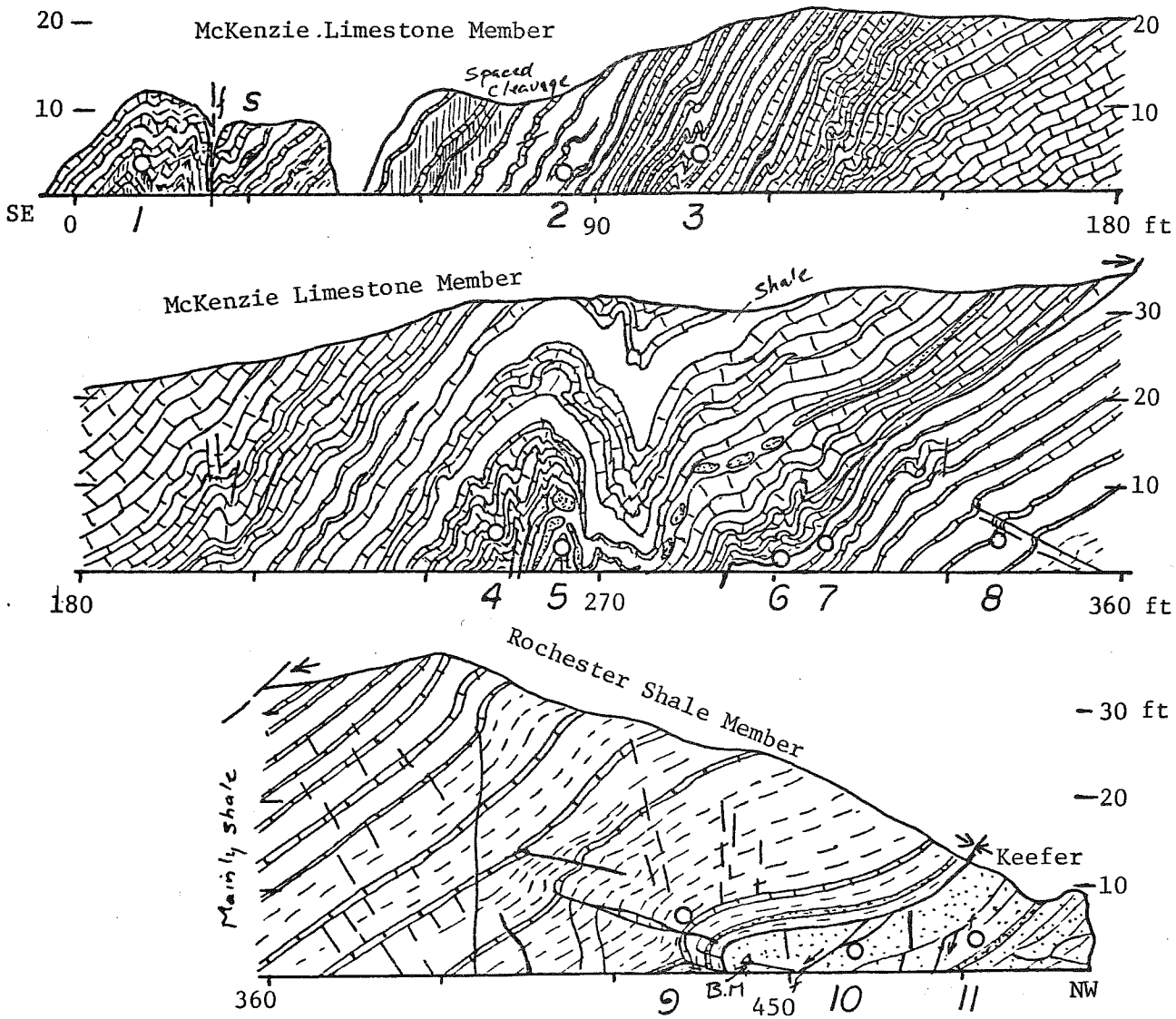

Figure 13. Schematic cross-section of railroad cut exposing the McKenzie and Rochester Members of the Mifflintown Formation in a complexly folded section overlying hematitic sandstone of the Keefer Formation.

THEME:

- Disturbed zone with 4th and 5th order folds and a small back thrust fault.

- Disharmonic mesoscopic scale folds, with curved axial surfaces that change vergence directions from southeast to northwest.
- Local northwest dipping cleavage.
- Early layer parallel shortening features such as wedge faults and snake-head folds, kink bands and box folds.
- Algal head limestone (possibly boudinaged) with a small (mesoscopic scale) fan fold near Station #5.
- Incompatible sense of folds (in the Keefer Sandstone with the 3rd order Barree anticline to the northwest.

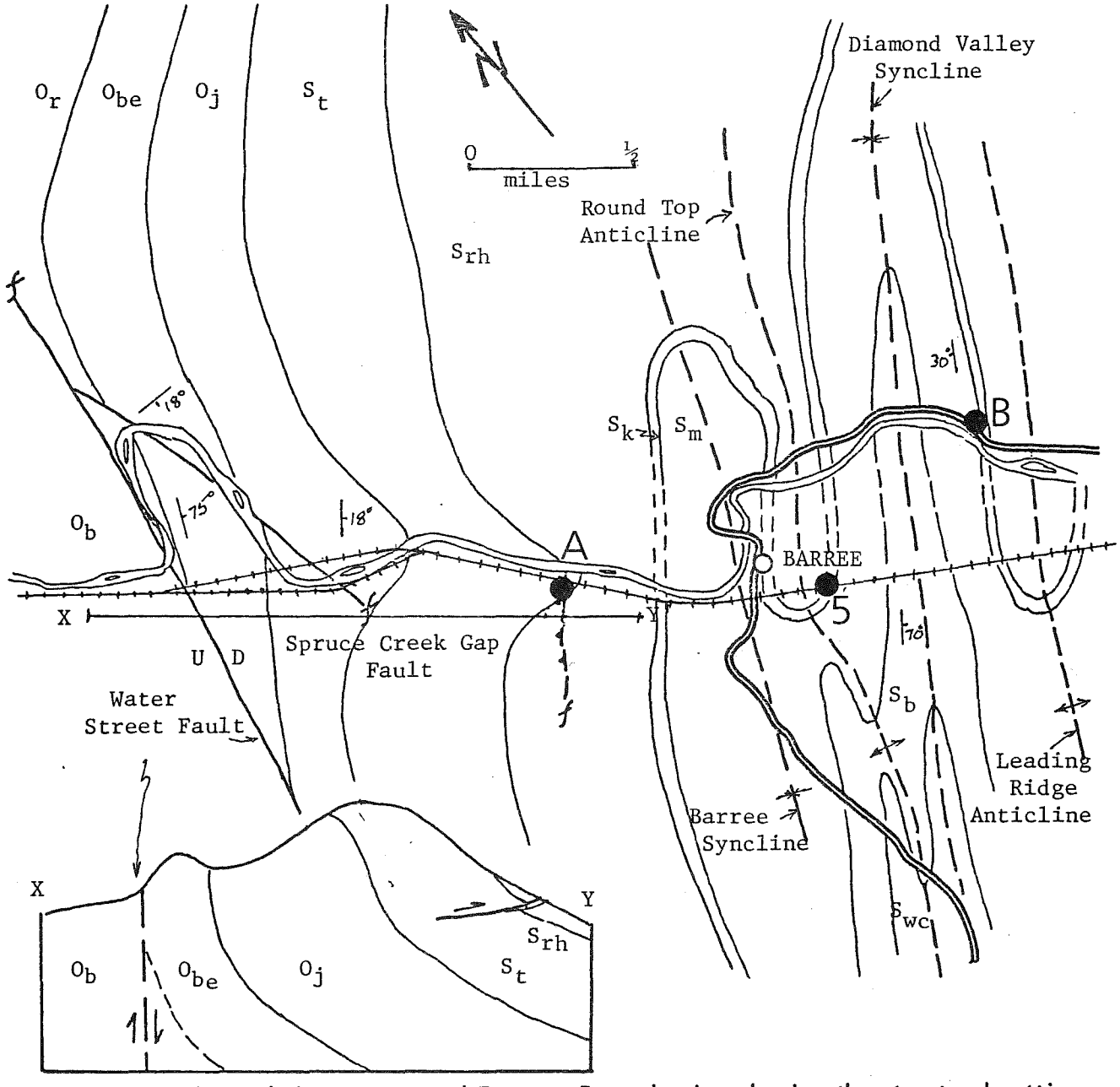

Figure 14. Geology of the area around Barree, Pennsylvania, showing the structural setting for STOP # 5, A and B. Unit symbols are: O_b - Bellefonte Dolomite; O_r - Reedsville Shale; O_{be} - Bald Eagle Sandstone; O_j - Juniata Formation; S_t - Tuscarora Formation; S_{rh} - Rose Hill Formation; S_k - Keefer Sandstone; S_m - Mifflintown Formation; S_b - Bloomsburg Formation; S_{wc} - Wills Creek Formation.

NARRATIVE: THE BARREE RAILROAD CUT.

Some of the best developed layer parallel shortening structures are exposed in two railroad cuts and one road-cut within one mile of the town of Barree. The unusual structural geology and geomorphology of the area, as well as the localities of these outcrops, are portrayed in the accompanying geological sketch map (see Figure 14). The Spruce Creek Gap, through which the Little Juniata River transgresses Tussey Mountain (Short Mountain) is evident to the northwest (direction of railway tracks). Although the location of the water gap is controlled by the Tyrone-Mt. Union lineament, the exact course of the river is governed locally by two faults, the Water Street fault and the Spruce Creek Gap fault. The Water Street fault is a high angle fault with east side down, and it appears to be related geometrically to the Spruce Creek Gap fault, whose presence is inferred from contrasting bedding attitudes across a fracture zone in Spruce Creek Gap. This fault acted as a domain boundary across which the Bald Eagle sandstone beds were rotated from a gently southeasterly dipping attitude to a near vertical attitude (see Figure 14).

The railroad cut at locality A, "highlighted" in Butts' 1939 Tyrone Quadrangle Report, shows beds of the Tuscarora Formation thrust antithetically over the contact between the Tuscarora Quartzite and beds of the Rose Hill Shale (lowermost Clinton Group). This low angle fault is exposed about 20 feet above the floor of the railroad cut and cuts up-section but down-topography. As seen at other outcrops, this indicates that the major thrust fault formed prior to the regional Round Top anticline. To the southeast this back-thrust fault splits into a duplex-type system, with possible footwall under-splays in the Rose Hill shale beds. Drag folds in the Tuscarora beds, and a counter-clockwise rotation of beds in the duplex wedge, indicate a southeasterly transport. Some S-type folds (counter-clockwise rotations) can be seen in the small disturbed zone that has been "snow-ploughed" in front of the advancing thrust fault. The displacement on this "back-thrust" fault is of the order of 200 to 300 feet.

About a mile to the southeast at STOP #5 is another railroad cut (see Figure 14) where the outcrops of "much crumpled" beds of McKenzie Limestone and Rochester Shale overlie Keefer Sandstone (Butts et al., 1939) are now interpreted as a disturbed zone. A structurally similar outcrop of these units is exposed at locality B, on the flank of Leading Ridge anticline. These outcrops are of interest for the mesoscopic scale analogs to those seen on some seismic reflection surveys.

The outcrop at STOP #5 begins with the Keefer Sandstone, which is about 40 feet (12 m) thick in this area, and contains some oolitic hematite beds. This unit was actively prospected and locally mined for its iron content during the 19th century. Note the wedge and tear faults near Stations #10 and 11. Farther to the southeast are the Lower (Rochester Shale) and Upper (McKenzie Limestone) members of the Mifflintown Formation. This formation is characterized by shales with interbedded limestones and some sandstones. Deformation of these interbedded competent and incompetent strata, yielded folds and faults in the relatively brittle units, and fan folds, boudins, axial plane

cleavage, and hinge zone thickening in the ductile units. Note the detached algal head masses that locally form boudins between Stations #5 and 6.

Some interesting mesoscopic scale structures are exposed along the contact between the Rochester Shale and the McKenzie Limestone beds, near Stations #6 and 7. The syncline portrayed at Station #6 is concentric in nature, with an axial trace that crosses a bedding plane detachment and passes upward into an anticline. Similar patterns are seen in some seismic sections (the over-riding anticline may be a reasonable analogy). One meter to the northwest is a thicker wedge-faulted bed of limestone, that forms the core of a small snake-head anticline (Station #7). This anticline shows an antithetic vergence at the base. Higher in the fold the axial surface becomes vertical and near the top of the fold, the vergence is synthetic. Similar reversals in vergence are commonplace in this outcrop. The lower antithetic vergence may be related to the "back-thrusts" exposed about 1 mile to the northwest (at locality A), whereas the upper vergence may be connected to the general translation of the beds to the northwest, as part of the main Alleghenian movement.

Several meters to the southeast, near Station #5, is an upright, tight to almost isoclinal anticline, with a small displacement fault across from the southeast limb to the northwest limb. Adjacent to this anticline is another syncline-anticline pair, whose lower beds verge antithetically and whose upper beds verge synthetically. These folds are incompatible in sense with, and appear to predate the regional folds.

As you walk along the outcrop from northwest to southeast, note the following features:

1. A kink fold in a limestone bed, that attenuates over a short distance normal to the general bedding surface.

2. Mesoscopic faults in the core of 4th order folds.

3. A fanfold and other disharmonic features associated with tight anticlines and synclines.

4. Boudins and an axial plane cleavage associated with the 4th order folds.

The road-cut at locality B, on the western flank of the Leading Ridge anticline exposes successively McKenzie Limestone and Rochester Shale of the Mifflintown Formation, and calcareous sandstones of the Keefer Formation above shales of the Rose Hill Formation. The Keefer Formation is only about 11 m thick, and locally contains oolitic siderite and hematite lenses. The competent beds in the underlying Rose Hill Shale are calcarenites 5-25 cm thick. About 40 m of Rochester Shale is exposed overlying the Keefer sandstone in the core of an inclined 4th order syncline. Bedding-slip surfaces with slickenlines perpendicular to the axial line of the fold suggest a flexural slip mechanism. An axial plane cleavage, inclined to the southeast, is developed mainly in the hinge zones of the syncline and its companion anticline to the southeast. This cleavage is more closely spaced in the Rose Hill shale in the anticlinal

hinge than in the Rochester shale (3-8 mm apart) in the synclinal hinge. To the northwest, the dominant shale beds grade into thinly interbedded limestones and shales of the McKenzie Formation.

The sense of these mesoscopic scale folds is not compatible with the macroscopic scale anticlinal axis to the east. The westerly vergence of these mesoscopic scale folds and associated easterly dipping cleavage, suggest they may be part of a "disturbed zone" representing the upper portion of a splay fault at depth. Mesoscopic scale concentric folds, with a dominant western vergence, box folds, snake-head folds, and wedge faults are best developed in the McKenzie lithologies, and attest to an early layer parallel shortening event.

* * *

Miles	Interval	
49.2	0.2	Return to vehicles, turn around and drive to Barree intersection. Turn left on road to Alexandria.
50.95	1.75	Turn left at intersection near Mead Products, Inc.
51.55	0.6	Turn right at traffic light.
51.6	0.05	Cross over bridge to south.
51.7	0.1	Take right fork at Y intersection to junction with Rte 22E.
52.05	0.35	At intersection, turn left onto Rte 22E.
52.95	0.9	Stop in parking area on the left side of the road at the axis of the right-hand curve in the road. Walk across the highway to the exposure of limestones of the Wills Creek Formation.

CAUTION: We will be examining approximately 0.2 mile of road-cut on the blind curve of a busy highway.

STOP #6. CHARLIE HILL ROAD-CUT. (Also see Figure 15). We conclude the field trip with an exposure of a probable "disturbed zone", that disappears to the northeast under the Broadtop synclinorium, and may continue southwestward as a branch of a major north-northeast striking thrust fault in the western part of the Spruce Creek quadrangle.

THEME:

- Disturbed zone with antithetic and synthetic faults and associated folds.
- Kink band in the thinly laminated limestone/shale beds.
- Variable attitude to axial plane cleavage, suggesting a late rotation along splay faults.
- Cyclical nature of beds with intertidal carbonates (algal limestone, mudstone, dolomite, shales and siltstones).
- Solution pits (probably of evaporite material) deformed in axial plane direction.

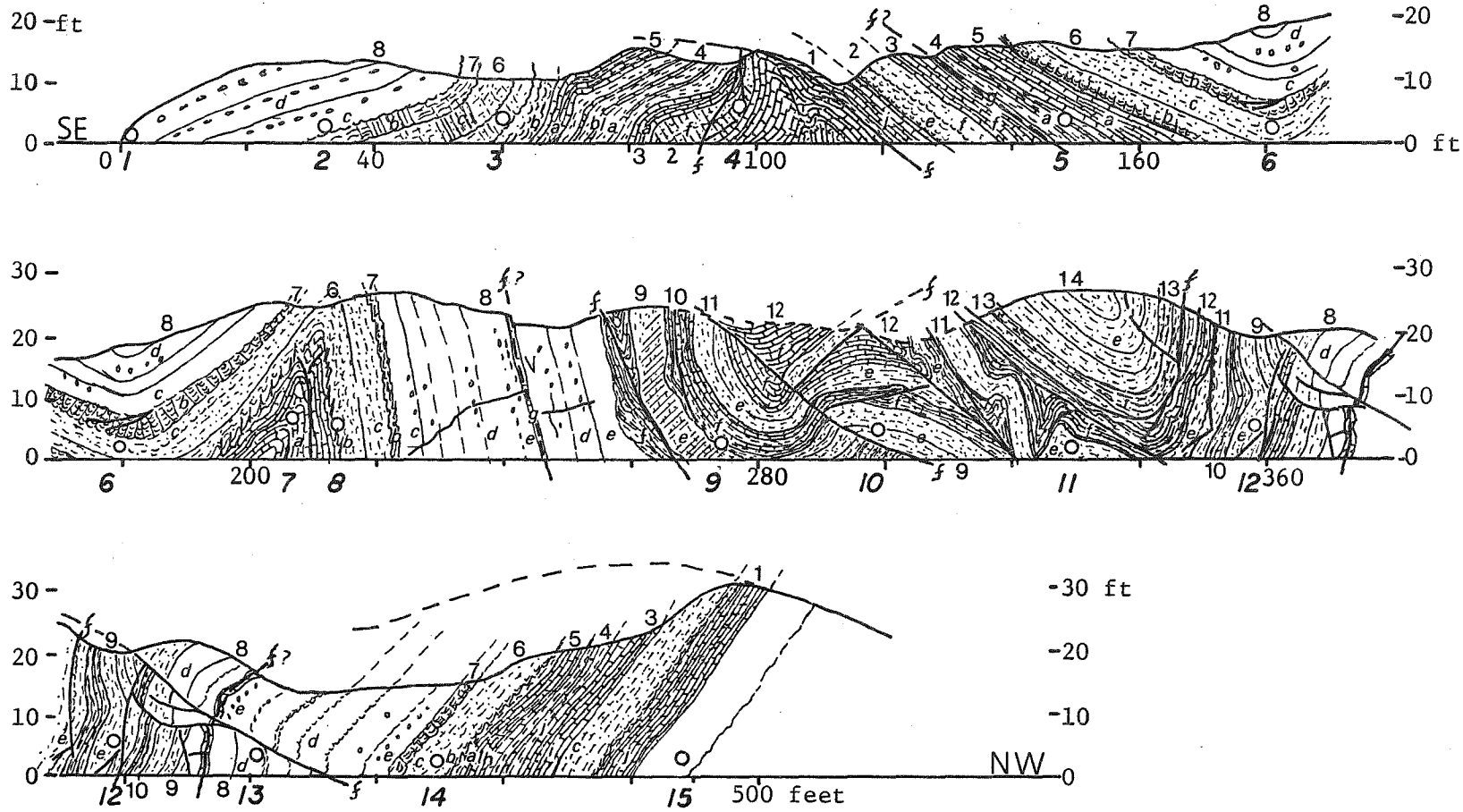

Figure 15. Schematic cross-section for 450 feet of the Charlie Hill road-cut. The orange blaze numbers (1 to 15) and letters (a to l) represent, respectively, marker stations and sedimentary facies units. The litho-structural units are labelled from 1 to 14 in the sketch above, and in white paint on the outcrop. The litho-structural units portrayed in the sketch may include more than one facies unit. Stratigraphically these rocks are assigned to the upper part of the Wills Creek Formation.

Miles Interval

- Late fractures trending 140°.
- Variation in fold style from upright open to overturned tight in the same outcrop.

QUESTIONS:

- Do the ostracods (Leperditia in Unit 5 (STOP #5) represent a tidal environment?
- Are the spherical quartz grain layers in Unit 8 near Station #2 wind blown?
- Are the druzy vugs in Unit 8 deformed?
- Do they represent dissolved gypsum balls or concretions?
- Are the algal mattes deformed by a coarsely spaced (5 cm) fracture cleavage?
- Is there a bedding fault or decollement between Units 8 and 9?
- Are the star-like forms a few mm across that occur in Unit 5 (e.g., near Station #3) relects of salt crystals?
- Why are the kink bands in Unit 7 stratabound?

NARRATIVE: CHARLIE HILL ROAD-CUT

This outcrop is located about 6 miles (10 km) northwest of Huntingdon in the Seven Mountains anticlinorium, and we conclude the field trip at a road-cut (see Figure 15) in deformed cycles of dark limestone, laminated and massive mudstones, and light grey to buff weathering dolomite near the top of the Wills Creek Formation. We will look at depositional cycles, with both Wills Creek and Tonoloway affinities, that are repeated in a "disturbed zone" with locally developed kink bands and axial plane cleavage. The geology of this outcrop will be treated in two parts, one dealing with sedimentation (by A.L. Guber), and the other with structural interpretation (H. Pohn and D.P. Gold).

Part I: Late Silurian Shallowing Upward Cyclic Sedimentation at Charlie Hill

by

Albert L. Guber

Shallowing upward sedimentary cycles are characteristic of the rocks of Late Silurian and Early Devonian age in central Pennsylvania, but surprisingly few researchers have commented on their widespread and temporally pervasive nature. Swartz (1955) recognized "obscure cycles" in the Wills Creek and Tonoloway formations at Mount Union, Pennsylvania. His descriptions of the facies comprising the cycles were scant, and he attempted little environmental interpretation. His "ideal" Wills Creek cycle (see Figure 16) would appear to contain a basal, non-laminated, argillaceous, dolomitic limestone which might be oolitic and/or fossiliferous and would exhibit a sharply defined base. This limestone

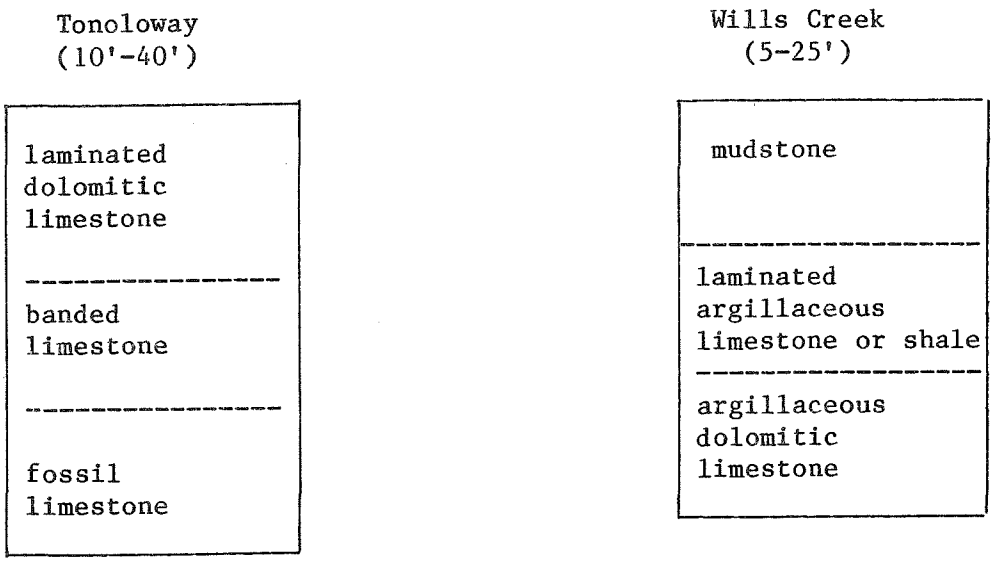

Figure 16. Swartz's ideal Wills Creek and Tonoloway cycles.

would grade upward into a laminated argillaceous limestone or dark calcareous shale which, in turn, would be gradationally overlain by red and green mudstones. Swartz's Wills Creek cycles seem to range from 5 to 25 feet thick.

Swartz's Tonoloway cycles (see Figure 16) would be similar to his Wills Creek cycles in that both cycles commenced with an oolitic or fossiliferous limestone. The ideal Tonoloway cycle, however, would contain no mudstones, and the basal limestone would grade upwards through banded limestones to laminated dolomitic limestones. More massive vugular dolomites occur in places in the upper part of the cycle.

Gwinn and Bain (1964) and Gwinn and Clack (1965) interpreted Swartz's Wills Creek and Tonoloway cycles as shoaling upward cycles in which the salinity of the environment increased up-cycle. They considered the limestones to be subtidal and the dolomites to be inter- to supratidal. Vinton Gwinn spent a year at Penn State in 1964, during which time he gathered additional data and sharpened his arguments for thin-skin deformation of the central Appalachians. At this time he also persued his interest in cyclicity in the Upper Silurian rocks exposed at Mt. Union. This writer joined Gwinn in visiting the Mt. Union section, at which time Gwinn gave the writer several dittoed diagrams illustrating his concept of cyclicity in the Wills Creek and Tonoloway formations. Unfortunately, Vinton met an accidental death at a relatively young age, and, as far as the writer can ascertain, did not publish the results of his cyclicity studies.

Figure 17 shows Gwinn's ideal Wills Creek and Tonoloway cycle sequences as deduced from his analysis of the Mt. Union section. The most marine portion of both cycles is their basal part (symbol (a) in Figure 17 and this may be a fossiliferous and/or oolitic and/or intraclastic limestone or limey shale. The contact of this unit with its underlying facies is sharply defined in contrast to most other contacts in the sequence. Gwinn's ideal Wills Creek cycle would then grade upward into a vaguely laminated greenish-grey mudstone (b) to a greenish (c) to

reddish (d) and back to greenish (e) massive mudstone. The upper part of this mudstone is usually more dolomitic than the lower part which is more calcitic. The massive mudstones would grade upward into dolomitic laminated mudstones (f) and the Wills Creek cycle would terminate with a massive dolomite (g) whose base and top are sharply defined.

The basal massive limestones (h) of Gwinn's Tonoloway cycle would grade up into laminated limestones (i), thence, to laminated dolomites (j) followed by a porous zone (k). The facies of the porous zone would include argillaceous laminated limestones and dolomites which generally are deeply weathered and poorly exposed. These rocks commonly are vugular and highly brecciated. The Tonoloway, like the Wills Creek cycle, would terminate with a sharply defined massive dolomite (l).

Tonoloway
(3'-21')

Facies	Facies Symbol	Type of Carbonate
massive dolomite	l	D
porous carbonate zone	k	C or D
laminated dolomite	j	D>>C C+D
laminated limestone	i	C>>D
massive limestone	h	C

Wills Creek
(5'-25')

Facies	Facies Symbol	Type of Carbonate
massive dolomite	g	D
greenish gray laminated mudstone	f	D
greenish massive mudstone	e	C or D
reddish massive mudstone	d	C
greenish massive mudstone	c	C
vaguely laminated greenish mudstone	b	C
dark shale ± limestone	a	C

-----gradational contact
C = calcite

_____sharp contact
D = dolomite

Figure 17. Gwinn and Bain's ideal Wills Creek and Tonoloway cycles.

Shallowing upward cycles have also been reported from the Keyser Formation (Head, 1969) which overlies the Tonoloway and from the Lower Devonian Helderberg Group (Anderson and Goodwin, 1980) of New York state. In these formations, as in the Wills Creek and Tonoloway, a rapid transgressive stage is followed by a gradual aggradational shallowing upward stage. Anderson and Goodwin (1980) have referred to such

sequences as punctuated aggradational cycles (PACs). Such cycles are noteworthy in the central Appalachians because of their widespread geographic distribution, and their temporal persistence over the diversity of lithofacies embraced by the Wills Creek through Helderberg formations.

At Charlie Hill, the uppermost part of the Wills Creek Formation is exposed, and interbeds of some of the Tonoloway facies are also present. Because of the presence of units from two different cyclic sequences, the Charlie Hill cycles are not as obvious as at Mt. Union. Most of the Charlie Hill cycles are incomplete, but all of the units of the ideal Wills Creek cycle shown on Figure 17 are present in the outcrop. Letters on the outcrop correspond to facies letters shown on Figure 17.

Part II: General Geology and Structural Interpretations

by H. A. Pohn and D. P. Gold

In addition to the facies units described above, and identified by the symbols a to g in 450 feet of the road-cut at Charlie Hill (see Figure 15), 14 litho-structural units have been recognized and labelled in black (Numbers 1-14 in Figure 15). The typical sedimentary facies change upward from thinly bedded dark marine limestones and shales (locally with salt(?) crystal molds), through buff weathering grey oolitic limestone beds, edgewise conglomerates and shale, into finely laminated algal matte limestone and greenish mudstone that grade into massive green calcareous mudstones about 2 m thick. These mudstones exhibit similar coincidal fracture and plumose decorations on the joint surfaces to the overlying massive red and gray mudstones (about 5 m thick), followed by a green dolomitic mudstone about 1 m thick that contains druzy vugs, 2-20 cm across, generally in distinct stratigraphic horizons. The top of a cycle is marked by a buff weathering fine-grained dolomite, generally about 30 cm thick, that locally contains rip-up clasts conglomerates.

The exposure at Charlie Hill contains an excellent example of antithetic folds and faults, formed in the hanging wall of a synthetic fault, possibly against a sharp flexure abutment. The southern part of the outcrop show folds shortening in wavelength as a small displacement fault is approached. The more northerly part of the exposure shows the wavelength again decreasing as the buttressing fault or flexure is approached (see Figure 18a). This is illustrated in the reconstruction sketch (Figure 18b) depicting the northerly part of the folded sequence at some time prior to the development of the faults, but after the initiation of the folds. The dashed lines show the location of the incipient faults. The decrease in wavelength towards the bounding fault is so pervasive in the central Appalalchians that a fold train decreasing in wavelength (commonly attentend with an increase in amplitude) is an almost certain indicator of a nearby bounding fault.

The variable attitude of the cleavage is perplexing, and suggests late rotation on splay faults(?). Small ramps and snake-head faults (Station #7), and uplimb thrust faults (antithetic and synthetic) attest to an early layer parallel shortening event. The wedge faults in Unit 7 in the

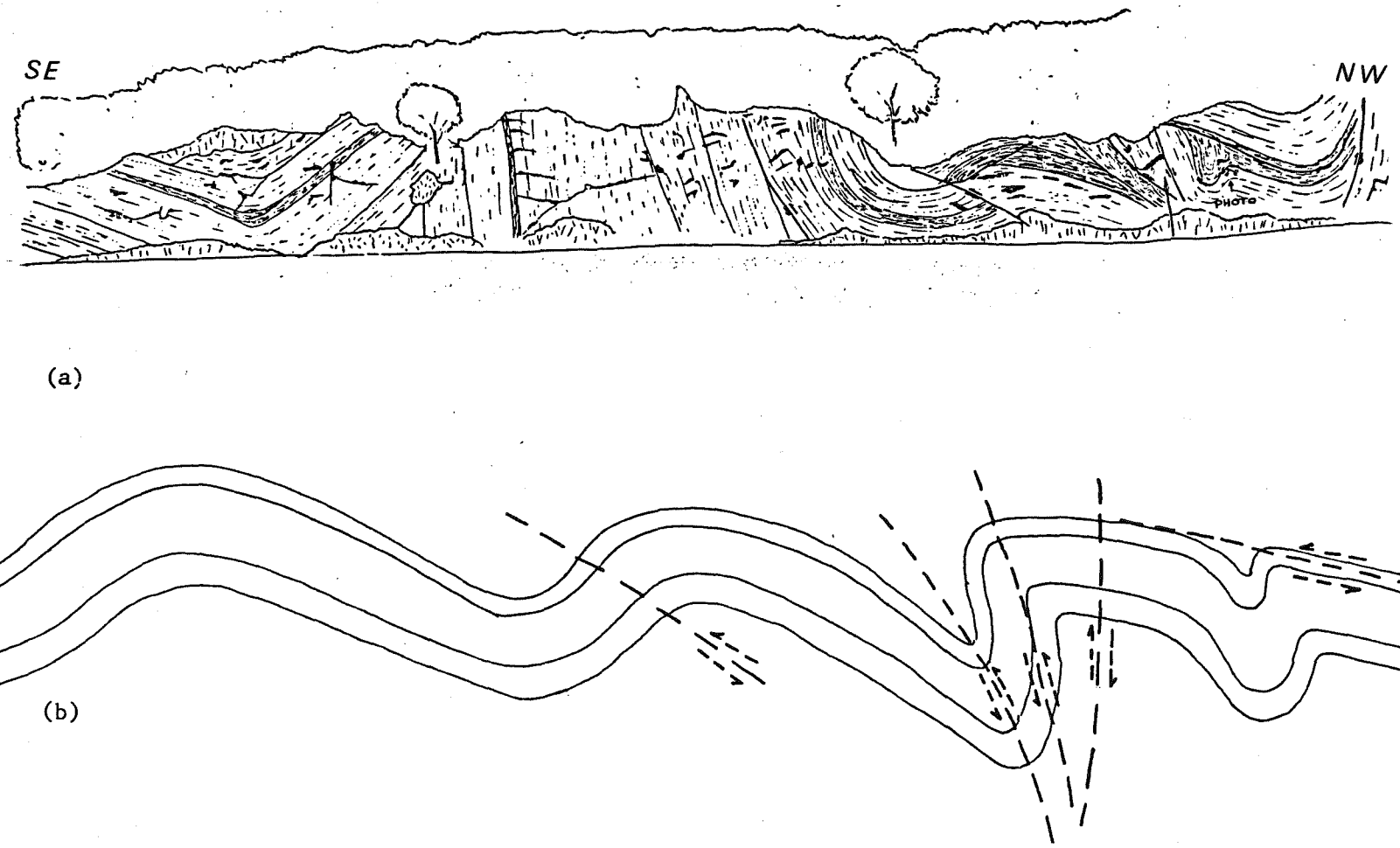

Figure 18. Schematic cross-section of part of the Charlie Hill road-cut, showing the present day configuration (a), and a reconstruction if the splay faults are removed.

hinge zone of the syncline at Station #6 are anomalous because they usually are found in competent beds coring anticlines. The kink bands are restricted to the laminated argillaceous algal limestone beds, and Faill (1973) noted that the asymmetry of the kink bands is a function of the dip of the enveloping surface. Local solution vugs, up to 20 cm across, appear to be deformed and elongated in the direction of the axial plane cleavage. The conclusion that the leached material from the vugs is anhydrite or gypsum is not unreasonable when one considers that these beds intertongue with the Salina (salt) Formation farther to the west.

This outcrop illustrates several space accommodation features associated with asymmetric and inclined synclines in the Valley and Ridge province, and in overthrust belts elsewhere. They are characterized by a single uplimb thrust fault on the steep limb and several uplimb thrust faults on the shallow limb, e.g., the synclines exposed at Stations #6 and #11. Also note the tight overturned syncline that repeats Units 10 and 11 near the road sign. Similar features have been noted in a 10 m wavelength syncline, 1 km east of Keyser, West Virginia, and in a 200 m wavelength syncline north of the dam site at Medley, West Virginia, as well as in a 3 km syncline in the Brooks Range, Alaska (John Kelley, pers. comm., 1985). Recognition of the uplimb thrust faults in some of the larger synclines of the Valley and Ridge province of the eastern overthrust belt may be difficult unless there is duplication of a marker unit, such as the doubling of the Tuscarora beds at Judy Gap, West Virginia (Perry, 1978), because these faults (particularly on the steep limb) are nearly bed-parallel. Disparity in limb thickness might be only a few percent if the faults are nearly bed-parallel, but could be as high as several tens of percent if the uplimb thrust are inclined 20° to 30° to bedding.

Miles	Interval	
		Return to vehicles and drive southeast for about 200 yards.
53.05	0.1	Turn left on Petersburg road, Rte 305N.
	2.55	Bridge.
	0.6	Right turn, and cross over bridge.
56.3	0.1	Cross over railroad bridge, and turn right at junction with Barree road. Follow Rte 305N to Petersburg.
57.2	0.9	Left turn in Petersburg.
63.7	6.5	Village of Neffs Mills.
64.95	1.25	Mooresville. Leave Rte 305 at Y intersection and follow left branch to State College.
	2.75	Stone Valley Recreation Center; and outdoor facility operated by The Pennsylvania State University. Entrance to Civil Engineering Camp.
	1.4	Stone Valley Nature Center.
70.85	1.75	Turn left onto Rte 26 at intersection.
72.95	2.1	STOP #7. LOOK-OUT ON CREST OF TUSSY MOUNTAIN. This is an informal stop for a late afternoon view of Nittany Valley, an anticlinal valley underlain by Ordovician carbonate rocks. Bald Eagle and Tuscarora rocks are preserved in Nittany Mountain, a 3rd order syncline on the broader 2nd order Nittany Arch. It is

		the first major valley into the Appalachian Valley and Ridge Province east of Bald Eagle Valley and the Appalachian Front. This arch terminates south of Birmingham, where the Sinking Valley anticline plunges beneath Canoe Mountain. The Birmingham fault, seen at Stop #3, has been mapped along the far side of the valley to a point beyond the line of site with Nittany Mountain.
74.9	1.95	Village of Pine Grove Mills. Turn right at junction with Rte 45 at the traffic light.
76.2	1.3	Keep left on Rte 26N at junction with Rte 45.
77.15	0.95	Turn right at traffic light onto Whitehall Road.
80.55	3.4	Turn left at traffic light onto Rte 322.
80.65	0.1	Turn left into Holiday Inn parking lot - end of Field Trip.

REFERENCES FOR FIELD TRIP 4

Anderson, E. J., and Goodwin, P. W., 1980, Application of the PAC hypothesis to limestones of the Helderberg Group: SEPM Eastern Section Field Trip, p. 1-32.

Berg, T. M., and Dodge, C. M., 1981, Atlas of preliminary geologic quadrangle maps of Pennsylvania: Pennsylvania Geological Survey, 4th ser., Map 61, 636 p.

Berg, T. M., Edmunds, W. E., Geyer, A. R., and others, compliers, 1980, Geologic map of Pennsylvania: Pennsylvania Geological Survey, 4th ser., Map 1, scale 1:250,000, 3 sheets.

Berg, T. M., McInerney, M. K., Way, J. H., and MacLachlan, D. B., 1983, Stratigraphic correlation chart of Pennsylvania: Pennsylvania Geological Survey, 4th ser., General Geology Report 75, 1 sheet.

Berger, P. S., Perry, W. S., Jr., and Wheeler, R. L., 1979, Three stage model of brittle deformation in the central Appalachians: Southeastern Geology, v. 20, no. 2, p. 59-67.

Blanchet, P. H., 1957, Development of fracture analysis as an exploration method: American Association of Petroleum Geologists Bulletin, v. 41, p. 1748-1759.

Boyer, S. E., and Elliott, D., 1982, Thrust systems: American Association of Petroleum Geologists Bulletin, v. 66, no. 9, p. 1196-1230.

Butts, Charles, 1918, Geologic section of Blair and Huntingdon Counties, central Pennsylvania: American Journal of Science, v. 46, p. 523-537.

Butts, Charles, Swartz, F. M., and Willard, Bradford, 1939, Tyrone quadrangle: Pennsylvania Geological Survey, 4th ser., Atlas 96, 118 p.

Canich, M. R., 1976, A study of fractures along the western segment of the Tyrone-Mount Union lineament: University Park, Pennsylvania State University, M.S. paper.

Chamberlain, R. T., 1910, The Appalachian fold of central Pennsylvania: Journal of Geology, v. 18, p. 228-251.

Charlesworth, H. A. K., and Gagnon, L. G., 1985, Intercutaneous wedges, the triangle zone and structural thickening of the Mynheer coal seam at Coal Valley in the Rocky Mountain foothills of central Alberta: Bulletin of Canadian Petroleum Geology, v. 33, no. 1, p. 22-30.

Cloos, Ernst, 1940, Crustal shortening and axial divergence in the Appalachians of southern Pennsylvania: Geological Society of America Bulletin, v. 51, p. 845-872.

_____, 1964, Wedging, bedding plane slips, and gravity tectonics in the Appalachians, In Tectonics of the southern Appalachians: Virginia Polytechnic Institute, Geological Studies Memoir 1, p. 63-70.

Currie, J. B., Patnode, H. W., and Trump, R. P., 1962, Development of folds in sedimentary strata: Geological Society of America Bulletin, v. 73, p. 655-674.

Dahlstron, C. D. A., 1969, Balanced cross section: Canadian Journal of Earth Sciences, v. 6, no. 4, p. 743-757.

_____, 1970, Structural geology in the eastern margin of the Canadian Rocky Mountains: Bulletin of Canadian Petroleum Geology, v. 18, p. 332-406.

DeSitter, L. M., 1956, Structural geology: New York, McGraw-Hill Book Co.

Diment, W. H., Muller, O. H., and Lavin, P. M., 1980, Basement tectonics of New York and Pennsylvania as revealed by gravity and magnetic studies, In The Caledonides in the USA: Virginia Polytechnic Institute and State University, IGCP Project 27, Proceedings, Memoir 2, p. 221-227.

Donaldson, A. C., 1959, Stratigraphy of Lower Ordovician Stonehenge and Larke Formations in central Pennsylvania: University Park, Pennsylvania State University, Ph.D. thesis, 393 p.

Dyson, J. L., 1963, Geology and mineral resources of the New Bloomfield quadrangle, Pennsylvania: Pennsylvania Geological Survey, 4th ser., Atlas 137ab, 63 p.

Elliott, D., 1976, The energy balance and deformation mechanisms of thrust sheets: Royal Society of London, Philosophical Transactions, Series A, v. 283, p. 289-312.

Engelder, T., 1979, Mechanisms for strain within the Upper Devonian clastic sequence of the Appalachian Plateau, western New York: American Journal of Science, v. 279, p. 527-542.

Engelder, T., and Engelder, R., 1977, Fossil distortion and decollement tectonics of the Appalachian Plateau: Geology, v. 5, p. 457-460.

Engelder, T., and Geiser, P., 1979, The relationship between pencil cleavage and lateral shortening within the Devonian section of the Appalachian Plateau, New York: Geology, v. 7, p. 460-464.

Engelder, T., and Geiser, P., 1980, On the use of regional joint sets as trajectories of paleostress fields during the development of the Appalachian Plateau, New York: Journal of Geophysical Research, v. 85, p. 6319-6341.

Epstein, A. G., Epstein, J. B., and Harris, L. D., 1977, Conodont color alteration--An index to organic metamorphism: U.S. Geological Survey Professional Paper 995, 27 p.

Faill, R. T., 1969, Kink band structures in the Valley and Ridge province, central Pennsylvania: Geological Society of America Bulletin, v. 80, p. 2539-2550.

_____, 1973, Kink-band folding, Valley and Ridge province, Pennsylvania: Geological Society of America Bulletin, v. 89, p. 1289-1314.

_____, 1979, Geology and mineral resources of the Montoursville South and Muncy quadrangles and part of the Hughesville quadrangle, Lycoming, Northumberland, and Montour Counties, Pennsylvania: Pennsylvania Geological Survey, 4th ser., Atlas 144ab, 63 p.

Fox, H. D., 1950, Structure and origin of two windows exposed on the Nittany Arch at Birmingham, Pennsylvania: American Journal of Science, v. 248, p. 158-170.

Gary, Margaret, McAfee, Robert, Jr., and Wolf, C. L., eds., 1972, Glossary of geology: Washington, D. C., American Geological Institute, 805 p.

Gay, S. P., Jr., 1973, Pervasive orthogonal fracturing in the earth's continental crust: Salt Lake City, Utah, American Stereo Map Company.

Geiser, Peter, and Engelder, Terry, 1983, The distribution of layer parallel shortening fabrics in the Appalachian foreland of New York and Pennsylvania: evidence for two non-coaxial phases of the Alleghanian orogeny, In Hatcher, R. D., Jr., and others, eds., Contributions to the tectonics and geophysics of mountain chains: Geological Society of America Memoir 158, p. 161-175.

Gold, D. P., 1980, Structural geology, In Siegal, B., and Gillespie, A., eds., Remote sensing in geology: New York, John Wiley and Sons, p. 419-483.

_____, 1983, Application of remote sensing to structural geology and tectonics, In Manual of remote sensing: American Society of Photogrammetry, 2nd ed., vol. 2, p. 1777-1782.

Gold, D. P., Alexander, S. S., and Parizek, R. R., 1973, Application of remote sensing to natural resources and environmental problems in Pennsylvania: Earth and Mineral Sciences, v. 43, no. 7, p. 49-53.

Gold, D. P., and Parizek, R. R., 1976, Field guide to lineaments and fractures in central Pennsylvania: International Conference on New Basement Tectonics, 2nd, Newark, Del., University of Delaware, Guidebook, 27 p.

Gold, D. P., Pohn, H. A., and Canich, M. R., 1984, Strike parallel and cross-strike structures in Tyrone-Mt. Union lineament in central Pennsylvania: American Association of Petroleum Geologists, Eastern Section, Field Guide, 71 p.

Grout, M. A., and Verbeek, E. R., 1983, Field studies of joints: Insufficiencies and solutions with examples from the Piceance Creek Basin, Colorado: Symposium on Oil Shale, 16th, Proceedings, Colorado School of Mines, p. 68-80.

Gwinn, V. E., 1964, Thin-skinned tectonics in the Plateau and northwestern Valley and Ridge provinces of the central Appalachians: Geological Society of America Bulletin, v. 75, p. 863-900.

_____, 1970, Kinematic patterns and estimates of lateral shortening, Valley and Ridge and Great Valley provinces, central Appalachians, south-central Pennsylvania, In Fisher, G. W., and others, eds., Studies of Appalachian geology: central and southern: New York, Interscience Publishers, p. 127-146.

Gwinn, V. E., and Bain, D. M., 1964, Penecontemporaneous dolomite in Upper Silurian cyclothems, south-central Pennsylvania [abs.]: American Association of Petroleum Geologists Bulletin, v. 48, p. 528.

Gwinn, V. E., and Clack, W. C., 1965, Penecontemporaneous dolomite, Upper Silurian, Pennsylvania [abs.]: Geological Society of America Special Paper 82, p. 80-81.

Harris, A. G., Harris, L. D., and Epstein, J. B., 1978, Oil and gas data from Paleozoic rocks of the Appalachian basin: maps for assessing hydrocarbon potential and thermal maturity (conodont color alteration isograds and overburden isopachs): U.S. Geological Survey Miscellaneous Geological Investigations Map I-917-E, scale 1:2,500,000, 4 sheets.

Harris, L. D., and Milici, R. C., 1977, Characteristics of thin-skinned style of deformation in the southern Appalachians, and potential hydrocarbon traps: U.S. Geological Survey Professional Paper 1018, 40 p.

Head, J. W., III, 1969, An integrated model of carbonate depositional basin evolution: Late Cayugan (Upper Silurian) and Helderbergian (Lower Devonian) of the central Appalachians: Brown University, Ph.D. dissertation, 390 p.

Hodgson, R. A., 1961, Classification of structures on joint surfaces: American Journal of Science, v. 259, p. 493-502.

Hollister, L. S., Crawford, M. L., Roedder, E., and others, 1981, Practical aspects of microthermometry, In Hollister, L. S., and Crawford, M. L., eds., Short course in fluid inclusions: applications to petrology: Calgary, Mineralogical Association of Canada, p. 278-304.

Hood, A., Gutjahr, C. C. M., and Heacock, R. L., 1975, Organic metamorphism and the generation of petroleum: American Association of Petroleum Geologists Bulletin, v. 59, no. 6, p. 986-996.

Hower, J. C., 1978, Anisotropy of vitrinite reflectance in relation to coal metamorphism for selected United States coals: University Park, Pennsylvania State University, Ph.D. thesis, 339 p.

Jacobeen, F., Jr., and Kanes, W. H., 1974, Structure of Broadtop synclinorium and its applications for Appalachian structural style: American Association of Petroleum Geologists Bulletin, v. 58, no. 3, p. 362-375.

_____, 1975, Structure of Broadtop synclinorium, Wills Mountain anticlinorium and Allegheny frontal zone: American Association of Petroleum Geologists Bulletin, v. 59, no. 7, p. 1136-1150.

Kiemic, Harry, Warman, J. C., and Taylor, A. R., 1963, Geology and uranium occurrences of the northern half of the Lehighton, Pennsylvania quadrangle and adjoining areas: U.S. Geological Survey Bulletin 1138, 97 p.

Kowalik, W. S., and Gold, D. P., 1974, The use of LANDSAT-1 imagery in mapping lineaments in Pennsylvania: International Conference on the New Basement Tectonics, 1st, Proceedings, Utah Geological Association Publication 5, p. 236-249.

Krohn, M. D., 1976, Relation of lineaments to sulfide deposits and fractured zones along Bald Eagle Mountain: Centre, Blair, and Huntingdon Counties, Pennsylvania: University Park, Pennsylvania State University, M.S. thesis, 104 p.

Lattman, L. H., 1958, Techniques of mapping geologic fracture traces and lineaments on aerial photographs: Photogrammetric Engineering, v. 24, p. 658-673.

Lattman, L. H., and Nickelsen, R. P., 1958, Photogeologic fracture trace mapping in Appalachian Plateau: American Association of Petroleum Geologists Bulletin, v. 42, p. 2238-2248.

Lavin, P. M., Chaffin, D. L., and Davis, W. F., 1982, Major lineaments and the Lake Erie-Maryland crustal block: Tectonics, v. 1, no. 5, p. 431-440.

Lesley, J. P., 1885, [The Little Juniata section and Warriors Mark], In White, I. C., The geology of Huntingdon County: Pennsylvania Geological Survey, 2nd ser., Report T3, p. 359-384.

Levine, J. R., 1983, Coal rank patterns in the Pennsylvania Anthracite Region, In Nickelsen, R. P., and Cotter, Edward, eds., Silurian depositional history and Alleghanian deformation in the Pennsylvania Valley and Ridge: Annual Field Conference of Pennsylvania Geologists, 48th, Danville, Pa., Guidebook, p. 67-73.

Matzke, R. H., 1961, Fracture trace and joint patterns in western Centre County, Pennsylvania: University Park, Pennsylvania State University, M.S. thesis, 39 p.

Moebs, N. N., and Hoy, R. B., 1959, Thrust faulting in Sinking Valley, Blair and Huntingdon Counties, Pennsylvania: Geological Society of America Bulletin, v. 70, p. 1079-1088.

Nickelsen, R. P., 1963, Fold patterns and continuous deformation mechanisms of the central Pennsylvania folded Appalachians, in Cate, A., ed., Tectonics and Cambro-Ordovician stratigraphy in the central Appalachians of Pennsylvania: Pittsburgh Geological Society and Appalachian Geological Society, Guidebook, p. 13-29.

_____, 1966, Fossil distortion and penetrative rock deformation in the Appalachian Plateau, Pennsylvania: Journal of Geology, v. 74, p. 924-931.

_____, 1974, Early jointing and cumulative fracture patterns: International Conference on the New Basement Tectonics, 1st, Proceedings, Utah Geological Association Publication 5, p. 193-199.

Nickelsen, R. P., 1979, Sequence of structural stages of the Alleghany orogeny, at the Bear Valley strip mine, Shamokin, Pennsylvania: American Journal of Science, v. 279, p. 225-271.

_____, 1983a, Aspects of Alleghanian deformation, in Nickelsen, R. P., and Cotter, Edward, eds., Silurian depositional history and Alleghanian deformation in the Pennsylvania Valley and Ridge: Annual Field Conference of Pennsylvania Geologists, 48th, Danville, Pa., Guidebook, p. 29-52.

_____, 1983b, Ambient temperatures during the Alleghany orogeny, in Nickelsen, R. P., and Cotter, Edward, eds., Silurian depositional history and Alleghanian deformation in the Pennsylvania Valley and Ridge: Annual Field Conference of Pennsylvania Geologists, 48th, Danville, Pa., Guidebook, p. 64-66.

Nickelsen, R. P., and Hough, V. N. D., 1967, Jointing in the Appalachian Plateau of Pennsylvania: Geological Society of America Bulletin, v. 78, no. 5, p. 609-629.

Norris, D. K., 1958, Structural conditions in Canadian coal mines: Geological Survey of Canada Bulletin, v. 44, 54 p.

Orkan, N., and Voight, B., 1983, Fracture geometry and vein mineral paleothermometry-barometry from fluid inclusions, Valley and Ridge province, Pennsylvania: Geological Society of America Abstracts with Programs, v. 15, no. 6, p. 656.

Parker, J. M., 1942, Regional systematic jointing in slightly deformed sedimentary rocks: Geological Society of America Bulletin, v. 53, p. 381-408.

Parrish, J. B., and Lavin, P. M., 1982, Tectonic model of kimberlite emplacement in the Appalachian Plateau of Pennsylvania: Geology, v. 10, p. 344-347.

Paxton, S. T., 1983, Relationships between Pennsylvanian age lithic sandstone and mudrock diagenesis and coal rank in the central Appalachians: University Park, Pennsylvania State University, Ph.D. thesis, 503 p.

Perry, W. J., 1978, The Wills Mountain anticline; A study in complex folding and faulting in eastern West Virginia: West Virginia Geological and Economic Survey Report of Investigations RI-32, 29 p.

Platt, Franklin, 1881, The geology of Blair County: Pennsylvania Geological Survey, 2nd ser., Report T, 311 p.

Pohn, H. A., and Purdy, T. L., 1979, Thrust fault zones in the Allegheny Plateau of north-central Pennsylvania: U.S. Geological Survey Open-File Report 79-1604, 8 p.

_____, 1982, Disturbed zones: Indicators of deep-seated surface faults in the Valley and Ridge and Appalachian structural front of Pennsylvania: U.S. Geological Survey Open-File Report 82-967, 82 p.

Price, P. A., 1931, The Appalachian structural front: Journal of Geology, v. 39, no. 1, p. 24-44.

Rich, J. L., 1934, Mechanics of low-angle overthrust faulting as illustrated by Cumberland thrust block, Virginia, Kentucky, and Tennessee: Geological Society of America Bulletin, v. 18, no. 12, p. 1584-1596.

Rodgers, J., 1963, Mechanics of Appalachian foreland folding in Pennsylvania and West Virginia: American Association of Petroleum Geologists Bulletin, v. 47, no. 8, p. 1527-1536.

Roedder, Edwin, 1962, Ancient fluids in crystals: Scientific American, v. 207, p. 38-47.

_____, 1970, Application of an improved crushing microscope stage to studies of the gases in fluid inclusions: Schweiz. Mineral. Petrogr. Mitt., v. 50, Pt. 1, p. 41-58.

_____, 1972, The composition of fluid inclusions, Chapter JJ, in Fleischer, Michael, ed., Data of geochemistry: U.S. Geological Survey Professional Paper 440-JJ, 6th ed., p. JJ1 -JJ164.

_____, 1979, Fluid inclusions as samples of ore fluids, in Barnes, H. L., ed., Geochemistry of hydrothermal ore deposits: New York, Wiley, p. 684-737.

Roedder, Edwin, and Bodnar, R. J., 1980, Geologic pressure determinations from fluid inclusion studies: Annual Review of Earth and Planetary Science, v. 8, p. 263-301.

Rogers, H. D., 1858, The geology of Pennsylvania: Philadelphia, J. B. Lippincott and Co., v. 1, 586 p.

Rogers, M. R., and Anderson, T. H., 1984, Tyrone-Mt. Union cross-strike lineament of Pennsylvania: a major Paleozoic basement fracture and uplift boundary: American Association of Petroleum Geologists Bulletin, v. 68, no. 1, p. 92-105.

Root, S. I., 1971, Geology and mineral resources of northeastern Franklin County, Pennsylvania: Pennsylvania Geological Survey, 4th ser., Atlas 119ab, 104 p.

_____, 1974, Structure, basin development and tectogenesis in the Pennsylvania portion of the folded Appalachians, In De Jong, K. A., and Scholten, Robert, eds., Gravity and tectonics: New York, John Wiley and Sons, p. 343-360.

Schafer, K., 1979, Recent thrusting in the Appalachians: Nature, v. 280, p. 223-226.

Schmiermund, R. L., and Palmer, C. D., 1973, Plane table and geologic map of an area near Birmingham, Pennsylvania: University Park, Pennsylvania State University, unpublished class project.

Sheppard, R. A., 1956, A systematic joint study in the folded Appalachians: Pennsylvania Academy of Science Proceedings, v. 30, p. 142-145.

Smith, R. C., II, 1977, Zinc and lead occurrences in Pennsylvania: Pennsylvania Geological Survey Mineral Resource Report 72, 318 p.

Smith, R. C., II, Herrick, D. C., Rose, A. W., and McNeal, J. M., 1971, Zinc-lead occurrences near Mapleton, Huntingdon Co., Pennsylvania: Pennsylvania State University, College of Earth and Mineral Sciences Experiment Station Circular 83, 37 p.

Swartz, F. M., 1955, Stratigraphy and structure of the Ridge and Valley area from University Park to Tyrone, Mt. Union, and Lewistown: Annual Field Conference of Pennsylvania Geologists, 21st, Guidebok, p. S1-1-38.

_____, 1966, Subsurface faults in the vicinity of Birmingham and Jacksonville, Pennsylvania: Pennsylvania State University, College of Earth and Mineral Sciences Experiment Station Report, Trip 2, Appendix to S1-1955, p. SA-1-8.

Ver Steeg, K., 1942, Jointing in the coal beds of Ohio: Journal of Geology, v. 52, p. 131-138.

_____, 1944, Some structural features of Ohio: Journal of Geology, v. 52, p. 131-138.

Voight, B., 1976, Editor's comments on "The mechanics of overthrust faulting: a critical review, by J. L. Roberts," In Voight, B., ed., Mechanics of thrust faults and decollement: Stroudsburg, Pa., Dowden, Hutchinson and Ross, 471 p.

Voight, B., and St. Pierre, B. H. P., 1974, Stress history and rock stress: International Society of Rock Mechanics, IIA, 3rd Congress, Proceedings, p. 580-582.

Wells, R. B., and Bucek, M. F., 1980, Geology and mineral resources of the Montoursville North and Huntersville quadrangles, Lycoming County, Pennsylvania: Pennsylvania Geological Survey, 4th ser., Atlas 143cd, 68 p.

Williams, H., 1978, Tectonic lithofacies map of the Appalachian orogen: Memorial University of Newfoundland, Map 1.

Willis, B., 1891, The mechanics of Appalachian structure: U.S. Geological Survey, 13th Annual Report, p. 211-281.

Wood, G. H., Arndt, H. H., and Carter, M. D., 1969, Systematic jointing in the western part of the Anthracite Region of eastern Pennsylvania: U.S. Geological Survey Bulletin 1271-D, p. D1-D17.

Woods, T. L., Bethke, P. M., Bodnar, R. J., and Werre, R. W., Jr., 1981, Supplementary components and operation of the U.S. Geological Survey gas-flow heating/freezing stage: U.S. Geological Survey Open-File Report 81-954, 12 p.

Zeller, R. A., 1949, The structural geology and mineralization of Sinking Valley, Pa.: University Park, Pennsylvania State University, M.S. thesis, 71 p.

FIELD TRIP #5

ORIGIN OF THE MERCER HIGH-ALUMINA CLAY

by
E. G. Williams and William Bragonier

Among the most unique deposits in the coal fields in western Pennsylvania are the underclays which lie below the Lower Mercer coal; unique because they contain the minerals diaspore, boehmite, and gibbsite which occur together with kaolinite and are confined to one stratigraphic position and to a relatively restricted area in the northeastern part of the Appalachian Basin, encompassing parts of Clearfield, Centre, Cameron, and Clinton Counties (Fig. 1). Clays of this composition are known from only one other area in the United States--the Cheltenham fire clays from Missouri. In both areas, the clays are the basis for an extensive refractory brick industry. The deposits in western Pennsylvania have been studied by Foose (1944), Bolger and Weitz (1952), Williams (1960b), Erickson (1963), and Bragonier (1970). These studies deal mainly with the genesis of the high-alumina deposits. Weitz and Bolger (1964) have prepared a geologic map of the Mercer clay horizon and associated formations and members (Pocono, Mauch Chunk, Lower Mercer coal, and the Lower Clarion coal in the four counties where the clays are found). This map is most useful in prospecting for the clays and will be discussed later.

The location of the principal high-alumina clay deposits is shown in Figure 1 and their stratigraphic position in Figure 2. The areas in Clearfield County (west of State College) and in Clinton County (west of Lock Haven) are commercial strip or deep mines and all contain both diaspore and flint clays. All other localities contain only flint clay. The exact stratigraphic position of the clay shown in Figure 2 is at the base of the Pennsylvanian, where it overlies sandstones and red beds of the Mauch Chunk Formation. However, the correlation and identification of this sandstone has been a matter of debate, Edmunds (1968) calling it upper Pocono. Although differing as to formation, most investigators now believe such sandstones to be Mississippian in age, based on plant fossils. The high-alumina clays there-

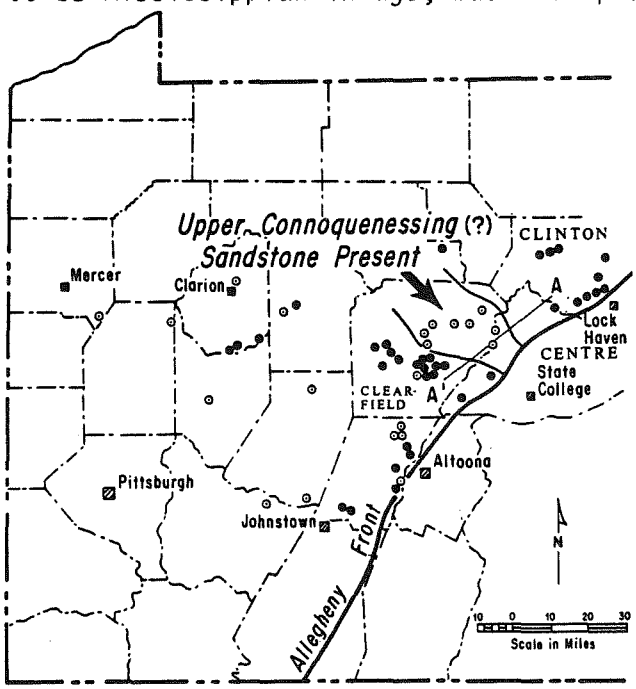

Figure 1. Areas of occurrence of the principal mines and outcrops of the Lower Mercer flint and nodule clays. Modified from Williams (1960). Closed dots are areas containing minable clay; open dots are areas where hard clay is absent.

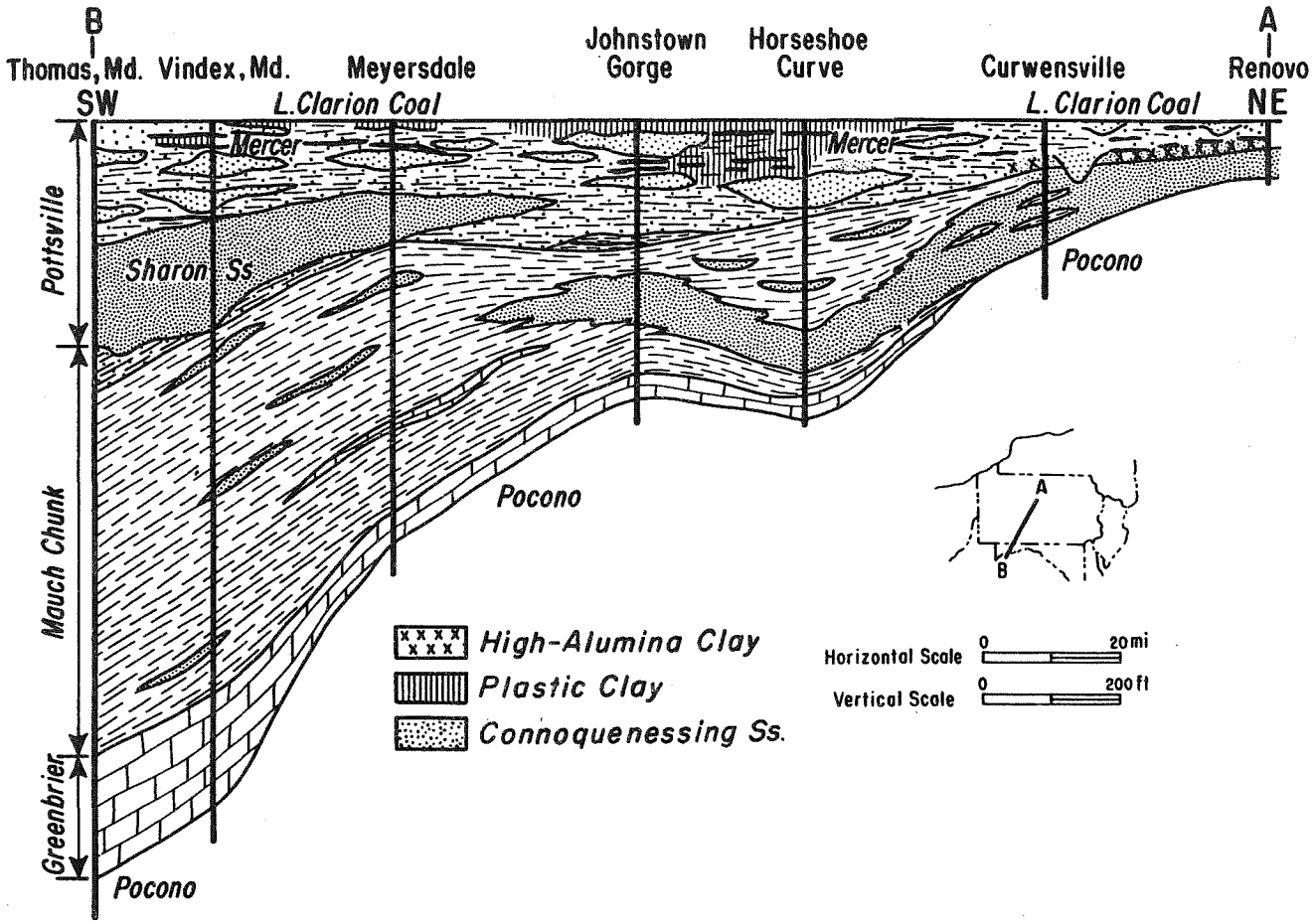

Figure 2. Stratigraphic cross section of the Upper Mississippian and Pennsylvanian Pottsville rocks in western Pennsylvania. The Mercer high-alumina clay occurs between Curwensville and Renovo and is marked by x's. After Williams and others (1969).

fore occur in the areas where the Pottsville and Upper Mississippian formations are thinnest, a fact we interpret to mean that the occurrence of the clay has been tectonically controlled.

A classification of the high-alumina clays is given in Figure 3. Flint and block clays are volumetrically the most important types. They consist of a very fine grained groundmass (10 microns) of well-crystallized kaolinite with lesser amounts of coarsely crystalline stringers, veinlets, and patches of kaolinite. Flint clays are very dense, smooth, with a conchoidal fracture producing sharp edges and points, and frequently brecciated. The alumina content of flint clays is about 40 percent.

Diaspore and boehmite constitute the high-alumina minerals occurring in the nodule clay fraction of the deposit. Both of these minerals occur as fine-grained groundmass or as nodular masses in a kaolinite matrix. Nodules may become so abundant that they comprise the whole deposit, thereby producing what is called burnt nodule clay, a gray to brown, porous material with a cindery appearance, having an alumina content of about 70 percent. Quartz and illite, although abundant in the plastic clays, are absent in the high-alumina clays. However, tourmaline and zircon are common in the high-alumina clays and rare in the plastic clays. Pyrite, siderite, and limonite are the main iron-bearing minerals whose presence, generally less than two percent, is critical to the use of the clay in making refractory brick since these minerals have a pronounced, undesirable effect on melting temperature.

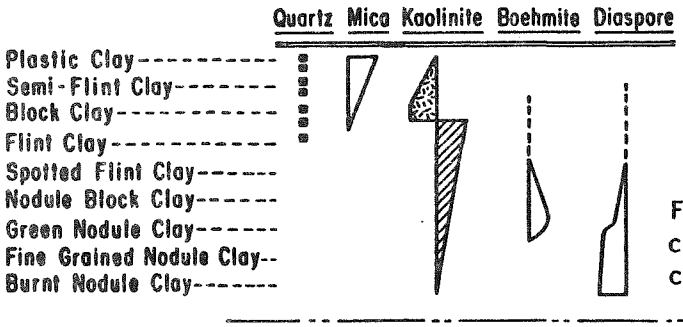

Figure 3. Mineral composition of the megascopic clay types of the Mercer high-alumina clay. Reconstructed from Erickson (1963).

NOTE: Width of band denotes relative concentration of mineral.
Dashed line (- - -) denotes a phase which may or may not be present in the particular rock type

Poorly-Crystalline Kaolinite

Well-Crystalline Kaolinite

Organic constituents preserved within the Mercer clays occur as either remains of cellular tissues (mostly roots) or remains of microbiological organisms and lower forms of life. The general dirty appearance of kaolinite is believed to be due to the fine-grained organic particles incorporated within the groundmass.

The local variation in the mineralogy of the high-alumina clays appears to be largely controlled by paleotopography developed on the quartzitic sandstone which, in almost all localities, lies directly below the clay, usually with sharp contact. Figure 4 shows that the nodule clays of the Mercer are located on the sides of

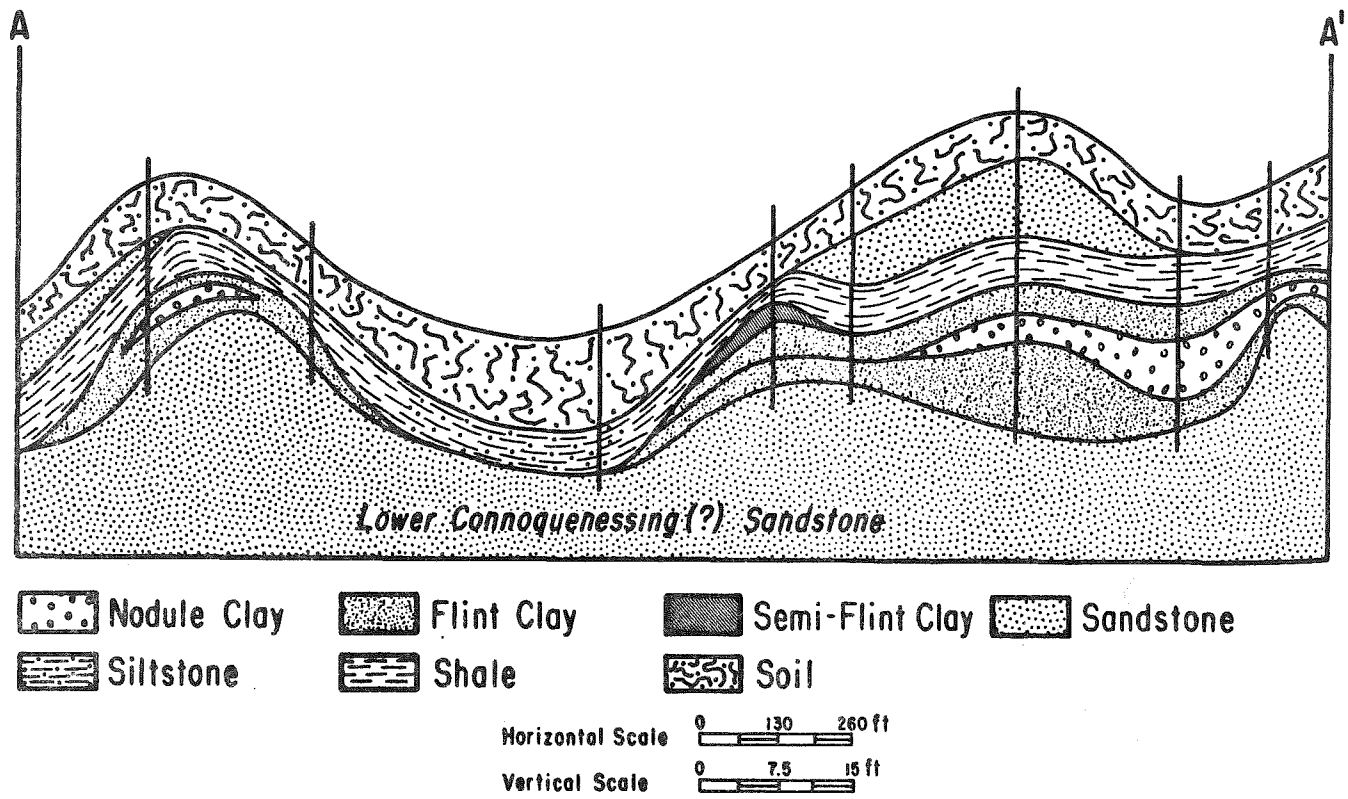

Figure 4. A typical cross section of the Lower Mercer high-alumina clay in the Anderson Creek area several miles north of Curwensville, Pennsylvania.

elevated areas and are absent in low areas in between. Observe that the nodule clay is bounded by flint clay, and that both clays thin toward the adjacent low. It is not clear whether the flint clays thickened into the low and were subsequently eroded or were confined to the topographic high. However, it is quite evident that the nodule clays were developed on the more topographically elevated areas. Petrographic evidence shows that the diaspore and boehmite replace both the coarsely and finely crystalline kaolinite, so that we infer that this process was favored by more intense leaching on the topographic highs.

Reference to Figure 1 shows the nature of the subregional variation in the Mercer high-alumina clay. In the northeast part of Clearfield County, the clay is absent and, as shown in Figure 5, replaced by sandstone, called the Upper Connoquenessing. The upper diagram illustrates the idea that the Mercer clays were developed over the eroded edges of several sandstone bodies within the Mauch Chunk Formation. The lower diagram conveys the hypothesis that the distribution of the clays is primarily controlled by Pennsylvanian erosion. This interpretation would imply that the clays are largely depositional features and that no major hiatus occurs between the clay and underlying sandstone.

We tend to favor the first interpretation for the following reasons. Paleobotanical studies quoted in Edmunds (1968) demonstrate that the underlying sandstone is Middle Mississippian and the Mercer clays uppermost-Lower Pennsylvanian. In addition, the sandstone below the Mercer clay, at every locality, shows evidence of intensive chemical weathering; namely these sandstones, unlike any others in the upper Paleozoic, do not contain chlorite, have very high kaolinite contents, contain an abundance of chert cement, and exhibit, in the upper 20 feet, well-rounded and etched quartz grains as well as concentrations of well-rounded tourmaline. And although some of these properties might have been inherited from an adjacent, deeply weathered shield, all of them together suggest considerable in situ alteration.

Because the high-alumina clay rests sharply on the underlying sandstone, whose composition prior to cementation by quartz and kaolinite was probably greater than 90 percent quartz, many investigators (Erickson, 1963; Bragonier, 1970) have

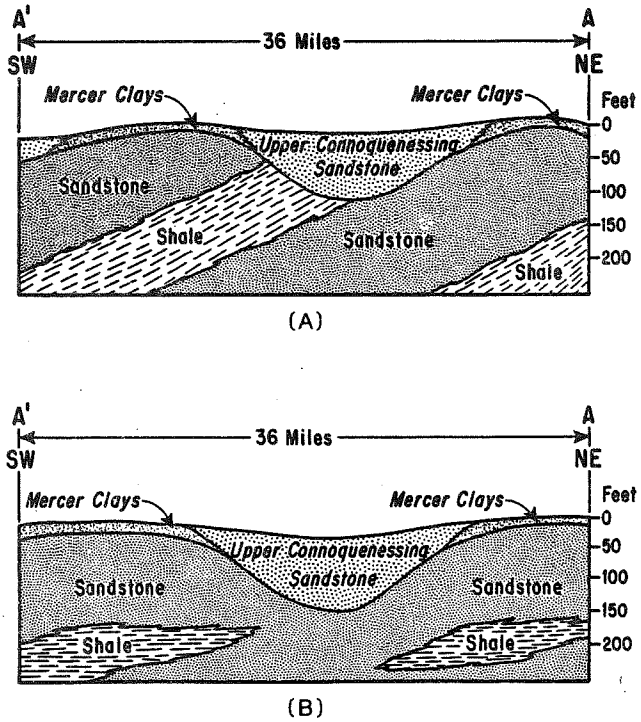

Figure 5. A hypothetical cross section through Centre and Clearfield Counties illustrating the ideas that the Mercer clays were confined to paleotopographic highs (5A) or limited by post-clay erosion (5B). Line A-A' is shown on Figure 1. Scales are approximate.

inferred that the source for the nodule clay must have been colloidally precipitated flint clays, which formed by flocculation in swampy coastal environments, or perhaps a more complex detritus of illite, kaolinite, and quartz, which was purified by contact with organic-rich, acid swamp waters. One of the principal lines of evidence which suggests that at least a part of the clay was derived from rocks like the underlying sandstone is the presence, in local areas of the clay, of lense-shaped concentrations of rounded tourmaline, similar in size, shape, and roundness to that in the underlying sandstone. Surrounding all such occurrences are wavy and contorted structures in the kaolinite matrix which suggest that there has been collapse and flowage. Since the volume of tourmaline in the sandstone is about one quarter of one percent, the removal of all the quartz would involve a considerable loss of volume, which might account for the flow structures. And lastly, the development of kaolinitic and bauxitic clays on quartzites is not so rare as might be imagined--the Gatesburg Formation, a formation consisting of quartzite and dolomitic quartzite, is the source for extensive kaolinite and local bauxite deposits formed during the late Tertiary in central Pennsylvania. Loughnan (1962) also reports thick bauxite deposits overlying quartzite formations in Australia. Given the high permeability of these rocks, sufficient water, and time, it is not out of the reach of probability that the Mercer high-alumina clays were largely derived from the underlying sandstones.

In addition to exhibiting marked local and subregional variations, the Mercer clay also manifests significant regional change, as illustrated in Figure 6. Although the high-alumina clays are lenticular bodies whose lateral dimensions are commonly only a few acres, the diaspore and boehmite are restricted to the most northeastern parts of the Appalachian Bituminous Coal Basin, where they occur together with flint clays. To the south and west occur isolated lenses of flint clay which are replaced to the southwest toward the basin center by plastic clays composed of illite, kaolinite, and quartz. These regional facies are very similar to those exhibited by the Cheltenham clays of Missouri (Fig. 7) described by Keller

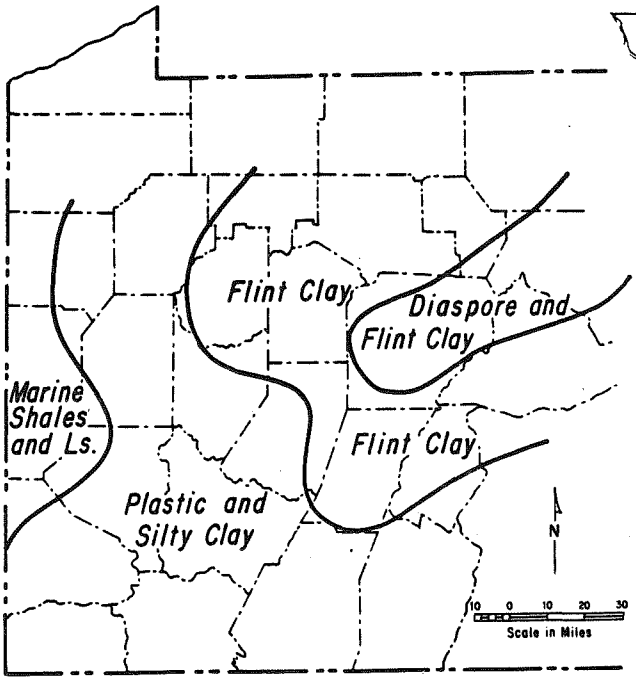

Figure 6. Map of the distribution of the various clay mineral facies in the Mercer underclay. From Williams and others (1969).

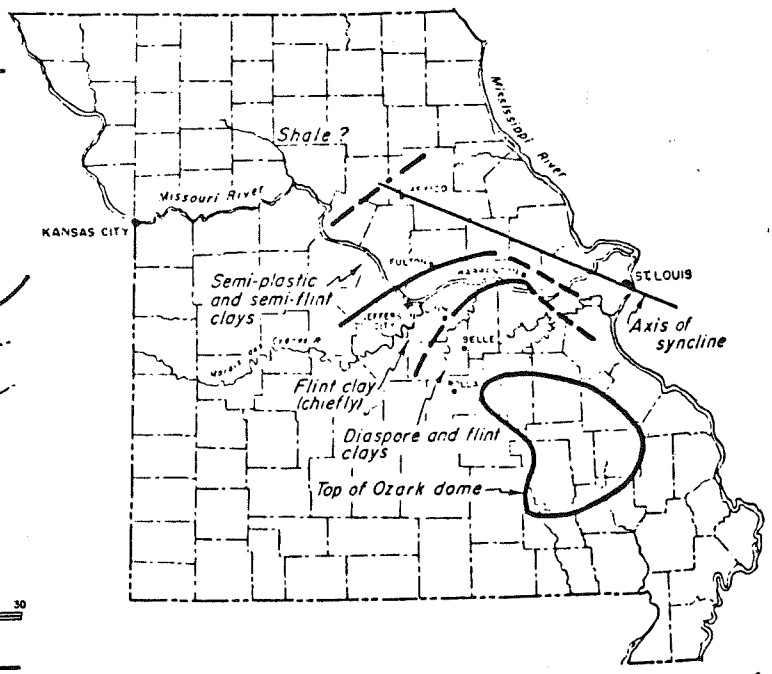

Figure 7. Map showing the distribution of the clay types in the lower Pennsylvanian Cheltenham clay. From Keller and others (1954).

and others (1954). Keller attributes the regional facies changes to increased intensity of leaching with increasing tectonic relief on the northern flank of the Ozark Dome, as well as to increasing time of exposure to weathering processes. We believe that the regional thinning of the Upper Mississippian and Lower Pennsylvanian sections in a northeasterly direction along the axis of the basin is caused by both erosion and nondeposition in areas of elevated topography, which existed during the time of clay formation. Areas of tectonic doming in the northeastern parts of the basin during the Upper Paleozoic have been discussed by Williams and Bragonier (1974).

We propose the following theory of origin for the Mercer high-alumina clays. During Late Mississippian and Early Pennsylvanian time, the northeastern portion of the Allegheny Plateau was a stable shelf or slightly elevated area as a result of tectonic doming in north-central Pennsylvania. This paleotectonic framework provided the conditions necessary for the formation of the high-alumina clay; namely, a prolonged period of environmental stability, relatively large supplies of silica and alumina and a relatively low amount of detrital material, and extensive chemical weathering possibly enhanced by an underlying, permeable sandstone. The initial material from which the nodule clays were derived is not known, but might have ranged from colloidal precipitates of kaolinite and illite to quartz-rich sand. Within the clay-forming environment that existed over significant paleotopography on sandstones of the Mauch Chunk Formation, extensive chemical leaching took place, enriching the deposit in alumina. During this sustained period of chemical purification, the clays were subjected to physical reworking. Alternative periods of oxidation and reduction caused by water-table fluctuations within the environment resulted in intermittent drying and shrinking of the deposit, especially near paleotopographic highs. These circumstances, combined with effects of minor en masse gravitational adjustments on paleotopographic slopes, eventually led to a considerable amount of fragmentation within the deposit.

The dark color and the presence of root traces and dispersed organic matter, in the clay, suggest that the environment was both reducing and capable of removing silica and alumina at the same time. Since it has been shown that organic complexing may dissolve silica and alumina, a swampy, coastal-plain environment with some local relief and periodic change in the water table might be the environment envisioned as illustrated in Figure 8.

The ability to predict the occurrence and properties of the Mercer high-alumina clay depends upon our capacity to relate these properties to features which are more easily observable. We have done this in the areas of good exposure of the clay and the following are the most useful exploration guides:

1. The Mercer high-alumina clay is everywhere underlain by a resistant, outcropping sandstone of distinctive mineralogy and physical appearance. In contrast to other Upper Paleozoic sandstones, this sandstone is a light-gray orthoquartzite with a kaolinite and chert cement and containing, in the upper 20 feet, rounded and pitted quartz and tourmaline. This sandstone formation lacks chlorite and low-rank metamorphic rock fragments, components which characterize almost all Mississippian and Pennsylvanian sandstones. Williams and Griffiths (1961) demonstrated that these characteristics statistically separate clay- from nonclay-bearing areas.

2. Distribution of the clay on a subregional scale is controlled by the presence of sandstones which either replace the clay or erode it. Such

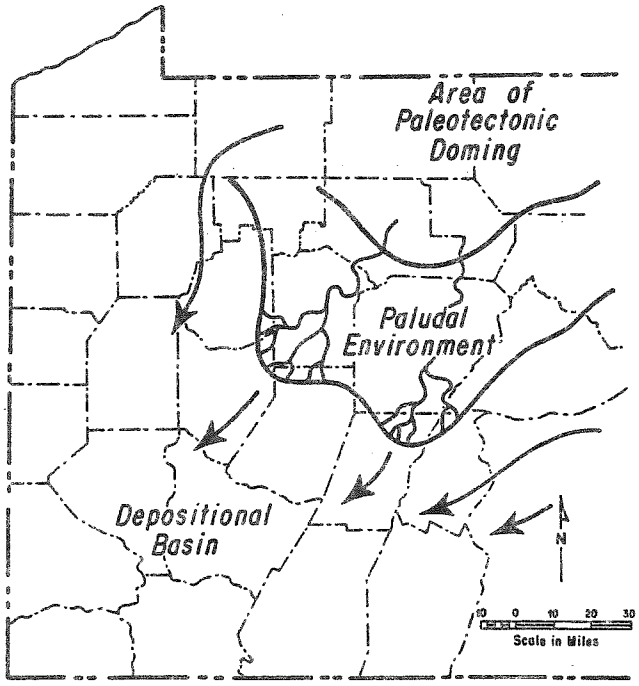

Figure 8. Proposed paleogeographic map of western Pennsylvania during the time of the formation of the Lower Mercer high-alumina clay. Arrows indicate avenues of detrital influx into the basin; high-alumina clay would occur in parts of the paludal area. Boundaries are approximate.

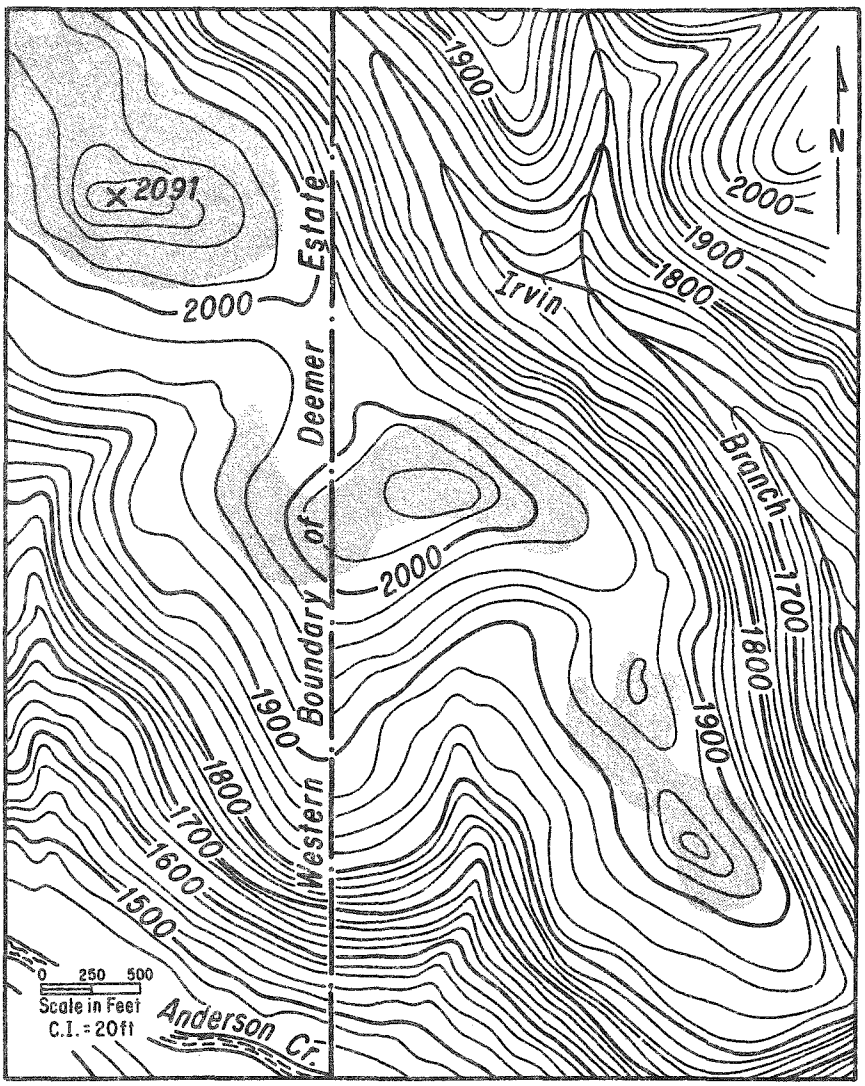

Figure 9. Relation between the present topography and the distribution of the Mercer high-alumina clay in a portion of the USGS 7.5-minute Elliott Park, Pennsylvania, quadrangle. The shaded pattern defines the area where the clay is present. The structural dip is to the southeast.

sandstones are typical low-rank graywackes, containing chlorite and abundant low-rank metamorphic rock fragments. Unlike the crossbed dip directions of the Mauch Chunk sandstones, which are mainly southwest, those in the graywackes are mainly northwest. Their presence below the Mercer coal means that the high-alumina clay is absent.

3. The nodule facies are most abundant in the vicinity of paleotopographic highs, although often the thickest nodule sections occur on the slopes near the higher areas, rather than directly over the summits. This is especially true on the more significant paleotopographic summits where the nodule facies may have been entirely removed by later erosion.

4. Usually both the size and percentage of nodules increase upward through the clay, although a deposit of flint clay often overlies the nodule facies.

5. In general, iron-bearing minerals are more prevalent in paleotopographic lows and also increase toward the bottom of the deposit.

6. In areas where the Mercer coals and associated rocks occur on the highest parts of hills, as is the case in anticlinal areas, the present topography may reflect the paleotopography which existed during and after the formation of the high-alumina clays, as illustrated in Figures 4 and 9. The reason for this association is that the high-alumina clay is more resistant than siltstones and shales which filled the adjacent paleotopographic lows, so that upon exposure to later Mesozoic and Cenozoic erosion, sediments in the low would be more easily removed. The resulting topography therefore represents exhumed, early Pennsylvanian topography.

Application of the above criteria to areas shown by Weitz and Bolger (1964) to be underlain by the Mercer coal leads us to believe that there are still relatively large quantities of flint and diaspore clay yet to be developed.

ORIGIN OF PLASTIC UNDERCLAYS

by
E. G. Williams and Philip Holbrook

Many of the shales, underclays, and coals of the Pottsville and lower and middle Allegheny of western Pennsylvania exhibit systematic mineralogical changes from basin margins to basin center; namely shales and underclays contain higher amounts of illite, chlorite, and pyrite in the basin center in contrast to the margins where kaolinite is more abundant, and pyrite and chlorite are low or absent. Coals show the same trends in addition to petrographic variation where vitrain is more abundant along basin margins. The causes of these regional facies changes in silicate mineralogy have been variously interpreted as due to differential settling, differential flocculation, different sources, authigenesis in marine and freshwater environments, diagenesis, and in the case of the underclays, weathering before, during, or after peat deposition. The main purpose of this paper is to make a regional analysis of a single underclay in order to establish the standard against which to compare other underclays. Accordingly, quantitative X-ray analyses of 70 sections of the Lower Kittanning underclay, taken at 1-foot intervals, were made. The sampling localities are shown in Figure 7 and the stratigraphic position in Figure 1.

The Lower Kittanning underclay can be grouped into four main classes as illustrated in Figure 2. Because chlorite is present in almost all Pennsylvanian sediments, its absence in underclays suggests weathering. Accordingly, we first grouped the clays into classes without chlorite and those containing this mineral in some part of the profile. Next, each of these groups was further subdivided based on whether a distinctive vertical sequence of minerals was present. As shown in the figure, four criteria were used to determine if in situ weathering had occurred; namely, an absence of chlorite in the upper part of the profile, a progressive increase in the kaolinite/illite ratio upward, an increase in vermiculite upward, and a decrease in mica basal spacing upward. The underclays without chlorite and exhibiting this vertical variation were interpreted to have formed in situ by pedogenic processes; those underclays without chlorite or a discernible vertical variation were thought to represent transported clays derived locally from the residual clays. Clays containing chlorite but lacking any vertical variation in mineralogy were thought to be unweathered. And lastly, those underclays containing chlorite and exhibiting some vertical variation were thought to have undergone some weathering but less than that experienced by class 1.

Figure 3 shows a typical example of a weathered profile and Figure 4 the corresponding X-ray patterns. Kaolinite-mica ratio increases exponentially upward and mica diminishes in thickness of basal spacing in the same direction; vermiculite increases in the upper part of the profile; and chlorite is absent through the entire section of clay. In contrast, Figure 5 illustrates a clay which shows no systematic variation in clay mineralogy but contains no chlorite, conditions we interpret to mean that the clay is a transported one whose source was an adjacent, deeply weathered soil.

Figure 6 shows the appearance of a typical chloritic underclay. The upper foot is plastic, light gray, rooted, and contains no chlorite. The lower portion of the profile is medium gray (N-4), hard, and has a laminated structure. Siderite nodules are present below the fifth foot. Here, as in most chloritic profiles, the mica is

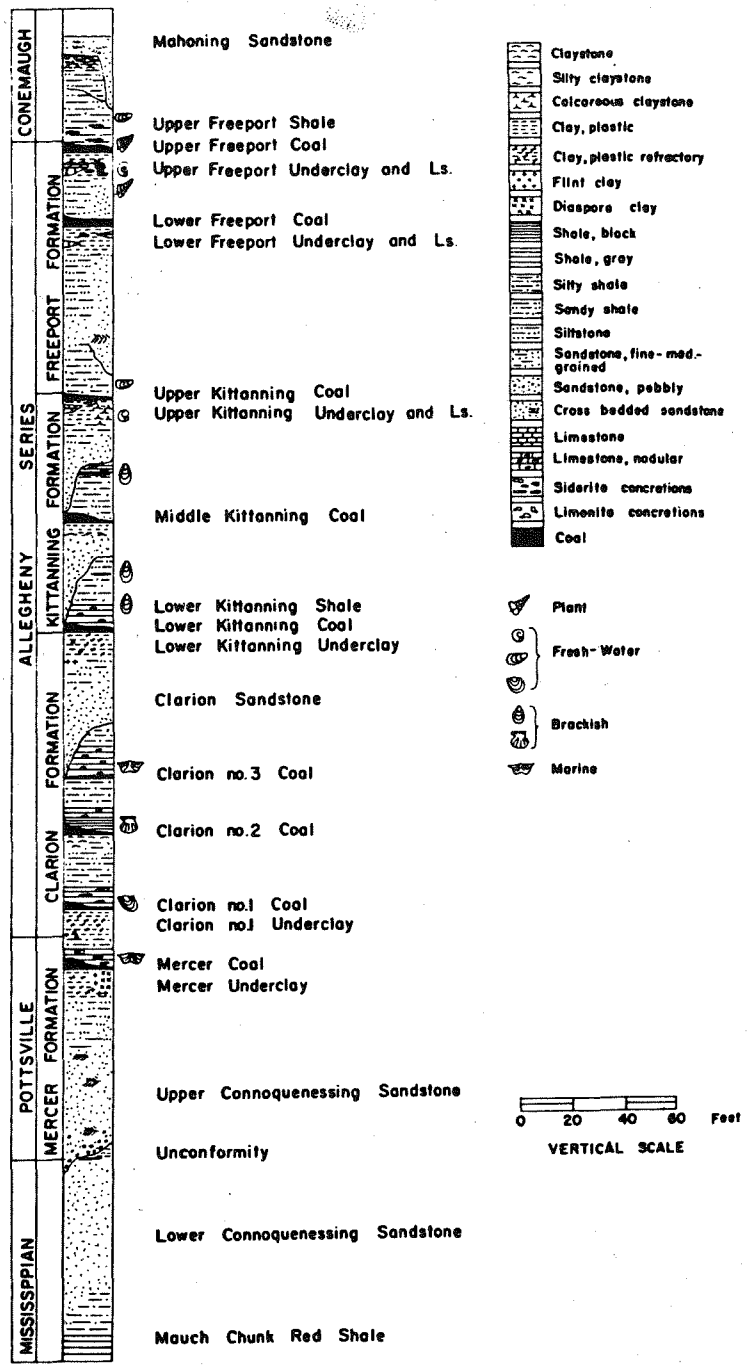

Figure 1. Stratigraphic column of the Pottsville and Allegheny Series in Clearfield County, from Williams, Bergenback, Falla, and Udagawa (1968).

better crystallized with sharper X-ray diffraction peaks and greater apparent mica thicknesses.

Table 1 summarizes the mineralogic properties of the four underclay categories classified in Figure 2. The parameters describe the average clay mineralogy of each category as well as parameters sensitive to weathering within profiles. The weathering ratio is the kaolinite/mica ratio of the top foot of a profile divided by the same ratio of the bottom foot. The mica-loss ratio is the cubed basal thickness of the mica in the bottom foot divided by the same value in the top foot. Both

78 MINERALOGIC PROFILES

PRESENCE OF CHLORITE IN SOME PORTION OF THE PROFILE

NO(57) — DECISION — YES(21)

WEATHERED

LITTLE OR NO WEATHERING

SYSTEMATIC VERTICAL VARIABILITY IN UPPERMOST 3 FEET

1. ABSENCE OF CHLORITE IN UPPER FEET OF A PROFILE.
2. STEADY INCREASE IN THE KAOLINITE/MICA RATIO TOWARD THE CLAY-COAL CONTACT.
3. INCREASE IN VERMICULITE TOWARD THE CLAY-COAL CONTACT.
4. DECREASE IN "APPARENT MICA" THICKNESS TOWARD THE CLAY-COAL CONTACT.

NO(31) — DECISION — YES (26)

NO (18) — DECISION — YES(3)

C WEATHERED TRANSPORTED SOIL

A DEEPLY WEATHERED SOIL

D UNWEATHERED BEDROCK

B SLIGHTLY WEATHERED SOIL

Figure 2. A classification of Lower Kittanning underclay profiles.

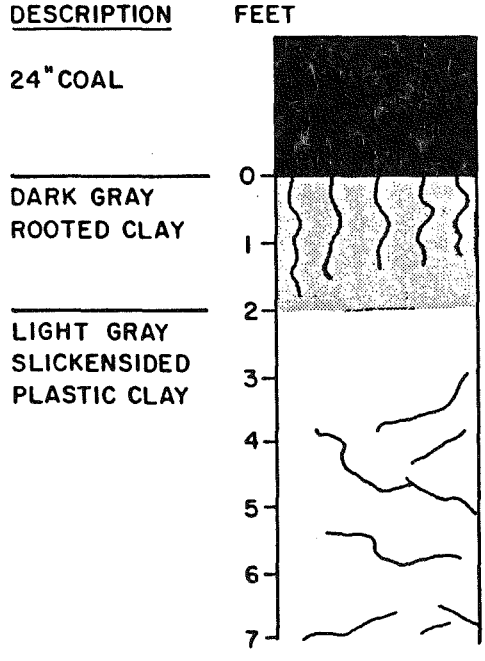

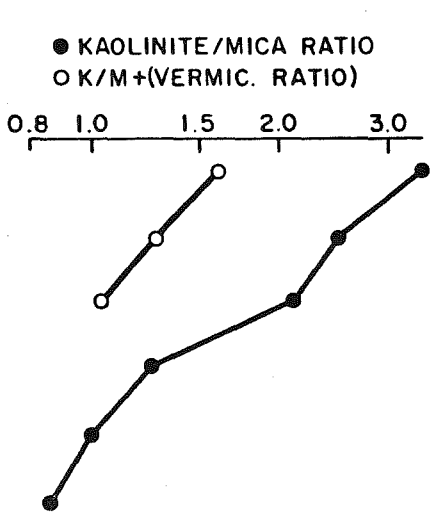

APPARENT MICA THICKNESS Å	PERCENT QUARTZ
96	19
88	32
145	30
156	33
178	32
156	39

Figure 3. Underclay profile characteristic of deeply weathered soil, class A on Figure 2.

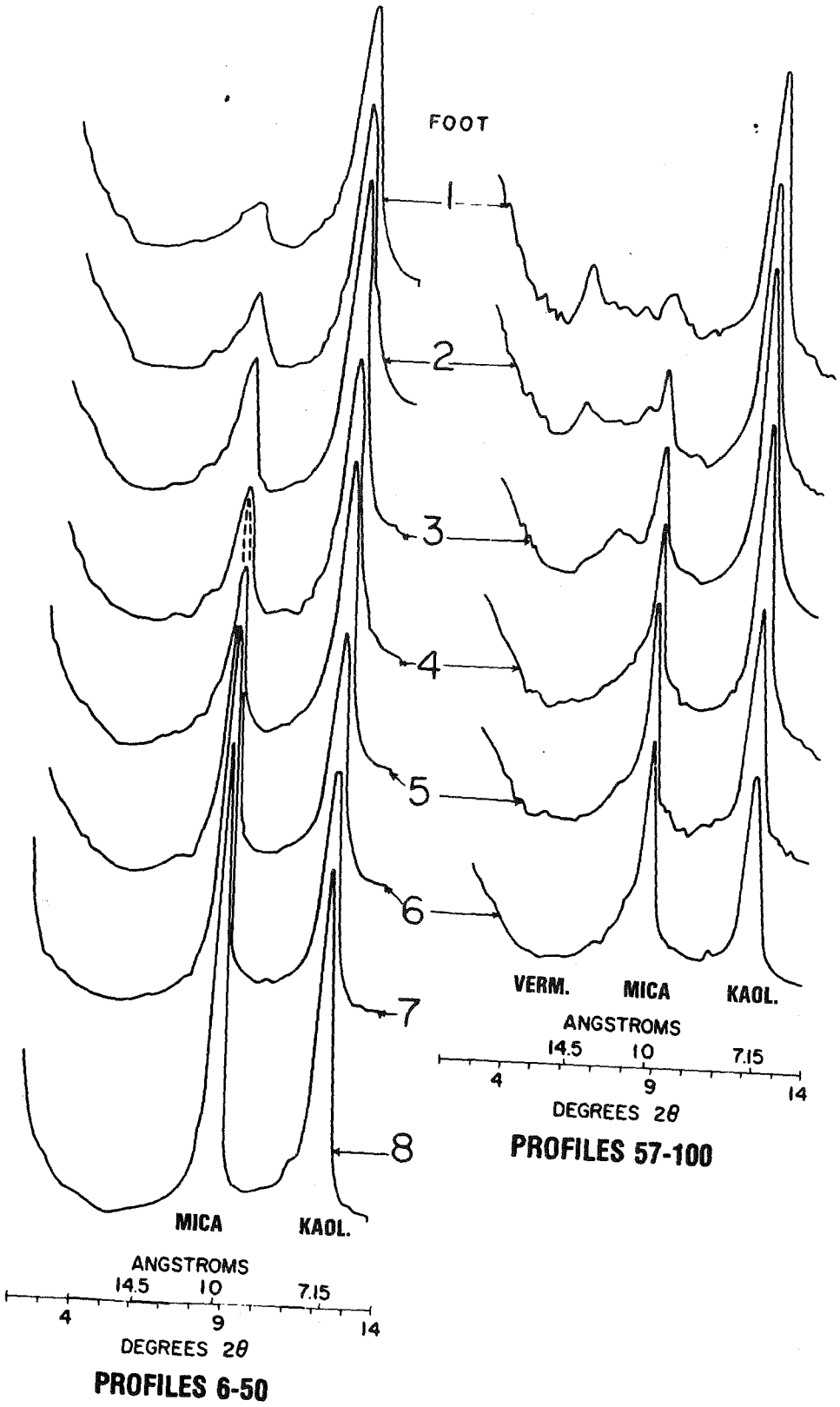

Figure 4. X-ray diffraction pattern of two deeply weathered underclay profiles.

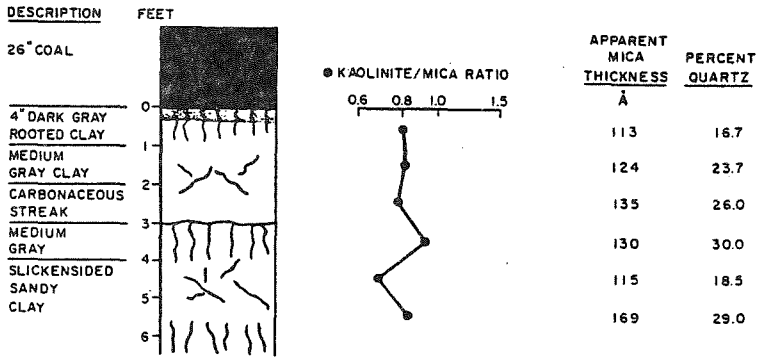

Figure 5. Underclay profile characteristic of weathered, transported clay or soil, class C on Figure 2.

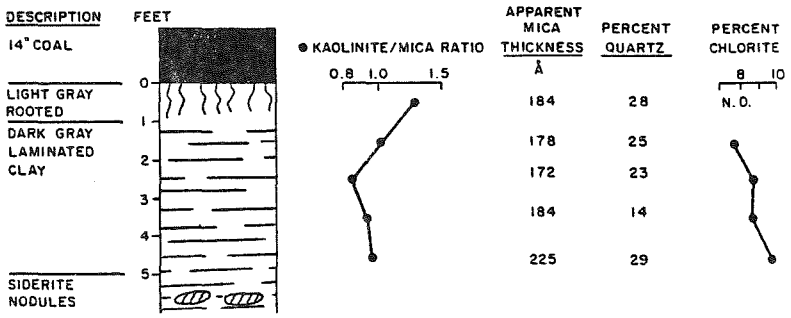

Figure 6. Underclay profile characteristic of unweathered bedrock, class D on Figure 2.

Table 1. Summary of the clay mineralogy of the various categories of the Lower Kittanning underclay and associated Allegheny shales.

Profile type	Average kaol./mica ratio	Average percentage of chlorite	Weathering ratio $\frac{K_T \times M_B}{K_B \times M_T}$	Mica-loss ratio $(TM_B)^3/(TM_T)^3$	Number of profiles
Deeply weathered soil (A)	1.39	0.0	2.29	6.66	26
Weathered transported soil (C)	1.27	0.0	1.16	3.03	31
Slightly weathered soil (B)	0.97	2.0	3.92	9.30	3
Unweathered bedrock (D)	0.61	7.5	1.41	4.28	18
Allegheny shales	0.56	8.3	--	--	9

ratios are designed so that a value of 1.0 means no vertical mineralogical gradient and therefore no evidence for weathering, a conclusion which assumes the clay-rich sediments were deposited without a vertical mineralogical gradient.

The foregoing analysis of vertical variability has shown fairly strong evidence for weathering. Two new parameters, weathering ratio and mica-loss ratio, were designed to document this vertical variability. These same parameters also permit

the study of areal variability. Where these parameters are areally related to each other and to paleotopography, weathering is a probable cause of some of the regional variability.

Contoured on Figure 7 is the average kaolinite/mica ratio for the Lower Kittanning underclay. Kaolinite/mica ratios are high along the northern basin margin, and also high in the folded Allegheny Mountain region to the southeast. Underclays that occur in the aforementioned basin axis have the lowest kaolinite/-mica ratio. Thus, there is a general correspondence between paleotopographic control as defined by Williams and Bragonier (1974) and average underclay mineralogy. It is suggested that kaolinite content is greater on paleotopographic highs because these sites have better soil drainage and are exposed for longer times. Also observe that the sections containing chlorite occur primarily in topographic and structural lows where the K/M ratio is less than 1, whereas flint clays (pure kaolinite) occur on topographic and structural highs where the K/M ratios generally exceed 1.50.

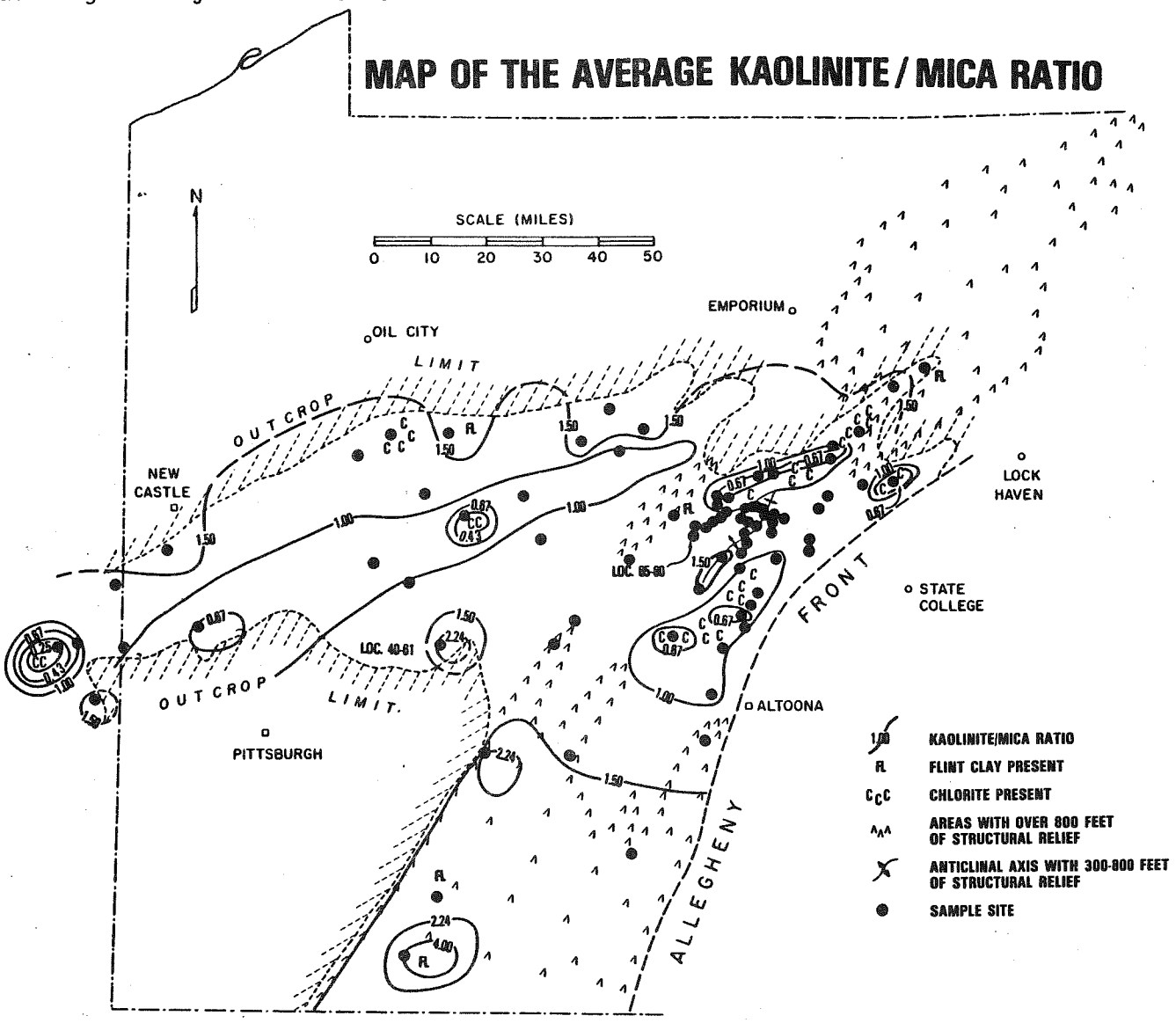

Figure 7. Map of the average kaolinite/mica ratio for the Lower Kittanning underclay, showing distributions of chlorite, flint clays, and major structural elements.

Figure 8 is a map of the weathering ratio of the Lower Kittanning plastic underclay. There is a great deal of similarity between this map and the average K/M map (Fig. 7). Weathering ratios are highest (>3.0) along the stable northern basin margin, and lowest in the basin axis where the 1.0 value indicates that no significant weathering has occurred. These different weathering ratios probably reflect different soil drainage conditions which can be inferred from paleotopography.

There is a striking contrast between the tectonically passive northern basin margin and the more deformed eastern basin margin. Average weathering ratios are much lower and more variable along the eastern margin, although most of the values are above 1.0, indicating that some weathering has occurred. Third-order paleotopography as well as sedimentary cut and fill probably controls much of this local variability. Our sampling is sufficient to demonstrate the aforementioned regional paleotopographic controls but not to demonstrate local paleotopographic ones.

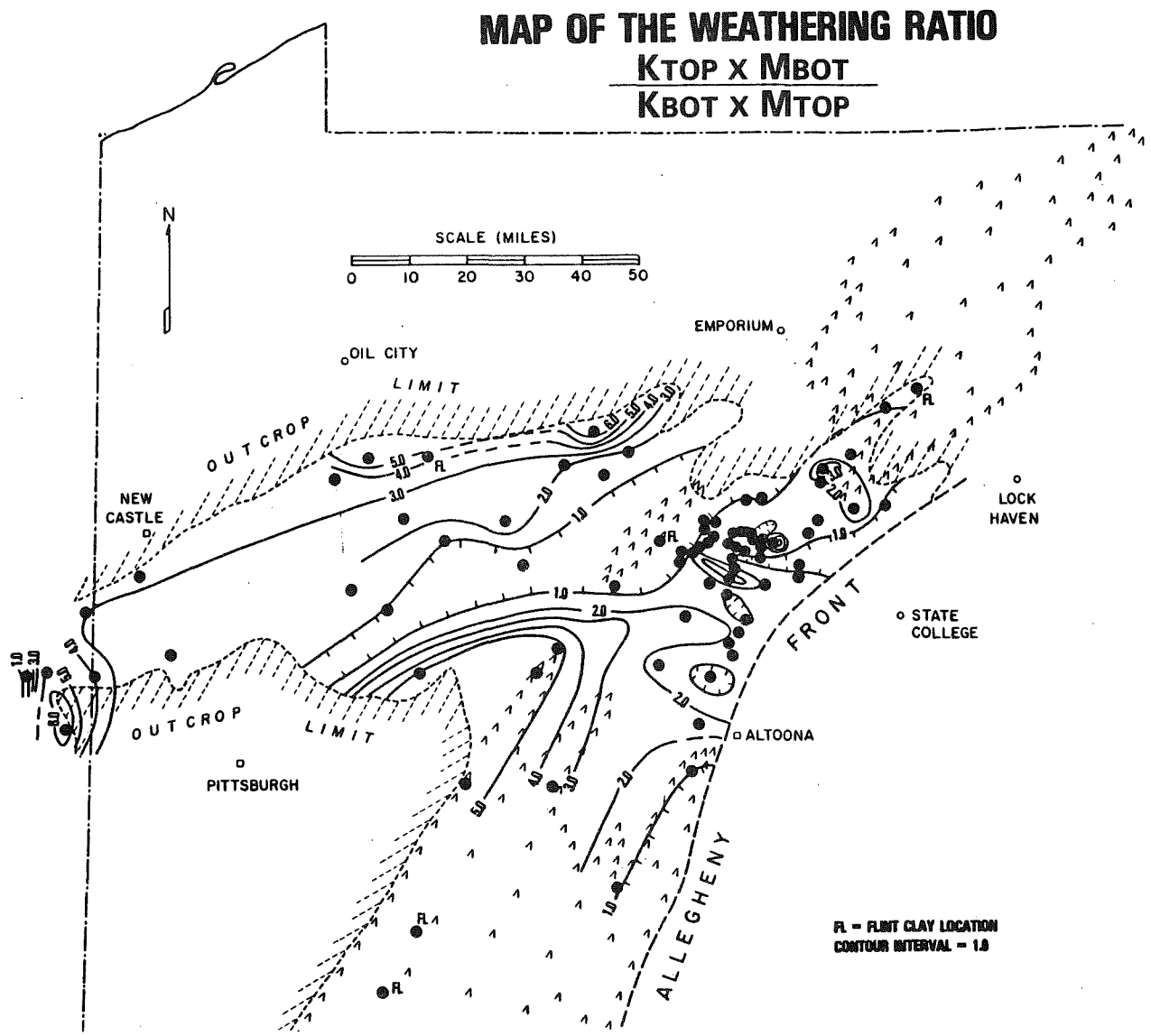

Figure 8. Map of the weathering-ratio index based on the kaolinite/mica ratio in the top foot of the underclay divided by the kaolinite/mica ratio in the bottom foot.

Figure 9 is a map of the mica-loss ratio. It is similar in many respects to the weathering-ratio map (Fig. 8) and the average kaolinite/mica ratio map (Fig. 7). The variability of this parameter can also be related to paleotopography. The sample locations along the northern basin margin generally have high mica-loss ratios (above 5.0), whereas the lowest ratios are in the basin axis. Values near 1.0 indicate negligible mica loss.

As in Figures 7 and 8, the mica-loss ratios are lower and more variable along the eastern basin margin. The Allegheny Mountain region to the south has high mica-loss ratios (above 5.0), suggesting a strong second-order paleotopographic control. This region also has a relatively high K/M ratio as shown in Figure 7.

The determination of the exact amount of weathering would depend on estimation of the regional variability of unweathered parent material of the underclay. Williams and others (1974) have studied such variations in the shales and siltstones above the Lower Kittanning coal, rocks which vary from marine to fresh water from

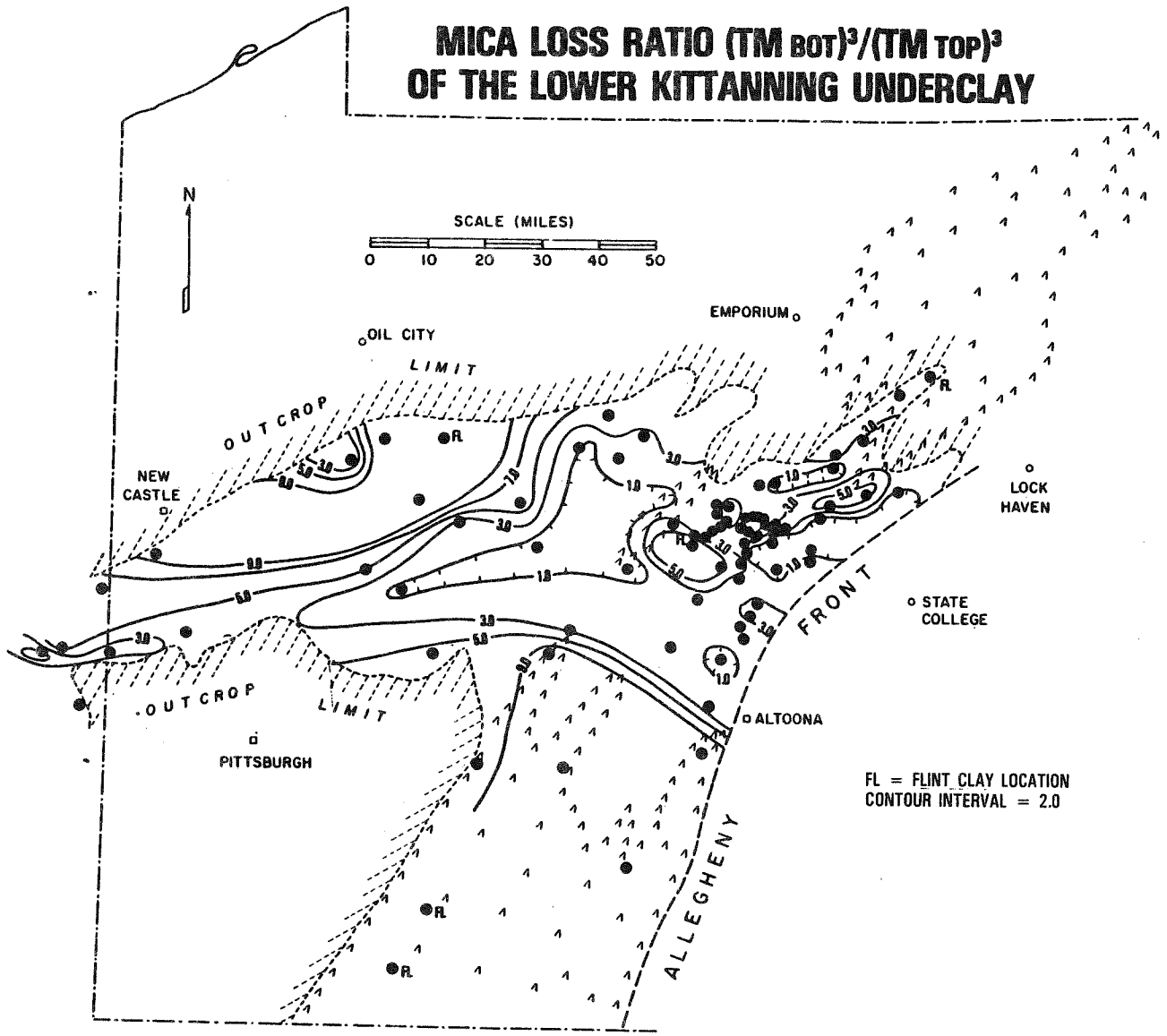

Figure 9. Map of the mica-loss ratio, based on the volume of mica in the top foot divided by the volume of mica in the bottom foot.

basin axis to margins, and which we believe would approximate the composition of parent material for any of the lower Pennsylvanian underclays. The kaolinite/illite ratios for the shale vary from 0.20 in the basin center to 0.50 along the northern and eastern margins. Williams and others (1974) believed such variation was probably produced by selective size sorting or differential flocculation. Corresponding values for the Lower Kittanning underclay are 0.43 and 1.50, respectively. Thus, approximately 30 percent of the regional variation in the underclay could have been inherited from the parent sediments. Furthermore, compared to the shale, the kaolinite/illite ratio has been increased in the underclay by a factor of 2 in the basin center and by 3 at the margins, a condition which supports the differential-weathering theory developed from the weathering and mica-loss maps. Figure 10 illustrates the relations in graphic form between underclays and shales from which they were derived. The form of the underclay curve resembles that of the shale. Williams, Bergenback, Falla, and Udagawa (1968) concluded that the variation in the clay mineralogy of the shale is caused by differential settling or differential flocculation of kaolinite in the nearshore environment, thus accounting for the lower mica/kaolinite ratio at the margin of the bituminous coal basin. The difference between the shale and the underclay, which is greatest at the elevated basin margin, we believe has been produced by in situ weathering. The remainder of the regional variation in the underclay is produced by inheritance of the mineralogy from the underlying shales and sandstones.

Of great significance to the theories of underclay genesis is the length of time required to form underclays. An attempt has been made to estimate this duration by comparing the potassium loss between the top and bottom feet of the underclay with corresponding values from accurately dated Wisconsinan tills, where Hensel and White (1958) found an average loss of 0.1 percent K_2O per thousand years. Table 2 gives the estimates for the sections that showed evidence of weathering.

Despite the evidence for strong weathering in many sections, the underclays do not exhibit the marked zonation of modern well-drained soils, which led McMillan (1956) to interpret them as analogues of modern gleys, which are gray, poorly drained soils. Because the gleying process involves mainly the removal of iron

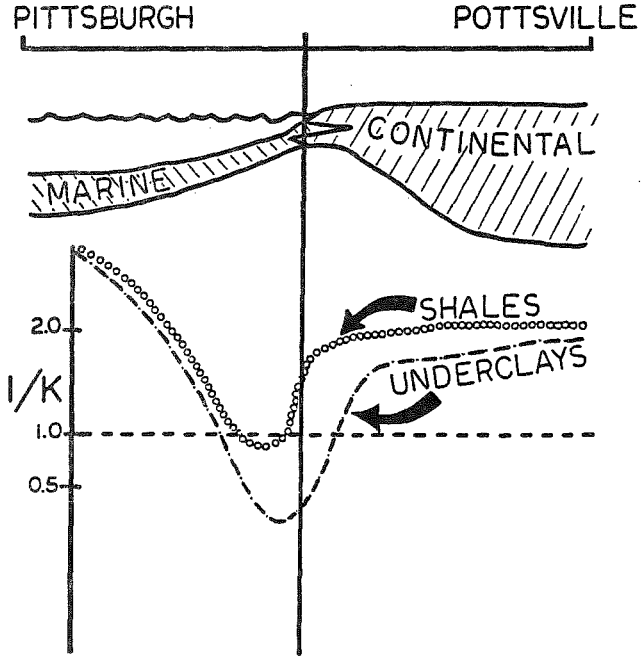

Figure 10. Graph showing the regional variation in clay mineralogy of the Lower Kittanning underclay and associated shale and its relation to the position of marine and continental sedimentation (modified from Williams and Oldham, 1977).

Table 2. Estimated ages of the various weathered profiles of the Lower Kittanning underclay as determined by potassium oxide loss.

Location	Percentage K_2O		Difference	Estimated age of profile	Depth of foot immediately below weathered zone
	Foot below	Top foot			
4-59	5.20	(2.22+0.33)	2.65	26,500	4
6-50	5.13	1.54	3.59	35,900	6
7-69	4.70	2.90	1.80	18,000	2
9-58	5.04	3.50	1.54	15,400	3
13-75	4.45	(1.88+0.18)	2.30	23,900	3
32-91	4.52	2.39	2.13	21,300	2
35-95	5.38	2.05	3.33	33,300	3
39-85	4.70	2.82	1.88	18,800	5
45-43	2.82	(1.37+0.18)	1.27	12,700	4
45-81	5.22	(1.63+0.18)	3.41	34,100	5
48-85	4.87	3.16	1.71	17,100	2
50-79	4.10	3.08	1.02	10,200	3
52-62	4.10	(1.46+0.15)	2.49	24,900	3
53-65	3.59	(1.62+0.21)	1.16	17,600	4
57-100	4.65	(1.11+0.80)	2.74	27,400	6
58-93	4.71	(3.50+0.33)	0.88	8,800	4
66-81	3.93	2.99	0.94	9,400	2
67-46	4.86	(1.79+0.33)	2.74	27,400	3
68-53	4.95	2.90	2.05	20,500	3
68-77	4.18	(2.48+0.21)	1.49	14,900	3
69-84	5.30	4.86	0.46	4,600	5
70-75	4.61	(3.50+0.21)	1.49	14,900	3
71-65	5.45	(2.82+0.42)	2.21	22,100	3
73-82	4.78	3.42	1.36	13,600	3
77-78	4.44	3.59	0.85	8,500	3
79-88	4.52	3.59	0.93	9,300	4
79-96	4.86	(2.48+0.09)	2.20	22,900	5
82-90	4.35	2.39	1.96	19,600	3
85-106	4.27	2.82	1.45	14,500	3
AVERAGE			2.04	20,400	3.5

under reducing conditions, it does not seem likely that it can account for the strong mineralogical gradient observed in some of the underclays. Accordingly, we envision a two-stage process of underclay formation similar to that initially proposed by Williams and others (1965); namely, a well-drained phase of podzolization followed by the poorly drained gleying process, the former occurring during times of highest relief produced by either tectonic or sea-level lowering, the latter during the period of lowest relief when peat swamps transgressed across the region of low relief. The gleying process would remove the iron oxide zonation produced during the phase of podzolization.

In addition to vertical and lateral variation within particular underclays, there also occurs variation between underclays, the most notable examples being the

contrast between the lower and upper Allegheny along the basin margins in the eastern part of the Plateau. In contrast to the highly weathered, noncalcareous, kaolinitic underclays of the lower Allegheny, the upper Allegheny clays are largely unweathered, illitic, and calcareous. Figure 11 shows typical examples of the Upper Freeport underclay, which shows a characteristic increase in the illite/kaolinite ratios toward the top of the bed whereas in the last foot or so there is a marked increase in kaolinite. Beds and lenses of limestone occur throughout the lower and middle parts of the clay. The presence of limestone, the relatively high illite content, and the fact that the illite is a low-temperature variety which increases upward, are all interpreted to mean that the illite formed in alkaline lakes undergoing high rates of evaporation during the dry season of a monsoonal climate. During the wet season, the lacustrine clays would be leached of carbonate in the upper part. But considering the whole deposit, pedogenic processes would be inhibited by the relatively large amount of limestone and calcareous clay. Only in the upper foot or so, where the carbonate was leached, was illite altered to kaolinite. Here the rate of kaolinite increase is as great as that exhibited by the lower Allegheny clays over a much greater thickness interval, suggesting that the Freeport clay may have experienced a comparable period of exposure.

In order to determine the extent of weathering in the center of the basin compared to the margin, vertical mineralogical and chemical profiles were made on six underclays selected to encompass the entire Pennsylvanian and range of paleoenvironments. The Waynesburg, Pittsburgh, and Upper Freeport underclays all occur in sections containing beds of nonmarine origin, whereas the Upper Mercer, Lower Clarion, and Middle Clarion underclays are associated with marine shales and limestones. Table 3 summarizes the results of this analysis and Figure 12 shows the clay profiles. In addition to the mineralogical criteria for weathering applied in the Lower Kittanning study, a set of chemical criteria is also presented. The presence of chlorite in some part of all the profiles, and the fact that all but one of the underclays show no increase in the illite/kaolinite ratios, suggests that these clays are less weathered than the Lower Kittanning along the basin margins. However, the Allegheny underclays exhibit most of the chemical criteria for moderate weathering. Thus, although the lower and middle Allegheny clays are characterized by extensive weathering along basin margins, there is evidence to suggest that some, but lesser, weathering has taken place in the basin center. Conemaugh and Monongahela rocks have been eroded along the basin margins so nothing is known about the soil-forming processes in these regions. However, based on the similarities of the underclays to the Allegheny and Pottsville clays, we surmise that the regional pattern of the former might have been similar to that of the latter.

Recent work by Busch and Rollins (1984) concludes that the interval between coals in the Pennsylvanian of the Appalachian coal basin represents a transgressive-regressive cycle produced by glacial sea-level changes over a 400,000-year period. Critical to such a theory would be the occurrence of a major disconformity within the sequence. Estimates of the times required to deposit the sediments of a single coal-measure cycle are based on the sedimentation rates of Sadler (1981) and are in the range of 20,000 to 40,000 years. The difference of approximately 350,000 years must either be accounted for by distributing it among numerous bedding planes or assigning it to a single surface of erosion or nondeposition. We believe that the weathered, residual underclays and their correlated erosion surfaces beneath some sandstones might represent this single surface. Our estimates of the average and maximum length of time of underclay formation of 20,000 and 40,000 years, respectively, are much smaller than the postulated time interval. However, it is possible that the erosional hiatus between coal and underclay is much longer than these

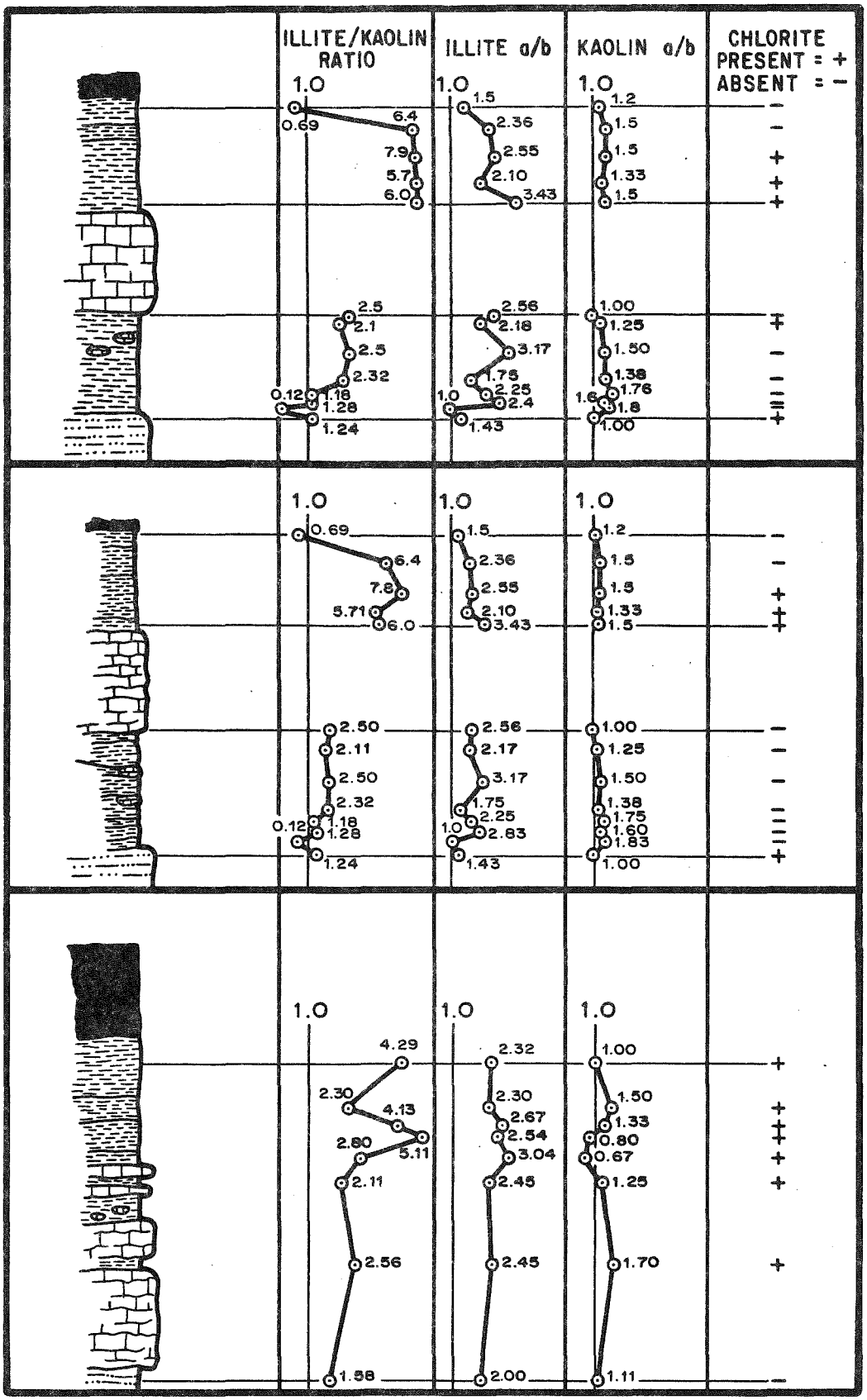

Figure 11. Clay mineral profiles of three typical Upper Freeport underclays. a/b is a measure of the degree of asymmetry of the clay mineral peaks, a value of 1 meaning perfect symmetry.

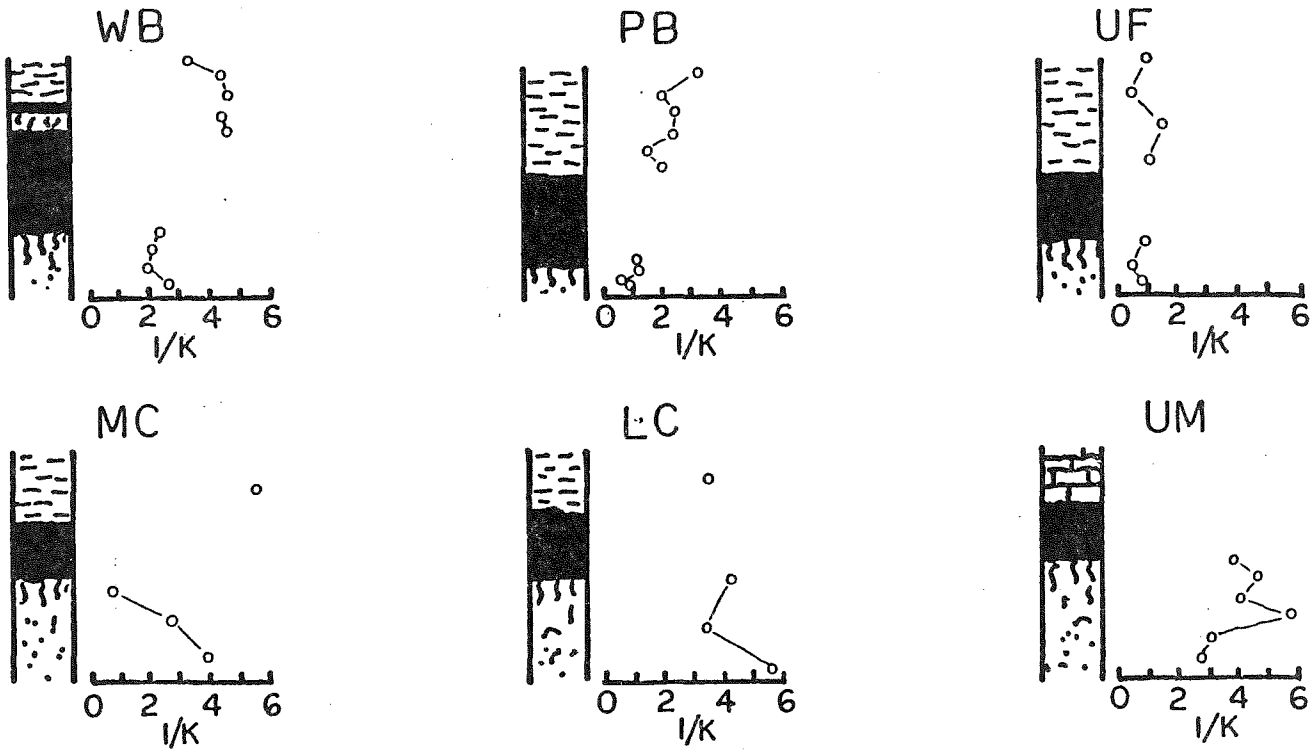

Figure 12. Clay mineral profiles of underclays and shales from selected sequences in the Pittsburgh area. Vertical distances not to scale. WB - Waynesburg, PB - Pittsburgh, UF - Upper Freeport, MC - Middle Clarion, LC - Lower Clarion, UM - Upper Mercer (from Oldham, 1979).

Table 3. Criteria used to determine the degree of weathering undergone by underclays from the Pittsburgh area (from Oldham, 1979).

	Criterion	WB	PB	UF	MC	LC	UM
MINERALOGICAL	Presence of chlorite	X	-	X	X	X	X
	No chlorite at top	X	X	-	X	X	-
	Decrease in I/K upward	-	-	-	X	-	-
	Increase in vermiculite upward	X	-	X	-	-	X
	Decrease in mica thickness upward	X	-	X	X	X	X
	Decrease in kaolinite thickness upward	X	-	X	X	X	X
	Decrease in quartz upward	-	-	X	X	-	-
CHEMICAL	Increase in Al_2O_3 upward	X	?	X	X	-	X
	Increase in TiO_2 upward	X	?	X	X	-	X
	Decrease in Fe_2O_3 upward	X	?	X	X	X	X
	Decrease in MgO upward	X	?	X	X	X	X
	Decrease in CaO upward	-	?	X	-	X	X
	Decrease in K_2O upward	-	?	-	X	X	X
	Decrease in MnO upward	-	?	X	X	X	X

X.....Present
-.....Absent
?.....Not available

WB.....Waynesburg
PB.....Pittsburgh
UF.....Upper Freeport

MC.....Middle Clarion
LC.....Lower Clarion
UM.....Upper Mercer

values. Williams and others (1965) have shown that in some areas in western Pennsylvania the hiatus between coal and underclay is represented by at least 35 feet of sediment, the removal of which on lower delta plains might require a relatively long time. The estimate of 200,000 years for the formation of the underclays made by Weller (1930) does not, therefore, seem excessive. However, even if this longer estimate is not deemed realistic, the shorter ones would seem to create some difficulties for the theories which produce coal-measure cycles by periodic, lateral migration or switching of delta lobes, similar to that proposed by Ferm (1970) using the Mississippi delta as an example. In that delta complex, subdelta migration occurs every 500 to 1000 years, which would not be sufficient time to develop the thickness or mineralogy of the type of inferred soils observed in the coal fields. Therefore, we conclude that the coal-measure cycles are caused by more regional tectonic and eustatic factors.

THE DISTRIBUTION OF SULFUR AND CARBONATE MINERALS IN PENNSYLVANIAN ROCKS AND THEIR SIGNIFICANCE IN PREDICTING ACID MINE DRAINAGE

by
E. G. Williams, A. W. Rose, S. A. Waters, and J. Morrison

It is probably not surprising that research on Pennsylvanian rocks has discovered that the principal factors governing the production of acid mine drainage are the amounts and types of sulfur, especially pyrite, and the amounts and types of carbonates, especially calcite. The purpose of this report and the associated field trip is to demonstrate that the abundance of these elements and minerals is closely related to specific rock types and inferred paleoenvironments. Because the latter have been accurately mapped in western Pennsylvania and other areas in eastern and central United States, estimates of pre-mining acid mine drainage can be made by comparison to laboratory and controlled field experiments.

The first attempt in western Pennsylvania to relate sulfur to specific rock types and paleoenvironments was made by Williams and Keith (1963), who concluded that coals overlain by marine shales or limestones were higher in sulfur than coals of the same age overlain by freshwater beds, a condition attributed to the higher content of sulfur in sea water. Reidenouer and others (1967) studied the controls of local paleogeography on sulfur distribution in coals, and found that sulfur and the amount and types of clay minerals, as well as coal petrography, were correlated; high sulfur was found with dull coals containing the highest illite/kaolinite ratios, whereas the lowest sulfur values occurred with brighter coals having the highest kaolinite amounts. Generally, the highest sulfur occurred in paleogeographic lows.

These results were explained assuming that the distribution of sulfur in the form of pyrite was controlled by the presence of iron which was brought into the swamp in oxidized form attached to detrital illite. Upon encountering the reducing environment in the coal swamp, the ferric iron was reduced to soluble ferrous iron, part of which migrated into the peat, where it reacted with sulfide formed by sulfate-reducing bacteria, to form pyrite. This action occurred preferentially in topographic lows where detrital clay was most abundant, presumably carried into the swamp during periods of higher water, a time when the peat was undergoing some oxidation, thus explaining the association of the high sulfur and dull coal. During periods of quiet water in the swamp, pH and Eh conditions were lower, favoring the formation of kaolinite, and brighter coal with lower sulfur compositions, which also were favored in paleotopographic lows. Dull coals, which occupied the adjacent highs, were lower in sulfur because they lacked the detrital clay component. Reidenouer and others (1967) concluded that the distribution of pyrite in coal was controlled by the pH and Eh of the swamp environment, and the concentration of sulfur and iron, all of which were related to rates of water movement, depth of water, and water chemistry, factors which themselves are dependent upon paleogeography.

The first detailed study of the distribution of sulfur in the detrital rocks and inferred paleogeographies of the intervals between coals in western Pennsylvania was made by Guber (1972). He found that Lingula-bearing shales deposited in brackish conditions contained the highest amounts of sulfur (greater than 1.5 percent), whereas marine and fresh shales and siltstones were low in sulfur. Guber

explained these relations by showing that brackish-water environments would contain high concentrations of both sulfate and iron under reducing conditions, the situation most favorable for the production of pyrite. Guber and others (1971) made the first controlled field study of acid mine drainage in western Pennsylvania, the main results of which are shown in Table 1. Strip mines containing only nonmarine overburden, such as the Freeport, produced no acid mine drainage; mines containing brackish-water shales, such as the Kittanning and Clarion, produced large amounts of acidity, sulfate, and iron. Most interesting is the fact that the method of backfilling seems to have little effect on acid mine drainage abatement, a fact

Table 1. Chemistry of effluent from strip mines, according to coal seam and method of reclamation of spoil (after Guber and others, 1971).

	1 Contour backfilled	2 Normal backfilled	3 Untouched
Freeport 1	pH = 6.57 Ta = 10.69 Fe = 1.27 Al = 0.36 Ca = 37.64 Su = 599.8 N = 11	pH = 6.24 Ta = 7.54 Fe = 0.81 Al = 0.40 Ca = 29.10 Su = 275.5 N = 10	pH = 6.97 Ta = 5.80 Fe = 1.12 Al = 0.0 Ca = 17.67 Su = 119.7 N = 3
Kittanning 2	pH = 4.65 Ta = 153.6 Fe = 2.28 Al = 21.47 Ca = 39.64 Su = 1075.7 N = 11	pH = 3.94 Ta = 141.3 Fe = 10.53 Al = 19.86 Ca = 42.67 Su = 878.4 N = 18	pH = 3.38 Ta = 970.9 Fe = 297.4 Al = 83.20 Ca = 40.60 Su = 1766.6 N = 5
Clarion 3	pH = 3.20 Ta = 156.7 Fe = 2.16 Al = 28.00 Ca = 50.00 Su = 1385.00 N = 1	pH = 3.52 Ta = 340.5 Fe = 20.95 Al = 56.20 Ca = 24.82 Su = 1111.0 N = 5	pH = 4.35 Ta = 79.46 Fe = 7.05 Al = 7.40 Ca = 13.88 Su = 365.5 N = 4

All units except pH in parts per million

Ta = titratable acidity
Su = sulfate
N = no. of observations in cell

1) Land restored to original topographic contour
2) Coal covered within five feet of spoil
3) No backfilling; coal exposed

which can be explained by the occurrence of high sulfur in brackish shales whose stratigraphic position is directly above the coal, and would therefore occupy the surface of most spoil piles; that is, the sequence in spoil banks would be reversed from the normal stratigraphic sequence above coal beds. As shown in Table 1, backfilling the Clarion coal mines actually produced more acidity, probably as the result of increasing the total surface area of the exposed brackish shale. Another important conclusion which can be drawn from the table is that the coals are unlikely to be important acid producers even though they may contain more sulfur than associated shales. This is evident in the Freeport mines where the acid production of mines not backfilled does not differ from those that have been backfilled.

Caruccio (1967) was the first to attempt to relate quantitatively sulfur amounts and types to the production of acidity. In laboratory leaching tests of coals associated with both marine and nonmarine rocks, Caruccio found that acidity was related to the type rather than the amount of pyrite, the greatest amount being produced by coals containing framboidal forms, whose surface areas are much greater than coarse-grained euhedral forms. Hornberger and others (1981), although confirming the relation between framboidal pyrite and coals associated with marine beds, were unable to demonstrate any relation between framboids and acidity, either in the field or laboratory. Waters (1981) and Williams and others (1982), in addition to confirming Guber's conclusion that brackish shales contained the highest amounts of pyritic sulfur, demonstrated that the relation between sulfur and acidity was an exponential one, with a dividing point between 1.0 and 1.5 percent sulfur. Brackish and marine shales generally plotted above this point, and all nonmarine shales and all sandstones (except one), siltstones, and limestones below this value. As shown in Figure 1, most brackish shales and coals produce maximum 1-week acidities in excess of 100 mg/l $CaCO_3$/100 g in the laboratory test used and all freshwater samples less than this as do the marine samples. The low values for the marine samples are explained by the presence of small amounts of calcite which are absent in the coals and brackish shales.

The laboratory results were tested in a set of field experiments, the results of which are illustrated in Figures 2, 3, and 4. As predicted, drainage from mines in brackish shales has the highest average acidity (section 2) and nonmarine shales (section 6) the lowest. Sections with limestone beds (1 and 3) had low acid but high sulfate, indicating that acid had been produced but was subsequently neutralized by the limestone. The acidity values in sections 4 and 5 were not predicted by the laboratory experiments, since the sandstones had low sulfur and produced little acid. Our explanation is that the greater porosity of these rocks permits greater rates of oxidation of the pyrite, which, if extended over a relatively large volume of sandstone, might produce larger amounts of acidity even though the total volume of pyrite is small. Another important feature exhibited by section 6, Figure 4, is that the sulfate contents are low in comparison to the other sections, which means that the low acidity in the section cannot be explained by neutralization but by the fact that insufficient pyrite is being oxidized upon exposure to the atmosphere. As shown in Figure 1, very little acidity was produced in the laboratory when sulfur values were below 1.0 percent sulfur.

In addition to the controlled field experiments, 40 mines, representing a wide range of geologic, hydrologic, and mining factors and conditions, were studied. Each mine was classified according to lithologic criteria, and the pH of water flowing from the mines was measured. The results are summarized in Table 2, which generally confirms the laboratory and controlled field experiments. All mines

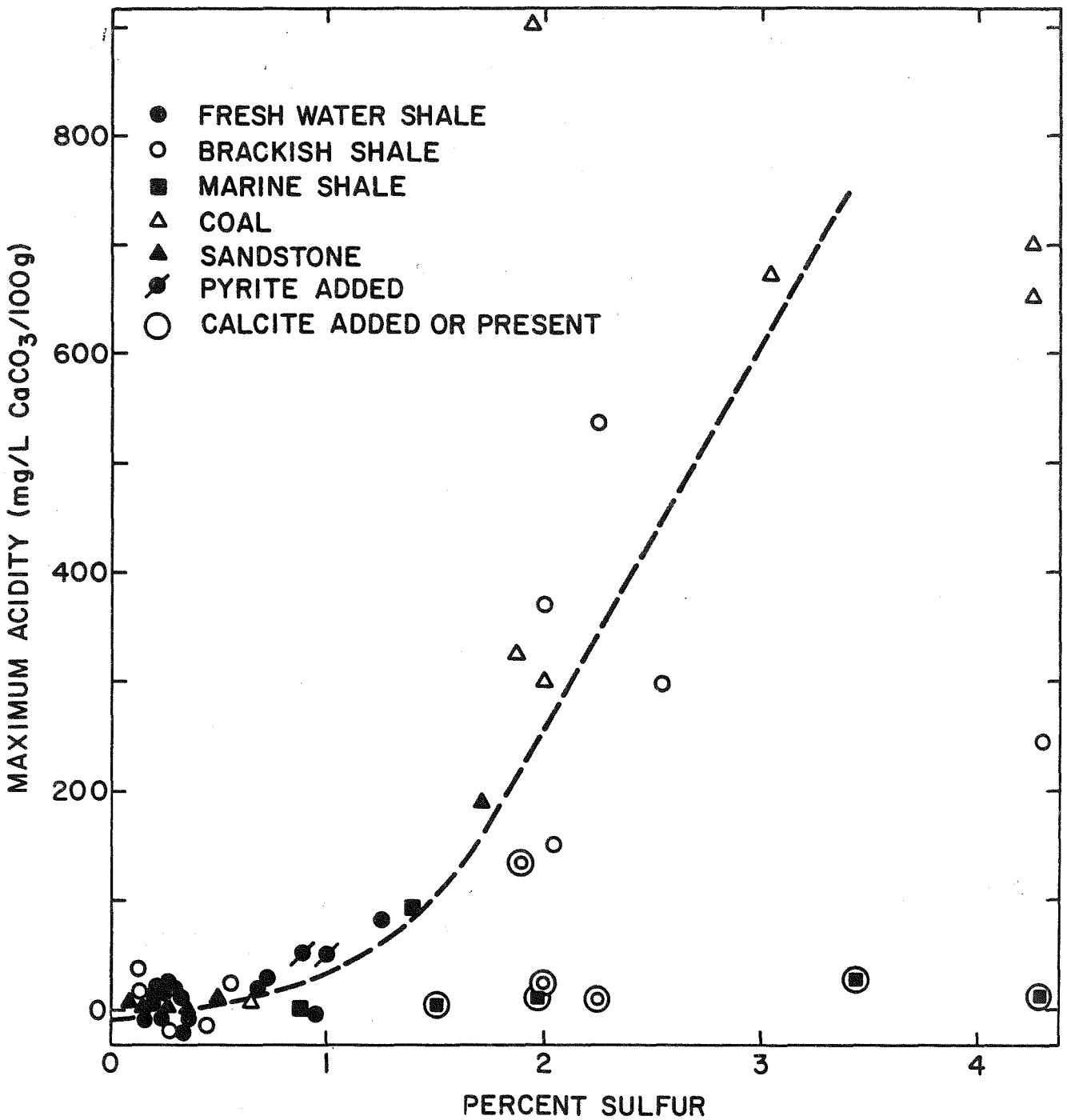

Figure 1. Graph illustrating the exponential rise in acidity with increasing total sulfur.

containing brackish or marine shales or both, but lacking $CaCO_3$ present in the highwall (a total of nine mines), produced acid mine drainage in amounts sufficient to be classified as bad (pH <4.5). Of the eight mines containing marine shale and observable $CaCO_3$ in the highwall, only one was classified as an acid producer. Of 12 mines containing both freshwater shales and channel sandstones but lacking calcite, all but one was classified as an acid producer, a condition predicted from the controlled field experiments. The four mines with only freshwater shales but no sandstone produced little acid.

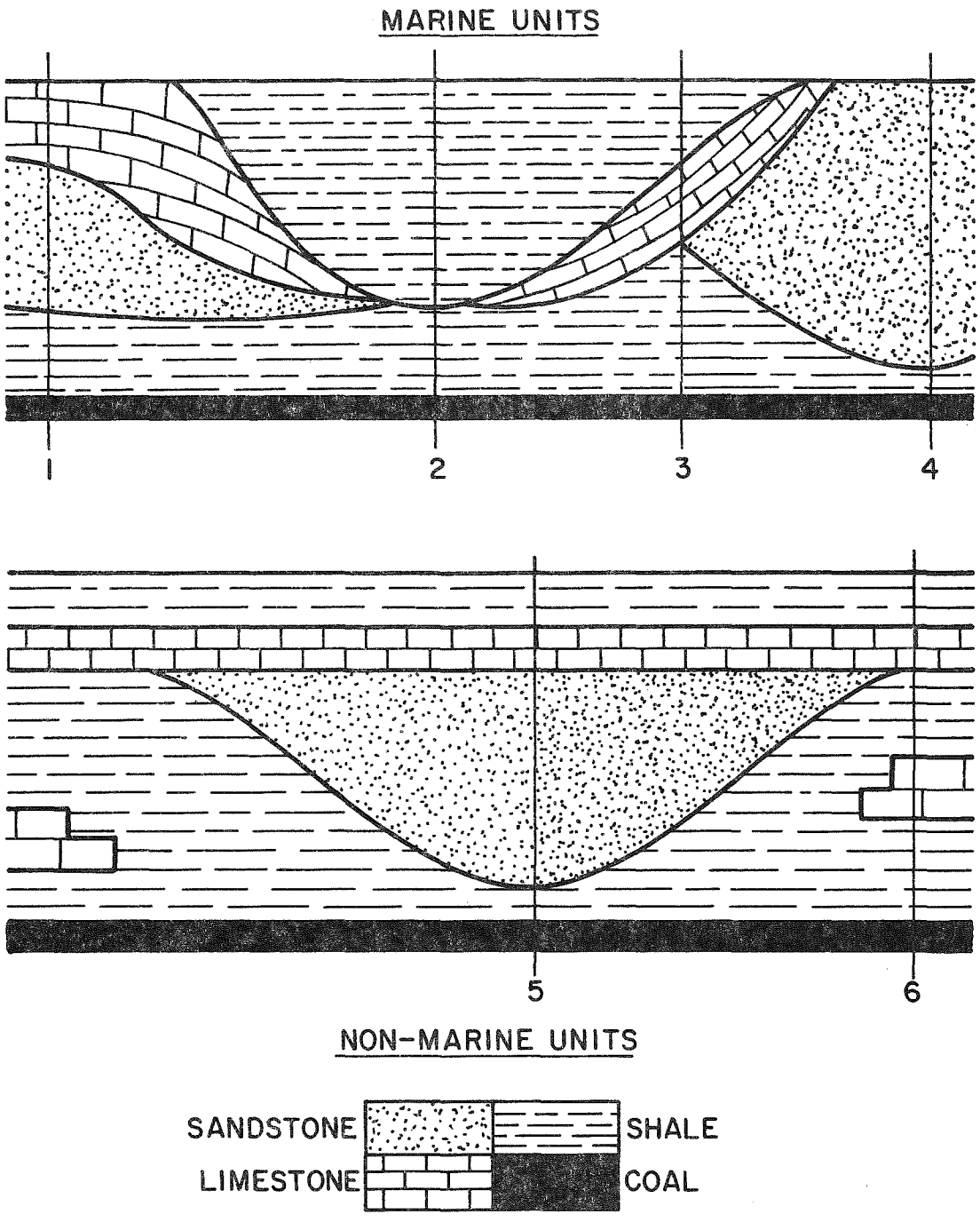

Figure 2. Schematic diagram representing the maximum variation in lithofacies characteristics of the lower and middle Allegheny Series in western Pennsylvania. Each of the localities represents a mine or group of mines which were chemically monitored.

Based on all of our experiments and field observations, we conclude that the amount of sulfur, the amount of $CaCO_3$, and the presence of channel sandstones are the three most important factors in producing acid mine drainage. Other factors involving aspects of mining and hydrology did not seem to be major factors since we examined a wide range of them and the geological factors were in almost all cases still plainly evident. Since the geological factors are well known, that is, they have been mapped over large areas of the Appalachian Basin, pre-mining prediction of the acid problems can be made, the accuracy of which depends on the accuracy of the estimated mineralogy, petrology, and geochemistry of the mapped units. We have

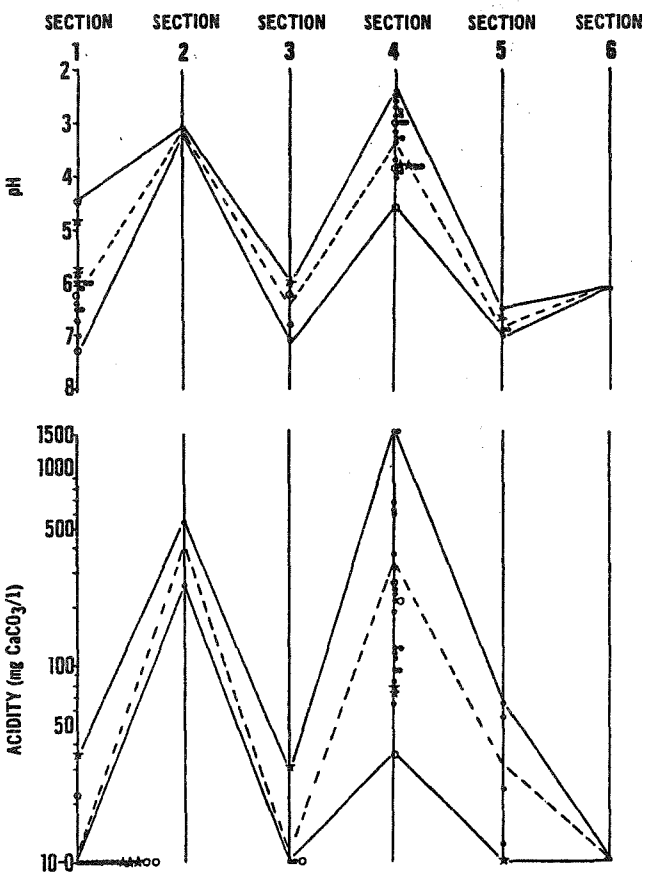

Figure 3. Graphs of acidity and pH for the various localities shown in Figure 2. Dotted line connects the mean values; solid lines connect the upper and lower ranges.

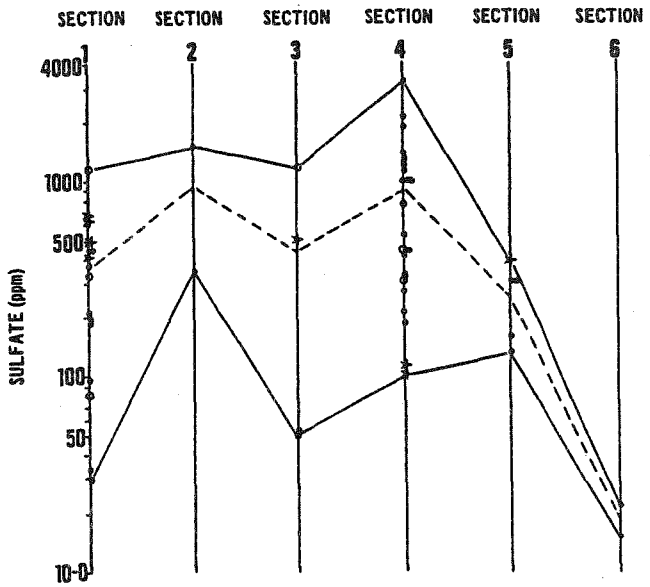

Figure 4. Graph of sulfate for the various sections shown in Figure 2. Dotted line connects the mean values; solid lines the upper and lower ranges.

accumulated a large body of quantitative data of this kind which will be discussed in the following sections.

Morrison (1985) has made the most recent and extensive study of acid mine drainage in western Pennsylvania, from which the following tables have been extracted. Examination of Table 3 reveals that brackish and marine shales and coals are the only rocks in the Carboniferous with sulfur contents in excess of 1.0 percent. The lowest values occur in freshwater shales and underclays. Although the variation in sulfur, as measured by the range and standard deviation, is relatively large for most of the rock types, it should be noted that except for sandstones, the low-sulfur rocks (freshwater shales, siltstones, underclays, freshwater and marine limestone) do not overlap the high-sulfur rocks (brackish and marine shales and coals).

Table 4 summarizes the amounts and types of carbonate and Table 5 the amount of carbonate carbon found in coals and various types of shales. Observe that freshwater shales have the highest calcite, dolomite, and siderite contents, brackish shales and coals have negligible calcite, and marine shales have intermediate amounts of calcite, dolomite, and siderite. The validity of these differences is supported by some field and mineralogical evidence, namely that freshwater shales are frequently associated with limestone beds, whereas limestones are unknown in brackish-water shales and rare in marine ones. The calcite/sulfur ratios for

Table 2. Summary of the mineralogy, lithology, paleoenvironments, and water quality of effluent from strip mines in the Allegheny Group of western Pennsylvania.

Mine no.	Location	Formation	$CaCO_3$	$CaCO_3$ criteria	Paleo	SS	Weath.	pH values	Water quality
1	N. Washington, Butler Co.	LF	X	ab, 1&4	FW			6.0	Good
4	Grant City, Lawrence Co.	MK	X	ab, 3	M			5.7-6.5	Good
5	Grant City, Lawrence Co.	MK	X	ab, 3	M			6.5	Good
7	Boydstown, Butler Co.	U&LF	X	bl, 1&4	FW			7.0	Good
9	Rock Spring Crk., Butler Co.	C	X	ab, 2	M			7.2	Good
14	Rodgers Mills, Fayette Co.	U&LF	X	bl, 4	FW			3.8	Bad
15	Laurelville, Westmoreland Co.	F	X	ab, 1	FW			6.0	Good
17	Stoystown, Somerset Co.	LK-UF	X	ab, 1	FW-B			3.0-3.7	Bad
18	Stoystown, Somerset Co.	LK-UF	X	ab, 1&4	FW-B			3.5	Bad
30	Rodney, Westmoreland Co.	U&LF	X	bl, 1&4	FW				Good
71	Falls Creek, Jefferson Co.	LK	X	bl, 2	B&M			7.1	Good
13	Rogers Mills, Fayette Co.	U&LF	X	bl, 4	FW	X		6.8	Good
28	Rodney, Fayette Co.	U&LF	X	bl, 1	FW	X		6.1	Good
44	Clearfield, Clearfield Co.	UF	X	ab, 1	FW	X		7.6	Good
64	Glasgow, Cambria Co.	MK	X	bl, 1	FW	X		4.0	Bad
96	Homer, Clarion Co.	LK	X	ab, 4	M	X	X	6.3	Good
108	Rimersburg, Clarion Co.	C	X	ab, 2	M	X		6.0	Good
122	Emlenton, Butler Co.	C	X	bl, 2	M	X		5.0	Good
124	Perryville, Clarion Co.	C	X	bl, 2	M	X	X	3.7	Bad
2	Hilliards, Butler Co.	UF			FW	X			Bad
3	Eldorado, Butler Co.	F			FW	X		3.8	Bad
10	Elliotsville, Fayette Co.	M			FW	X	X	3.8	Bad
11	Elliotsville, Fayette Co.	M			FW	X	X	3.0	Bad
12	Flatrock, Fayette Co.	UF			FW	X	X	4.0	Bad
16	Somerset, Somerset Co.	LK			FW	X		3.5-4.0	Bad
19	Lambertville, Somerset Co.	LK-UF			FW	X		3.3-3.5	Bad
22	Kregar, Fayette Co.	LK			B&M	X	X		Bad
24	Kecksburg, Fayette Co.	M			FW	X	X		Bad
25	Kecksburg, Fayette Co.	LK			B	X	X	2.9	Bad
26	Kecksburg, Fayette Co.	LK			B&M	X		3.4-3.9	Bad
45	Clearfield, Clearfield Co.	MK			B&FW	X		3.2-7.0	Bad&Good
47	Clearfield, Clearfield Co.	F			FW	X	X	4.5	Bad
53	Lecontes Mills, Clearfield Co.	UF			FW	X		6.3	Good
56	Lecontes Mills, Clearfield Co.	M			FW	X			Bad
63	Glasgow, Cambria Co.	C			B	X		3.3	Bad
66	Blandburg, Cambria Co.	C			B	X		4.3	Bad
75	Clearfield, Clearfield Co.	UF			FW	X		2.6	Bad
128	Rimersburg, Clarion Co.	C			M	X	X		Bad
6	Grant City, Lawrence Co.	MK			M			3.5-4.7	Bad
142	Homer, Clarion Co.	LK			M			4.5	Bad

Key to Table 2:

Formation:
M=Mahoning
F=Freeport
K=Kittanning
C=Clarion

U=Upper
M=Middle
L=Lower

$CaCO_3$:
X=present
ab=above acid producer
bl=below acid producer

1=freshwater limestone
2=marine limestone
3=glacial till
4=calcareous siltstone

Paleoenvironment:
FW=freshwater
B=brackish
M=marine

Sandstone:
X=channel sandstone present

Weathering:
X=weathered deeply

Water quality:
Good=pH above 5.0
Bad=pH less than 5.0

freshwater, brackish, and marine shales are 5.13, 0.025, and 0.27, respectively. Since 3 units of calcite will neutralize 1 unit of sulfur, any acid produced by freshwater shales would be completely neutralized, whereas this process would be negligible in brackish and marine shales.

Estimates of pre-mining acidity will depend upon a knowledge of the arrangement and distribution of the major rock types as manifested in stratigraphic cross sections and lithofacies maps. Figure 5 is an example of the former and illustrates the vertical and lateral facies which characterize the Allegheny Group in western Pennsylvania. The upper Allegheny, consisting mainly of nonmarine shales, siltstones, sandstones, clays, and freshwater limestones, seldom produces acid mine

Table 3. Total sulfur values for the major rock types in the Allegheny Group of western Pennsylvania. (N - number of samples; $\bar{x}$ - mean; s - standard deviation.)

	N	$\bar{x}$	s	Range	Conf. level (95%)
Overall (shale & coal)	332	1.82	2.15	0-14.30	1.59-2.05
All shales					
Total	237	1.36	2.07	0-14.30	1.00-1.72
Marine	70	0.95	0.90	0-4.27	0.74-1.16
Brackish	102	2.40	2.69	0.10-14.30	1.88-2.92
Freshwater	65	0.15	0.20	0.00-0.95	0.10-0.20
Freeport shales (freshwater only)					
Total	21	0.29	0.25	0.03-0.95	0.17-0.40
Kittanning shales					
Total	213	1.47	2.15	0.00-14.30	1.18-1.76
Marine	70	0.95	0.90	0.00-4.27	0.74-1.16
Brackish	99	2.45	2.72	0.10-14.30	1.91-2.99
Freshwater	44	0.09	0.13	0.00-0.74	0.05-0.13
All coals					
Total	95	2.99	1.89	0.50-9.13	2.62-3.36
Kittanning	76	2.93	1.84	0.55-9.13	2.52-3.34
Freeport	13	2.70	1.75	0.50-7.40	1.64-3.76
Clarion	6	4.34	2.59	0.89-7.20	1.62-7.06
All sandstones					
Total	24	0.45	0.42	0.13-1.72	0.27-0.63
Freeport and Mahoning	13	0.51	0.54	0.13-1.72	0.18-0.84
Kittanning	11	0.40	0.18	0.23-0.79	0.28-0.52
All siltstones					
Total	8	0.32	0.15	0.13-0.57	0.19-0.45
Freeport	3	0.25	0.10	0.13-0.31	0.00-0.50
Kittanning	5	0.37	0.17	0.19-0.57	0.16-0.58
All clays					
Total	7	0.28	0.19	0.08-0.67	0.10-0.46
Underclays	4	0.37	0.21	0.22-0.67	0.04-0.70
Calcareous	3	0.17	0.09	0.08-0.26	0.00-0.39
All carbonates					
Total	10	0.45	0.37	0.13-1.40	0.19-0.71
Freshwater	2	0.51	0.22	0.35-0.66	---
Marine	3	0.24	0.10	0.13-0.30	0.00-0.49
Siderite	5	0.56	0.50	0.25-1.40	0.00-1.18

Table 4. Carbonate carbon of all shale types and coals in the Allegheny Group in western Pennsylvania. (N - number of samples; $\bar{x}$ - mean; s - standard deviation.)

	N	$\bar{x}$	s	Range	Conf. level(95%)
Overall (shale & coals)	46	0.33	0.49	0.00-1.64	0.19-0.47
All shales					
Total	36	0.43	0.52	0.00-1.64	0.26-0.60
Marine	15	0.65	0.61	0.00-1.64	0.31-0.99
Brackish	15	0.16	0.24	0.00-0.88	0.03-0.29
Freshwater	6	0.54	0.58	0.00-1.60	0.00-1.05
All coals					
Total	10	0.00	0.00	0.00-0.01	0.00-0.00

Table 5. Carbonate mineralogy of all shale types in the Allegheny Group in western Pennsylvania. (N - number of samples; $\bar{x}$ - mean; s - standard deviation.)

	N	$\bar{x}$	s	Range	Conf. level(95%)
Marine environment					
Siderite	15	4.05	3.60	0.03-11.00	2.06-6.04
Calcite	15	0.26	0.52	0.00-2.05	0.00-0.55
Dolomite	15	0.74	0.53	0.03-1.75	0.45-1.03
Brackish environment					
Siderite	14	1.79	2.11	0.00-7.55	0.57-3.01
Calcite	14	0.06	0.13	0.00-0.50	0.00-0.14
Dolomite	14	0.48	0.36	0.05-1.55	0.27-0.69
Freshwater environment					
Siderite	6	5.41	2.58	1.30-9.10	2.70-8.12
Calcite	6	0.77	0.79	0.05-1.75	0.00-1.60
Dolomite	6	1.59	0.80	0.08-2.35	0.75-2.43

drainage because all beds have low sulfur contents and abundant limestone is usually present. The lower part of the diagram illustrates the typical regional variation in lithofacies characteristic of the Pottsville Group and the lower and middle Allegheny Group in western Pennsylvania. The highest acid production is estimated to be geographically in the middle zone, where brackish shales are the principal rock type, containing the highest sulfur and lowest carbonate. Areas to the east, containing freshwater beds, will have mines which produce little acid except in areas of channel sandstones. Areas in the west contain both brackish and marine

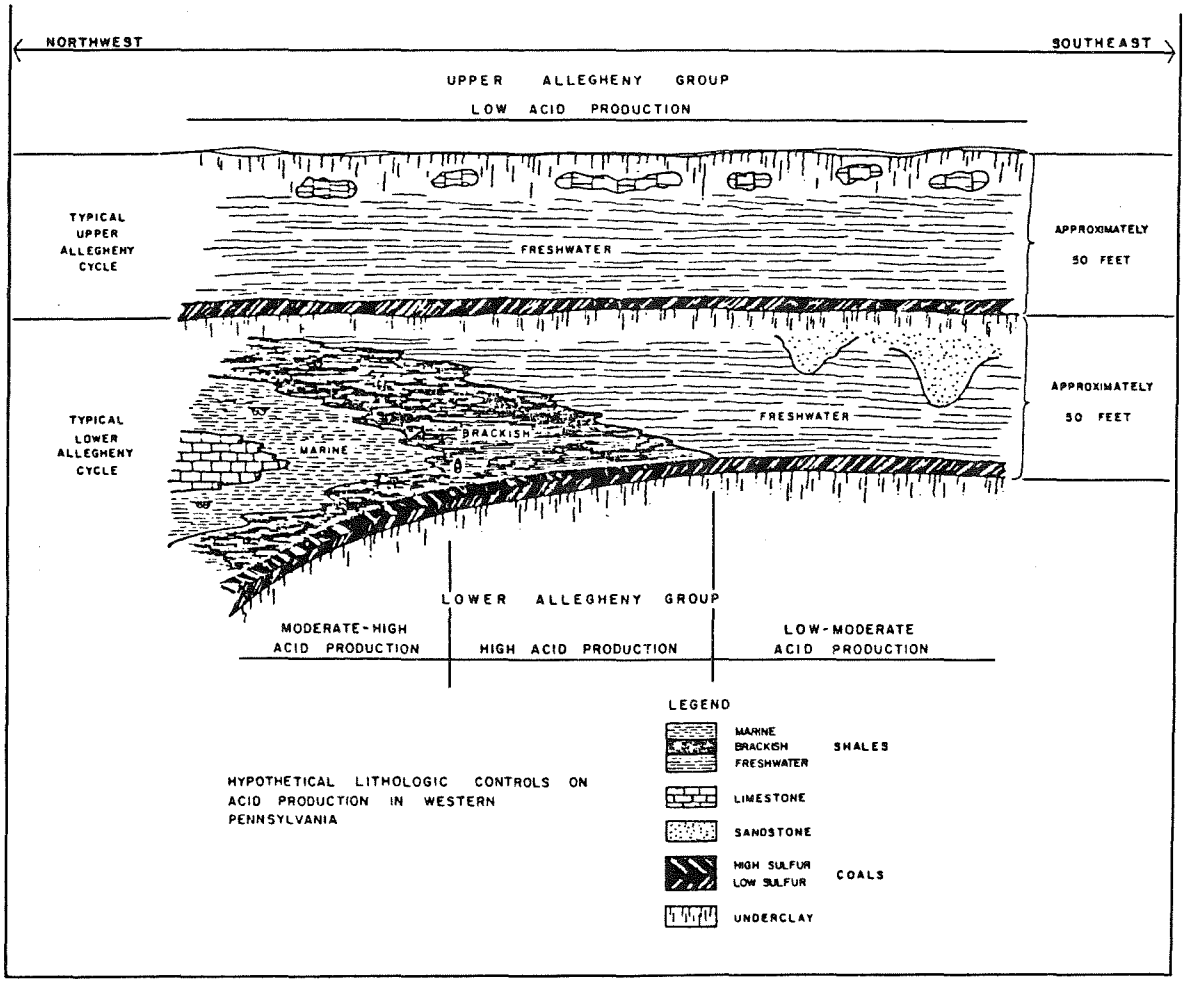

Figure 5. Schematic summary of hypothetical, lithologic, stratigraphic, and paleoenvironmental controls on acid mine drainage on the Allegheny Group in western Pennsylvania. From Hornberger and others (1981).

beds as well as minor marine carbonates. Whether acidity is produced depends on the proportion of sulfur to $CaCO_3$, the ratio of which would be variable. Figure 6 is a biofacies map with inferred amounts of acid mine drainage for each facies, based primarily upon the controlled field experiments as well as the laboratory leaching experiments. We believe the boundaries for the "Low" class are accurate, since the sulfur values are always low. Boundaries for the other classes are less precise since two factors are involved, sulfur and carbonate. Maps of this kind exist for most coal beds in western Pennsylvania (Williams and others, 1982).

In addition to statements attempting to predict acid mine drainage prior to mining, our studies permit some conclusions to be drawn about reclamation procedures. Figure 7 illustrates the common method of backfilling a strip mine, whereby the stratigraphy of the final spoil bank is inverted with respect to the original sequence, a condition which places the brackish-water shale, unit A, on the top of the pile; further backfilling spreads this unit out and makes it the main lithology exposed to oxidation. This may explain the results obtained by Guber and others (1971), in which the backfilled mines produced more acid than those unfilled. Figure 8 suggests alternative methods of backfilling whereby the main acid-producing unit is buried and covered with the more impermeable and low-sulfur underclay.

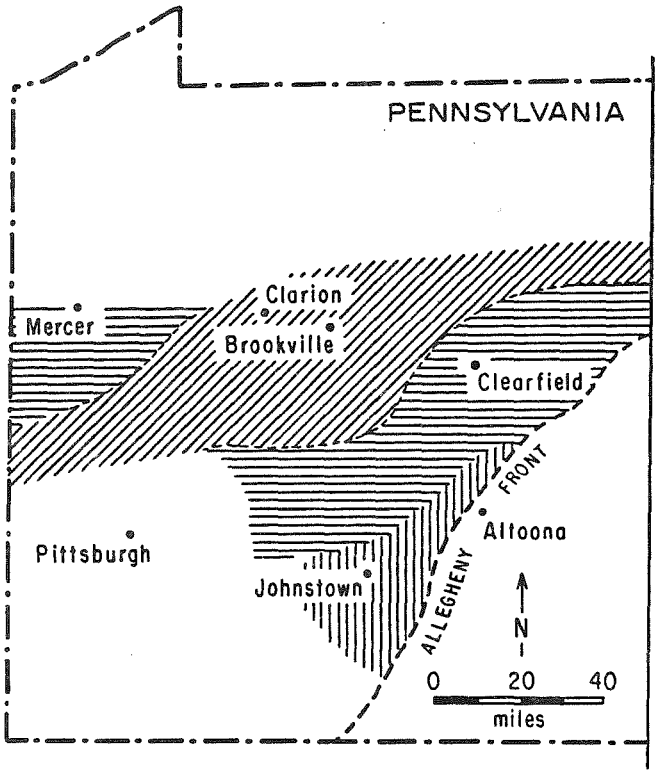

Figure 6. Map showing the distribution of paleo-environments for the Lower Kittanning shale and estimated amounts of acid production (upper left).

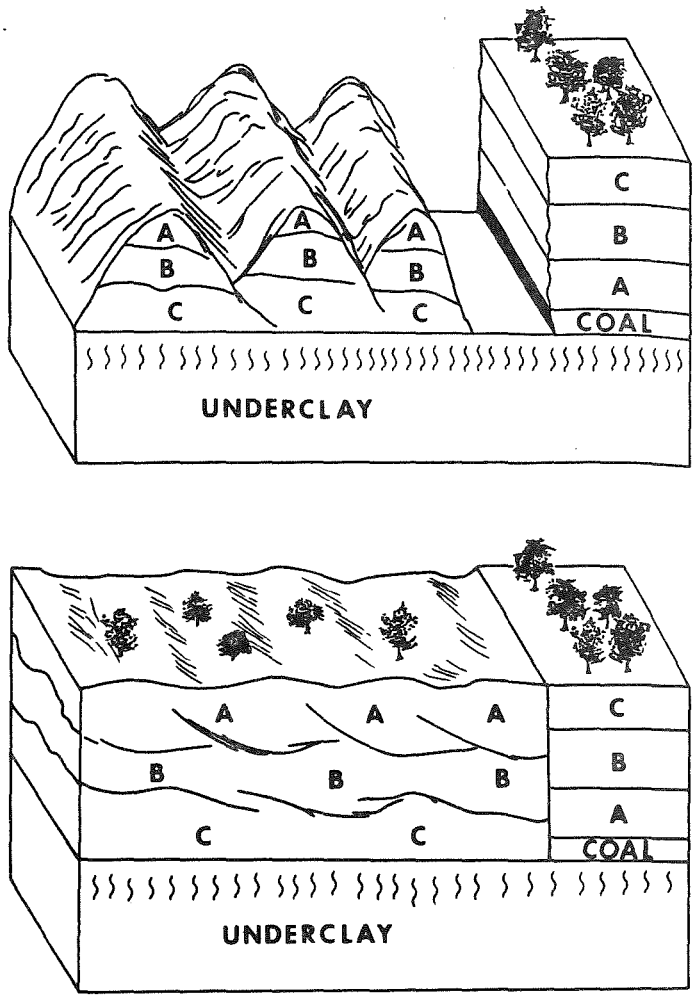

Figure 7. Diagrams illustrating common methods of backfilling strip mines (upper right).

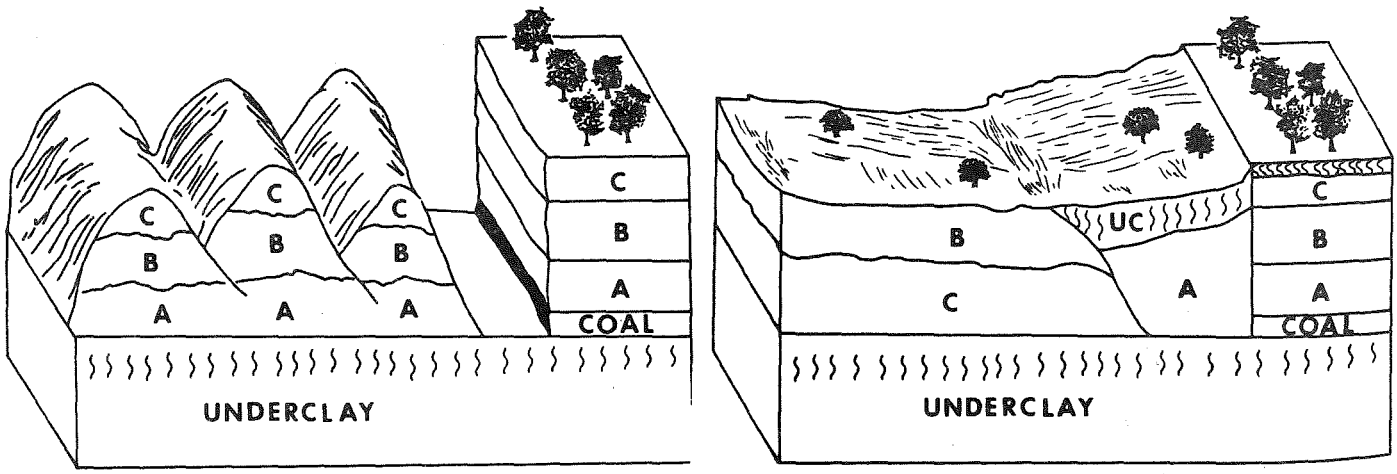

Figure 8. Diagrams illustrating alternative methods of backfilling strip mines designed to minimize the production of acid mine drainage (lower left).

ENVIRONMENTS OF DEPOSITION OF THE LOWER KITTANNING SEAM IN PENNSYLVANIA AND OHIO AND THEIR INFLUENCE UPON COAL PETROGRAPHIC, MINERALOGIC, AND CHEMICAL COMPOSITIONS

by
Susan M. Rimmer*, Deborah W. Kuehnt, Sharon D. Allshouse+, and Alan Davis
Department of Geosciences, The Pennsylvania State University

Introduction

The Lower Kittanning seam and its stratigraphic equivalents extend throughout much of the northern part of the Appalachian coal basin. It is second only to the Pittsburgh seam as a source of bituminous coal in the region (U.S. Geological Survey and U.S. Bureau of Mines, 1968). The wide extent and accessibility of this seam, together with the opportunity it provides to study a single coal deposited in a range of environments and modified to varying degrees by subsequent metamorphism, have made it the most intensively studied in the eastern U.S. This paper describes some of the results obtained since 1980 by several researchers, mostly graduate students, at The Pennsylvania State University.

Lateral and Vertical Variability

Lateral Variability in Petrographic Character

It can be expected that the distribution of organic and inorganic constituents in coals will reflect, to some extent, local and regional variations in environmental conditions as well as subsequent diagenetic and metamorphic influences. One broad indication of the influence of depositional environments is the varying character of the shales which overlie the Lower Kittanning seam. These environments are depicted in Figure 1 together with the location of samples used to study the lateral variability in the coal petrology and mineralogy. A total of 43 channel samples from Pennsylvania were used as the basis for the contouring; they represent a wide range of environments and rank. Present geographic limits of the seam are not shown.

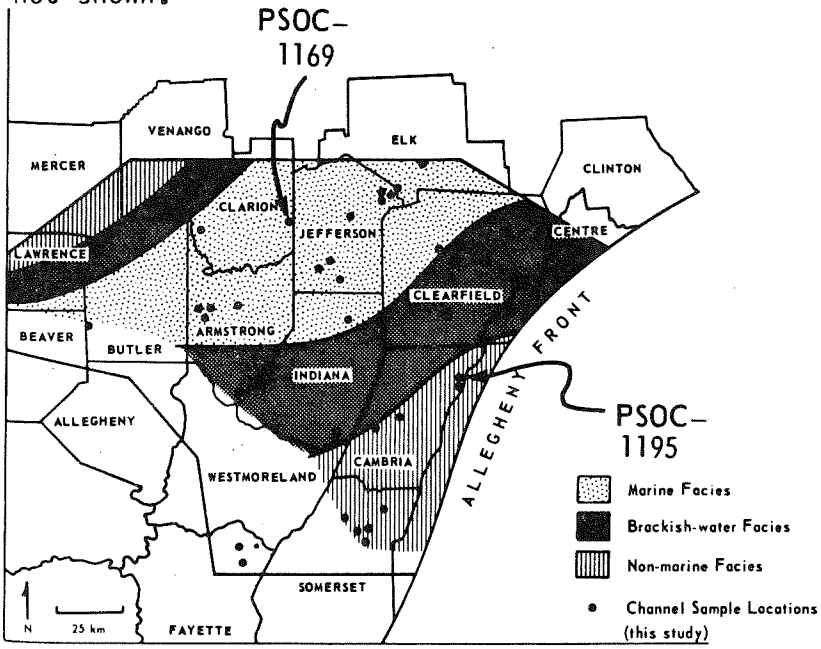

Figure 1. Distribution of samples in western Pennsylvania in relation to suggested environments of deposition for the overlying shale (from Rimmer, 1985).

Present addresses:
*Department of Geology
Bowman Hall
University of Kentucky
Lexington, KY 40502-0059
†Department of Geography
and Geology
Western Kentucky University
Bowling Green, KY 42101
+2109 Forest Street
Rapid City, SD 57701

Vitrinite group macerals are the major petrographic constituents of the Lower Kittanning seam and provide the clearest indications of environmental changes in these studies. Senftle (1981) and Rimmer (1985) have described the distributions of certain other macerals. To obtain more insight into the factors which may have influenced the vitrinite maceral content, the distributions of total vitrinite, desmocollinite, and telocollinite were mapped. Following a description of these trends, various controls on the distributions will be considered.

Total vitrinite ranges from 74 to 98 percent, with low values occurring in an area trending southwest-northeast across the basin (Fig. 2), a trend which roughly coincides with the marine facies of the overlying shale (Fig. 1). Locally, vitrinite content increases to over 92 percent in the southeast (in Somerset County), is relatively high in Clearfield County, and low in the Centre and Cambria County areas.

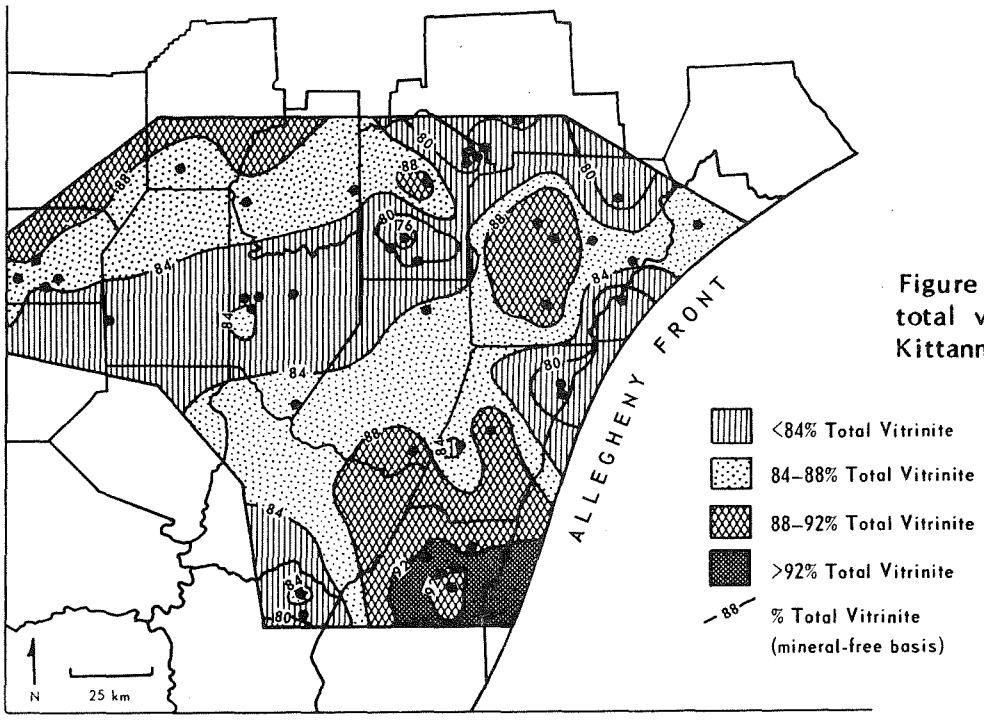

Figure 2. Lateral variability in total vitrinite content: Lower Kittanning seam.

Desmocollinite is that vitrinite which originates from smaller plant tissues such as grass and reeds, and tissues which have been degraded into finer sized fragments; it often occurs in detrital admixture with other coal macerals and minerals. Low desmocollinite contents (less than 25 percent) occur in the central part of the basin, and highest desmocollinite contents (over 35 percent) occur along the basin margins (Fig. 3). Locally, a low desmocollinite content is seen in the Clearfield County area and also in the Cambria County area. Along the Allegheny Front, to the north and south of Cambria County, desmocollinite increases to over 40 percent. The regional trend is clear in the second-order trend surface (not shown) which is highly significant (at the 1 percent level).

Telocollinite is vitrinite which occurs in distinct, homogeneous layers generally devoid of other macerals; it represents the coalified products of the roots, bark, and stems of plants. In general, the telocollinite content is highest in the central part of the basin, and decreases towards the margins; an exception to this is an area of high telocollinite content observed in Somerset County (Figure 4). In other local areas, telocollinite is very high in much of Clearfield County; low

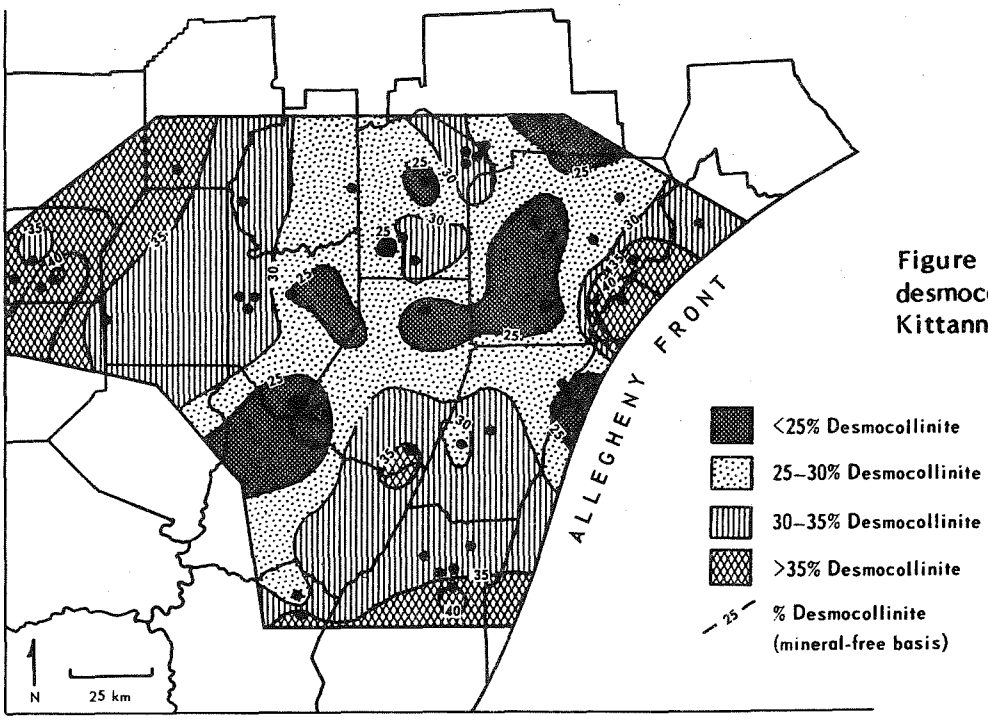

Figure 3. Lateral variability in desmocollinite content: Lower Kittanning seam.

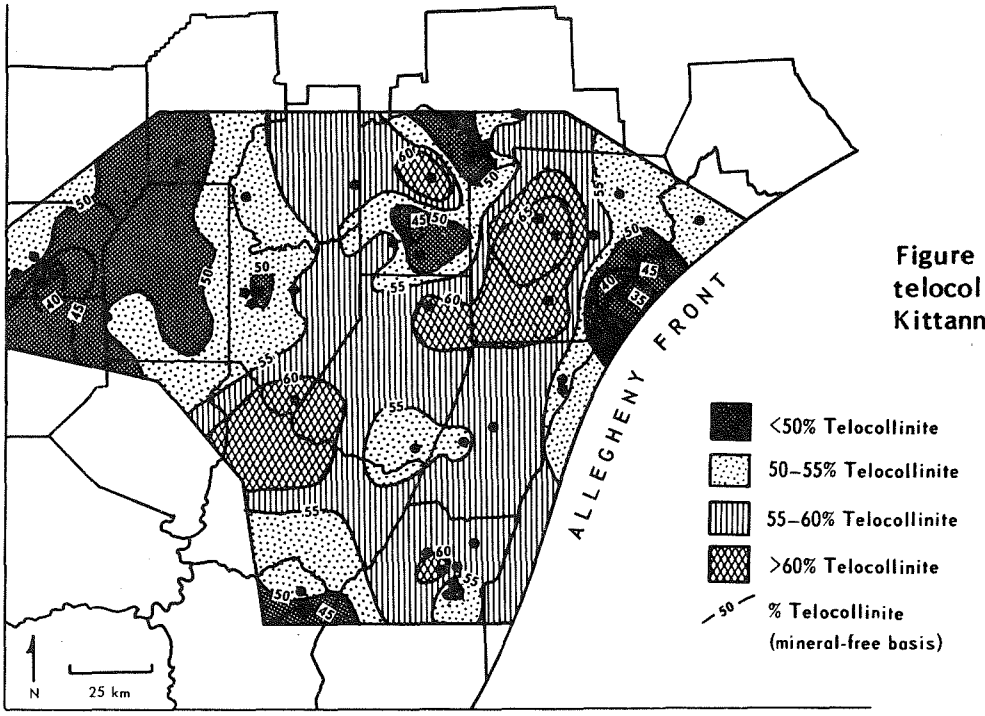

Figure 4. Lateral variability in telocollinite content: Lower Kittanning seam.

telocollinite contents are observed in Cambria and Centre Counties. The telocollinite distribution appears to be quite variable, an observation emphasized by trend surface analysis (analysis of variance shows levels of significance reaching only 25 percent).

In previous studies, variations in petrography and palynology of the Lower Kittanning seam have been attributed primarily to different plant assemblages, which may have changed in response to the encroaching marine conditions (Habib, 1964; Ting, 1967). According to this explanation, areas along the margins of the basin

supported a freshwater, arborescent vegetation, dominated by lepidodendrids as indicated by the dominance of Lycospora. This type of vegetation would produce high-vitrinite coals. The marine-influenced central part of the basin supposedly supported a cover of smaller plants, dominated by the presence of Densosporites, and produced a low-vitrinite coal.

The distribution of total vitrinite observed in the present study could be explained in part by the change in vegetation type suggested by Habib (1964). A comparison of Figures 1 and 2 shows that in the central part of the basin, where the coal is overlain by marine shales, the total vitrinite content of the coal is low. If this area did support vegetation of smaller plants, woody tissues would constitute a smaller proportion of the material available for preservation, and thus low-vitrinite coal would result.

Alternatively, or in addition, the level of peat degradation may be a factor in determining vitrinite content. High vitrinite contents would have resulted where there was little degradation, i.e., where relatively rapid burial prevailed. Low vitrinite contents would have resulted from peats which had undergone degradation, due to either periodic subaerial exposure or to the influx of oxygenated waters or waters of relatively high pH. The decrease in vitrinite observed in the center of the basin may thus reflect higher levels of degradation associated with the influx of marine or brackish waters late in the development of the peat swamp. Neutral pH values associated with such waters would have enhanced decomposition by allowing more bacterial activity.

Areas along the basin margins which have low vitrinite contents may have resulted either from the influx of well-oxygenated fresh water into topographically low areas, or from repeated exposure to the atmosphere due to fluctuations in the ground-water table on topographic highs. These possibilities will be considered as other variables are examined.

Additional insight concerning controls on vitrinite distribution may be provided by examining variations in vitrinite submaceral content. A zone of low desmocollinite and high telocollinite (Figs. 3 and 4) crosses the center of the basin. In addition, it should be noted that this area does not coincide with the low vitrinite area, i.e., the area overlain by marine shale, but is shifted slightly to the southeast.

If vegetation was the only control of the vitrinite submaceral content, then desmocollinite and telocollinite distributions might be expected to follow established trends in vegetation type. Whole-seam sample data presented here show a relative increase in telocollinite towards the center of the basin, and an increase in desmocollinite towards the margins. This would imply that, overall, throughout the life of the peat swamp, arborescent vegetation was dominant in the central part of the basin. Habib's (1964) palynological data, however, suggest an increase in herbaceous types towards the top of the seam in the center of the basin, and a dominance of arborescent types on the basin margins and in the lower portion of the seam in the center of the basin. The observations suggest that vitrinite type may not be entirely dependent on the type of vegetation.

An alternative explanation is that vitrinite submaceral content may reflect the degree of preservation. In an area which underwent more rapid subsidence, in this case the center of the basin as compared to the margins, burial would have been more rapid and plant materials would have undergone less degradation. A higher proportion

of telocollinite would thus be preserved. Higher overall desmocollinite contents are observed along the basin margins where more decomposition could take place owing to the low burial rates, oxidation, and reworking.

Even greater subsidence during the late stages of the peat swamp in the central part of the basin led to a marine incursion which may have influenced the total vitrinite content. An increase in desmocollinite, the fine-grained type of vitrinite, towards the top of the seam has been noted by Allshouse (1984) and Rimmer (1985). Other than by a change in vegetation type, as suggested by Habib (1964), this could be explained by a change in chemical conditions accompanying the marine incursion, enhancing the breakdown of woody tissues.

Still within the central part of the basin, but somewhat removed from the marine influence, the peat continued to be buried quite rapidly, resulting in the continued preservation of telocollinite. This produced the southwest-northeast-trending area of high telocollinite and low desmocollinite which is parallel to, but shifted slightly towards the southeast from, the zone of marine influences. In addition to the possibility of high levels of preservation, the type of vegetation could have had an important influence: this area was not strongly influenced by marine conditions so that larger arboreal types might have developed.

The extent of degradation may also be used to explain some of the local variations in vitrinite submaceral content. Along the basin margins, an influx of oxygenated waters would partially neutralize acidic swamp waters resulting in increased degradation. This may have occurred in the Centre County area where very high desmocollinite contents are observed together with thick inorganic partings, suggesting a topographic low into which sediment-laden, oxygenated waters were carried. Other areas along the margins, such as Somerset County, may also have been topographic lows, but differed from the area in Centre County in that there was limited influx of oxygenated waters and sediment. As a result, the peat was well preserved as the area subsided. Occasionally such influxes did occur, and the resulting short-lived periods of oxidation are represented by an increase in desmocollinite content within the coal column and the deposition of thin inorganic partings. There is some independent evidence for the existence of a depositional center being situated in this area; several units are reported to thicken in this direction (E. Koppe, pers. commun.).

Clearfield County is typical of conditions existing in the center of the basin where very high telocollinite and low desmocollinite contents are seen. Conditions in this area probably included relatively rapid subsidence and acidic conditions, with little influx of oxygenated water. Within this more stagnant environment, the preservation of woody tissue would be optimized.

In summary, the type of vitrinite may reflect not only the vegetational type, but how well the woody material was preserved. This, in turn, would reflect rates of subsidence and pH/Eh conditions within the peat swamp. Rapid subsidence and acidic conditions would enhance telocollinite preservation, whereas desmocollinite would be associated with lower subsidence and more neutral or oxidizing conditions, and possibly with areas which experienced fluctuating water levels and some subaerial exposure.

Lateral Variability in Mineralogy

Pyrite and Marcasite

The major minerals occurring in the Lower Kittanning seam are pyrite, marcasite, quartz, and clays.

The highest sulfide concentrations are found in the central part of the basin, particularly in the areas overlain by brackish shales in the southern side of the basin (Fig. 5). This observation supports a similar finding by Guber (1972), rather than the conclusion of other workers that higher pyrite contents were associated with marine rocks.

Whether iron was transported in organic-rich colloids which flocculated upon entering the brackish water (Sholkovitz and others, 1978) or was associated with detrital clay particles, the eastern margin probably would have more iron available from sources in that direction. The brackish zone would represent an optimization of iron and sulfate availability and pH of the swamp waters.

The presence of marcasite may provide some clues to the timing of sulfide emplacement. Edwards and Baker (1951) indicated that pyrite forms in marine environments whereas marcasite forms under more acidic conditions. In recent experimental work, pyrite formed at a pH of 5.0, whereas marcasite formed at a pH of 3.5, a result which was interpreted as being controlled by the dominance of various polysulfide species (Murowchick and Barnes, 1983). The occurrence of marcasite in what apparently are marine facies may therefore indicate subsequent acidification (Edwards and Baker, 1951).

In the Lower Kittanning seam, marcasite occurrence does not appear to be closely related to the depositional environments shown by facies of the overlying shale. Coals associated with freshwater to marine shale facies contain both pyrite and marcasite. Marcasite is absent or only a minor constituent in the low-sulfide (less than 20 percent sulfide, low-temperature ash (LTA) basis) samples, although

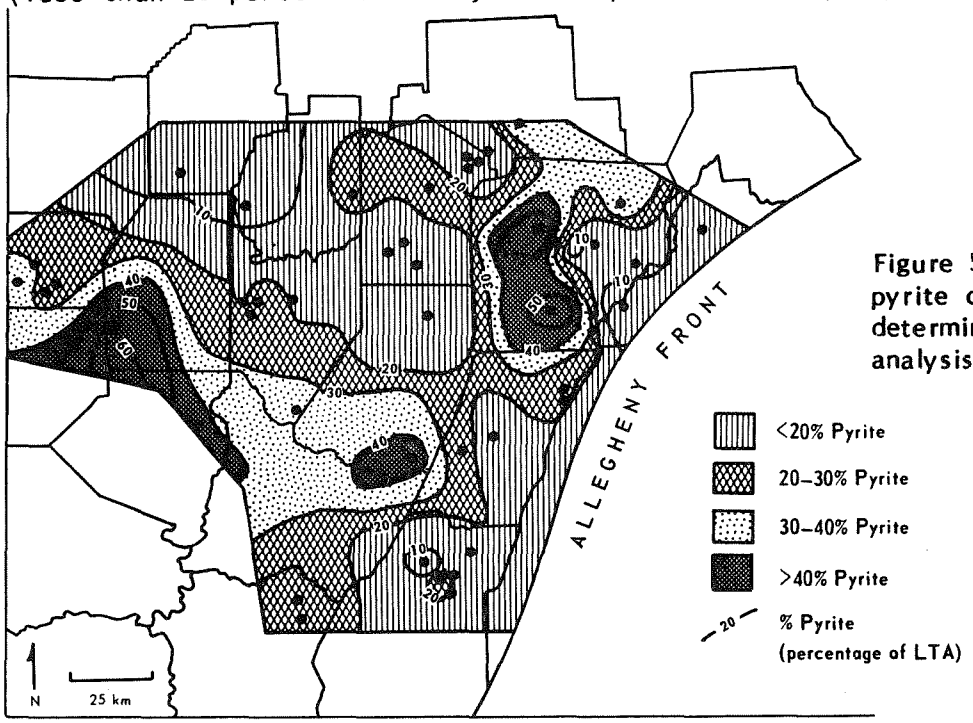

Figure 5. Lateral variability in pyrite content (%, LTA basis), as determined by X-ray diffraction analysis: Lower Kittanning seam.

dominance of marcasite over pyrite might have been expected on the basis of an inferred more acidic swamp environment. In fact, marcasite is more abundant in high-sulfide coals. A possible explanation is that the marcasite may be authigenic and formed in the presence of acidic interstitial waters. Its emplacement may have occurred at any time following burial, and would reflect a change in the pH of the waters moving through the coal. This conclusion regarding the authigenic nature of marcasite in the Lower Kittanning seam appears to be supported by petrographic observations. The mineral tends to occur in the more massive sulfide bodies, as overgrowths on pyrite spherules and in cell infillings.

Quartz

In this coal seam, quartz contents tend to be relatively low, with many samples containing less than 15 percent (Fig. 6). Highest quartz contents as determined by X-ray diffraction (15-20 percent and above) are seen in the north-central part of the region, in Clarion and Jefferson Counties, and in several isolated areas along the basin margins, such as Centre County. Lowest quartz contents occur in a band running from the south and southeast towards the northwest, and in Clearfield County. The linear trend surface (not shown) for quartz indicates an increase towards the north. This first-order surface is significant at the 1 percent level and seems to adequately express the basinal trend.

The distribution of quartz may be helpful in indicating the origin of this mineral in the Lower Kittanning seam. Quartz may be transported into the peat swamp by water and wind (detrital), as envisaged by Mackowsky (1968), Stach and others (1975), Davis and others (1984), and others. However, others have suggested that some quartz may precipitate within swamps from silica that was originally contained within the plants which gave rise to the coal (Renton and Cecil, 1980; Renton and others, 1980).

Some of the quartz grains observed in this study were 30-50 μm or larger, and tended to be concentrated in attrital coal bands associated with clay minerals. These observations suggest that much of the quartz in the Lower Kittanning seam is of detrital origin.

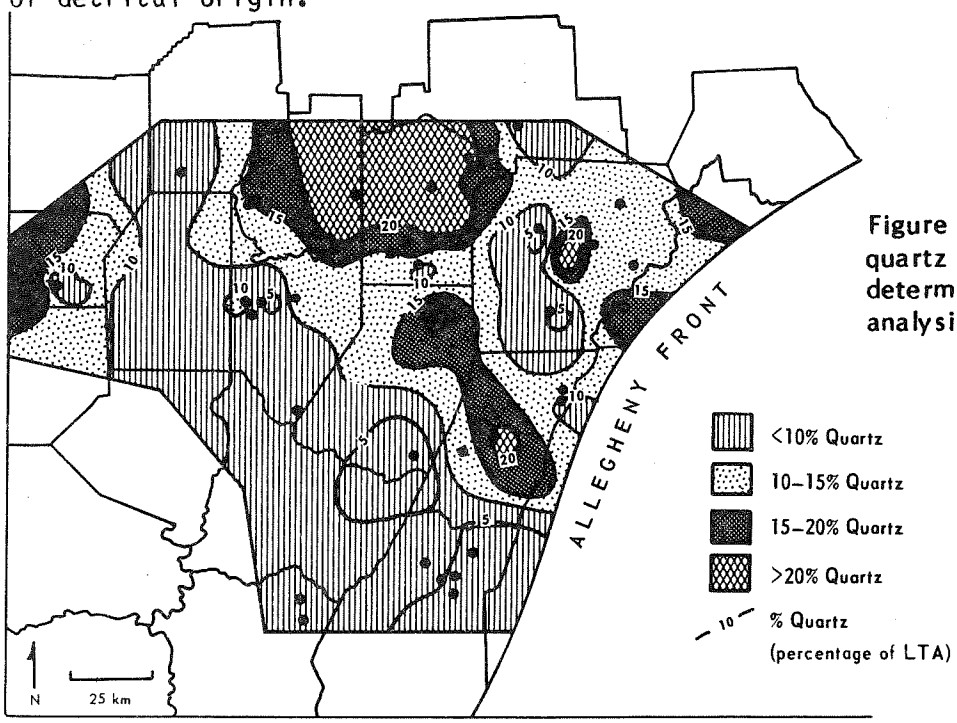

Figure 6. Lateral variability in quartz content (%, LTA basis), as determined by X-ray diffraction analysis: Lower Kittanning seam.

Williams and Bragonier (1974) suggested that a second-order control on sedimentation during Pennsylvanian times was a basement high situated in the north-central part of western Pennsylvania. The existence of this high is indicated by Bouguer anomalies in the area and by the thinning of sedimentary units from Cambro-Ordovician through late Pennsylvanian times. It is possible that quartz-rich sediments were shed from this high into the peat swamp. Transportation of sediment within a swamp is restricted by the filtering effect of the vegetation (Otte, 1984). It would be unlikely, therefore, that detrital quartz would be dispersed evenly throughout the swamp, but rather would tend to concentrate close to the source area.

Holbrook (1973) showed that the quartz content of the Lower Kittanning underclay was highest directly over a clastic wedge in Clarion and Jefferson Counties and over another wedge in Lawrence County. An increase in the quartz content of the Lower Kittanning coal seam itself has now been noted in these areas. Quartz-rich sediment from the north may have continued to be received into these areas during peat accumulation. Alternatively, mixing of underlying sediments with the lower peat layers, perhaps aided by bioturbation, may have occurred; however, the vertical distribution of quartz in the seam (Rimmer, 1985) does not support this hypothesis.

Clay Minerals

Clay minerals may be transported into the swamp during peat accumulation (detrital), precipitate from solutions rich in aluminum, silicon, and various cations (syngenetic and epigenetic), or may form by the alteration of other minerals either within the swamp or during burial (transformation and/or diagenesis) (Davis and others, 1984).

Clays in the Lower Kittanning seam include kaolinite (well-crystallized), illite/mica, and expandable clays. The term total clays includes kaolinite, as determined by infrared spectroscopy, plus "illite," as determined by normative analysis. The "illite" term includes not only illite (s.s.) but also well-crystallized, fine-grained mica. Lowest total clay contents are observed in areas high in pyrite, as in the center of the basin, and those high in quartz, as in the north-central region (Fig. 7). Highest total clay contents are seen on the north-

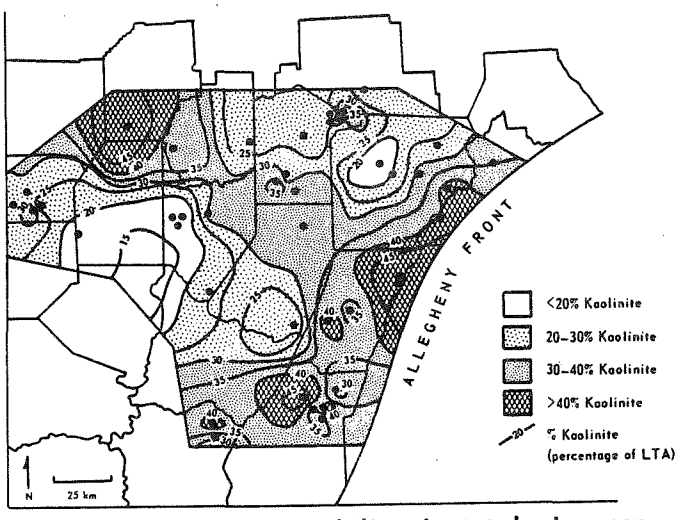

Figure 7. Lateral variability in total clay content (kaolinite plus "illite," LTA basis): Lower Kittanning seam.

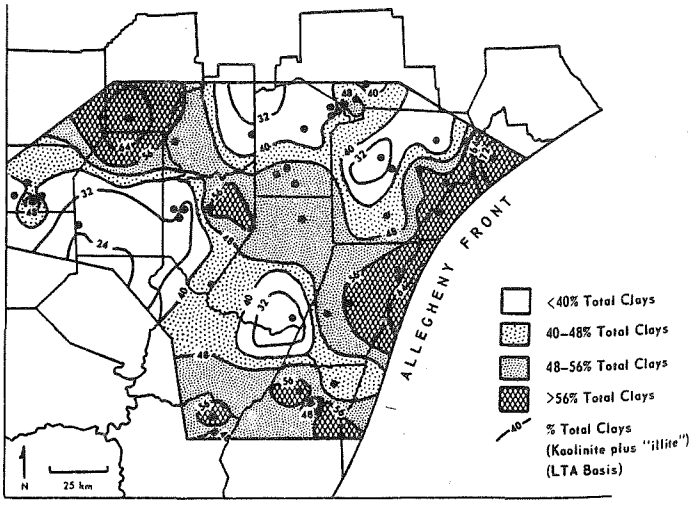

Figure 8. Lateral variability in kaolinite content (LTA basis), as determined by infrared spectroscopy: Lower Kittanning seam.

western and eastern margins of the basin. The effect of closure on the distribution of clays and other minerals clearly is important; variation in the absolute amounts of quartz and pyrite will strongly influence the proportionate distribution of clay.

The distribution of kaolinite shows a low in the central part of the basin and high kaolinite contents in the northwest and along sections of the Allegheny Front (Fig. 8). This distribution is very similar to that for total clays because kaolinite is the major clay constituent of this coal. Trend-surface analysis gives very high levels of significance for the first- through fourth-orders; the cubic surface is significant at the 0.05 percent level and explains 51.1 percent of the data variability, indicating a significant basinal trend.

To avoid the problem of data closure, it is possible to examine variations in individual clays on a basis that is unaffected by fluctuations in other minerals, that is by examining the relative amounts of various clays in the less than 2 μm fraction. The overall distribution of kaolinite in the clay (<2 μm) fraction, however, still shows many similarities to that on a whole LTA basis and so is not shown.

The well-crystallized nature of much of the kaolinite suggests an authigenic origin for at least some of this clay. The possibility that authigenic kaolinite may mask trends in detrital kaolinite has been discussed by Gluskoter (1967), who concluded that kaolinite could in fact be used as an indicator of depositional environment, and that authigenic kaolinite did not mask previously existing trends. Assuming this also to be the case in the present study, the distribution of kaolinite and other clays may be explained in terms of the depositional environment.

Illite in the less than 2 μm fraction increases away from the margins of the basin, with the exception of one sample in the south in Somerset County (Fig. 9). This local fluctuation may be explained by the presence within the coal at that locality of thick clay-rich partings which may contain abundant detrital illite or mica. Variations in the amount of expandable clays (not shown), demonstrate little relationship to trends noted for kaolinite and illite. High expandable clay contents occur locally in Centre, Somerset, and Indiana Counties. These samples all

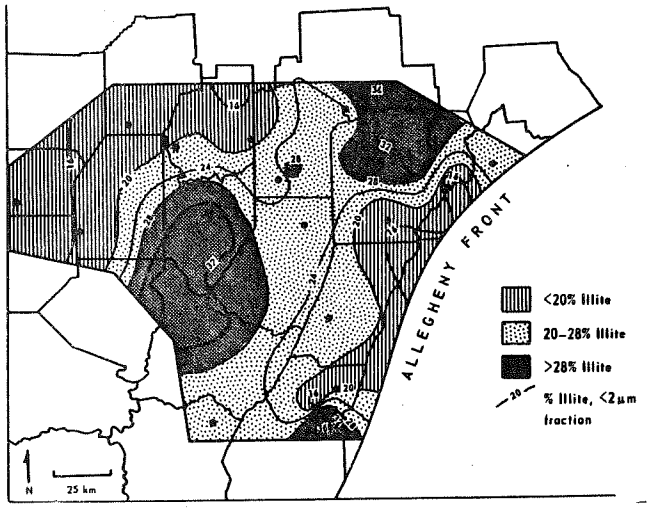

Figure 9. Lateral variability in illite content of the <2 μm fraction: Lower Kittanning seam.

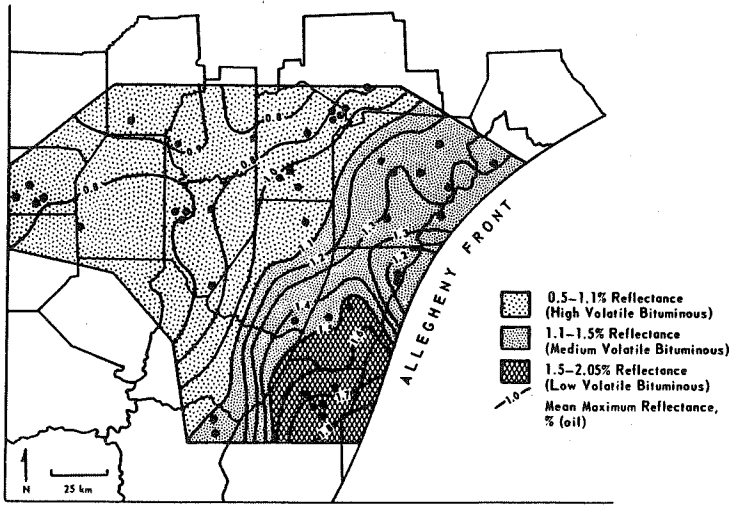

Figure 10. Lateral variability in reflectance: Lower Kittanning seam.

have low kaolinite contents, moderate to high illite contents, and the seam contains clay partings. It is likely that fine-grained mica and illite introduced into the swamp was altered to expandable clays, possibly by the leaching action of organic acids within the peat swamp. With the removal of potassium from the illite/mica interlayers, the clay layers gradually expand. Such a mechanism has been suggested to explain the alteration of illite to mixed-layer clays in the underclay of the Herrin (No. 6) coal (Rimmer and Eberl, 1982). Assuming that the distribution of expandable clays reflects alteration of detrital illitic parent material, the distribution of kaolinite versus illite plus expandables must be explained.

Holbrook (1973) has related high kaolinite contents of underclays to topographic highs, where kaolinite enrichment resulted from excessive subaerial leaching. Thus, in the underclay of the Lower Kittanning seam, high kaolinite contents are found along the margins of the basin and other areas which exhibited positive relief.

The distribution of kaolinite in the Lower Kittanning seam closely resembles that found in the underclay. There are several mechanisms which may have influenced the kaolinite content of the coal, including physical processes, such as in situ mixing and bioturbation of the underlying sediment, and chemical processes including differential flocculation, and either transformation or precipitation in response to conditions within the swamp. Comparison with data presented in Holbrook (1973) suggests that many of the coal samples which contain more kaolinite overlie kaolinite-rich underclays. This is particularly true in the north, northwest, and southeast. Mixing of peat with the underlying sediment could have increased the kaolinite content in these areas, although there is no support for this hypothesis from kaolinite variation within the vertical seam profiles reported by Rimmer (1985). Sharp contacts were observed between coal and underclay, but any evidence of intermixing could have been obscured during compaction.

Parham (1962, 1966) suggested that higher kaolinite contents reflect more shoreward areas. Owing to larger particle size, kaolinite particles flocculate out first, with illite and expandable mixed-layers clays being carried farther out into the basin. The second possible explanation for the observed distributions of the clays, then, is that differential flocculation occurred across a salinity gradient. According to this theory, some authigenic formation or regrading of illite would also take place. Holbrook (1973) argued against this latter process on the basis that most of the mica in the Lower Kittanning underclay is the $2M_1$ polytype, which forms only at temperatures far in excess of those experienced during burial of these sediments. Whereas not all of the illite in the Lower Kittanning coal could be identified as the $2M_1$ polytype, due to the presence of only minor amounts and the somewhat degraded appearance of some of this material, this high-termperature polytype does exist, particularly in clay partings and high-ash samples (Davis and others, 1984). The degraded nature of this mineral is suggested by a very broad 10 Å diffraction peak. Such degradation is not surprising because, under the conditions that existed within the peat swamp and during burial, leaching by organic acids would most likely have occurred.

The third explanation for the distribution of clays relates to the chemistry of the swamp environment. A comparison of Figures 1 and 8 shows that kaolinite occurs in marginal areas which may have been influenced by freshwater conditions, whereas higher illite (Fig. 9) and expandable clay contents are generally seen in the central part of the basin which may have experienced more brackish conditions. Under conditions that existed in freshwater areas, kaolinite would be the stable

clay mineral, forming either from solution or as the stable alteration product of incoming sediment. The high degree of crystallinity of the kaolinite suggests in situ formation which could result from either of these mechanisms. In the more neutral basinward areas, illite/mica would be better preserved than under freshwater conditions. This trend would have been even more pronounced with the onset of the marine invasion. Alteration could still proceed in these areas, producing degraded illite and expandable clays. Around the margins, sudden influxes of sediment, now represented by clay partings within the coal, introduced illite/mica-rich sediments, some of which may have been altered to expandable clays by organic acids.

To examine further the influence of peat chemistry on the clay mineral composition, the clay mineral composition of the channel samples was compared to that of selected floor, roof, and parting samples. Channel samples tend to be enriched in kaolinite compared to other samples (Table 1). Floor rocks tend to have the highest expandable clay contents, whereas roof rocks have the highest illite/mica contents. These observations are quite consistent with the ideas just presented and indicate the importance of chemical conditions within the peat swamp. If it is assumed that the composition of the overlying shales is the closest representation of parent mineralogy available, the clay sediments entering the depositional basin included considerable amounts of illite/mica, relatively small amounts of expandable clays, and moderate amounts of kaolinite, with some chlorite. While some modifications may have taken place since deposition of these sediments, they probably have been affected less by the organic acids than clays in the underclays, coals, or partings. The presence of chlorite suggests that acidic conditions have not been experienced, because this mineral is usually unstable in such environments.

Table 1. Clay composition of the less than 2 μm fraction of coals and associated sediments: summary statistics. (n = number of samples; $\bar{x}$ = mean; s = standard deviation.)

Sample type	Sample size (n)	Kaolinite + chlorite $\bar{x}$	Kaolinite + chlorite s	Illite/mica $\bar{x}$	Illite/mica s	Expandable clays $\bar{x}$	Expandable clays s
Coals	28	62.2	12.58	23.6	8.03	14.1	8.55
Floors	18	42.2	11.53	33.7	12.45	23.9	8.94
Roofs	16	31.2	11.03	50.4	12.71	18.3	10.00
Partings	4	43.5	17.89	41.5	9.88	15.0	8.16

Conditions within the peat swamp would favor the formation and/or preservation of kaolinite. This would result in the observed enrichment in kaolinite within the coal relative to the surrounding sediments. Relatively low illite/mica contents are observed in the coals, possibly due to alteration to expandable clays and ultimately to kaolinite.

The inorganic partings within the coal have slightly higher illite contents; however, very few samples were examined and the results must be interpreted with care. Most of the clay in these partings is detrital rather than the result of in situ formation, as suggested by the presence of $2M_1$ mica and the low degree of crystallinity of the kaolinite. This is in contrast to most of the kaolinite within the coal which probably formed in place.

The floors have greater amounts of expandable clays relative to the coals and roof rocks. Kaolinite is less abundant than in the coals, but more abundant than in the roofs. Only one sample contained any chlorite. These observations are consistent with alteration of underlying sediment by organic acids as suggested by Rimmer and Eberl (1982). Acting on a typical sedimentary clay assemblage, such as that observed in the overlying shales, organic acids would leach the clays and result in the destruction of chlorite and the gradual alteration of illite to expandable clays. As suggested by the slight relative increase in kaolinite, some alteration may also have progressed to kaolinite.

A final control on clay mineral composition could be variations in the extent of metamorphism experienced by the coals. Figure 10 is a map showing the variation in vitrinite reflectance across the study area. The rank range for this suite of coals and clay mineral assemblages that have been reported are indicated in Figure 11. This diagram may help explain some of the observations concerning the clay mineralogy of

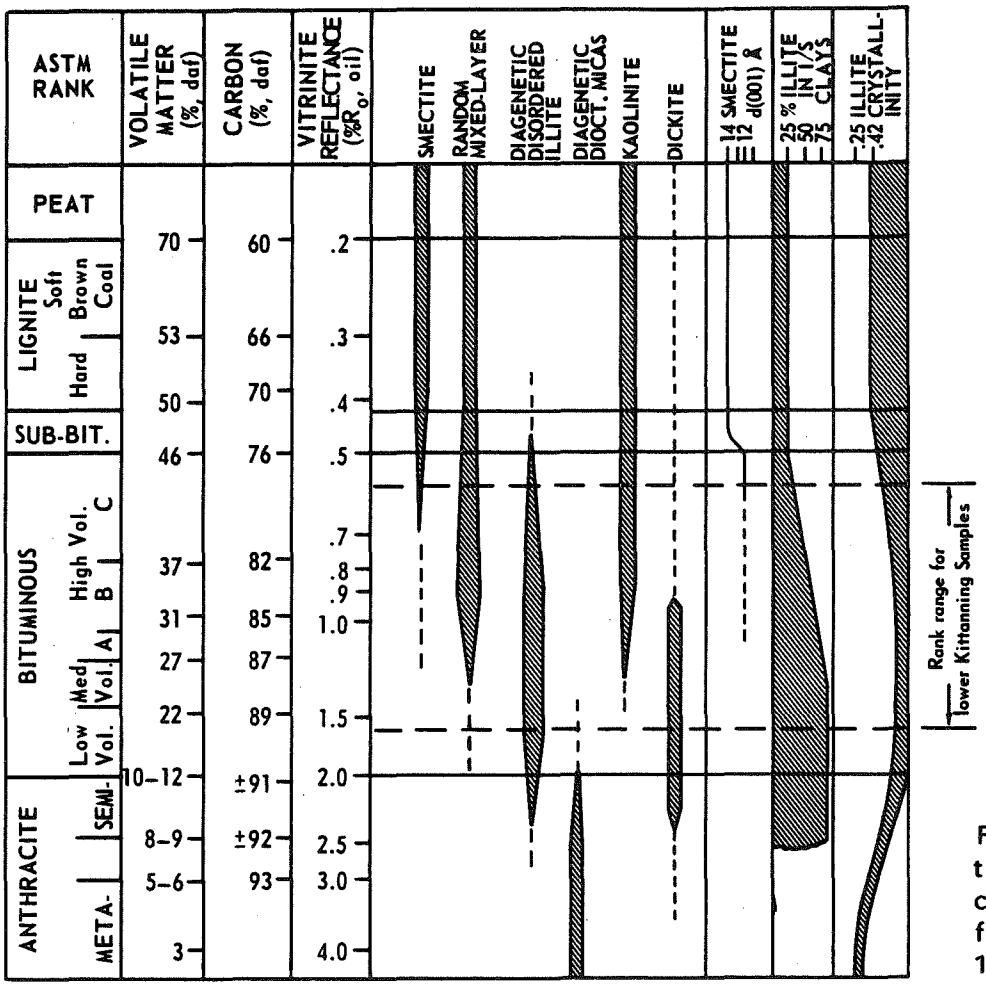

Figure 11. Suggested relationships between rank and clay mineralogy (modified from Heroux and others, 1978).

the Lower Kittanning coal and underclay. According to this diagram the occurrence of smectite should be minimal. Holbrook (1973) noted the presence of this mineral in only 6 percent of his samples (30 out of a total of 478), and no smectite was observed in the LTA's of the coal in the present study. This is not surprising not only because of the level of metamorphism, but also because smectite could be altered under conditions existing in the swamp. Staub and Cohen (1978) noted that smectitic material alters to kaolinite within the Snuggedy Swamp.

Random mixed-layer (expandable) material can occur throughout the rank range included in this study. Holbrook (1973) compared data on the Lower Kittanning underclay to those presented by Parham (1962) for the Illinois underclays, and indicated that although mixed-layer material is present in western Pennsylvania it is much more abundant in the Illinois Basin. In the Lower Kittanning coals, expandable clays are degraded random mixed-layer clays. It has been suggested above that these clays resulted from the alteration of mica-rich sediments. Figure 11 indicates that the amount of random mixed-layer material may decrease from high-volatile B through A bituminous ranks, and percent illite in illite/smectite (I/S) should undergo a dramatic increase over this rank range. No relationship between expandable clay content and rank was noted in the present study.

Within the rank range of samples used in this study, diagenetic illite could form under the appropriate chemical conditions. However, there is no evidence for diagenetic illite formation along cleats in the Lower Kittanning seam, although the possibility has not been ruled out. The $2M_1$ polytype discussed above is interpreted as being detrital.

Thus, it appears that thermal maturity (rank) may help explain the absence of smectite and the paucity of mixed-layer expandable clays in general, but no distinct relationship exists between the amount of expandable clays and rank. The most significant control appears to be chemical conditions within the swamp which produced alteration of a parent material that included kaolinite and fine-grained illite/mica, with lesser amounts of chlorite, vermiculite, and smectite. Within the freshwater facies, alteration of other clays to kaolinite may have occurred, in addition to the precipitation of kaolinite from solution. In more neutral brackish or marine conditions, kaolinite formation was not favored, resulting in a relative increase in illite/mica content. Some of this illite/mica may have formed diagenetically, but the presence of the high-temperature polytype indicates a detrital origin for most of this material. Regrading of degraded illites in potassium-rich waters may also have taken place. Local increases in expandable clays are unrelated to coal rank and may reflect chemical alteration of mica-rich sediments introduced into the peat swamp.

Lateral Variability in Chemical Properties (by FTIR)

Kuehn (1983) used Fourier transform infrared spectroscopy (FTIR) to determine some structural characteristics of hand-picked vitrinites and seam channel samples for Lower Kittanning occurrences in Pennsylvania and Ohio. Some of these data were contoured by hand in a series of maps and related to the regional coalification pattern and the distribution of depositional environments.

The trends for aromatic 4 adjacent hydrogens (750 cm^{-1} band) and phenolic OH (1770 cm^{-1} band) in the vitrinite specimens, and the aromatic stretching region (3100-2990 cm^{-1}) (Fig. 12) of the channel samples show a parallelism to coalification trends in the basin (Fig. 10). A components analysis performed by Kuehn confirmed that these absorption bands were strongly related to reflectance.

Figure 13 shows the distribution of aliphatic CH_3 groups at 2956 cm^{-1}. The amount of lateral variability of this band relating to coalification (reflectance) is about 40 percent. There is, however, a prominent trend which is not related to coalification. The values for CH_3 groups increase toward the center of the basin in Pennsylvania with the lowest values near the margins; unfortunately, there are insufficient data for Ohio to make an interpretation there. This trend can be interpreted as having a chemical control related to the paleoenvironment. The highest values for aliphatic CH_3 groups are in the brackish facies and the lowest values are in the freshwater facies. Varying pH/Eh conditions within the peat swamp may have selectively preserved plant material, giving rise to different amounts of aliphatic CH_3 groups. Stach and others (1975) have observed that coals deposited in a relatively more marine-influenced environment may be enriched in hydrogen.

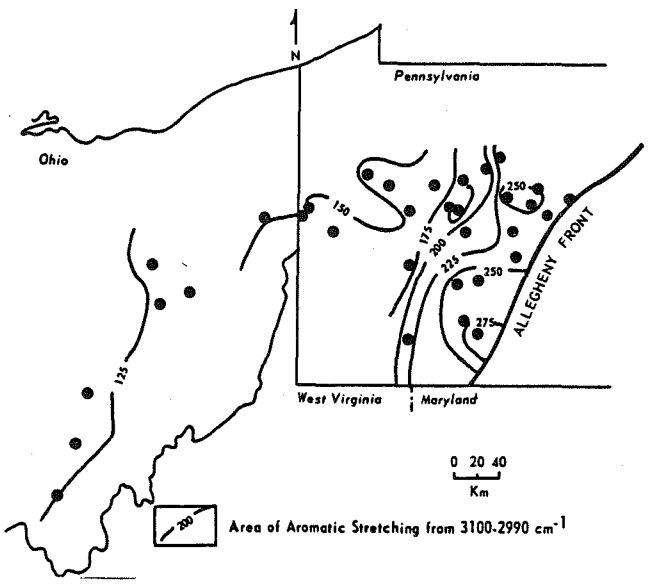

Figure 12. Distribution of the area of aromatic stretching from 3100-2990 cm^{-1} for channel samples of the Lower Kittanning seam.

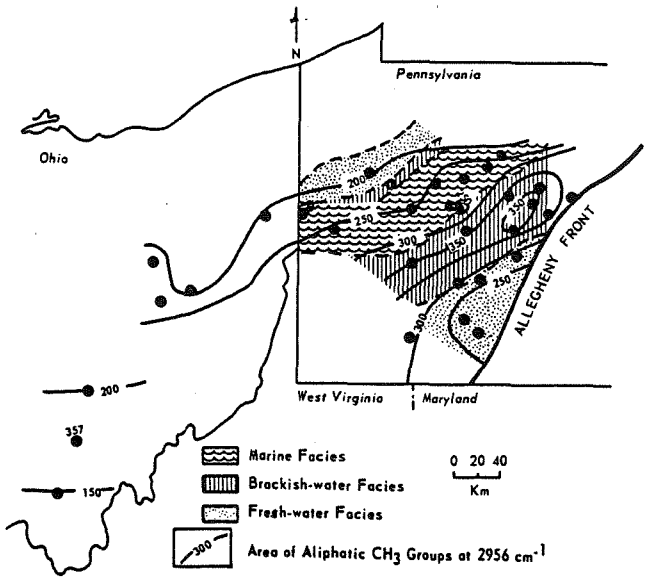

Figure 13. Distribution of aliphatic CH_3 groups at 2956 cm^{-1} for channel samples and facies of shales above the Lower Kittanning seam (facies distribution from Williams, 1960a, and Ting, 1967).

The distribution across the area of aliphatic stretching at 2853 cm^{-1}, representing the symmetric stretching of CH_2 groups, likewise indicates that the environment of deposition may have exerted a control upon the chemistry of the coal, although a major part of the distribution is still explainable by the regional rank pattern. Fig. 14 shows this trend for the channel samples, although a similar pattern was obtained for the vitrinite concentrates. The high values for aliphatic CH_2 coincide with the marine facies. As was the case with the aliphatic CH_3 groups, it seems that an enrichment of aliphatic material could have occurred as a result of exposure to a relatively more marine influence.

In speculating as to how such an enrichment might have occurred, one recognizes the possibility that at relatively higher pH, bacterial activity would have been increased resulting in a more extensive breakdown and loss of humic material. The more resistant plant tissues are likely to have been those which were relatively

enriched in hydrogen. Further, with more extensive loss of the humic components, the greater would have been the possibility of enrichment in liptinitic material. In fact, there is a definite, though only minor, increase in the liptinite content in the central part of the basin where the seam is overlain by marine shale (Rimmer, 1985). Ting (1967) observed that a lithotype rich in alginite occurred in parts of the seam influenced by marine conditions; although no alginite was noted in Rimmer's study, it seems likely that the breakdown products of algal matter could have been incorporated into the coal in the area. The mobility of lipid matter derived from algae has been inferred by, for example, Teichmüller (1974) and Davis (1985); consequently, an enrichment in aliphatic material need not be restricted to zones in which algal remains have been observed. Finally, lipids also might have been enriched in organic sediments where the pH of circulating waters was favorable for bacterial growth.

Vertical Variability in Petrographic Character

The vertical variability in petrography across the study area will be examined by comparing a pair of petrographic profiles representing the seam at both the basin center and margin (Figs. 1 and 15). These profiles have been taken from the study by Rimmer (1985), who examined a number of other profiles along two traverses across the basin. Similar results were obtained in an earlier study made by Allshouse (1984).

In general across the basin there is a decrease in vitrinite content towards the top of the seam, a change that is pronounced in the central part of the basin. Also, as total vitrinite decreases, there appears to be a change in vitrinite type: the base of the seam is enriched in telocollinite, and desmocollinite increases towards the top of the seam at the expense of telocollinite. Again, the trend is more pronounced for the coal overlain by a marine shale.

Towards the top of the seam, both total liptinite and inertinite contents increase. In coals where rank is sufficiently high to obscure the liptinite group macerals, increases in inertinite macerals towards the top of the seam are still evident. Among the inertinite group macerals, degradofusinite, inertodetrinite, and micrinite show the greatest increases towards the top of the seam. These increases are generally more pronounced in the central part of the basin, in association with the brackish and marine facies of the overlying shale.

In several seam sections described by Rimmer (1985), the existence of thin to moderately thick shale partings was noted. Although these are not always associated with changes in the overall vertical petrographic trends, those profiles which show any deviation from the general trends described above more often than not contain inorganic partings. These partings represent periodic influxes of sediment into the swamp, possibly as overbank or splay deposits. In several instances an increase in telocollinite was noted directly above them. Some sections showed little or no decrease in total vitrinite, or even a slight increase towards the top of the seam. Sediment-laden waters would be attracted to low-lying areas where because of rapid burial plant tissues would have stood a better chance of preservation as telocollinite. An increase in vitrinite above partings has been related to changes in the type of vegetation; arborescent types might have been more able to establish themselves in deeper water (Shibaoka and Smyth, 1975).

Regardless of the cause, it does appear that the interruption of peat accumulation as represented by the deposition of an inorganic parting can modify the overall petrographic character of the seam. This may explain the lack of clear megascopic vertical zonation reported by Allshouse (1984) for columns from the freshwater environment in Somerset County: the seam at this locality contains thick inorganic partings.

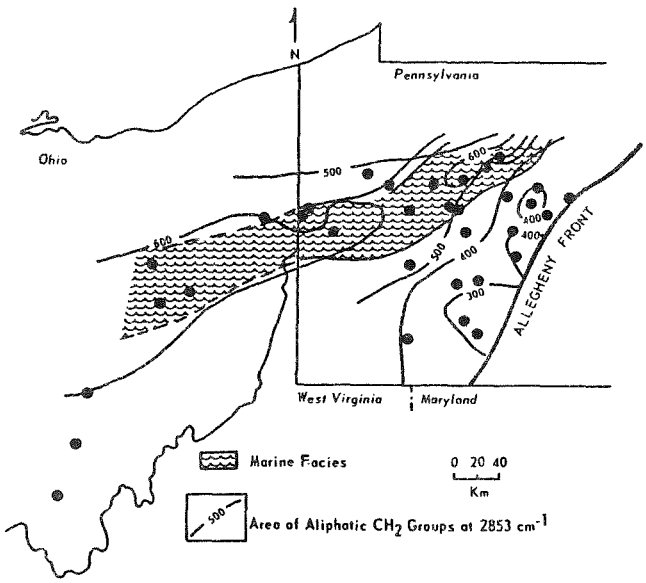

Figure 14. Distribution of aliphatic CH_2 groups at 2853 cm^{-1} for channel samples and marine facies of shales above the Lower Kittanning seam (facies distribution from Williams, 1960a, and Ting, 1967).

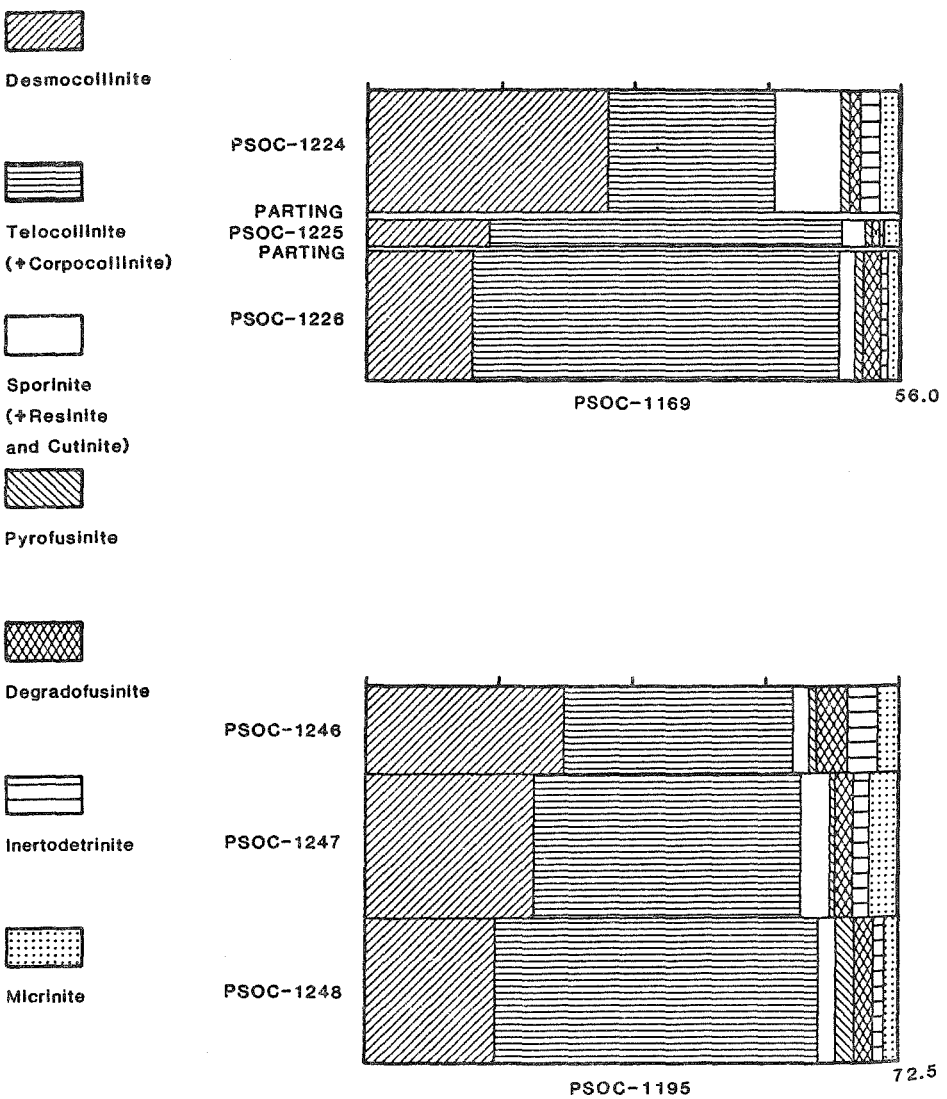

Figure 15. Petrographic seam profiles: Lower Kittanning seam (after Rimmer, 1985).

The lateral increase in telocollinite towards the central parts of the basin was explained above, in part, by increased subsidence which allowed better preservation of woody tissues. Vertical variation within the profiles suggests that during the early stages of peat accumulation fairly rapid subsidence existed across the entire basin, but especially in the center of the basin, resulting in high telocollinite contents at the base of the seam. Comparison of the desmocollinite ratios for lowermost subsections of columns provided as examples in Figure 15 indicates lowest desmocollinite and highest telocollinite content at the base of the seam in the center of the basin (PSOC-1169). Towards the margins of the basin, there are higher desmocollinite contents, not only in the overall channel sample composition (as indicated by the study of lateral variability, see Figure 3), but also in the base of the seam (PSOC-1195). This could be due to slower rates of subsidence in the marginal areas, compared to those found in the center of the basin. Of course, there are exceptions from the general trend just described, representing variation in local conditions.

Throughout the basin, the majority of sections show an increase in the desmocollinite ratio towards the top of the seam. The observation is consistent with the conclusion that subsidence rates increased late in the history of the peat swamp, resulting in an influx of relatively more alkaline, oxygenated waters. This would have accelerated the breakdown of woody tissues, and could have produced the increase in desmocollinite contents observed in the topmost subsections of the seam. Naturally the effects of inundation by marine waters were felt most strongly in the area underlain by marine roof rocks.

An additional control could have been the type of vegetation. It has been suggested by Habib (1964) that the area underlain by marine rocks had a more herbaceous vegetative cover during the final stages of peat accumulation, compared to the margins of the basin which continued to support arborescent vegetation. While the petrography can be explained in terms of chemical conditions within the swamp without requiring a change in vegetation, the spore data of Habib cannot be ignored. The presence of well-preserved telocollinite at the base of the seam across the entire basin may be explained by a more arborescent vegetation which prevailed throughout the swamp up until the initial effects of the marine invasion were experienced. Thus, in the center of the basin, during the final stages of peat accumulation, there may have been some change in vegetation type, which influenced the petrography and palynology of the upper section of the seam.

The increase in inertinite content, particularly degradofusinite and inertodetrinite, observed towards the top of the seam (Fig. 15) may also be related to the incursion by marine waters. One possible explanation is that it was washed as a fine, low-density debris into the deepest part of the basin. Alternatively, if a tidal influence was effective in the center of the basin, alternate periods of wetting and drying could have occurred, resulting in the higher degradofusinite content. It has also been suggested by Timofeev (see Stach and others, 1975, p. 220) that oxygenated waters brought in by tides might contribute to the formation of degradofusinite. Reworking, which could take place in a tidal zone, is indicated by the increased amounts of inertodetrinite in the top of the seam. Allshouse (1984) noted the presence of organic clasts in the top section of the seam which may have formed by reworking.

Under the alkaline conditions associated with the influx of marine waters, spores, cuticles, and resins would have been more resistant than woody tissue, and thus liptinite macerals should occur in increased proportions at the top of the seam.

Summary and Conclusions

Areal distribution of vitrinite maceral types within the seam can be interpreted as a response to pH/Eh of waters within the swamp and the influence of the rate of subsidence. Relatively high contents of telocollinite, the vitrinite type which represents larger, undegraded fragments of humic tissue, occur within the central part of the basin; this is concluded to be the result of the rapid burial, and thus preservation, of such material. In contrast, desmocollinite contents are highest at the swamp margins to the northwest and east; in this case more neutral, oxygenated fresh waters are thought to have aided decomposition of the plant tissues into a more finely divided type of vitrinite precursor.

The same explanation is offered to account for the vertical variation in telocollinite and desmocollinite contents. Telocollinite is enriched in the lower part of the seam, again because the rate of burial was sufficiently rapid to permit preservation of the tissues. By the time the upper peat layers were being deposited, subsidence had permitted the influx of relatively more alkaline, oxygenated waters, leading to the degradation of plant tissues and the enrichment of desmocollinite. Alternatively, in response to the greater influence of marine waters a change in vegetation type towards a community more enriched in herbaceous types could account at least in part for the shift from the coarser telocollinite to finer desmocollinite.

These effects upon the upper peat layers were more pronounced within the central part of the basin; the possibility that sedimentation here took place under relatively high energy conditions in a marine setting is supported by the presence of organic clasts, the corrosion of spores, detrital quartz grains, and an increased proportion of inertodetrinite. The proportion of sporinite also increases at the top of the seam, and it is known that this part of the seam is enriched in densospores. It is concluded that the duller, upper part of the seam in the central part of the basin represents a peat influenced by relatively more alkaline, possibly deeper, waters and supporting a more herbaceous vegetation. This interpretation supports the conclusions reached for this seam by Habib (1964) and Ting (1967), but is contrary to that suggested by Smith (1968) for similar petrographic and palynologic trends in the profiles of some British coals.

Certain inorganic components of the Lower Kittanning seam show clear areal patterns which can be related to depositional and other factors. The highest pyrite contents appear to be associated with that part of the seam which is overlain by brackish shales. The distribution of marcasite, however, is explained as being due to epigenetic formation. Relatively high quartz contents are found towards the north of the study area; the coincidence with a known basement high suggests that a source of this mineral lay in that direction. Kaolinite is enriched at the margin of the basin; a predominantly authigenic origin under relatively acidic freshwater conditions is supposed. Illite, on the other hand, increases toward the center of the basin and less alteration has presumably taken place. The existence of high-temperature illite/mica polytypes indicates that a significant proportion must be detrital.

Functional groups were determined by FTIR for hand-picked vitrinites and seam channels from the Lower Kittanning seam. Certain groups (aromatic 4 adjacent hydrogens and phenolic OH in the vitrinites and the aromatic stretching region for the channel samples) show a strong parallelism with the regional rank trends. Aliphatic CH_3 and aliphatic CH_2 stretching groups are not just rank related but show highest values in coals associated with the brackish and marine roof facies, respectively. It is suggested that the coals in these zones may have adsorbed relatively more lipid material which might be favored by such environments.

PROPERTIES AND OCCURRENCE OF BLOATING SHALES AND CLAYS IN THE PENNSYLVANIAN OF WESTERN PENNSYLVANIA

by
E. G. Williams, R. Holbrook, and E. Lithgow

Underclays and shales are two natural resources associated with the coal measures. Underclays are widely used as a raw material for refractory, semi-refractory, and face bricks. Shales are useful for sewer pipe and lightweight aggregate. This study concentrates on the geologic controls over the properties of shales for use in the manufacture of lightweight aggregate, and the geologic controls over the properties of underclays for use in the manufacture of bloating ladle refractories. Ladle bricks are used in lining the ladles which transport molten steel. In use, they expand irreversibly, sealing any cracks in the ladle lining. The industrial processes are similar in that both involve the trapping of a gas phase to cause bloating. They differ in that the bloating of lightweight aggregate occurs at lower temperatures (1000-1200°C) than ladle bricks (1350-1470°C). Lightweight aggregate bloats during an initial rapid firing. Ladle bricks are manufactured by slow firing at 1100°C for up to 80 hours. Bloating occurs when these bricks are reheated to 1350°C.

Bloating shales are those which expand twice or more times their original volume during fairly rapid firing. Commercial bloating is usually done by rotary kiln processing or sintering; in both cases the firing rate is much faster than the experimental rate (5/8°C/minute). Bloating results from the entrapment of gases which are evolved during firing. The material must have adequate viscosity to trap gas bubbles throughout the temperature range of bloating. The finished product contains a high percentage of closed pores with a bulk density between 35 and 75 pounds per cubic foot. Expanded shale finds its most important use as a substitute for heavy concrete aggregate (crushed stone, sand and gravel) where low bulk density is desired or required.

The extent of bloating in lightweight aggregate is a function of the mineralogy and chemistry of the shale. Figure 1 shows a corner of the three phase diagram, kaolinite-quartz-(illite and chlorite). Several areas on the diagram are outlined which contain predominantly marine shales, freshwater and brackish-water shales, and underclays. Each sample was fired and the resulting expansion was plotted on the phase diagram.

Approximately 63 percent of the samples falling in the area of marine shales were classified as bloaters. Approximately 17 percent of the samples falling in the area occupied by brackish and freshwater shales were classified as fair bloaters. And lastly, about 13 percent of the samples classified as underclays exhibited fair bloating characteristics. Therefore, classification of shales based on mineralogy or sedimentary environment permits a gross discrimination in bloating properties.

The correspondence between mineralogy, chemistry, depositional environment (marine, brackish, freshwater, and underclay), and bloating can be used to develop a rational geologic-mineralogic prospecting technique. Williams (1960a) mapped the freshwater, brackish-water, and marine shales in western Pennsylvania on the basis of fossils. His maps can be used to determine the probable mineralogy of a shale at a given location. Figure 2 shows the distribution of freshwater, brackish-water, and marine fossils in the Lower Kittanning shale. Marine shales are generally the

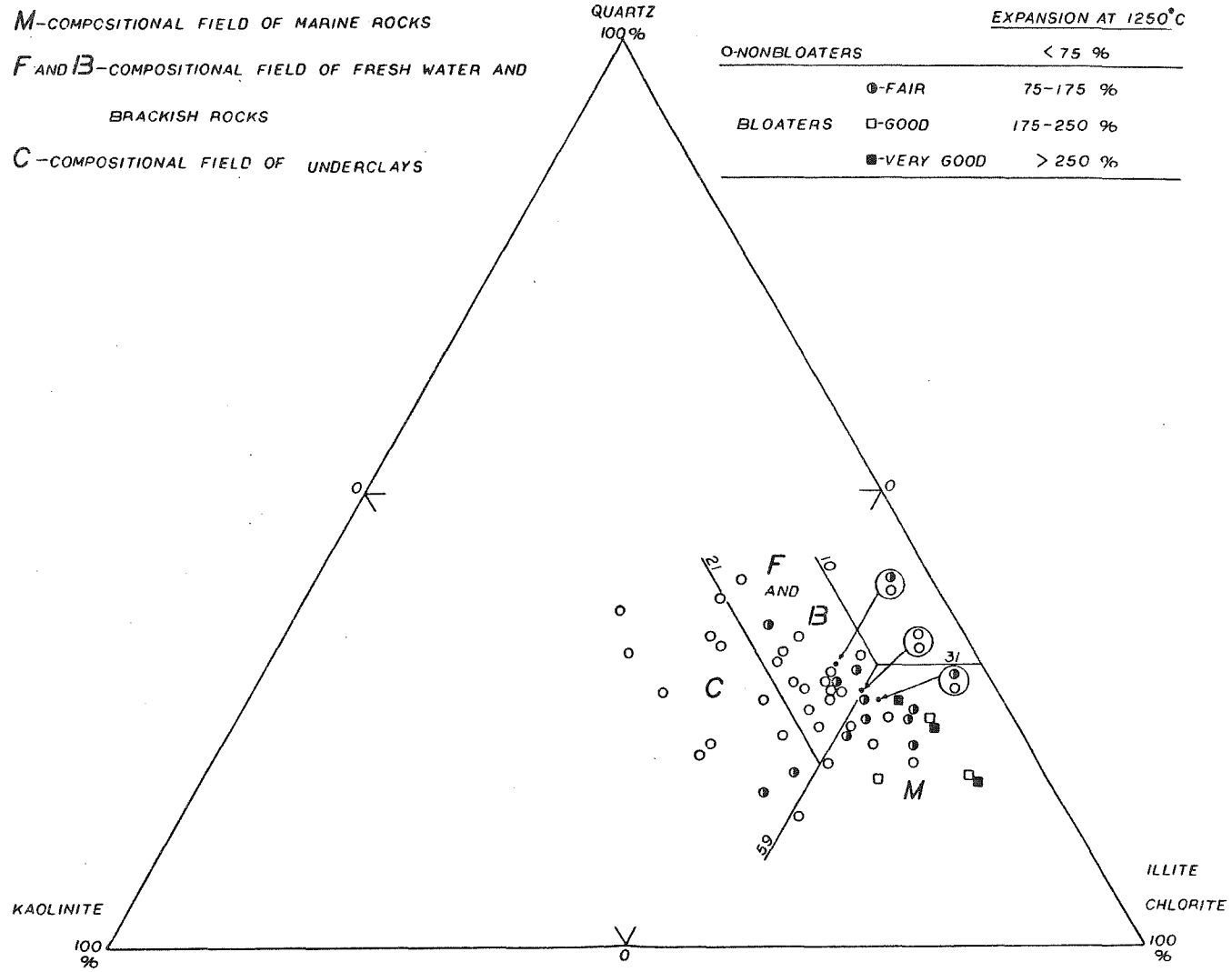

Figure 1. Three phase mineral diagram illustrating the relationship between mineral composition, paleoenvironment, and expanding characteristics of shales and underclays from the Allegheny Group in western Pennsylvania (from Williams and others, 1974).

best bloaters. Additional study has shown that within the marine environment, the best bloaters are found in the basinal axes. This relation should greatly reduce the prospecting and testing costs for anyone interested in the manufacture of light-weight aggregate.

The phenomenon of bloating in refractory ladle bricks is also caused by the trapping of a gas phase. The ASTM requires that they have a P.C.E. of 15 (M.P. = 1470°C) or greater, and a linear reheat expansion of 15 percent or more. In ladle bricks, the expansion occurs only after the bricks have been manufactured and burned for over 30 hours at 1100°C. Most of the reactions which generate gas for light-weight aggregate occur below 1100°C. Analysis reveals that over 97 percent of the gas evolved from a ladle brick is oxygen. The two possible reactions which could produce the gas at these temperatures (1200-1350°C) are the reduction of hematite:

$$Fe_2O_3 \xrightarrow[\log pO_2 = 10^{-2}]{1350°C} 2FeO + 1/2\ O_2$$

and the dissociation of mica anhydride.

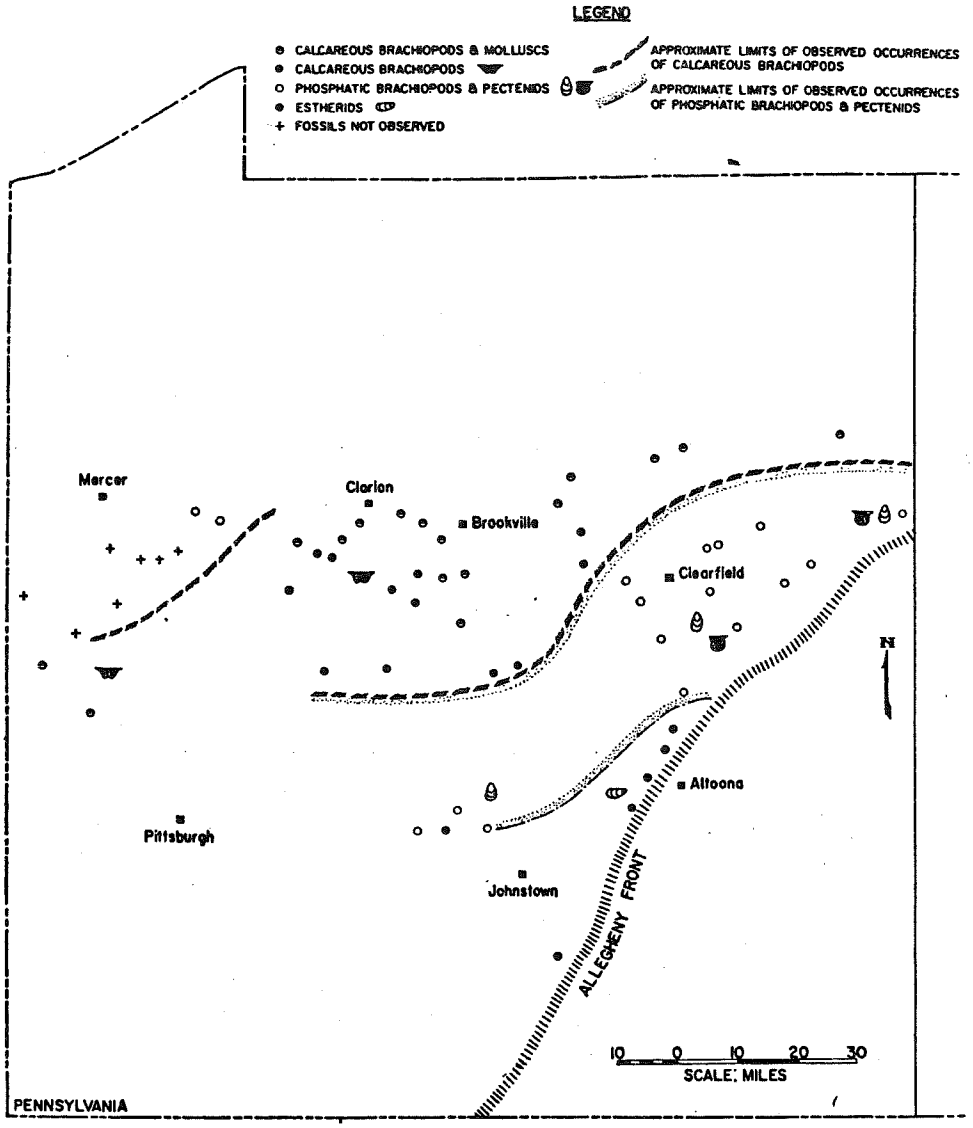

Figure 2. Biofacies map of the Lower Kittanning shale in western Pennsylvania. Calcareous brachiopods are marine; phosphatic brachiopods and pectins are brackish; estherids are freshwater. Bloating shales are largely confined to the marine area (from Williams, 1960).

Whether or not the bricks meet their 15 percent reheat expansion requirement depends upon the ability of the brick to trap gas. Only bricks with less than 10 percent porosity exceeded 15 percent linear reheat expansion. Percent reheat expansion is probably also a function of the volume of gas released.

The development of low porosity is a function of the mineralogy of the raw materials. Clays with high plasticity can be pressed into less porous green bricks. The amount of mica in an underclay is critical, because it forms the glassy phase that fills open pores, thus decreasing porosity. Bricks which exceeded 15 percent reheat expansion could be separated from those that failed to meet specifications with 85 percent reliability, using 37 percent (mica + vermiculite) as a discriminant. Figure 3 is the three phase diagram kaolinite-quartz-(mica + vermiculite). Two areas are defined on this diagram as "optimum clay" and "useable clay." Both areas contain over 37 percent (mica + vermiculite). The optimum clay has over 40

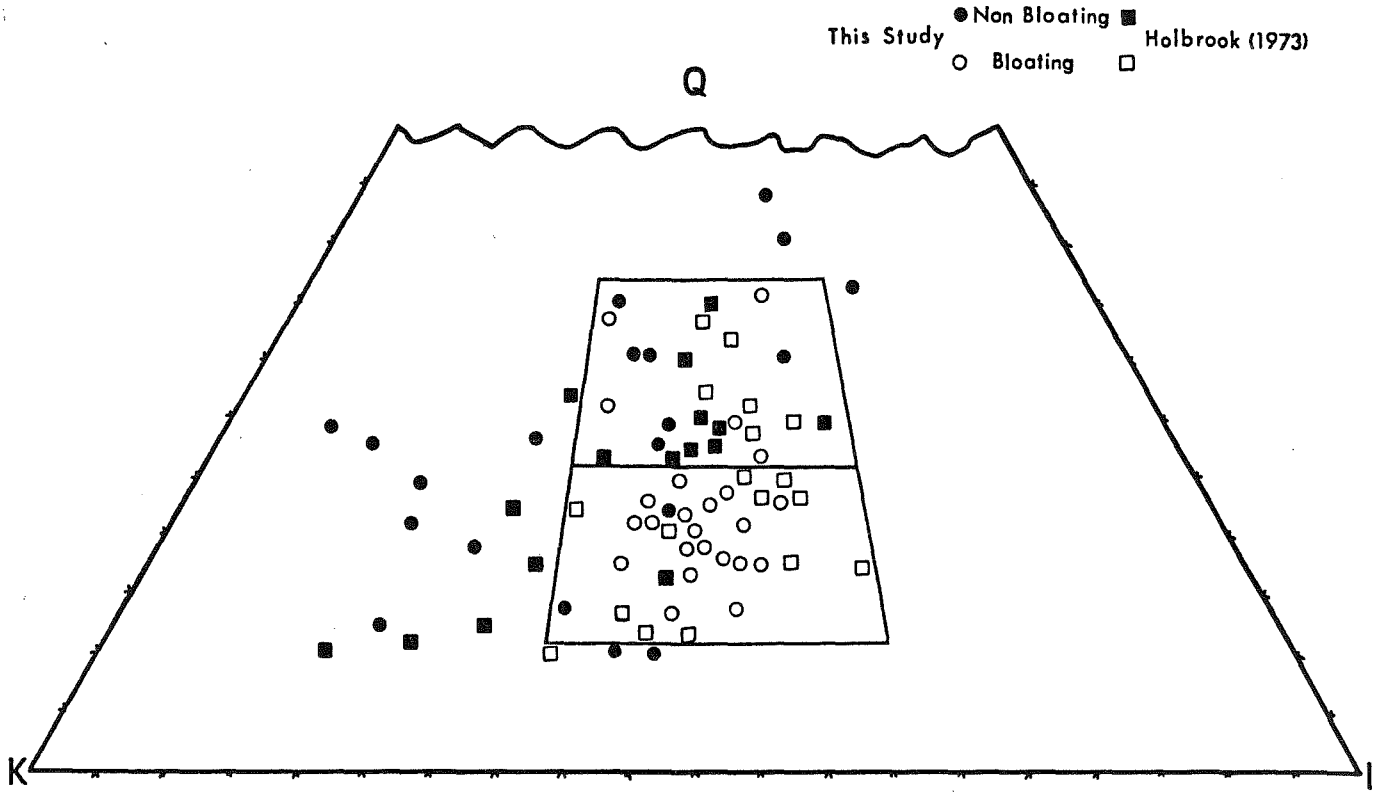

Figure 3. Three phase mineral diagram illustrating the relationship between mineralogy and linear reheat expansion of ladle bricks. Open dots indicate bricks which have experienced more than 15 percent linear reheat expansion; closed dots are those samples which have experienced less than 15 percent. Circles are data from Holbrook (1973); squares are data from Onasch (1976).

percent kaolinite (to maintain high P.C.E.) and less than 25 percent quartz; quartz has a marked detrimental effect upon porosity. The useable clay has less than 40 percent quartz and less stringent kaolinite requirements.

The development of the above mineralogic criteria for ceramic behavior allows a rational geologic-mineralogic prospecting technique. The kaolinite/(mica + vermiculite) ratio and the percent quartz in the Lower Kittanning underclay were mapped throughout western Pennsylvania. Seventy-eight locations were sampled in order to construct the maps shown as Figure 4. In general the kaolinite/(mica + vermiculite) ratio decreases from the basin margin toward the basin axis. The underclays around the basin margin contain too much kaolinite, and those in the basin axis contain not enough to meet the defined mineralogic criteria. The area marked with vertical lines contains a generally satisfactory clay mineralogy. However, the percent quartz exhibits much greater variation than does the clay mineralogy and therefore cannot be accurately predicted on a regional basis. Hence, after a favorable location has been selected on the basis of clay mineralogy, additional tests for quartz must be made.

Parts of the results reported here are taken from Lithgow (1972), Holbrook (1973), Oldham (1979), and Onasch (1976). The research was supported by the Mineral Conservation Section and Small Industries Research of The Pennsylvania State University.

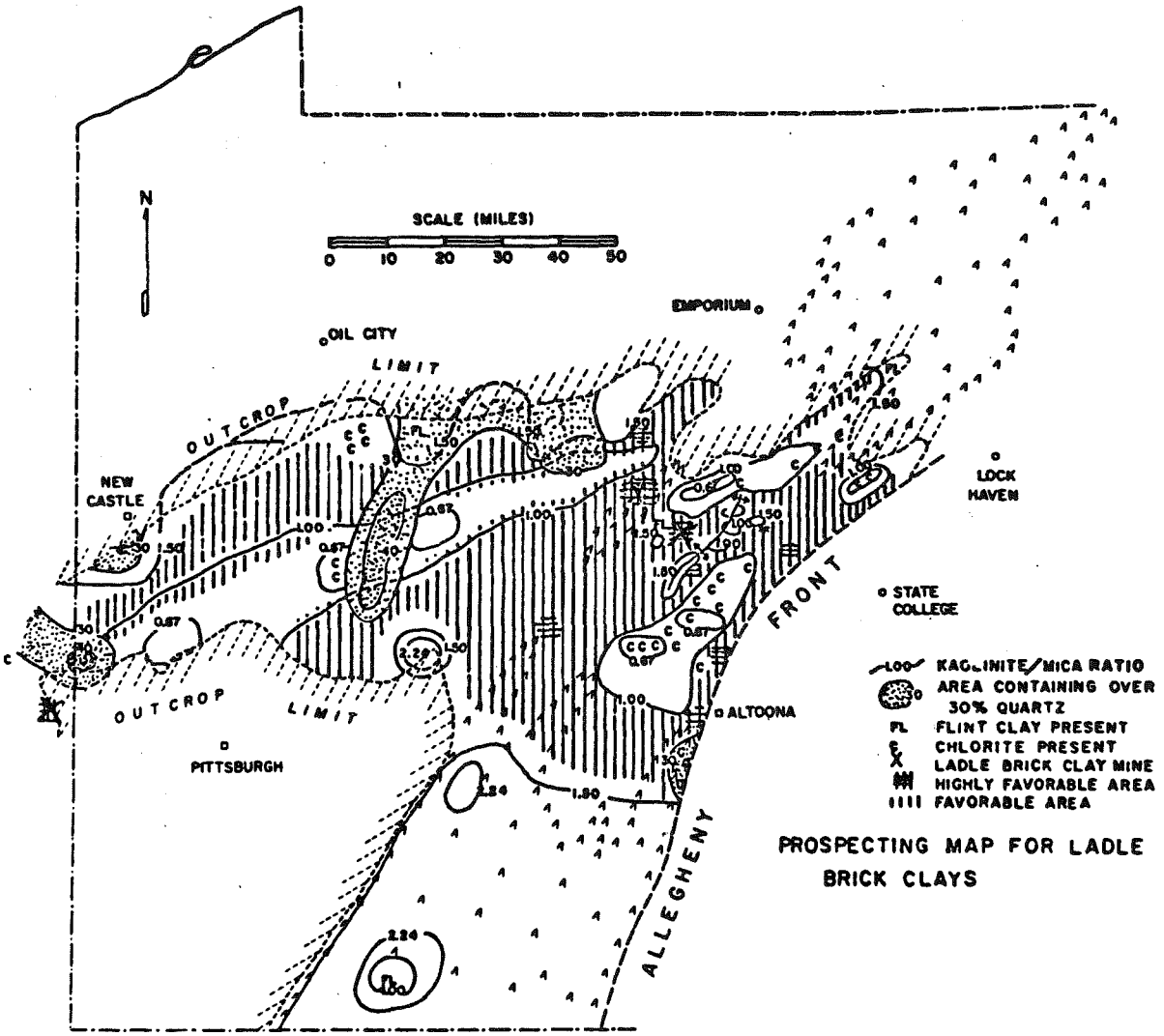

Figure 4. Map of the kaolinite/mica ratio, and the percent quartz in the Lower Kittanning underclay, showing the areas most favorable for the occurrence of ladle brick clays (from Holbrook, 1973).

AN ANALYSIS OF FACTORS CONTROLLING THE VARIATION IN POROSITY OF PENNSYLVANIAN SANDSTONES IN THE ALLEGHENY PLATEAUS OF WESTERN PENNSYLVANIA

by
Hue Chung Chou

It has long been known that the fixed-carbon contents of the coals in Pennsylvania systematically increase from west to east at rates which are greatest in a direction approximately perpendicular to regional structural trends (White, 1925, Fig. 1). Also as shown in Figure 1, the rate of increase is greatest at the location of Chestnut Ridge, which marks the boundary between the High Plateaus to the east and the Low Plateaus to the west. Chestnut Ridge is the surface expression of one of the two largest anticlines in the Allegheny Plateaus, and so represents a significant structural change from the essentially flat lying rocks of the Low Plateaus to the broadly arched rocks of the High Plateaus.

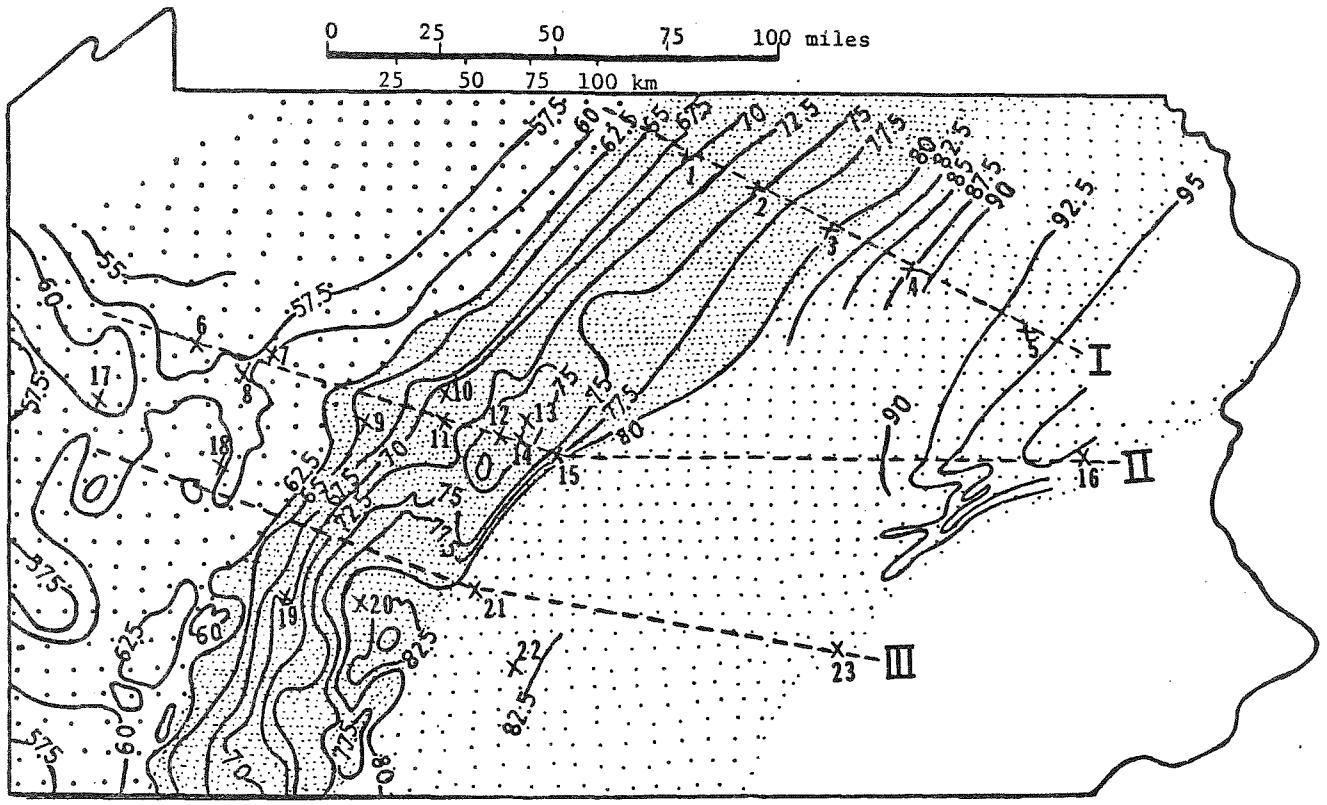

---- I (PAXTON) : —1.Gaines Basin(B) 2.Blossburg B. 3.Barclay B. 4.Bernice B.5.N.Anthracite B.

TRAVERSES : ---- II (CHOU) : { 6.Emelton 7.Clarion 8.Rimmersburg 9.McGees Mill 10.Hyde Town
11.Curwensville 12.Bogg Town 13.Free Port Mine 14.Philipsburg
15 Port Matilda 16.Jim Thorpe

---- III (CHOU) : { 17.New Castle 18.Kittanning 19.Chestnut Ridge 20.Laurel Ridge
21.Cresson 22.Broad Top 23.Harrisburg

SHADED AREA : Valley and Ridge High Plateau Low Plateau

Figure 1. Coal isocarb (fixed carbon, dry, ash-free) distribution across Pennsylvania. Dashed lines indicate three traverses from both Paxton's (1983) thesis and this study. X represents sample locality. (Modified after White, 1925.)

Paxton (1983) demonstrated that Pennsylvanian sandstones sampled along a traverse extending across the northern Allegheny Plateau into the northern Anthracite Basin exhibited systematic increases in bulk density and corresponding decreases in porosity, both closely correlated with fixed carbon. Paxton's values are shown on Figures 2 and 3. Because bulk density and porosity are highly correlated, it is only necessary to show one; because porosity is the more important variable, it is the one illustrated. Paxton explained the regional porosity changes by assuming an increased depth of burial from 3 km in the Allegheny Plateaus to 9 km in the Anthracite Basin to the east, almost all of which would have been removed by later erosion.

Levine and Davis (1984), studying anisotropy of coals in the Anthracite Basins, concluded that the coal rank and reflectance were produced before folding and thus supported the burial-depth view of Paxton. However, Levine believed that the 9 km of overburden required in the Anthracite Basins was partly produced by thrust faulting.

Hower and Davis (1981), in studying reflectance of coals in western Pennsylvania, showed that this variable changed with fixed carbon, exhibiting the most rapid increase at the Chestnut Ridge anticline. They concluded that, because the existing Pennsylvanian and Permian sections decrease in thickness eastward across the Plateau, the increase in rank of coals was caused by increase in geothermal gradient.

In the present study, we have studied the bulk density, porosity, and petrography of lower Allegheny sandstones in two traverses across Pennsylvania, shown on Figure 1. At each locality, coarse-, medium-, and fine-grained sandstones of the

POROSITY/ DISTANCE

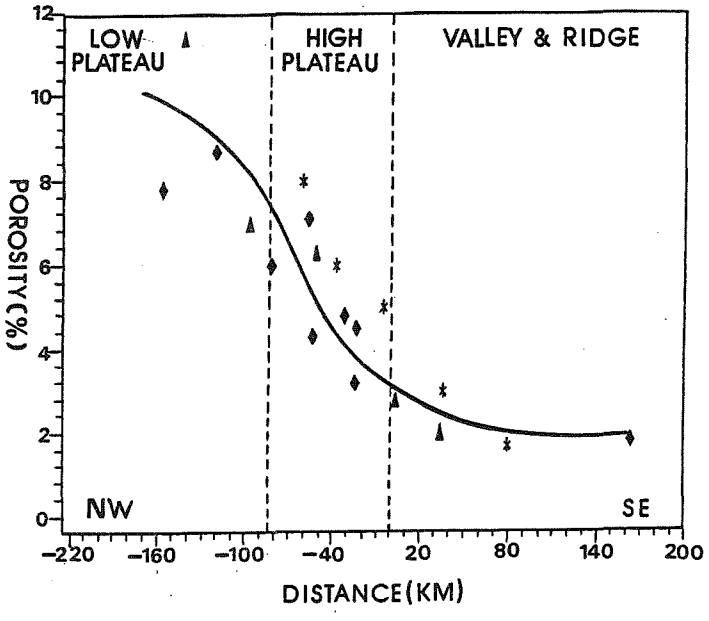

LEGEND: TRAVERSE ✱✱✱ I ♦♦♦ II ▲▲▲ III

Figure 2. Variation in sandstone mean porosity with distance of three traverses across Pennsylvania.

POROSITY / FIXED CARBON

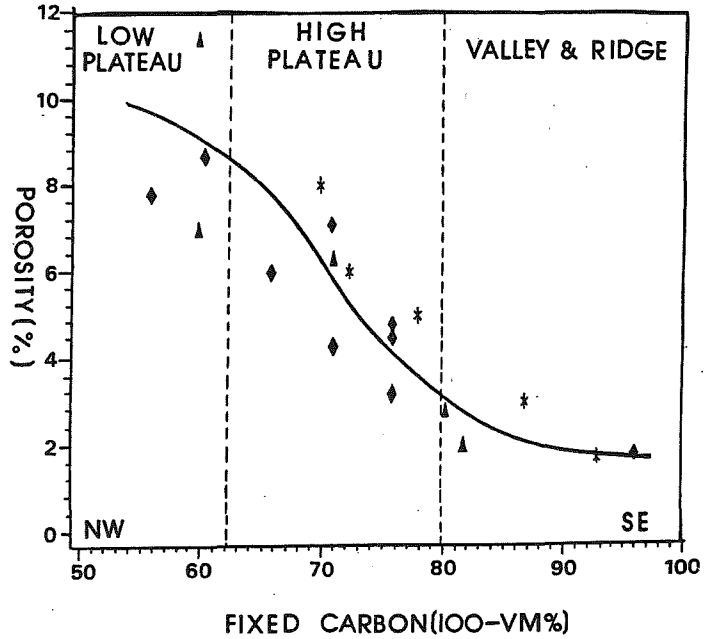

LEGEND: TRAVERSE ✱✱✱ I ♦♦♦ II ▲▲▲ III

Figure 3. Variation in sandstone mean porosity with fixed carbon of three traverses across Pennsylvania.

same mineral composition were sampled. These sandstones are low-rank graywackes consisting of approximately 70 percent quartz and 30 percent labile rock fragments and clays. The porosity values shown in Figures 2 and 3 are the averages of the measurements made on the three sizes. Observe that the maximum rate of decrease in porosity occurs in the area between Chestnut Ridge and the Allegheny Front, a distance of about 35 miles and coinciding exactly with the area of the High Plateaus. Because we do not observe any significant regional changes in the mineralogy of the matrix or cement of these sandstones, we conclude, as did Paxton, that the changes in porosity and bulk density have resulted from physical processes attendant upon either increased depth of burial or lateral compression or both. Because 10 percent layer-parallel shortening has been documented in the area of the High Plateaus by Nickelsen (1966), and because the Pennsylvanian and Permian sections thin in the direction of decrease in porosity, we believe that the compression of sandstones by layer-parallel shortening is a possible mechanism to explain the porosity changes. The decrease in porosity across the Allegheny Plateau can be accounted for by the 10 percent lateral shortening estimated by Nickelsen (1966) for the High Plateaus area.

Further evidence for lateral compression as the mechanism for explaining the decrease in porosity is the fact that little or no change occurs east of the Allegheny Front or west of Chestnut Ridge. Subsequent to porosity reduction to 2 percent, further compaction or compression would likely not have much effect on porosity. In the areas west of Chestnut Ridge, the amount of lateral shortening has been negligible and so the porosity remains unchanged even though the fixed-carbon content of the coals increases to the east.

Arguments against lateral compression as the mechanism for porosity reduction come by comparing the porosity values for the three traverses shown in Figure 2. Traverses 1 and 3 occur in the areas of highest structural amplitude in the Allegheny Plateaus; traverse 2 occurs in an area of less structural amplitude and presumably less shortening by folding. However, as the graphs show, the porosity values are not appreciably different. Because the fixed-carbon contents of coals are temperature dependent and because compaction may be the principal process in porosity reduction, these relations would lend support to the increased-overburden hypothesis of Paxton (1983) and Levine and Davis (1984). This would require approximately 9 km of section to have been removed at the Allegheny Escarpment, most of it post-Paleozoic in age. It would also require an equal amount to have been removed in the folded Appalachians, which is about twice that estimated by Gilluly (1964) from computations based on the thickness of post-Paleozoic sediments in the Atlantic coastal plain and shelf.

The above argument would only hold if all the shortening was produced by folding. If most was produced by layer-parallel shortening, then the amount of shortening might not be different in the structurally different parts of the High Plateaus. We have not yet investigated this possibility. However, if differences are present, this would lend credence to the depth-of-burial concept.

I am attempting to test the vertical vs. lateral compression hypotheses by a petrographic analysis of oriented thin sections to see if a preferred direction of pressure solution in quartz can be found. For now, however, it would appear that the detection of porosity and bulk-density changes in three traverses across the Allegheny Plateaus, with the maximum rate occurring in the area of the High Plateaus, represents a real trend which is likely to have significance in evaluation of these areas for oil and gas as well as groundwater and the production of acid mine drainage.

GEOMORPHOLOGY AND HYDROLOGY OF SURFACE-MINED WATERSHEDS, BITUMINOUS COAL FIELDS, CENTRAL PENNSYLVANIA

by
Thomas W. Gardner, Jeffrey J. Gryta, Corinne R. Lemieux,
David W. Jorgensen, and Kimball C. N. Touysinhthiphonexay

Introduction

As of 1972 surface coal mines covered over 4000 km^2 of Appalachia (Gregory and Walling, 1973) with the possibility that the total disturbed area could double by the turn of the century (National Research Council, 1981). In an attempt to reduce surface erosion and acid mine drainage from surface coal mines, federal and state agencies have promulgated regulations which require the reclamations of mine pits and spoil banks. The general reclamation procedure is designed to return all disturbed areas to their approximate original contour by transporting, back-filling, compacting, and regrading spoil to eliminate all highwalls, spoil piles, and depressions. After grading, all surfaces are covered with topsoil and revegetated. Regrading overburden and topsoil to the approximate original topography requires the passage of heavy machinery which results in compaction of the replaced topsoil to such an extent that infiltration rates can be significantly reduced (National Research Council, 1981, p. 138) and the volume of surface runoff is materially increased over that of ungraded spoil (Sawyer and Crowl, 1968). Comparison of hydrographs for mined and unmined watersheds in Kentucky (Collier and others, 1970) and Tennessee (Minear and Tschantz, 1974) shows a considerable difference in the response of these basins to intense rainstorms. For a given intensity of precipitation, the mined basin hydrographs for sediment concentration and water discharge have sharper peaks and attain much greater magnitudes than those of the unmined basins. Furthermore, compaction and lack of moisture retention greatly reduce both the survival and growth rates of vegetation planted on graded spoil, thereby delaying complete reclamation and extending the period of surface erosion, sediment production, and increased peak discharge (Sullivan, 1967; Sawyer and Crowl, 1968) for periods extending over tens of years (National Research Council, 1981, ch. 6).

High rates of water and sediment discharge per unit area are manifestations of landscape instability which exists to varying degrees on many reclaimed surface mines (Fig. 1). The causes of, changes in, and appropriate reclamation design for this instability are the subject of this paper.

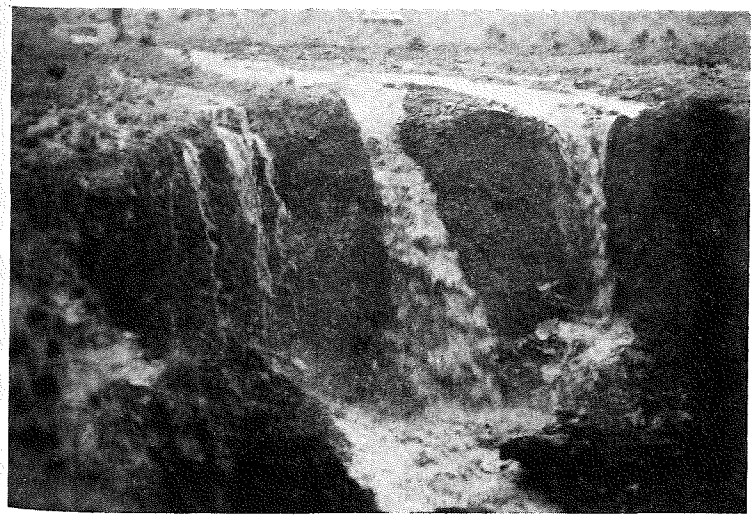

Figure 1. During a typical summer thunderstorm turbid water plunges over a four-meter-high waterfall into a gully formed in a reclaimed surface mine. The gully network is eroding through a convex-up toeslope of overburden reclaimed five years earlier. Large sections of the gully wall have collapsed into the channel supplying large volumes of poorly sorted sediment to the ephemeral stream. Flume used to measure discharge is visible in upper left corner. The gully drains 0.2 km^2, has eroded 2100 m^3 of reclaimed overburden, and is 660 m long.

Watersheds which have been disturbed by surface coal mining provide an excellent field laboratory for the study of hydrologic and geomorphic processes for several reasons. First, because of the potentially rapid rates of landscape modification in disturbed watersheds, it is possible to investigate the nature of landscape response as reclaimed surfaces move toward an equilibrium state. Second, given the relatively small size of the disturbed watersheds (10^2 to 10^5 m^2) it is possible to quantify mass balance equations for water and sediment, and to investigate the sources, allocations, and residence times of sediment in sinks (depositional sites). Third, data from these studies can be used to evaluate laboratory-scale, experimental geomorphic models of landscape dynamics and evolution which provide the basis for much of our knowledge of landscape evolution (Schumm, 1977). Furthermore, a better understanding of the fundamental processes that control the hydrology and geomorphic evolution of these disturbed watersheds should result in effective reclamation designs that are stable over long time intervals (10^3 yrs).

Dominant Geomorphic Processes

Causes of Instability

Examination of undisturbed watersheds in central Pennsylvania indicates that existing drainage networks and hillslopes are relatively stable (Hack, 1960). The driving force determined by water discharge/runoff and channel slope is in approximate equilibrium with the force resisting erosion which is determined, to a large degree, by soil shear strength and particle grain size. When equilibrium exists, channel erosion, sediment transfer, and deposition tend to be minimized.

It can be shown that the equilibrium form which a slope tends to attain is dependent upon the type of process acting on it. Operating over geomorphically long time intervals, soil creep tends to produce convex-up slopes, whereas channelized flow tends to produce concave-up slopes (Carson and Kirkby, 1972). Regrading surface coal mines to the approximate premining topography, as required by the Surface Mining Control and Reclamation Act of 1977, produces convex-up slope forms for two reasons. First, convex-up slope elements dominate upper hillslope segments in humid temperate climatic zones typical of the Appalachians. Second, backfilled areas typically have higher porosity than undisturbed bedrock; a 20 percent increase in porosity is typical. This volumetric expansion can create convex-up bulges in the slope form during reclamation. The convex slope segment often occurs on the toe of many reclaimed backfills where the downhill cast of spoil from the first cut meets the undisturbed land.

Fluvial erosion (slope wash, rilling, and gullying), not soil creep, is the dominant geomorphic process on newly reclaimed surfaces (Gryta and Gardner, 1983, 1984), and the stable fluvial profile is concave-up (Leopold and Langbein, 1962). Therefore, reclamation that permits channelized flow to pass across convex-up slopes can result in high rates of sediment transport as the process of gullying establishes stable, concave slope elements. In essence, a drainage network will develop on the reclaimed surface. Thus, the surface forms of many reclaimed coal mines are not in equilibrium with the geomorphic processes that erode those surfaces over the long term (up to 10^3 yrs).

Surface Mine Hydrology

The hydrologic system of reclaimed surface mines (Fig. 2) determines the nature and degree of landscape instability as well as the short- and long-term geomorphic evolution. Initially, rainfall is apportioned between surface runoff and ground-

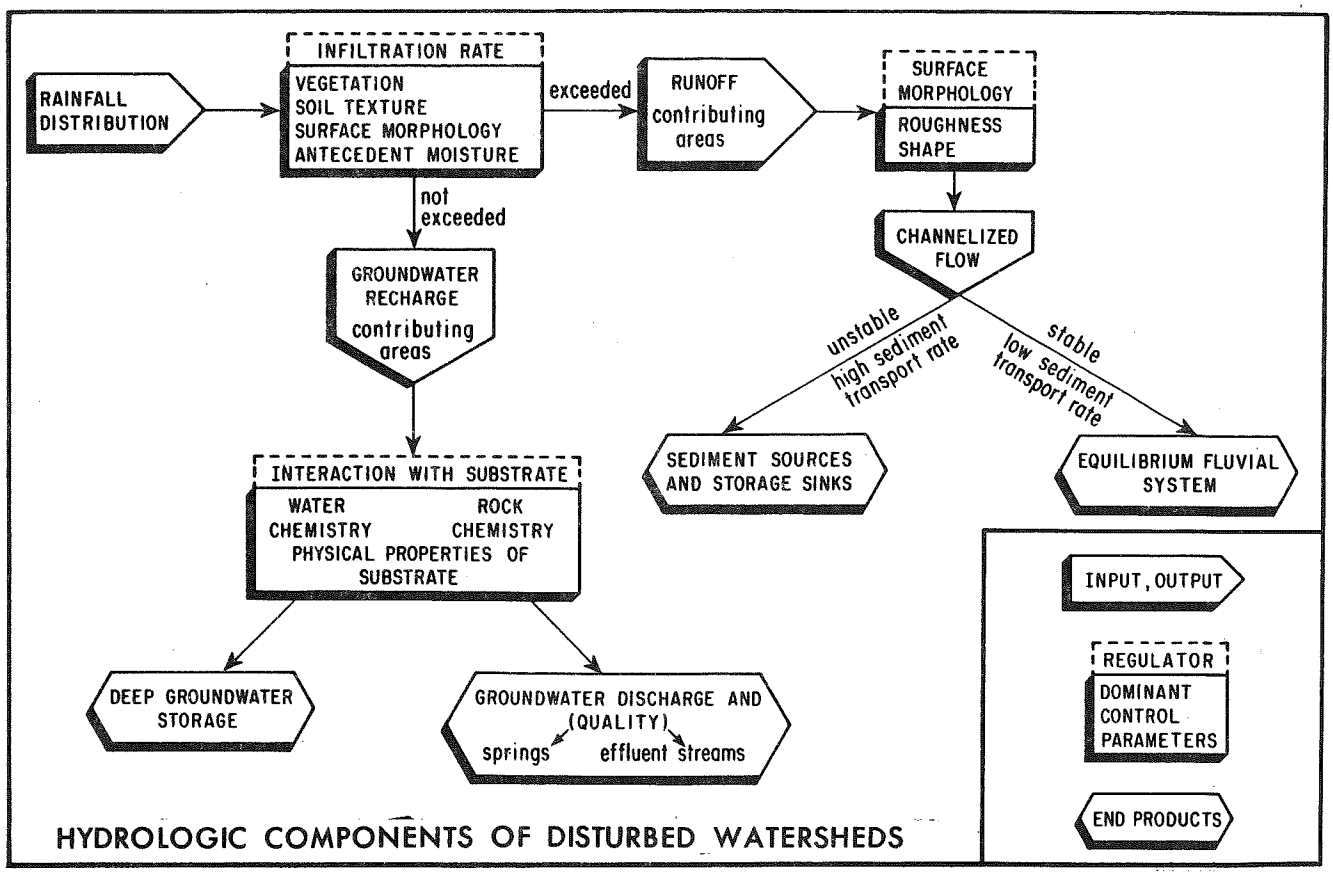

Figure 2. Flow diagram illustrating the hydrologic components, fluid pathways, and independent variables that control the hydrology of disturbed watersheds. The evapotranspiration component can be neglected for the short-duration, high-intensity storms that tend to drive this particular geomorphic system.

water recharge by the infiltration characteristics of the reclaimed spoil surface. The initial value of, and subsequent change in, the infiltration capacity are critical parameters that will determine, to a large degree, the geomorphic evolution of reclaimed surfaces. Seventy-eight dripping infiltrometer tests performed on one- to four-year-old reclaimed surfaces of five coal mines demonstrate the mining-induced changes in infiltration and changes in infiltration characteristics through time following reclamation (Jorgensen and Gardner, in press). First, infiltration rates in the year following reclamation are uniformly low, almost an order of magnitude lower than undisturbed forest soil infiltration rates (Byrnes, 1961), and are independent of soil texture, slope, and surface character. Secondly, infiltration rates steadily increase in the second through fourth years following reclamation (Fig. 3). In addition, soil and surface properties can be used to predict infiltration capacity at each age of reclamation; the variables contributing the most to multiple regression equations of infiltration rates and volumes are slope, percent silt and clay, percent vegetation, and bulk density. Lastly, recovery of infiltration rates toward their premine level is not uniform at all mines. Figures 4 and 5 demonstrate the variability of infiltration rate change over four surface ages. Extrapolation of the temporally limited data indicates that anywhere from five to 500 years may be required to establish premining infiltration rates on reclaimed mine surfaces. The mine site properties which control the magnitude of this change are soil texture (predominantly the amount of silt and clay which can plug the soil surface), vegetation cover, and, possibly, surface slope. Ultimately, these factors may themselves be controlled by overburden lithology and chemistry, premine soil conditions, and mining method.

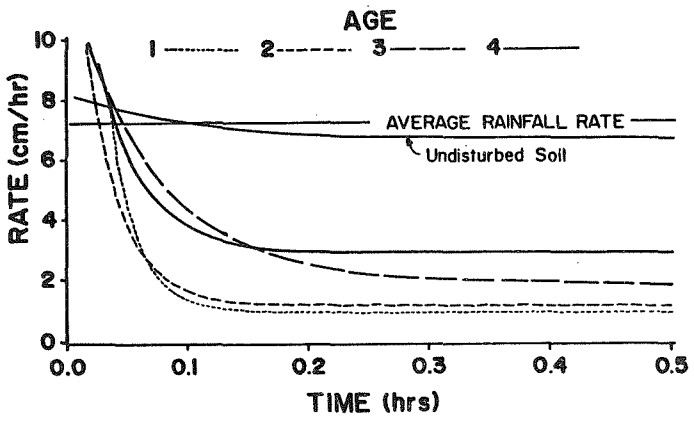

Figure 3. Average infiltration curves of reclaimed surface mines as a function of time; 1, 2, 3, and 4 indicate age in years since reclamation.

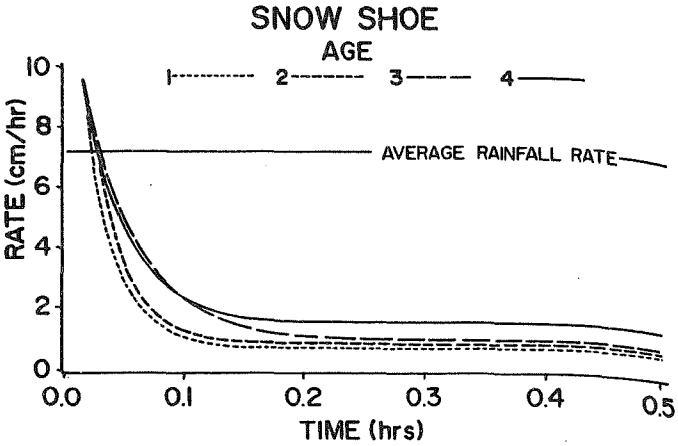

Figure 4. Change in infiltration rates over a four-year period for one reclaimed surface mine near Snow Shoe, Pennsylvania. Note the poor recovery compared to Figure 5.

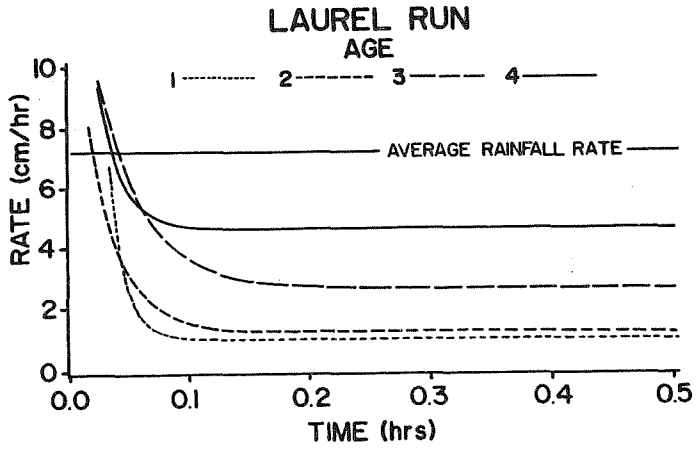

Figure 5. Change in infiltration rates over a four-year period for one reclaimed surface mine near Laurel Run. Note the nearly five-fold increase in infiltration rate.

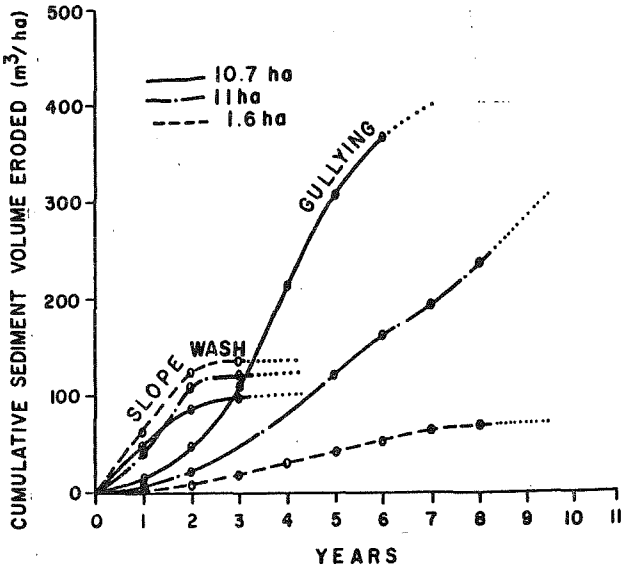

Figure 6. Volume of sediment eroded from reclaimed spoil surfaces as a function of soil age, drainage basin size, and surface process.

Given these low infiltration rates, a given rainfall event will produce a significantly larger volume of water per unit area from reclaimed surfaces than from undisturbed forest soils. Low infiltration rates will apportion most rainfall to the surface runoff segment of the flow diagram (Fig. 2). This is precisely the desired effect if the long-term goal is to minimize acid mine drainage, but it also necessitates careful design of the surface topography to conduct the runoff discharge from the reclaimed surface with minimal erosion. Furthermore, the surface must remain stable over the long term until higher infiltration rates are produced by vegetation growth and soil development.

Runoff initially flows as sheet wash across a reclaimed surface, but surface morphology, slope length, and roughness eventually concentrate sheet wash into channelized flow. Although much reclamation is directed toward the control of sheet

wash, data indicate that channelized flow in the form of gullying can produce much more sediment in the long term, and thus is more deleterious to spoil stability and downstream ecosystems than sheet wash (Fig. 6). This is particularly true with increasing drainage basin size and drainage network integration.

During the first several years after reclamation, sheet wash is the dominant surface process, eroding an order of magnitude more sediment than gullying. However, as a vegetation mat and surface armor develop, sediment contribution from sheet wash falls off drastically. On larger surfaces generally exceeding 25 acres (10 hectares), sufficient runoff is available to produce large gully networks on convex-outward slopes within about three years. These unstable gully networks, which form as a consequence of runoff volume and slope configuration, continue to expand in a positive feedback loop, where an increase in gully development promotes more efficient drainage integration and sediment transport, in turn causing more gullying. This model explains the rapid increase in the volume of eroded sediment (Fig. 6) and the transfer of large volumes of sediment through the gully network and onto alluvial fans adjacent to the mine site (Fig. 7). Studies of gully-fan systems on reclaimed surface mines in central Pennsylvania (Gryta and Gardner, 1983, 1984) have documented cyclic episodes of degradation and aggradation which occur during fall through spring and summer seasons, respectively (Figs. 8 and 9). Gully filling is initiated in the fall by mass wasting of sidewalls during periods of low-intensity steady rain and accelerates in the winter and early spring from freeze-thaw cycles. During the fall-winter-spring cycle most sediment is stored within the gully although higher intensity storms can cause local erosion along oversteepened channel slopes in the gully. Along fans episodic cutting or filling occurs simultaneously during individual storm events in the fall-winter-spring cycle depending upon storm characteristics and local slope (Fig. 10, see time = T_2 for an example). During more intense summer thunderstorms, gully channels erode (Fig. 10, time = T_3 and T_4) but fans alternately cut and fill (Fig. 10, time = T_2, T_3, and T_4) producing a complex sequence of cut-and-fill terraces (Fig. 11).

Rapid evolution of these disequilibrium gully-fan systems permits analysis of the allocation and grain size distribution of sediment in fluvial storage sites.

Figure 7. Large gully-fan system on convex-out toeslope of a five-year-old reclaimed surface mine as seen during an average summer thunderstorm. Note coalescing alluvial fans at bottom of photograph. See Figure 1 for gully size.

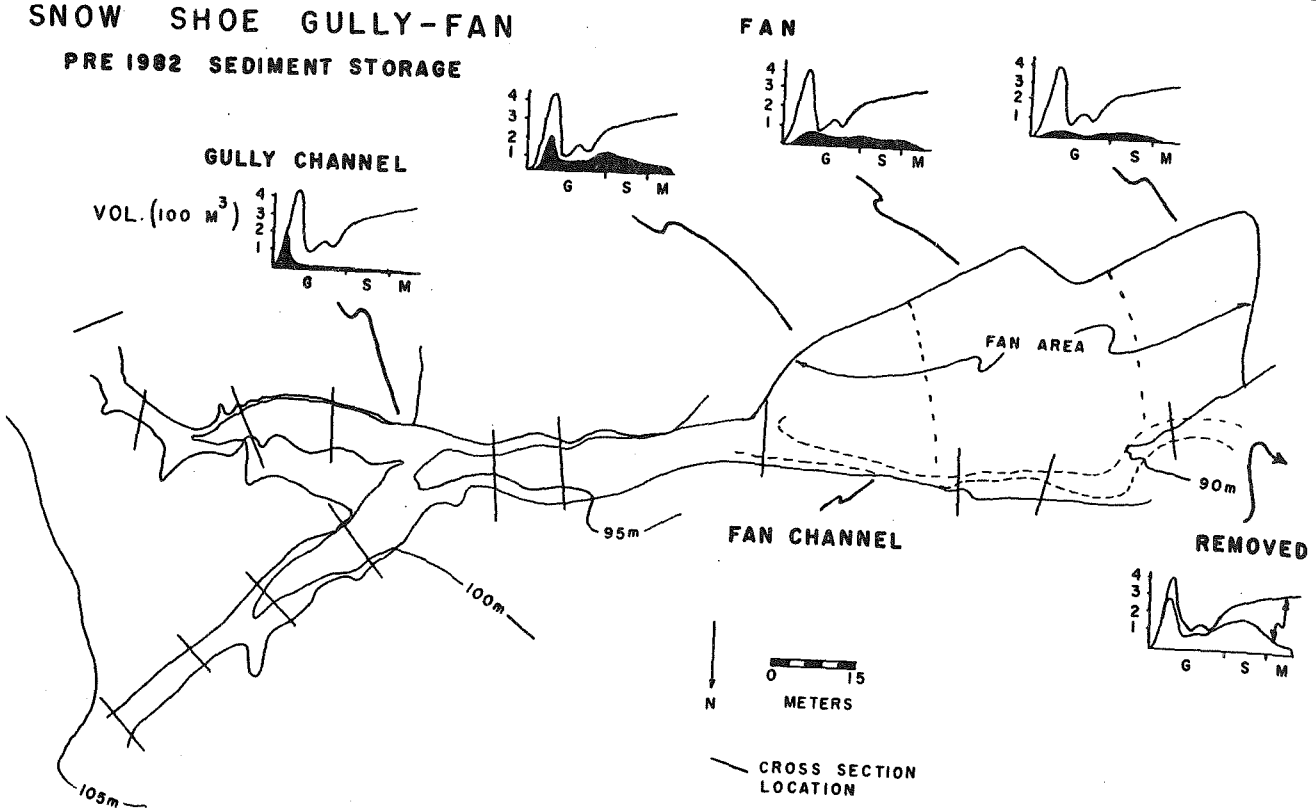

Figure 8. Plan view of one of the larger gully systems at Snow Shoe, Pa. Climatic data, sediment aggradation and degradation cycles, cross sections, and longitudinal profile changes are summarized in Figures 9, 10, and 11. The distribution of sediment (g = gravel, s = sand, m = silt + clay) is discussed later.

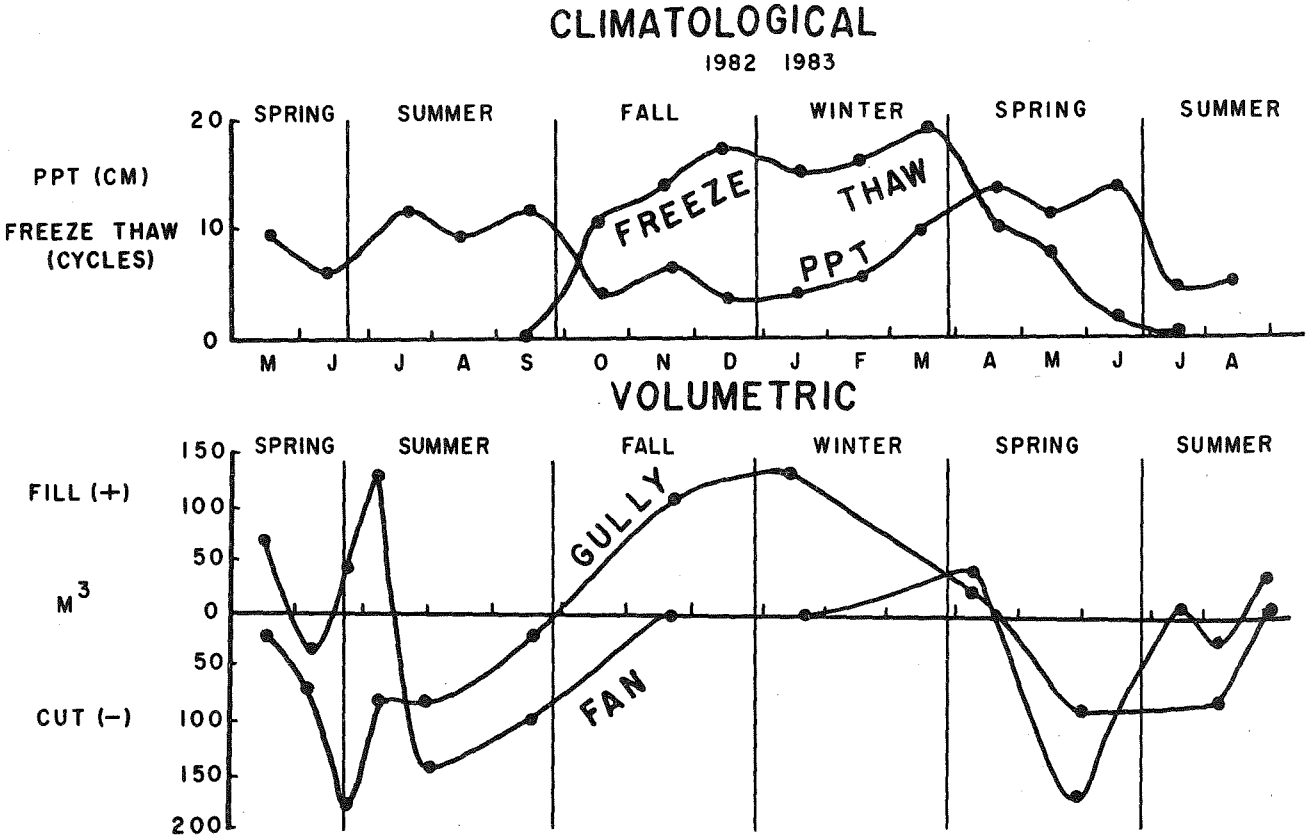

Figure 9. Typical yearly cycle of cut and fill on a gully-fan system (see Fig. 8) and a summary of concurrent climatic data (Clearfield, Pa.). Gully aggradation during fall, winter, and early spring coincides with an increase in number of freeze-thaw cycles. Subsequent aggradation (fill) on the fan downstream of the gully occurs during the following summer when the gully is degraded (cut).

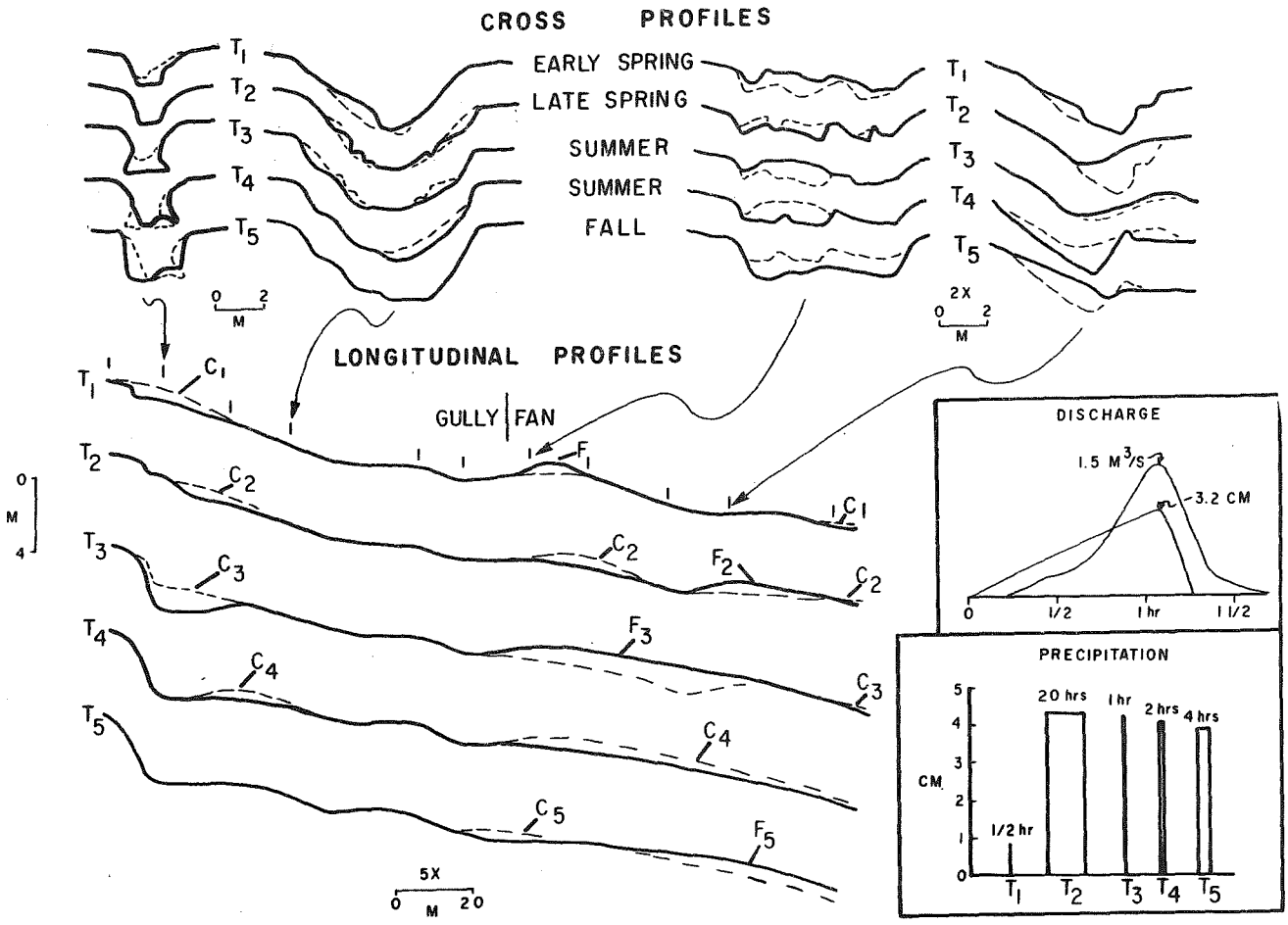

Figure 10. Climatic, cross section, and longitudinal profile summary for late spring to early fall cycles of the Snow Shoe gully (Fig. 8). Precipitation for event t, through T_5, is shown in lower right box. Timing of events is shown in the cross section at top. Dashed lines on longitudinal profiles and cross sections indicate channel shape preceding storm event; C = cut and F = fill.

Location of storage sites, amounts of deposition, mean grain size, and degree of sorting depend upon seasonal sediment production, local slope, and storm events (Fig. 12). Large amounts of boulder to clay size sediment are supplied to the gullies by bank collapse of overburden and bottom scour during storm events and from mass wasting of gully walls during freeze-thaw cycles. Most of the coarse-grained sediment is stored at least temporarily near the mine site in terraces and alluvial fans. Discontinuous, poorly sorted fills develop along gully channels during short-duration, high-intensity rainfall events. Oversteepened reaches on the downstream side of these gully fills are cut when rainfall and sediment productions are low. More continuous, longer lived, and better sorted terraces occur along fan segments. Mean grain size, sorting, and thickness of fills decrease downfan. Nearly all fine-grained silt and clay is discharged downstream (Figs. 8 and 12) to sediment ponds or to the main fluvial system, where it can drastically disrupt aquatic ecosystems. Storage sites in these disequilibrium fan gully systems display a complex response of cutting and filling that is dependent upon grain size distribution of the source, climatic variations, and antecedent drainage basin conditions (Fig. 11). Studies of this type of small alluvial fans may be very useful in understanding development and evolution of large, semiarid alluvial fans in the American southwest.

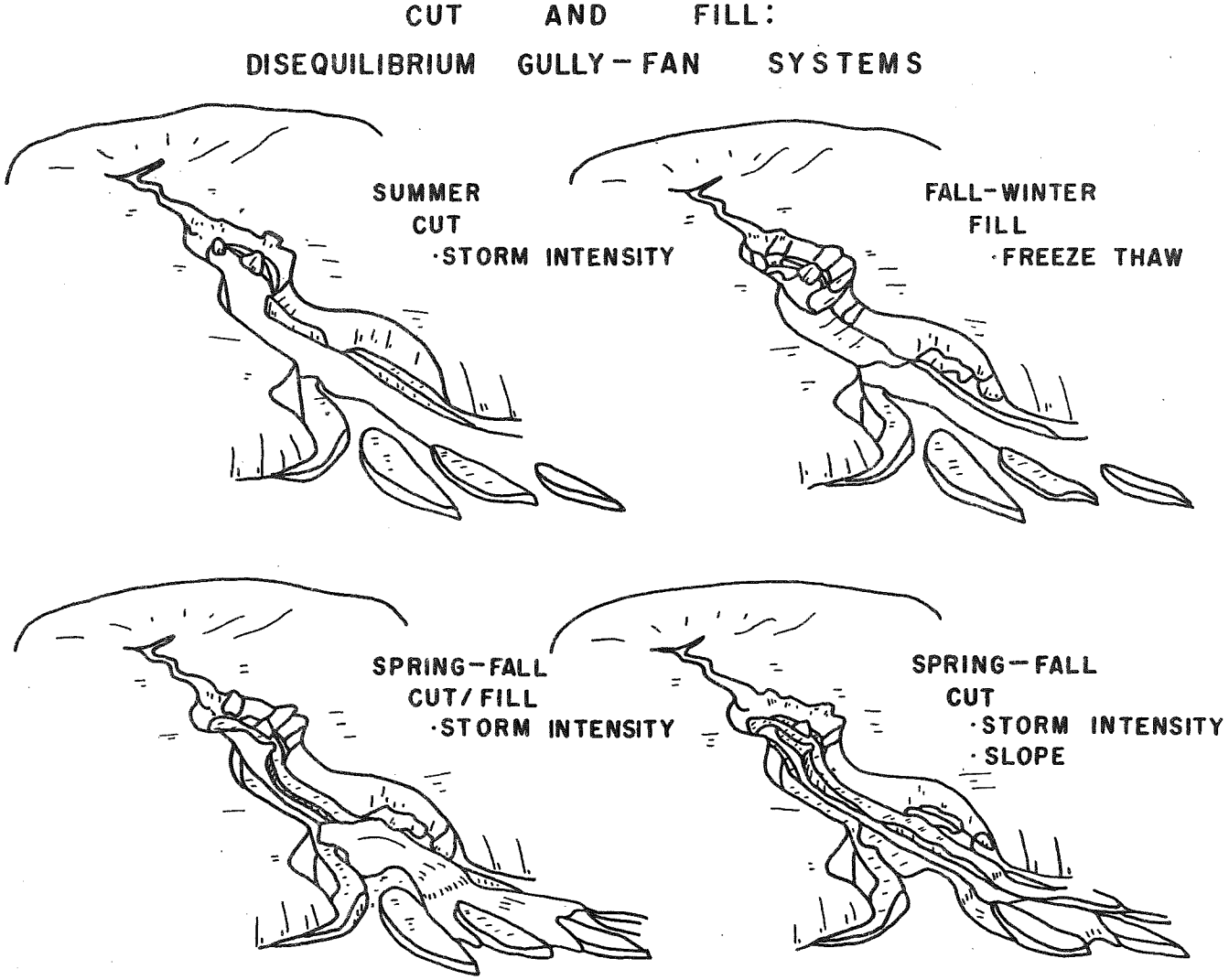

Figure 11. Cartoon diagrams illustrating the seasonal cut-and-fill cycles in gully-fan systems on reclaimed surface mines as conditioned by storm intensity and slope.

Surface mines not only cause an increase in the total volume of water and sediment discharge, but also result in greatly increased peak discharges (Collier and others, 1970; Touysinhthiphonexay and Gardner, 1984). In basins where more than 50 percent of the area has been mined and the total mined area exceeds 0.45 km^2, channel shear stresses associated with peak discharges exceed the combined resistance to erosion of floodplain vegetation and channel sediment. A critical threshold is exceeded and channel erosion increases abruptly. The stepped response of these first-order tributaries takes the form of enlarged channels and an increase in the size of moving blocks (Fig. 13). In these basins, severe erosion and high rates of sediment transport catastrophically degrade aquatic and floodplain habitats. There is an extended period of extreme morphologic adjustment until the streams attain a new equilibrium compatible with the discharge conditions imposed by mining and reclamation.

Equilibrium Landscape Components

Data from these detailed geomorphic studies of surficial processes associated with surface coal mines in central Pennsylvania are being used to design and model

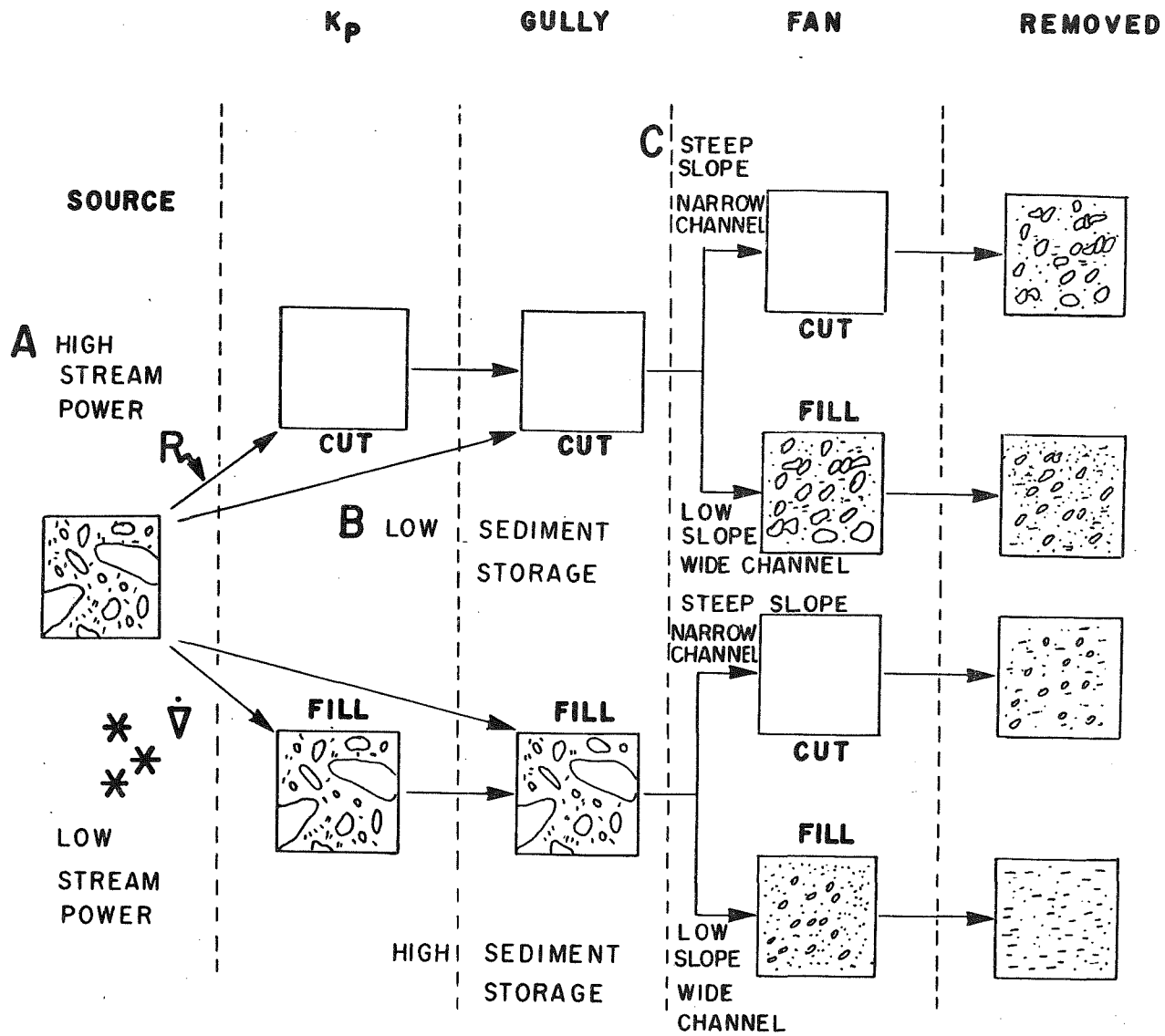

Figure 12. Schematic diagram illustrating the grain size distribution of sediment deposited in different storage sites under different climates and channel slope conditions. Source material is poorly sorted, polymodal overburden. Knickpoint (K_p), gully, and fan are shown in Figure 8.

equilibrium landscape components that are stable to the dominant, long-term, surficial geomorphic processes on reclaimed mines. We are investigating the infiltration, runoff, and discharge characteristics of surface strip mines to enable prediction of discharge hydrographs from a computer program, ANSWERS (Beasley and Huggins, 1980). A computer program, GRADE (Snow, 1983), recently developed at Penn State, solves for an optimum, equilibrium longitudinal profile of a gully, essentially a slope that minimizes erosion. Input variables to the model consist of water discharge from ANSWERS (as determined by basin area and infiltration/runoff characteristics), sediment grain size on gully bottoms (as determined by the grain size distribution of the spoil material), and channel widths. Given the range of conditions demonstrated to exist on large reclaimed surfaces, the equilibrium profiles are concave-up, while the actual shape of the concavity is determined generally by site-specific basin size and spoil grain size. Using GRADE, these concave profiles or valleys are easy to calculate, generally easy to construct during reclamation, and insensitive to small miscalculations of profile shape, in contrast

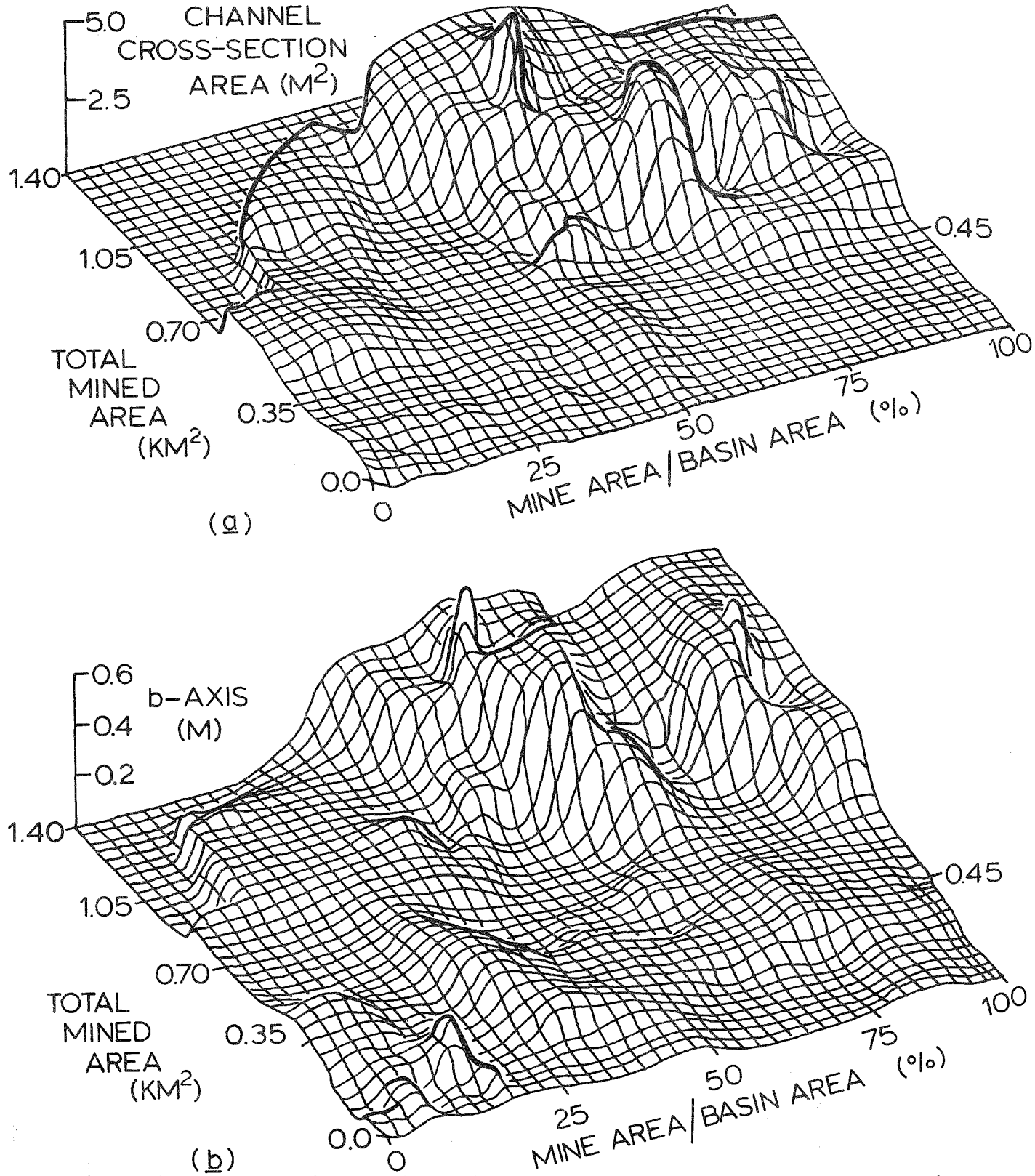

Figure 13. Three-dimensional plots of (a) channel cross-sectional area, and (b) b-axis of largest moving blocks versus total mined area and percent of mined area for streams affected by mining. System threshold exists at 0.45 km^2 of mined area and 50 percent of basin area mined. Data sets consist of 262 cross-section measurements on 29 first-order tributaries of Beech Creek in Centre County, Pennsylvania.

to terraced slopes which can often fail if not maintained properly. More importantly, they are designed to minimize erosion by channelized flow, the dominant surficial geomorphic process on large reclaimed strip mines. We are currently using this model to design the topography of a reclaimed area near Clearfield, Pennsylvania.

It is critical to understand the erosional and depositional processes in the rapidly eroding gully systems because they are the most significant long-term sediment sources, and also the dominant mechanism for breaching impermeable topsoil caps that are used to inhibit spoil oxidation and prevent acid mine drainage. Certainly the key to a successful reclamation effort is the establishment of a continuous, dense vegetation cover that will ultimately reestablish "natural" soil profiles, increase infiltration rates, and reduce peak discharges. One of the many important factors in establishing a vegetation cover is a stable land surface. However, even vegetation is ineffective in stabilizing the large, rapidly growing gully systems that will ultimately form on some larger reclaimed surfaces. Hence, it is critical that the initial landscape design be stable to the dominant geomorphic process, channelized flow.

Stop localities for Field Trip #5, plotted on Landsat Image of part of Central Pennsylvania (scene E 1243-15253, band 7, of March 23, 1985).

FIELD TRIP #5

FIELD GUIDE - ECONOMIC AND MINING ASPECTS OF THE COAL-BEARING ROCKS IN WESTERN PENNSYLVANIA

E. G. Williams, T. Gardner, A. Davis,
R. R. Parizek, A. W. Rose, and W. Bragonier
Field Leaders

Introduction

During the past 20 years, efforts have been made by several investigators at Penn State, working mainly in the Carboniferous of western Pennsylvania, to determine the mineralogy, petrology, and geochemistry of the main rock types and to relate these to paleoenvironments, paleotectonics, and paleoclimates. Work on the shales, underclays, and limestones has been mainly the research of Williams and associates, that of the coals by Davis and associates. The second half of this field trip will illustrate the results of this research, using exposures of the Pottsville and Allegheny Groups in Clearfield County in the vicinity of the Curwensville Dam.

More recently, research at Penn State has been directed at attempting to predict and control the deleterious effects of mining coal, namely acid mine drainage and increased erosion rates. This involves both field and laboratory studies encompassing a wide range of rock types and mining conditions. The acid mine research has been conducted by Rose, Williams, and Parizek and their students; the erosion rate studies have been by Gardner and students. The first half of the field trip will attempt to illustrate the results of this research, from strip mines in Centre and Clearfield Counties.

In addition, during the past 10 years, research has also been conducted attempting to relate the petrography of coals, clays, and shales to various industrial products and processes such as lightweight aggregate, refractory brick, ladle bricks, coking coal, etc. The results of these studies will be discussed at the appropriate stops during both parts of the trip.

The results of all of this research are presented in comprehensive form in the preceding papers.

Stop 1: The first stop, located several miles north of Pine Glen, Pennsylvania, off State Route 879 is on a surface mine reclaimed in 1978 and 1979. At this site, we have instrumented the watershed and have been collecting rainfall, infiltration, and runoff data during the past 3 years. In addition, we have collected data on the hydrology, sediment transport, and geomorphic evolution of several large gully-fan systems. The discussion will focus on the hydrology and geomorphology of this reclaimed mine (see chapter by Gardner and others) and use this mine as a basis for comparison at Stop 2.

Stop 2: The second stop is located 2 miles south of Glen Richey, Pennsylvania, on Township Route T579. It is an active mine, Browncrest No. 3--MDP No. 17800119, operated by the Pennsylvania Coal Company. This site is being reclaimed under an experimental practice program sponsored by the Office of Surface Mining as part of a variance to deviate from approximate original contour (AOC) requirements. The objective of the reclamation program is to demonstrate that regrading of generally

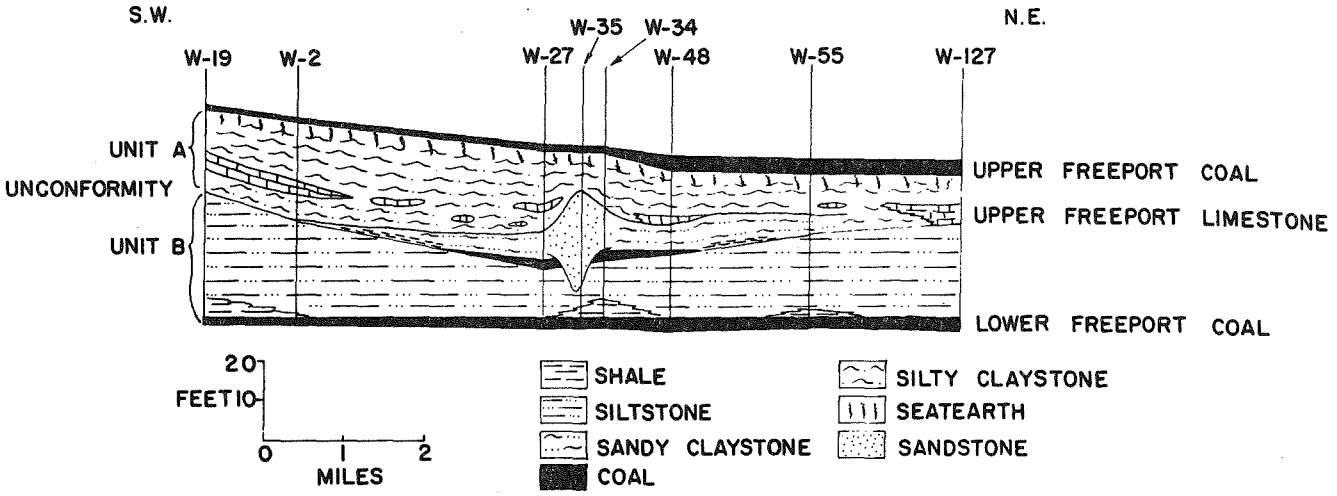

Figure 1. Stratigraphic cross section of the Upper Freeport underclay and associated rocks in Clearfield County (from Williams, Bergenback, and Weber, 1968).

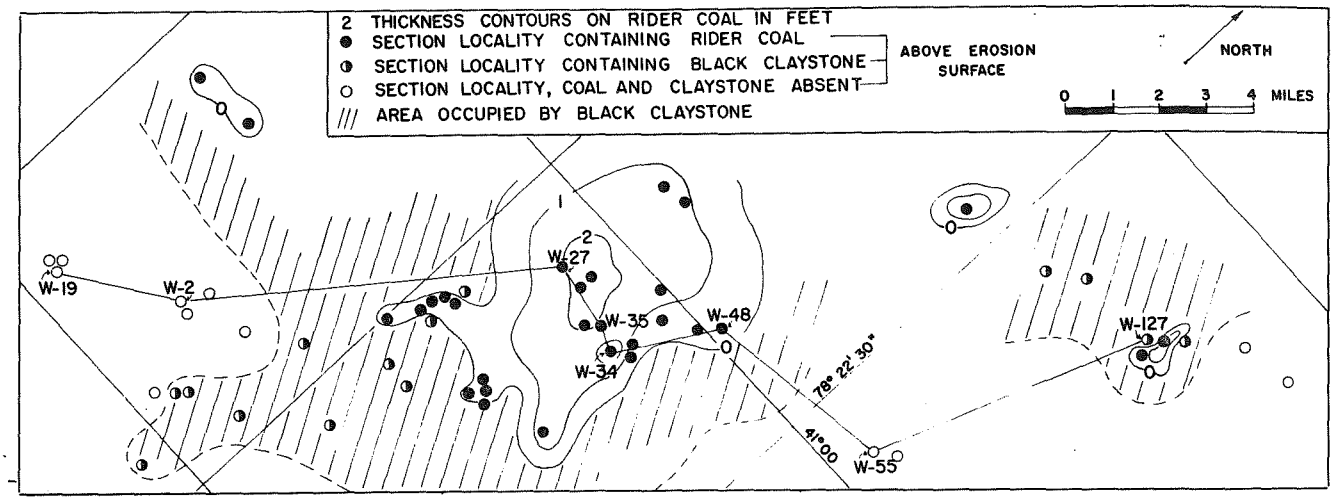

Figure 2. Combined isopach map of rider coal and lithofacies map of rocks resting on the unconformity at the base of the Upper Freeport underclay (from Williams, Bergenback, and Weber, 1968).

convex backfilled slopes to contain channels with concave-longitudinal profiles, which are adjusted to fluvial runoff, will significantly reduce the potential for gullying and topsoil erosion. The reclamation design is based on hydrologic data from numerous reclaimed surface mines (especially at Stop 1) and several computer models described in the chapter by Gardner and others. The coals mined here are the Upper and Lower Freeport, the two highest minable coals in the Allegheny. Their properties as well as those of the overlying shales can be obtained from the fresh-water column in Figure 4 at Stop 3. For the characteristics of the Freeport underclays, see the chapter on the origin of plastic underclays by Williams and Holbrook and their Figure 10. Throughout western Pennsylvania, the upper Allegheny rocks seldom produce acid mine drainage since shales, sandstones, and clays contain very little sulfur and relatively large amounts of carbonate.

Of most interest at this locality is the nature of the lithologic variation in the Upper Freeport underclay, the interval extending from the base of the Lower Freeport rider coal to the base of the Upper Freeport coal. Figure 1 shows the local and regional variability of this interval. Section W-27 approximates the measured section at the mine we will visit and W-35 is the section a short distance

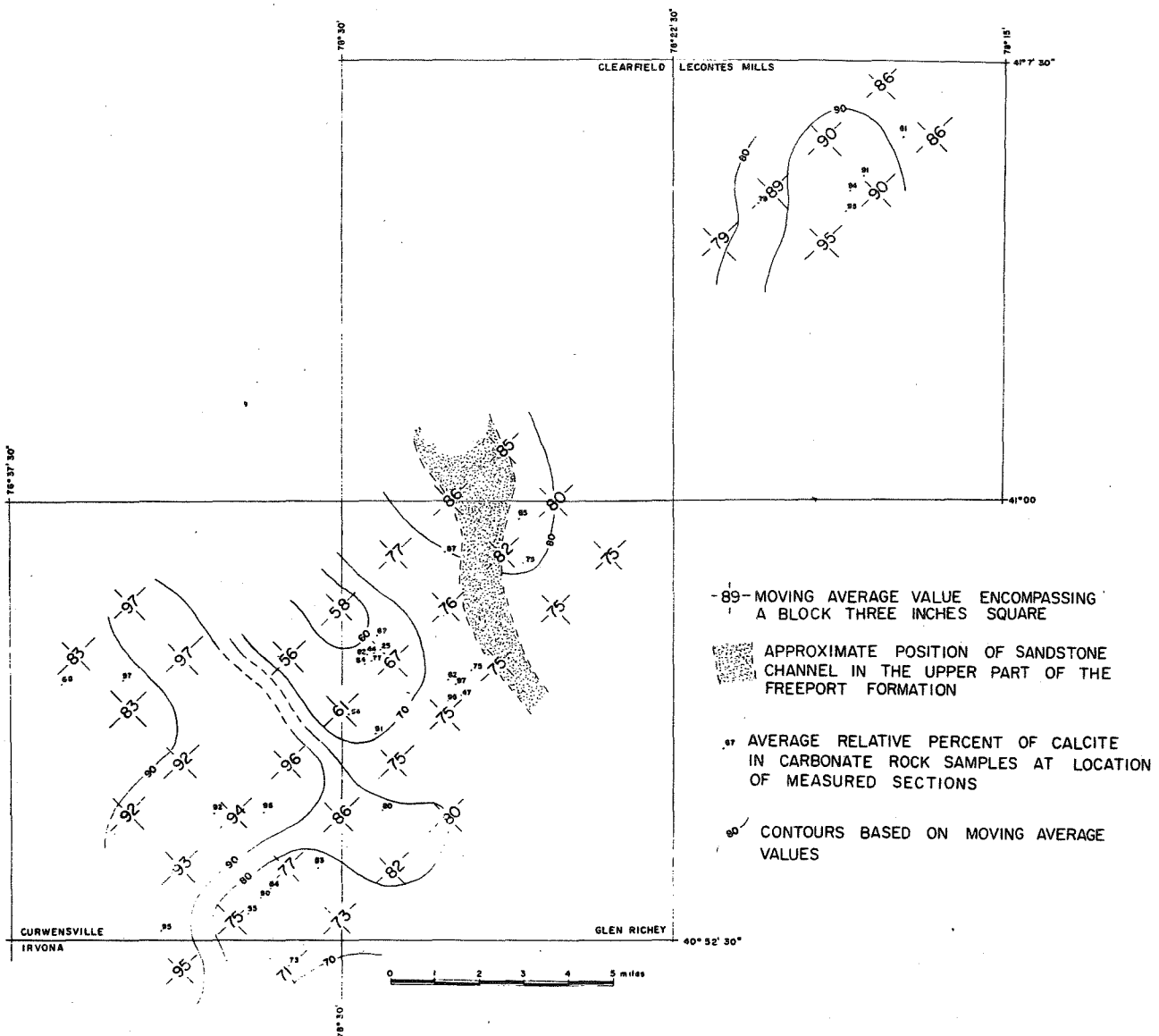

Figure 3. Moving-average map of the percent calcite in the freshwater carbonate beds in the Upper Freeport underclay (from Williams, Bergenback, and Weber, 1968).

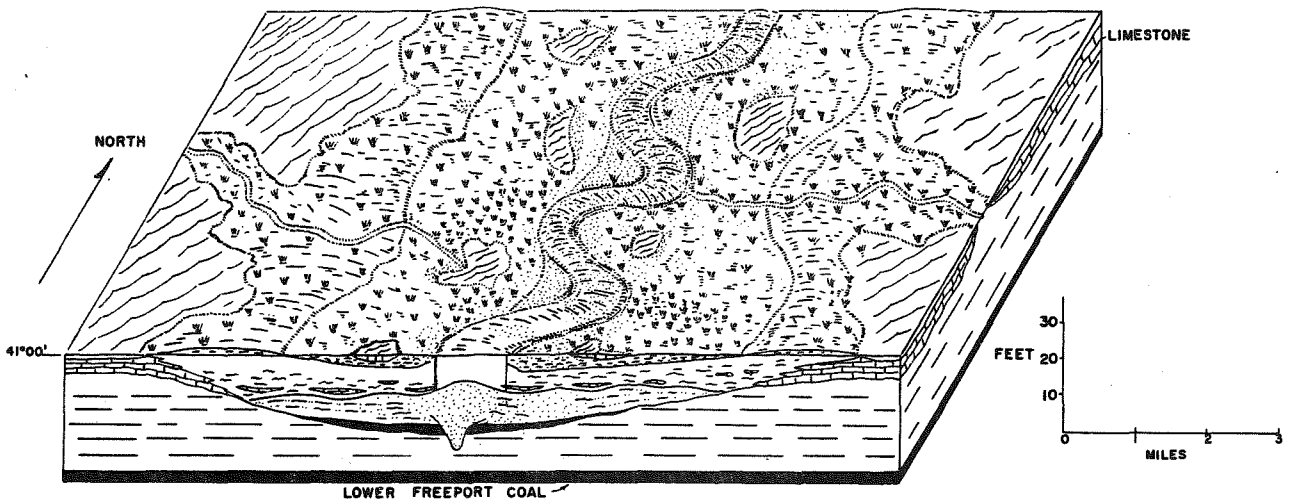

Figure 4. Paleogeographic map during the time of formation of the Upper Freeport limestone and associated rocks (from Williams, Bergenback, and Weber, 1968).

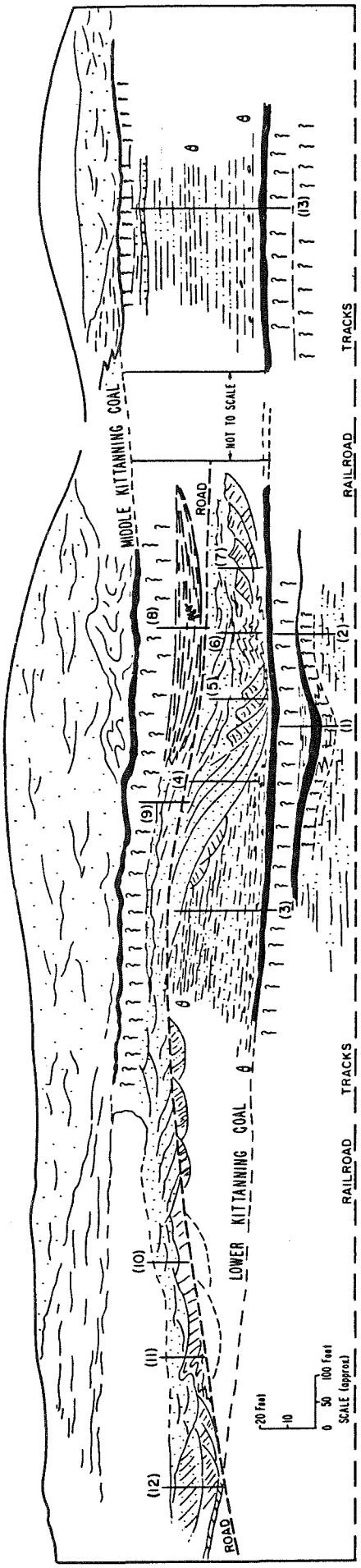

Figure 5. Sketch of railroad cut, roadcut, and strip mine highwall at the flood spillway of the Curwensville Dam, Stop 3.

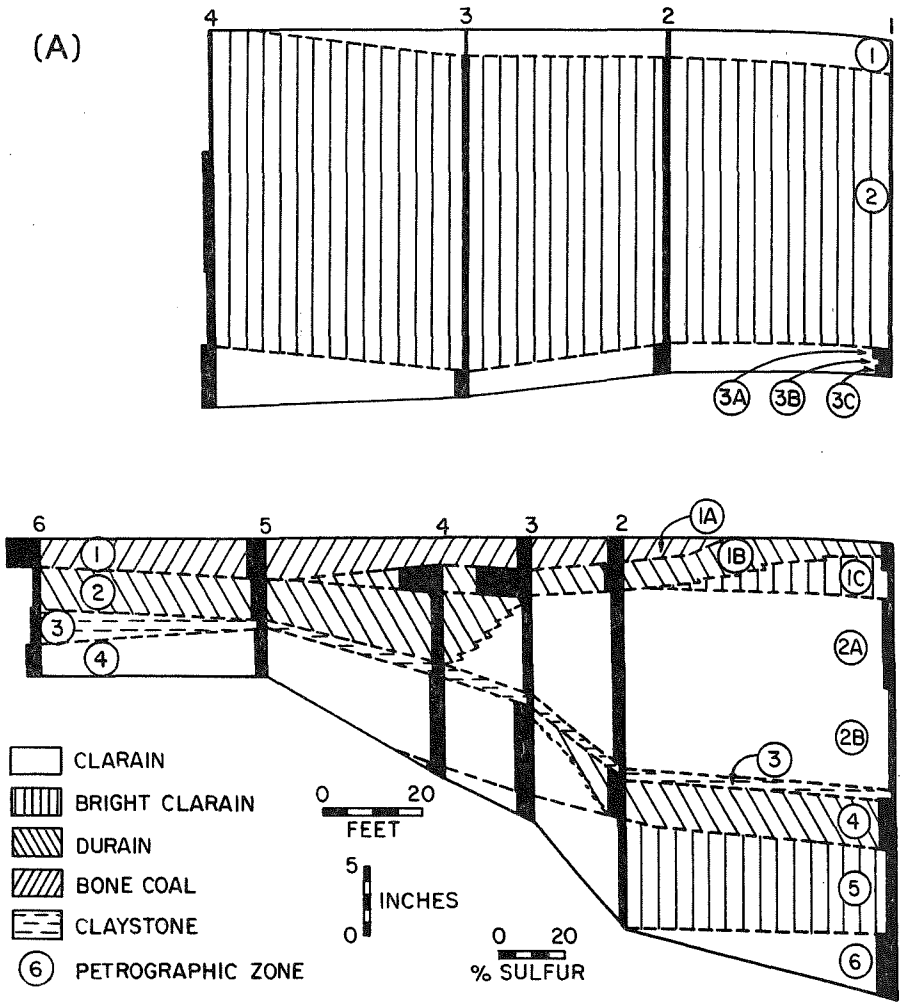

Figure 6A. Petrographic and mineralogical variation of the two Lower Kittanning coals exposed in the railroad cut shown on Figure 1 (from Reidenouer and others, 1967).

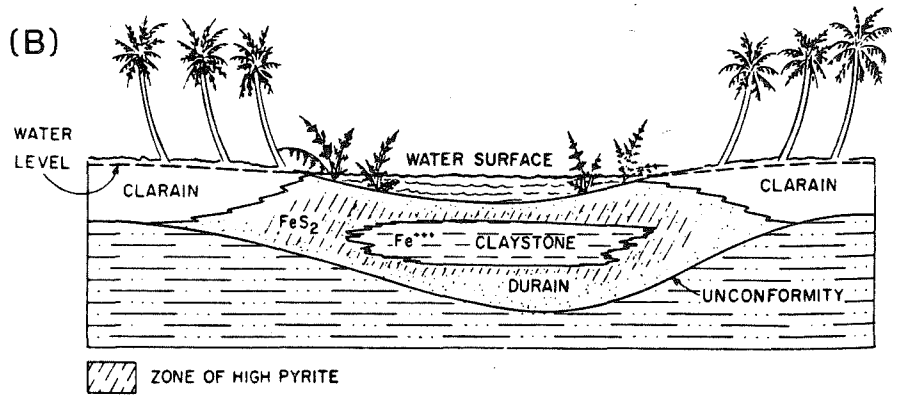

Figure 6B. Hypothetical diagram showing the relation between paleotopography, water depth, and the distribution of coal types and pyrite (from Reidenouer and others, 1967).

to the east. As illustrated in Figures 1, 2, and 3, the thickest channel sandstones occur where the rider coal is thickest and the freshwater limestones thin or absent. Further from the channel, the interval thins and the freshwater limestones thicken and increase in the proportion of calcite (dolomite and clays decrease). Figure 4 is a paleogeographic reconstruction during the time of formation of the Upper Freeport underclay and associated freshwater limestone. The clays and claystones are interpreted as overbank deposits of the channel whose orientation is controlled by differential subsidence and compaction. The smaller lakes proximate to the channel have the highest dolomite and clay contents whereas the thickest, most chemically pure limestone forms in the lakes at the greatest distance from the channel. As shown in Figure 11 (in the chapter by Williams and Holbrook, this volume), the illite content generally increases upward, except in the upper foot, where it is drastically reduced (decrease in illite is accompanied by increase in kaolinite). We believe that some of the illite is authigenic and its upward increase as well as the presence of freshwater limestones probably reflect an increase in the rate of evaporation over that present in the lower and middle Allegheny, where freshwater limestones are absent and the kaolinite contents of underclays are much higher and increase rather than decrease upward. We believe that these stratigraphic differences are related to a change to drier climates in the upper Allegheny.

Stop 3: Roadcuts and strip-mine highwalls in middle Allegheny rocks at the Curwensville Dam site along Route 969, 2 miles southwest of Curwensville, Pennsylvania.

The rock mined at this locality was the underclay below the Lower Kittanning coal which was used in making ladle bricks, a product which expands at high temperatures. Figure 5 is a sketch of the roadcut and adjacent strip mines. Local paleogeographic control of the morphology and composition of all the rock types is well illustrated at this locality. The most obvious relationship is exhibited by the lowest coal at sections 1 and 2, where it thickens into an erosional paleotopographic low with marked changes in mineralogical and petrographic character as shown in Figure 6A. Brighter coal generally is found in the low, dull coal on the adjacent high. Sulfur is highest in the dull layers where they are interbedded with claystone partings, the latter, as illustrated in Figure 6B, providing the source of the iron for the pyrite. The upper coal in Figure 6A shows no lateral change in petrographic properties, suggesting it was deposited at constant water depth.

As shown in Figure 8, similar petrographic and mineralogical changes in the Lower Kittanning coal have been observed on a regional scale (see chapter by Davis and others, this volume). The amounts of pyrite are highest in areas overlain by brackish shales and lowest in areas of freshwater shale deposition. Framboidal pyrite is abundant in coals overlain by marine and brackish shales and absent in the freshwater areas. The total amount of clay in the coal is highest in the areas of freshwater shales as is the proportion of kaolinite in the coal ash. All of these changes are believed to be related to changes in water chemistry of the peat-forming swamps which in turn are controlled by regional paleoslope and eustatic sea-level changes.

The underclays below the Lower and Middle Kittanning coals are thought to represent both residual and transported soils, the evidence for which can be observed at sections 1, 2, and 9. The genesis of the underclays is illustrated in Figure 7, where the residual clays form on paleotopographic highs and the transported clays in the adjacent lows. Based on vertical mineralogical changes and estimates of the amount of denudation, we have concluded that residual underclays represent an erosional interval of tens of thousands of years involving tens of feet

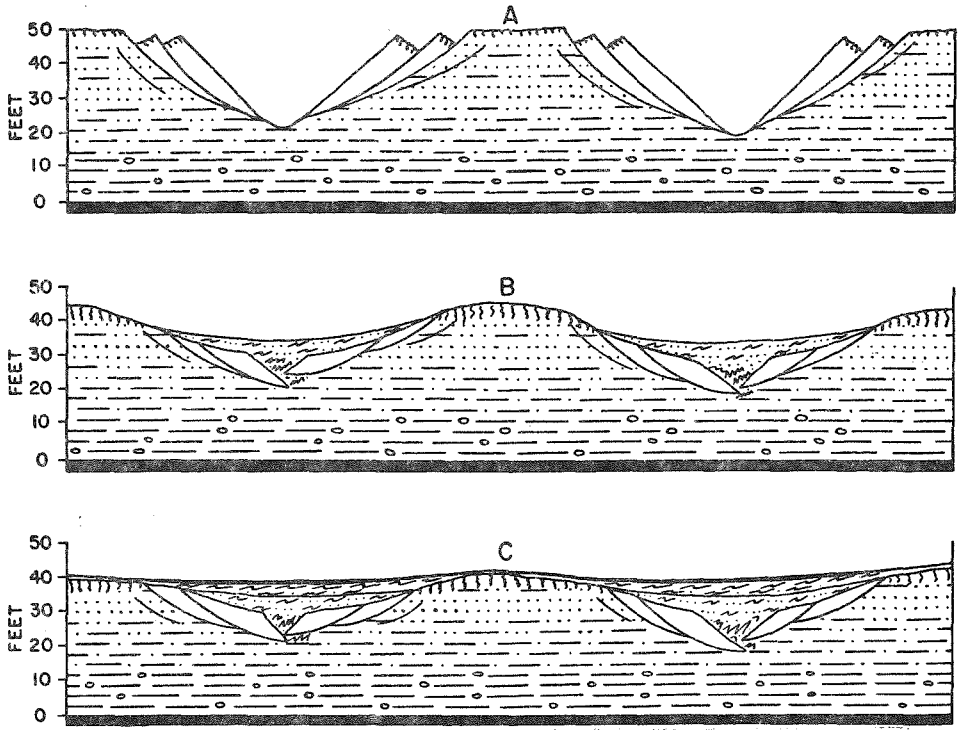

Figure 7. Erosional history of slumping and the development of residual and transported underclays (from Williams and others, 1965).

of section. As shown in Figure 8, underclays exhibit pronounced regional changes, the greatest degree of weathering, as manifested by greater thickness, vertical variation, and kaolinite contents, occurring in areas of continental sedimentation on basin margins (also see chapter by Williams and Holbrook, this volume).

Section 3, which is characteristic of 75 percent of the lower and middle Allegheny rocks of this area, consists of a coarsening-upward sequence--dark, Lingula-bearing shales at the base grading up into laminated siltstones and fine-grained sandstones. The Lingula shales are brackish, and, as shown in Figure 8, have the highest sulfur and lowest carbonate and lowest calcite content of any of the shale types in western Pennsylvania, which makes them the main acid-producing rocks (see chapter by Williams, Rose, Waters, and Morrison, this volume). Thus, areas such as those near Curwensville have the greatest acid mine drainage problems, which are further exacerbated by the presence of relatively thick sandstones whose presence in the spoil banks increases porosity and therefore rates of oxidation of pyrite. The sandstones exhibit pronounced regional changes in porosity from about 9 percent in the Clarion area to 2 percent near the basin margin, with the area at Curwensville having values of about 6 percent. Our explanation of these porosity changes is that they are the result of layer-parallel shortening, evidence for which was first observed by Nickelsen who estimated the amount of shortening from calculations based on the amount of shape distortion in Lingula at this and nearby localities (see also chapter by Chou, this volume).

The sandstone at section 4 consists of accretion beds on a point bar building into a northwestward-trending channel. The features at section 5 are rotated slumps produced in the toe of the point bar as it prograded over the Lingula-bearing shales. The faulted blocks caused the underlying shales to be folded and faulted to the center of the channel (section 6), where they met similar shales produced by rotating slumps forming along the cut banks of the stream (section 7). These slump

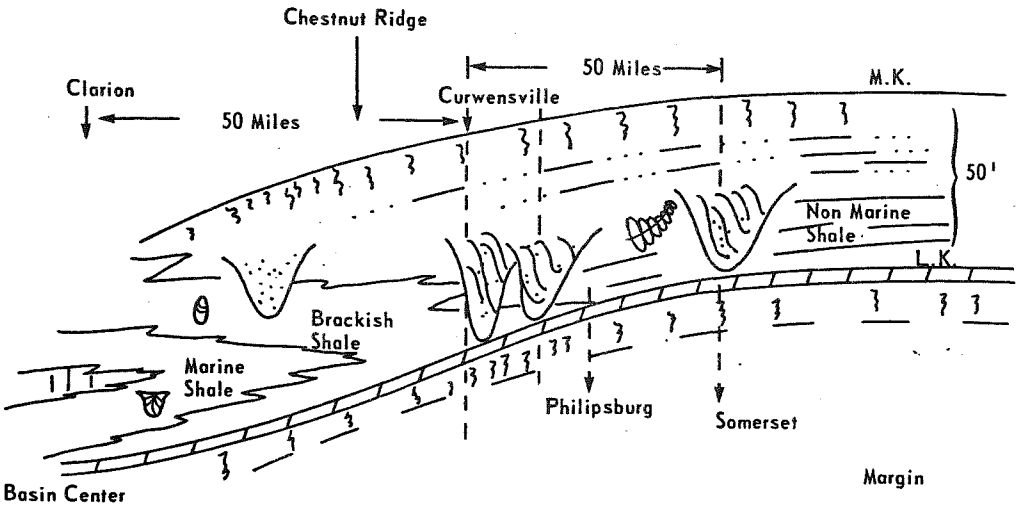

ENVIRONMENT OF OVERBURDEN				
MARINE	BRACKISH	FRESH WATER	VARIABLE	ROCK TYPE
high volatile	med volatile	low volatile	rank	COAL
84	88	88	% vitrinite	"
20-30	>40	<20	% pyrite in ash	"
45	<40	>50	% total clay in ash	"
>20	<10	<10	% quartz in ash	"
20-30	20-30	30-40	% kaolinite in ash	"
framboidal + +	framboidal +	euhedral	pyrite type	"
<24"	24-39"	39-55"	thickness	"
>3:1	2:1	<1:1	illite/kaolinite ratio	UNDERCLAY
present + +	present +	absent	chlorite	"
absent	absent	present	vermiculite	"
none	moderate	pronounced	vertical change	"
5-10	10-20	20-40	age (years x 10^3)	"
<2	2-4	5-6	thickness of weathered zone	"
6:1	4:1	3:1	illite/kaolinite ratio	SHALES
<15	15-30	>30	% quartz	"
0.95	2.40	0.15	% sulfur	"
abundant framboids	abundant framboids	rare framboids	pyrite type	"
nodular	lenticular	banded	siderite morphology	"
0.65	0.16	0.54	% carbonate carbon	"
0.26	0.06	0.77	% calcite	"
4.05	1.79	5.41	% siderite	"
0.74	0.48	1.59	% dolomite	"
2.435	2.502	2.633	bulk density	Channel Sandstones
8.7	6.3	2.0	porosity %	"
absent to serious	serious	absent to mod.	acid mine drainage	

Figure 8. Summary of the regional variation in the mineralogical and petrographic properties of the Lower Kittanning coal and associated rocks for western Pennsylvania.

blocks, when rotated back to their original position, extend above the present position of the Middle Kittanning coal, which means that removal of the section in undeformed areas has occurred subsequent to slumping but prior to the deposition of the Middle Kittanning peat. The quartzitic sandstone, called a ganister, occurring at section 9, we believe is one of the weathering products of this erosional interval. The quartzite interfingers with the black, carbonaceous shale at section 8, a deposit which represents an abandoned channel fill, probably of an oxbow lake. The sandstones and associated slumped shales at sections 10, 11, and 12 may represent the formation of the new channel which developed following the abandonment of the old one at section 8. The locations of the sandstones above the Lower and Middle Kittanning coals are controlled by the processes of differential erosion, sedimentation, and compaction, producing a rhombohedral stacking pattern. The sandstone at locality 4 presumably occupied a paleotopographic low produced by the compaction of the underlying peats and shales. The sandstone above the Middle Kittanning coal lies directly above the sandstone at locality 4. The fact that the Middle Kittanning coal is thickest at the place where the overlying sandstone is thickest suggests that both were formed in topographic lows related to the differential compaction caused by a buildup of sand bodies at localities 10, 11, and 12, where the topography would have been higher.

Stop 4: Riprap quarry, railroad cuts, and roadcuts along Route 969, 2 miles southwest of Stop 3, exposing upper Mississippian and lower Pennsylvanian strata, the latter comprising the Pottsville and lower Allegheny Groups.

Figure 9 is a sketch of the exposed sequence and Figure 10 is the same sequence in which, at the various stages illustrated, the compactional effects have been removed. It shows that the effects of the undulating surface upon which the Mercer no. 2 coal was deposited have been propagated throughout the entire section, eventually affecting the thickness and composition of the Lower Kittanning coals and underclays. The locations of the sandstone bodies above the Mercer no. 2 coal were

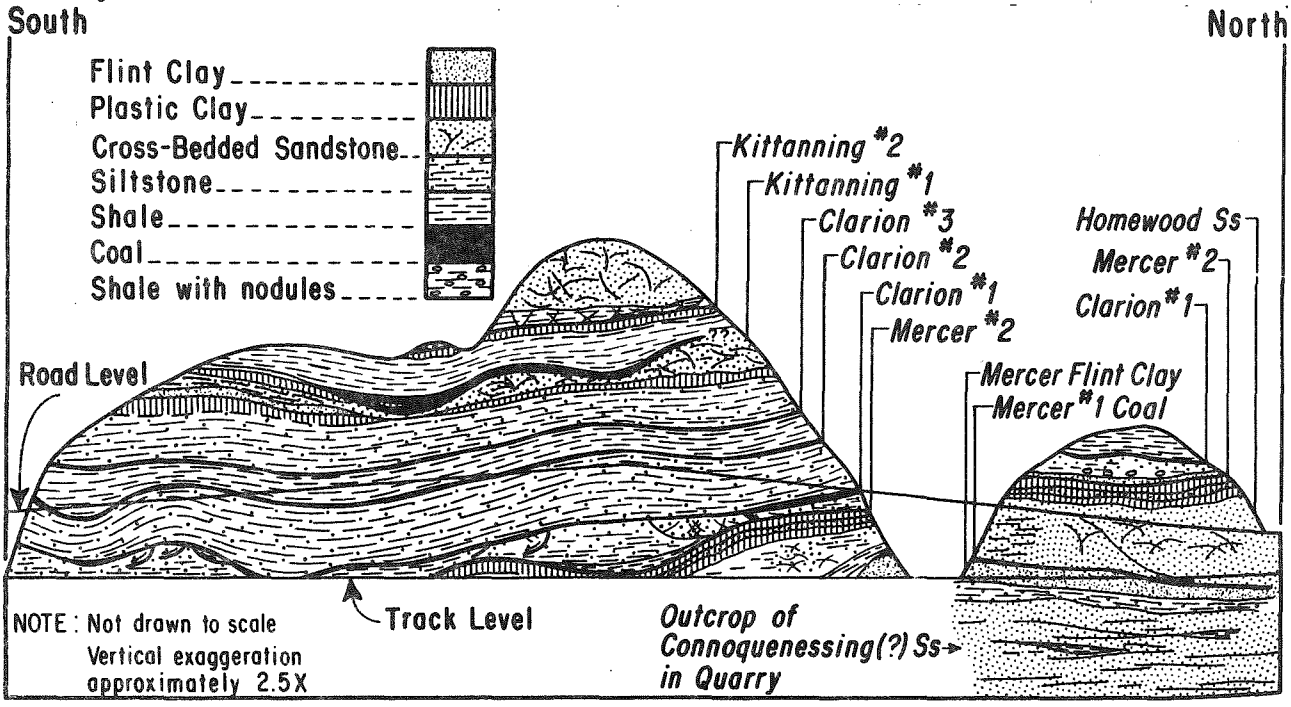

Figure 9. Sketch of railroad cut, roadcut, and quarry in Pottsville and Lower Allegheny rocks at Stop 4, 2 miles west of the Curwensville Dam (from Williams and Bragonier, 1974).

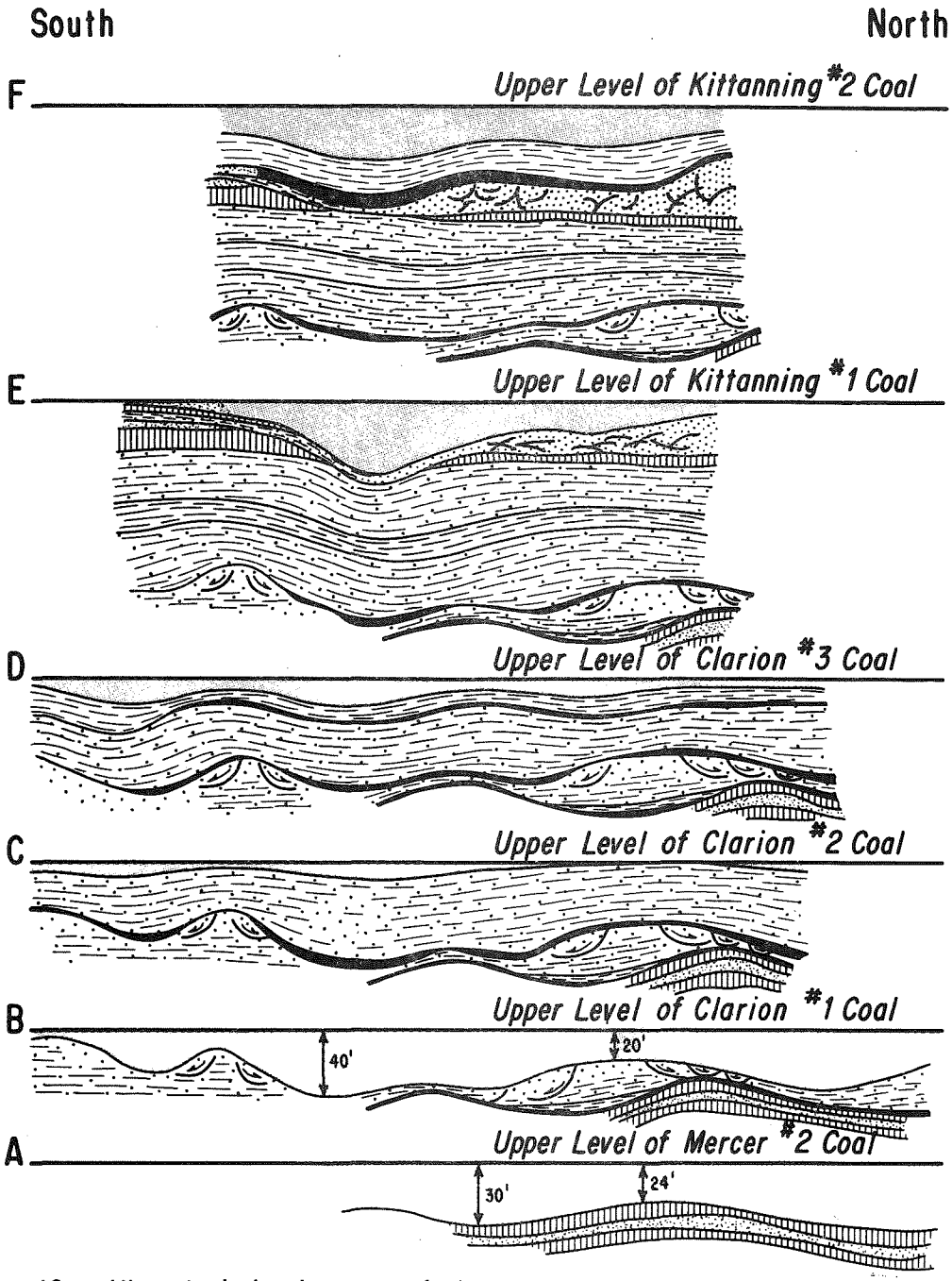

Figure 10. Historical development of the sequence at Stop 4 (from Williams and Bragonier, 1974).

controlled by the compaction of the varying thickness of this coal so that the sand is thickest where the coal is thickest. Since the sandstones compact less than coals and shales, those above the Mercer no. 2 coal would produce topographic highs, so that the next coal, the Clarion no. 1, would be thickest in the topographic lows between the two sand bodies. With the deposition of mud on this peat, more compaction would occur in the areas of thickest peat, thus creating more space for more mud, etc., a process which continues to the deposition of the Kittanning no. 2 coal. The thickest plastic clays with a layer of flint clay (pure kaolinite) occur beneath the Lower Kittanning no. 1 coal over the paleogeographic high which has been propagated over the sand body on the south end of the outcrop.

The Mercer high-alumina clay is well exposed at the top of the stone quarry below the railroad tracks at the north end of the outcrop, Figure 5. The clay is 10 feet in thickness and consists, from bottom to top, of flint and spotted flint clay (well-crystallized, very fine grained kaolinite) with siderite, 2 feet of burnt nodule clay (80 percent diaspore, 18 percent pyrite, 3 percent kaolinite), 1 foot of green nodule clay (100 percent diaspore), and several feet of flint clay. The clay is underlain by the light-gray, quartzose graywacke whose correlation is in doubt, having been variously identified as Lower Connoquenessing of Pottsville age, a sandstone in the Mauch Chunk Formation of Late Mississippian age, or the lower Mississippian Pocono. The relationship of this sandstone to the overlying Mercer high-alumina clay at this and adjacent areas is illustrated in Figures 11 and 12, where it can be seen that the high-alumina clay is everywhere present where the Upper Connoquenessing sandstone is absent so that the clay is always underlain by the Lower Connoquenessing. The identifying features of the two sandstones are given

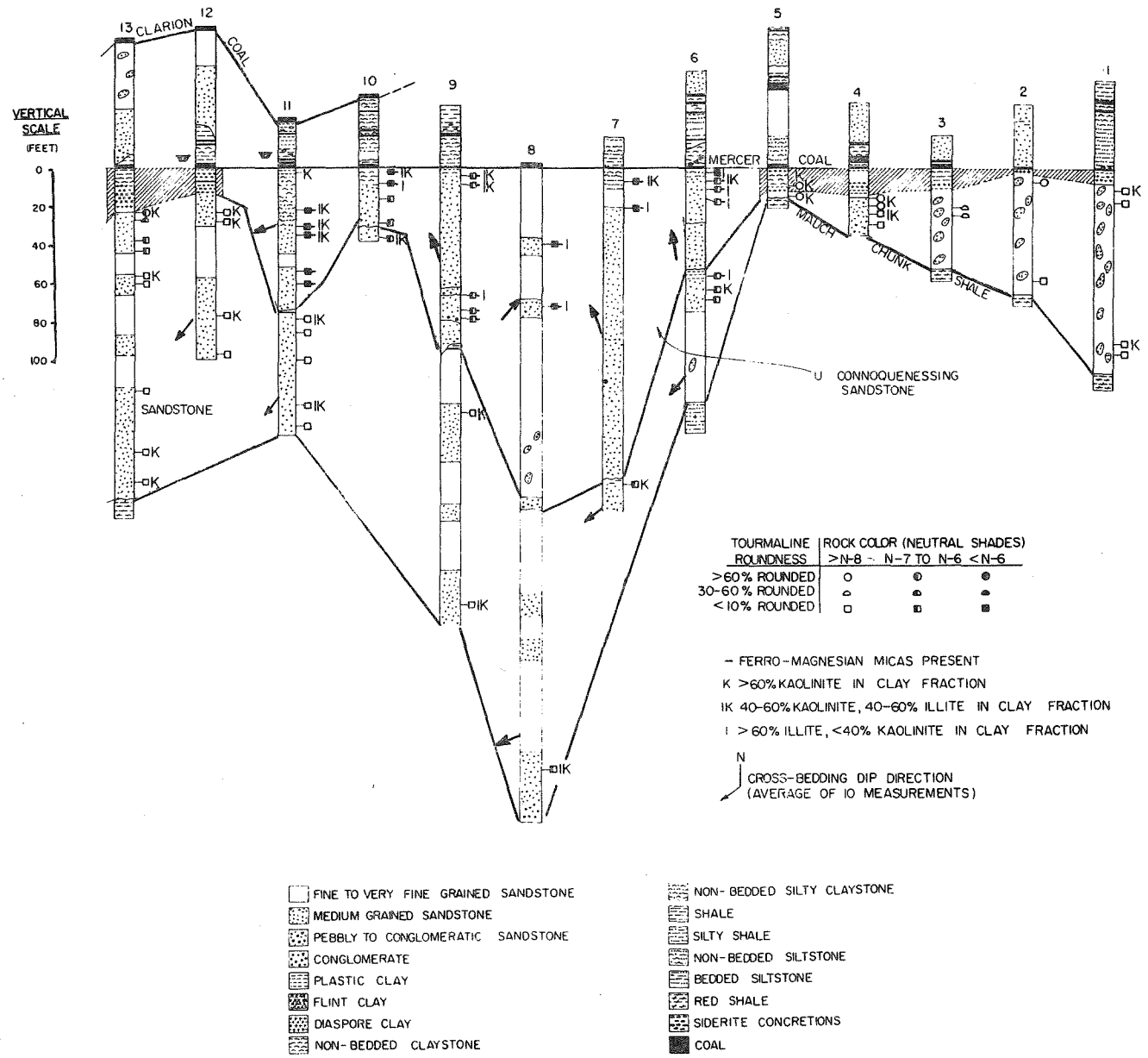

Figure 11. Correlation diagram of the Mercer clay and associated rocks in Clearfield County (from Williams, 1960).

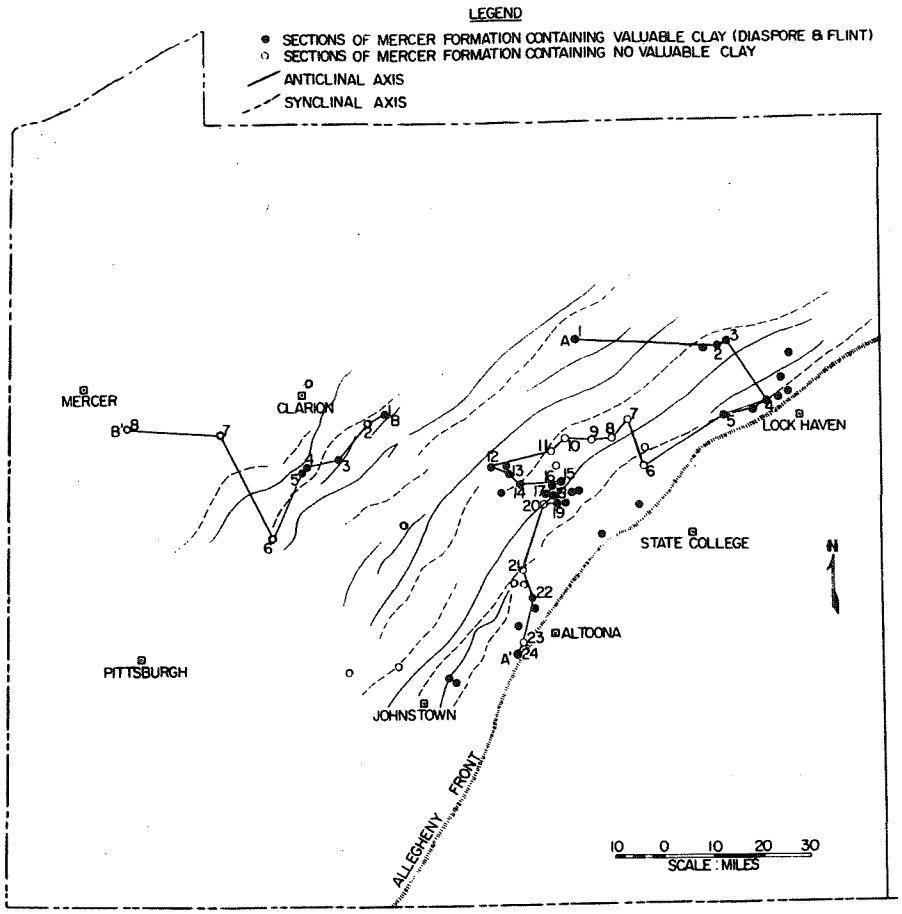

Figure 12. Map of sections of the Mercer clay and associated rocks (from Williams, 1960).

in Table 1 and Figure 13. The high quartz content, absence of chlorite, high kaolinite, and large proportions of rounded tourmaline plus the southwest crossbedding dip directions all suggest that the Lower Connoquenessing was derived from a cratonic dispersal system and deposited in a tectonically stable environment. The low quartz, high illite and chlorite contents, angular tourmaline, and northern crossbedding directions point to a southeastern tectonic dispersal system for the Upper Connoquenessing sandstone. At almost all localities where the Mercer high-alumina clay is present, the upper 10-20 feet of the Lower Connoquenessing contains moderately well rounded tourmaline. We believe that the above data show that the

Table 1. Summary of petrographic data for the Lower and Upper Connoquenessing sandstones (from Williams, 1960).

Sandstone member	Chlorite or biotite present	<7 Micron fraction			Color: >N-8*	>30% Rounded tourmaline	>70% Quartz in med. grain size
		>60% Kaolinite	Kaolinite ≈illite	>60% Illite			
U. Connoquenessing	39	30	30	30	39	39	10
	87%	6%	47%	47%	0%	5%	20%
L. Connoquenessing	82	58	52	52	82	82	22
	0%	64%	27%	13%	76%	34%	96%

Upper figure, number of samples analyzed.
Lower figure, percent of samples possessing sedimentary property.
*N-8 (neutral color shade).

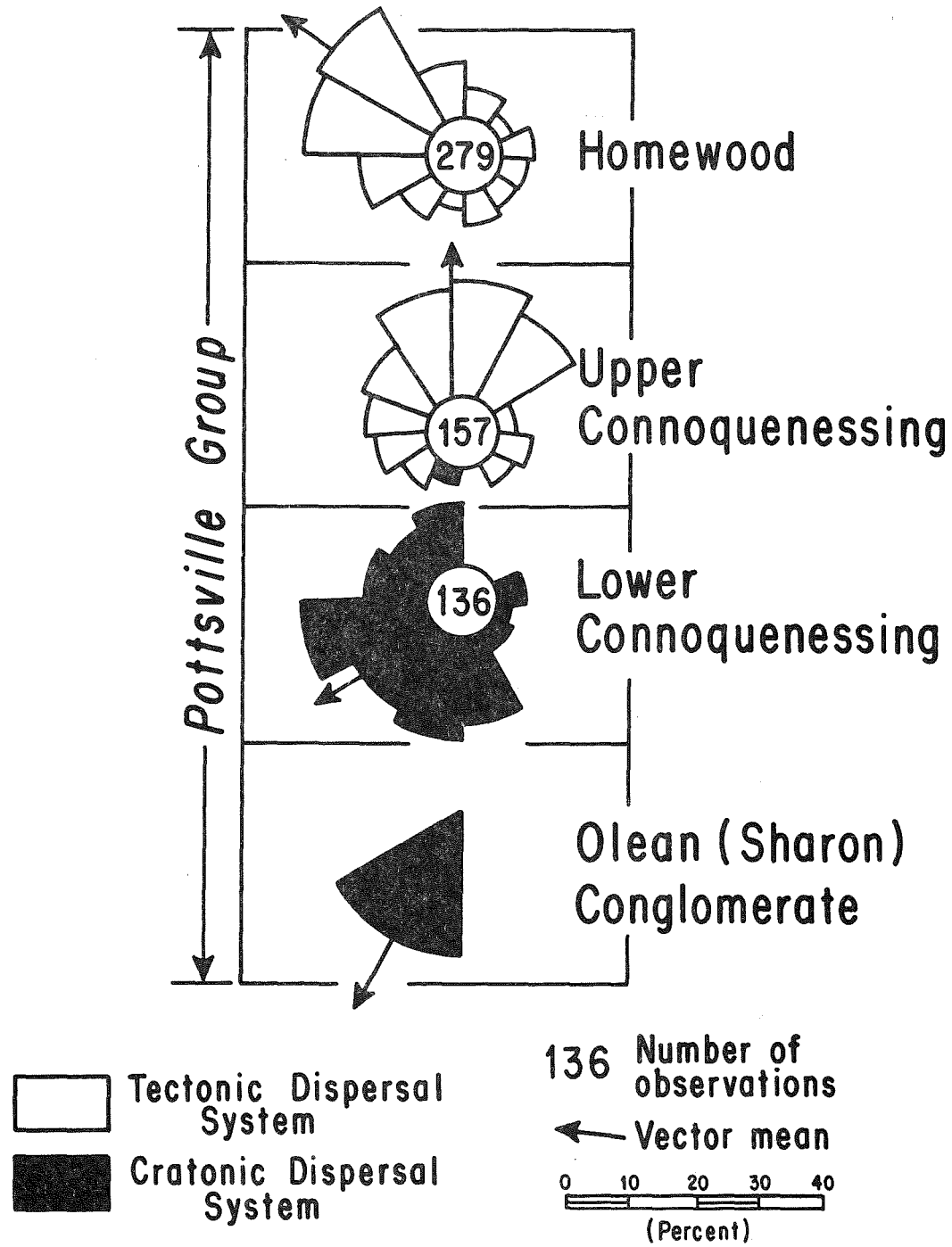

Figure 13. Paleocurrent directions of the Pottsville sandstones in the Allegheny Plateau (from Meckel, 1967).

high-alumina clay was deposited during very long periods of tectonic stability and consequent sedimentary bypassing and ceased with the onset of orogenic activity to the southeast. The local and subregional occurrence of the clay was related to weathering on erosional or depositional highs. The presence of sand-sized rounded tourmaline within the hard clay suggests that much of the clay was derived from the in situ weathering of the Lower Connoquenessing sandstone throughout Late Mississippian and Early Pennsylvanian time. In areas to the southwest, the Mercer high-alumina clays are replaced by plastic clays whose illite and chlorite content increases toward the basin center (see chapter by Williams and Bragonier, this volume).

REFERENCES FOR FIELD TRIP 5

Allshouse, S. D., 1984, Petrographic variation due to depositional setting of the Lower Kittanning seam, western Pennsylvania: University Park, Pennsylvania State University, M.S. thesis, 96 p.

Beasley, D. B., and Huggins, L. F., 1980, ANSWERS users manual: Department of Agricultural Engineering, Purdue University, Lafayette, 55 p.

Bolger, R. C., and Weitz, J. H., 1952, Mineralogy and origin of the Mercer fireclay of north-central Pennsylvania, in Problems of clay and laterite genesis [Symposium, St. Louis, Mo., 1951]: New York, American Institute of Mining and Metallurgical Engineers, p. 81-93.

Bragonier, W. A., 1970, Genesis and geologic relations of the Mercer fire clay, western Pennsylvania: University Park, Pennsylvania State University, Master's thesis, 212 p.

Busch, R. M., and Rollins, H. B., 1984, Correlation of Carboniferous strata using a hierarchy of transgressive-regressive units: Geology, v. 12, no. 8, p. 471-474.

Byrnes, W. R., 1961, Hydrologic balance of three soils supporting natural hardwood, planted red pine, and old field plant communities in central Pennsylvania: University Park, Pennsylvania State University, Ph.D. thesis.

Carson, M. A., and Kirkby, M. J., 1972, Slope profiles, in Hillslope form and process: Cambridge, Cambridge University Press, p. 369-389.

Caruccio, F. T., 1967, An evaluation of factors influencing acid mine drainage production from various strata of the Allegheny Group and ground water interactions in selected areas of western Pennsylvania: University Park, Pennsylvania State University, Ph.D. thesis, 213 p.

Collier, C. R., Pickering, J., and Musser, J. J., 1970, Influence of strip mining on the hydrologic environment of parts of Beaver Creek basin, Kentucky: U.S. Geological Survey Professional Paper 427-C, 20 p.

Davis, A., 1985, Coal petrology and petrographic analysis, in Ward, C., ed., Coal geology and coal technology: Blackwell, Oxford.

Davis, A., Russell, S. J., Rimmer, S. M., and Yeakel, J. D., 1984, Some genetic implications of silica and aluminosilicates in peat and coal: International Journal of Coal Geologists, v. 3, p. 293-314.

Edmunds, W. E., 1968, Geology and mineral resources of the northern half of the Houtzdale 15-minute quadrangle, Pennsylvania: Pennsylvania Geological Survey, 4th ser., Atlas 85ab, 150 p.

Edwards, A. B., and Baker, G., 1951, Some occurrences of supergene iron sulphides in relation to their environments of deposition: Journal of Sedimentary Petrology, v. 21, p. 34-46.

Erickson, E. S., 1963, Mineralogical, petrographic and geochemical relationships in some high-alumina and associated claystones from the Clearfield basin, Pennsylvania: University Park, Pennsylvania State University, Ph.D. thesis, 190 p.

Ferm, J. C., 1970, Allegheny deltaic deposits, in Morgan, J. P., ed., Deltaic sedimentation, modern and ancient: Society of Economic Paleontologists and Mineralogists Special Publication 15, p. 246-255.

Foose, R. M. (1944), High-alumina clays of Pennsylvania: Economic Geology, v. 39, p. 557-577.

Gilluly, J., 1964, Atlantic sediments, erosion rates and the evolution of the continental shelf: some speculations: Geological Society of America Bulletin, v. 75, p. 783-792.

Gluskoter, H. J., 1967, Clay minerals in Illinois coals: Journal of Sedimentary Petrology, v. 37, p. 205-214.

Gregory, K. J., and Walling, D. E., 1973, Drainage basin form and process, a geomorphological approach: New York, John Wiley and Sons, 456 p.

Gryta, J. J., and Gardner, T. W., 1983, Episodic cutting and filling within gully-fan systems in disequilibrium [abs.]: Geological Society of America Abstracts with Programs, v. 15, p. 587.

_____, 1984, Complex response and sediment allocation in disequilibrium gully-fan systems [abs.]: EOS (American Geophysical Union Transactions), v. 65, p. 217.

Guber, A. L., 1972, Pyritic sulfur as a paleoecologic indicator in Carboniferous cycles, in Stratigraphy and sedimentology: International Geological Congress, 24th, Montreal, Canada, 1972, Proceedings, Section 6, p. 389-396.

Guber, A. L., Berlin, T., Froehlich, D., and others, 1971, A study of the effectiveness of backfilling: Pennsylvania State University, College of Earth and Mineral Sciences Special Publication.

Habib, D., 1964, Distribution of spore and pollen assemblages in the Lower Kittanning coal of western Pennsylvania: University Park, Pennsylvania State University, Ph.D. thesis, 310 p.

Hack, J. T., 1960, Interpretation of erosional topography in humid temperate regions: American Journal of Science, v. 258A, p. 80-97.

Hensel, D. R., and White, J. L. (1958), Time factor and the genesis of soils on early Wisconsin tills: Clays and Clay Minerals, v. 7, p. 200-215.

Héroux, Y., Chagnon, A., and Bertrand, R., 1978, Compilation and correlation of major thermal maturation indicators: American Association of Petroleum Geologists Bulletin, v. 63, p. 2128-2144.

Holbrook, P. W., 1973, Geologic and mineralogic factors controlling the properties and occurrences of ladle brick clays: University Park, Pennsylvania State University, Ph.D. thesis, 318 p.

Hornberger, R. J., Parizek, R. R., and Williams, E. G., 1981, Delineation of acid mine potential of coal-bearing strata of the Pottsville and Allegheny Groups in western Pennsylvania: U.S. Department of Interior, Research Project Technical Completion Report, OWRT Project B-097-PA, 359 p.

Hower, J. C., and Davis, A., 1981, Application of vitrinite reflectance anisotropy in the evaluation of coal metamorphism: Geological Society of America Bulletin, Part 1, v. 92, p. 350-366.

Jorgensen, D. W., and Gardner, T. W., in press, An analysis of soil and surface properties which affect infiltration and runoff on mined lands, Centre County, Pennsylvania: Proceedings, Wetlands and Water Management on Mined Lands, Pennsylvania State University.

Keller, W. D., Westcott, J. F., and Bledsoe, A. O., 1954, The origin of Missouri fire clays, in Swineford, Ada, and Plummer, N. V., eds., Clays and clay minerals [National Conference on Clays and Clay Minerals, 2nd, Columbia, Mo., 1953]: National Research Council Publication 327, p. 7-46.

Kuehn, D. W., 1983, Characterization of the organic structure of the Lower Kittanning coal seam using Fourier transform infrared spectroscopy and optical properties: University Park, Pennsylvania State University, Ph.D. thesis, 392 p.

Leopold, L. B., and Langbein, W. B., 1962, The concept of entropy in landscape evolution: U.S. Geological Survey Professional Paper 500-A, 20 p.

Levine, J. R., and Davis, A., 1984, Optical anisotropy of coal as an indicator of tectonic deformation, Broad Top coal field, Pennsylvania: Geological Society of America Bulletin, v. 95, p. 100-108.

Lithgow, E. W., 1972, An analysis of the factors controlling the occurrence of bloating shales in the Pennsylvanian System of western Pennsylvania: University Park, Pennsylvania State University, M.S. thesis, 209 p.

Loughnan, F. C., 1962, Some Tonstein-like rocks from New South Wales, Australia: Neues Jahrbuch fuer Mineralogie, Stuttgart, v. 99, no. 1, v. 8, p. 756-761.

Mackowsky, M-Th., 1968, Mineral matter in coal, in Murchison, D., and Westoll, T. S., eds., Coal and coal-bearing strata: Edinburgh, Oliver and Boyd, p. 309-321.

McMillan, N. J., 1956, Petrology of the Nodaway underclay (Pennsylvanian), Kansas: Kansas State Geological Survey Bulletin 119, pt. 6, p. 121-247.

Meckel, L. D., Jr., 1967, Origin of Pottsville conglomerates (Pennsylvanian) in the central Appalachians: Geological Society of America Bulletin, v. 78, no. 2, p. 223-257.

Minear, R. A., and Tschantz, B. A., 1974, Contour coal mining overburden as solid waste and its impact on environmental quality: Appalachian Resources Project Report 30, University of Tennessee, Knoxville.

Morrison, J., 1985, A study of factors controlling acid mine drainage: University Park, Pennsylvania State University, M.S. thesis.

Murowchick, J. B., and Barnes, H. L., 1983, The role of polysulfides in pyrite and marcasite formation [abs.]: Geological Society of America Abstracts with Programs, v. 15, p. 649.

National Research Council, 1981, Soil, coal, and society: Washington, D.C., National Academy Press, 233 p.

Nickelsen, R. P., 1966, Fossil distortion and penetrative rock deformation in the Appalachian Plateau, Pennsylvania: Journal of Geology, v. 74, p. 924-931.

Oldham, I. W., 1979, Analysis of the relationship between composition and the occurrence of bloating shales and clays in the Pennsylvanian System of western Pennsylvania: University Park, Pennsylvania State University, M.S. thesis, 166 p.

Onasch, C. C., 1976, An analysis of the variability of underclays for use as ladle bricks: University Park, Pennsylvania State University, M.S. thesis.

Otte, L. J., 1984, Controls over the quantity and distribution of mineral sediment in North Carolina peat deposits: Geological Society of America Abstracts with Programs, v. 16, p. 185.

Parham, W. E., 1962, Clay mineral facies of certain Pennsylvanian underclays: University of Illinois, Ph.D. thesis, 122 p.

_____, 1966, Lateral variations of clay mineral assemblages in modern and ancient sediments: International Clay Conference, Proceedings, v. 1, p. 135-145.

Paxton, S. T., 1983, Relationships between Pennsylvanian-age lithic sandstone and mudrock diagenesis and coal rank in the central Appalachians: University Park, Pennsylvania State University, Ph.D. thesis, 503 p.

Reidenouer, D. R., Williams, E. G., and Dutcher, R. R., 1967, The relationship between paleotopography and sulfur distribution in some coals of western Pennsylvania: Economic Geology, v. 62, p. 632-647.

Renton, J. J., and Cecil, C. B., 1980, Coal composition relationships in support of a chemical coal model, in Donaldson, A. C., and others, eds., Carboniferous coal short course and guidebook: American Association of Petroleum Geologists, Seminar, Morgantown, West Virginia, v. 3, p. 103-128.

Renton, J. J., Cecil, C. B., Stanton, R., and Dulong, F., 1980, Compositional relationships of plants and peats from modern peat swamps in support of a chemical coal model, in Donaldson, A. C., and others, eds., Carboniferous coal short course and guidebook: American Association of Petroleum Geologists, Seminar, Morgantown, West Virginia, v. 3, p. 57-101.

Rimmer, S. M., 1985, Lateral and vertical variability in petrography and mineralogy of the Lower Kittanning seam, western Pennsylvania and Ohio: University Park, Pennsylvania State University, Ph.D. thesis.

Rimmer, S. M., and Eberl, D. D., 1982, Origin of an underclay as revealed by vertical variations in mineralogy and chemistry: Clays and Clay Minerals, v. 30, p. 422-430.

Sadler, P. M., 1981, Sediment accumulation rates and the completeness of stratigraphic sections: Journal of Geology, v. 79, p. 569-584.

Sawyer, L. E., and Crowl, J. M., 1968, Planning and engineering design of surface coal mines; land reclamation, in Pfierder, E. P., ed., Surface mining: New York, AIME, p. 247-266.

Schumm, S. A., 1977, The drainage basin, in The fluvial system: New York, Wiley-Interscience, p. 57-94.

Senftle, J. T., 1981, Relationships betwen coal constitution, thermoplastic properties and liquefaction behavior of coals and vitrinite concentrates from the Lower Kittanning seam: University Park, Pennsylvania State University, Ph.D. thesis, 223 p.

Shibaoka, M., and Smyth, M., 1975, Coal petrology and the formation of coal seams in some Australian sedimentary basins: Economic Geology, v. 70, p. 1463-1473.

Sholkovitz, E. R., Boyle, E. A., and Price, N. B., 1978, The removal of dissolved humic acids and iron during estuarine mixing: Earth and Planetary Science Newsletter, v. 40, p. 130-136.

Smith, A. H. V., 1968, Seam profiles and seam characterization, in Murchison, D., and Westoll, T. S., eds., Coal and coal-bearing strata: Edinburgh, Oliver and Boyd, p. 31-40.

Snow, S. R., 1983, A mathematical model of river longitudinal profile adjustment: University Park, Pennsylvania State University, Ph.D. thesis.

Stach, E., Mackowsky, M-Th., Teichmüller, M., and others, 1975, Stach's textbook of coal petrology: Berlin, Gebrüder Borntraeger, 428 p.

Staub, J. R., and Cohen, A. D., 1978, Kaolinite-enrichment beneath coals: a modern analog, Snuggedy Swamp, South Carolina: Journal of Sedimentary Petrology, v. 48, p. 203-210.

Sullivan, G. D., 1967, Current research trends in mined-land conservation and utilization: Mining Engineering, v. 19, p. 63-67.

Teichmüller, M., 1974, Entstehung und Veränderung bituminöser Substanzen in Kohlen in Beziehung zur Entstehung und Umwandlung der Erdols: Fortschritte in der Geologie von Rheinland und Westfalen, v. 24, p. 65-112.

Ting, F. T. C., 1967, The petrology of the Lower Kittanning coal in western Pennsylvania: University Park, Pennsylvania State University, Ph.D. thesis, 137 p.

Touysinhthiphonexay, K. C. N., and Gardner, T. W., 1984, Threshold response of small streams to surface coal mining, bituminous coal fields, central Pennsylvania: Earth Surface Processes and Landforms, v. 9, p. 43-581.

U.S. Geological Survey and U.S. Bureau of Mines, 1968, Mineral resources of the Appalachian region: U.S. Geological Survey Professional Paper 580, 492 p.

Waters, S. A., 1981, Factors controlling the generation of acid mine drainage in bituminous surface coal mining: University Park, Pennsylvania State University, M.S. thesis, 247 p.

Weitz, J. H., and Bolger, R. C., 1964, Map of the Mercer clay and adjacent units in Clearfield, Centre, and Clinton Counties, Pennsylvania: Pennsylvania Geological Survey, 4th ser., Map 12, scale 1 in. = 1.5 mi.

Weller, J. M., 1930, Cyclical sedimentation in the Pennsylvanian Period and its significance: Journal of Geology, v. 38, p. 97-135.

White, D., 1925, Progressive regional carbonization of coals: AIME Transactions, v. 71, p. 253-281.

Williams, E. G., 1960a, Marine and fresh water fossiliferous beds in the Pottsville and Allegheny Groups of western Pennsylvania: Journal of Paleontology, v. 34, p. 908-923.

_____, 1960b, Relationship between the stratigraphy and petrology of the Pottsville sandstones and the occurrence of the high-alumina Mercer clay: Economic Geology, v. 55, p. 1291-1302.

Williams, E. G., Bergenback, R. E., Falla, W. S., and Udagawa, S., 1968, Origin of some Pennsylvanian underclays in western Pennsylvania: Journal of Sedimentary Petrology, v. 38, p. 1179-1193.

Williams, E. G., Bergenback, R. E., and Weber, J. N. (1968), Relationship between paleotopography and the thickness and geochemistry of a Pennsylvanian freshwater limestone: Journal of Sedimentary Petrology, v. 38, no. 2, p. 501-509.

Williams, E. G., and Bragonier, W. A., 1974, Controls of Early Pennsylvanian sedimentation in western Pennsylvania: Geological Society of America Special Paper 148, p. 135-152.

Williams, E. G., Bragonier, W. A., and Swinehart, J. B., 1969, Sedimentation in the Carboniferous of western Pennsylvania: American Association of Stratigraphic Palynologists, Annual Meeting, 2nd, State College, Pa., 1969, Guidebook, 78 p.

Williams, E. G., and Griffiths, J. C., 1961, Application of statistical methods in prospecting for high-alumina clay: Pennsylvania State University Mineral Industries Experiment Station Bulletin 77, p. 29-34.

Williams, E. G., Guber, A. L., and Johnson, A. M., 1965, Rotational slumping and the recognition of disconformities: Journal of Geology, v. 73, p. 534-547.

Williams, E. G., Holbrook, R. P., Lithgow, F. W., and Wilson, B. R., 1974, Properties and occurrences of bloating shales and clays in the Pennsylvanian of western Pennsylvania: AIME Transactions, v. 256, p. 237-240.

Williams, E. G., and Keith, M. L., 1963, Relationship between sulfur in coals and the occurrence of marine roof beds: Economic Geology, v. 58, p. 720-729.

Williams, E. G., and Oldham, D. W., 1977, Mineralogy of fine-grained Carboniferous sediments and paleotectonic and paleogeographic significance [abs.]: Geological Society of America Abstracts with Programs, v. 9, no. 3, p. 330.

Williams, E. G., Rose, A. W., Parizek, R. R., and Waters, S. A., 1982, Factors controlling the generation of acid mine drainage: Final Report on Research Grant G5105086, U.S. Bureau of Mines, 265 p.